BIB. NAT. LAB.
REG.BIB.CENTR.
31 MEI 1941
N.V. PHILIPS' GLOEILAMPENFABRIEKEN.

PHILIPS TECHNICAL REVIEW

556

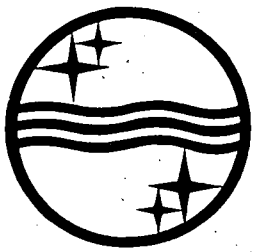

VOLUME V

1940

PHILIPS RESEARCH LABORATORY - EINDHOVEN

CONTENTS

VOLUME V - 1940

LIGHT SOURCES

	page
The new luminous standard	1
Tungsten ribbon lamps for optical measurements	82
Technical photometry of gas-discharge lamps	166
Subjective photometry	280
Rear lights and reflectors for bicycles	335
The blended-light lamp and other mercury lamps with improved colour rendering	341

RADIATION AND ILLUMINATION

The new luminous standard	1
Reflecting surfaces in the neighbourhood of linear sources of light	16
Interesting lighting effect of the Liége water-exhibition	42
Tungsten ribbon lamps for optical measurements	82
Black-out by the filter method	93
The distribution of the light reflected by different ceiling and wall materials	125
Technical photometry of gas-discharge lamps	166
A new fitting for roadlighting	222
Subjective photometry	270
Natural illumination and visibility at night	296
The blended-light lamp and other mercury lamps with improved colour rendering	341

RADIO

The electrometer triode and its applications	54
Testing amplifier output valves by means of the cathode ray tube	61
The hum due to the magnetic field of the filaments in transmitting valves	100
The reproduction of high and low tones in radio receiving sets	115
Electron trajectorics in multigrid valves	131
The accuracy of measurements of field strength	149
A new push-pull amplifier valve for decimetre waves	172
Output and distortion of output amplifier valves under differents loads	189
Measurements of phase angles with the help of the cathode ray tube	208
Wireless telephony with moving motor cars	315
A variable amplifier valve with double cathode connection suitable for metre waves	357

SOUND AND ITS AMPLIFICATION

The laryngophone	6
Perspectives in the development of the violin	36
The transport of sound film in apparatus for recording and reproducing	74
Stereophonic sound reproduction	107
The reproduction of high and low tones in radio receiving sets	115
Microphones	140
Experiments with stereophonic records	182
Output and distortion of output amplifier valves under different loads	189
Standardization of acoustic quantities	243
A photocell with amplification by means of secondary emission	253
A tone generator	263
The perception of pitch	286
Optical experiments with models of the directional distribution of sound in halls	321

CATHODE RAYS

The investigation of rapidly changing mechanical stresses with the cathode ray oscillograph	25
Testing amplifier output valves by means of the cathode ray tube	61
Measurement of phase angles with the help of the cathode ray tube	208
An electrodynamic pick-up for the investigation of mechanical vibrations	230
A cathode ray tube with post-acceleration	245
A cathode ray tube for use in toolmaking	277
An electrical pressure indicator for internal combustion engines	348

X RAYS

	page
X ray photographs with extremely short exposure times	22
X ray apparatus for the macroscopic examination of materials	69
The use of X rays and cathode rays in chemical and metallographic investigations	157
X ray photography with the camera	258
The localization of objects in the human body	309
An apparatus for the measurement of the photographic density of films	331

ELECTROTECHNICAL APPARATUS AND METHODS

	page
The use of selenium valves in rectifiers	199
Measurement of phase angles with the help of the cathode ray tube	208
An electrodynamic pick-up for the investigation of mechanical vibrations	230
A photocell with amplification by means of secondary emission	253
A tone generator	263
A cathode ray oscillograph for use in tool making	277
The measurement of very small phase displacements	300
Geometrical configurations and duality of electrical networks	324
An electrical pressure indicator for internal combustion engines	348

MATERIALS AND THEIR RESEARCH

	page
Drilling diamond dies	14
The investigation of rapidly changing mechanical stresses with the cathode ray oscillograph	26
The use of modern steels for permanent magnets	29
X ray apparatus for the macroscopic examination of materials	69
Measurements in the Philips rare gas plant	88
The use of X rays and cathode rays in chemical and metallographic investigations	157
A permanent magnet which can left 3500 times its own weight	195
Metals as getters	217
Adsorption phenomena at metal contacts	238

MISCELLANEOUS

	page
Drilling diamond dies	14
Quantitative considerations in colour photography by the additive method	48
Measurements in the Philips rare gas plant	88
The use of X rays and cathode rays in chemical and metallographic investigations	157
A permanent magnet which can lift 3500 times its own weight	195
Technical temperature measurement with thermoelements	214
Adsorption phenomena at metal contacts	238
A photocell with amplification by means of secondary emission	253
The localization of objects in the human body	309
Geometrical configurations and duality of electrical networks	324
An apparatus for the measurement of the photographic density of films	331
An electrical pressure indicator for internal combustion engines	348
Alphabetical Index, vol. 1-5	363
Chronological Index, vol. 1-5	368

VOL. 5 No. 1 JANUARY 1940

Philips Technical Review

DEALING WITH TECHNICAL PROBLEMS
RELATING TO THE PRODUCTS, PROCESSES AND INVESTIGATIONS OF
N.V. PHILIPS' GLOEILAMPENFABRIEKEN

EDITED BY THE RESEARCH LABORATORY OF N.V. PHILIPS' GLOEILAMPENFABRIEKEN, EINDHOVEN, HOLLAND

THE NEW LUMINOUS STANDARD

by G. HELLER.

535.241.42

Beginning January the 1st, 1940, the international candle power is to be replaced by a new unit which is based upon the radiation of a black body at the temperature of melting platinum. In this article the considerations are examined which have led to the development of the new light unit. In conclusion the properties of the light of the "new candle" are discussed in detail.

Introduction

When towards the end of the last century, chiefly due to the invention of the carbon filament lamp, the use of electric light was becoming more and more general, the problem of expressing the light produced in numbers also became more and more urgent. It will be obvious that this could be done by comparing the intensity of the light produced with that of a carefully standardized source of light. This luminous standard took the form of a flame, fed with some kind of combustible liquid. It was found possible to render the light intensity of such a light source reproducible with sufficient accuracy by choosing the diameter of the wick, the chemical composition of the fuel, the height of the flame and the direction of observation according to definite specifications. In this way the so-called Hefner candle was established in 1896 in Germany as unit of light intensity. In other countries similar standard lamps were adopted, such as the pentane lamp, the spermaceti candle and the Carcel lamp, and soon attempts were made to reach agreement on an international standard of light intensity.

In these attempts it was found that none of the standard flames could be considered absolutely satisfactory. The use of open flames with precisely determined radiation properties requires very elaborate precautions as to the condition of the atmosphere. Moreover the colour of the light usually deviates very much from that of the sources to be measured (electric lamps), which makes photometric comparison difficult. This difficulty early led to the construction of auxiliary standards for practical use in the form of carbon filament lamps. It was then found that these auxiliary standards could be compared with each other with much more accuracy than with the various primary standards. This led finally to the use of a set of these standard lamps, which had been compared with the national standards in the different countries, as a basis for the establishment of the international unit of light intensity. In 1909 the unit of light intensity so defined was adopted by France, England and the United States, while Germany, in agreement with these countries, established the fact that the Hefner candle was equal to $^9/_{10}$ of an "international candle" (IC).

Objections to the international light unit

Although the fixing of a light unit by means of a set of electric lamps makes possible very simple and accurate measurement, there are serious objections to this method in principle. The most important requirement made of a standard is that it either be absolutely constant or that it be possible to reproduce it with the necessary precision at any moment. Neither of these two conditions is fulfilled in the case of the light unit in question: the light intensity of an electric lamp decreases, although very slowly, in the course of time due to the evaporation of the filament and the blackening of the bulb; it is also impossible — at least until now — to standardize the manufacture of an electric lamp to such a point that a lamp made according to the specifications shall always have the same light intensity within the accuracy of measurement.

In order to avoid the decrease in light intensity, much use is made of secondary and tertiary standards, and the primary standard is used as little

as possible. Nevertheless the situation is far from satisfactory. The various derived standards are not only carbon filament lamps, but also tungsten filament lamps. The latter burn at a considerably higher temperature, and therefore have a different spectral composition of light. This makes a photometric comparison of the different standards so difficult that there still exists some doubt as to the intensities of the various standard lamps.

The difficulties are further increased when the different standard electric lamps have to be compared not only with each other, but also with the Hefner candle, which still remained the basis of photometry in certain countries. It was discovered that different values result for the numerical ratio between the Hefner candle and the international candle, according as a carbon filament lamp or a tungsten filament lamp are used as standard of the international candle. The difference amounts to about 5 per cent: with the help of a carbon filament standard the ratio mentioned is:

$$\text{Intern. candle} : \text{Hefner candle} = 1.11,$$

while the tungsten filament lamps give values between 1.14 and 1.17, depending on their colour temperature. It is clear that this discrepancy considerably decreases the comparability of measurements obtained in Hefner units and those in international units [1]).

The difficulties which are encountered in the comparison of the Hefner candle with the international candle must be ascribed to the fact that in using the Hefner candle one is compelled to work with extremely low brightnesses of the photometer screen. Every measurement of intensity is based upon an illumination of the photometer screen by the light source investigated, and a calculation of the intensity by means of the inverse square law. This law will, however, not apply at small distances of the Hefner candle because the light is produced not only at the surface of the flame but partially also in the interior, so that the distance will differ by several millimetres for different parts of the radiation. In order to obviate this difficulty the candle must be placed far enough away from the photometer screen, for instance 1 m. The intensity of illumination is then 1 lux, a value with which it is no longer possible to apply the methods of photometry with great accuracy, and with which moreover an appreciable Purkinje effect already appears [2]).

In order to make the influence of this effect clear, we shall suppose that two photometer screens are illuminated by a tungsten filament lamp and a carbon lamp respectively, with an intensity of about 25 lux (this is a suitable value for photometry), and that the photometer is adjusted for equal brightnesses of the two screens. If we now decrease both light intensities by a factor 25, for instance, by making the distances from the sources five times as great, we will observe that the brightnesses of the photometer screens are no longer equal, but that that of the white photometer screen (tungsten filament) is several per cent higher than that of the yellow screen (carbon filament). The measured ratio between the light intensities of the yellow lamp and the white lamp thus changes in photometry with low intensities of illumination in favour of the white lamp, and it is therefore clear that the latter will give a larger number of Hefner candle powers per international candle power than the former.

The new luminous standard

In order to overcome the above-mentioned difficulties an attempt was made to develop a light unit which combines the advantages of the Hefner candle with those of the international candle. On the one hand therefore the new unit could not be fixed by an existing set of lamps, but it had to be able to be made in a reproducible way according to definite specifications. On the other hand it was desirable for the sake of avoiding photometric difficulties that the new light source should have a considerably greater brightness and also a higher colour temperature than the Hefner candle.

As early as 1879 Violle had suggested a light source which it was hoped would satisfy these requirements. Violle proposed as light unit the intensity of the light radiated by 1 sq.cm of a surface of glowing platinum at the temperature at which platinum is just melting. One twentieth part of this light intensity, which corresponds approximately to the international candle power, was actually considered as the primary light standard in France from 1889 until 1909. After that date this standard light source was, how-

[1]) Although in principle the ratio IC : HK should be able to be fixed absolutely, no one has ever succeeded in removing these discrepancies. The seriousness of this difficulty may be seen from the fact that the I.C.I. in 1928 was forced to recommend different values for the ratio between the international candle and the Hefner candle, depending on the colour temperature, namely:

2000°	1.11
2360°	1.145
2600°	1.17.

[2]) This effect is discussed in detail in Philips techn. Rev. 1, 142, 1936.

ever, discarded because the accuracy with which it could be reproduced was found not to come up to expectation.

The reason is that the radiation of a glowing body is determined not only by its temperature but also by the reflective properties of its surface. Experience showed that by carefully freeing platinum of impurities its melting point could be reproduced to within less than one degree. The reflective properties of the surface, however, even in the case of the most carefully purified material, were not found to be so constant that the light source could be reproduced with the desired accuracy.

There is, however, another method of obtaining a surface with known radiation properties: the body to be heated is given such a form that part of its surface possesses no reflective power at all. Such a "black body" can be realized by a tube which is so narrow and deep that light entering it cannot escape through the opening. Upon heating the tube to a given temperature the absolutely "black" opening of such a tube radiates more intensely than any material surface, possessing certain reflection, and there is moreover the advantage that the intensity of this black body radiation and the variation of the intensity as a function of the wave length is independent of any possible irregularities in the radiating surface of the tube.

It has been found experimentally that the brightness which a black body assumes at the temperature of melting platinum can be reproduced with the desired accuracy, and that this light source is suitable for precise photometric measurements. After these investigations had been concluded it was decided in 1937 [3]) to introduce a "new luminous standard" as unit of light intensity beginning with January the 1st 1940, and that this unit should be defined in such a way that a black body at the temperature of melting platinum has a brightness of 60 new candles per square centimetre. This new light unit has been adopted by all the countries which have until now used either the Hefner candle or the international candle.

Construction of the new luminous standard

Fig. 1 shows the arrangement used by the "Bureau of Standards" for the realization of the new candle. A crucible of thorium oxide is filled with pure platinum. The black radiator is situated at the axis of the platinum ingot and takes the form of a tube also made of thorium oxide. For the purpose of better heat insulation the crucible is placed in a larger container filled with powdered thorium oxide.

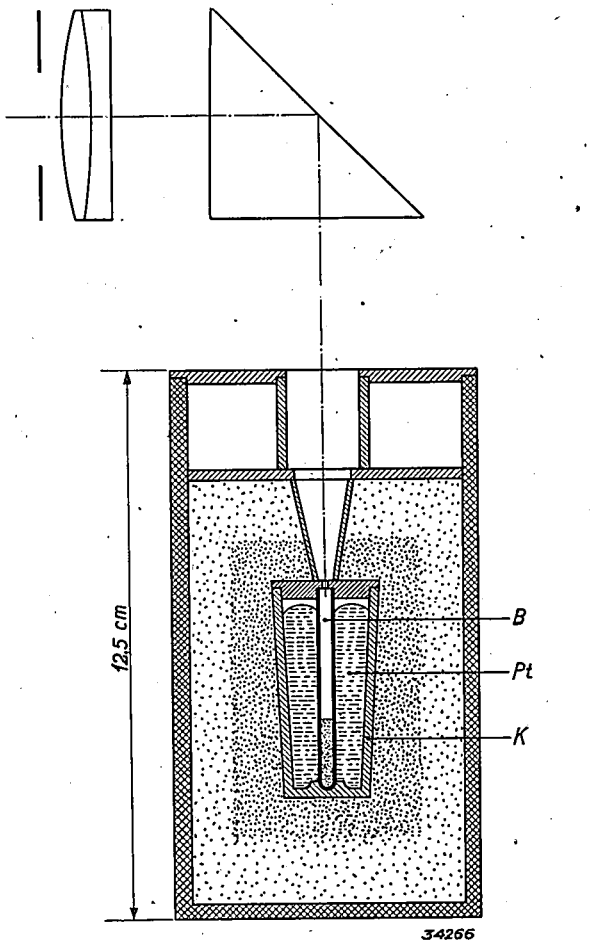

Fig. 1. Experimental arrangement of the "new candle". *B* tube of thorium oxide (black body), *K* crucible of thorium oxide, P_t platinum.

The platinum is heated by means of high-frequency eddy currents which are generated in the platinum itself by means of an induction coil. When the platinum is melted a strong circulation is maintained by the electrodynamic forces occurring in the liquid [4]), which promotes uniformity in the temperature distribution. By means of a prism and a lens the light emerging in a vertical direction from the tube is transformed into a horizontal beam. The intensity of this beam can be compared with that of the substandard to be calibrated by the well known methods of photometry.

Properties of the new luminous standard

The very careful measurements of the Bureau of Standards (U.S.A.), the National Physical Laboratory (England), the Physikalisch-Technische

[3]) Rev. Gén. d'El. XLII, 5, p. 129. Comité internationale des Poids et Mesures, Réunion de juin 1937. Unités photometriques: Résolution I.

[4]) This subject was treated in detail in an article about a high-frequency furnace: Philips techn. Rev. **1**, 53, 1936.

Reichsanstalt (Germany) and G. Ribaud (France) found, in good mutual agreement, a value of the brightness of the black body at the temperature of melting platinum of

58.8 IC/cm², and 65.3 HK/cm²,

which are equivalent when the ratio IC : HK is considered equal to 1.11.

filament standard lamps for the international candle, and it is due to this circumstance that the new candle and the international candle could be compared to each other down to one part in a thousand.

The spectral light distribution of the new candle can be found by calculating the intensity distribution by means of Planck's radiation for-

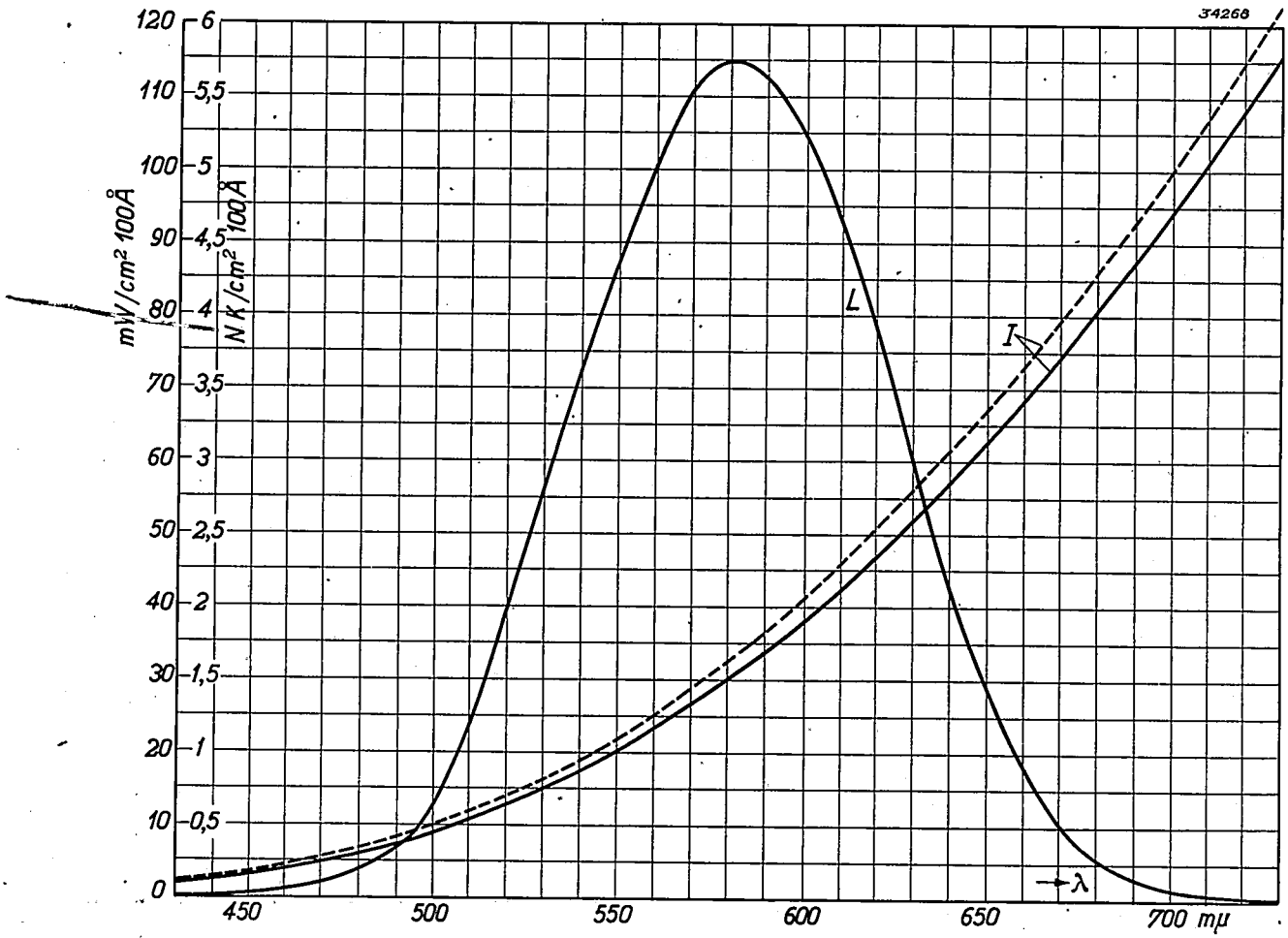

Fig. 2. Radiation intensity I in mW per cm² per 100 Å and light intensity L in new candles per cm² per 100 Å of a black body at the temperature of melting platinum as a function of the wave length. In calculating the full line curves (see equation (1)) we used the constants $c_1 = 3.743 \times 10^{-5}$, $c_2 = 1.439$, $T = 2041.3$, while the broken line curves were calculated with the constants $c_1 = 3.699 \times 10^{-5}$, $c_2 = 1.432$, $T = 2046.6$.

Since by definition this brightness corresponds to 60 new candles per sq.cm, it is clear that the intensity of the new candle lies between that of the Hefner candle and that of the international candle [5]).

The colour of the light from the new candle corresponds approximately to that of the carbon

mula, and then multiplying the intensity at each wave length by the corresponding relative luminosity factor. For this purpose several experimentally determined constants must be accurately known, namely the melting temperature of the platinum T_p and the constants c_1 and c_2 in Planck's formula:

$$I_\lambda \, d\lambda = \frac{c_1}{\lambda^5} \frac{1}{e^{c_2/\lambda T} - 1} \, d\lambda, \quad \ldots \quad (1)$$

which indicates the radiation intensity I_λ of a black body having the temperature T in the wave range between λ and $\lambda + d\lambda$.

[5]) As for Philips lamps, beginning with Jan. 1st 1940 the new luminous standard will be adopted as well as the appropriate new photometric method of bridging the colour difference between the standard light source and the electric lamp. The result of this change will be that there will be little or no change in the intensity of the lamps.

Quite recently some doubt has arisen as to the correctness of the values of these constants accepted in the past [6]). While on the basis of investigations carried out before about 1935 the following values were considered most probable:

$$c_2 = 1.432,\ T_p = 2046.6\ °K,$$

the latest investigations give the results:

$$c_2 = 1.439,\ T_p = 2041.3\ °K.$$

Although the change in the constants only amounts to several parts in a thousand, the theoretical aspect of the spectral intensity distribution is hereby very considerably altered. Further consideration of equation (1) shows that the intensity in the region of visible wave lengths varies approximately with the tenth power of T/c_2. Since T_p has become about 0.25 per cent lower, while the constant c_2 has increased 0.5 per cent, Planck's formula now gives about 7.5 per cent lower values in the visible region than formerly when the old values of the constants were used. A small change also occurs in the value of c_1, which, however, only feably affected the results.

The difference is clearly visible in *fig. 2* where the spectral intensity I is plotted in mW per sq.cm. per 100 Å as a function of the wave length. The broken line refers to the former values of the constants c_2 and T_p; the continuous line is calculated with the new values of the constants. If now we use the spectral intensities to compute the light distribution curve (new candles per sq.cm per 100 Å), which is given by $L(\lambda)$ in fig. 2, we note that the change of constants only has a very small influence. The light distribution curve is found by multiplying the spectral distribution of the intensity (new constants) by the international relative luminosity factors, and in addition by a factor such that the total light intensity becomes equal to 60 candle powers. Since the total light intensity is fixed by means of this factor, the influence of a change in the constants c_2 and T_p on the light intensity curve is much smaller than was to be expected from the intensity curve; practically the same shape is found with the new as with the old values of the constants.

This influence is much greater in the spectral variation of the efficiency given in *fig. 3* as calculated from the data used in fig. 2. The shape of the curve naturally corresponds with that of the international relative luminosity curve. The broken-line curve (old constants) has a maximum of 636 new lumens/watt (624 international lumens per watt) which agrees very well with the values of the so-called mechanical equivalents of light generally given in the literature. With the new constants, however, one finds a maximum of 688 new lm/W (675 int. lm/W), and this high value is difficult to reconcile with the results of other determinations of the light yield. Further investigation on this point is thus called for.

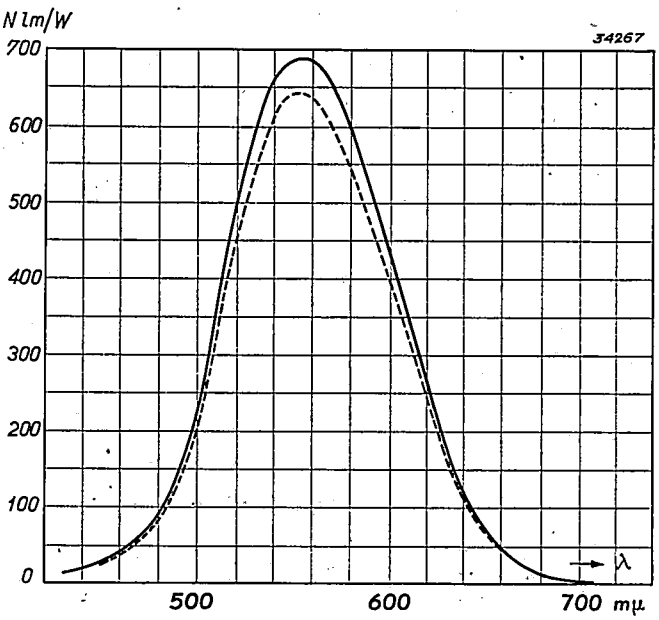

Fig. 3. Efficiency (new lumens per watt) as a function of the wave length, calculated from the data used in fig. 2. When the old constants are used a value for the maximum light yield is found which agrees well with the results of more direct determinations. The new constants, however, give a considerably higher maximum.

These uncertainties naturally do not affect the usefulness of the new candle as a photometric standard; only when energy measurements must be carried out in addition to light measurements must this be taken into account.

[6]) A critical study of the constants c_2 and T_p is given by W. de Groot, Ned. T. Natuurk. **7**, 35, 1940.

THE LARYNGOPHONE

by J. de BOER and K. de BOER.

621.395.61

In telephoning it is possible to use as excitation agent the mechanical vibrations of the speaker's throat instead of the air vibrations which occur in front of the mouth of the speaker. This method makes it possible to use the telephone in places where there is so much noise that the human voice is drowned. The picking up of the throat vibrations is done with a laryngophone, the principle and several structural details of which are described in this article. Two different types have been developed: a crystal microphone in which the chief aim has been the best possible quality of reproduction, and a carbon microphone whose sensitivity can be made so great that it can be used directly in a telephone apparatus instead of the usual microphone. A consideration of the sensitivity of the laryngophone for air vibrations as well as a series of intelligibility tests show to what degree the desired purpose has been realized in the laryngophones described.

In the electrical transmission of sound as in the telephone the first step consists of converting the sound vibrations into voltage alternations by means of a microphone. In general the action of the latter is on the following principle: a body is introduced into the sound field. This body follows the vibrations of the air, and by its movement causes for instance a resistance, a capacity or a magnetic flux to vary. From these variations, by suitable electrical connections, a voltage variation is obtained.

Since the microphone cannot distinguish between the desired air vibrations and any other vibrations which may be present, in order to attain sufficient intelligibility it is necessary that there shall not be too much disturbing sound in the chamber where the microphone is used. What, however, is the situation when the telephone must be used in a place where the disturbance level is so high that one can scarcely make oneself understandable to ones neighbour even by shouting? Consider for example the cabin of an aeroplane, a boiler factory, a ship-building yard, a mine shaft — places where it is often necessary to conduct a telephone conversation, or at least to give orders by telephone, in the midst of deafening noise.

In such places telephoning can be made possible if the speech vibrations are picked up, not out of the noise-filled air but on the throat of the speaker. The "laryngophone" by means of which this is accomplished, could in fact better be compared with an electrical gramophone pick-up than with one of the ordinary types of microphone, since the transmission takes place in this case not by way of air vibrations, but by way of mechanical vibrations, of the throat. And just as we are accustomed to being able to converse calmly in a room while a gramophone record is being played without the gramophone pick-up reacting to the speech vibrations in the air, so we may also expect that a laryngophone will be able to reproduce the vibrations of the larynx without appreciable disturbance from possible noise in the surrounding air.

A laryngophone can of course only be used instead of an air microphone if the throat vibrations have the same form as the air vibrations which occur during speech. To what degree is this true? In order to obtain some insight into this matter we shall first devote our attention to a brief consideration of the mechanism of the excitation of sound in speech.

Mechanism of the excitation of sound in speech

The air which is compressed in the lungs flows along the vocal chords through the pharynx and the mouth or nose to the outside. In pronouncing certain sounds the energy of flow of the air is converted into vibration energy at certain points where the air flux experiences a constriction. This may take place for example in the slit between the vocal chords, in the space between tongue and uvula, between the teeth, between the lips. The vibrations occurring are generally relaxation vibrations caused by the growth and dispersion of tiny air whirls, and they therefore comprise a large number of harmonics. If such an air flux, modulated by such a relaxation vibration, enters the mouth cavity, the latter acts as a resonator, and certain frequencies of the original vibration are reinforced. In this way sounds are formed which are then radiated through the mouth opening as audible sound. The vibrations of the air in the mouth are, however, also communicated to the surrounding fleshy and bony parts of face and neck and can be felt plainly on the outside as vibrations. The most suitable spot for picking up these vibrations is the throat, since here the damping layer between the cavity and the outer skin is thinnest (*fig. 1*); this is the origin of the laryngophone.

From the above it is clear that only those sounds

will be manifested in the face and throat vibrations which are formed by the resonating cavities, or for which these cavities act as resonators to a considerable degree. The farther forward in the mouth the primary relaxation vibration is excited, the less this will be the case. The "explosive" consonants p, t, k and the s sounds, s, f, sh, are therefore poorly represented in the throat vibrations. Most of the other consonants, however, and all the vowels, which are practically the conveyers of speech, are formed chiefly with the collaboration of the resonating cavities. It may therefore be expected that the throat vibrations will be able to form a very acceptable substitute for the actual speech vibrations. This expectation is fully met in the intelligibility tests which we shall describe later.

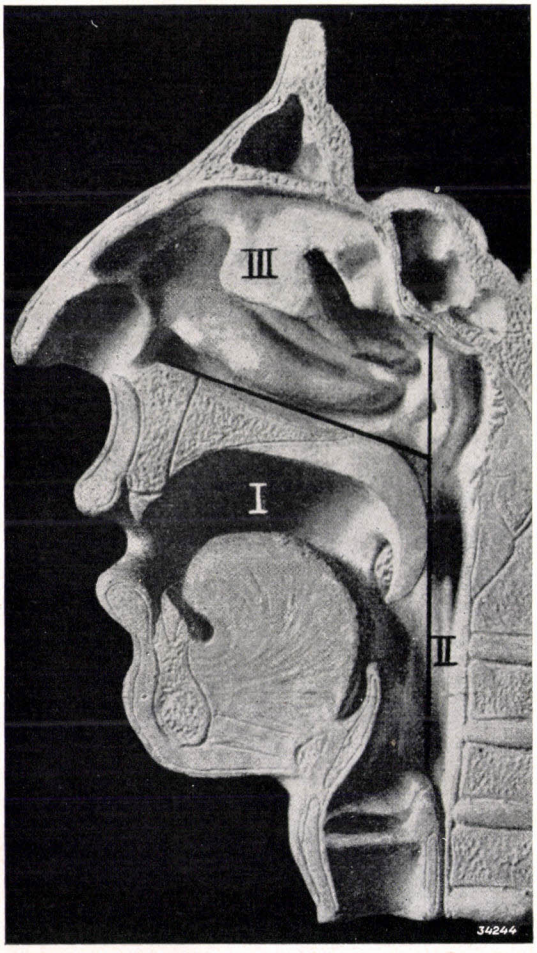

Fig. 1. Cross section of a model showing the wind pipe and the mouth, throat and nose cavities *I*, *II* and *III*. (From Panconcelli-Calzia, Einführung in die angewandte Phonetik, Fischers mediz. Buchh. Berlin 1914).

Frequency characteristic of the radiating body

When the vibrations in the oral cavity are radiated through the mouth as sound, their frequency spectrum ("timbre") experiences a certain additional alteration: the relatively small opening of the mouth radiates high frequencies better than low ones [1]). On the other hand the vibrations in the oral cavity also experience a change in "timbre" in their transmission *via* flesh and bone to the skin of the throat, due to a certain dependence of the damping on the frequency. These two facts can be given common expression by saying that the vibrations of the throat — which we here consider as the primary phenomenon for convenience' sake — must pass another organ having a certain "frequency characteristic" before they are radiated. For this statement to be valid it is necessary that all the sounds be affected according to approximately the same characteristic, which is actually found to be true. In order to make the voltage alternations resemble as much as possible the speech vibrations observed by the ear, in the case where the vibrations of the throat are picked up by the laryngophone, an element must be included in the circuit which has a frequency characteristic similar to that of the "radiator", or provision must be made that the laryngophone itself possesses a sensitivity curve which guarantees the required change in timbre.

What is the appearance of the above-mentioned frequency characteristic? In other words, what is the ratio between the velocity of the air particles and the velocity of the throat for each frequency? In order to discover this a number of speech sounds (vowels and consonants) were recorded at the same time with a calibrated band microphone and with a provisional, likewise calibrated laryngophone on two different gramophone records. For each record the average distribution of the intensity over the different frequencies was measured [2]). With the help of the calibration curves of the two microphones the velocities of the band microphone and of the laryngophone respectively were measured at every frequency. The ratio of the velocities of the air and of the throat, respectively, found in this way, is plotted in *fig. 2* as a function of the frequency (on a logarithmic scale), for three different speakers. By approximation the average characteristic obtained in the frequency range from 200 to 3 000 cycles per sec can be represented by a straight line of slope 2, which means that the "amplification factor" of the hypothetical organ

[1]) By approximation we may consider the radiating mouth as a pulsating sphere. For the behaviour of such a radiator *cf.*: A. Th. van Urk and R. Vermeulen, The radiation of sound, Philips techn. Rev. **4**, 213, 1939.

[2]) As is usual in speech measurements these intensity distributions are recorded with a series of filters each of which passes a frequency band, half an octave broad.

which converts the throat vibrations into air vibrations is proportional to the square of the frequency.

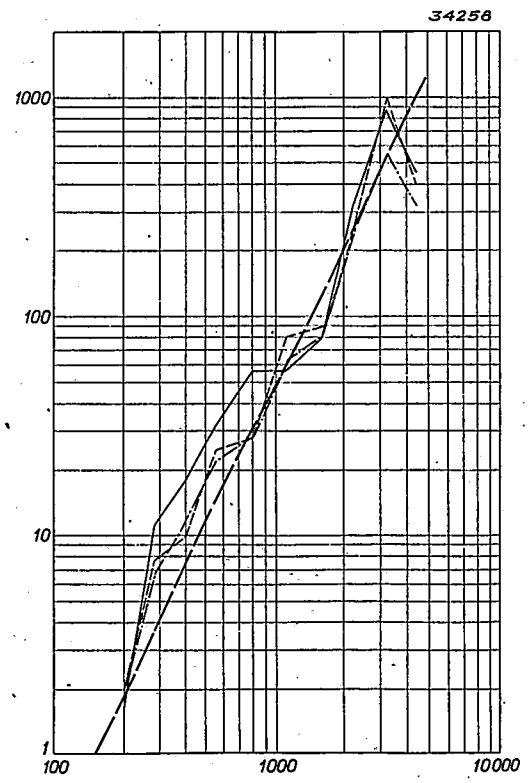

Fig. 2. Frequency characteristic of the "radiator". The average ratio between the velocity of the vibrating air particles in front of the mouth and the velocity of the vibrating throat is recorded as a function of the frequency (in c/sec) upon the pronunciation of different sounds by three different speakers. The characteristic can be represented approximately by a straight line of slope 2.

In order to obtain a voltage amplitude proportional to the velocity of the air particles, therefore, at a constant velocity of the throat the output voltage of the laryngophone plus amplifier must increase with the square of the frequency. If the laryngophone gives a voltage proportional to the velocity of the throat, then an amplifier must be used with a frequency characteristic which increases quadratically. If the output voltage of the laryngophone is not proportional to the velocity, but to the displacement of the throat, then the sensitivity of the amplifier must increase with ω^3.

For ease in replacement of separate links in the transmission it is easier when all the amplifiers occurring can have the usual flat characteristic. One will therefore attempt to construct a laryngophone which already possesses the desired characteristic and which can therefore immediately be combined with normal amplifiers. This is *a fortiori* true when a laryngophone is to be used entirely without amplifier [3]).

Excitation of the laryngophone

It has actually been found possible to construct a laryngophone with a quadratic characteristic, and the construction is even found to be quite simple.

In the case of ordinary air microphones and also in that of the gramophone pick-up the vibrating element (a membrane for instance) is set in motion directly by the vibration to be registered, while the holder in which the element is elastically suspended or clamped remains practically at rest (*fig. 3a*). In a laryngophone on this principle the amplitude of the relative velocity between membrane and holder is identical with the amplitude of the velocity of the throat, *i.e.* instead of the desired quadratic characteristic we obtain a flat characteristic. The laryngophone can also, however,

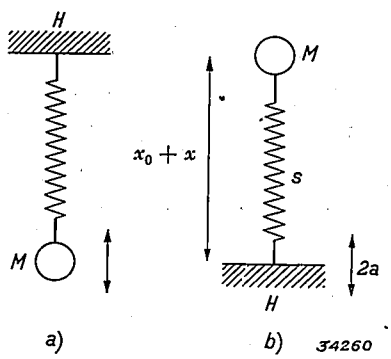

Fig. 3. a) Diagram showing the principle of a directly excited microphone. The holder H remains at rest, the exciting forces act directly on the vibrating element M.
b) Diagram of an indirectly excited microphone. A certain motion is communicated to the holder H and the vibrating element takes on a certain alternating deviation x with respect to the holder; x_0 is the distance between M and H when at rest.

be excited indirectly, namely by allowing the holder to follow the throat vibrations and leaving the vibrating element entirely free. This is represented schematically in fig. 3*b*. If the holder H (the throat) moves according to $a\,e^{j\omega t}$, then the following differential equation is valid for the relative displacement x between the holder H and the vibrating element M:

$$m\,\frac{d^2\,(x+a\,e^{j\omega t})}{dt^2} + sx = 0, \quad \ldots \quad (1)$$

where m is the mass of the vibrating element and s the stiffness of the elastic suspension. The damping has been neglected. Equation (1) can be written in the form:

[3]) A decrease of the sensitivity at low frequencies is moreover also accompanied by the advantage that, at a constant velocity amplitude, the deviations at low tones do not become very large, which might otherwise lead to non-linear distortion.

$$m\frac{d^2x}{dt^2} + sx = ma\omega^2 e^{j\omega t}$$

and its solution is:

$$x = A e^{j\omega t},$$

with

$$A = \frac{a}{\left(\frac{\omega_0}{\omega}\right)^2 - 1}, \quad \ldots\ldots \quad (2)$$

where $\omega_0 = \sqrt{s/m}$, the resonance frequency of the system. If the throat moves with the same velocity amplitude $a\omega$ at all frequencies, the relative velocity amplitude $A\omega$ of the laryngophone varies according to

$$\left|\frac{1}{\left(\frac{\omega_0}{\omega}\right)^2 - 1}\right|, \quad \ldots\ldots \quad (3)$$

which is drawn in *fig. 4.*

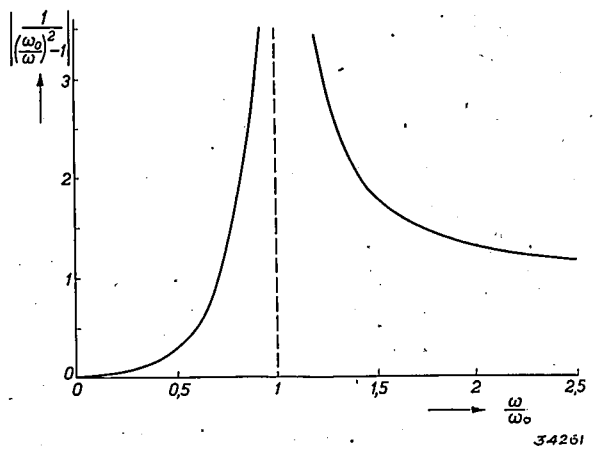

Fig. 4. Variation of the factor (3) as a function of ω/ω_0.

This frequency characteristic has the desired quadratic character in the region $\omega \ll \omega_0$, since (3) can here, by approximation, be replaced by

$$(\omega/\omega_0)^2. \quad \ldots\ldots \quad (4)$$

Practical construction

From the above it is clear that an indirect excitation of the vibrating element is indicated for the laringophone, when its resonance frequency ω_0 lies higher than the frequency region to be reproduced. On the other hand, however, the resonance frequency may not be given any arbitrarily high value since according to (4) the sensitivity of the microphone is inversely proportional to ω_0^2. For the reproduction of speech the frequencies between 500 and 2 000 c/sec are the most important ones; a suitable value for the resonance frequency therefore is in the neighbourhood of 2 000 c/sec.

Two different systems have been chosen for the actual construction: a crystal microphone in which particular attention has been paid to the quality of the reproduction, and a carbon microphone in which the main effort has been to attain the greatest possible sensitivity. We shall describe several details of the construction of these two systems.

Crystal laryngophone

The action of a crystal microphone is based on the piëzo-electric effect: certain kinds of crystals, such as Rochelle salt, assume an electric charge when they are deformed. When a plate cut from such a material at a certain angle to the crystal axes is stretched it becomes positive on one side and negative on the other; under pressure the charges are reversed. If two plates are stuck together in a suitable manner, a plate is obtained which, not by stretching, but by bending, exhibits a certain electrical tension between the upper and the lower sides. In the Philips crystal laryngophone such a plate is clamped in a holder at one end as shown in *fig. 5.* On the upper and lower sides of the plate electrodes making good contact are fastened. The voltage alternations occurring when the plate is in vibration are taken up by these electrodes.

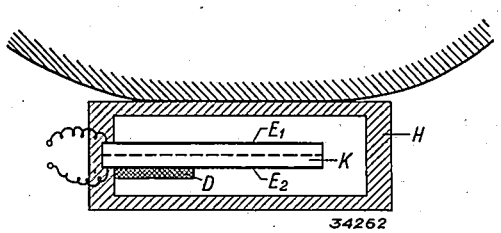

Fig. 5. Construction of the crystal laryngophone. *H* holder, one side of which is pressed against the throat of the speaker; *K* crystal composed of two discs; E_1, E_2 electrodes; *D* damping material.

The simple diagram of fig. 3*b* does not actually apply in the case of this vibrating system, since here the stiffness and the mass are distributed uniformly through the system. Nevertheless a closer consideration leads to the same result, namely that with a vibration of the holder with the frequency ω and the velocity amplitude $a\omega = b$, the plate moves with a relative velocity amplitude $\sim b\omega^2$ (as long as ω lies below the resonance frequency). If the output voltage of the crystal microphone were proportional to the velocity of the crystal the problem would be solved. The piëzo-voltage is, however, proportional to the displacement of the plate, so that at constant velocity amplitude b of the throat against which the holder of the microphone is pressed we obtain a microphone voltage of only $\sim b\omega$ instead of $\sim b\omega^2$.

The required correction of the microphone characteristic is obtained by connecting a relatively low resistance R in parallel with the crystal (*fig. 6*).

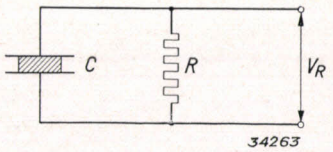

Fig. 6. Connections of the crystal laryngophone. The crystal may be considered as a condenser C upon which an alternating piëzo-voltage V acts during vibration. Resistance in parallel R, output voltage V_R.

If C is the capacity of the crystal, V the amplitude of the piëzo-voltage, then the output voltage obtained is

$$V_R = \frac{RV}{\sqrt{R^2 + \left(\frac{1}{\omega C}\right)^2}} \quad \cdots\cdots \quad (5)$$

When the resistance R is chosen so that

$$R\omega C \ll 1, \quad \cdots\cdots \quad (6)$$

then

$$V_R \approx R\,\omega\,C \cdot V \sim b\omega^2 \quad \cdots \quad (7)$$

and this is the desired relation. The improvement of the characteristic is obtained at the expense of the sensitivity; condition (6) means that according to equation (7) $V_R \ll V$.

With the crystals used, capacity $C = 1000\ \mu\mu$F; with a resistance $R = 10^5$ ohms in parallel, therefore the characteristic has the desired shape up to frequencies of about 1 600 c/sec, where $R\omega C$ becomes equal to unity. The slackening of the rise in the characteristic in this region is compensated partially by the fact that the crystals come into resonance at about 1 700 c/sec [4]). The resonance peak is reduced to the desired proportions by the introduction of a strip of damping material on one side of the crystal (fig. 5).

Fig. 7 shows the frequency characteristic obtained. The ideal curve is shown by the broken line; this is seen to be fairly well approached with a resistance of 10^5 ohms in parallel, in the frequency region between 100 and 3 000 c/sec. The (mean square of the) voltage which is obtained in this case amounts to 20 mV when the speech is of normal intensity.

By the indirect method of excitation, in which no moving parts need to project outside the holder, an unusually compact and sturdy construction is

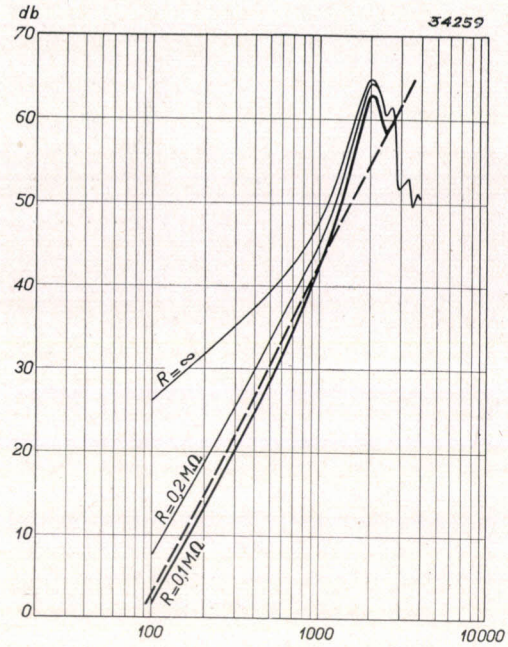

Fig. 7. Frequency characteristic obtained from the crystal laryngophone with different resistances R is parallel. With $R = 10^5$ ohms the ideal relation (broken line) is fairly well approached in the frequency region of greatest importance for speech.

made possible. Moreover, the microphone is small and light in weight. *Fig. 8* shows two microphones, while *fig. 9* shows the manner in which such a microphone can be fastened into an aviator's helmet.

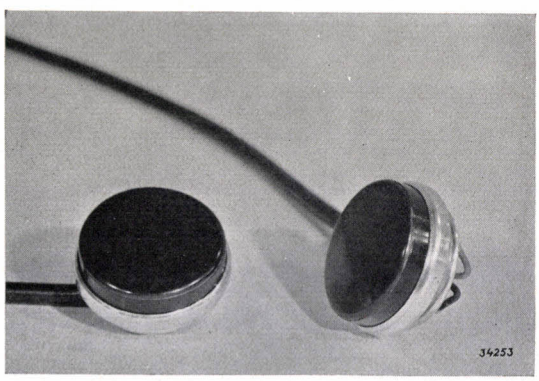

Fig. 8. Two laryngophones. Crystal type and carbon type cannot be distinguished by their appearance.

Carbon microphone

The construction of the carbon microphone is shown diagrammatically in *fig. 10*. Use is again made of the principle of indirect excitation. The vibrating system in this case is a circular membrane M which is stretched across the inside of the microphone holder. Between the membrane and the metal plate P there is a layer of granulated carbon. The electrical resistance of this layer depends closely upon the pressure at which the grains of

[4]) It is unnecessary to take into account the resonance frequencies of higher order which occur with a vibrating continuum, since in this case they lie above 10 000 c/sec.

Fig. 9. The laryngophone can easily be fitted into an aviator's helmet.

carbon are pressed together. Upon vibration of the membrane with respect to the holder the carbon is compressed to different degrees, and the resulting resistance variations lead to variations in an electric current sent through the carbon. The variations are, as in the case of the piëzo- crystal, proportional to the amplitude of the membrane, so that here again the frequency characteristic (at constant velocity amplitude of the excitation) increases with ω instead of with ω^2 as desired. The too great intensity of the low tones which is hereby caused can here also be corrected if necessary in a simple manner. We shall not discuss this point here, but we shall discuss on the other hand the dimensions of the microphone in some detail since they are very important in connection with the desire to attain the greatest possible sensitivity.

The following points must be considered:

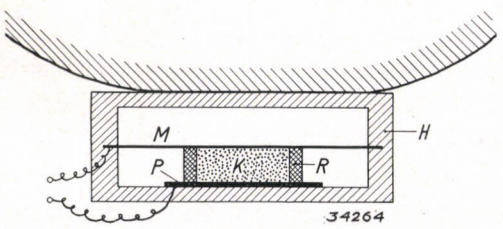

Fig. 10. Cross section of the carbon laryngophone. *M* membrane; *P* metal plate; *K* carbon in the space surrounded by the ring *R* of flexible insulating material.

1) The thinner the layer of carbon the greater the relative variations of the thickness of the layer, and thus of the resistance for the same amplitude of the membrane. If the layer is too thin, however, the non-linear distortion may become too great. Further consideration shows that maximum amplitudes of the membrane of about 0.003 mm may be expected. With this in view a thickness of the carbon layer of about 1 mm has been chosen, and with this no appreciable non-linearity was observed.
2) The bending of the membrane is greatest at the center and zero at the edges. The change in resistance is determined by an effective value of the bending, an average over the whole surface. It is therefore desirable to allow only the centre of the membrane to press upon the carbon (see fig. 10) and thus to make the membrane relatively very large. A limit is set to its size by the requirement that the mass of the membrane must be small enough to give the necessary high value of the resonance frequency. The diameter of the carbon layer may also not be decreased at will. The requirement that the laryngophone must be able to be connected in the place of the ordinary microphone in standard telephone connections had to be taken into account, and this meant that the average resistance of the carbon layer had to have a prescribed value (about 75 - 100 ohms here).
3) The size of grain of the carbon was also influenced by the latter consideration. Since the sensitivity increases with the size of grain it would seem preferable to choose a coarse grain. However, the resistance also depends upon the grain size, so that in connection with the chosen thickness and diameter of the carbon layer the choice of grain size is limited.

The sensitivity obtained is about 200 times as great as that of the above-described crystal laryngophone at a frequency of 1 000 c/sec (the resonance lies at about 2 000 c/sec). Measured during speech, at normal speech intensity and in normal connections (see *fig. 11*) an average power 0.2 mW is obtained.

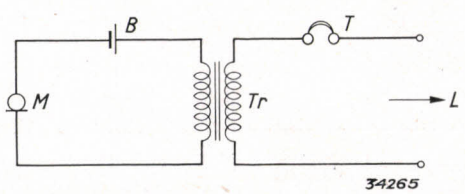

Fig. 11. Normal connections when the carbon microphone is used. *M* microphone, *B* battery of 4 volts, *Tr* transformer 1 : 2, *T* telephone, *L* telephone line.

Fig. 12. By means of a rotating intermediate section a laryngophone can be attached to the ordinary combination of receiver and microphone of a telephone apparatus.

Fig. 12 shows how the laryngophone can be added to the usual combination of receiver and microphone of a telephone apparatus by means of a removable and adjustable intermediate section. When the arm with the laryngophone is turned to such a position that the laryngophone rests against the throat when the apparatus is held in the usual way (*fig. 13*), the air microphone of the apparatus is automatically disconnected, so that the disturbing air vibrations are no longer transmitted.

Fig. 13. When the arms to which the laryngophone is attached are turned into such a position that the laryngophone rests against the throat when the apparatus is held in the ordinary way, the air microphone is automatically disconnected by a switch situated in the intermediate section.

The effect of noise

How does the laryngophone react towards air vibrations? To use a simplified image, we may consider the microphone holder to be a flat plate with the area O and the mass m, which is fastened to a very weak spring (the throat), and upon one side of which the sound pressure p acts. For the displacement y of the plate the following equation is roughly valid:

$$m \frac{d^2y}{dt^2} = p\,O.$$

When p varies with the frequency ω, the plate moves with the same frequency, and an amplitude

$$a = \frac{p\,O}{m} \cdot \frac{1}{\omega^2} \cdot \quad \ldots\ldots \quad (8)$$

Since in the ideal case (a crystal microphone with as mall resistance in parallel) the laryngophone gives an output voltage which is proportional to ω^3 when the amplitude of the holder is constant, the sensitivity of the laryngophone for air vibrations increases proportional to ω. At low frequencies therefore it is least sensitive to air vibrations, which is fortunate, since in many cases the disturbing sounds in question (the noise of motors for example) have their greatest intensity at lower frequencies than speech.

The influence of air vibrations can be calculated with the above-described simple model. In the cabin of an aeroplane there is an average disturbance level of 114 phons. By definition we hear a noise of 74 phons as loud as a tone of 1 000 c/sec with a sound pressure of 1 dyne/cm². We may therefore substitute for the noise in an aeroplane a tone of 1 000 c/sec with a sound pressure of:

$$10^{\frac{1}{20}(114-74)} \cdot 1 = 100 \text{ dyne/cm}^2.$$

With an area $O = 10$ cm² and a mass $m = 18$ g of the laryngophone, the latter, according to (8), has an amplitude

$$a = \frac{100 \cdot 10}{18 \cdot (2\pi \cdot 1000)^2} = 1.41 \cdot 10^{-6} \text{ cm}.$$

From the calibration of the laryngophone it is found that at this amplitude (with a low resistance in

parallel) a voltage of about 4 mV is obtained. Actually the interference observed by the listener will be less than would be represented by 4 mV, since, as stated above, the low frequencies in which the noise is concentrated are transmitted in less intensity than the frequency of 1 000 c/sec taken as a basis, due to the nature of the frequency characteristic of the laryngophone. If we now take into account that this same crystal microphone gives an output voltage of 20 mV in normal speech, and that, even when the intensity of speech and disturbing noise is the same, the intelligibility is satisfactory [5]), it is clear that when a laryngophone is used the noise surrounding the speaker is practically absent for the listener. The only effect of the noise is that the speaker, not hearing his own voice, begins to articulate less clearly or in an unnatural manner.

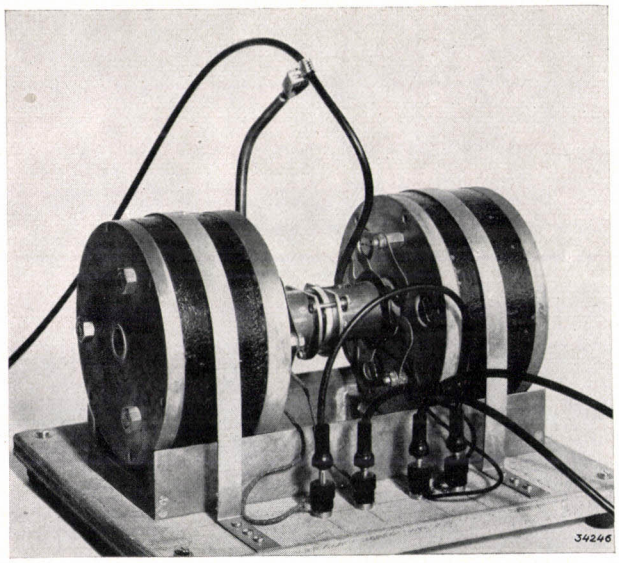

Fig. 14. Apparatus with which the calibration of an indirectly excited laryngophone may be calibrated. Two loud speaker systems are activated by two identical alternating currents differing in phase by 180°, while the laryngophone to be tested is clamped between the two coils.

It will perhaps interest the reader to know how the repeatedly mentioned calibration of the laryngophone is carried out. The apparatus shown in *fig. 14* is used for this purpose. Two loud speaker systems without cones are set up facing each other so that they can be slid back and forth. A brass plate is fastened to the coil of each system. The laryngophone is clamped between these two plates, and alternating currents of equal frequency and amplitude but with 180° difference in phase are sent through the coils, so that the laryngophone is moved back and forth as a whole. The output voltage produced, given by the laryngophone when excited in this way, is measured with the help of an amplifier and a thermocouple, while at the same time the deviations of the laryngophone are determined by setting the needle of a calibrated gramophone pick-up on it and measuring the output voltage of the pick-up.

Intelligibility tests

The utility of the laryngophone can be tested directly by quantitative determinations of the intelligibility. Both types of laryngophone have been examined in this respect in the following way. A number of listeners were placed in a quiet room where they could hear the speech from a loud speaker (in the case of the crystal microphone) or with head phones (in the case of the carbon microphone). At the spot where the speakers (three in our case) were situated the normal noise level of an office prevailed, or a disturbance level of 123 phons could be created. The speakers then read 50 unconnected words in the native language (Netherlands) of the listeners.

In the test on the crystal microphone, which was provided with only a small resistance (10^5 ohms) in parallel for the sake of obtaining the best possible reproduction, an intelligibility of 86 per cent was found without extra disturbing noise. Since normal telephone apparatus give no greater intelligibility than about 90 per cent, the quality of reproduction of the crystal laryngophone may be considered quite satisfactory. When the speakers were surrounded by the above-mentioned noise of 123 phons, the intelligibility decreased by only a few per cent; it then became 80 per cent. The decrease in this case could be ascribed almost exclusively to the less clear articulation of the speakers. For the sake of comparison it may be mentioned that the intelligibility with an ordinary telephone apparatus diminishes to zero when the speaker is surrounded by a noise of only 90 phons!

As was to be expected, the carbon laryngophon gave somewhat lower intelligibility than the crystal microphone. The value without disturbing noise was 77 per cent. After adding the noise of 123 phons the intelligibility decreased to 68 per cent. This is still high enough to enable one to follow a conversation, and thus certainly high enough to be able to make understandable orders, or similar communications of a familiar, recurring nature. If desired, the intelligibility can moreover still be considerably increased by using telephones with a better frequency characteristic than that

[5]) See R. Vermeulen, Auditorium acoustics and intelligibility, Philips techn. Rev. **3**, 1938, 1938.

possessed by the commonly used telephone.

The most important possibilities of application for the laryngophone have already been mentioned at the beginning. Another application would be the use of the laryngophone in combination with gas masks. An air microphone is quite useless in this case due to the resonances in the small sealed air space inside the mask. When a laryngophone is used this difficulty is met, with the added advantage that the microphone can be passed from one speaker to another without it being necessary to open the mask.

DRILLING DIAMOND DIES

In the Philips factory for drilling diamonds, which may be considered one of the largest of its kind in the world, dies for drawing wire are made with diameters from 10 microns up. Part of the production is destined for use in the other departments, namely for drawing wire of tungsten, molybdenum and various other metals.

The diamonds which are made into dies, are first cut off flat on the two opposite sides of the future bore. Facets are then ground in two mutually perpendicular planes parallel to the direction of the bore (see *fig. 1*), which make it possible to follow the drilling process and continually to control it by means of a microscope (title photograph). The diamond so prepared is fastened into a holder. The drilling is done with a needle of a special shape

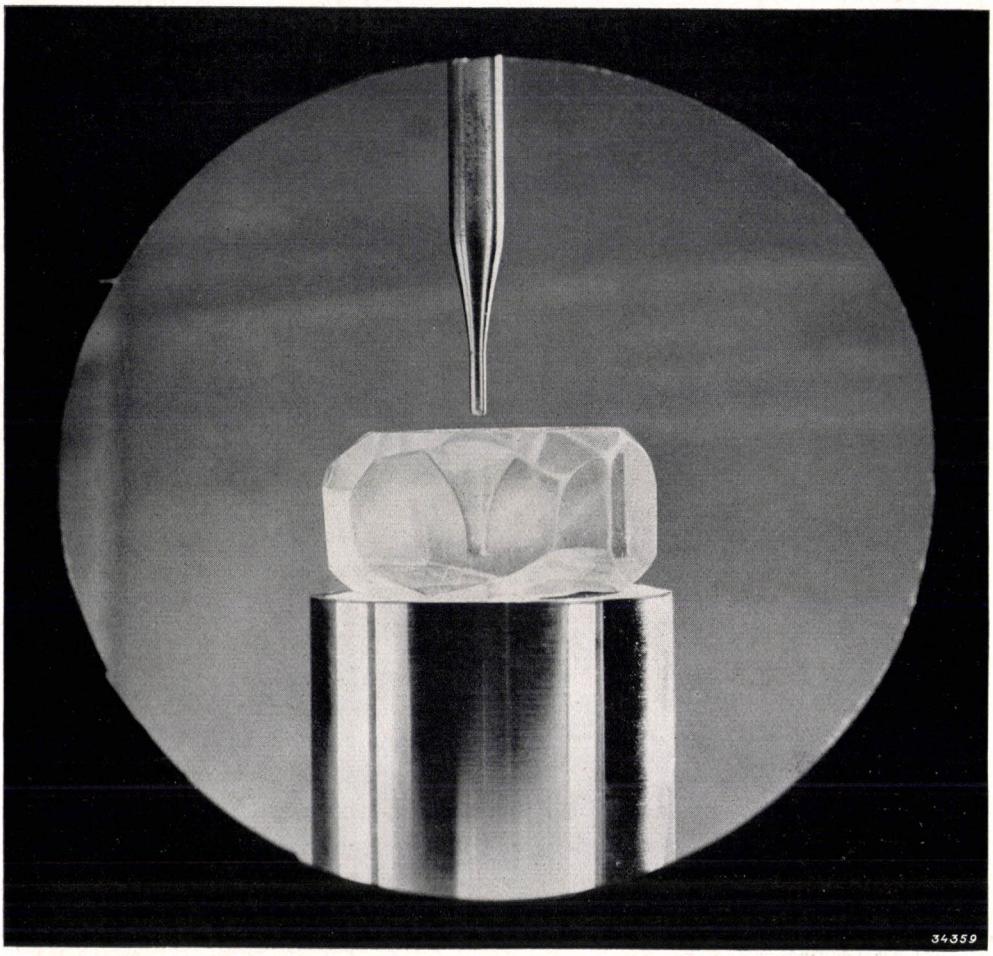

Fig. 1

(fig. 1) which is allowed to take up diamond dust mixed with oil in the pores of its surface. The bore must be given a very definite shape and polish for each material to be drawn in order that the die may have a long life. On the side where the wire leaves the die the drawing channel opens out into a wider depression as may clearly be seen in the photomicrograph *fig. 2* (magnified 120 times).

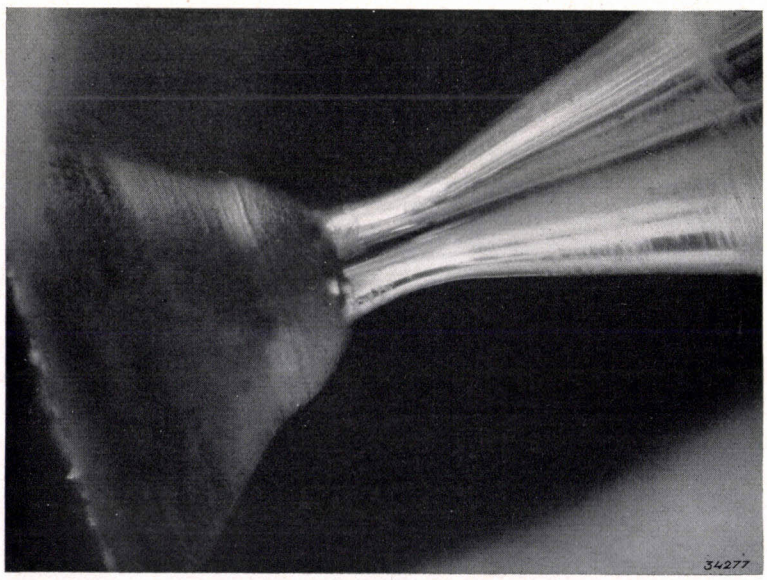

Fig. 2.

REFLECTING SURFACES IN THE NEIGHBOURHOOD OF LINEAR SOURCES OF LIGHT

by N. A. HALBERTSMA.

628.936

Because of the low surface brightness of tubular sources of light it is not necessary to take precautions against glare by means of fixtures. It may, however, be advisable to introduce in the neighbourhood of such light sources specularly or diffusely reflecting surfaces of such shape that they prevent the loss of part of the emitted light for the desired illumination purpose.

In illumination by means of point sources of light, or at least with sources of light of sufficiently small dimensions use is nearly always made of reflectors. This is for two reasons:

1) To decrease the maximum brightness seen by the eye of the observer, thus preventing glare,
2) By means of suitable reflectors to employ the total light flux more efficiently for the illumination of given surfaces than would be the case without such reflectors.

When tubular sources of light are used, the first reasons for using reflectors is no longer valid, since in this case the brightness is generally low enough lower so that there is no risk of glare. While for example with an electric lamp of 150 dlm with a clear glass bulb the brightness of the incandescent coil is 500 c.p./cm^2, and with an inside frosted lamp it is still 3 c.p./cm^2 on an average, and reaches a maximum of 15 to 20 c.p./cm^2, it falls to about 0.3 c.p./cm^2 when the filament is mounted in an opal glass tube, like the „Philinea" lamp. For a mercury-discharge lamp [1]) where the discharge takes place in a glass tube covered on the inside with a layer of luminescent material the brightness is also about 0.3 c.p./cm^2.

When these brightness values are considered, it is obvious that "Philinea" lamps as well as the luminescent discharge lamps can be used entirely without reflectors as far as the danger of glare is concerned, if only the background is light coloured and is sufficiently illuminated. The second reason for the use of reflectors, namely the more efficient use for the desired purpose of the light flux produced retains, however, its full force even in the case of linear sources of light.

The question now is whether it is possible to render the distribution of the light emitted over the different directions in space much more satisfactory by at introducing reflecting surfaces in a suitable way into the neighbourhood of a linear source of light. In the lengthwise direction of the source these surfaces must be at least as long as the source itself. Since in general it is desirable to avoid giving the combination of reflecting surfaces a clumsy and heavy appearance, the dimension of the reflector perpendicular to the axis of the slender light source should be kept small, and it should be mounted close to the source of light. This consideration leads to the use of cylindrical mirrors which need not be less decorative than the light source itself. With such mirrors curved around the tubular light source in one direction only it is of course never possible to obtain such a concentration of the light as can be obtained with a point source by means of surfaces of revolution such as paraboloids.

If the reflecting surfaces are actually very close to the tubular source there is a danger that a large part of the reflected light will again strike the surface of the tube, so that only after several reflections, in which part of it is absorbed, will the light succeed in leaving the space between source and reflector and contribute to the desired illumination. It is therefore important to study the best possible construction of the reflecting surfaces keeping this danger in mind.

In the first place we shall consider the effect of specularly reflecting surfaces on the distribution of the light flux. We shall then consider the influence of diffusely reflecting surfaces.

The action of specularly reflecting surfaces

We shall begin our discussion with a study of the reflection of the light from a tubular source by a plane mirror parallel to the source. *Fig. 1* shows a cross section of this arrangement perpendicular to the axis of the tube. The centre M_2 of the circular cross section of the source lies at a distance $d/2$ from the plane mirror AB. At a distance $d/2$ beyond the mirror lies the mirror image of the actual source of light, and this is again a luminous tube, whose

[1]) Philips techn. Rev. 4, 353, 1939.

centre lies at M_1. The rays reflected by the mirror AB all seem to come from the cylindrical surface of the mirror image of the original light source. If we neglect the loss of light upon reflection the problem is reduced to that of the light distribution of two similar parallel cylinders whose surfaces radiate diffusely, *i.e.* in such a way that the brightness is the same in all directions. This is called radiation according to Lambert's law.

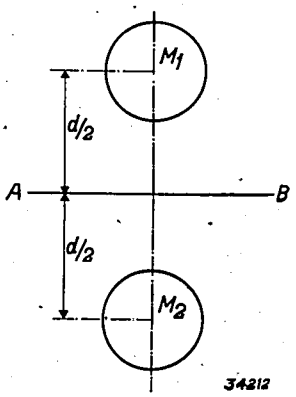

Fig. 1. Cross section of a tubular source of light, centre M_2 and of its mirror image, centre M_1, with respect to the plane AB.

The cross section of the two luminous tubes of diameter $2\ r$ and with a distance d between their axes is shown in *fig. 2*. The light intensity I_α at any given angle α in the plane perpendicular to the axes of the two tubes at their middle point, when the radiation is entirely diffuse, is proportional to the apparent size of the total luminous surface observed at an angle α. The light intensity in our case is therefore equal to the sum of the light intensity of the first cylinder [2]) $C \cdot 2\ r$ and that of that part of the second cylinder which is not screened by the first one. This latter contribution to the total light intensity is variable and amounts to: $C\ (r + y) = C \cdot d \sin \alpha$. The total luminous intensity is therefore:

$$I_\alpha = C\ (2r + d \sin \alpha) \quad . \quad . \quad . \quad . \quad (1)$$

For $\alpha = 0°$ one cylinder entirely screens the other, and the light intensity becomes:

$$I_0 = C \cdot 2r, \quad . \quad . \quad . \quad . \quad . \quad . \quad (2)$$

which is supplied by one cylinder alone, and represents the minimum light intensity for this pair of tubes. At angles equal to or greater than the limiting angle α_1, where:

[2]) The constant factor C in all these expressions is determined by the brightness of the surface of the cylinder and its length.

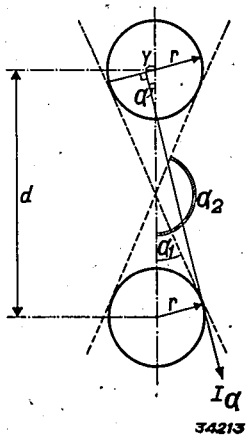

Fig. 2. Cross section of two similar, parallel tubular sources of light. I_α represents the luminous intensity occurring on the plane perpendicular to the axes of both tubes at their middle point, at any given angle α.

$$\sin \alpha_1 = 2\ r/d, \quad . \quad . \quad . \quad . \quad . \quad (3)$$

the total light intensity assumes its highest value:

$$I_{\alpha_1} = C \cdot 4\ r, \quad . \quad . \quad . \quad . \quad . \quad . \quad (4)$$

which is twice the minimum value and is indeed the sum of the equal light intensities of the two tubes.

Fig. 3 shows how the light intensity varies for different distances between the tubes when the angle α varies from 0° to 180°. When the tubes touch one another ($d = 2\ r$) the limiting angle is reached at $\alpha_1 = 90°$ and an intensity equal to twice that of one lamp is observed only in a direction perpendicular to the plane through the axes

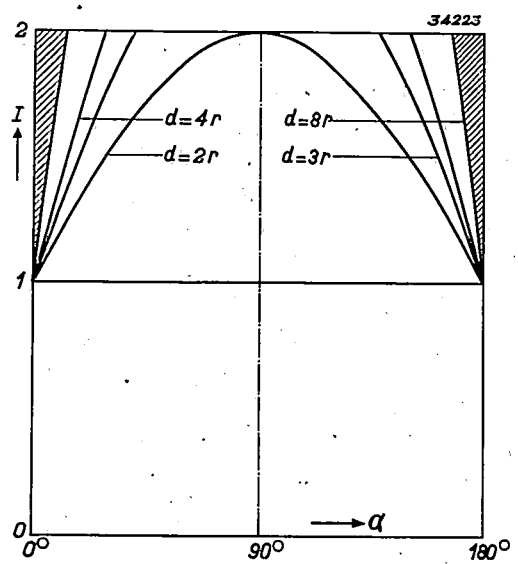

Fig 3. Under the assumption that no light is reflected by their surfaces, the variation of the combined luminous intensity of two parallel lamps at different distances is calculated as a function of the angle α in fig. 2. The results are sine curves. For 0° and 180° the luminous intensity is at a minimum, and is equal to the intensity of a single tube. At $\alpha = 90°$ the intensity reaches a maximum equal to twice the intensity of one tube.

of the two lamps. When the lamps are farther apart the limiting angle α_1 becomes smaller according to formula (3), so that the doubled light intensity prevails throughout a much larger angle, namely from α_1 to $\alpha_2 = 180° - \alpha_1$. When $d = 8r$ only the shaded section of the total light flux is intercepted. It follows from fig. 3 by calculation of the areas bounded by sine curves that, at different distances between the axes of the tubes, the percentages given in the second column of *table I* of the total light flux emitted by the two lamps together are intercepted.

Table I

Percentage of light flux intercepted at different distances between two parallel luminous tubes.

	calculated; without reflection	measured; with reflection
$d = 2r$	17%	6,2%
$d = 3r$	11%	3,4%
$d = 4r$	8%	2,9%
$d = 8r$	4%	1,7%

The figures in the second column of table I would indicate the total loss of light flux only if the lamps could absorb completely all radiation falling upon them. This is of course by no means the case; the diffusing layer on the tube wall will always reflect a considerable part of the incident light. This is proved by the third column of table I and by *fig. 4* which represents measured light distribution for two similar parallel luminous tubes. It may be seen that in the horizontal direction ($\alpha = 90°$) the light intensity is actually greater than twice the intensity of one tube of the pair in question. This excess is provided by that part of the light which is able to escape from the space between the two lamps after having been diffusely reflected one or more times by the tube walls.

While the surface of a single cylinder obeying Lambert's law appears uniformly bright, two parallel luminous tubes exhibit a greater brightness on the sides facing each other than on the sides away from each other due to the reflection of each others' light. This phenomenon will be more intense the closer the tubes are brought to one another, and we therefore may conclude that *the maximum luminous intensity of the pair of tubes will be greater the closer the two tubes are brought to each other.*

If we now determine the loss of light from the measured light distribution curves of fig. 4 we find it to be about $^1/_3$ of the loss calculated when the diffuse reflections are neglected. The results are given in the last column of table I. The fact that about $^2/_3$ of the primarily intercepted light flux is saved is due to the high diffuse reflection factor of the milk glass of which the tubes used in these experiments are made. If, however, we are concerned with the luminescent discharge lamps described in an earlier number of this periodical (see footnote[1]) it is necessary to take into account the fact that the luminescent layer has a smaller coefficient of reflection than milk glass, so that the values in the third column will be larger.

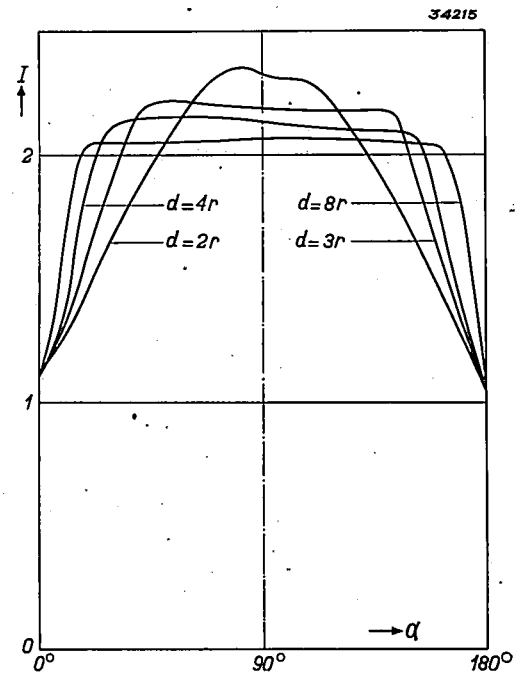

Fig. 4. Measured variation of the luminous intensity for two parallel luminous tubes. At $\alpha = 0°$ and 180° the intensity is again at a minimum and equal to that of a single tube. Perpendicular to this plane, however, the maximum intensity is found to be greater than twice that of a single tube, due to the fact that the light reflected at the surface of the tube can be emitted in a lateral direction.

The practical conclusion from the table is that in order to avoid appreciable losses of light it is advisible not to bring the linear sources of light closer together than a distance equal to their diameter ($d > 4\ r$). In agreement with this they must also not be brought closer to a specularly reflecting plane surface than a distance at least equal to their own radius. Keeping the transverse dimension of the mirrors small, they should be so placed that the reflected light cannot again strike the tube because of the absorption. If we examine what parts of a horizontal plane mirror placed above a

horizontally suspended tubular lamp are most important for the reflection of the light directly downward, we find that these are only relatively narrow strips of the plane mirror (*fig. 5*). These

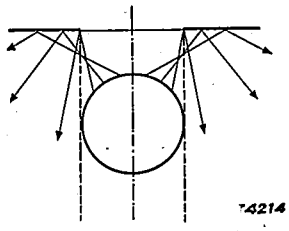

Fig. 5. Reflection of the light of a luminous tube on a plane mirror parallel to the tube. Strips of mirror which do not lie just above the mirror are able to reflect the light which is radiated upward in a downward direction again, without its striking the tube.

most effective strips begin at the lines of intersection of the plane of the mirror with the vertical tangent planes of the luminous cylinder, and continue further away from the cylinder. The strip of the plane mirror lying just above the lamp is less well able to reflect light from the lamp directly downward, so that this part is actually of little practical use. It is better to place the strips of mirror somewhat to the side above the lamp.

In a very simple way, with the aid of two plane mirrors, it is possible to cause all the light emitted upward to be reflected downward again along the sides of the lamp. The two mirrors should have a V-shaped cross section. This combination is placed directly above and parallel to the axis of the lamp (*fig. 6*). The two plane mirrors S_1 and S_2 are now

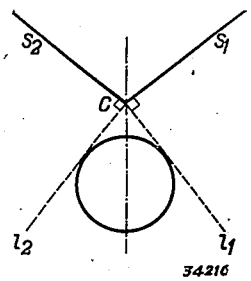

Fig. 6. Cross section of a tubular source of light with two plane mirrors arranged in V-form above it. The tangents l_1 and l_2 from C to the surface of the tube are perpendicular to S_1 and S_2 respectively.

placed at such an angle that they are perpendicular to the tangents l_1 and l_2 respectively in fig. 6. The surface of the mirrors in this position will not reflect any light on to the lamp. The closer the point of intersection C of the two plane mirrors is brought to the lamp, the steeper the angle at which the plane mirrors must be set and the more the upward radiation of the lamp is reflected laterally (*fig. 7*).

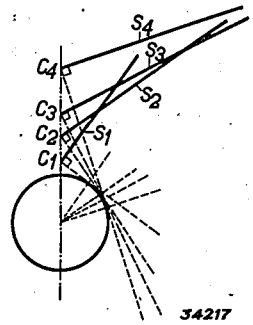

Fig. 7. Positions of plane mirrors which reflect the light downwards as much as possible without causing it to strike the surface of the tubular light source.

As a final problem relating to specular reflection we shall study the shape of a mirror which reflects downward all the light incident upon it from the tubular lamp, and yet in such a way that it does not strike the lamp again. *Fig. 8* shows the shape of the cross section of such a reflector. It may be considered as built up of infinitesimally small strips each of which is oriented as favourably as possible for its position in the manner explained above. Each of these strips is thus perpendicular to the tangent drawn from it to the circular cross section of the lamp. The final shape of the cross section of the mirror therefore becomes that of the involute of the circular cross section of the lamp.

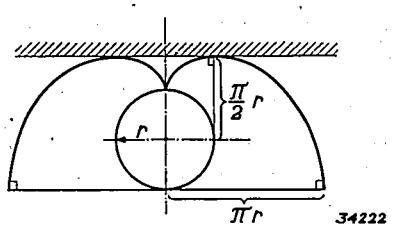

Fig. 8. Shape of a curved mirror to give the best possible downward reflection of the upward radiations of a tubular lamp. The cross section of the mirror is the involute of the circular cross section of the tube.

If we let the edge of the mirror touch the top of the lamp, the plane tangent to the mirror at that point is vertical. If we continue the mirror so far that it catches all the light reflected upwards the tangent plane of the mirror at the end point is again vertical, and the width of this reflecting cove around the linear source of light is only π times the diameter of the tube itself.

The axis of the tubular lamp lies at a distance $\pi/2$ times its own radius lower than the surface of the the ceiling. The distance from the tube wall to the ceiling, in the case of this involute cross section, is thus found to be only $(\pi/2-1)\ r = 0.507\ r$. The lamp may therefore in this case be placed only

half as far away from the ceiling as was found advisable in the case of plane horizontal mirrors.

Reflection by diffusely reflecting surfaces

As stated in the introduction it is possible to employ linear sources of light without any shade or reflector because of the low brightness of the types now in use. In order to avoid exessive contrasts it is, however, advisable to take care that the ceiling, the walls or other diffusely reflecting surfaces in the neighbourhood of the linear sources are white, or at least light in colour.

In this way it is possible at the same time to obtain a great improvement in the effective illumination. The diffuse reflection of a white surface may in fact very well be compared with the specular reflection of ordinary mirrors. In the case of a glass mirror a specular reflection of 85 to 90% per cent is obtained, while the diffuse reflection of a freshly whitewashed ceiling may also amount to 85 to 90 per cent. If it is not specially necessary to concentrate the light in a certain direction, whitewashed ceilings and walls may be considered suitable reflectors.

Upon reflection by a diffusely reflecting surface in the neighbourhood of a tubular source of light it is inevitable that part of the reflected light should again strike the lamp itself. By repeated reflections between the lamp and the white surface part of the light radiated is always lost. The magnitude of this loss has been investigated in the following experiments.

Diffuse reflection by a plane surface

The intensity was measured of the illumination which is provided at a distance of 425 cm by a tubular lamp 50 cm long and 3 cm in diameter with a white plane surface of the same length and a width of 80 cm set up behind it. The measurement was carried out on planes (see *fig. 9*) which made angles of 0°, 15°, 30° and 45° with the reflecting plane surface. The distance between the surface of the tube and the reflecting surface varied from 0 to 24 cm. By subtracting each time from the results of the measurement the intensity of illumination determined without a reflecting surface, the intensities of the reflected light are found. They are indicated in *table II* and in *fig. 10* for two of these angles.

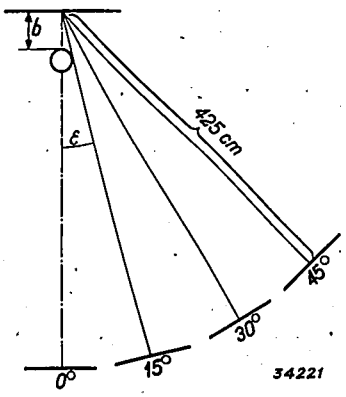

Fig. 9. Cross section of a luminous tube with a diffusely reflecting plane parallel to it and at a distance of b above it. The illumination is measured on a plane parallel to the source and at various angles ε with the diffuse reflector, and at a distance of 425 cm from it.

Table II

Intensity of illumination due to diffusely reflected light, measured in the case illustrated in fig. 9 at various angles ε and for different distances b, expressed in per cent of the intensity of direct illumination provided by the tubular lamp.

	$\varepsilon = 0°$	15°	30°	45°
$b = 0$ cm	64%	64%	63,5%	60%
1,5	70	70	68	63
3	67	67	65	59
6	63,5	63	60	53
12	53	52	48	42
18	42	41	38	32
24	34	33	31	26

As might have been expected the intensity of illumination on the measuring surface due to reflection increases when the source of light is brought closer to the reflecting surface. More light falls upon that surface so that it is able in turn to send out more light. If, however, the lamp comes closer than 6 cm, *i.e.* twice its diameter, to the white surface, the increase in the intensity of illumi-

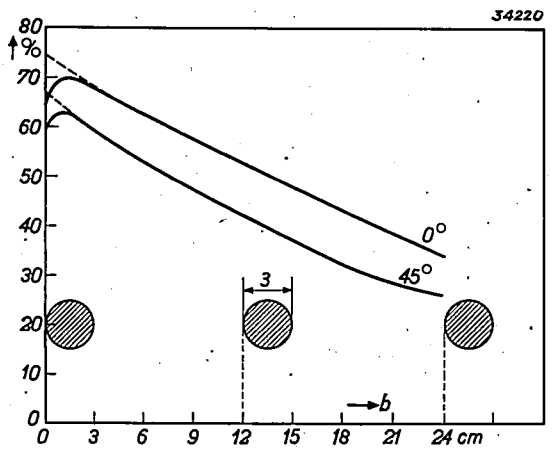

Fig. 10. Intensity of the reflected light measured in the case shown in fig. 9 in directions at angles of 0° and 45° with the normal to the diffusely reflecting plane placed at a variable distance b from the luminous tube.

nation due to reflection becomes less than was to be expected from the values at greater distances, and finally it changes to a decrease. When the surface of the tube touches the reflecting surface, *i.e.* when $b = 0$, the illumination intensity due to reflection at an angle of 0 and 45° amounts to 64 and 60 per cent respectively of the direct illumination intensity, while one might have expected the values 75 and 67 per cent, respectively, from the shape of the curves for greater distances between the lamp and the diffusely reflecting plane.

The relative decrease in the intensity of the light obtained by diffuse reflection for a tubular lamp touching the reflecting surface amounts to 15 per cent and 10 per cent at the angles 0° and 45°, respectively, according to the results of above measurements. The fact that the reflection at 45° is somewhat better than that at 0° may be ascribed to the fact that in the former case the light reflected toward the light source itself has a greater chance of escaping in a lateral direction than in the latter case, perpendicular to the reflecting surface. If we inquire, for example, what is the loss at a distance b of 1.5 cm (this is equal to the radius of the tubular lamp used) compared with the expected increase of the intensity of illumination, it is found to be only 3 per cent as with specular reflection. It is therefore obvious that care must be taken that the distance between the diffusely reflecting surface and the surface of the tube is at least equal to the radius of the tube, just as in the case of specular reflection.

Diffuse reflection by a cylindrical concave surface

As we have seen in the foregoing, a plane white surface introduced into the neighbourhood of a tubular lamp will always reflect a considerable portion of the light falling upon it back into space. If, however, curved white surfaces are used the situation may be much less favourable, because the light has more difficulty in escaping from the space between the lamp and its surrounding curved surface. As an example we shall consider the case in which the tube of diameter d is surrounded by a concentric semi-cylindrical reflector of diameter D whitened on its inner surface.

In *fig. 11* the situation is sketched for the case in which the ratio $D : d$ of the diameters is fairly large. The angle α_1 ($\sin \alpha_1/2 = d/D$), within which the diffusely reflected light is screened by the tubular lamp, is therefore small. The light which is reflected within the angle α_1 will again be partially reflected by the surface of the source and then contribute once more to the emission of the lamp. Part of the light flux which falls outside α_1 is again incident on the diffusely reflecting surface, and then finally contributes to the desired illumination.

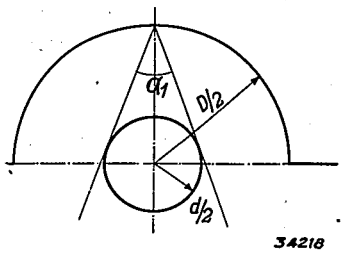

Fig. 11. Cross section of a luminous tube of diameter d surrounded by a large semi-cylinder of diameter D. The diffusely reflected light is intercepted only within a small angle α_1 by the tube.

If the ratio between D and d is only slightly greater than unity, *i.e.* if the cove is made to surround the lamp more closely, as indicated in *fig. 12*, the angle α_2 within which the reflected light is intercepted becomes much larger then α_1 in fig. 11. Only an extremely small part of the light flux from the diffusely reflecting white surface will then be able to escape directly through the narrow opening. In the limiting case in which the two diameters are equal ($D = d$), of the half of the total light flux emitted upward, only that part will not be lost for the purpose in view which returns through the glass wall to the interior of the tube.

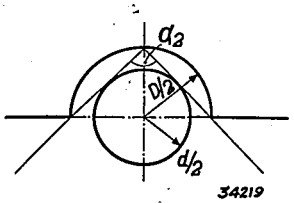

Fig. 12. Cross section of a luminous tube of diameter d closely surrounded by a semi-cylinder of diameter D. The diffusely reflected light is now intercepted by the tube within a wide angle α_2.

If the choice of the diameter of the surrounding semicylinder is determined by the brightness which one desires the whole to possess, it is necessary to know how this brightness can be calculated from the given brightness of the surface of the tube. As has already been explained in this periodical [3]), at sufficiently short distances from linear sources of light the propagation of the light may be considered to take place by way of concentric cylinders, so that the brightness is then inversely proportional to the distance from the axis of the tube. The light which, coming directly from the tubular lamp, is reflected for the first time by the diffusely re-

[3]) Philips techn. Rev. 4, 181, 1939.

flecting concave surface, would, with a reflection coefficient of 1, give a brightness of d/D times that which the surface of the tube itself provides. Actually we may for instance be concerned with a reflection coefficient of 0.8, so that we would then calculate with 0.8 d/D times the brightness of the tube wall. Over against this however is the fact that we must not consider only the light which has been once reflected at the concave surface, but must consider numerous successive reflections between the different parts of the diffusely reflecting concave surface. If the diameter of the latter is large compared to that of the tube ($D \gg d$), then upon reflection according to Lambert's law we find that about 36 per cent of the reflected light is once more incident on the concave surface, so that the light reflected for the second time gives a contributory brightness which is $0.86 \times 0.36 = 0.29$ times the original calculated brightness. Due to the successive reflections therefore there is a geometrical series of contributions to the brightness with a ratio of 0.29, so that finally a brightness is obtained which is $0.8/(1 - 0.29) = 1.13$ times the originally calculated brightness.

X RAY PHOTOGRAPHS WITH EXTREMELY SHORT EXPOSURE TIMES

by W. J. OOSTERKAMP.

621.386.8 : 778.33

When an X-ray tube is loaded for a very short time the specific focus loading may be considerably higher than normal. The amount of radiation available therefore decreases relatively slowly with the time during which loading is applied. The experiments which are described in this article show that simple objects may be photographed with an ordinary X-ray tube with exposure times of the order of one millionth of a second.

In order to take an X-ray photograph a certain amount of X-radiation is necessary, which amount depends upon the nature of the object to be photographed. The amount of X-radiation obtained is, except for a proportionality factor depending upon the tube voltage, given by the product of three quantities the area of the focus of the X-ray tube, the power supplied per unit of this area (the so-called specific focus loading W) and the time of exposure (τ).

When the object to be photographed is moving, the time of exposure may not exceed a certain limit in order to restrict the lack of sharpness due to the motion. The two other factors also have their limits: the focus may not be too large for the sake of sharpness in the image, while the specific focus loading is limited by the permissible increase in temperature (T_m) of the material of the anode.

There is thus a limit to the amount of X-radiation available. The permissible specific focus loading W_m however depends upon the time of exposure τ, according to the equation [1])

$$W_m = \frac{T_m \sqrt{\pi k c}}{2} \cdot \frac{1}{\sqrt{\tau}} \quad \ldots \quad (1)$$

k is here the thermal conductivity, c the specific heat of the anode material. Thus when full use is always made of the permissible focus loading the available X-ray energy (which is proportional to $W\tau$) does not decrease proportionally with τ, as might be expected in the first instance, but only with $\sqrt{\tau}$.

With the present quality of sensitive material (films and intensifying screens) large objects whose photography requires a considerable amount of radiation, such as the thorax, can be photographed with exposure times of the order of 1/100 sec. Because of the fact that the available X-radiation according to the above decreases only slowly with decreasing exposure time, it may be expected that photographs of simple objects which require a much smaller amount of radiation will be possible with extremely short exposure times.

Experiments which have been carried out in this direction show that this is indeed the case. As example a photograph of a hand is given in *fig. 1*. This was taken with an ordinary X-ray tube with an exposure of several millionths of a second. The fact that the

[1]) A. Bouwers, Z. techn. Phys. 8, 271, 1927. The formula has already been used in this periodical in connection with the discussion of the "Rotalix" X-ray tube, in the article by J. H. van der Tuuk, Philips techn. Rev. 3, 292, 1938.

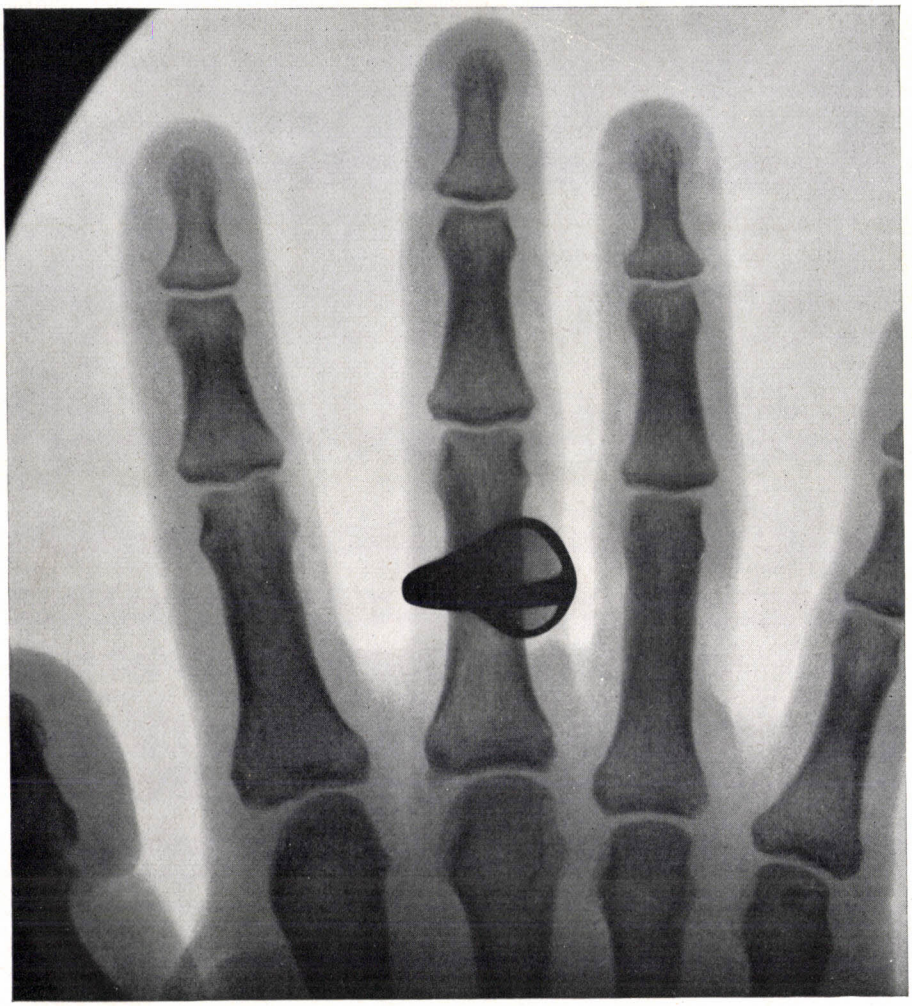

Fig. 1. X-ray photograph of a hand, taken with an ordinary X-ray tube and an exposure time of 5×10^{-6} sec. The bony structure is clearly visible.

photograph is by no means underexposed may be seen by the easily visible bone structure.

Description of the experiments

The X-ray tube used had a tungsten anticathode. If the appropriate values:

$$T_m = 3400^\circ \text{ K}$$
$$k = 1.6 \text{ watt/cm. degree,}$$
$$c = 2.7 \text{ W sec/cm}^3 \text{ degree,}$$

are substituted in equation (1), one finds for an exposure time $\tau = 10^{-6}$ sec. a permissible specific focus loading $W_m = 63$ kW/sq.mm. Since about 20 per cent of the energy supplied to the tube is not dissipated on the focus, but at other spots in the tube (because of secondary electron emission), the specific tube loading may have a still higher value, namely about 80 kW/sq.mm.

This extremely brief heavy loading of the X-ray tube is realized by discharging a condenser across the tube. The circuit is shown in *fig. 2*. The speed of the discharge, *i.e.* the exposure time and the tube load can be adjusted by choosing suitable values for the capacity of the condenser and the tube current. The necessary current can easily be calculated. The focus of the X-ray tube used for the experiments was 8 mm long and 3 mm

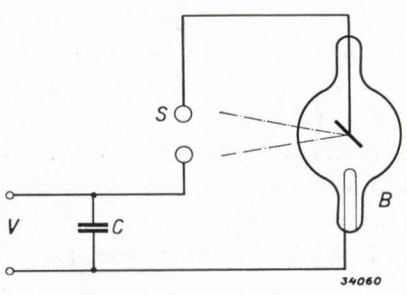

Fig. 2. Circuit diagram for taking "X-ray snapshots". The condenser C is charged by the high voltage source V. At a certain optional value of the voltage the spark gap S breaks down and the condenser is discharged very rapidly across the X-ray tube B.

wide [2]). From this in the case where $\tau = 10^{-6}$ sec. the value of $80 \times 24 =$ about 2 000 kW for the total permissible tube load follows, *i.e.* a current of 20 A with a tube voltage of 100 kV. Such great emission currents can be obtained by temporarily increasing the saturation current of the hot cathode by strong overheating. In the experiments the X-ray tube was provided with a hot cathode such as is used in the "Rotalix" X-ray tubes. The arrangements for the focussing of the beam of electrons cause only a weak electrostatic shielding of the heated filament, so that the saturation current was already reached at relatively low voltages.

In normal X-ray photography the tube current is only about 400 mA. In the case of the experiments here described where the current was 50 times as great, a certain broadening of the focus must be expected due to the mutual repulsion of the electrons in the electron beam. The fact that this broadening nevertheless has no appreciable effect may be seen from *fig. 3* where two photographs of the focus at the two different values of the current are shown side by side for comparison.

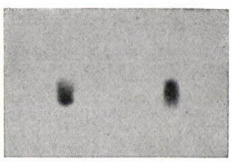

a b

Fig. 3. Photographs in natural size of the focus of the X-ray tube. The tube has a line focus of 8 × 3 mm, which is here photographed at an angle of 13° to the surface of the anode. The photographs were obtained by allowing the X-radiation to pass through a diaphragm of 0.5 mm diameter.
a) Ordinary photograph with a tube current of 0.4 A and an exposure time of several tenths of a second.
b) Instantaneous photograph; tube current 20 A, exposure time one millionth of a second.

In the foregoing we have spoken of a certain exposure time which was tacitly assumed to be equal to the time during which the tube was loaded. When however the X-ray tube is loaded by means of the discharge of a condenser, the loading decreases with the time, and we must define more carefully the terms exposure time and loading time. The voltage on the tube decreases linearly with the time as long as we are still within the region of saturation of the cathode emission. Since the X-ray intensity is proportional to a high power of the tube voltage, we may in practice consider the exposure as concluded when the voltage has fallen to for instance 3/4 of its initial value (*fig. 4*).

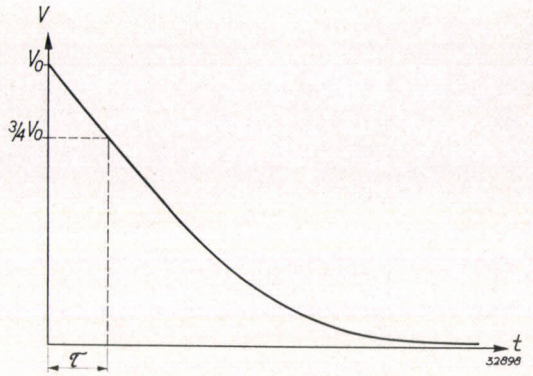

Fig. 4. Voltage V on the tube as a function of the time, during discharge of the condenser. As long as one is still in the region of saturation of the cathode emission, the voltage falls linearly, after that it falls approximately exponentially. One may consider as "effective exposure time" τ the time during which the voltage drops to 3/4 of its initial value V_0.

Similar considerations hold for the loading time: since the "tail" of the condenser discharge contributes much less to the increase in temperature of the focus, and also since the heat conduction toward the inside of the anode takes place very quickly due to the high temperature gradient, the temperature of the focus will no longer increase after a given time which we shall call the "effective loading time". This effective loading time will be of about the same magnitude as the above "effective exposure time". Equation (1) may therefore again be applied if one takes for the specific focus loading a value corresponding to an average

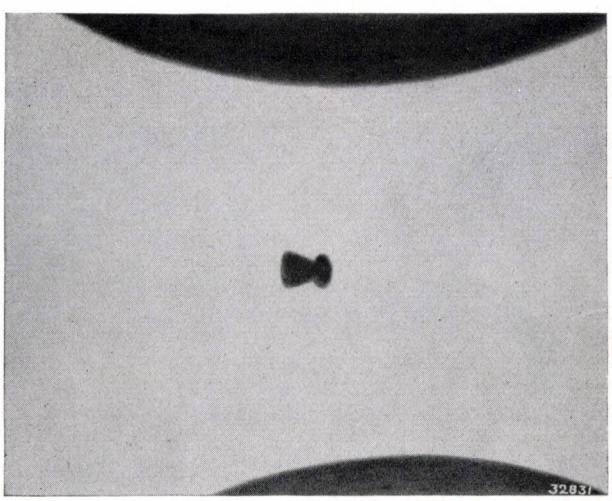

Fig. 5. Photograph of a bullet shot between the two spheres of the spark gap (*5* in fig. 2). The bullet had a velocity of 200 m/sec., the exposure time was 1.5×10^{-6} sec. Further details: capacity of the condenser 0.01 μF, maximum voltage 100 kV, maximum current 20 A. The X-ray tube is hereby loaded with 1800 kW.

[2]) For the exposure an oblique projection of such a "line focus" is used, whereby the "brightness" of the source of radiation is considerably increased. This is explained at length in the article by J. F. de Graaf and W. J. Oosterkamp. An X-ray tube for the analysis of crystal structure, Philips techn. Rev. **3**, 259, 1938.

value in the first section of the voltage drop in the curve of fig. 4.

In fig. 1 a photograph of a hand has already been shown which was taken as an X-ray snapshot in the way described above. It is obvious that the sphere of application of such instantaneous photographs will be the photography of very rapidly moving objects. In *fig. 5* for example a photograph is given of a bullet shot from a gun taken in the above-described way. The bullet had a velocity of 200 m/sec., the effective exposure time was 1.5×10^{-6} sec. This time is short enough, because the lack of sharpness due to the motion, 0.3 mm, is still less than the lack of sharpness caused by the intensifying screens (0.4 mm). In order to obtain the exposure at the moment when the bullet was passing the field, a spark gap was used as high voltage switch. The spheres were placed at such a distance apart that the spark potential is just not reached at the voltage to which the condenser is charged. By dropping a metal object between the spheres, or by shooting the bullet to be photographed between them, the spark discharge is started and the condenser is discharged. With the X-radiation produced the spark gap is photographed, so that the bullet is captured on the photograph. After the exposure, details of which are given under the figure, the anticathode was examined. No traces of overheating were found [3]).

Cinematographic X-ray photographs can also be taken in this way. As an example we may mention the photography of the drops of metal being transferred during the process of welding [4]). The number of exposures which can be made per second in this way is limited only by the charging time of the condenser, and by the condition that the focus must have sufficient time to cool between two successive loads. A rate of several hundred pictures per second is easily attained.

[3]) With the same purpose in view other workers have followed quite a different method (Kingdom and Tanis Phys. Rev. **53**, 128, 1938; Steenbeck, Wiss. Veröff. Siemenswerke **17**, 363, 1938). They constructed a special X-ray tube in which the anode consisted of a pool of mercury. In this case the focus can be strongly overheated if desired since the surface is always restored. In Steenbeck's experiments he estimated a temperature of 100 000° K at the focus, so that he employed much higher specific focus loading than we have used. The total X-ray energy obtainable here is however limited by the fact that the cloud of vapour given off by the anode causes breakdown, *i.e.* a decay of the tube voltage. The higher the load the sooner breakdown occurs, and with it the conclusion of the loading period.

[4]) J. Sack, Philips techn. Rev. **1**, 26, 1936; **2**, 138, 1937; **4**, 9, 1939. The photographs in these articles were however taken with much longer exposure times.

THE INVESTIGATION OF RAPIDLY CHANGING MECHANICAL STRESSES WITH THE CATHODE RAY OSCILLOGRAPH

by S. L. de BRUIN.

621.317.755 : 620.178.5

By means of a specially made resistance strip which is firmly fastened to a part of the structure to be investigated, the changes in shape caused in the structure by rapidly changing mechanical stresses are converted into electrical voltage variations. These latter can then be made visible by means of a cathode ray oscillograph. The very sensitive, portable cathode ray oscillograph type GM 3 152 can be used in this way as a quick-reaction indicator in the study of certain mechanical problems.

Mechanical stresses, which occur in materials and parts of mechanical structures can be investigated by measuring the accompanying changes in shape. These changes are usually only extremely small, but they may nevertheless be investigated with special instruments constructed for that purpose. Such instruments, however, generally have too much inertia to allow the measurement of small, rapidly changing mechanical deformations, such for example as occur upon vibration in steel girder structures, high speed turbine shafts, aeroplane wings, etc. Moreover, the parts of the structure which must be tested are often difficult to reach, so that mechanical instruments can not be brought to bear.

A solution of this difficulty is offered in the possibility of replacing the mechanical measurement by an electrical one in which one may take immediate advantage of the already highly developed electrical measuring technique. It is for example possible in this way to use a cathode ray oscillograph [1]) as a very sensitive indicator with almost no inertia.

For this purpose a simple method has been worked out whereby the mechanical deformation in a structural element can be converted into variations in voltage. A specially constructed resistance strip whose electrical resistance varies practically linearly with its length is firmly attached to the outer surface of the part of some mechanical structure to be investigated. By an appropriate electrical circuit the changes in resistance are converted into changes in voltage which can be made visible directly on the screen of a cathode ray oscillograph. In order to obtain reproducible results, it is very important to take care that the resistance strip is attached as firmly as possible to the surface of the structural element being tested, so that one may be sure that the strip in its entirety undergoes the rapidly alternating expansions and contractions.

[1]) For instance the cathode ray oscillograph GM 3 152 which is described in Philips techn. Rev. 4, 198, 1939 and the employment of which in mechanical engineering is discussed in Ingenieur 54, W 29, 5 May 1939.

The resistance strip

The measuring strip consists of a piece of flexible insulation material (*fig. 1*), upon which a line is drawn with a suspension of powdered charcoal.

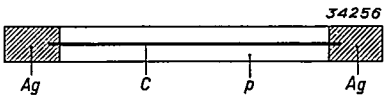

Fig. 1. Sketch of a resistance strip made of flexible insulation material (*p*) and provided with conducting silver ends (*Ag*). *C* is the carbon line whose resistance changes upon stretching or contraction.

The electrical resistance of this carbon line changes as the strip is stretched or shortened, because of the fact that the mutual contact of the carbon particles in it becomes poorer or better as the case may be. Just as in the case of the carbon microphone, where use is made of the fact that the resistance of a mass of carbon powder depends upon the pressure exerted upon it, we can employ this phenomenon in order to measure the deformations to which a mechanical construction is subjected at different conditions of loading. The great sensitivity of this method of measurement may be convincingly demonstrated by a very simple test. If the measuring strip is included in a sufficiently accurate resistance meter, a measuring bridge for example, and if the strip is then bent with the carbon line on the convex side of the resulting curve, so that it is stretched, the resistance is actually found to have increased compared with that in the non-deformed state. If the strip is bent so that the carbon line is on the inner, concave side, the resistance becomes smaller.

The resistance strip is prepared in the following way [2]). On a strip of insulation material 0.3 mm thick, 50 mm long and 8 mm wide (see fig. 1), between the ends, which have been rendered conducting by means of a layer of silver, a line is drawn with a drawing pen, using very finely divided carbon powder suspended in a liquid

[2]) The necessary components bear the type number GM 4 470.

binder. The binder is dried by heating. A strip is obtained in this way with a resistance of for instance about 10 000 ohms.

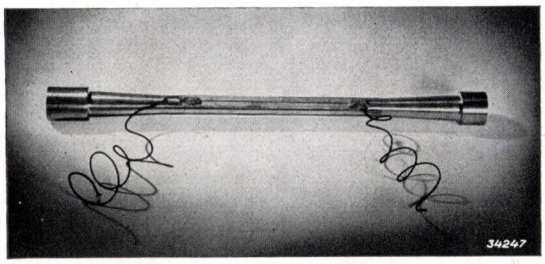

Fig. 2. Tie rod to which a resistance strip is fastened.

The resistance strip can easily be cemented to the surface of the object to be examined, for instance a tie rod (*fig. 2*) by means of celluloid lacquer. According as the temperature of the object tested is higher or lower the strip glued to it must be dried under pressure for $^1/_2$ to 1 hour. The copper wires, by means of which the strip can be included in an electrical circuit, are then fastened to the silvered ends of the resistance strip by means of a cement containing highly conducting metal. Finally, to avoid the absorption of moisture from the atmosphere, it is advisable to cover the whole resistance strip with a layer of celluloid lacquer before the measurements are begun.

Connections and sensitivity of the measuring arrangement

The resistance strip, prepared as described in the preceding section, is included in an electric circuit as indicated in the diagram of *fig. 3*. With a sufficiently high series resistance R_v, the voltage variations between the terminals of the measuring strip R_w, which is in parallel with the built-in amplifier of the cathode ray oscillograph giving an amplification of about 1 500 times, are in the first instance practically proportional to the resistance variations of the measuring strip. When the deformations are not too great, 0.05 per cent at the most, for instance, these resistance variations are also approximately proportional to the deformations, and the latter in turn, according to Hooke's law, are proportional to the mechanical stresses which cause them in the material tested. We therefore obtain as result a deviation on the fluorescent screen of the cathode ray tube which is practically proportional to the mechanical tensile stress to be measured.

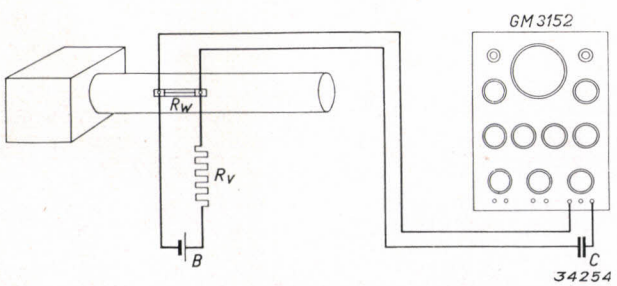

Fig. 3. Measuring arrangement with the cathode ray oscillograph 3 152. R_w is the resistance strip, R_v a series resistance, B a battery and C a condenser which serves to prevent direct current from passing through the oscillograph.

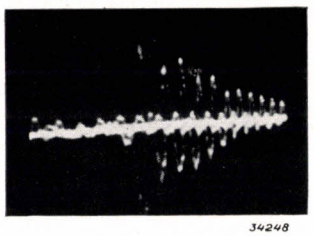

Fig. 4. Oscillogram of the variation with time of the mechanical tension in the outermost layers of a rod clamped at one end which is struck at a given moment and then allowed to come to rest unhindered.

Thanks to this proportionality it is possible to judge the vibration phenomenon to be investigated directly from the fluorescent screen of the oscillograph. As an example an oscillogram is reproduced in *fig. 4* which shows the change of tension with time for a rod clamped at one end which is set vibrating at a given moment and then allowed to return to rest without interference.

If it is desired to measure the mechanical deformations in absolute values, the relation between the change in resistance and the change in length of the measuring strip must be established by calibration. For this purpose a resistance strip is glued to a tie rod for instance (fig. 2) and included in a

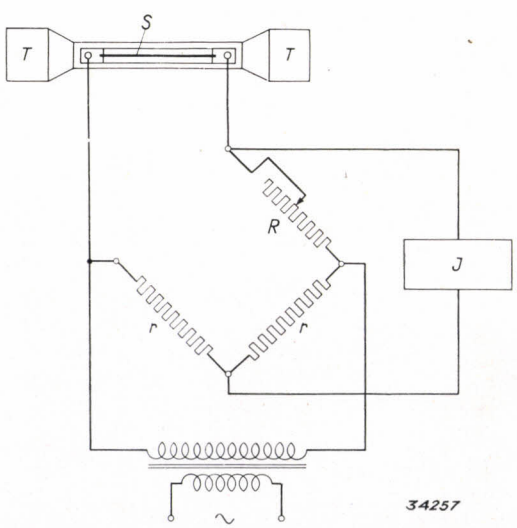

Fig. 5. Circuit of an electrical measuring bridge with which the resistance strip can be calibrated. T tie rod, S resistance strip, R resistance box, r fixed comparison resistances, J pentode amplifier with a tuning indicator.

bridge circuit [3]) as in *fig. 5*. The tie rod can then be stretched in a machine for testing tensile strength (*fig. 6*).

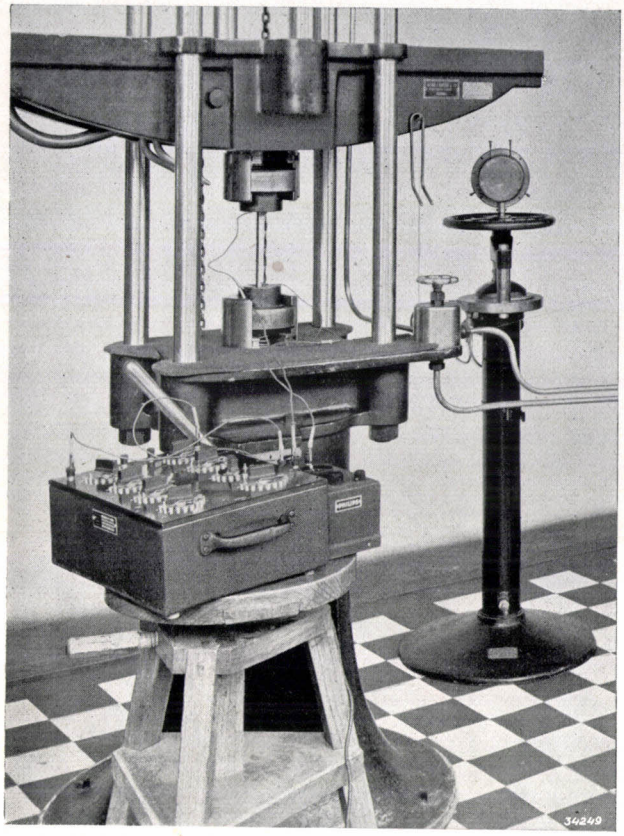

Fig. 6. Measuring arrangement for the calibration with the help of a machine for testing tensile strength.

Between the specific change in resistance of the measuring strip and the specific change in length ϱ of the tie rod, measured with the above-mentioned machine, a satisfactorily reproducible [4]) relation can be found of a character such as that shown in curves *I*, *II* and *III* of *fig. 7* which were determined with several test objects. It may be seen from this that for deformations ϱ of not more than 0.03 per cent, the relation between the variation of electrical resistance λ and mechanical tension is in fact practically linear. In this region the quotient λ/ϱ has a value of about 15. With larger deformations the electrical resistance is found to increase more rapidly than proportional to the stretch.

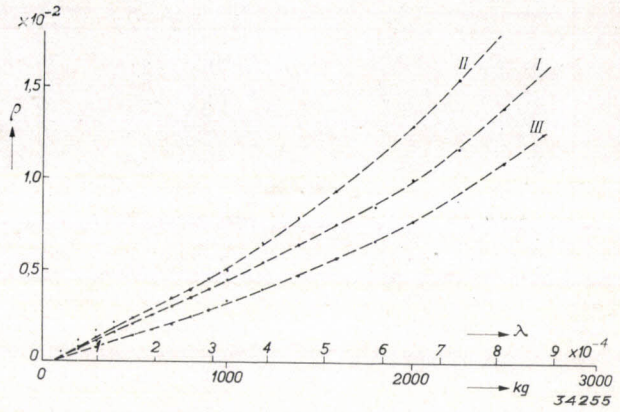

Fig. 7. Relation between the specific resistance variation ϱ of the measuring strip and the load on the tie rod in kg, or the specific stretch λ of this tie rod.

For the calibration of the measuring strip it is by no means necessary that one use a machine for testing tensile strength, it is only necessary to be able in some way or other to cause an accurately measurable change in length of the strip. In order to test a strip it may for instance be glued to a test rod (*fig. 8*) which is supported at two points at a distance $2\,l$ from each other. The rod is then bent between its points of support into a circular form over a distance d. The changes in length of the upper and lower surfaces of the rod then follow from the formulae for the circle. In this way the specific change in length of the rod can be determined and the relation between that and the specific change in resistance of the strip, measured in bridge connection, can be found.

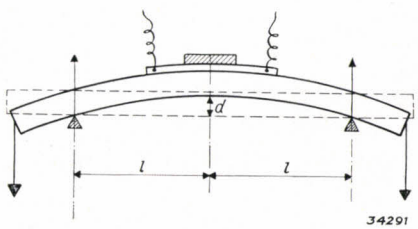

Fig. 8. Circularly bent test rod, supported at two points at a distance apart of $2l$ and with a bend of d.

[3]) For example the "Philoscope", type GM 4 140 which was discussed in Philips techn. Rev. **2**, 270, 1937.

[4]) For reproducibility it is necessary, as is usual in stretching tests, that the rod should have been prestretched.

VOL. 5 No. 2 FEBRUARY 1940

Philips Technical Review

DEALING WITH TECHNICAL PROBLEMS
RELATING TO THE PRODUCTS, PROCESSES AND INVESTIGATIONS OF
N.V. PHILIPS' GLOEILAMPENFABRIEKEN

EDITED BY THE RESEARCH LABORATORY OF N.V. PHILIPS' GLOEILAMPENFABRIEKEN, EINDHOVEN, HOLLAND

THE USE OF MODERN STEELS FOR PERMANENT MAGNETS

by A. TH. van URK.

In order to obtain a certain magnetic field strength in a given air gap with as little magnet steel as possible, the construction of the magnet must be so chosen that the product of induction and field strength in the interior of the magnet steel is as large as possible. In the case of modern magnet steels with very high coercive force and relatively low residual magnetism, this condition leads to quite different constructions than in the case of the older kinds of steel with low coercive force and high residual magnetism. It is explained in this article how one sets about the construction of a magnet. In the first part spreading is neglected: in the second part a semi-empirical method is given of taking spreading into account.

Introduction

If we wish to improve upon a magnet made of the tungsten steel [1]) formerly used, it would seem obvious simply to substitute for the tungsten steel a piece of modern magnet steel of the same shape. The result would, however, usually be found very disappointing: the magnet is scarcely improved at all. The modern magnet steel may even produce a weaker field than tungsten steel.

On the other hand it has been found that upon judicious construction of the whole magnet modern magnet steels do give very much better results than the steels formerly used, and that with the magnet steel "Ticonal 2A" for instance a field can be excited in a given air gap which could only be obtained with ten times as much tungsten steel. It follows from this that the disappointment mentioned above must not be ascribed to the steel itself, but to the fact that a design intended for tungsten steel is not suitable for making the most of the specific qualities of the modern magnet steels.

The aim of this article is to find out the reason for this, and to learn how a magnet should be designed in order to use a given kind of magnet steel to the greatest advantage.

[1]) Tungsten steel may be considered as the best representative of the older type of magnet steel. Modern magnet steels differ in physical respects from the steels used earlier mainly in the nature of the rearrangement processes in the material by which the magnetic hardness is obtained; see in this connection: J. L. Snoek, Philips techn. Rev. 2, 233, 1937.

Comparison of modern and older kinds of steel

The properties of a magnet steel are determined by its magnetization curve. The shape of this curve can be established approximately by the values of residual magnetism and coercive force (see *fig. 1*). The residual magnetism or remanence is the maximum induction which remains in the steel when the magnetizing field is reduced to zero after the steel has been magnetized to saturation. The coercive force is the magnetic field which must be applied in a direction opposite to the residual induction in order to reduce the latter to zero.

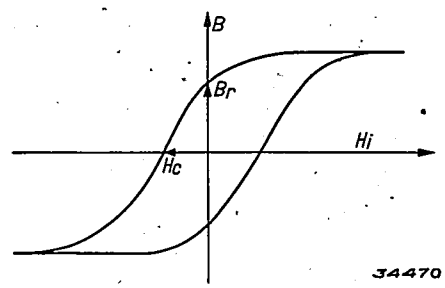

Fig. 1. Induction B of a magnet steel as a function of the internal field H_i. The remanence is B_r, the coercive force H_c.

Fig. 2 gives the magnetization curve of a modern nickel- aluminium steel, such for example as the previously mentioned "Ticonal 2A", compared with that of a tungsten steel. It may be seen that an increase of the coercive force of nearly tenfold is obtained by the sacrifice of part of the remanence, which has fallen back to nearly one half. In spite

of its lower remanence, however, the magnet steel "Ticonal" must in general be considered very much better than tungsten steel. In order to show why this is so, we shall examine the results obtained in solution of the problem of obtaining a certain field strength in a given air gap with as little magnet steel as possible.

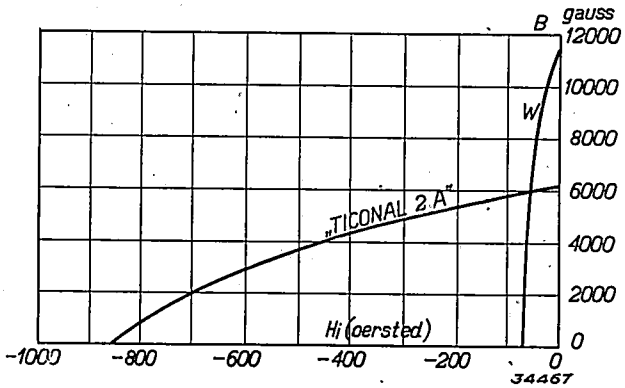

Fig. 2. Induction B of a tungsten steel (W) and of the magnet steel "Ticonal 2A", as functions of the internal field H_i which is opposite in direction to the induction in the part of the curve given.

Simplified calculation of a magnet

We shall begin with a magnet constructed as indicated in *fig. 3*, namely a magnet of length L and cross section S, upon which two pieces of soft iron are fastened, which together bound an air gap of length l and cross section s. For the sake of simplification we shall assume for the present that the lines of force of the magnet must all pass through the air gap in order to pass from the north to the south pole. Thus spreading is neglected. Furthermore, the fields in the magnet steel and in the air gap will be considered homogeneous, and we shall also assume that the soft iron is absolutely conductive for magnetic flux, *i.e.* at any arbitrary value of the induction B the field H_i in the soft iron is zero.

The magnetic condition of the model thus simplified can be described by three quantities: the external field strength H in the air gap, the internal field strength H_i and the induction B of the magnet

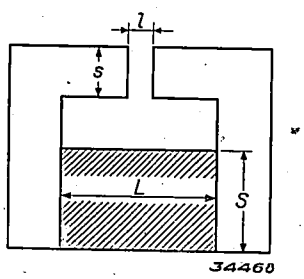

Fig. 3. Model for simplified calculation of a magnet. The air gap has a length l and a cross-section area of s; the magnet steel has a length L and a cross-section area S.

steel. Now three equations are sufficient for the calculation of a magnet in the first approximation.

The first equation is derived from the proposition that the total magnetic flux is the same through every cross section of the system, and therefore also through a cross section of the magnet and of the air gap. The equation is therefore as follows:

$$B\,S = H\,s. \quad \ldots\ldots\ldots \quad (1)$$

The second equation follows from the proposition that the line integral of the magnetic field strength is zero along every closed path. Since the field strength is assumed to be zero in the soft iron, this means that:

$$H\,l + H_i\,L = 0, \quad \ldots\ldots \quad (2)$$

$$H_i\,L = -\,H\,l. \quad \ldots\ldots\ldots \quad (2a)$$

H_i is therefore opposite in sign (opposite in direction) to H.

Finally as third equation we have the relation between B and H_i which is given by the magnetization curve of the magnet steel:

$$B = f\,(H_i) \ldots\ldots\ldots\ldots \quad (3)$$

We are practically concerned with the part of the curve in which the direction of the field strength is opposite to that of the induction (*cf.* fig. 2), so that the field has a demagnetizing action. Before we make use of this curve, we shall however first draw a general conclusion which becomes obvious when we multiply equations (1) and (2*a*) by each other. The result of this operation:

$$-\,B\,H_i\,L\,S = H^2\,l\,s \quad \ldots \quad (4)$$

expresses the fact that the volume l_s of the air gap, multiplied by the square of the field strength, is equal to the volume LS of the magnet, multiplied by the absolute value of the product BH_i. Since the problem is, with a given air gap and field strength in the air gap, *i.e.* with a given second term, to keep the volume LS of the magnet as small as possible, it follows from (4) that we must choose a magnet steel or a design of construction whereby the product BH_i is as large as possible. Now for a given magnet steel BH_i is not a constant, but depends upon the value of H_i. That is obvious, because the product disappears for $H_i = 0$ (B is equal to the remanence), as well as for $B = 0$ (H_i is equal to the coercive force), while at intermediate values it is not equal to zero. With a given value of H_i, therefore, the product will have a maximum (see *fig. 4*).

The height of the maximum of BH_i now provides us with a measure of the quality of a magnet steel, while the corresponding value of H_i determines the most favourable design of the magnet. For tungsten steel the maximum lies at 30 oersted and amounts to 2×10^5 gauss-oersted; for "Ticonal 2A" the maximum lies at 400 oersted and amounts to 1.8×10^6 gauss-oersted. According to equation (4), therefore, nine times less "Ticonal" steel than tungsten steel is necessary to produce the same field in a given air gap.

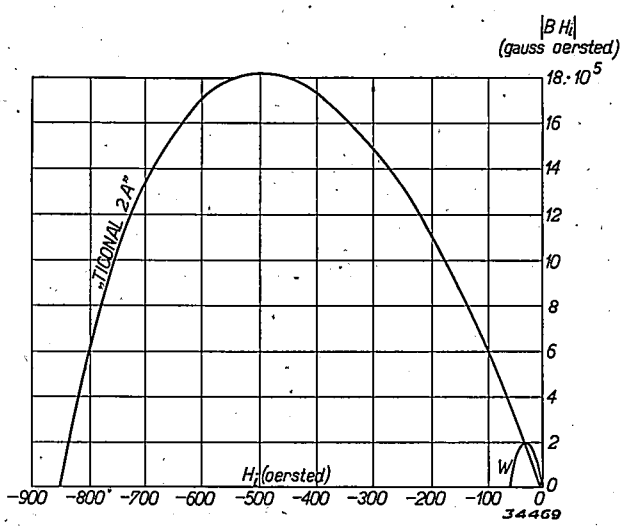

Fig. 4. Absolute value of the product BH_i (induction times internal field) as a function of H_i for a tungsten steel (W) and for the magnet steel "Ticonal 2A".

After we have calculated the volume of magnet steel needed, we can calculate the required length of the magnet with the help of equation (2). We find

$$L = -\frac{H}{H_i} l \quad \ldots\ldots\ldots \quad (5)$$

and we must substitute here for H_i the optimum value (with "Ticonal" 400 oersted). The cross section of the magnet is now of course also known. The following relation is valid, according to equation (1):

$$S = \frac{Hs}{B}, \quad \ldots\ldots\ldots \quad (6)$$

where B is the induction which, according to equation (3), corresponds to the optimum value of the demagnetizing field H_i.

From equations (5) and (6) it is clear how the design of a magnet must be changed when a tungsten steel is replaced by "Ticonal". The optimum field H_i has increased thirteen times and according to equation (5) this means that the length of a "Ticonal" magnet must be only $^1/_{13}$ of that of a tungsten steel magnet which produces the same field. On the other hand the induction B for optimum field strength in the case of the magnet steel "Ticonal" is slightly lower than with a tungsten steel; according to equation (6), therefore, the cross section S must be taken slightly larger.

We are now also able to understand why the replacing of a tungsten steel by the magnet steel "Ticonal" (without alteration in design) does not always lead to a better result. To show this we divide equation (1) by (2a):

$$\frac{B}{H_i} = -\frac{L}{S}\frac{s}{l}. \quad \ldots\ldots\ldots \quad (7)$$

Thus if we have a magnet and an air gap of known dimensions, the ratio B/H_i is known. In the diagram of the magnetization curve this gives us a straight line through the origin which cuts the magnetization curve at a point which gives us the values of B and H_i. Now it is quite possible (see *fig. 5*) for this line to cut the curve of the better steel at a point which gives a lower product of BH_i than the point at which it cuts the curve for the poorer steel. It is, however, clear that in this case the magnet of the better steel is very badly proportioned. By changing the design it is certainly possible to obtain a considerably better result with the same quantity of magnet steel.

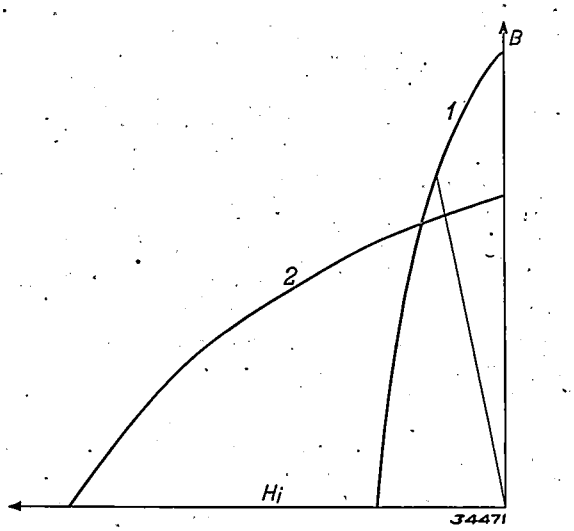

Fig. 5. The ratio between the induction B and the internal field H_i with a given design is independent of the properties of the magnet steel. With a sufficiently high value of this ratio (slope of the straight line B/H_i = constant) the product BH_i is greater for the magnet steel *1* than for the steel *2*, although the maximum value of the product is smaller for steel *1* than for steel *2*.

The spreading of lines of force

Until now we have failed to take into account the spreading of the lines of force. We reached the conclusion that the quality of a magnet steel is

determined solely by the maximum value of the product BH_i. A lowering of the remanence of the magnet steel therefore meets with no objections, if only it is accompanied by a corresponding increase in the coercive force. Such a change in the magnetic properties has, however, the result that the design must be altered, and the new design may have considerably more spreading than the old. An example will serve to illustrate this point.

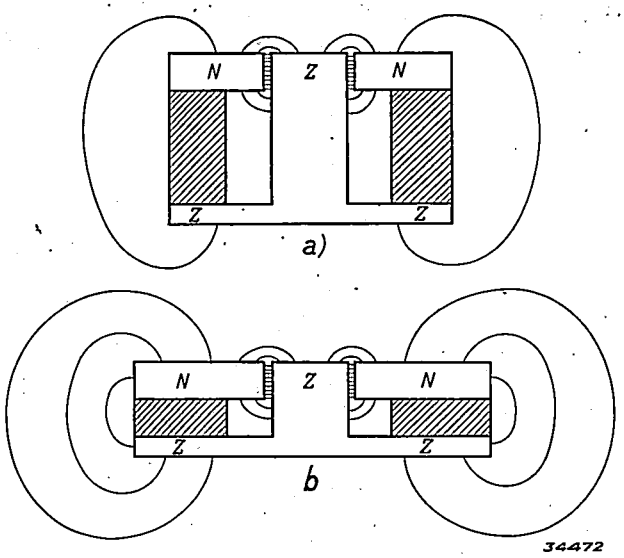

Fig. 6. a) Diagram of a cross section of a loud speaker magnet, constructed of the magnet steel "Ticonal 2A". b) Cross section of the same magnet, if the coercive force of the steel were three times as great, and the remanence one third. The shape changes in such a way that the spreading becomes considerably greater.

*Fig. 6*a shows the cross section of a magnet such as is used in loud speakers. The magnet steel is shaded, while the soft iron of the pole pieces is left white. The relative dimensions of this magnet are adapted to the B-H curve of the magnet steel "Ticonal 2A". If a tungsten steel were used, the height of the magnet would have to be considerably greater, while the diameter could be taken slightly smaller.

Let us now consider the imaginary case where, while the product BH_i is kept constant, the coercive force of the steel is three times as great as that of "Ticonal", while the remanence is only one third of that of "Ticonal". The magnet would then have the shape given in fig. 6*b*. As far as spreading is concerned, the design is much less satisfactory. In the first place, due to the increase in diameter, the surface from which the spread field originates is increased, and in the second place, due to the decrease in height, the resistance of the air path for the lines of force of the spread field is considerably decreased. Although when spreading is disregarded the second magnet steel is just as good as the first, it will not be possible to obtain as good results with it when it is used as a loud speaker magnet. It may be stated as a general conclusion, that the question as to which magnet steel is the most suitable for exciting a field of a certain strength in an air gap of a given form, cannot be answered by noting exclusively the maximum value of BH_i, but that B and H_i themselves also play a part. In particular the remanence of the magnet steel "Ticonal 2A" is found to be too low for certain applications. A new magnet steel has therefore been developed which has a slightly lower coercive force than "Ticonal 2A", but practically twice its remanence, namely 12 000 gauss. The maximum value of BH_i in the case of this steel is also twice as great. In *fig. 7* may be seen the magnetization curve of this magnet steel which has been called "Ticonal 3.8".

If we now return to the question of how a magnet must be constructed in order to use the magnet steel to the greatest possible advantage, our qualitative considerations of the influence of spreading are inadequate, and must be supplemented by a method of taking the spreading into account quantitatively in the calculation of the magnet.

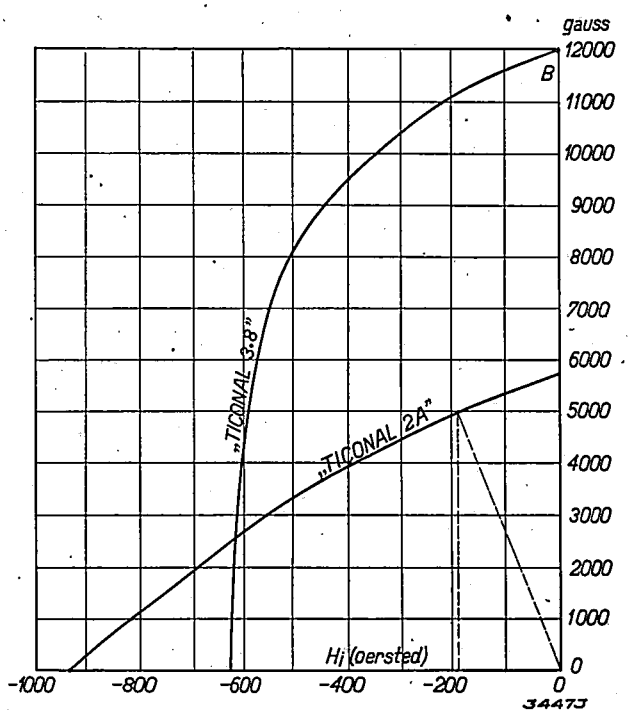

Fig. 7. Magnetization curve of the magnet steel "Ticonal 3.8", compared with that of "Ticonal 2A". The dotted lines refer to the examples treated in the conclusion.

More precise calculation of a magnet

The more elaborate calculation of a magnet which we shall carry out in the following differs from the above simplified treatment in the fact

that we determine not only the flux in the effective air gap, but the flux between each pair of surfaces between which lines of force pass through the air.

In calculating these different components of the total flux we can to our advantage make use of the concept of "magnetic potential", which is defined in the following way:

$$U_M = \int_{P_0}^{P} H_s \, ds,$$

where ds represents an element of a line drawn from a point P_0, at which the magnetic potential is considered to be zero, to the point P, at which the magnetic potential is indicated by the integral. H_s is the component of H in the direction of the line element ds.

The flux for each two surfaces between which lines of force pass can now be represented by the magnetic potential difference, multiplied by the magnetic conductivity. The latter quantity is therefore defined in exactly the same way as an electrical conductivity. The magnetic conductivity of a rod of length l, cross section s and permeability μ is:

$$g = \mu s/l .$$

The specific conductivity is thus nothing else than the permeability.

The conductivity of the air path between two surfaces is equal to the cross section of the bundle of lines of force which pass between the two surfaces. Actually both the cross section and the length must be considered as some kind of average values. The way in which these average values are determined will be discussed presently on the basis of an example.

If U_k is the potential difference between every pair of surfaces and g_k is the corresponding conductivity, the total flux

$$\Phi = \Sigma U_k g_k . \quad . \quad . \quad . \quad . \quad . \quad . \quad (8)$$

The total flux Φ is often compared with the effective flux $\Phi_0 = U_0 g_0$ which passes through the air gap. The ratio Φ/Φ_0 is called the coefficient of spreading σ.

When the coefficient of spreading is known, the calculation of the magnet can be carried out in the way discussed at the beginning of this paper. Equation (1) must be replaced by the more precise relation

$$B S = H s \sigma . \quad . \quad . \quad . \quad . \quad . \quad (9)$$

and this, together with equations (2) and (3) gives the three unknowns B, H_i and H.

The whole problem is thus reduced to the measurement or calculation of the terms $U_k g_k$ or $U_0 g_0$, which appear in the calculation of the coefficient of spreading σ. Often there is appreciable spreading only between the soft iron pole pieces, between which the air gap is situated. The different magnetic potential differences U_k are then practically equal to each other and to U_M. In that case only the conductivities g_k or g_0 occur in equation (8).

The conductivities can be calculated exactly in certain simple configurations. Usually, however, the calculation is very difficult or even impossible. Since this problem has great practical significance, for instance for the construction of measuring instruments, we shall explain in the following how formulae can be arrived at by a semi-empirical method which make it possible to calculate the field in the air gap of a magnet for different shapes and sizes of the magnet and different kinds of magnet steel.

As cross section of the bundle of lines of force which pass between two surfaces, we take the average size of the two surfaces. In order to determine the length of path in the air, we choose a simple shape for the lines of force, a straight line or part of a circle, for instance. The formula for the conductivity so obtained is finally completed by a numerical factor which is determined experimentally by measuring on a model the flux which passes between these two surfaces. It is clear that with the help of the formulae so obtained it is only possible to make precise calculations for a model which is an enlarged or reduced reproduction of the experimental model. The great value of the method, however, lies in the fact that the empirically found numerical factors apparently do not change when the relations between the various dimensions of the magnet and the nature of the magnet steel in the actual practical model are quite different from those of the experimental model. With the help of the same formula, therefore, it is possible to anticipate the properties of very different types of magnets. A simple example will be given in the following.

Complete calculation of a simple example

As example we have chosen the design represented in *fig. 8*, which consists of two cylindrical magnets M lying in a straight line, provided with iron pole pieces P and closed by an iron armature B which is thick enough to have practically no magnetic resistance. The distance a between the armature and the pole pieces is made so great that practically no appreciable flux will pass across this air space.

Let us assume that the left-hand pole piece is the north pole and the right-hand one the south pole. The flux through the air space can be divided as follows:

1) the flux Φ_1 from the left-hand magnet to the right-hand magnet;
2) the flux Φ_2 from the wall of the cylinder of the left-hand pole piece to that of the right-hand pole piece;
3) the effective flux Φ_3 from the flat surface of the left-hand pole piece to that of the right-hand pole piece.

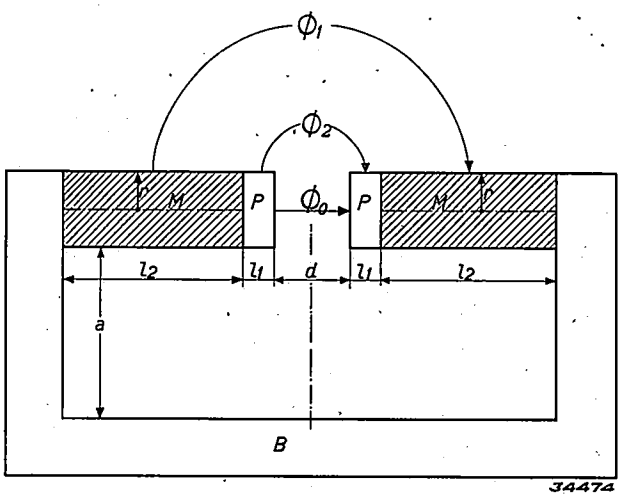

Fig. 8. Model of a magnet whose effective flux Φ_0 and spread flux $\Phi_1 + \Phi_2$ can be calculated by a semi-empirical method. Cross hatched: magnet steel, white: soft iron.

The flux Φ_1 will be proportional to the cylindrical surface $2\,\pi\,r\,l_2$ of the magnet, and inversely proportional to the length of the lines of force. For this latter length we take as average value the length of the semicircle drawn in the figure, which is equal to

$$\pi\left(\frac{d}{2}+l_1+\frac{l_2}{2}\right).$$

The magnetic potential then passes from the value 0 for the outermost line of force to the value $2\,l_2\,H_i$ for the innermost one; we have here taken as average value $l_2\,H_i$. In this way we arrive at the formula:

$$\Phi_1 = \alpha\,\frac{2\,\pi\,r\,l_2}{\pi\left(\frac{d}{2}+l_1+\frac{l_2}{2}\right)}\,H_i\,l_2 = \alpha\,\frac{4\,r\,l_2^2}{d+2\,l_1+l_2}\,H_i \quad (10)$$

It will be seen that in addition to the quantities already mentioned another factor α has been introduced. This factor is determined experimentally by measuring the flux Φ_1. The formula is in this way made to produce the correct result for a given model. In general it is found that the empirical correction factor does not change very much when one passes from the experimental model to a design with quite different dimensions, r, l_1, l_2, d; this is the basis of the whole method of calculation.

The flux Φ_2 through the side wall of the soft iron pole piece is calculated in exactly the same way as the flux Φ_1; the result is:

$$\Phi_2 = \beta\,\frac{2\,\pi\,r\,l_1}{\pi\left(\frac{d_1}{2}+\frac{l_1}{2}\right)}\,2\,H_i\,l_2 = \beta\,\frac{8\,r\,l_1\,l_2}{d+l_1}\,H_i, \quad (11)$$

where β is again a factor which must be determined experimentally.

Finally we calculate the effective flux. The length of the lines of force (d) and the cross section of the bundle of lines of force ($\pi\,r^2$) are well defined with a sufficiently narrow air gap, so that it is unnecessary to introduce a correction factor. The following result is obtained:

$$\Phi_0 = \frac{\pi r^2}{d}\,2\,H_i\,l^2 \quad (12)$$

The experiments for the determination of α and β were carried out with a magnet of "Ticonal 3.8" having the dimensions:

$r = 1.28$ cm,
$d = 0.515$ cm,
$l_1 = 0.2$ cm,
$l_2 = 3$ cm.

The following values were found:

$H = 4\,300$ oersted,
$\Phi_1 = 15\,100$ maxwell,
$\Phi_2 = 13\,300$ „ ,
$\Phi_0 = 22\,400$ „ ,
total flux $\Phi = 50\,800$ „ ,
$\sigma = \Phi/\Phi_0 = 2.27.$

From the measured value of Φ_0, with the help of equation (12) we can calculate the internal field H_i, and we find a value of 373 oersted. By means of equation (9) and (10) the spread flux Φ_1 and Φ_2 can now be calculated. The results are:

$\Phi_1 = \alpha \cdot 4\,400$ maxwell,
$\Phi_2 = \beta \cdot 3\,100$ „ .

By comparing these values with the measured values of Φ_1 and Φ_2 we find:

$$\alpha = 3.43$$
$$\beta = 4.14.\ ^{2})$$

All the quantities are now known which are necessary for setting up a formula for the coefficient of spreading with the help of equations (9), (10), (11) and (12):

$$\sigma = (\Phi_1 + \Phi_2 + \Phi_0)/\Phi_0 =$$
$$= \frac{2\,d}{\pi\,r}\left(\frac{3{,}43\,l_2}{d+2l_1+l_2} + \frac{8{,}28\,l_1}{d+l_1}\right) + 1. \quad (13)$$

Equation (13) forms the basis for the calculation of a magnet of the type described above. If the coefficient of spreading σ is known, equations (2), (3) and (9) give us the other unknowns, H, H_i and B.

In order to check the formula and thus to test the whole method, a second model was made with very different dimensions from those of the test model, while in addition a different kind of magnet steel "Ticonal 2A" was used instead of "Ticonal 3.8" (see fig. 7). The dimensions of the second model are the following:

$$r = 1.7 \text{ cm},$$
$$d = 2.05 \text{ cm},$$
$$l_1 = 1.0 \text{ cm},$$
$$l_2 = 5.6 \text{ cm},$$

cross section magnet [3]) 8.28 cm^2.

The field H in the air gap of this magnet was found to be 980 oersted. Let us now find the field strength which is to be expected on the basis of the formulae derived above.

According to (13) we find

$$\sigma = 4.6.$$

According to equation (9) $8.28\,B = H \times 9.08 \times 4.6$, while according to equation (2)

$$H_i = -\,H\,\frac{2{,}05}{11{,}2}.$$

If we eliminate H from these two equations (as was done in the derivation of equation (7)), it follows that:

$$\frac{B}{H_i} = \frac{9{,}08 \cdot 4{,}6 \cdot 11{,}2}{2{,}05 \cdot 8{,}28} = 27{,}6.$$

Now with the help of the magnetization curve we can also determine B and H_i themselves: the line $B/H_i = 27.6$ cuts the B-H_i curve of the magnet steel used ("Ticonal 2A") at the point

$$B = 5\,000 \text{ gauss}, \quad H_i = -182 \text{ oersted}.$$

We finally find for the field in the air gap

$$H = \frac{-11{,}2}{2{,}05}\,H_i = 994 \text{ oersted}.$$

The discrepancy with the measured result thus amounts to only 1·5 per cent, which must be considered fairly satisfactory, especially when it is kept in mind that the control model had quite different dimensions from the test model (the ratio between the spread flux and the effective flux is, for example, three times a great as in the test model).

Having seen how a magnet can be calculated, it remains to find out how a magnet can be designed in order to provide a given field in a given air gap. We begin by calculating the length and the cross-sectional area of the magnet steel according to the equations (2a) and (9). For H_i we choose a favourable value, and estimate the value of the coefficient of spreading σ. With the dimensions of the steel obtained we design a magnet and then calculate σ according to equation (13). If the calculated value agrees with the estimated one, the work is finished, otherwise we repeat the calculation with the new value of σ and the result will be attained after a second or third attempt.

---

[2]) α and β are much larger than one, which means that our estimation of the conductivity before the introduction of the correction factor was very inaccurate. The fact that the actual conductivity is very much higher is understandable. The area of the cross section of the bundle is very much greater at the middle than we have assumed. It is remarkable that this rough method of taking spreading into account gives fairly good results in the end.

[3]) The magnet had a hole along the axis so that its cross-section area was slightly less than $\pi\,r^2$.

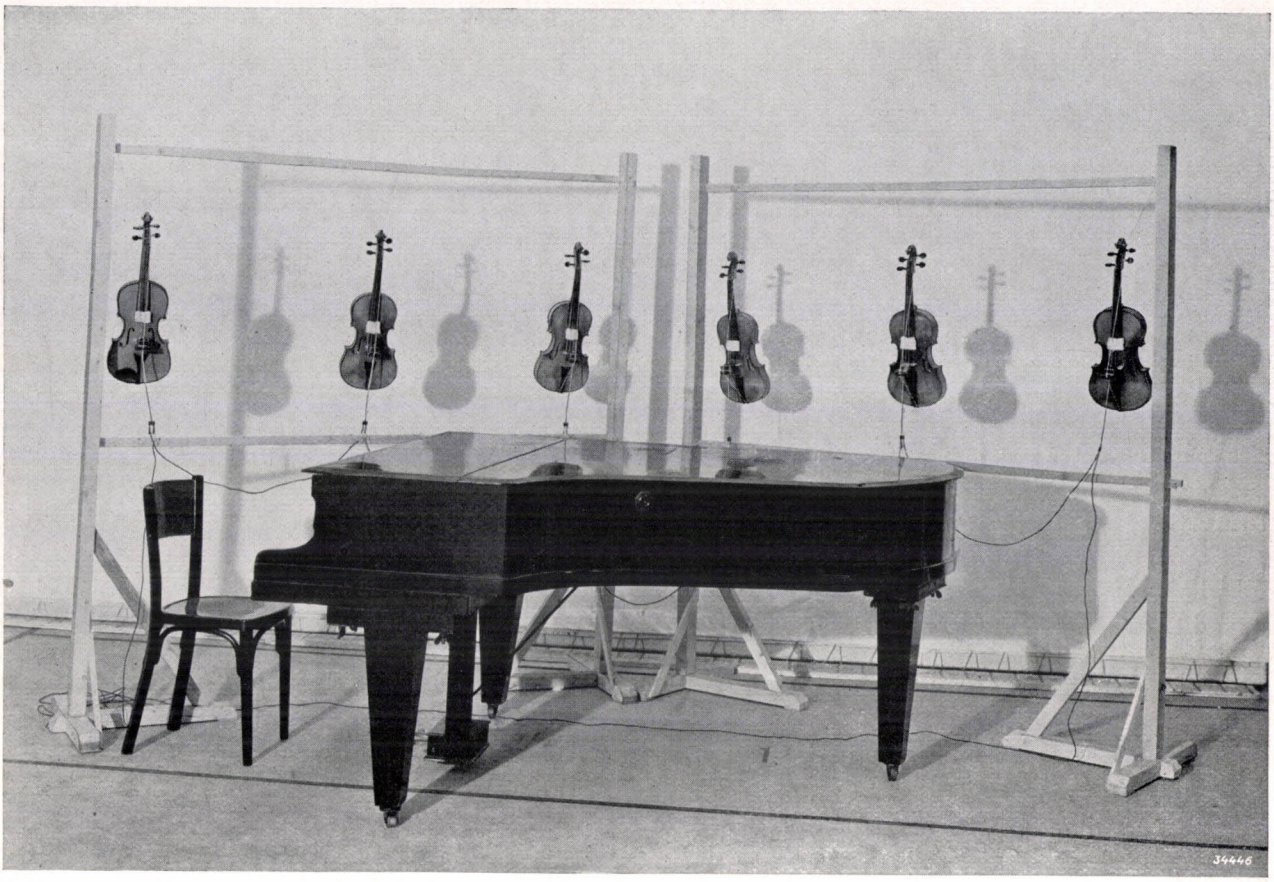

PERSPECTIVES IN THE DEVELOPMENT OF THE VIOLIN

by R. VERMEULEN.

534.86: 787.1

A discussion is given of a method of obtaining sufficient amplification of the sound of a solo violin with respect to the accompanying orchestra. The arrangement tested in the Philips Laboratory is described and various factors are discussed which would be of importance in its practical application.

In reading the title of this article one will probably be tempted to ask immediately: "Does the need of further development of the violin exist? Is not the situation rather that violin builders would like nothing better than to return to the standard already reached by Stradivarius and Guarnerius in the eighteenth century?"

Nevertheless it is not unreasonable to speak of a need of development for the violin. This need has arisen simply due to the fact that the purposes for which the violin is used have changed with time. While in the beginning — we are thinking of the sixteenth century, since which time no further fundamental changes in the construction of the violin have occurred — the violin was used chiefly for chamber music and for musical programmes in the reverberating spaces of churches, the present day practice of music makes it necessary that the violin be played in concert halls often of enormous size, and before huge audiences. This practice makes much higher demands on the volume of sound which must be produced by the source. These demands are reflected clearly in the greatly increased size of orchestra: each instrumental voice occurring in the score is played by a group of representatives in unison; each violin voice is played by a large number of violins, as many as 25, for example.

This method of increasing the intensity, namely by the multiplication of the number of musicians, gives no difficulty as long as nothing more than average skill upon his instrument is demanded of each collaborator. The situation, however, is quite different when it is a question of musicians of exceptional talent who appear as soloists, for instance in a violin concert with orchestral accompaniment. The soloist must then play against the whole orchestra with his single violin, and even though

the conductor imposes the greatest restraint on the orchestra, it often becomes a "concert" in the truest sense of the word, a "competition", in which it costs the soloist the greatest effort to bring out his instrument sufficiently strongly above the accompaniment. It is obvious that this is not exactly desirable. There is not only the danger that the artist will be distracted by the exertion from complete surrender to the music he is interpreting, but moreover the quality of the tone may suffer because of the fact that non-linear distortion may occur with too great amplitudes of the strings and sounding boards, and result in squeaking and scratching. Every violin soloist will acknowledge the fact that it would be an improvement very much to be appreciated if it were possible to increase the volume of sound from the violin while retaining its other qualities.

How could this be done? It is known from experience that the instruments of the above-mentioned famous violin builders of the 18th century not only possess a more beautiful tone, but that they produce a greater intensity with much less effort. The knowledge of the methods used to obtain these qualities seems to have been lost, so that until now we have been unable to equal these old violins. Some people even believe that efforts in this direction are doomed to failure because the old violins owe their fine quality to the fact that they are so old and have been played for so long a time by so many excellent violinists. Aside from this, however, the desired effect could not be achieved even if it were possible to copy the old violins exactly, since even a Stradivarius does not produce enough volume to come out above the accompaniment of a large orchestra.

A second possibility of amplifying the sound of the instrument would be to increase its dimensions. As was explained some time ago in this periodical in connection with the simplest sound radiator, the pulsating sphere [1]), the acoustic power produced increases with the size of the radiator. In our case, however, this method cannot be considered for obvious reasons: the size of a violin determines to a large extent its timbre. If we make it larger we do not obtain a louder violin, but a viola or a cello.

A solution of this difficulty may be sought by making use of modern electro-acoustic aids. The sound of a violin can be picked up with a microphone, the microphone voltage amplified at will and fed to a loud speaker. But the question now arises: where must we place the microphone? It would be most reasonable to pick up the sound of the violin at the position of the hearers. If we do this, however, we are no further ahead, since the sound of the orchestra is then amplified together with the violin solo. In order to shift the ratio of the two sound contributions in favour of the solo instrument the microphone would therefore have to be hung in the immediate neighbourhood of that instrument. Such a solution is employed for example in the analogous case in which a singer's voice must be clearly heard above a jazz band. Placing the microphone close to the source of sound, however, has the objection that the sound may differ considerably in timbre from that at a greater distance. In the example mentioned of the jazz singer this fact has led to the development of a special singing technique known as "crooning". The violin is, however, much larger than the mouth opening of a jazz singer, and moreover, the violinist needs a certain freedom of movement, so that the placing of the microphone close to the solo violin cannot be considered.

These difficulties are avoided if, instead of the acoustic vibrations around the violin, the mechanical vibrations of the body of the violin are picked up [2]) with the help of a kind of electrical gramophone pick-up, and then amplified. The practical realization of this principle, which has been tested in the Philips Laboratory, involves several other considerations which we shall discuss briefly.

When the bow slides over a string a relaxation vibration sets in, in which the deviation of the string varies as a function of the time approximately according to a saw-tooth relation (*fig. 1*).

Fig. 1. The deviation of a bowed violin string as a function of the time. The shadow of a point of the string is photographed during vibration on a constantly moving film (H. Backhaus, Naturwiss. 17, 811, 1929).

This vibration of the string, which is composed of a large number of harmonics, is communicated *via* the bridge to the body of the violin, which then in turn begins to vibrate and radiates the vibrations in the form of sound. By the very pronounced resonances of the body of the violin (see the frequency characteristic *fig. 2*) harmonics in certain regions are amplified and the typical violin quality

[1]) A. Th. van Urk and R. Vermeulen, Radiation of sound, Philips techn. Rev. 4, 213, 1939.

[2]) Similar considerations have already been discussed in this periodical in the description of the laringophone which makes telephone communication possible in places where there is much noise: Philips techn. Rev. 4, 6, 1940.

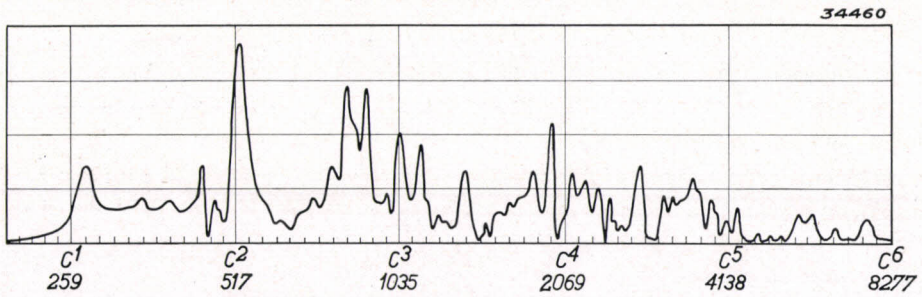

Fig. 2. Frequency characteristic of a violin (from H. Meinel, Akust. Z. 4, 89, 1939).

is obtained: the body of the violin thus determines the timbre. To each of the resonances mentioned there corresponds a certain form of vibration of the body of the violin which could be made visible by Chladni sound figures. From this it follows, however, that it is impossible to use the mechanical vibrations of the body of the violin itself for the purpose in view. If one should set the needle of a vibration pick-up at any point on the sounding board for a given frequency, this point might just lie at a node of the vibration occurring, so that this frequency would not be communicated. The only spot on the whole violin where all the vibrations will certainly be encountered is the bridge, which passes the vibrations of the strings on to the sounding board.

On the other hand we have just seen that the vibrations of the bridge can by no means represent the sound of the violin, since they have not yet passed through the timbre-determining organ. If therefore we should reproduce the vibrations of the bridge by means of an ordinary loud speaker, the sound so obtained would not resemble the sound of a violin. In this way we arrive at the remarkable conclusion that in reproducing the vibrations we must still include the organ which determines the timbre, namely by using a violin body as loud speaker. *The vibrations which are picked up from*

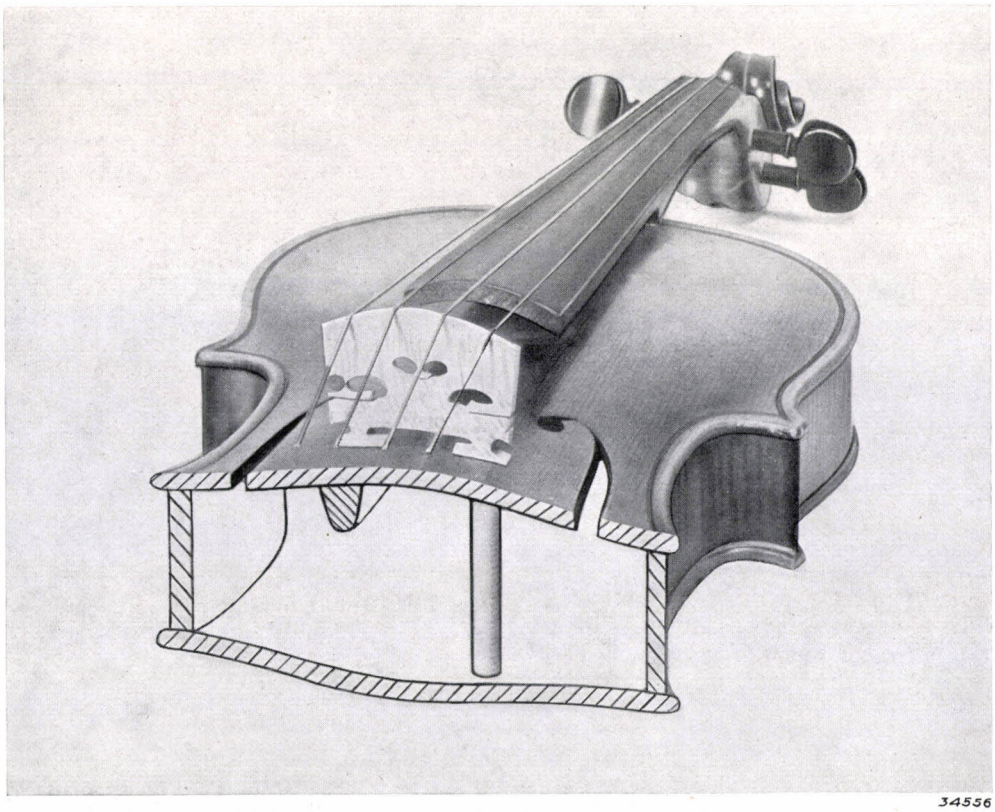

Fig. 3. Cross section through a violin at the position of the bridge. To the right (under the E-string) the sound post, to the left (under the G-string) the bass bar. The strings vibrate chiefly in a horizontal direction.

the bridge of the solo violin are communicated to the bridge of a second violin which then in principle radiates the same sound as if it were made to vibrate by the vibrations of the strings of the first violin [3]).

In picking up the vibrations it is not a matter of indifference what spot on the bridge is chosen. *Fig. 3* shows a cross section of a violin through the bridge. Under the right hand end of the bridge, *i.e.* under the E-string there is a vertical wooden peg between the belly and the back of the violin, the so-called sound post. The amplitude of the belly at this point is therefore practically zero, and we may say that the bridge can only execute a rotating motion about its right hand point of support. The rotating motion of the bridge is caused by the strings vibrating mainly in a horizontal direction. By the left-hand point of support the belly of the violin is then brought into transverse vibration. In order to spread this vibrating motion over a larger surface the sounding board at this point (under the G-string) is reinforced by a thicker oblong piece of wood, the so-called bass bar.

As point of contact for the point of the vibration pick-up with which we wish to amplify the sound of the violin, we choose the spot on the bridge indicated by a circle (*fig. 4*), since we can expect

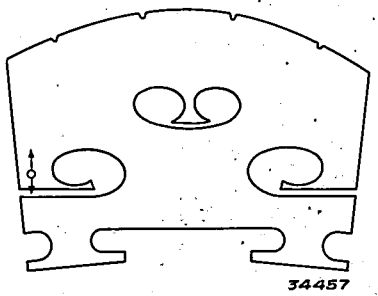

Fig. 4. Bridge of a violin (natural size). Since the bridge executes chiefly a rotating motion around its right-hand point of support, the greatest amplitudes occur on the left. The point of the vibration pick-up is placed on the spot indicated by a circle; it can move in the direction of the arrow.

to find the greatest amplitudes here. The point then moves in the direction of the arrow (perpendicular to the sounding board). *Fig. 5* shows the method of attaching the vibration pick-up, details are described in the text below the figure.

The excitation of the bridge of the "loud speaker violin" is by means of an apparatus similar to that used for the recording of gramophone records which has previously been described in this periodical [4]).

[3]) When loud speaker technology was still in its infancy, a violin or mandolin body was sometimes used as loud speaker. This was done, however, to amplify the normal sound of speech or music. The fact that this was a mistaken idea is clear after the above.

[4]) K. de Boer and A. Th. van Urk, A simple apparatus for sound recording, Philips techn. Rev. 4, 106, 1939.

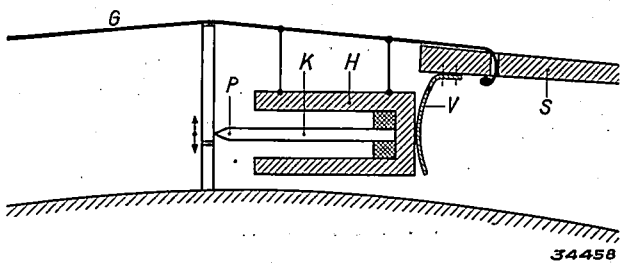

Fig. 5. The vibration pick-up consists of a piëzo-crystal K which is fastened elastically in a holder H and which carries the point P excited by the bridge. The construction and action of this resembles closely that of the crystal laringophone described in the article already cited [2]). The holder H is suspended on the dead end of the G-string G, and is pushed in the direction of the bridge by the spring V which is attached to the tail piece of the violin. When the bridge vibrates the relatively heavy holder H remains practically at rest and the crystal K executes vibrational bending movements upon which a piëzo-voltage occurs between the upper and lower sides of the crystal. This voltage is picked up by means of electrodes stuck to the crystal, and, after amplification, fed to the "loud-speaker violin".

In order to apply the principle entirely consistently the excitation should take place at the spot on the bridge corresponding to that at which the vibrations were picked up on the solo violin. In practice this was not found possible since the spot indicated in fig. 4 is not suitable for the firm attachment of the

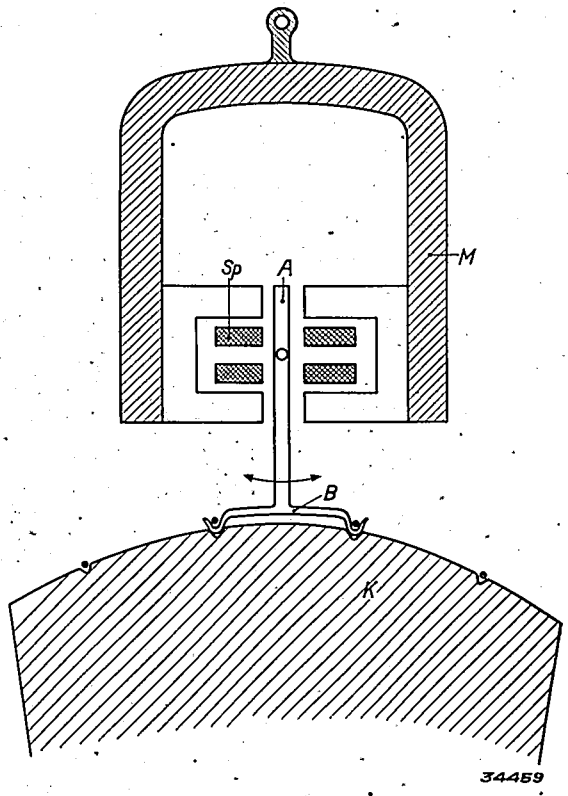

Fig. 6. Excitation of the loud-speaker violin. A bent strip of metal B is set on top of the bridge and held in place by the two middle strings. The metal strip is fastened to the electrically excited armature A, and upon vibration of the armature it exerts a couple in the plane of the bridge. The heavy mass of the magnet M and the pole pieces remain practically at rest. The weight of these parts is supported by a cord bound to the extremities of the violin (see fig. 7).

recorder to the bridge, which is necessary because of the fairly large forces to be communicated. The recorder was therefore fastened to the top of the bridge by means of a bent strip of metal clamped under the two middle strings, as is shown diagrammatically in *fig. 6*. This arrangement was found to be very satisfactory. When in use the strip of metal which moves with the vibrating armature of the recorder tends to execute a tipping motion whereby a couple is exerted on the bridge in the same direction as by the original movement of the strings. The strings themselves on the loud speaker violin may not of course take part in the vibration, since they are not continually being tuned to the correct pitch by stopping. The motion of the strings is therefore entirely damped by means of a wad of cotton. The strings cannot be omitted, since, by the tension which they communicate to the body of the violin, they affect fundamentally the properties of the latter in its function as organ which determines the timbre [5]).

[5]) The variation in the tension due to the varied stopping during playing is in this respect a second order effect which may be neglected.

The amplification which can be obtained by means of such a loud-speaker violin is of course limited by the above-mentioned non-linear distortion which becomes noticeable at too great amplitudes of the components of the violin. If it is desired to increase the amplification still further, as many more loud-speaker violins as desired must be connected in parallel (*fig. 7* and title photograph).

Let us return for a moment from the laboratory to the concert hall. When the above-described method of amplification is applied the sound of the solo violin is reproduced by five or ten violins at the same time. This raises the question of whether this method might not make it possible to dispense with a large number of musicians in the orchestra. Instead of 25 first violins, could one use a single violinist, and allow 24 other violins to amplify his performance? If the multiple performance of every violin voice had as its only aim an increase in the intensity, this conclusion would in fact be justified. Actually, however, the situation is much more complicated. From the point of view of the composer, without doubt the choral effect

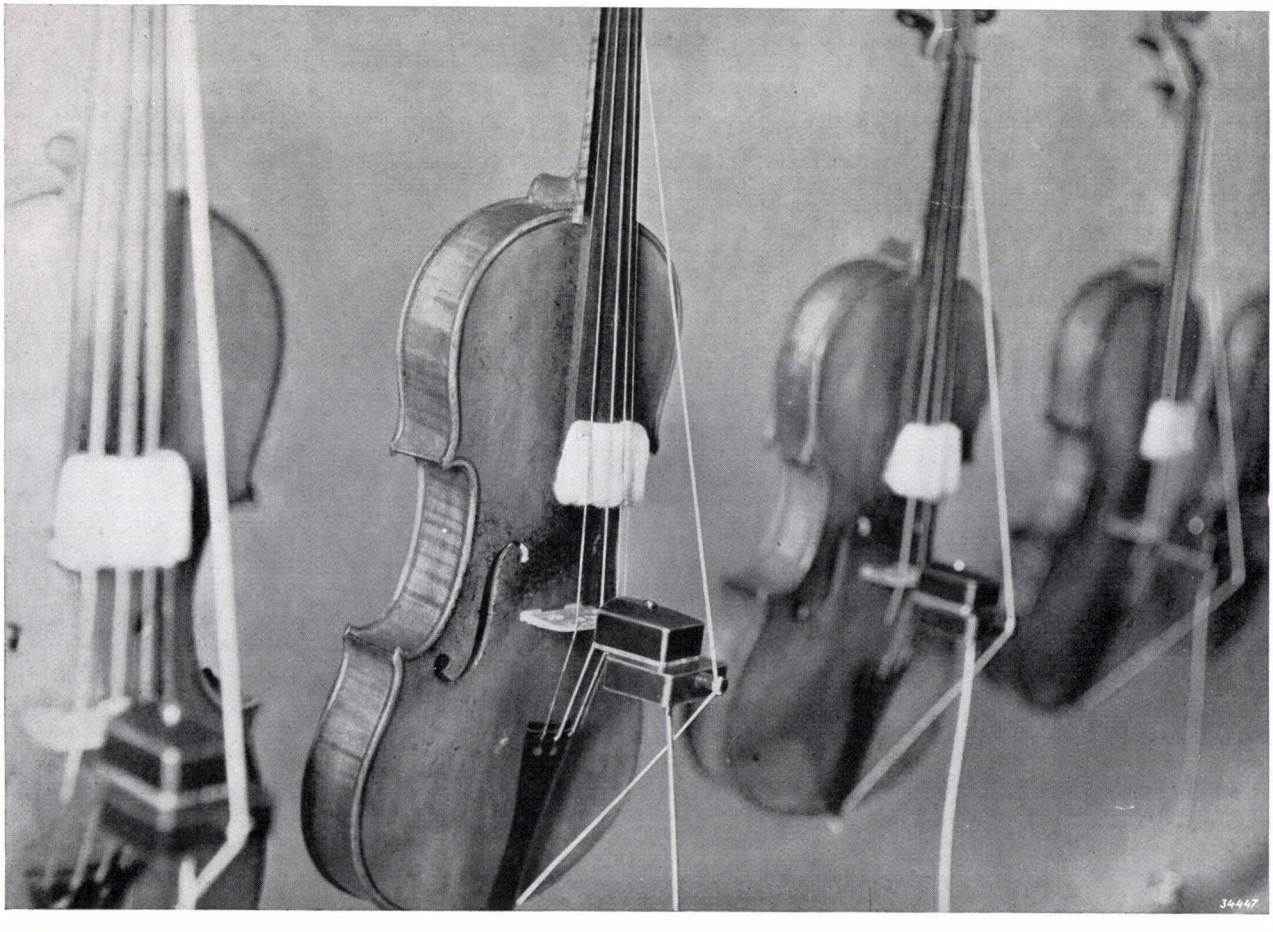

Fig. 7. Series of loud-speaker violins.

of the multiple representation of each voice also plays an important part. This effect is obtained by the slightly differing moment of attack, by the small differences in pitch and in the vibrato, as well as by somewhat differing timbres of the violins and the scattering of the sources of sound over a larger area. The first two of these four factors would be lost if we substituted for the 24 violinists simply 24 loud-speaker violins. It is quite possible that this would be a serious objection. Experience alone can decide the question.

The consideration of the choral effect also however has consequences in the application of the method to the solo violin. The two last mentioned factors — differences in timbre and scattering of the radiating surface — now enter as additional factors in the case of the solo violin, and it is not impossible that the impressions received by the listener will be appreciably altered thereby. Whether the change is permissible, or whether it may even be an improvement, these are questions which cannot be answered by means of laboratory experiments.

INTERESTING LIGHTING EFFECTS OF THE LIEGE WATER EXPOSITION

by L. C. KALFF.

628.974

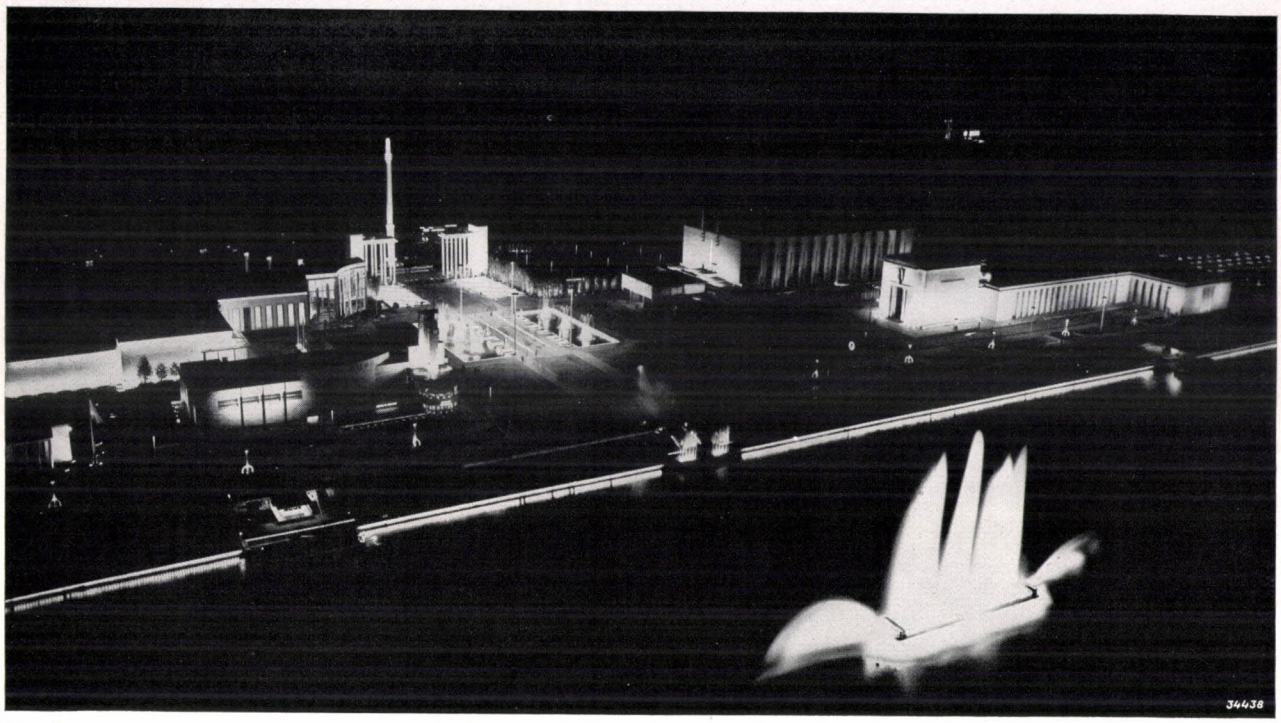

The Liége water exposition, which was opened in 1939, and which was planned primarily to call attention to this busy industry centre of eastern Belgium, was unfortunately compelled by the outbreak of the war to close its gates prematurely. It had already proved a great success, and the attendance and interest of the public were very great. This was undoubtedly due in some part to the logical arrangement which avoided the confusing and fatiguing effect of a too comprehensive world exposition, and to the aesthetically successful building construction under the direction of the young architect Falise.

In planning this exposition the importance of keeping the design and execution as much as possible under a unified direction was immediately understood. A fruitful and interesting coöperation with the Philips consulting bureau for illumination resulted from this conviction.

The grounds of the exposition were laid out on a very generous scale with two permanent boulevards 40 m wide along the banks of the Meuse which is about 180 m wide at this point. The lighting elements had to be in good proportion to these broad open spaces and to the high and massive buildings of the exposition. It is to the credit of the architect that he did not hesitate to accept the unusually large dimensions to which this consideration of proportion led.

In the first place there were the wide boulevards along the Meuse, along which were erected standards 13 m high at distances of 50 m, each bearing six lamps of 300 dlm, which together gave a very uniform illumination of 40 lux over a width of 40 m. The six simple enamelled reflectors in which the lamps were fixed housed in a dome-shaped cap made of eternite (*fig. 1*) in such a way that any one looking along the boulevard was not disturbed by glaring points of light (see *fig. 2*). The standards were manufactured by the Liége steel industry from steel plates bent into circular form and welded. The result was beautifully slender smooth columns which will form part of the permanent lighting system in the future. One of the leading ideas in planning the exposition was the desirability of being able to use the exposition material for practical purposes later on, as well as that of using as far as possible materials (rolled and profile steel,

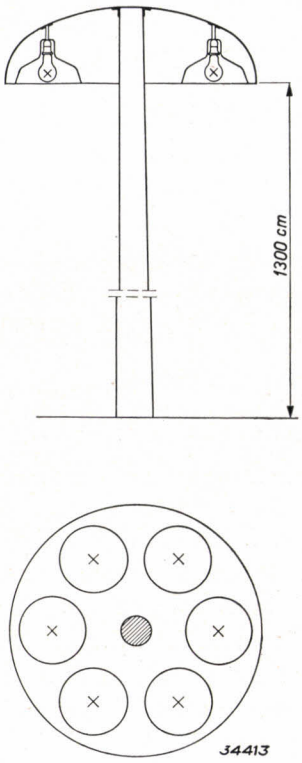

Fig. 1. Construction of the standards for lighting the boulevards along the Meuse. Six 300 dlm lamps are arranged under an eternite dome.

eternite, plates of wood fibre, glass) which could be supplied by the industries in the neighbourhood of Liége.

In order to break the monotony of the main traffic highways a strip of grass was sown along the middle, and lower, more decorative lighting ornaments were placed between the high ones. These lower lamps also provided an extra illumination of the flower beds surrounding them (fig. 2). The ornaments consisted of five m standards crowned by a double cone. The upper cone contained a loud speaker and the lower one three milk-glass globes each containing a 150 dlm lamp. Three arches containing a total of 54 small Argenta lamps shed most of their light upon the flowers. Three strips of netting, painted white, were stretched along the standards and were illuminated from below by three "Cornalux" mirror lamps of 100 watts (for the installation of these lamps see *fig. 3*). As may be seen in fig. 2, these simple motives gave a very pleasing effect, thanks to their correct proportions.

The imposing square directly behind the main entrance, of which the title page photograph gives some impression, was transformed into a water garden. It contained decorative flower mosaics, small fountains, statues and paths. The paths were paved with heavy plates of cast glass lighted from

Fig. 2. Between the stadards for the boulevard lighting, stand the light ornaments for illuminating the flower beds. They are five m high and bear a loud speaker and three milkglass globes each with a 150 dlm lamp. The strips of netting are lighted with "Cornalux" lamps.

below. In contrast with this effect were four enormous standards 20 m high of the same construction as the 13 m standards described above. In this case the eternite cap contained three mercury lamps type NO 2 000 with three ordinary electric lamps of 1 500 watts, which together gave a light source of 13 500 dlm. The centre of the square was in this way very well lighted with an intensity of 60 lux (*fig. 4*).

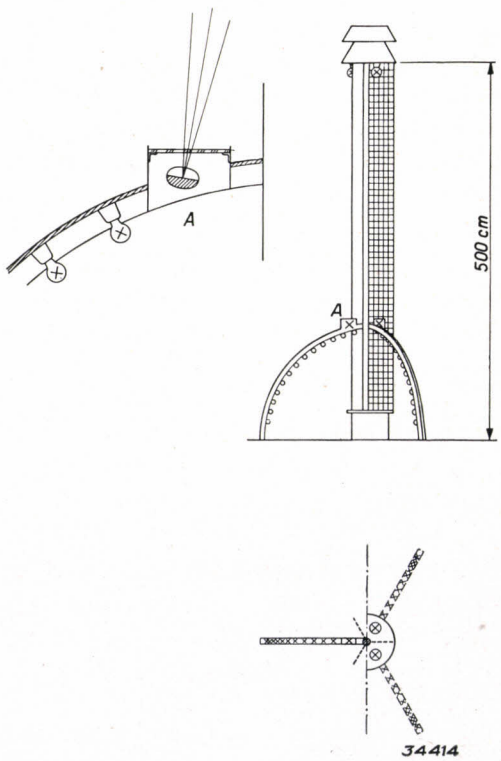

Fig. 3. Construction of one of the ornaments of fig. 2. The detail sketch *A* shows the position of one of the three "Cronalux" lamps illuminating the netting.

The flower mosaic (*fig. 5*) consisted of square flower beds alternating checker-board fashion with square pools of water. At the centre of each pool was a fountain about two m high, which was illuminated at night by means of four "Altrilux" lamps. These are lamps of a special shape and construction (*fig. 6*) intended to be used under water. The bulb is silvered on the inside over half its surface so that a concentrated beam is obtained and a special water-tight reflector is unnecessary. The lamps are cemented into a small cylinder which also contains the lamp socket. The cylinder must be firmly anchored to the bottom of the pool, because, due to the large volume of the lamp, it has a fairly great floating power ($\pm$ 2 kg). The lamps are placed as near as possible to the surface of the water in

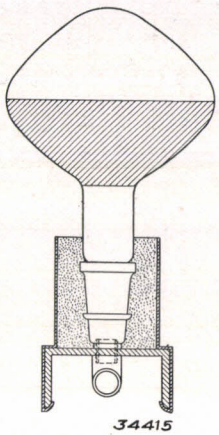

Fig. 6. Construction and assembly of the "Altrilux" under-water lamps.

Fig. 4. The great square behind the entrance is illuminated by four 20 m high standards of construction similar to that in fig. 1. The cap on each standard in this case however contains three mercury lamps, type NO 2000, and three 1500 watt electric lamps, which together give a light flux of 13 500 dlm.

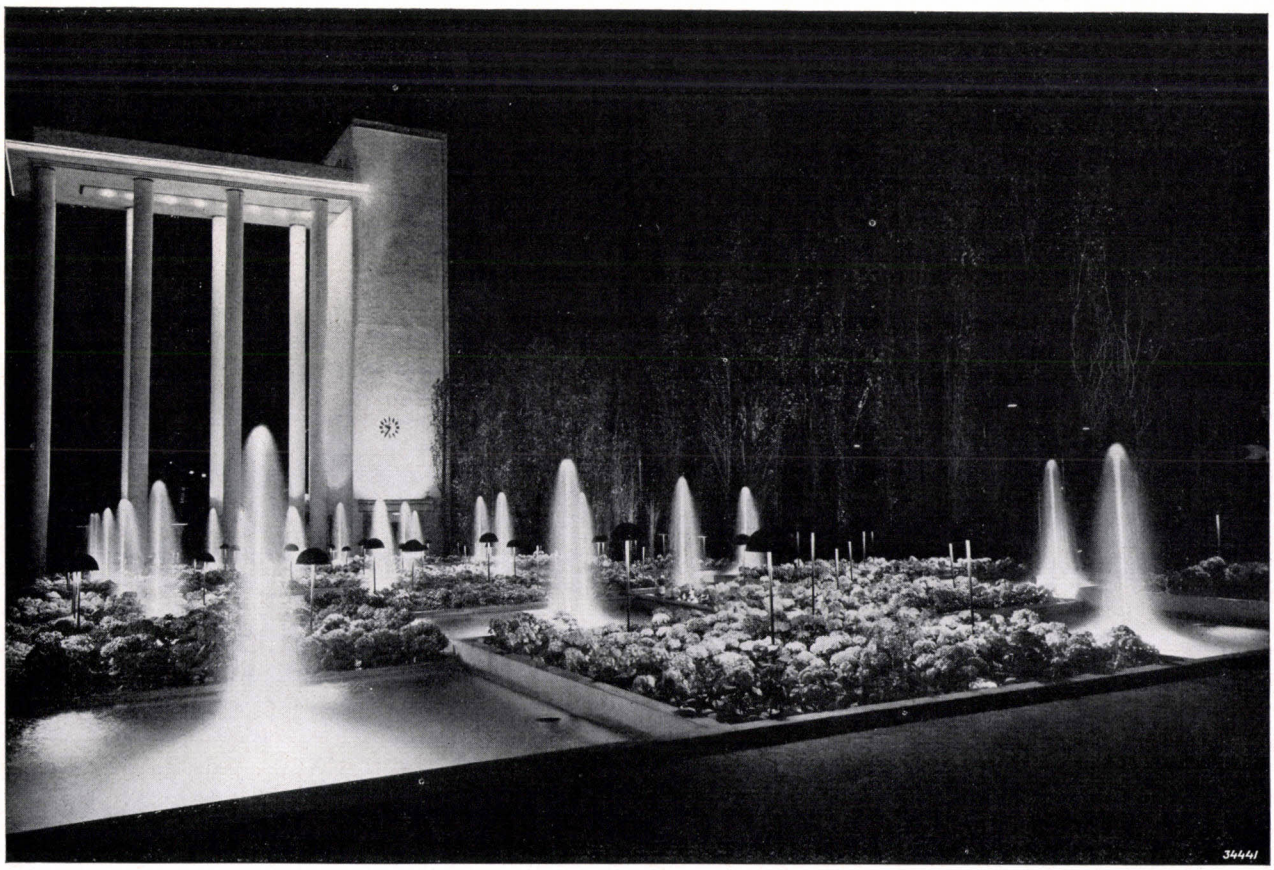

Fig. 5. The flower mosaic of the great square was formed by a checker-board of flower beds and pools. The two m high fountain in each pool was illuminated from below by four "Altrilux" under-water lamps. Each flower bed receives its light from four "Philiflor" reflectors.

order to limit the loss of light, but there must be a layer of water of a certain thickness above the lamp since it would otherwise be broken by the falling water from the fountain. Moreover the high calcium and phosphate content of the water in Liége was a disturbing factor. Within a few days a layer of scale formed on the lamp which was very difficult to remove and which caused considerable loss of light. For that reason the originally planned power of these under-water lamps was doubled

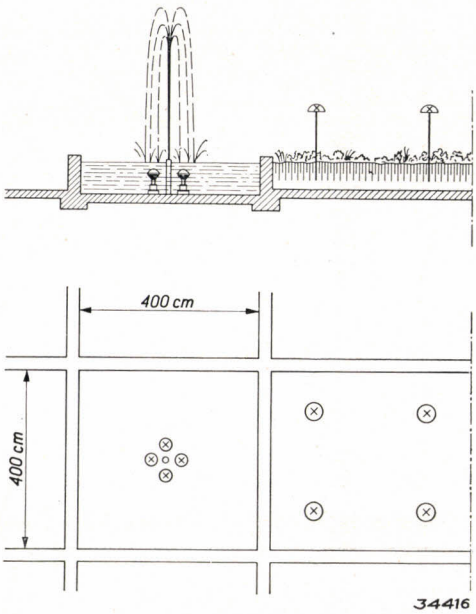

Fig. 7. Ground plan and vertical cross section of a square flower bed and pool.

Each square flower bed was illuminated with four "Philiflor" reflectors with 125 dlm lamps (*fig. 7*).

In the centre of the great square, as may be seen in the title photograph, were two pools and six large statues. These pools were bordered by a sinuous luminous line formed by a row of 40 dlm lamps in an eternite light cove (*fig. 8*). The lamps themselves were invisible but their reflection could always be seen in the water which was kept in continual motion by the play of the fountains. A total of 1 800 lamps were used in this detail. Twelve

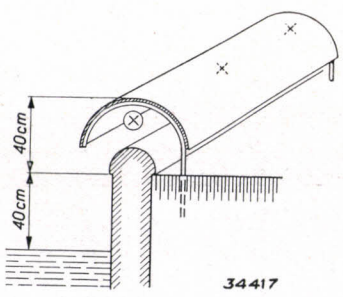

Fig. 8. Construction of the light coves along the pools in the main square. The reflection of the 40 dlm lamps placed in the cove is visible in the water.

Fig. 9. Illumination of the groups of statuary bordering the pools. The sinuous luminous outlining of the pools by means of the light cove can also be seen.

mirror reflectors type FLD with 250 watt searchlight lamps illuminated the groups of statuary (*fig. 9*).

Another interesting part of the illumination of the exposition was formed by the decorations along the 180 m wide Meuse. This broad strip of water had to be incorporated into the illumination so that the exposition should not be cut in two in the evening by the dark strip of water. It is nearly impossible to render a stagnant water surface visible with light sources of limited dimensions, since the water reflects only specularly. Due to the current however the water of the Meuse is in continual motion. Just as the image of the moon is drawn out into a long path of light by a rippling water surface, in the same way a long row of lamps along the bank should transform the whole stream into a brilliant glittering surface for an observer on the opposite bank. Experiments were found to confirm this expectation. Therefore eternite light coves

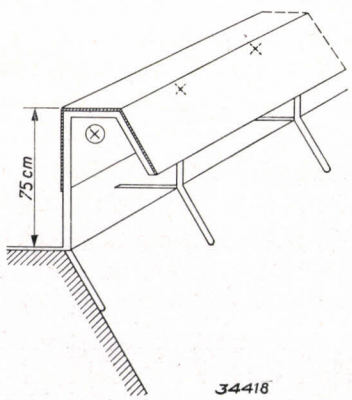

Fig. 10. Construction of the eternite light coves along the banks of the Meuse. The row of 40 dlm lamps in the coves illuminates the stone embankment of the river, and by reflection in the rippling water makes the whole surface of the water visible to an observer on the opposite bank.

Fig. 11. The effect of the illumination along the banks of the Meuse.

(*fig. 10*) $3^1/_2$ km long were set up on both sides of the river, containing 40 dlm lamps at half meter intervals. These lamps illuminated the embankment and together with the lighted buildings were reflected in the rippling surface of the water (*fig. 11*).

It would have been possible to construct numerous illuminated fountains in the river, but it is necessary to keep in mind that the huge dimensions of the water surface would have rendered any ordinary fountain insignificant. It was therefore decided to build a single simple illuminated fountain (*fig. 12*). on a pontoon, but of dimensions in scale with those of the river. The fountain had a jet which could reach 200 m, for which pumps with motors of 1 200 h.p. were necessary. The illumination of this floating fountain was by means of yellow and white light by 64 reflectors with three kW lamps, which were mounted water-tight in the pontoon. Fig. 12 shows another remarkable lighting effect. It was the desire of the architect that there should also be a lighted boundary in an upward direction. For this purpose two flat beams of blueish-white mercury light were projected at a height of 100 m from the top of the mast of the cable railway over the exposition. Due to the scattering by dust particles and mists these fan-shaped beams were visible from below and formed in this way a kind of ceiling over the exposition grounds. The beams were obtained by means of the apparatus shown in *fig. 13*. Two water-cooled super high pressure mercury lamps with a total light flux of 24 000 dlm were mounted in parabolic

Fig. 12. Large fountain in the middle of the Meuse. After dark the fountain is illuminated with yellow and white light.

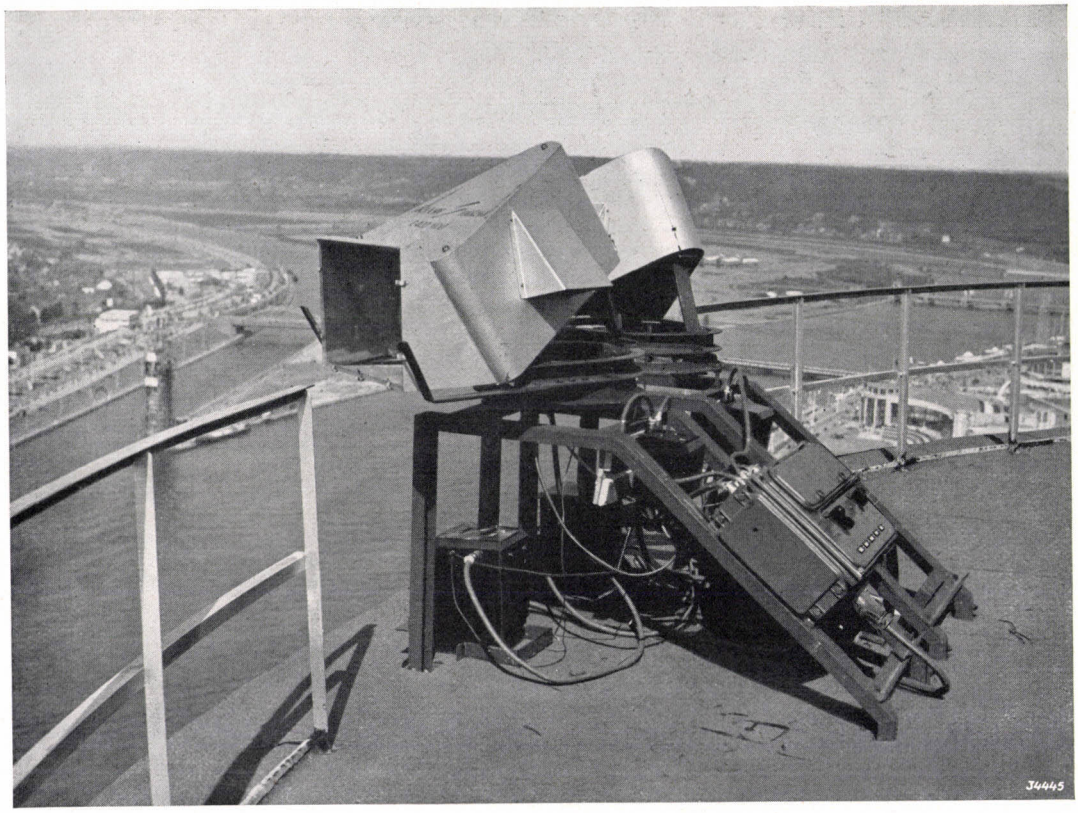

Fig. 13. By means of two searchlights with a total light flux of 24 000 dlm two broad flat beams of light were projected as a "ceiling" over the exposition.

cylindrical mirrors. The lamps, type SP 2 000, consume only 2.3 kW for a light flux of 12 000 dlm. The beams obtained are very flat and wide (2° in height and 120° in a horizontal direction), and are otherwise quite similar to the beams used to illuminate landing fields in aerodromes (Philips techn. Rev. 4, 93, 1939).

The importance of illumination in the laying out of the exposition is most clearly seen from the fact that a total of 12 000 kW was installed for lighting and 16 000 kW for power. In the middle of July the current consumption was 35 000 k.w.h. per day. Before the premature closing a consumption of 50 000 k.w.h. per day was anticipated for the month of September.

QUANTITATIVE CONSIDERATIONS IN COLOUR PHOTOGRAPHY BY THE ADDITIVE METHOD

by J. F. H. CUSTERS.

535.623 : 771.534.53 : 778.6

The principles and the natural limitations of the photographic reproduction of colours are discussed. On the basis of a fundamentally very simple method of colour reproduction, in which pictures in three colours are projected over one another, the importance for faithful reproduction of a strict linear relation between the amounts of light at the beginning and the end of the whole photographic process is pointed out. The requirement of linearity can be satisfied when the photographic materials used in combination for negative and positive transparency have certain characteristics. In particular it is desirable that the transmission curves of the two materials should be mirror images of each other, as pointed out by Kremer. Various methods are described by which such transmission curves can be realized practically. The methods described have been tested in the Philips Laboratory with different photographic materials, and it has been found that a faithful colour reproduction can be obtained with it for all practical purposes.

Principles of colour photography

When light of two different colours falls simultaneously on the same point of the retina we generally do not observe either of the original colours, but a mixed colour. Spectrally pure red and green, for example, mixed in a certain ratio of illumination intensities on the retina, give together yellow; red and violet together give purple, all the spectral colours together give daylight (white). Experience has shown that it is possible to produce in this way any colour, except some of the spectrally pure colours themselves, by the mixture of other colours. In particular it has been found possible to produce a majority of all existing tints with only three correctly chosen "primary colours" [1]).

This fact forms the basis of almost every method of colour photography. No matter how different the details of the methods may be, they always proceed on the following principle. Three photographs of the object are made in such a way that the transmissibility in each of these pictures is a measure of the amount of light of one of the three primary colours chosen which is observed in the object. In reproduction the three primary colours are remixed in the relation which is determined for every point of the object by the three pictures taken.

Reproduction can be made in two different ways, namely by the "additive" method or the "subtractive" method. If we confine our discussion to reproduction by projection we may describe the two methods as follows. In additive reproduction the three pictures (transparencies) are placed side by side and three coloured light beams each of which passes through only one of the pictures are added together. In the subtractive method the three transparencies which must be coloured in the complementary colours of the three primary colours, are placed one behind another, and the excess light of each primary colour present in a beam of white light is successively removed by the three pictures. This has the same effect on the resulting mixed colour as the addition of the three primary colours. The subtractive method has the advantage that less light is lost in reproduction. This is easily understood when we compare the way in which the impression "white" is brought about in the two methods. In additive reproduction the three coloured light components are obtained by appropriate filtering of the available white light. When this is done and the three light components have to be added together to give "white", only $1/3$ at the most (roughly estimated) of the original white light remains. In subtractive reproduction on the other hand "white" occurs when no part of the available white light is removed by any of the three transparencies, and thus the original white light remains quite unweakened.

With this advantage in view the subtractive method has obtained greater practical importance, especially when it is a question of projection in large cinemas where all the available light must be used if the screen is not to appear too dark. Nevertheless the additive method deserves attention since it is simpler in principle and involves fewer possible sources of incorrect reproduction of the colours. In the following discussion we shall confine ourselves to the additive method.

Limitations and conditions of colour photography

For the sake of example we shall examine a method of colour photography which is very simple

[1]) This is explained in detail in the article by P. J. Bouma: The representation of colour sensations in a colour space-diagram or colour triangle, Philips techn. Rev. 2, 39, 1937.

in principle (*fig. 1*). Three filters *a, b, c* are used each of which has a spectral transmission curve such that upon irradiation with white light the transmitted part of the light is of one of the primary colours, *A, B, C* (red, green and blue, for instance). Three photographs are made of the object in the usual way with one of the three filters placed before the lens in each case. Three positive transparencies α, β, γ, are made from the three negatives obtained. The transparency α is then projected through the filter *a*, β through *b* and γ through *c*, simultaneously, in such a way that the three pictures coincide on the screen. At each point of the picture a colour mixture occurs which corresponds to the colour of the object.

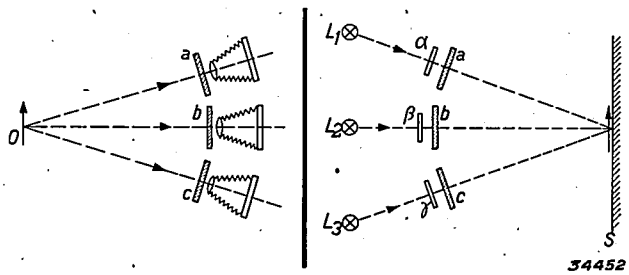

Fig. 1. Diagram of a method of additive colour photography. The object *O* is photographed three times with three filters *a, b, c* (red, green and blue, for example). Three positive transparencies $\alpha\ \beta, \gamma$, are then made from the three negatives in the ordinary way. These transparencies are then simultaneously projected on a screen *S* with three sources of white light $L_{1,2,3}$ with the same three filters *a, b, c*. (For the sake of clarity three cameras are shown here side by side, while actually the three photographs are made one after another with the same camera).

We have been cautious and have used the word "corresponds", because a completely faithful reproduction of all colours cannot be attained in this way. At the beginning of the article we stated that some of the pure spectral colours cannot be produced by mixing. The limitation to which we must submit in this respect can be illustrated by means of the representation of colours in the colour triangle [1]), see *fig. 2*. Each point within the boundaries of the figure represents a tint, and conversely, every tint is represented by a point within this area. The spectral colours lie on the curvilinear boundary. A colour obtained by mixing two colours, lies on the line joining the two colours mixed. With two primary colours, *P* and *Q*, therefore, all the colours can be produced which lie on the line *PQ* in the figure. With three primary colours *ABC* all the colours can be realized which fall within the triangle *ABC*. If a colour lies outside the triangle it means that one of the two ratios of mixing of the primary colours becomes negative, *i.e.* light of one primary colour would have to be used in the mixture in a negative intensity. Since this cannot be done in practice, and since a triangle with three colours at its angles can only include part of the colour area with curved boundaries, it is obvious that some of the colours (very pure colours) fall outside the scope of colour photography with three primary colours.

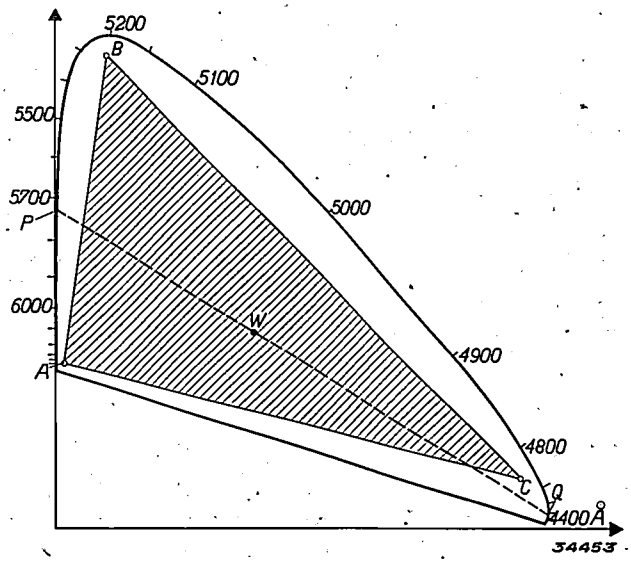

Fig. 2. Colour diagram. Each point represents a tint. The line joining two colours (*P* and *Q* for example) includes all the possible colour mixtures of these two colours. The pure (spectral) colours lie along the curvelinear boundary. With three primary colours, *A, B, C*, all the colours within the triangle *ABC* can be obtained by mixing. *W* represents white. (By means of the coordinate system indicated the position of each colour can be indicated numerically).

Experience shows that this limitation is not so serious in practice if the primary colours are suitably chosen (namely so that the most important part of the colour diagram is included in the triangle). Even when we have accepted the above-mentioned limitation, we cannot immediately expect that the process of colour photography as here described will result in absolute correspondence between the colour produced and the original colour. In the first place it is not enough that the filters possess the desired primary colours. The same colour can be obtained with entirely different spectral transmission curves of the filters. It has been found [2]) that for a faithful colour reproduction the transmission curve of each filter (combined with the spectral distribution of the light source and the spectral sensitivity curve of the photographic material) must have a very definite shape, derived from the properties of the human eye and the primary colours chosen. The remarkable point in all this is that in the three filter curves calculated negative portions also occur, *i.e.* that the system

[2]) A. C. Hardy and F. L. Wurzburg, Jr., J. Opt. Soc. Am. **27**, 227, 1937.

filter plus photographic emulsion should have a sensitivity less than zero for light of certain wave lengths (see article cited [2])). This can only be realized in a very elaborate way, which is scarcely applicable in practical cases. Approximations of the required filter curves must therefore be accepted, and this is found quite satisfactory in practice.

In the second place, for a faithful reproduction the mixture of the three light components transmitted by the positive must be in the correct proportions for every point of the object. The importance of this condition can again be illustrated by an example. Suppose that the colours P (spectral yellow of about 5700 Å) and Q (spectral blue of about 4470 Å) are mixed in such proportions that the colour W (white) is obtained (see fig. 2). With the help of available experimental data [3]) it is found that upon increase in the intensity of P by only 3.7 per cent a yellow tint is already observed.

The proportions of the three primary colours for a given point of the object can be very simply adjusted to the correct value by suitable adjustment of the light sources in the projection of the three pictures. In order, however, to arrive at the correct proportions for all other points as well, it must be

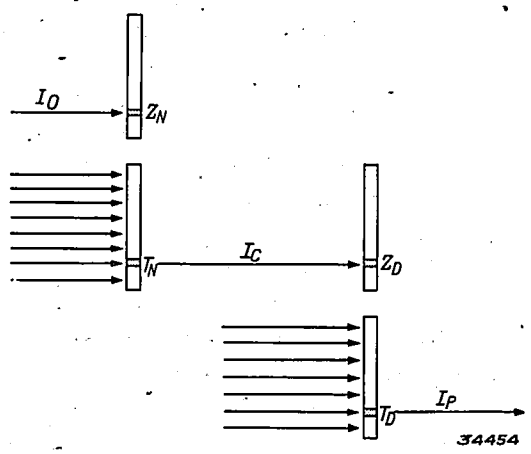

Fig. 3. Upon exposure an amount of light I_O gives a density Z_N (the negative). In copying the fraction T_N of the incident light is transmitted by this point of the negative. Thus the amount of light I_C is incident on the material of the positive transparency and there causes a density Z_D. Upon projection the transparency allows the fraction T_D of the incident light to pass at this point, and the amount of light I_P is incident on the screen.

true of all three transparencies that the amount of light transmitted I_P at every point is proportional to the amount of light I_O which that point received from the corresponding negative when it was photographed.

The way in which this fundamental requirement can be satisfied will be the subject of the following discussion.

Consequences with respect to the density and transmission curves

In order to elucidate the object of the above-mentioned requirement we shall consider in somewhat more detail the process of photographing, copying and projecting (*cf.* the diagrammatic representation *fig. 3*). For the sake of simplicity we shall in the following speak of only one primary colour.

Due to the amount of light I_O which falls on the photographic plate during exposure a density Z_N occurs on the plate (the negative). The density is defined in the following way:

$$Z_N = \lg \frac{1}{T_N} ,$$

where T_N represents the transmission, *i.e.* the fraction of a quantity of incident light which the blackened plate transmits. There exists a relation between Z_N and I_O which is characteristic of the photographic material used [4]), and which is described by a "density curve", in which Z_N is plotted as a function of log I_O, or by a "transmission curve" in which T_N is plotted as a function of I_O. In *fig. 4* the two curves have been drawn for one kind of material. It is characteristic of most density curves that they rise only slowly at small values of I_O (they have a "toe") and then gradually pass on to a longer or shorter straight section, to reach a kind of saturation at high values of I_O.

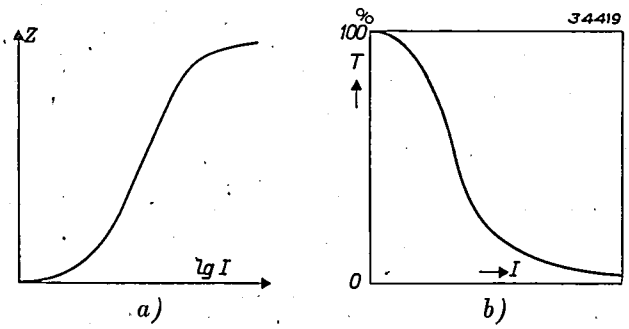

Fig. 4. *a*) Density curve of a photographic material. *b*) Transmission curve.

In copying a negative (see fig. 3 once more), an amount of light I_C falls upon the material used which is proportional to T_N, and which causes a density Z_D (the positive transparency). Z_D is determined by the density curve of the positive

[3]) L. A. Jones and E. M. Lowry, J. Opt. Soc. Amer. **13**, 25, 1926.

[4]) It is assumed that development is always carried out in the same way.

material. In projection an amount of light I_P falls upon the screen which is proportional to the transmission T_D of the positive transparency.

Whether or not the above-formulated condition that

$$I_P \sim I_O \quad \ldots\ldots\ldots \quad (1)$$

is satisfied will obviously depend upon the nature of the two density curves Z_N and Z_D. We shall here examine different forms which satisfy equation (1).

Rectilinear density curves

Let us assume that the two density curves Z_N and Z_D are straight lines, and that Z_N has the slope γ_N and Z_D the slope γ_D. Then the following

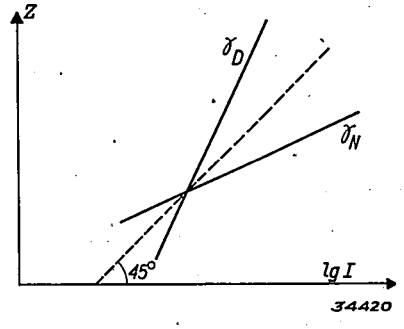

Fig. 5. Two rectilinear density curves for the negative and the positive transparency. The slopes γ_N and γ_D are such that the lines are mirror images of each other with respect to a 45° line.

equations hold where $c_{1,2\ldots}$ represent various constants which are of no importance for our purposes:

$$\lg \frac{1}{T_N} = \gamma_N \lg I_O + c_1,$$

$$\lg \frac{1}{T_D} = \gamma_D \lg I_C + c_2.$$

With the help of $I_C = c_3 T_N$

and $I_P = c_4 T_D$

it follows directly that

$$\lg I_P = \gamma_N \gamma_D \lg I_O + c_5.$$

Equation (1) is therefore satisfied when

$$\gamma_N \gamma_D = 1 \quad \ldots\ldots\ldots \quad (2)$$

This means that the two rectilinear density curves must be each other's mirror images with respect to a line at 45° (*fig.* 5).

In ordinary photography also equation (2), which is called Goldberg's condition, is important when it is a question of faithful reproduction of all the various degrees of brightness. The permissible deviations in that case, however, are considerably greater than in colour photography, since incorrect degrees of dark and light do not so easily give the impression of "unnaturalness" as do incorrect tints of colours.

We have assumed here that the density curves are straight lines. The density curves of most photographic material do indeed possess a longer or shorter rectilinear portion. Equation (2) can therefore be satisfied if only all the light quantities occurring — in photography and in copying — fall within the rectilinear portions. This is however a very unfortunate limitation, especially for colour photography, since it means that small quantities of light which still fall within the toe of the density curve have no effect, while, due to the losses of light in colour photography, it is often just this part of the curve which must be used, and small amounts of one primary colour may have a very great influence on the colour mixture.

Non-rectilinear density curves

It has been found possible to satisfy equation (1) even without a rectilinear density curve. Since the logarithmic representation is mainly used in a density curve because of the simple rectilinear form thereby obtained, if we no longer desire the rectilinear form we can give up the logarithmic representation and use the transmission curve (fig. 4*b*) directly.

In *fig.* 6 the transmission curves of a negative and of a positive transparency are given, which in logarithmic representation would not give a straight line, but with which nevertheless a linear reproduction according to equation (1) would be obtained. A definite quantity of light, that which causes the greatest density occurring, and thus

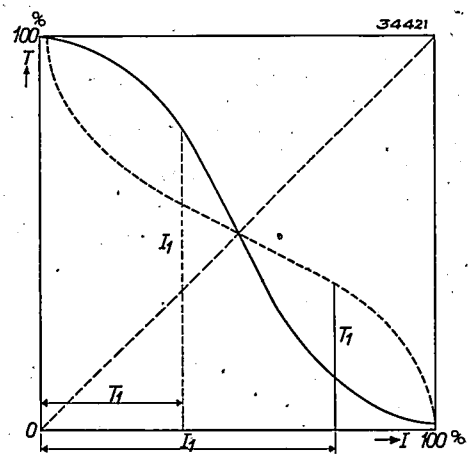

Fig. 6. Transmission curves which are mirror images of each other with respect to the 45° line (full line for the positive transparency and broken line for the negative, for example).

the smallest possible transmission, is set equal to 100 per cent in the figure. In the same way the transmission of an unexposed spot (where there is only fogging) is set equal to 100 per cent. It is characteristic of the two curves that they are mirror images of each other with respect to the 45° line. Thus if an amount of light I_1 causes a transmission T_1, an amount of light numerically equal to T_1 causes a transmission numerically equal to I_1. Equation (1) is therefore satisfied when care is taken that the proportionality factor between I_C and T_N is equal to unity in the process of copying. This amounts to the fact that the amount of light used for copying must be exactly equal to the amount indicated as 100 per cent in the figure.

Is it possible in practice to fulfil the condition mentioned, that the two transmission curves must be mirror images of each other? We have given the full-line curve in fig. 6 a form which is typical of most photographic materials. (The slowly falling first section of the curve corresponds to the toe of the density curve). The broken line curve, its mirror image, has, on the other hand, a form which differs very widely from what is encountered with ordinary emulsions.

The astronomer Dr P. Kremer of Utrecht has suggested an interesting process whereby the mirror image curve can be very approximately realized. Assume that with normal exposure of the negative curve *1* of *fig. 7* is obtained. If the negative is exposed with f times the normal amount of light, a transmission curve of the type 1*a* or 1*b* is obtained, which can be constructed simply by drawing out the section $0 - f \cdot 100\%$ of curve *1*, or compressing it to the abscissa scale 0 - 100%. In the case of curve 1*a*, $f < 1$, the negative is underexposed, the transmission curve is flatter than with normal exposure (*1*). In curve 1*b* $f > 1$, the negative is overexposed, the transmission curve is steeper than with normal exposure. The mirror image of curve *1* (broken line curve) has, however, the property that in the section to the right of the point of intersection with curve *1* it is flatter, and in the section to the left it is steeper than curve *1*, when the extremities in the neighbourhood of $I = 0$ and 100 are disregarded. It is actually found possible to approximate the mirror image curve by means of a combination of an underexposed and an overexposed negative which are copied successively on the same positive transparency. In copying the two negatives a fraction F_1 and F_2, respectively, of the normal amount of light must be used. The required factors f_1 and f_2 for the under and overexposure of the negatives, as well as the factors F_1 and F_2 for the copying can be derived according to Kremer from the shape of the transmission curve *1* by a simple construction. This is explained in *fig. 8* and the text below the figure. The approximation of the mirror image curve obtained by this construction is generally quite good, so that when the positive has the original transmission curve I, the condition for linear reproduction (1) is satisfied in a very wide region of intensities; greater discrepancies occur only at the largest and smallest amounts of light. A certain limitation is laid on the otherwise quite arbitrary shape of the transmission curve I with which we begin, by the permissible amount of error in these regions.

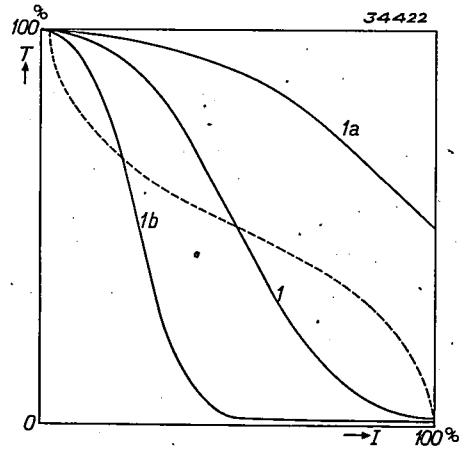

Fig. 7. Transmission curve *1* of the normally exposed negative (its mirror image is indicated as a dotted line). An underexposed negative has the transmission curve *1a* and an overexposed one the curve *1b*.

A series of experiments carried out according to this method in the Philips Laboratory have shown that very good colour reproductions can indeed be obtained. It was found at the same time, however, that in many cases the condition involving the mirror image curves can also be approximated by a simpler device, namely by choosing two suitable emulsions for the negative and positive and pre-exposing one of them with a certain amount of light. The effect of this is demonstrated clearly in *fig. 9*. Fig. 9*a* shows a normal transmission curve; if the whole plate is exposed before the picture is taken (afterward or at the same time is also possible) to the amount of light V the result is fogging corresponding to the point A, and there remains only the portion A-B of the transmission curve for further variations (fig. 9*b*). If this section is plotted anew with abscissae and ordinates from 0 to 100 per cent it represents a new transmission curve as shown in fig. 9*c*. With a suitably chosen value of V it is possible to make this transmission curve the mirror image of another (given) emulsion.

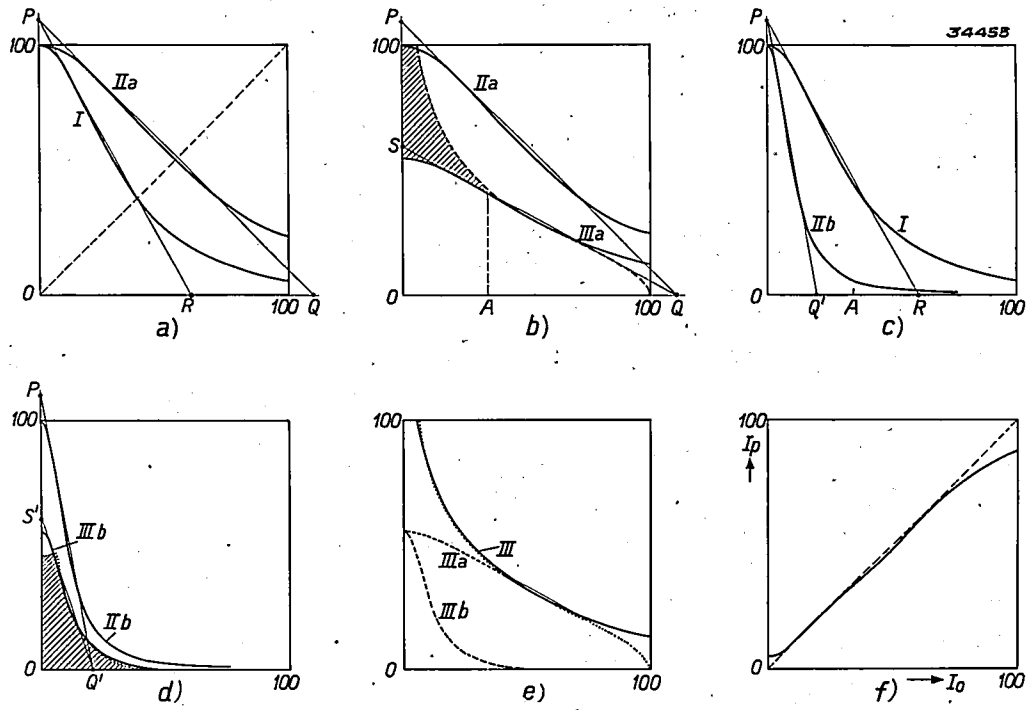

Fig. 8. *a*) Curve *I* is the normal transmission curve of the material to be used for negative and positive transparency. A large part of the curve is approximately a straight line, as indicated, which cuts the axes at *P* and *R*. If *OQ* is drawn equal to *OP*, then $f_1 = OR/OQ$, the factor for the underexposure of the first negative which then attains the transmission curve *IIa*.

b) In copying the underexposed negative with the normal amount of light (100%) the ordinates of *IIa* would indicate the amounts of light incident on the positive. What is however desired is the amounts of the dotted line (mirror image of curve *I*). Therefore only the fraction F_1 of the normal amount of light is used for copying, so that one is concerned as it were with transmission curve *IIIa* when $F_1 = OS/OP$. In the construction here given $F_1 = f_1$. The left-hand portion of *IIIa* is too low and would have to be completed by the shaded portion.

c) For this purpose the overexposed negative is used. The factor $f_2 = OR/OQ'$ for overexposure is so chosen that the negative transmits practically no light from the point *A* on the abscissa, from which point *IIIa* is a sufficiently close approximation of the mirror image curve.

d) The required fraction F_2 for copying the overexposed negative is found by plotting the part of the mirror image curve to be completed (shaded area of *b*), and approximating it by a straight line *Q'S'*. Then $F_2 = OS'/OP$ and the apparent transmission curve *IIIb* is obtained.

e) In the successive copying of the two negatives on one positive transparency, the same total amount of light is incident on the latter as if only one negative with the transmission curve *III* were used; *III* is the sum of *IIIa* and *IIIb* and approaches the desired mirror image curve of *I* (dotted line) very satisfactorily. The relation between I_P and I_O which is finally obtained is represented in

f) The 45° line represents the ideal case.

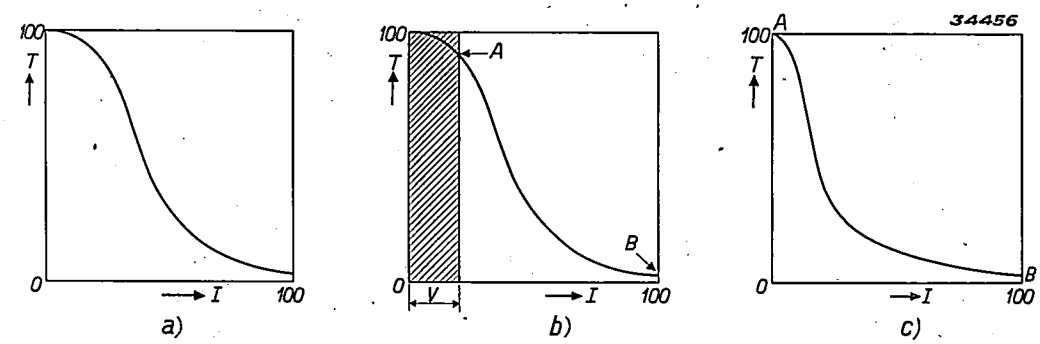

Fig. 9. By pre-exposure with a suitably chosen amount of light *V* (*b*) the nature of the transmission curve of a photographic material can be influenced in a definite way (*c*), so, for example, that it becomes the mirror image of the curve of another given material.

In *fig. 10* an example is given which was obtained in the experiments under consideration. It may be seen that a satisfactory approximation of the linear relation between I_P and I_O has been obtained by this simple method.

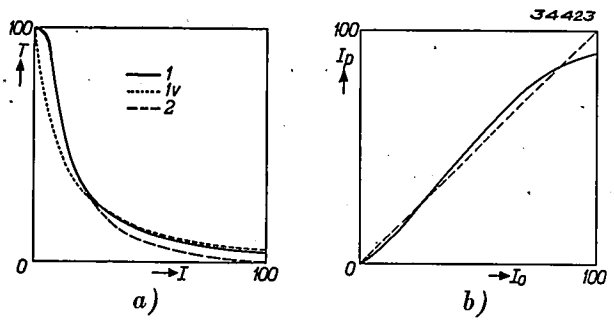

Fig. 10.*a*) The transmission curve *1* of the negative material is changed by pre-exposure into the curve *I v* which is a close approximation of the mirror image of the transmission curve *2* of the positive material.
b) The ratio obtained between I_P and I_O.

In conclusion it may be pointed out that a special case of this condition involving mirror images occurs when a transmission curve is given which is symmetrical with respect to the 45° line. The curve is then at the same time its own mirror image and the material can therefore be used for both negative and positive. In our experiments we actually found certain emulsions among the usual kinds which possess approximately such a transmission curve, and with which therefore it is sufficient to secure accurate dosage of the amounts of light in photographing and copying in order to obtain satisfactorily linear reproduction. With certain materials symmetry of the transmission curve could be achieved by appropriate pre-exposure; in that case the pre-exposure must of course be applied not only in the case of the negative but also in that of the positive.

THE ELECTROMETER TRIODE AND ITS APPLICATIONS

by H. van SUCHTELEN.

621.317.723 : 621.385.3

Since the anode current of a triode can be influenced by a change in voltage of the control grid when there is no current flow in the grid circuit, a triode is in principle suitable for electrostatic measurements of potential. In this article the characteristics and the possibilities of application are discussed of the electrometer triode, type 4 060, which was designed especially for this purpose.

In many physical and electrotechnical experiments the problem is encountered of measuring the voltage of sources of voltage which possess a very high internal resistance. It is of course essential that the voltage meter used should consume as little current as possible, so that the terminals voltage measured will remain equal to the EMF of the source.

Very small currents also are sometimes measured by sending them through a high resistance and then measuring the voltage across the resistance. In such cases also a voltage meter with a high resistance is called for, since the meter shunts the measuring resistance, and thus limits the magnitude of the total resistance to be applied, thereby also limiting the sensitivity of the circuit.

In such cases an electrometer is best used whose deflection is caused by the electrostatic action of charges, and which in principle therefore consumes no current at all.

The electrometer in its different types (quadrant electrometer, string electrometer, etc.) is a fairly expensive and delicate instrument, so that its possibilities of application are limited. A much sturdier arrangement can be obtained by replacing the electrometer by a triode which also allows a currentless measurement of the voltage. The anode current can be influenced by voltage variations of the control grid without any current flowing through the grid circuit.

The term currentless must in this case be taken with a grain of salt. As is generally known a grid current immediately occurs when the grid becomes positive with respect to the cathode. This can, however, easily be avoided by a correct circuit arrangement, but even when the grid potential is negative a small current often remains which may be due to various causes.

In the first place, in the "pinch" of an ordinary radio valve, *i.e.* in the glass holder of the various electrodes, there will be a certain leakage between the grid and one of the other electrodes. This weak leakage current is permissible in ordinary radio and amplifier connections, but it is usually not

permissible when a triode is used as electrometer.

In the second place, it is inevitable that a vacuum tube, instead of being an absolute vacuum, contains a small residue of gas. If gas molecules are ionized by the anode current the positive ions are drawn toward the electrode with the lowest potential, *i.e.* the control grid, and neutralized. This amounts to a grid current.

In the third place the control grid may have a certain thermionic emission, because it is fairly strongly heated by the glowing cathode, and moreover in some cases it becomes covered in spots with a highly emissive material, due to the evaporation of the surface of the cathode. Besides the thermionic emission there may also be photoelectric emission due to light incident from the outside and to soft X-rays which come from the anode bombarded by electrons.

The total grid current which occurs as a result of the various causes here mentioned is less than 0.1 microampere in ordinary amplifier valves. For certain electrometrical applications the degree of insulation of the control grid found in these valves is sufficient without further measures being taken. In order however to satisfy the much higher requirements which are made in certain cases, a special electrometer triode has been constructed in which measures have been taken to make the grid current considerably smaller.

Construction of the electrometer triode

In *fig. 1* the construction of the Philips electrometer triode, type 4 060, is shown. The grid is fastened to two long glass rods in order to make the path of creeping currents as long as possible. In order to make this arrangement possible, control grid and anode have different positions than is usual in amplifier triodes; they are situated on opposite sides of the filament. Both the electrodes are flat plates. The wire lead of the grid is fused through the glass at the top of the bulb, thus as far as possible away from the lead-in of the other electrodes. When the outside of the bulb is well cleaned and dry the leakage current over the glass of the supports and the bulb may be neglected.

From the point of view of thermionic emission also, this placing of the control grid is more satisfactory than the ordinary arrangement, because the temperature of the grid is kept lower due to the great heat radiation of the flat plate. It will usually be unnecessary to take special precautions against photoelectric emission because the shielding from external electric fields which is usually present will give sufficient shielding against the light as well. The illumination of the grid by the glowing cathode is avoided by using an oxide cathode which emits at a very low temperature.

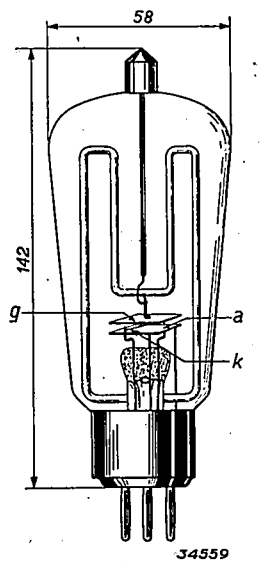

Fig. 1. Construction of the electrometer triode, type 4 060. The control grid is mounted on long glass rods; the lead-in of the grid is fused in through the top of the bulb. Very good insulation is obtained in this way.

Finally, considerable decrease in the grid current caused by ions and X-rays is obtained by choosing a very low anode voltage, namely 6 volts. At this voltage no ions are yet formed, because the energy which an electron obtains in passing through a potential difference of 6 volts is not enough to ionize an atom of the gas, while the X-rays excited at this voltage are much weaker than at the usual anode voltages of about 250 volts.

The result of these precautions is expressed in the valve characteristic reproduced in *fig. 2*. It may be seen that the total grid current becomes practically zero when the anode current is zero. From this it may be concluded that the leakage current over the glass may be neglected compared with the currents connected with the anode current. With normal grid voltages the grid current is of the order of 10^{-15} A, *i.e.* at least 10^6 times as small as may be expected in valves of the ordinary type [1]).

The other characteristics of the electrometer triode, type 4 060, are given below:

Heating voltage	about 0.7 V	Specific values for every tube are given in the instructions.
Heating current	about 0.6 A	
Anode voltage	max. 6 V	
Slope	25 μA/V	
Amplification factor	1	
Grid current	$< 10^{-14}$ A.	

[1]) To give some idea of the size of this current, it may be stated that it corresponds to 6 000 electrons per second.

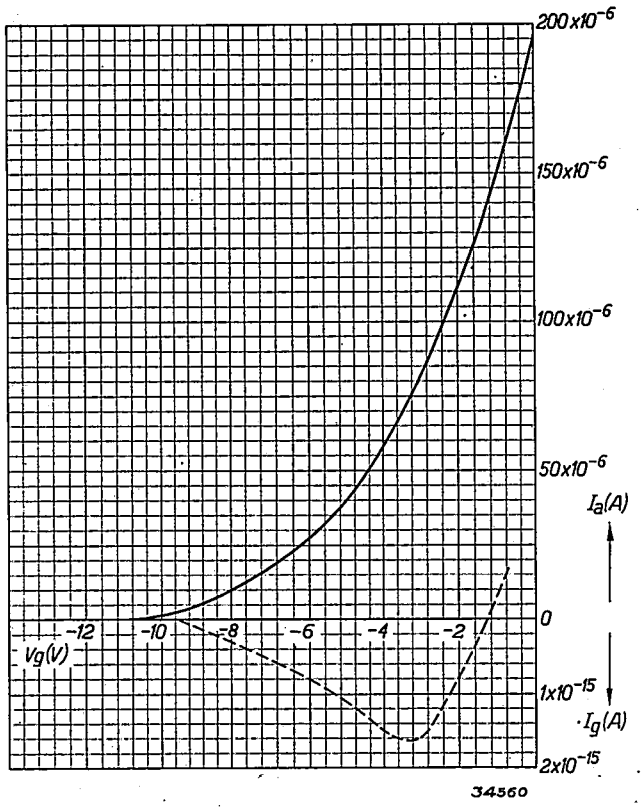

Fig. 2. Grid current and anode current as functions of the grid voltage for an anode-voltage of 4 V. At negative grid voltages the grid current is smaller than 10^{-14} A. For a certain grid voltage the grid current is exactly zero.

Connections of the electrometer triode

In most of its connections the electrometer triode is used as a zero indicator. The voltage to be measured is compensated by a variable counter voltage which can be read off. Both voltages are connected in series in the grid circuit of the electrometer triode. If there is an excess voltage due to insufficient compensation, this is manifested in the anode current. The compensation can therefore be adjusted using the reading of the anode current as indicator.

This method has two advantages. In the first place the form of the characteristic, anode current as a function of the grid voltage, plays no part. The required value follows from a direct reading of the compensation voltage, and the slope of the valve affects only the accuracy with which the compensation can be regulated.

In the second place, the actual voltage on the grid always retains about the same value, independent of the voltage measured. Arrangements can therefore be made so that one always works at a voltage at which no grid current flows (fig. 2), and at which therefore the measurement is entirely electrostatic in character.

A fairly general scheme for the measurement of voltages by the compensation method is indicated in *fig. 3*. The grid voltage V_g is adjusted approximately at the value at which no grid current flows. This value can be determined empirically in the following way. When the grid of the triode is entirely insulated, it automatically assumes the potential in question. If it did not originally have that potential, electrons will flow to it or away from it until the potential is reached at which the current becomes zero, and then the situation becomes stationary. In fig. 3 the switch is set at the insulated middle position S_1, and the grid then takes on the required potential. The corresponding anode current is then read off, and with S at the lowest position, V_g is so adjusted that the same anode current is again obtained.

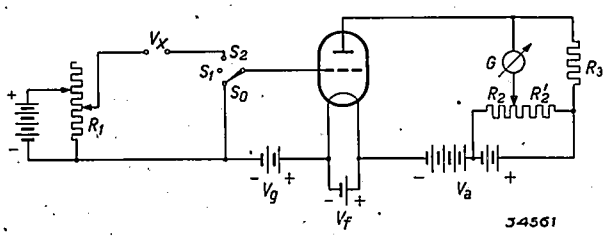

Fig. 3. Circuit for the comparison of a voltage to be measured with an accurately known compensation voltage (from R_1). The galvanometer is in the so-called currentless connection, *i.e.* the potentiometer R_2. R_2 is so adjusted that the galvanometer indicates zero when the voltage applied to the grid, other than V_g, is zero. This is the case when the grid switch is set on S_0, or when the correct compensation has been obtained (with the grid switch on S_2).

On the extreme left may be seen the compensation voltage tapped off from the resistance R_1, in series with the voltage V_x to be measured. The point on R_1 where it is tapped off must be so adjusted during the measurement that the anode current does not change when the switch S is moved from the lowest to the highest position. V_x is then equal to the compensation voltage used, which is known from the part of the resistance R_1 tapped off, through which an accurately known current flows. As a rule this arrangement is calibrated by connecting a standard element in place of the voltage V_x to be measured.

In order to be able to read off very small current variation, as is necessary for accurate compensation, a connection is used in the anode circuit in which the normal anode current does not pass through the galvanometer. The anode current flows through the resistance R_3, and there causes a certain voltage drop, so that the voltage on the anode is lower than that of the anode battery. At the lowest terminal of the galvanometer G, by means of an adjustable tap on the potentiometer R_2, the same voltage R'_2 can be applied so that G carries no current. If however the anode current

changes, the equilibrium is disturbed, and a current flows through the galvanometer. If the internal resistance of the galvanometer and potentiometer is sufficiently small compared with R_3, this current is practically equal to the change in the anode current. Thus the entire scale is available for the measurement of the current fluctuations, and one may choose as sensitive a galvanometer as desired without taking into account the normal anode current.

The measurement is now carried out as follows. The switch is first set in position S_0, and the potentiometer R_2 so adjusted that the current through the galvanometer is zero. When one now switches over to S_2, a deflection of the galvanometer will generally occur. Potentiometer R_1 is then adjusted so that this deflection disappears.

Since the slope of the electrometer triode is 25 μA/V an error of 1 mV in the compensation voltage will cause an anode current variation of 0.025 μA, a value which can be registered with a relatively simple instruments. In practice however the accuracy is determined not only by the sensitivity of the galvanometer, but also by the stability of the circuit arrangement. When, for example due to a fluctuation in the temperature of the cathode, the anode current changes slightly, the equilibrium of the galvanometer connections is upset. This drift can cause an error of several hundredths of a volt in the measurement of the compensation voltage, and is therefore much more important than the error caused by the limitation of the sensitivity of the galvanometer. Fortunately the drift generally takes place very gradually, so that it is of little importance when the measurements in position S_0 and that in position S_2 are carried out in quick enough succession.

The drift would however be disturbing when a series of measurements had to be carried out, for instance of a voltage which itself slowly varies. One would then be compelled by the drift to note the zero position of the galvanometer each time anew, or to adjust it to the same value.

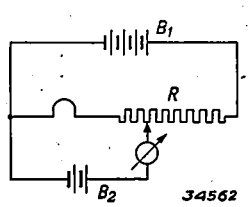

Fig. 4. Connections for the purpose of keeping the voltage of the heating current battery constant. The filament is fed by the battery B_1; the battery B_2 is made currentless by adjusting the potentiometer R. If however the voltage of B_1 changes, the missing portion is supplied by B_2. Since B_2 is very lightly loaded its voltage is quite constant.

Since the drift is caused mainly by fluctuations in the heating current, considerable improvement can be obtained by very carefully keeping the voltage of the heating current constant. A simple connection making this possible is given in *fig. 4* and explained in the text beneath.

In connections in which the electrometer triode does not serve as a zero instrument, but as an actual meter, the problem of fluctuation is still more important. In such a case the effect of any voltage fluctuations can be eliminated to a large degree by using the arrangement reproduced in *fig. 5* [2]). These connections, used here for measuring a photocurrent, are so arranged that any fluctuations of battery voltage do not lead to a change in the current through the galvanometer, because upon such fluctuations the potential of both connections of the galvanometer change by the same amount.

The circuit has two identical electrometer triodes whose cathodes are connected in parallel. The voltage drop V_x to be measured is applied to the grid of the first electrometer triode. The galvanometer is connected in the anode circuit of this electrometer triode in a manner corresponding in principle with fig. 3, except that the resistance R_2' is replaced by the internal resistance of the second electrometer triode.

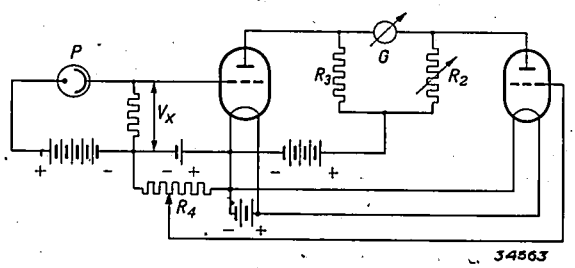

Fig. 5. Symmetrical connections of two electrometer triodes. If a voltage V_x acts between the terminals the galvanometer G shows a deflection. Variations of the battery voltages have equal effects in both the anode circuits, so that they do not cause a deflection of the galvanometer.

By means of the potentiometer R_1 the grid voltage of the second valve is so adjusted that the two valves have about the same anode current in the absence of the measuring voltage [3]). By fine regulation of the resistance R_2 (which corresponds approximately with R_3) the galvanometer is finally rendered currentless.

The two valves now function under practically the same conditions. They have the same battery for the heating current, the grid voltage and the

[2]) J. F. H. Custers, Z. techn. Phys. **14**, 153, 1933.

[3]) In order to do this when the triodes differ slightly, one takes as second triode the one which has a slightly lower anode current at a given grid voltage.

anode voltage. If a change occurs in one of the battery voltages it has the same effect on both valves, and it is very probable that the two anode currents will remain alike, and therefore also that the galvanometer will remain currentless. Only when a measuring current is applied to the first valve is the equilibrium upset and G shows a deflection.

The fluctuation is reduced to about one tenth by the use of these connections.

Applications of the electrometer triode

As already stated the electrometer triode can be used in general in every setup in which an electrometer would otherwise be used. There are however several types of measurements in which in the course of time the electrometer triode has won special recognition. We shall deal with them separately.

p_H measurements

The quantity p_H is a measure of the concentration of hydrogen ion c in a solution, $p_H = -\lg c$. Measurements of p_H are repeatedly made in chemical laboratories, in the testing of foods and farm products, in medical research, etc.

The commonest method of measuring p_H makes use of the fact that the potential of special electrodes immersed in the solution changes proportionally with p_H. Among the various electrodes which exhibit this property, the most suitable is the so-called glass electrode. Besides certain advantages, however, this electrode has the less desirable property that its internal resistance is very high, namely of the order of 10^7 ohms.

In order to determine the EMF of a source of voltage with this high internal resistance, an electrostatic method of measurement is indicated. The compensation circuit arrangement reproduced in fig. 3 is usually employed with an electrolytic cell with a glass electrode in the place of V_x. If the potential is measured accurately to within 1 mV, the value of p_H is determined with an accuracy of 1.7 hundredths of a unit [4]), which is more than adequate for most practical purposes.

A sensitivity of 1 mV can easily be attained, as explained above. If we examine to what extent the result of the measurement could be influenced by the residual grid current, we find that it is quite unnecessary to have the electrometer triode work at an especially favourable point; the maximum grid current is less than 10^{-14} A within a large range of grid voltages, and with this current a voltage loss of only $^1/_{10\,000}$ mV would occur at an electrode with an internal resistance of 10^4 ohms.

Radiation measurements with the ionization chamber

The intensity of radioactive radiation can be measured by determining its ionizing action. In most cases the ions formed by the radiation are collected on a very well insulated condenser whose voltage varies with the time. Since one is here concerned with extremely small charges it is here again important that the voltage meter should consume practically no current. Since the electrometer triode consumes a current of less than 10^{-14} A, an ion current of 10^{-12} A can be measured with an accuracy of 1 per cent.

A current of 10^{-12} A corresponds to a radioactivity of the order of 10^{-9} Curie, which may be considered very weak. If the same instrument is used to measure X-rays, with a sufficiently sensitive ionization chamber a current of 10^{-12} A corresponds to such a low radiation intensity that it cannot be made visible by means of a fluorescent screen. In both cases therefore the grid current of the electrometer triode has no bad effects, so that it is unnecessary to choose the working point such that the grid current is exactly zero.

In another important application of the ionization chamber, namely for the measurement of cosmic rays, the attainable ion currents are much smaller, of the order of 10^{-14} A. In this case the grid current at a given adjustment of the grid voltage cannot in general be neglected. According to a method indicated by Prof. Clay [5]), however, the grid current can be kept practically at zero during the measurement.

The method has also been used in this laboratory for the measurement of very weak photocurrents, and has been described in detail in this periodical [6]). In the circuit given the photocell can immediately be replaced by an ionization chamber.

As stated previously all of these measurements can also be made with an ordinary electrometer, and the advantage of the electrometer triode lies especially in the great sturdiness of the apparatus. In the measurements by Clay referred to some of the experiments were carried out on board ship, and the ionization chamber with the electrometer triode was even lowered overboard to a considerable depth below the surface.

[4]) The potential of a glass electrode at room temperature varies — 0.058 volts per unit of p_H. A change in the potential of 1 mV thus corresponds to a change in p_H of 0.017 units, which means that the hydrogen ion concentration changes by 4 per cent.

[5]) J. Clay, Physica 4, 124 and 654, 1937.

[6]) P. M. van Alphen, Philips techn. Rev. 4, 71, 1939.

The measurement of photocurrents

A photocell gives a current which is proportional to the incident light flux, and which amounts for instance to 20 or 30 microamperes per lumen. In certain measurements the light flux becomes so small that special devices must be used in order to be able to measure the photocurrent. This is the case for example in the photometry of stars or of lines in the spectrum [7]).

It is possible to carry out the measurement of the photocurrent in the same way as the measurement of the current through an ionization chamber in which the voltage on a condenser is determined when the condenser is charged by the current. As to the connections, we refer to the article cited in footnote [6]), in which the precautions are also discussed which must be taken in order to obtain a sufficiently high insulation and satisfactory shielding at all sensitive spots.

If the currents are not extremely small, but of the order of 10^{-13} A, for example, a simpler method may be used. Liquid resistances of the order of 10^9 to 10^{10} ohms may be made up. Currents which are just too small for direct measurement with a galvanometer (10^{-10} to 10^{-11} A) give voltages of the order of 0.1 V over such resistances. Since, as we have seen, the electrometer triode makes possible voltage measurement with an accuracy of 1 mV, a sensitivity of 10^{-13} to 10^{-14} A is obtained in this way. This is also about the limit of sensitivity set by the residual grid currents.

[7]) A star of first magnitude gives an illumination intensity of 10^{-6} lux. If, for example, the telescope has a lens (or mirror) of 40 cm diameter one obtains a light flux of 10^{-7} lumen. Such a small light flux, and even smaller ones, also occur in the spectral photometry of sources of light. See in this connection the article cited in footnote [6]).

ABSTRACTS OF RECENT SCIENTIFIC PUBLICATIONS OF THE N.V. PHILIPS GLOEILAMPENFABRIEKEN

1438: J. Sack: Forces acting during the transfer of material through the welding arc (Weld. Industr. 7, 234-240, July 1939).

For the contents of this lecture held before the Institute of Welding in London the reader is referred to: Philips techn. Rev. 4, 9, 1939.

We take the opportunity at this point to draw attention to an inaccuracy in the article referred to. For the theoretical estimation of the kinetic energy with which the drop is thrown off the welding rod, it is of some concern at what length of *radius of the neck of te drop* the moving force of electrodynamic nature is in equilibrium with the total sum of the opposing forces, and not with the weight of the drop alone. This consideration is developed further in the above-mentioned lecture, with as result that the electrodynamic forces are found to contribute only very little to the total energy. The mechanism of the transfer of the weld material may therefore be summed up in the following way. *The electrodynamic forces cause the constriction at the neck of the drop and the drop is then thrown off by the explosive forces.*

1439: F. A. Kröger: Some optical properties of zinc silicate phosphors (Physica **6**, 764-778, Aug. 1939).

Zinc silicate phosphors and zinc beryllium silicate phosphors activated with manganese are mixed crystals of zinc silicate and zinc beryllium silicate with manganese silicate. Mixed crystals with from 0 to 50 molecules per cent of manganese emit two bands at 25° and —180° C with maxima at 5 200 and 6 100 Å. The emission bands of zinc silicate-manganese phosphors are caused by electron jumps in the bivalent manganese. The 0 to 50% mixed crystals of zinc and manganese silicate absorb light in three different wave-length ranges. The first absorption range also exists with pure zinc silicate and must be considered as a crystal absorption. The second absorption range only appears when manganese is present but it also has the properties of a crystal absorption. In the third absorption range we are concerned with a band system; each band corresponds to a definite electron transition in the ion Mn^{++}. Upon irradiation with light from each of these absorption regions luminescence occurs in the emission bands characteristic of the bivalent manganese ion. Upon irradiation with wave lengths of the two regions of crystal absorption phosphorescence and fluorescence occur together, while irradiation with the manganese absorption bands gives only fluorescence.

1440: F. A. Kröger: Fundamental absorption of ZnS-MnS and ZnS-CdS-MnS mixed crystals (Physica **6**, 779-784, Aug. 1939).

Zinc sulphide possesses a fundamental absorption region with a long-wave limit at about 3 380 Å.

When manganese sulphide is taken up in the lattice a new absorption band appears with its edge at 3 650 Å. This band is similar to the fundamental absorption band found with manganese sulphide. When cadmium sulphide is taken up by zinc sulphide-manganese phosphors the fundamental absorption region of the zinc sulphide is shifted toward the red of the spectrum.

1441: J. L. Snoek: Magnetic after-effects at higher inductions (Physica **6**, 797-805, Aug. 1939).

Continuing with the investigations described in **1339** and **1399** on magnetic after-effect phenomena, a sample of pure iron was prepared, with which, by the addition of very small amounts of carbon homogeneously dispersed, an extremely strong magnetic after-effect could be observed. The magnetic after-effect with stronger fields was studied on this sample. Since it followed from the investigations with weaker magnetic fields that the permeability and the magnetic field were not the most important quantities, but the reciprocal of the permeability and the magnetic induction B, all the experimental data were recalculated for these latter quantities. The relative intensity of the after-effect remains constant to $B = .6$ gauss, and falls at $B = 100$ gauss to about 10% of the original intensity. This follows from the curves which indicate the manner in which the reciprocal of the permeability depends upon the temperature, and also from its behaviour at low temperatures and high inductions. It is remarkable that a demagnetization, at which the induction is 100 gauss at the most, results in no appreciable decrease in the reciprocal of the permeability at the same temperatures. Much higher inductions are required for this, for instance up to 10 000 gauss. The substance thus has a tendency to return to the old state of magnetization after demagnetization.

1442: H. Bruining and J. H. de Boer: Secondary electron emission, part IV. Compounds with a high capacity for secondary emission (Physica **6**, 823-833, Aug. 1939).

A pure compound of an alkali metal has a higher secondary emission than the metal itself. It is further described how the electrons, which are bound to the atoms of the electronegative element in the highest occupied energy band have the greatest chance of being emitted as secondary electrons. It is shown that it is impossible that all the secondary electrons should come from the metal atoms within or on the surface of the compound. These metal atoms provide only the conduction electrons.

1443: H. Bruining and J. H. de Boer: Secondary electron emission, part V. The mechanism of secondary electron emission (Physica **6**, 834-839, Aug. 1939).

On the basis of a simple energy scheme it is easily understood that the compounds of metals with a low ionization energy, which consist of ions with closed electron shells, can give a high secondary emission, while the compounds of metals with a high ionization energy must exhibit a relatively low secondary emission.

1444: J. A. M. van Liempt and W. van Wijk: The rare gas content of air dissolved in water (Chem. Wbld. **36**, 555, Aug. 1939). Original in Dutch language.

Air dissolved in water contains about twice as much of the rare gases as is present in the ordinary atmosphere.

1445: A. Claassen: The volumetric and quantitative determination of zirconium and hafnium single and together with selenious acid (Z. anal. Chem. **117**, 252-261, Aug. 1939). Original in German Language.

When zirconium and hafnium solutions are heated for some time with an excess of selenious acid, the initially formed insoluble basic selenite passes over into a crystallized compound of the composition $Zr(SeO_3)_2$ and $Hf(SeO_3)_2$ respectively.

Since these compounds have exactly the composition expressed by the formula, they are useful for the quantitative determination of zirconium and hafnium. For the volumetric determination the precipitate is dissolved in sodium fluoride and sulphuric acid and the selenious acid form is determined iodimetrically. In the case of zirconium correct results are obtained in this way, but with hafnium the results are from 1.0 to 1.4% too high. For the gravimetric determination the precipitate is dried at 120 to 200° C and then weighed. Since small amounts of selenium precipitate out, the results are often somewhat too high. By converting a known amount of a mixture of ZrO_2 and HfO_2 into the selenite, and determining the selenious acid radical volumetrically, the content of hafnium can be determined with an accuracy of about 1%.

VOL. 5 No. 3 MARCH 1940

Philips Technical Review

DEALING WITH TECHNICAL PROBLEMS RELATING TO THE PRODUCTS, PROCESSES AND INVESTIGATIONS OF N.V. PHILIPS' GLOEILAMPENFABRIEKEN

EDITED BY THE RESEARCH LABORATORY OF N.V. PHILIPS' GLOEILAMPENFABRIEKEN, EINDHOVEN, HOLLAND

TESTING AMPLIFIER OUTPUT VALVES BY MEANS OF THE CATHODE RAY TUBE

by A. J. HEINS van der VEN.

621.317.755 : 621.396.645

In testing amplifier output valves, the most important data are contained in the I_a-V_a diagram if one knows over which part of the diagram the values of voltage and current prevailing during operation range, *i.e.* if the position of the load line is known. The I_a-V_a diagrams as well as the load lines can very easily be obtained with the help of a cathode ray tube. The necessary apparatus is described in this article. A number of auxiliary arrangements are also studied, by which the axes and the necessary calibration lines in the diagram can be traced on the fluorescent screen, and which make it possible to cause the diagrams of two output valves which are to be compared to appear simultaneously on the screen. In order to obtain the load line in the correct place in the diagram, use must be made of direct current push-pull amplifiers for the deflection voltages of the cathode ray tube. The position of the load line upon inductive loading is discussed and explained by a number of examples. In conclusion one application of the installation in the development of output pentodes is dealt with.

If one wishes to characterize briefly the performance of an output valve of an amplifier or radio set, it is enough to give the sensitivity, the distortion as a function of the power output, and in some cases the maximum power which can be delivered without grid current flowing. For a more careful examination, however, particularly for the discovery of causes of deviations or errors, such for example as differences in distortion in different valves, one must in general have reference to the I_a-V_a diagram, which forms the actual basis for the judgement of the properties of an output valve. This diagram (*fig. 1*) gives the variation of the anode current I_a as a function of the anode voltage V_a with the negative control grid voltage V_g as parameter [1]). From the series of curves the primary quantities of the valve: slope, internal resistance and amplification factor, may be read off immediately for every operating point, as is explained in the text under the figure. A connection may, however, also be found between the shape of the curve and the above-mentioned quantities such as distortion and power output. Since these quantities are to some degree dependent on the loading impedance which is included in the anode circuit, it is first necessary to find out how the loading of the valve is expressed in the I_a-V_a curve.

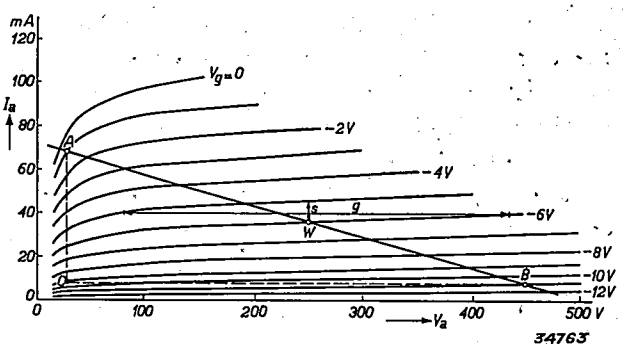

Fig. 1. The I_a-V_a diagram of the output valve EL_3. W is the operating point; in this valve it ordinarily lies at V_a = 250 volts, I_a = 36 mA, V_g = −6 volts. The screen grid voltage is permanently fixed at 250 volts. The slope S is given by the vertical distance between two successive curves, the amplification factor g by the corresponding horizontal distance, the internal resistance by the slope of the I_a-V_a curve at the operating point. AB is the load line for a pure resistance of 7 000 ohms.

If the valve is loaded with a resistance R which is connected to the anode circuit through a transformer in order to have no D.C. voltage drop in R (*fig. 2*), an alternating current I_R will begin to

[1]) The screen grid voltage, which forms a second parameter in the case of pentodes, is kept constant for the whole diagram.

flow in R when an A.C. voltage is applied to the grid of the valve. The A.C. voltage on the loading resistance is then $V_R = R \cdot I_R$. The total anode voltage V_a and anode current I_a of the valve are given by the sum of V_R or I_R and the values of the anode D.C. voltage or current indicated by the operating point. The relation between I_a and V_a of the loaded valve, the socalled load line, is therefore in this case represented by a straight line through the operating point (AB in fig. 1), with the slope $\tan \alpha = R$ with respect to the I_a axis.

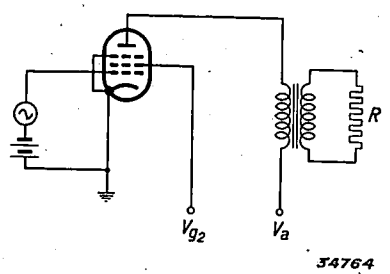

Fig. 2. A loading resistance R is included in the anode circuit of the output valve *via* a transformer 1 : 1.

If one considers the grid voltage to be varying, the values of I_a and V_a at any moment are always determined by the point of intersection of the load line with the I_a-V_a curve corresponding to the value of the grid voltage at that moment. If, for instance, the operating point lies on the curve for $V_g = -6$ volts and the grid excitation voltage is sinusoidal with a peak value of 5 volts, then the points of intersection of the line AB with the curves $V_g = -1$ volt and $V_g = -11$ volts give the extreme values of I_a and V_a. The distance AC is therefore twice the amplitude of the alternating current occurring, the distance BC twice the amplitude of the A.C. voltage. The power output to the loading resistance at the grid excitation voltage in question is thus given by $^1/_4$ of the area of the triangle ABC.

Insofar as the successive I_a-V_a curves cut off equal segments of the line AB, a proportional change in anode voltage and current corresponds to any change in the grid voltage. There is therefore no distortion. With large amplitudes along the load line, however, the segments cut off on AB become gradually smaller (fig. 1). The variation of anode voltage and current with a sinusoidal grid excitation voltage is then no longer sinusoidal, but exhibits a flattening. The distortion occurring could be calculated by careful measurement of the segments cut off on the load line.

If the loading impedance is not a pure resistance, the load line is not straight in the I_a-V_a diagram. Depending on the grid excitation voltage a larger or smaller portion of the whole diagram is then covered by the load lines. A knowledge of this region makes it possible to estimate the importance for the reproduction, of any irregularities occurring in the I_a-V_a diagram.

In the following a method will be described by which not only the I_a-V_a diagram, but also the load line can very easily be obtained. The principle of this method, which makes use of the cathode ray tube, has already been outlined in this periodical [2]), at least as far as the recording of I_a-V_a diagrams is concerned. We shall here go more deeply into the practical execution of the method and also give several examples of its application.

Installation for the recording of I_a-V_a diagrams.

An I_a-V_a characteristic can be registered on the screen of a cathode ray tube in the following way. A given D.C. voltage is applied to the control grid of the output valve to be investigated, while the anode voltage is made to vary periodically from zero to a maximum value. This anode voltage is applied, *via* a potentiometer and an amplifier, to the plates for horizontal deflection of the fluorescent spot. The voltage on a small measuring resistance, through which the anode current flows, causes the vertical deflection, which is therefore proportional to the anode current at every moment.

In order to trace different I_a-V_a curves on the screen successively, the grid bias must be given different values successively for short times. A voltage which varies in steps must therefore be applied to the grid, and in order to obtain a lasting image on the screen of the cathode ray tube, this voltage varying in steps must be run through completely several times per second.

The stepwise varying voltage is obtained by means of a rotating switch S_1 which passes over 28 contacts (*fig. 3*). Sixteen of these are connected to the taps of a potentiometer which correspond to the 15 steps of the desired voltage series, see *fig. 4*. On the following 6 contacts (*17* to *22*) there is a high negative voltage, so that the valve to be examined passes no anode current at all during this time. By this means, and by the great rapidity at which the switch rotates (1 000 to 1 500 r.p.m.) it is possible to record the whole I_a-V_a diagram without the valve becoming overloaded.

For the sake of orientation in the diagram, the two axes and the corresponding scale are necessary in addition to the I_a-V_a curves. The remaining

[2]) H. van Suchtelen, Applications of cathode ray tubes, Philips techn. Rev. **3**, 339, 1939. See also Philips techn. Rev. **4**, 56, 1939, where a related problem had to be solved in a different way.

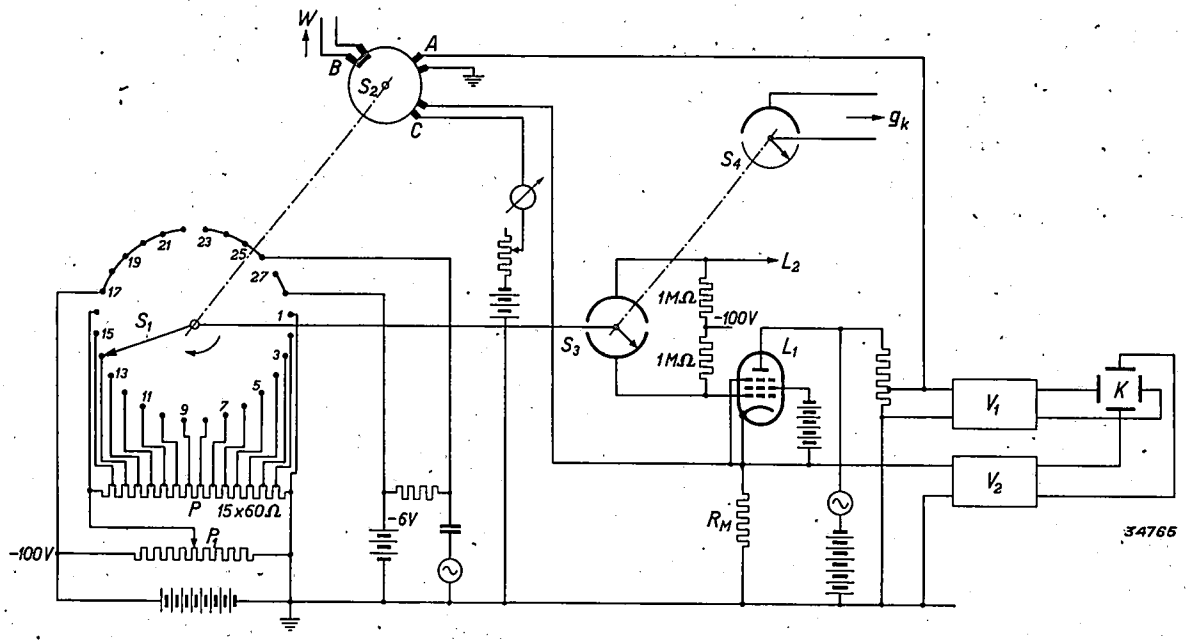

Fig. 3. The anode voltage of the output valve L_1 to be investigated is applied to the plates for horizontal deflection of the cathode ray tube K *via* the amplifier V_1; the voltage over the measuring resistance R_M, through which the anode current flows, is applied *via* the amplifier V_2 to the plates for vertical deflection. By means of the rotating switch S_1 the grid bias of the output valve is varied in steps. The auxiliary switch S_2 which is fastened to the axis of S_1 short circuits the pairs of brushes A, B, C at certain moments, and thus causes the various auxiliary lines of the diagram to be traced on the fluorescent screen. The switches S_3 and S_4 which rotate with half the velocity of S_1 serve to record the diagrams of two output valves L_1 and L_2 at the same time, while the voltage on the grid g_k of the cathode ray tube is lowered for the diagram of one of the valves. With the help of the potentiometer P_1 the current through the potentiometer P can be regulated and the grid bias stepwise variation can be made more or less steep.

contacts and the auxiliary switch S_r which is fastened to the axis of the rotating switch and passes over the pairs of brushes A, B, C (fig. 3) serve these purposes.

The horizontal axis is produced automatically due to the fact that during the currentless periods (contacts *17-22*) the fluorescent spot moving back and forth is not deflected in a vertical direction. The vertical axis is traced in the diagram when the switch passes over contacts *23* and *24*. At this moment the input of the amplifier for the voltage for horizontal deflection is short circuited *via* the brushes A. On the contacts *23* and *24*, which now feed the grid, an A.C. voltage now acts so that the anode current may vary sufficiently to describe the whole I_a axis. The same is true for the following two contacts, *25* and *26*. At the moment at which these contacts are connected to the grid, the second pair of brushes B brings about a substitution of the anode A.C. voltage by the normal anode D.C. voltage of 250 volts, for instance. The vertical line $V_a = 250$ volts is therefore now drawn in the diagram, which facilitates finding the operating point, and at the same time provides the scale for the horizontal axis. The scale for the vertical axis is obtained by passing a direct current of known magnitude through the measuring resistance R_m during the resting period of the valve (contacts *17* and *18*). This is done by means of the two brushes C, and gives in the diagram a horizontal line at a definite height above the V_a axis.

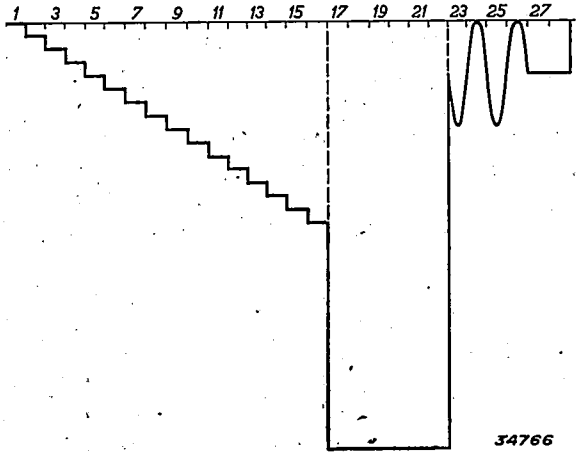

Fig. 4. The variation of the grid bias of the output valve under examination during one revolution of the rotating switch (S_1 in fig. 3).

The remaining two contacts *27* and *28* are at a negative voltage of a given magnitude, —6 volts for instance. The I_a-V_a curve with the parameter $V_g = -6$ volts is traced *via* these contacts. By regulating the potentiometer current and thus the voltage on the contacts *1* to *16*, one of the

15 I_a-V_a curves can be made to coincide with the established curve for $V_g = -6$ volts, and the parameter value for all the other curves is thus also known.

It is, however, seldom necessary, and with regard to clarity, it is sometimes even undesirable to record 15 I_a-V_a curves of the diagram. In that case the stepped voltage in fig. 4 is made so steep by increasing the potentiometer current, that on part of the contacts *1* to *16* the voltage is high enough to completely suppress the anode current of the output valve. The valve then has a longer resting period.

The comparison of two output valves

In addition to the rotating switch S_1 and the auxiliary switch S_2 there is a rotating contact S_3 which rotates at one half the speed of the first switch (fig. 3 and *fig. 5*). By means of this contact the grid bias according to fig. 4 may be applied alternately to two output valves. On the screen of the cathode ray tube the I_a-V_a diagrams of first one and then the other valve are drawn alternately, and since this takes place for each valve about 8 to 12 times per second, the two diagrams appear simultaneously on the screen. This makes it easy to detect quickly small differences between two valves of the same type. In order to be able to distinguish the two sets of curves from each other, the current of the cathode ray is diminished slightly with the help of the contact S_4 during the time when one of the valves is in circuit, so that the set of curves for this valve appears on the screen with a lower light intensity.

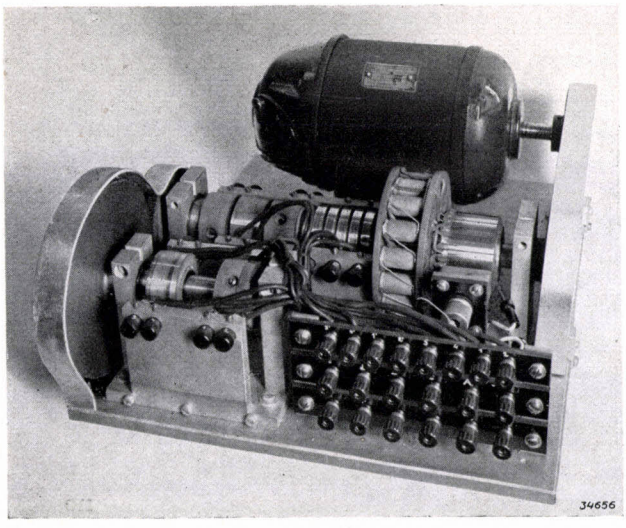

Fig. 5. The combination of rotating switches (S_1 to S_4 in fig. 3). For structural reasons, the switch arm of S_1 (a brush) is stationary while the 28 contacts (lamellae of a collector, middle axis on the right) rotate beneath it. The 15 resistances of the potentiometer P turn with the collector, the necessary voltages are applied *via* five slip rings. The auxiliary switch S_2, also for practical reasons, is divided into three contact makers (middle axis, left). The front axis turns at half speed and moves to two switches S_3 and S_4.

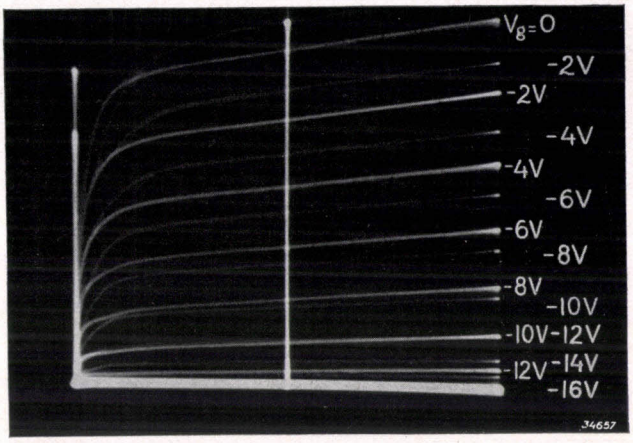

Fig. 6. Photograph of the I_a-V_a diagrams of two valves taken at the same time. One diagram is traced with lower intensity for the sake of distincion.

Fig. 6 gives an example of such an application of the apparatus. One valve (curves with lower intensity) has a smaller slope and a higher maximum anode current at $V_g = 0$ (highest curve). Furthermore the I_a-V_a curves of this valve do not run as close to the I_a axis as those of the other curve, a fact which has an unfavourable effect on the distortion at high values of the grid excitation current. Without going more deeply into this matter it may be noted that these deviations are caused by the fact that the cathode of this valve was not accurately centred with respect to the control grid.

Tracing the load line

When the I_a-V_a diagram has been photographed with a camera set up in front of the fluorescent screen, the load line may also be recorded on the same negative. For this purpose the output valve is first brought into the correct operating conditions, *i.e.* by means of suitable D.C. voltages on grid and anode the operating point is arrived at, and the loading impedance is put into the anode circuit *via* a transformer. If the anode current is now projected on the screen as a function of the anode voltage once more, the load line is obtained. There is however still a complication: without special precautions the load line is not in the correct position in the diagram. Ordinary amplifiers, such for example as those built into cathode ray oscillographs, do not pass D.C. voltages. When a voltage, whose mean value is not equal to zero, and which therefore has a certain D.C. component, is applied to the cathode ray tube, the image on the screen

always adjusts itself so that this average value of the voltage lies at the centre of the screen. When such amplifiers are used, therefore, the I_a-V_a diagram is projected on the screen in such a way that the centre of the screen is the point of greatest density of all the values of voltage and current occurring. The same is true in the case of the load line. Actually, however, the centre of the load line must coincide with the operating point of the diagram, which means that amplifiers used for this purpose must not suppress the D.C. voltage component.

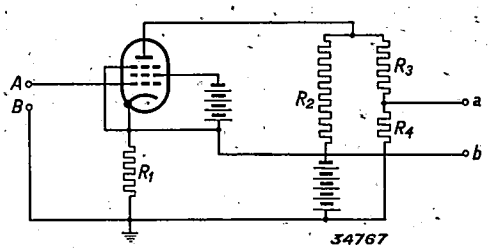

Fig. 7. First stage of the D.C. push-pull amplifiers for the deflection voltages. By giving the resistances R_1-R_4 suitable dimensions, upon application of an A.C. voltage to AB, the potential at a is made to increase by the same amount as that at b falls. The D.C. voltage potential at both points is adjusted to the same value by regulation of the anode direct current.

In order to obtain an accurately focussed image on the screen of the cathode ray tube, the potential in the middle of each set of deflection plates must remain constant (the focussing of the electron beam depends upon this). This means that the voltages must be applied to the deflection plates in a push-pull connection. One thus arrives at the somewhat unusual requirements of D.C. push-pull amplifiers.

Fig. 7 shows diagrammatically how the first stage of these amplifiers is arranged. The value of the resistance is for example the following: $R_3 = 18\,R_1$, $R_4 = 2\,R_1$, $R_2 = R_3 + R_4 = 20\,R_1$. If an A.C. voltage is applied to the input side AB, an A.C. voltage occurs over $R_3 + R_4$ which is ten times as great as that on R_1. The A.C. voltage over R_4 is thus equal to that over R_1, but in opposite phase. Since the potential of a at every moment rises as much as that of b falls, the tension between a and b is the desired push-pull voltage, provided a and b have the same D.C. voltage potential. This may be realized by regulation of the anode direct current, for instance by means of an adjustable resistance in series with the cathode, or by a suitable adjustment of the screen grid voltage. The further amplification of the symmetrical halves of the push-pull voltage is carried out in the manner usual for D.C. amplifiers. A diagram of the complete circuit is given in *fig. 8*. The points a and b correspond to the points a and b in fig. 7. It may be seen that in the practical application no special battery has been used for the screen grid. In addition to the anode current the screen grid current now also flows through the cathode resistance. Therefore the ratios between the resistances R_1 to R_4 (fig. 7) are slightly altered.

Fig. 9 is a photograph of the whole apparatus.

Load lines for different cases

In the simplest case in which the loading of the output valve consists of a pure resistance, the load line is a straight line through the operating point, as was indicated in fig. 1. *Fig. 10* is a photograph of such a case. The loading resistance in this case was equal to the so-called optimum resistance with which the output valve delivers the maximum power at a definite distortion (10% in this case). For output pentodes the optimum value is usually equal to the quotient of anode D.C. voltage and current. In that case the amplitudes of the anode A.C. voltage and current can simultaneously reach their maximum values, which are approximately equal to the anode D.C. voltage and current, respectively.

In practical cases the load on an output valve usually consists of one or more loud speakers. The

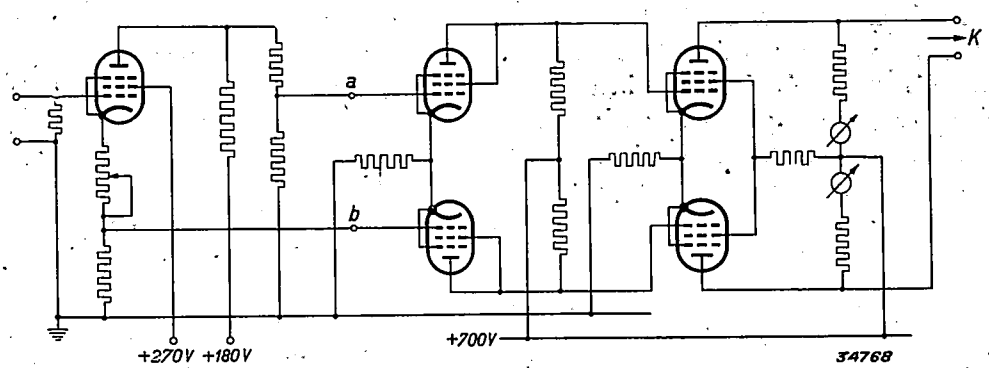

Fig. 8. Diagram of the complete circuit of the D.C. push-pull amplifiers a and b correspond to the points a and b in fig. 4.

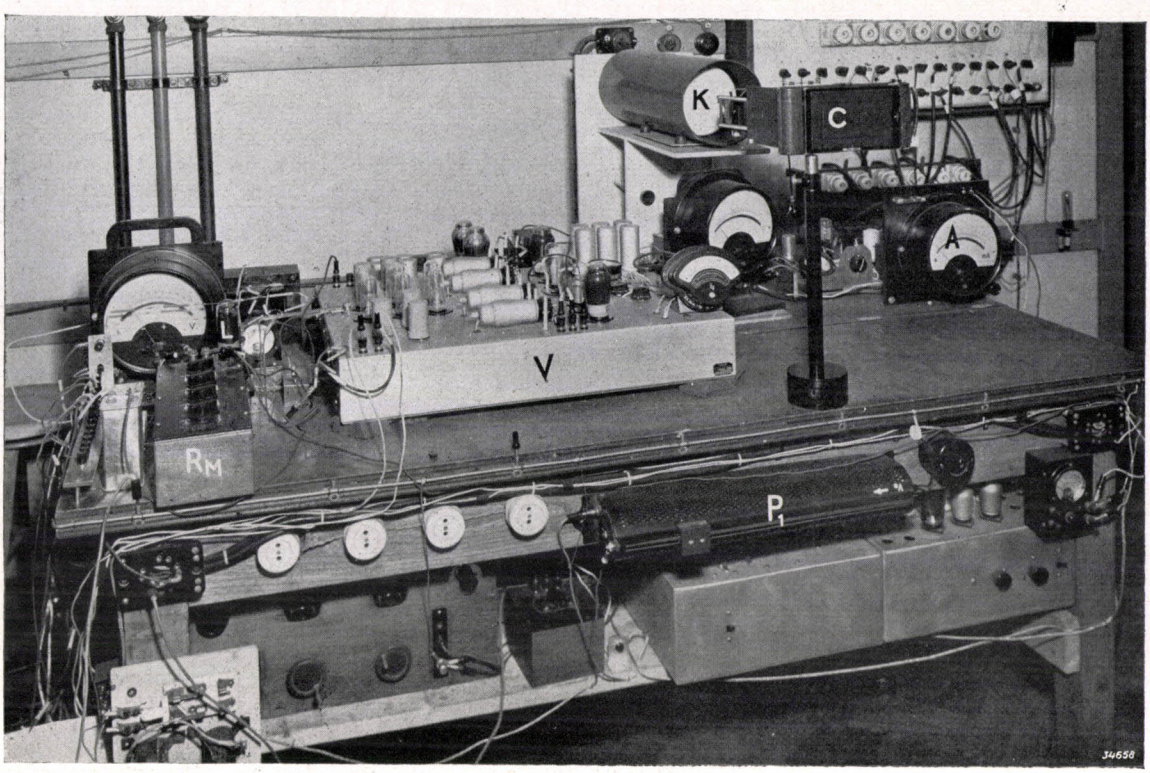

Fig. 9. View of the complete installation. L is the output valve under investigation, R_M the measuring resistance for the anode current, V the two amplifiers for the deflection voltages, K the cathode ray tube, C the camera set up in front of the screen. On the meter A the calibration current can be read off which is sent through the measuring resistance R_M during the resting period of the output valve (contacts *19-20* in fig. 4). With the potentiometer P_1, the steepness of the grid bias stepwise variation is regulated.

impedance of these is not a pure resistance but is inductive for a large part of the frequency range, due to the self-induction of the loud-speaker coil. The variation of the absolute value and the phase angle of the impedance of an ordinary loud speaker of good quality with appropriate transformer is represented in *fig. 11*. As a measure of the magnitude of the impedance the value at 1 000 c/sec is generally taken. In our case this amounts to about 7 000 ohms, which corresponds to the optimum resistance for the 9 watt pentode EL_3. The phase angle at the frequency mentioned is about 45°.

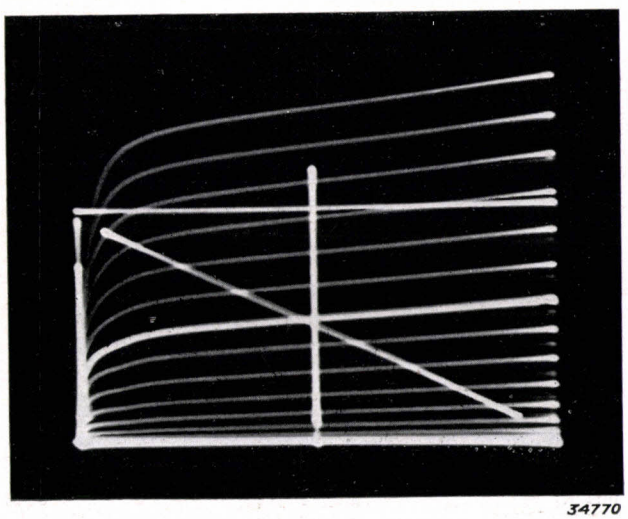

Fig. 10. Load line for the case in which the output valve is loaded with a pure resistance. The resistance here has the optimum value: the operating point lies in the middle of the section which is cut off on the straight load lines by the axes.

As a result of the phase shift between anode A.C. voltage and current a straight line is in general not obtained in the I_a-V_a diagram of the output valve. With a grid A.C. voltage of given frequency and amplitude, a more or less elliptical load line is obtained around the operating point. In *fig. 12* a number of such ellipses are shown which are obtained at different amplitudes of the grid A.C. voltage. If the grid A.C. voltage contains different frequencies more complicated figures occur. Examples are shown in *figs. 13* and *14* in which two frequencies, having the ratios 1 : 4 and 1 : 15, respectively, were applied to the grid, and in *fig. 15* in which three frequencies were combined. Finally, in *fig. 16* the image is given which is obtained when the output valve, loaded with a loud speaker, is allowed to amplify music for some time. One can no longer speak of a load line, but of a load field which occupies a more or less extensive portion of the I_a-V_a diagram.

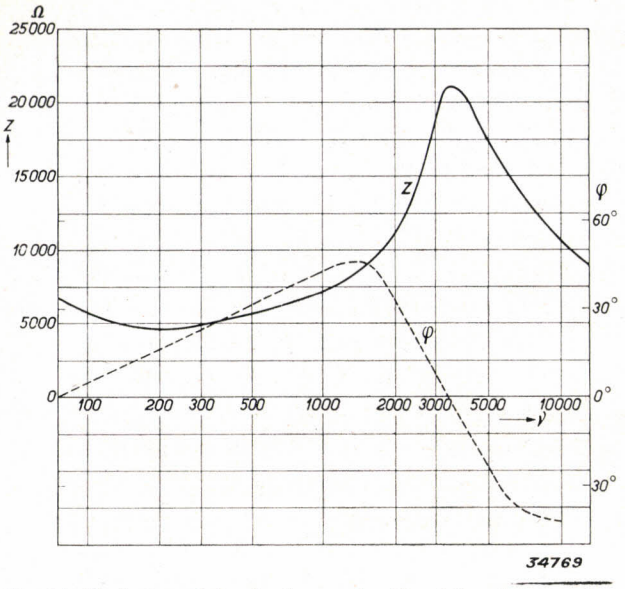

Fig. 11. Variation of the absolute value Z and the phase angle φ of the impedance of a normal loud speaker of good quality as a function of the frequency ν in c/sec. In this measurement a condenser of 2 000 μF was connected in parallel with the primary winding of the loud-speaker transformer, as is the case in many radio receivers. At 1 000 c/sec, $Z = 7\,000$ ohms. At lower frequencies Z changes only slightly: the minimum lies at 200 c/sec and amounts to about 5 000 ohms. At higher frequencies Z first increases sharply to about 21 000 ohms at 3 000 c/sec, it then decreases again due to the influence of the condenser. Cheaper types of loud speaker show in general a greater variation of Z and φ with the frequency.

The form of the I_a-V_a diagram

After an idea has been obtained in this way of the size of the region used in the I_a-V_a diagram, the requirements can be more precisely defined which the I_a-V_a diagram must satisfy in order to obtain as little distortion as possible in the reproduction and as large an output as possible.

Since the anode A.C. voltage and with it the output is limited by the crowding of the I_a-V_a curves near the vertical axis, it is desirable that the curves should run as closely as possible along the vertical axis at low anode voltages or in other words that in this region the anode current should increase very rapidly with the anode voltage. By the introduction of the screen grid it was possible to satisfy this requirement, without being compelled to use positive grid voltages, involving a consumption of energy by the grid as in triodes. At the same time, however, in the tetrode thus formed the phenomenon occurs that secondary electrons, formed at the anode, may pass to the screen grid, which causes a kink in the I_a-V_a curve (*fig. 17a*). In order to avoid these kinks which are accompanied by great distortion, a third grid (suppressor grid) is introduced, which is at cathode potential, and which suppresses the secondary emission from the anode to the screen grid. In the older types of pentodes, however, this sup-

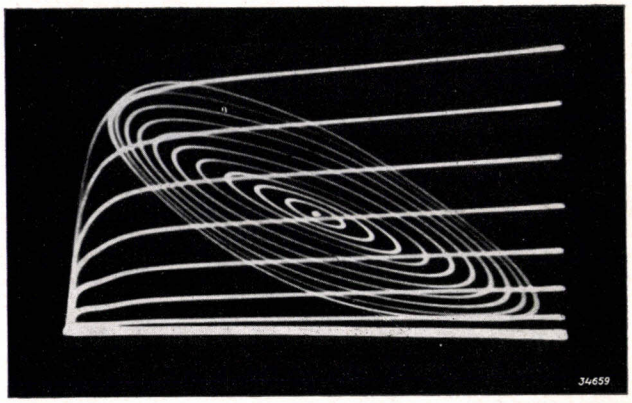

Fig. 12. With inductive loading of the output valve (connection to loud speakers) the load line becomes a more or less distorted ellipse around the operating point when the grid excitation voltage is sinusoidal. In this recording the amplitude of the grid excitation voltage was varied in steps with the frequency constant.

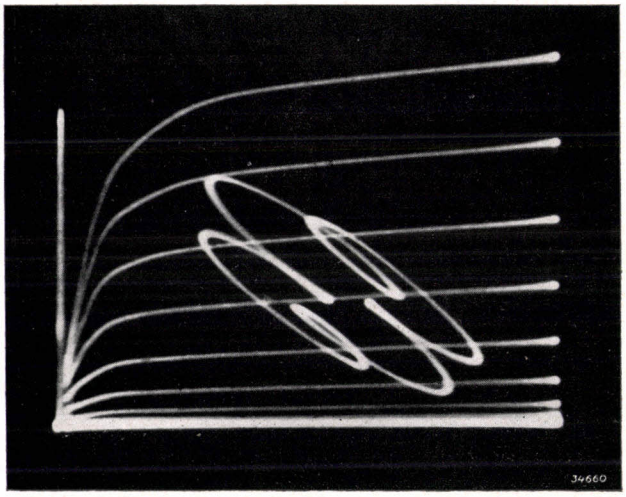

Fig. 13. Two A.C. voltages with a frequency ratio of 1 : 4 are applied to the grid of the inductively loaded output valve.

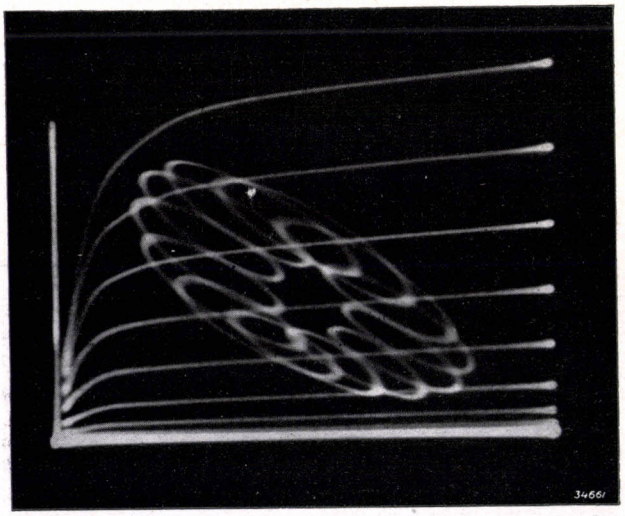

Fig. 14. Like fig. 13, but with a frequency ratio of 1 : 15.

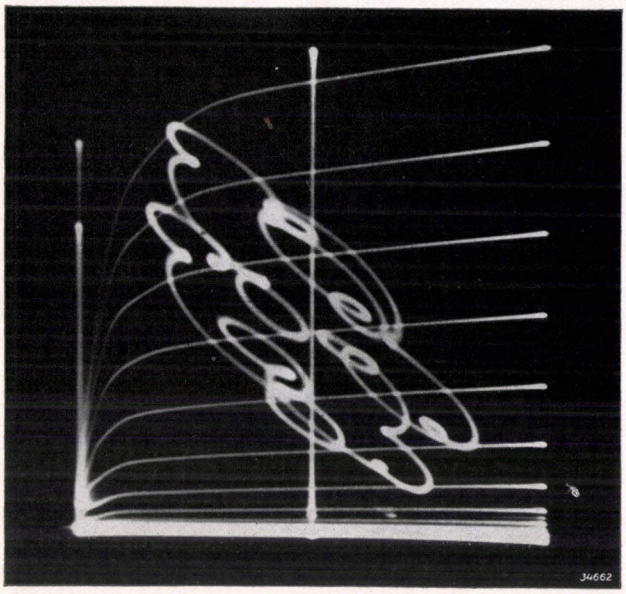

Fig. 15. Three frequencies are supplied to the grid.

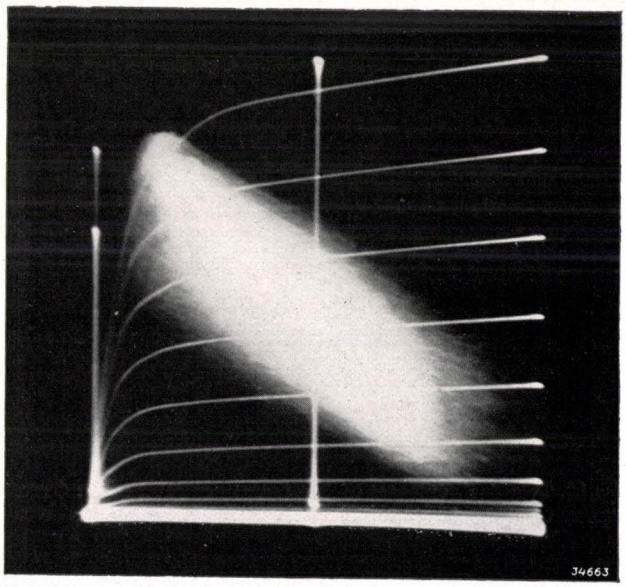

Fig. 16. The A.C. voltage of music is applied for some time to the grid of the output valve. A certain "load field" is now covered in the I_a-V_a diagram.

pression was often so thorough that at low anode voltage part of the primary electrons emitted by the cathode were also forced to reverse their direction in front of the third grid. These electrons were then lost for the anode current, and the result was that the anode current increased less rapidly with the anode voltage.

By a correct choice of position and dimensions of the suppressor grid the decrease in power output which hereby occurs can be kept very small. In the work involved in this development the method described in this article for the recording of I_a-V_a diagrams has proved very useful. A change in position and dimensions of the suppressor grid is to a certain extent equivalent to a definite change in its potential. By applying different negative or positive voltages to the suppressor grid — which in contrast to the ordinary construction must have leads to the outside — and by inspecting the I_a-V_a diagram in each case, it is possible to discover the voltage at which the most favourable form of the diagram is obtained. *Fig. 17* shows three records from such an investigation. In *a* the kinks are very pronounced, in *b* they have entirely disappeared, but at the same time the anode current increases much more slowly with the anode voltage, in *c* the correct compromise has been found in which the curves mount as steeply as possible while the kinks are only present in a region of the diagram which, according to the investigation of the load field (see above), is not used in practical cases.

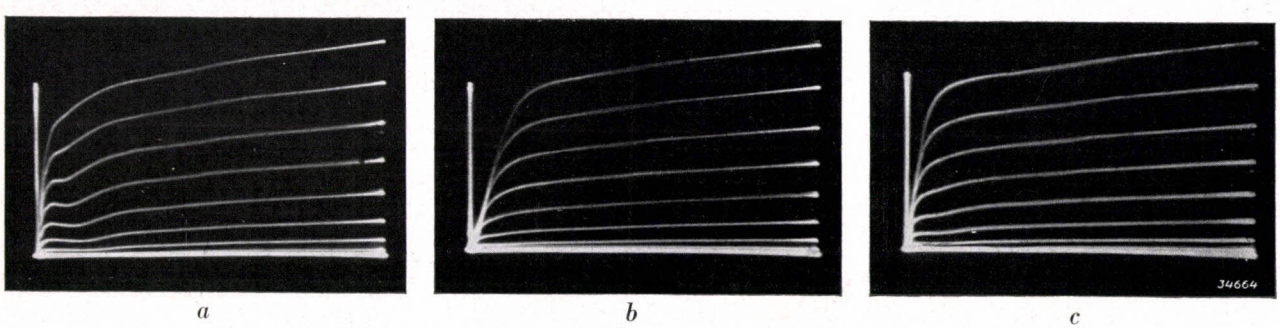

a *b* *c*

Fig. 17. The I_a-V_a diagram of a pentode at different potentials of the suppressor grid.
a) The suppressor grid is too strongly positive, the kinks in the characteristics due to secondary emission from the anode are not sufficiently suppressed.
b) The suppressor grid is too strongly negative. The kinks in the characteristic have disappeared, but at low anode voltages the curves rise less steeply.
c) The suppressor grid has the optimum potential. This value of the potential gives an indication of the sense in which position and dimensions of the grid must be changed in order to obtain the same result with this grid at cathode potential.

X-RAY APPARATUS FOR THE MACROSCOPIC EXAMINATION OF MATERIALS

by J. E. de GRAAF.

621.386.1 : 539.26

In the construction of X-ray apparatus to be used for the macroscopic examination of materials several problems occur which are connected with the use of high voltages and currents, such as the problem of the insulation of the apparatus and cables, and the dimensions of the focus of the X-ray tube. These problems are discussed in this article.

Introduction

Special X-ray apparatus have been constructed by Philips for the macroscopic examination of materials, a subject on which a series of articles has appeared in this periodical [1]). These apparatus are simple in operation and are not dangerous for the operator. In this article we shall discuss the factors which were taken into account in the construction of these apparatus.

[1]) Philips techn. Rev. **2**, 314, 350, 377, 1937 en **3**, 92, 186, 1938.

The apparatus are intended for use in making X-ray photographs of a large number of articles which may have large dimensions. The economic factor of time-saving is of great importance. According as the examination is transferred more and more from the laboratory to the workshop, this consideration becomes steadily more significant. The time necessary to take a photograph may be divided into two parts, namely:

1) the exposure time proper, and

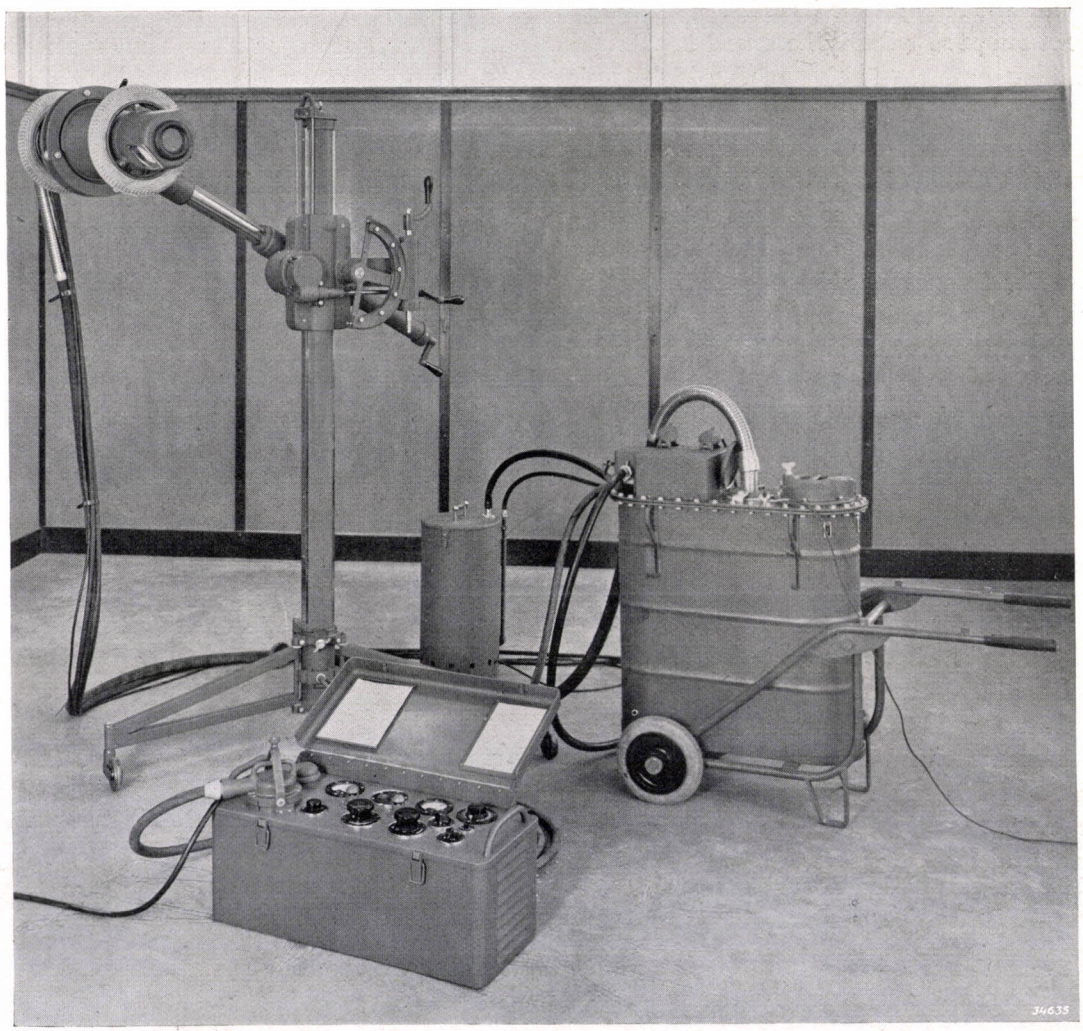

Fig. 1. The X-ray apparatus M 150 with earthed anode which is intended for a maximum voltage of 150 kV. By dividing it into components of small dimensions and light weight it has been made easily transportable. The connections are given in fig. 2.

2) the time necessary for moving about and adjusting the X-ray apparatus.

Consideration of the second item shows that it is desirable that the apparatus should be easy to handle. It should therefore be made as small and light as possible.

As for the necessity of keeping the exposure time itself short, this makes it necessary to use high tensions, even as high as several hundred kilovolts, especially in the examination of heavy pieces of work. With increasing voltage the exposure time needed for a given density on the film decreases very rapidly [2]). The problem is therefore reduced to that of obtaining as high voltages as possible with an apparatus which is easy to handle.

Since high-tension transformers and insulators are usually large and heavy, the X-ray apparatus for the purpose in view must immediately be divided into a number of components which can be transported separately, and each of which can easily be handled. The X-ray tube itself is suspended in a convenient support, as may be seen in *fig. 1*. The most difficult problem is that of the high-tension generator which always remains a heavy unit.

By means of special connections it is possible to obtain on the X-ray tube twice the voltage of the high-tension transformer, so that a much smaller transformer may be used to obtain a given voltage. In *fig. 2* a circuit is given which has previously been discussed in this periodical [3]). It employs for this purpose a rectifier valve V which is connected in parallel with the X-ray tube R. During the phase in which the rectifier valve has only a small resistance the buffer condenser C is charged to the peak voltage of the transformer T, since then practically no voltage acts on rectifier valve and X-ray tube. During the opposite phase this voltage on the condenser acts in series with the voltage of the transformer, so that about double the peak voltage of the transformer acts between the terminals of X-ray tube and rectifier valve. The voltage on the X-ray tube is always equal to the sum of the A.C. voltage on the transformer and a D.C. voltage equal to the peak value of this transformer voltage. A voltage equal to twice the transformer voltage thus occurs on the tube in the circuit according to fig. 2 only during short moments, so that the use of this circuit by no means gives the same X-radiation for a given power as would be obtained upon the use of a transformer with twice the peak voltage.

In order to obtain a practically constant voltage on the X-ray tube, which shall be approximately equal to twice the transformer voltage, use may be made of the connections shown in *fig. 3*, in which two condensers and two rectifier valves are used.

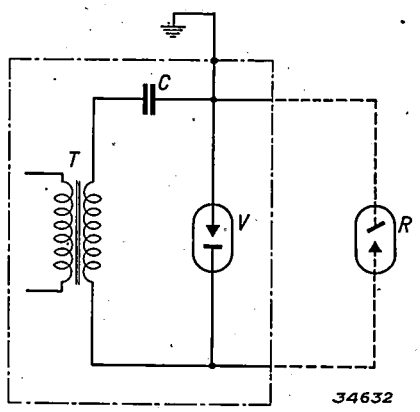

Fig. 2. Diagram of the connections, which supply to the X-ray tube R a pulsating voltage whose peak value is about double the peak voltage of the transformer T. C buffer condenser. V rectifier valve.

The condenser C_1 and the rectifier valve V_1 have exactly the same functions as in the circuit of fig. 2. At the moments when V_1 carries twice the peak voltage of the transformer, the rectifier valve V_2 connected counter to V_1 has a low resistance, so that the condenser C_2 can be quickly charged through V_2 to twice the peak voltage. Since the rectifier valves are connected counter to each other, condenser C_2 can only be discharged over the X-ray tube R, which has a resistance such that this discharge takes place only slowly, and the X-ray tube in this connection thus receives a practically constant voltage which is only slightly less than twice the transformer voltage.

As we shall see later, the apparatus are constructed according to the connections of fig. 2, and may be completed to give those of fig. 3 by means of a suitable auxiliary apparatus, which contains the condenser C_2 and the rectifier valve V_2.

As already mentioned, the density obtained on the

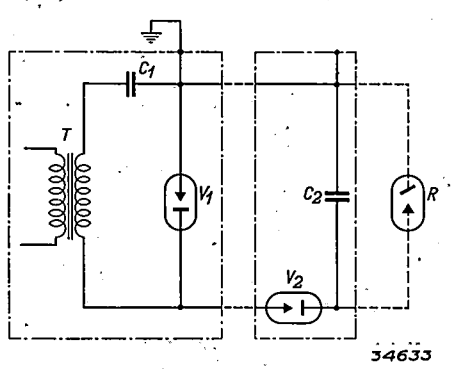

Fig. 3. Diagram of connections for obtaining a fairly constant voltage. C_1 and V_1 correspond to C en V in fig. 2. Another rectifier V_2 and a condenser C_2 have been added.

[2]) *Cf.*: fig. 5 in Philips techn. Rev. **2**, 314, 1937.

[3]) Philips techn. Rev. **1**, 6, 1936.

photographic plate increases very rapidly with the voltage on the tube. Since with the circuit according to fig. 3, the voltage is never far below its maximum value, with the same average tube current, the same density may be obtained with a much shorter exposure time than is the case when the circuit of fig. 2 is used. *Fig. 4* shows how the X-radiation acting on the photographic film depends upon the thickness of the article examined. The X-radiation is expressed in terms of röntgen [4]) per minute per mA, measured at a distance of 1 m from the focus. The thickness is indicated by the equivalent thickness of copper in mm. It may be seen in the figure that at great copper thickness the circuit of fig. 3 is about 3 times as efficient as that of fig. 2 in the case of our apparatus.

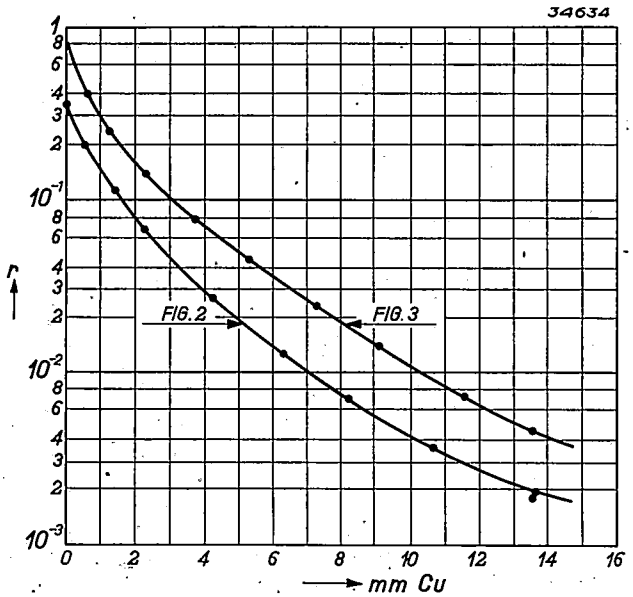

Fig. 4. For apparatus with connections according to fig. 2 and fig. 3 respectively, the amount of X-radiation acting on the photographic plate has been plotted. This is expressed in röntgen [4]) per minute per mA, and measured at a distance of 1 m from the focus through different thicknesses of the object examined, expressed in mm copper thickness. With large filter thicknesses the advantage of the circuit of fig. 3 over that of fig. 2 approaches a factor 3.

The insulation

In order to save weight in the construction of X-ray apparatus for testing materials, it is important to keep the relatively great weight of the insulation small. It would therefore seem advisable to use air as insulating medium as far as possible. Due, however, to the relatively low breakdown voltage of air such large dimensions would have to be used that the apparatus would become unwieldy, and unsuitable for use in limited spaces.

Since solid insulation materials have much higher breakdown voltages, much more compact designs can be arrived at with their use. Great care must, however, be taken that no air bubbles occur, either in the solid insulation itself or between the insulation and the parts insulated. The dielectric constant of air is smaller than that of all other dielectrics, so that the electric field in such air bubbles is greater than in the surrounding insulator. The danger thus arises that the gas in the bubbles will be ionized causing a discharge, corrosion and finally breakdown of the solid insulator [5]).

When it is only a question of simple constructions of porcelain, pertinax or "Philite", or, for example, of the rubber insulation of flexible high-tension connections, the occurrence of air bubbles can be avoided. With more complicated constructions, however, it is better to use a liquid insulation material, mineral oil for example. At the same time we insulate with this material the different parts of the generator not only with respect to each other but also with respect to the metal covering, which completely surrounds every part of a modern X-ray apparatus, and which is earthed in order to make it impossible for the operator to come into contact with any part under tension.

When mineral oil is used as insulation material it is possible that dust particles floating in it collect at spots with a high field strength and thus give rise to breakdown. Especially is this true if the dust particles contain moisture. Therefore care is taken by careful purification strictly to limit the number of dust particles and accompanying moisture, while care must also be taken that no impurities can enter the oil while it is in use. In this connection in our apparatus the space containing oil for the rectifiers, which must be accessible to the operator, is separated from that for the transformers and condensers. Furthermore by careful impregnation in a vacuum the air bubbles are driven out of the insulation.

In determining the required thickness of the layers of insulation, account must not only be taken of the difference of potential applied, but also of the nature of the surface of the conductors, which is an important factor. Irregularities, sharp angles and edges on a piece of metal to be insulated may cause unusually high fields in their neighbourhood. A simple example of an irregularity is the case of a hemisphere situated on one of two parallel planes and having a radius which is small compared

[4]) An object receives an X-ray dosage of 1 r when 100 ergs would be absorbed in 1 cc of water at that spot as a result of the radiation.

[5]) *Cf.* the more elaborate treatment of this problem in the article, Pressure condensers, Philips techn. Rev. 4 254, 1939.

with the distance between the planes. Such a hemisphere increases the field locally to about three times the field which would exist between the two parallel plates in the absence of the hemisphere. Care is therefore taken in the construction of the apparatus to give the conductors smooth flowing surfaces.

If the voltages are not too high, it is advisable to earth the anode of the X-ray tube, and supply the cathode by means of a high-tension cable. The focus lies at the earthed anode end of the tube, so that it is possible to introduce it relatively easily into small spaces. When for example it is necessary to project X-rays along the joining surface of two plates welded together at an angle, in order to discover faults in the joint, this can easily be done with a tube which has its focus at the end of the tube. An additional advantage of the earthed anode is that the heat developed at the focus, which amounts to about 2 kW with these tubes, can easily be dissipated by cooling water taken directly from the water mains.

A model of such a tube with earthed anode is shown in fig. 1. This tube can be used with voltages up to 150 kV. The connections of the apparatus are according to fig. 2. As already mentioned, by placing an auxiliary apparatus, in which condenser C_2 and rectifier valve V_2 are contained, between the tube and the supply apparatus of fig. 1, a unit is obtained with connections according to fig. 3, which can be moved about without much difficulty.

In the construction of such moveable apparatus it becomes difficult to insulate voltages higher than 150 kV with respect to earth. For such cases therefore a symmetrical construction has been employed as shown in *fig. 5* for a maximum tube voltage of 300 kV. In this case the focus lies at the middle of the tube; both cathode and anode are given opposite voltages of 150 kV with respect to earth by means of a high-tension cable. Since the focus is here not earthed, the anode is cooled by means of insulation oil which circulates through the anode and a cooler.

Since the voltages of cathode and anode are equal and opposite with respect to earth in a symmetrical tube, the electrical supply takes place with the help of two apparatus connected according to fig. 2, one of which is connected to the anode, while the other by reversing the rectifier supplies the reversed voltage to the cathode. Moreover, by adding two of the auxiliary apparatus mentioned above, one obtains the circuit of fig. 3 doubled, which gives a constant voltage between anode and cathode.

The focus

If we attempt to shorten the exposure time by using higher voltages, as was explained in the foregoing, the X-rays obtained are harder. As has previously been explained in this periodical [6]) this

[6]) *Cf.*: fig. 6 in Philips techn. Rev. **2** 314, 1937.

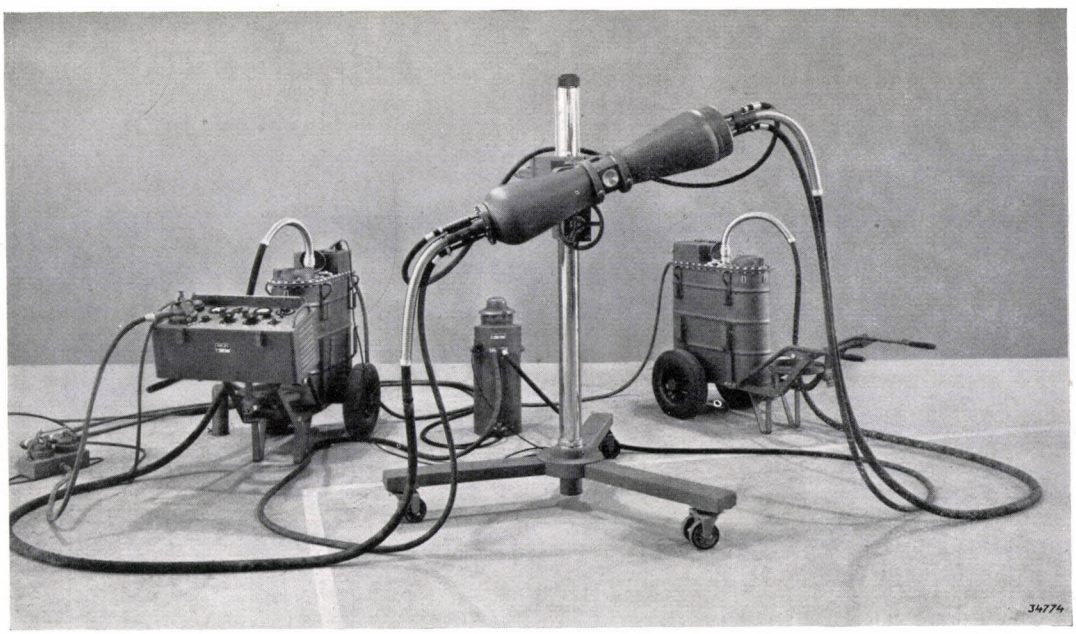

Fig. 5. The X-ray apparatus M 300 with symmetrical X-ray tube, supplied by two high-tension cables. It is designed for a maximum voltage of 300 kV. The generator is a symmetrical combination of two generators of the type M 150.

meets with the objection that the X-ray photographs will exhibit less contrast than when they are made with softer X-rays. In addition to raising the voltage, therefore, some other possibilities of increasing the X-ray intensity is desirable, such for example as the application of a high average tube current.

A high current can be obtained either by procuring a high current density or a large cross section area of the current. The first of these methods means a high specific loading of the focus, and it has already been explained in this periodical [7]) that this cannot be carried too far. The heat produced at the anode cannot otherwise be dissipated sufficiently well. The temperature of the anode might become so high that the anode would become rough due to evaporation, which could cause the efficiency of the tube to decrease too rapidly during operation. In the article cited it is also shown how it is possible to obtain the greatest permissible specific loading of the focus.

The second method of increasing the tube current is to increase the size of the focus. This method also has its limits since the lack of sharpness of the shadow image of the X-rays is proportional to the dimensions of the focus. If this lack of sharpness is not greater than the dimensions of the faults which one is desirous of discovering in the structure examined it is permissible. Depending on the nature of the object in view, therefore, there are corresponding optimum dimensions of the focus, which in turn correspond to a definite tube current.

For many uses of the tube shown in fig. 1 it is best to use a current source about 5 mm square with which a loading of 20 mA at 150 kV is possible with connections according to fig. 2. If it is necessary to introduce the focus into a small space, as is the case for instance in the examination of welds in steam boilers and pipes, the tube shown in *fig. 6* is very useful. In this tube the anode is situated at the end of a rodlike projection which is easily inserted into small spaces. Because of the small distance between focus and object in this case the dimensions of the focus must not be too large. In the tube shown in fig. 6 the focus is 2 × 3 mm.

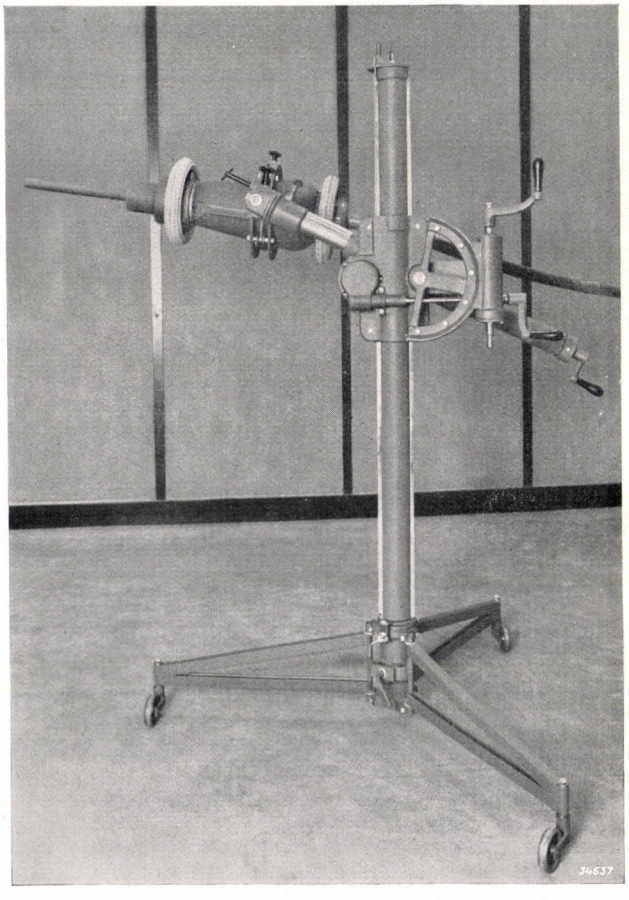

Fig. 6. X-ray tube with earthed rod-shaped anode designed for a maximum voltage of 150 kV. The focus lies at one end of the long projection.

The desired dimensions of the focus are in general obtained by applying a cap of a certain shape around the cathode, as may be seen in the construction diagram *fig. 7* of the tube of fig. 1. The cap *D* has such a shape that the electrons emitted by the cathode *K* are directed in a beam on to the anode *A*. Depending on the shape of the cap a larger or small-

[7]) Philips techn. Rev. **3**, 259. 1938.

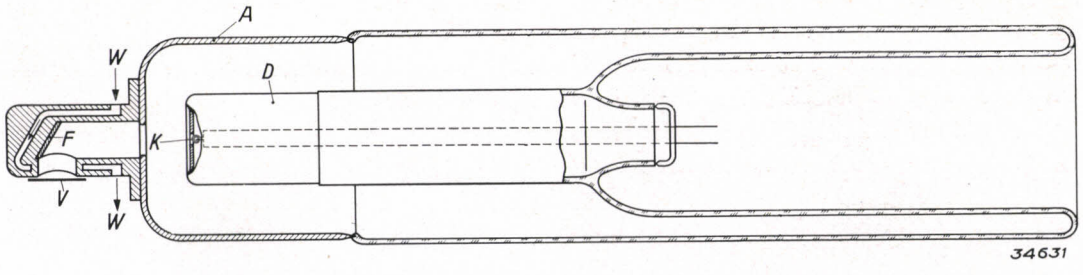

Fig. 7. Diagram of the structure of the X-ray tube belonging to the apparatus M 150 shown in fig. 1. The anode *A* is earthed and water-cooled. *F* focus, *K* cathode, *D* cap around cathode, *V* window and *W* cooling water.

er electron optical image of the cathode is formed on the anode. As may be seen in fig. 7 this focus F which emits the X-rays is situated in a short projection of the chrome-iron anode cylinder A to which the glass is fused which serves as insulation between anode and cathode. In the tube with projecting anode shown in fig. 6, however, the focus is too far away from the cathode for a cap D to be used to form a beam of electrons which is satisfactorily parallel. The beam in this case must be made to converge by means of a magnetic field [8]), for which purpose a magnet coil is applied around the anode cylinder.

[8]) *Cf.* Philips techn. Rev. 4, 153, 1939. In the tube for 1 MV there discussed a permanent magnet was used for focussing.

THE TRANSPORT OF SOUND FILM IN APPARATUS FOR RECORDING AND REPRODUCTION

by J. J. C. HARDENBERG.

778.533.1: 681.84.081

In order to avoid disturbing distortion in the reproduction of sound film, the film must be moved very uniformly past the spot where recording and scanning of the sound track takes place. In the combination of picture with sound track, in order to obtain a stationary picture the number of pictures per revolution of the driving mechanism is fixed, and therefore the velocity of the film is subjected to variations due to the shrinkage of the film material. The difficulties hereby ensuing for the transport of the film are discussed in this article, as well as several methods and types of constructions by which the problem is solved in modern machines for recording and reproducing sound film. In the Philips-Miller system of sound recording on the one hand more rigorous demands are made on the arrangement for film transport, and on the other hand for certain important applications the requirement of synchronization with the picture no longer holds, so that the construction may be considerably simplified. Several important structural details of the machines for the Philips-Miller system are described.

Sound recording involves the conversion of the temporal variations of the sound pressure into spatial variations of some physical quantity, such as the intensity or the width of an opacity along a band of film. In the reproduction, the spatial differences are reconverted into temporal differences. In order to ensure absolute similarity between the sound vibrations reproduced and those recorded the relation between "time" and "place on the band of film" must obviously be exactly the same in the recording and in the reproduction. In practice this means that high requirements must be made on the uniformity with which the film is transported in the machines for recording and reproduction, and on the stability (freedom from vibrations) of the spot where the recording or scanning of the sound track occurs. Every shortcoming in these respects is manifested as an undesired modulation and will make itself felt more or less audibly in the quality of the sound reproduced.

In satisfying the requirement mentioned certain difficulties occur which we shall discuss in the following. At the same time we shall describe several solutions to this main problem of sound film apparatus which have been proposed, and in particular the type of construction used in the machines for sound recording by the Philips-Miller system.

The sprocket roller

Sound film was originally developed as a supplement to the cinema film, and this is still its most important sphere of application. The transport of cinema film through the camera or projector always takes place by means of sprocket rollers, which catch in the perforations or sprocket-holes along both sides of the film. This method of transport makes it possible to draw the film past the projection window intermittently by means of the "Maltese cross" shutter — we shall confine ourselves to reproduction for the moment — and in this way give the audience the impression of a stationary picture. It is also possible, due to a so-called optical compensation, to draw the film past the film window at a uniform speed. Nevertheless the sprocket roller has persisted. The chief reason for this fact lies in the shrinking of the film which always occurs to some extent due to the drying out of the film

especially by the strong illumination in projection. The shortening due to shrinkage may amount to 0.5 per cent, and in extreme cases to 1 per cent. In spite of this change in length it is now required that the film shall move a distance exactly equal to the height of one frame each time the picture changes. If the change occurs a given number of times per revolution of the axis which drives the Maltese cross at a given velocity, then, because of the shrinkage, the same number of metres of film per second is not always transported. The same number of sprocket holes per second however is maintained. The sprocket roller now serves to determine this number of sprocket-holes transported, and in this way to ensure precise picture transport. If differences in the height of the frames have occurred due to shrinkage they are corrected whenever a sprocket engages a perforation. In *fig. 1* the manner

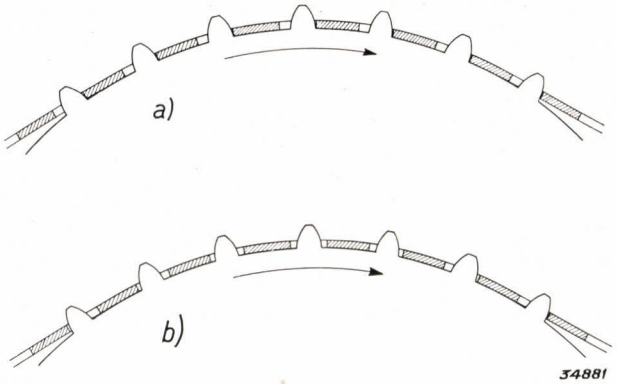

Fig. 1. a) If the distance between the film perforations corresponds to the thrust of the sprocket on the roller, the film rests against the flank of all the sprockets (10 for instance) which are engaged at the same time, and the transport of the film is taken over continuously by the sprockets which successively become engaged.
b) If the film is slightly shrunken, then, if we disregard the friction on the surface of the roller, it is only pulled along by the foremost sprocket, while the other engaged sprockets are loose in the perforations (the size of the perforations allows a play of about $^1/_2$ mm). At the moment when the foremost sprocket slides out of the perforation, the transport of the film has not yet been taken over by the following sprocket. The film thus decreases its speed relative to the roller for an instant until with a certain shock the following sprocket touches the edge of the perforation in which it previously stood free. This is repeated for each sprocket.

is shown in which this correction takes place. It may be seen that the film experiences a slight shock at each sprocket-hole. Since the film is normally projected with a speed of about 24 frames per second, and the height of a frame is equal to 4 sprocket-holes, the film undergoes about 96 shocks per second.

On the film intended for reproduction the sound track is added next to the pictures (*fig. 2*). If the film is more or less shrunk and if, after passing the projection window, it is drawn past the spot where the sound track is scanned by means of a sprocket

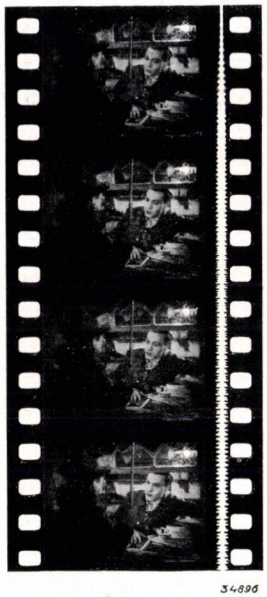

Fig. 2. Strip of film with pictures and sound track (recorded with amplitude modulation). The height of a frame corresponds to three sprocket-holes.

roller, the 96 discontinuities per second which occur in the film transport due to the corrective action of the sprocket roller become noticeable as so-called sprocket-hole modulation in the sound

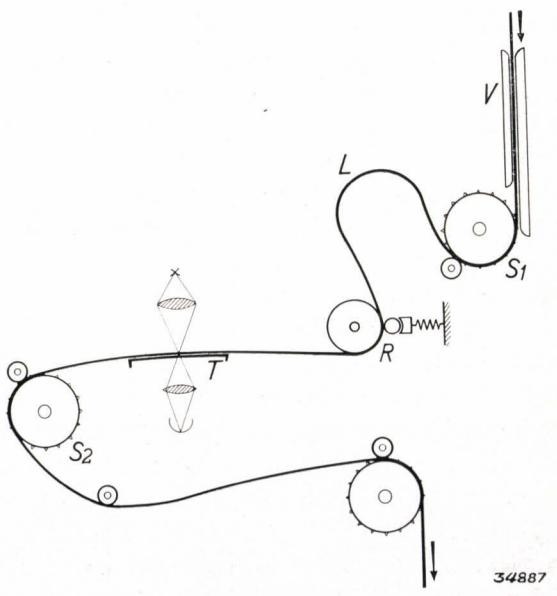

Fig. 3. After the film has been drawn intermittently by the sprocket roller S_1 on the shaft of the Maltese cross shutter past the projection window V, it is retarded by the rollers R (the loose loop L may periodically change its length unhindered upon change of picture). The sprocket roller S_2 then draws the stretched film through the gate T where the sound is scanned. Between V and T there is usually a length of film corresponding to about 19 frames. Picture and corresponding sound are thus relatively displaced by that amount on the film.

reproduction. In the initial stages of the development of sound film this was one of the most serious defects. The film was then always pulled by a sprocket roller S_2 in *fig. 3*, along a fixed gate where the sound was scanned, and it was retarded by the retarding rollers (R) in order to make sure that the film was firmly pressed into the gate. Due to the tension of the film between the gate and the sprocket roller pulling it, all the shocks were transmitted to the spot where the scanning took place. The reproduction of the frequencies between 2 000 and 6 000 c/sec were especially affected by the sprocket-hole modulation, since the combination tones occurring here give the impression of an unpleasant harshness.

A remedy was sought by damping the shocks of the sprockets by means of mechanical filters. Such a filter may for example consist of an elastic coupling between the sprocket roller and the axis driving it, or of a number of slack loops made in the film by stretching it around a series of guiding rollers between the sprocket roller and the spot where it is scanned. Fairly complex constructions are attained in this way and no decisive improvement is obtained.

The sound shaft

Considerable progress was made possible by the discovery of the fact, that as far as the sound is concerned it is not actually necessary to correct the variations in height of frame immediately, *i.e.* at every sprocket-hole. Care must only be taken that the length of film which passes the spot where the sound is scanned retains the same average value, over a period of a few seconds, as the length of the strip of film which passes the projection window, since otherwise either the film would break or become jammed. At the spot where the sound is scanned the film may be given a uniform velocity which only need correspond to the average length of film per picture in the course of several seconds, *i.e.* with inaudible "modulation frequency" [1]).

This idea is realized in the following way. At or very near the spot where the sound is scanned the film is laid over a smooth drum touching the surface over as great a length as possible (*fig. 4*). The drum is mounted on a shaft which rotates very uniformly, called the "sound shaft" or "tone shaft". The uniform velocity of the shaft is guaranteed by a fly-wheel. A braking mechanism or a pressure roller at the side where the film runs on to the drums provides high peripheral friction so that the film is coupled with the surface of the drum and no slipping takes place. The film thus has the desired uniform velocity at this point. It is obvious that the sound shaft must be perfectly centred in order that the circumference of the drum may have a constant velocity. An excentricity of the drum of 0.02 mm would be clearly audible in the sound.

As is clear from the above no definite number of revolutions may be forced upon the sound shaft, but it must be allowed to adapt its velocity of rotation to the length of film reeled off. This can be done in two ways.

a) By means of an adjustable mechanical drive. As regulator device a loopsetter roller may here be used which keeps the film slightly stretched between the sound axis and a sprocket roller further along which runs synchronously with the pictures on the film. When a change in picture height occurs the paths covered by the film on the sprocket roller and the sound shaft exhibit a difference, the loop of film between the two spots becomes longer or shorter, the loopsetter roller changes its position and thereby influences in one way or another the driving speed of the sound shaft.

b) The latest solution of the problem consists in allowing the sound shaft to be driven by the

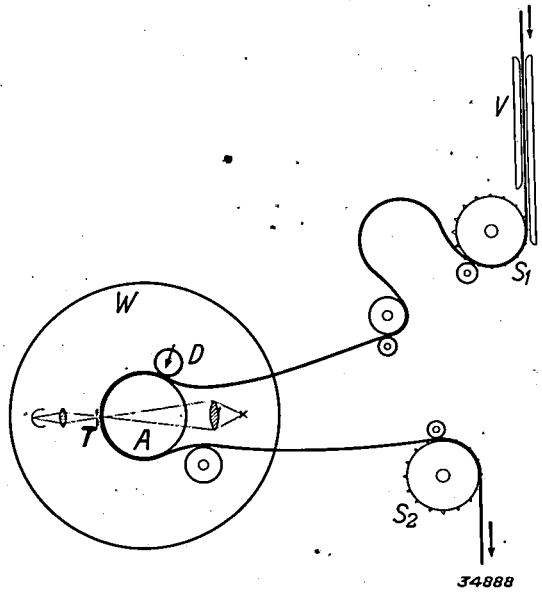

Fig. 4. The film is laid around the sound shaft A over a large angle. A rotates very constantly due to the action of the fly-wheel W. The pressure roller D, or some kind of braking arrangement, provides the necessary friction to prevent slip between sound shaft and film. The same symbols are used as in fig. 3.

[1]) Practically this average value varies so gradually, even with very irregular shrinkage of the film, that there are no noticeable deviations from synchronism between picture and sound.

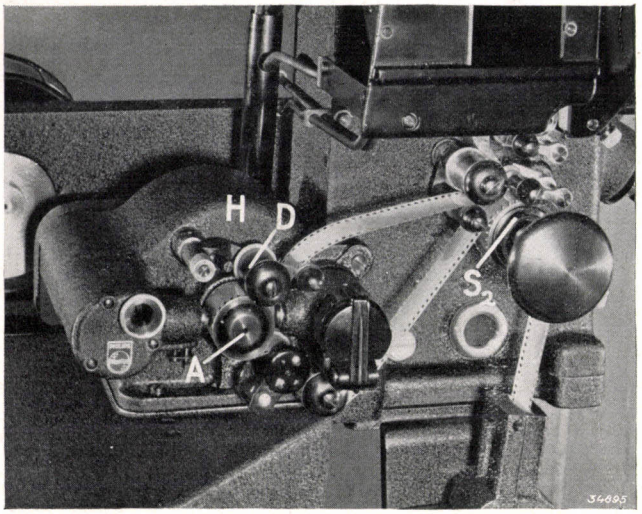

Fig. 5. Philips "sound head" type 3837 in combination with the projector FP 5. *A* is the sound shaft, *H* the housing of the fly-wheel, *D* the pressure roller, S_2 the sprocket roller which pulls the film through the sound head.

film itself. The film is fed to and reeled off from the sound shaft by sprocket rollers running synchronously with the pictures. The length of film reeled off is thus continually regulated by these rollers. The action of the freely running fly-wheel provides that variations in the film length per second cause gradual variations in the film speed on the sound shaft. It is however necessary that the coupling between the motion of the fly-wheel and the motion of the sprocket roller which pulls the film should be as loose as possible, *i.e.* that the strip of film between roller and sound shaft should be under as little tension as possible.

Of the above mentioned two possibilities of obtaining the necessary rolling friction a pressure roller or a braking arrangement, the first is to be preferred because it involves no extra tension on the film. In the new Philips "sound head" type 3837 (*fig. 5*) this method has therefore been used. The tension on the film is now determined practically only by the tension which the film must exert in order to overcome the frictional resistances which occur in the bearings of the sound shaft, the guiding rollers and the pressure roller. By the use of ball bearings it has been found possible in the case in question to reduce the frictional forces and thereby the pull on the film during reproduction to several tenths of a gram.

When reproduction is begun and the sound shaft must be set in motion by the film, the film must always exert a greater pulling force. Slipping hereby occurs during several seconds, either between sound shaft and film or between sound shaft and fly-wheel, if the latter is driven by the sound shaft *via* a friction coupling. The period before the operating state is reached depends upon the force which the film can transmit without danger of breaking, and on the energy which must be accumulated in the fly-wheel, *i.e.* at the moment of inertia of the latter.

Recording by the Philips-Miller system

In recording sound film the same construction may be used for the transport of the film as has been described above for the reproduction [2]). In general it is in this case even easier to keep the sprocket-hole modulation out of the sound, since one works with fresh film in which the distances between perforations are still relatively little changed by shrinkage, and with which therefore sprocket-hole shocks during transport occur to a much smaller extent.

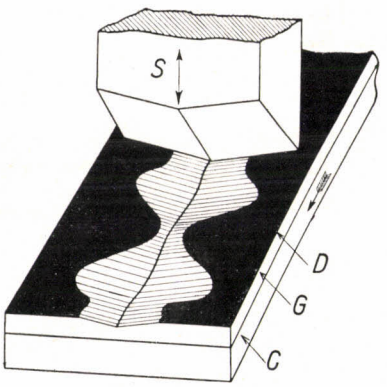

Fig. 6. The principle of sound recording by the Philips-Miller system. The "Philimil" film consists of the celluloid base *C* with the gelatin layer *G* and the very thin opaque covering layer *D*. The cutter *S* vibrating perpendicular to the film cuts a transparent sound track on the film which is moved in the direction of the arrow.

In sound recording by the Philips Miller system, however, a specific difficulty is encountered due to the unavoidable high tension on the strip of film. In order to explain this the principle of the Philips-Miller system must be briefly recalled [3]). The "Philimil" film on which the sound track is cut consists of a layer of gelatin deposited on a celluloid base and covered with a very thin black surface layer (*fig. 6*). A wedge-shaped cutter is

[2]) The sound track is usually recorded separately and then copied on the positive simultaneously with the pictures. Due to the requirement of synchronism between picture and sound however, this does not nullify the requirement that the number of perforations and not the length of film is fixed.

[3]) See also the articles: Philips techn. Rev. **1**, 107, 135, 211, 230, 1936.

moved up and down vertically over the moving film in the rhythm of the sound vibrations, and cuts a groove of varying width in the gelatin layer. By the cutting away of the thin covering layer over the groove thus produced, a transparent sound track is obtained on a black background, which can be scanned in the same way as a photographically recorded (amplitude-modulated) sound track.

The resistance experienced by the cutter in cutting the groove in the film depends on the width of the groove and amounts on an average to 1 kg. This is therefore also the force with which the film must be drawn through the machine. It is obvious that there would be very great danger of sprocket-hole modulation if the reaction against this force were sought in the pull of the sprockets. In the development of the Philips-Miller machines the above-described principle of construction was speedily adopted and the velocity of the film at the spot where the recording takes place is determined by the rotation of a sound shaft. From the high tension on the film it follows that in order to ensure synchronism (with a picture or another sound recording) the sound shaft cannot be driven by the film itself, which is the most preferable method, but only by an adjustable mechanical device.

Because of the lack of necessity of any photographic process in the treatment of "Philimil" film the Philips-Miller system is very suitable for use as a method of sound recording unconnected with cinema film. In particular the system has found an important sphere of application for sound recording in radio broadcasting studios. In this case the problem of film transport is considerably simplified by the disappearance of the requirement of synchronism with a certain picture rhythm. In the construction outlined above therefore the feeding and reeling off of the film by sprocket rollers, and the adjustable mechanical drive may be omitted. The film need not even be perforated. On the other hand the system introduces new demands on the film transport and opens new possibilities which we shall here consider.

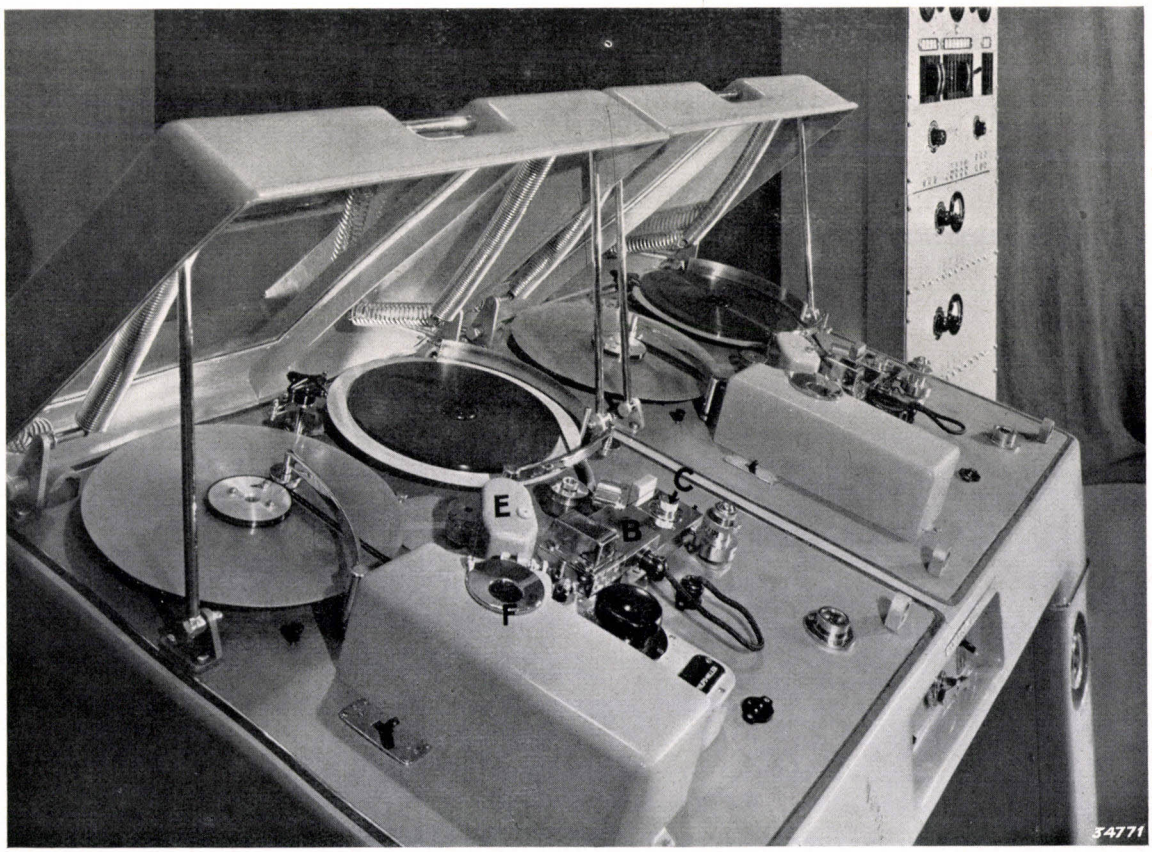

Fig. 7. Machine for sound recording by the Philips-Miller system. The machine, built especially for broadcasting purposes, consists of two quite similar halves each of which is arranged for both recording and reproduction. On the cover plate of each half may be seen the take-up reel to the left and the feed reel to the right. In the middle the sound recorder *B* which can be displaced by the micrometer screw *C* with respect to the film in order to adjust the cutting depth of the knife. The lamp and the photocell for scanning the sound track are housed in *E* and *F*.

The traject of the film and the driving mechanism of the sound axis

In *fig. 7* a view is given of a Philips-Miller recording apparatus as built for broadcasting studios. *Fig. 8* shows the sound shaft and the sound gate (the same apparatus also serves for the reproduction) on a larger scale. The very simple traject of the film is obvious. Aside from the S-shaped loop which is necessary in order to lay the film on the recording drum fastened to the sound shaft over the necessary large angle, the film runs practically free from one reel to the other. The cutting of the sound track takes place at the point where the film runs on to the recording drum (*s* in fig. 8); the pressure roller which provides the necessary friction between film and recording drum is situated at the point where the film leaves the drum. In

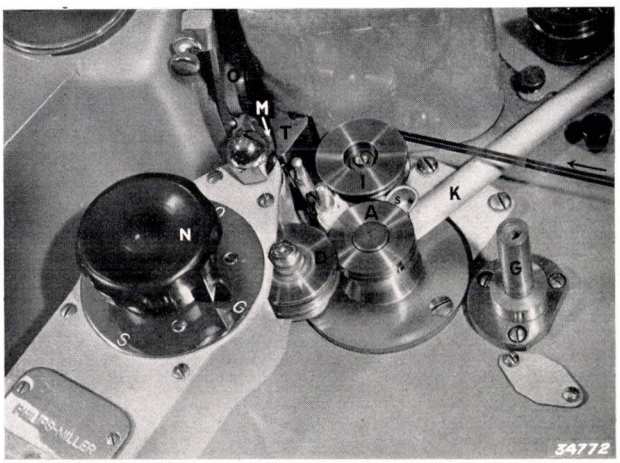

Fig. 8. The sound shaft of the machine shown in fig. 7. The cutter is set on the shaft *G*. In this case it has been removed to show the course of the film more clearly. By means of the fixed roller *I* a loop is laid in the film. This is necessary so that the film may make contact with the recording drum over as great a length as possible. The sound track is cut at *s*; the shaving is removed by suction through the tube *K*. *D* is the pressure roller, *M* the rubber finger for stopping the film. *D* and *M* are moved into position simultaneously by the knob *N*. *T* is the sound gate for scanning, at *O* part of the objective of the optical system may be seen.

contrast to the above described construction for cinema film the sound shaft may here be driven at a constant number of revolutions. It is of course necessary to prevent any vibrations from being transmitted from the driving motor to the sound shaft. The actual construction is shown in *fig. 9*. A driving wheel covered with soft rubber, which thus has a strong damping action, is attached to the shaft of the motor. This wheel presses against the smoothly finished inner surface of the rim of the fly-wheel which is attached to the sound shaft. The weight of the motor is supported by spiral springs which prevent motor vibrations from being transmitted to the cover plate of the machine *via* the frame, and which also supply the necessary pressure between rubber wheel and fly-wheel.

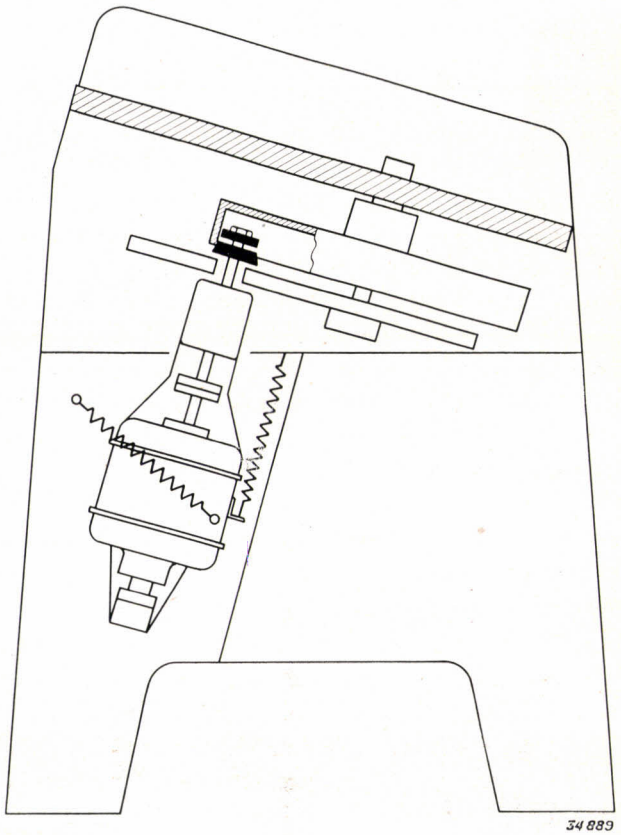

Fig. 9. Driving mechanism of the sound shaft. A friction wheel on the shaft of the motor, whose weight is entirely counterbalanced by springs, is pressed against the inside of the rim of the fly-wheel attached to the sound shaft.

When the machine is started there is a greater friction between the rubber driving wheel and the fly-wheel than when the machine is running at normal speed. In order to prevent excessive wear of the soft rubber wheel, the starting is accom-

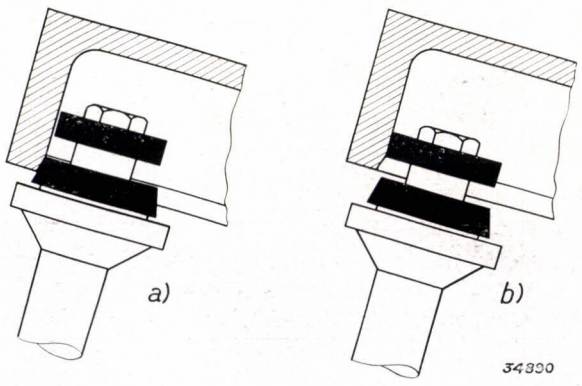

Fig. 10. a) Upon starting, the fly-wheel is accelerated by the conical starting wheel covered with hard rubber.
b) When the fly-wheel is once in motion the motor is allowed to drop slightly, and the fly-wheel is then driven by the driving wheel covered with soft rubber.

plished with a "starting wheel" covered with harder rubber. When the machine is at rest this conical wheel presses against the rim of the fly-wheel, (see *fig. 10a*). When the fly-wheel has been set in motion the whole motor is lowered slightly so that the soft rubber wheel takes over the work (fig. 10*b*).

Moreover it is unnecessary to stop and start the machine anew every time the recording must be interrupted. The moving film can very easily be uncoupled from the sound shaft be raising the pressure roller. When this is done the friction disappears between film and sound shaft, the film lies loosely around the steadily moving recording drum. Thanks to the very small mass of the moving film and the omission of perforations and sprocket roller the film may immediately be brought to a standstill by means of a rubber finger which clamps the film against the sound gate [4]) (see fig. 8). Conversely, by lifting the finger and pressing down the pressure roller the film almost immediately regains normal speed. This makes it possible to pass from the reproduction of one film on one machine (fig. 7) without interruption to the reproduction of a second film on a neighbouring machine.

In discussing the principle on which the sound shaft works we have mentioned the condition that it must be very accurately centred in order to avoid irregularities in the peripheral velocity. In the Philips-Miller recording machine much higher requirements are made in this respect, since an excentricity of the recording drum is manifested here not only as a variation in velocity, but, because of the principle used in recording (see fig. 6), as a direct variation in the width of the sound track, with an enlargement of about 40 times. The tolerance is here therefore much smaller than in the former case; it amounts to less than 1 micron. In order to obtain this great precision the bearing is conical. The steel peg upon which the shaft rests is pushed upward by a spring so that the shaft presses lightly against the conical bearing. The shaft thus continues to run centrically independent of any slight wear. The recording drum which is fastened to the end of the sound shaft is very carefully turned after it has been mounted.

The heavy fly-wheel which is fastened to the sound shaft may be undesirable for certain applications, particularly for installations which must be able to be transported. Since it is only a question of the energy which the flywheel accumulates, instead of a heavy fly-wheel on the relatively slowly turning sound shaft, one may in such cases also use a lighter fly-wheel attached to a rapidly turning auxiliary shaft closely coupled with the sound shaft. This method of construction has for example been chosen for machines which are intended only for the reproduction of "Philimil" film.

Velocity of the film transport

While in the case of sound film for the cinema the velocity of the film transport is fixed at about

[4]) The reel which pulls the film along must of course also stop, the driving mechanism of the reel slips during the interruption.

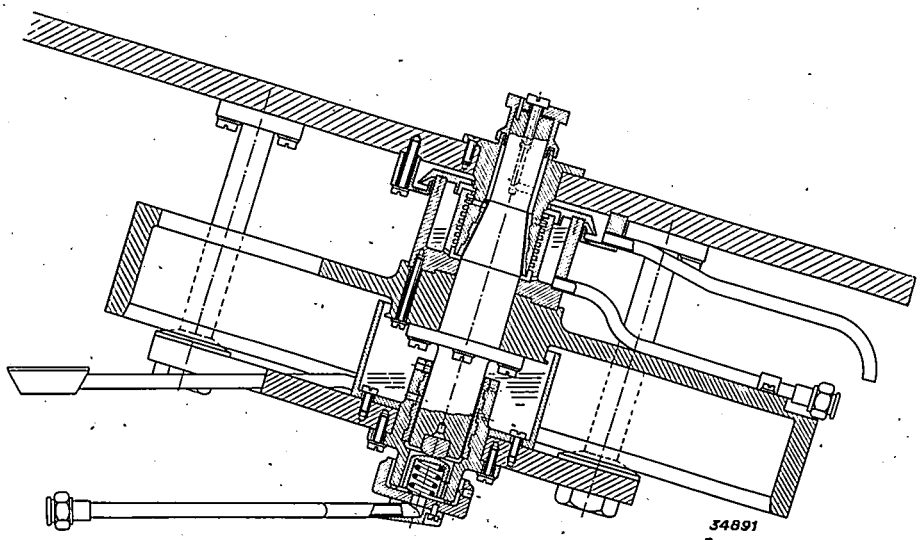

Fig. 11. Bearings and lubrication of the sound shaft. Due to the conical shape of the upper bearing and to the fact that the shaft is pushed against it by a spring under the peg below the end of the shaft, the latter continues to run centrically even after some time. The two bearings of white metal are surrounded by oil reservoirs. The reservoir for the upper bearing rests upon the fly-wheel and thus turns with it. The oil is hereby forced up along a screw thread and flows down along the shaft again. In this way, in spite of the oblique position of the shaft it is well oiled to the very top.

457 mm/sec by the standardized picture frequency and height, when the Philips-Miller system is used for broadcasting purposes, *i.e.* independent of any synchronization, the velocity of the film may be determined at will. From the point of view of saving material it is desirable to keep the velocity at which the film moves through the machine as low as possible. A velocity of 320 mm/sec has been chosen. It is impossible to decrease the velocity still more without disadvantage to the reproduction of the high frequencies of the sound. The lower the film velocity, the shorter the wave length of the sound track cut in the film at a given frequency. For various reasons the wave length may not fall below a certain limit:

1) A limit is set on the slope at which the cutter can penetrate into the gelatin layer by the size of the angle between the front and back surfaces of the cutter [5]). The ratio between the maximum amplitude and the wave length of the track cut is hereby limited. If a given amplitude is also demanded for the high frequencies, for which the wave lengths are the shortest, a lower limit for the film velocity is automatically prescribed.
2) The finite width of the light streak with which the sound track is scanned causes a certain loss of depth of modulation, which is greater the wider the streak compared with the wave length. The shortest wave length occurring must therefore be sufficiently long with respect to the width of the light streak. This limitation cannot be avoided by making the light streak as narrow as desired (it is 12 to 14 microns wide in practice) because the ratio between the level of interference and the desired signal becomes too large: a particle of dust on the film, for instance, which casts a shadow may then cover too large a proportion of the whole light-transmitting surface of the slit. For the same reason decrease in amplitude mentioned under 1) is even more undesirable.
3) The cutting edge of the knife in recording, and the light streak in reproduction are never both exactly perpendicular to the direction of length of the film. The two small deviations, whose effects must be added together, cause distortion which will be greater, the greater the unavoidable deviations in relation to the shortest wave length occurring.

The three effects mentioned only begin to be disturbing at wave lengths shorter than 40 microns. At the film velocity chosen of 320 mm/sec this corresponds to a frequency of 8 000 c/sec.

[5]) This has been carefully explained in the article by A. Cramwinckel. The sound-recording cutter in the Philips-Miller system, Philips techn. Rev. **1**, 211, 1936.

TUNGSTEN RIBBON LAMPS FOR OPTICAL MEASUREMENTS

621.326.3 : 535.24 : 536.52

The conditions are discussed which must be considered in the design of tungsten ribbon lamps for use as light sources in various optical measurements. Several different types are described.

For various types of optical measurements a uniformly radiating surface is needed whose intensity must be high and reproducible. Moreover in many cases the relative spectral distribution of the radiation of this surface must also be known. This is the case for instance in subjective and objective photometry, in pyrometry, in spectral photometry and in colorimetry. A few examples will serve to illustrate this statement.

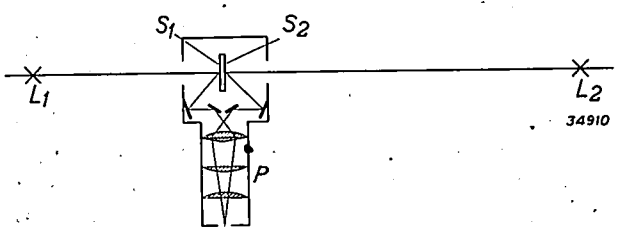

Fig. 1. Arrangement of apparatus for subjective photometry. L_1 and L_2 are the light sources to be compared. S_1 and S_2 are the comparison screens of the photometer P.

In subjective photometry one photometer screen S_1 is often illuminated by the light source L_1 to be measured, and the other photometer screen S_2 by a comparison lamp L_2 (*fig. 1*). The distance between L_2 and S_2 is so adjusted that upon looking through the photometer P the two screens appear to have the same intensity. In order to calculate the ratio of light intensity between L_1 and L_2 the law of the variation of brightness with the inverse square of the distance must be applied. This method involves the following requirements with respect to the comparison lamp L_2:

1) The light intensity must be reproducible.
2) The light intensity must be so high that the required illumination intensity of S_2 is obtained at a distance from L_2 to S_2 large enough to be measured accurately. The minimum value for this distance may be taken as 30 cm for accurate work.
3) The distance to all surface elements of S_2 concerned in the measurement must be very accurately equal, within two per cent if possible, for all points of the luminous surface, in order that it may be possible to use the above mentioned law in the calculation without further corrections. This requirement can easily be satisfied by a small luminous plane surface normal to L_1, L_2 in L_2. When the effective surface of S_2 is a circle with a radius of 10 mm, with a distance of 30 cm from L_2 to S_2 the luminous plane of L_2 must also fall within a circle of radius 10 mm.

The second example is taken from pyrometry. In the case of the much-used optical pyrometer of Holborn and Kurlbaum an image of the radiating body whose temperature is to be determined is projected on the plane of the pyrometer filament. This image and the filament are observed through a red filter by means of a simple microscope or with a magnifying glass. The current through the filament is so regulated that the filament appears just as bright as the image of the radiating body. In calibrating such a pyrometer the relation between the current through the filament and the "black body temperature" [1]) of the radiating body must be determined for the "effective wave length" used.

To do this the pyrometer is first set by means of a black body which has been raised to the melting temperature of gold. A small surface having a very great brilliancy is then observed through the pyrometer, and its brightness is then successively dimmed by known amounts. One observes how great the dimming must be in order that the brightness of the surface may be equal to that of the black body at the temperature of melting gold. Making use of Planck's radiation formula the black body temperature of the luminous surface can be calculated at the different degrees of dimming.

Means of carrying out such a calibration will not ordinarily be at hand, while it will nevertheless be considered necessary to be able to check a pyrometer occasionally, while it is in use. This may be done with the help of a calibration lamp which gives a uniform radiating surface large enough for accurate pyrometry. Moreover the black body temperature of this surface must be known for the effective wave length used, when the values of current or voltage of the calibration lamp are specified.

---

[1]) By "black body temperature" for a given wave length is meant the temperature of a black body which exhibits the same intensity of radiation at this temperature as the body in question.

Not only in primary but also in secondary pyrometer calibration, therefore, is a uniform radiating surface of reproducible high brilliancy needed.

A third example is encountered in spectal photometry. In this type of work it is often necessary, by means of a spectrograph for small wave length regions, to compare the brightness of an unknown light source with that of a comparison lamp of known spectral energy distribution. According to the method of measurement used the slit of the spectrograph must be entirely or partially illuminated by the comparison lamp. In practical cases this is usually accomplished by focussing the image of the luminous surface of this lamp on the slit. Thus here again is there need of a comparison lamp with a sufficiently large, uniformly radiating surface of reproducible high brilliance, whose spectral energy distribution must moreover in this case be known at least relatively.

It has been found that the need for such a lamp with a radiating surface can be met with the tungsten ribbon lamp, and such lamps are in common use for such optical measurements. The incandescent body of these lamps is formed by a tungsten ribbon about 20 μ thick, and for instance 2 mm wide and 20 mm long. This ribbon is heated to incandescence by means of an electric current.

Such a thin ribbon is particularly suitable for the purpose in view. Due to the small area of the cross section the heat conduction is small, so that the cooler sections at the ends are relatively short. Due to the favourable relation between radiating surface and electrical resistance per cm length, high temperatures can be obtained with relatively small currents. It is also important that the whole surface of the ribbon appears equally bright, in contrast to the case of a incandescent wire, where deviations from Lambert's law become appreciable along the edges.

Before we begin to discuss the different designs of tungsten ribbon lamps manufactured by Philips, we shall first examine the radiation properties of tungsten.

Light emission of tungsten

In general the radiation emitted by a substance depends very much upon its temperature. In addition the nature of the surface is also important. Let us consider that portion of the radiation which, at a temperature T, falls within the small wave length region $\Delta\lambda$ in the vicinity of the wave length λ. The current of energy, corresponding to the wave length region $\Delta\lambda$, which is emitted per unit solid angle by a surface element ΔS at an angle Θ with the normal to the surface may be represented by

$$I_{\lambda T\Theta}\,\Delta\lambda\,\Delta S.$$

As has already been mentioned in a previous article [2]), the radiation properties of a black body are accurately known. The way in which $I_{\lambda T\Theta}$ depends upon wave length and temperature is given by Planck's radiation formula. Furthermore the radiation of a black body satisfies Lambert's law, according to which

$$I_{\lambda T\Theta} = I_{\lambda T}\cos\Theta \quad . \quad . \quad . \quad . \quad . \quad (1)$$

For the radiation of other materials formula (1) is found to be approximately correct for not too large values of Θ. When however Θ approaches 90°, very great deviations may occur.

The radiation of a given substance at wave length λ, temperature T and sufficiently small values of Θ is often compared with that of a black body at the same length and temperature. The ratio of $I_{\lambda T}$ of the substance under consideration to $I_{\lambda T}$ of the black body is called the spectral emission coefficient $e_{\lambda T}$. Since no substance completely absorbs all incident radiation, as is the case with a black body, the emission coefficient is, according to Kirchhoff's law, always less than unity.

The value of $e_{\lambda T}$ for a given substance is found to be dependent on the purity and the degree of smoothness of the surface. Small depressions in the surface act more or less as black bodies, and therefore increase the emission. The smoother the surface the smaller the emission coefficient. In investigations of radiation properties of substances, therefore, one must always strive not only for great purity but also for very smooth surfaces.

In the case of tungsten the physical properties in general and the radiation properties in particular have been the subject of much research. On the basis of the results of these investigations we shall now discuss the questions which are of interest in connection with tungsten ribbon lamps, namely:

1) Is it possible with the help of tungsten ribbon to obtain a radiating surface whose brightness remains practically constant with the passage of time?

2) To what degree are the radiation properties of different ribbons equal?

3) Is it possible to give the relative spectral energy distribution of the radiation of an incandescent tungsten ribbon with reasonable accuracy?

---

[2]) *Cf.* The new unit of luminous intensity, Philips techn. Rev. 5, 1, 1940.

Reproducibility of the radiation of a tungsten ribbon in the course of time

It is also true of tungsten that the radiation depends upon the nature of the surface. It has been found that at a high temperature it makes little difference in the radiation emission of an ordinary drawn wire or rolled strip whether or not the surface has also been polished. The main point is that such a wire or strip should be "aged" for some time by heating it to a high temperature in a high vacuum or in an inactive atmosphere. During this process a bright shiny surface is formed whose radiation emission is found to be reproducible.

In order to prove this the current was determined of a gasfilled ribbon lamp, the ribbon of which had been heated in a high vacuum during evacuation when the lamp was being made. The true temperature at the middle of the ribbon was 2835 °K. This current was sent through the lamp for 100 hours, while the brightness of the middle of the ribbon was measured as a function of the time. This brightness was found to remain constant within the limits of error of the measurement (0.5 per cent).

Reproducibility of the radiation properties of different ribbons

The reproducibility for different ribbons is important in cases where the spectral emission coefficient must be used, for example, for the calculation of the temperature or of the spectral energy distribution from the black body temperature measured. The spectral emission coefficient $e_{\lambda T}$ must be known as a function of the temperature and wave length. This value is obtained from measurements of $e_{\lambda T}$ which are usually carried out in the investigations in question on several tungsten surfaces. For the wave length and temperature in question values of $e_{\lambda T}$ are found which exhibit slight differences from surface to surface. From these an average value of $e_{\lambda T}$ is found, which may be used in the calculation for any given ribbon lamp.

It is now important to know how great the maximum deviation between the average value and the actual value of $e_{\lambda T}$ will be for this ribbon lamp. The possible deviation consists of two parts. In the first place there is the actual scattering among the values of $e_{\lambda T}$ for different tungsten surfaces such as occurs, and is further heightened by experimental errors, in an investigation of different tungsten surfaces by a single method. In addition there is the possible deviation of the value of $e_{\lambda T}$ assumed to be the average one from the real average value, which may be due to systematic errors in measurement.

When the available material for observation is reviewed, it is found that the possible deviation of the emission coefficient of one ribbon with respect to the average for many ribbons must be placed at 1 per cent.

Furthermore the possible error in the assumed average value of the emission coefficient must be estimated.

Various investigators give different average values. This may be due partially to differences in methods of measurement. Moreover, the different degrees of purity and the different treatment of the surface of the tungsten investigated will play a part. In the case of the tungsten ribbons under discussion it would seen reasonable to give particular weight to the measurements by Hamaker[3]) which were performed on the very material in question. The possible error in the average values given by Hamaker may be considered 1 per cent. Therefore if we use his average value for a given tungsten ribbon, we must take into account a possible error of 2 per cent. This holds for the whole visible region of the spectrum. It is possible that the errors in the infra red and ultra violet regions are somewhat larger.

Calculation of the relative spectral energy distribution

For the calculation of the relative spectral energy distribution the temperature of the tungsten must be determined, the spectral energy distribution of the black body must be determined relatively for this temperature, and the value found must be multiplied by the corresponding spectral emission coefficient $e_{\lambda T}$ of tungsten for every wave length.

An example will show that this method leads to a fairly accurate knowledge of the relative spectral energy distribution.

Let us assume that the black body temperature for a definite, accurately known, effective wave length is 2500 °K, and that this is determined by pyrometry with a possible error of 10°. From this the true temperature is then calculated with the help of a value for the corresponding spectral emissions coefficient which may have an error of 2 per cent. As a result the possible error in the true temperature is increased by 6°. In total therefore the true temperature may contain an error of 16° at the most. Although such an error would be important in the calculation of absolute values of spectral intensities of the black body radiation, it has practically no effect on the relative spectral

[3]) H. C. Hamaker, dissertation, Utrecht, 1934; L. S. Ornstein, Physica **3**, 561, 1936.

energy distribution. The only uncertainty which yet remains is the possible error of 2 per cent in the spectral emission coefficient, by which the relative spectral intensity of the black body must be multiplied in order to obtain that of tungsten. This possible error of 2 per cent is valid for the visible region of the spectrum; in the infra red and ultra violet it is probably slightly larger.

For the visible spectral region the calculation of the relative spectral energy distribution of the radiation of tungsten can be shortened with the help of the concept of colour temperature. It has been found experimentally that between 4 000 and 7 000 Å the relative spectral energy distribution of the radiation of tungsten at every temperature T is practically equal to that of a black body at a temperature T_c which is slightly different from T. T_c is called the colour temperature of tungsten corresponding to T. In *table I* T_c is given as a function of T. In order to calculate the relative spectral energy distribution of tungsten, the true temperature is determined and the corresponding colour temperature T_c is found from the table. It is then only necessary to find the relative spectral energy distribution of the radiation of a black body for the temperature T_c in a suitable table.

Table I

T	1200 °K	1600	2000	2400	2800
T_c	1210 °K	1616	2023	2432	2844

From the data here discussed on the radiation properties of tungsten it may be seen that the tungsten ribbon lamp in principle is capable of satisfying the requirements of various optical measurements.

Design and construction of ribbon lamps

In connection with the very divergent applications it has been found desirable to construct different models of tungsten ribbon lamps. The differences lie chiefly in the shape of the bulb, the dimensions and the assembly of the ribbon and the construction as vacuum or gas-filled lamp. We shall discuss these points separately.

Shape of the bulb

When no very great demands are made of the optical focussing of the ribbon, and when moreover the spectral transmission curve of the wall of the bulb need only be known roughly, the simple cylindrical bulb shown in *fig. 2* may be used. This bulb is usually made of heat resistant glass. For the case in which the lamp must also be used in the ultra violet for wave lengths shorter than 3 500 Å or in the infra red for wave lengths longer than 25 000 Å a bulb of clear quartz may be chosen.

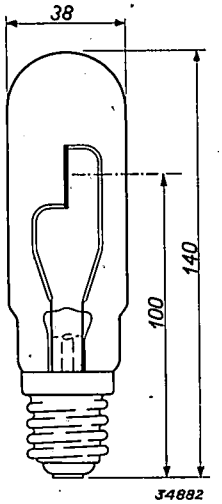

Fig. 2. Ribbon lamp with cylindrical bulb. The dimensions are indicated in mm.

If the optical focussing of the ribbon is important the horn-shaped bulb with the plane window fused on (*fig. 3*) is to be recommended. The radiation of the ribbon in this case passes through a ground plane parallel window which is fused to the bulb. The shape of the bulb is so chosen that the radiation from the back of the ribbon, which is reflected by the rear wall does not pass through the window. The combination of these two precautionary measures makes it possible to focus the image of the ribbon very well, and also makes it possible in the photometric application to apply

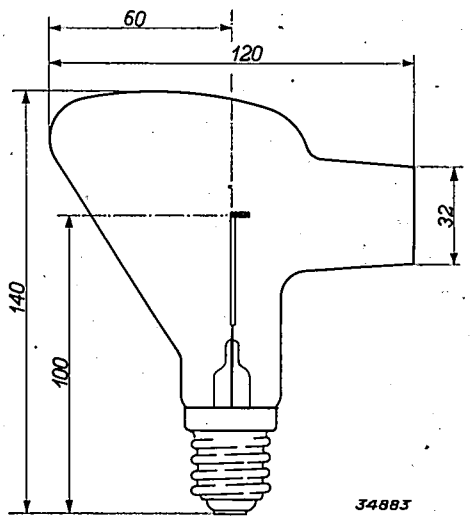

Fig. 3. Ribbon lamp with horn-shaped bulb provided with a fused-in plane window. The maximum transverse dimension of the bulb is 42 mm.

accurately the law of the variation of the intensity of illumination with the inverse square of the distance. The plane parallel window is made of heat resistant glass or quartz. In precise measurements it may be necessary to correct the spectral energy distribution of the radiation of the ribbon for the absorption by the window. To do this the spectral transmission curve of the window must be determined before it is fused into the bulb.

In spectral photometric investigations the bulb shown in *fig. 4* with two oblique plane windows may often be used. In such work it is often necessary to focus the image of the light source being investigated on the plane of the tungsten ribbon, and then to focus the image of this plane again on the plane of the slit of the photograph. With a vertical slit and a horizontal ribbon it is possible to illuminate part of the slit by the ribbon and the rest by the

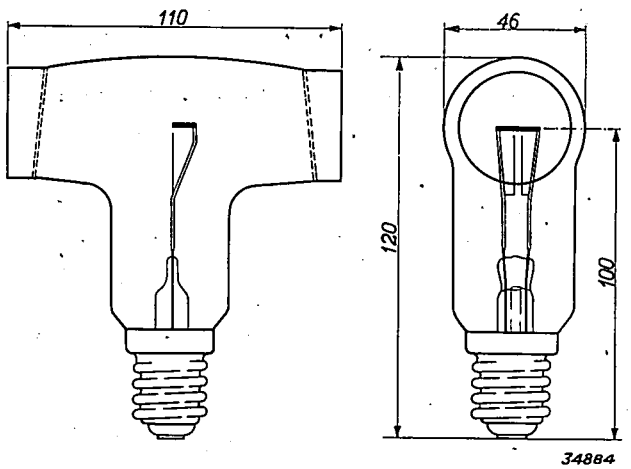

Fig. 4. Side and front views of a ribbon lamp with a bulb provided with two oblique plane windows. The dimensions are given in mm.

unknown source. When the bulb shown in fig. 4 is used the optical focussing through the plane windows is able to satisfy high requirements. By the oblique position of the window in the way shown in the figure disturbing reflections from front and rear walls are avoided. Windows of heat resistant glass or quartz may be used as in the horn-shaped bulb. The spectral transmission curve of each individual window may if necessary be determined before it is fused in.

In photometers of small dimensions, in simple spectral photometric arrangements and in many other cases there exists a need for a ribbon lamp with a small bulb and low power. This need is met by the lamp with small spherical bulb (*fig. 5*) which is made exclusively of calcium glass and in which only ribbons 0.5 mm wide are mounted.

Assembly and dimensions of the ribbon

The assembly is carried out in general as follows. Each end of the ribbon is welded to a nickel pole which must be relatively thick, since otherwise the temperature of the nickel at the weld would exceed the maximum permissible temperature for this metal.

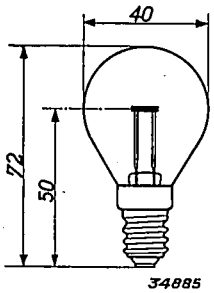

Fig. 5. Ribbon lamp with small spherical bulb.

The temperature at the ends of the ribbon naturally exhibits a sharp gradient due to the flow of heat toward the poles. In certain measurements these cooler end pieces might have a disturbing effect. In order to prevent this the ribbon is bent at both ends as shown in *fig. 6*. In this way the cooled ends are screened by the middle section of the ribbon whose radiation is to be used. By this means it is also brought about that the expansion of the ribbon upon heating has practically no tendency to cause disturbing stresses or deformations. The length of the ends bent under is always 5 mm. The useful length of the ribbon may be 10 or 20 mm, and its width 1 or 2 mm, in some cases 0·5 mm.

In choosing the most suitable ribbon lamp for a given application from the models given in *table II*, various factors must be considered. For spectral photometric uses the conditions of the desired optical focussing will be decisive. If the image of the ribbon is focussed transversally across the slit, a short ribbon is sufficient. If a vertical ribbon must be focussed on the slit a long ribbon is usually preferable.

In general photometric work the desired total luminous intensity may be the deciding factor.

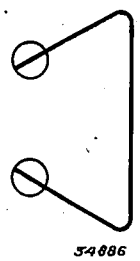

Fig. 6. The ribbon is bent so that the cooler end pieces are screened by the middle of the ribbon.

In any case the ribbon should always be chosen as small as possible in order to avoid unnecessary consumption of current. For many applications it is desirable that a certain point on the ribbon, usually the middle, should be indicated. In all lamps with a useful ribbon length of 20 mm such indication may be introduced in the form of a point of wire at one side in the plane of the ribbon.

Table II

Bulb	Width of ribbon in mm	Position of ribbon	Useful length of ribbon in mm
Cylindrical model of heat resistant glass or quartz	2 or 1	horizontal or vertical	10, 10 or 20*
Horn-shaped model with one plane window of heat resistant glass or quartz	2 or 1	horizontal or vertical	10 or 20*
Model with two oblique windows of heat resistant glass or quartz	1	horizontal	20*
	0.5	horizontal	10*
Small spherical model of calcium glass	0.5	horizontal	10

*) With index at the middle of the ribbon if desired.

Vacuum lamp or gas-filled lamp

The tungsten ribbon lamps may be vacuum lamps or gas-filled lamps. In general a gas-filled lamp will be preferred because with the same life a higher working temperature and thus a greater brightness can be obtained than with a vacuum lamp. For spectral photometric work in the blue and ultra violet this is an important advantage.

As we have already seen the gas has no harmful effect on the reproducibility of the radiation in the course of time if the lamp is always allowed to burn in the same position. The gas does, however, have some influence on the temperature distribution of the ribbon. In the vacuum lamp this temperature distribution is determined by accidental slight irregularities in dimensions and properties of the ribbon and by the flow of heat toward the poles. In the gas-filled lamp the flow of the heated gas is also an influential factor. In the most unfavourable case, namely that of a gas-filled lamp with a vertical ribbon 2 mm wide and 20 mm useful length, at an average temperature of 2 500 °K, the upper end of the ribbon is not more than 25° warmer than the lower end. This difference in temperature is however not important.

Due to the dissipation of heat by the gas a larger current must be used to obtain a given temperature with a gas-filled lamp than with a vacuum lamp. For example, in the case of the gasfilled lamp with a ribbon 2 mm wide, a normal working temperature of 2 800 °K is reached with a current of 17.5 A, a temperature of 2 300 °K with 12.8 A. In the case of a vacuum lamp a normal working temperature of 2 300 °K is reached with a current of 10.8 A.

Compiled by J. VOOGD

MEASUREMENTS IN THE PHILIPS RARE GAS PLANT

by H. C. A. HOLLEMAN.

545.7 : 661.93

In connection with the manufacture of electric lamps large scale measurements must be carried out in the Philips rare gas plant on the composition of mixtures of argon and nitrogen. Two methods used in these measurements are described in this article. The first is based upon a determination of the specific weight of the mixture with the help of a spring scale, and the second upon a measurement of the vapour pressure of the mixture at the temperature of boiling oxygen.

In carrying out the measurements necessary for the control of products or of the process of manufacture methods are used in many industries which differ very much from the ordinary laboratory methods. This is due on the one hand to the fact that the methods have been adapted to the peculiar requirements of the industry, and on the other hand to the fact, that use may be made of possibilities not otherwise offered. Both factors have played their part in the Philips rare gas plant in determining the choice of methods to be applied to determine the composition of gas mixtures.

One of the most important gas analyses is the determination of the composition of argon-nitrogen mixtures which are used as filling for electric lamps, the argon content of which influences the efficiency of the lamps. Great accuracy or sensitivity of the measuring method is in general not demanded. It is however desirable that the measurement should be rapid and capable of being performed without too great skill.

In an earlier article in this periodical [1]), it was stated that the composition of an argon-nitrogen mixture can be determined chemically with the help of metallic lithium, which has been brought into a condition in which it is able to absorb large quantities of nitrogen. This method is suitable for very precise measurements (which, however, also demand considerable time and experience), and also for the determination of very small quantities of rare gas. It is therefore suitable for controlling the purity of nitrogen.

For the purpose outlined above, namely the rapid and easy determination of large as well as of small quantities of argon in nitrogen, the method mentioned is less appropriate. Since, however, we are here concerned with a mixture consisting of two gases only, the analysis may also be carried out physically by measuring some physical quantity which varies in a definite way for different proportions of the gases in the mixture from 100 per cent nitrogen to 100 per cent argon. Two quantities have been found suitable: the specific weight and the vapour pressure of the mixture.

[1]) Philips techn. Rev. 4, 128, 1939.

Anlysis of argon-nitrogen mixtures by a determination of the specific weight

The specific weight of nitrogen (with respect to air) is 0.9672 and that of argon 1.3796. The difference is thus 0.4124, and 1 per cent difference in composition gives a change of 0.0041 in the specific weight. This shows, that the determination of the specific weight must take place with an accuracy of several tenths of one per cent.

A very easy indirect method of determining the specific weight of gases is that of Bunsen-Schilling, in which the velocity of effusion through a small aperture is measured. At a given difference in pressure and a given temperature this velocity is inversely proportional to the square root of the specific weight. The internal friction and other factors, however, prevent strict application of the law, so that no greater accuracy than 1 to 2 parts in the second decimal place can be attained. The method is therefore useless for our purpose.

A direct determination of the specific weight, consisting of accurate weighing of a bulb filled with gas would be accurate enough, but it is fairly elaborate and requires great skill in execution. Instead of filling the bulb with the gas being analyzed, a simplification was attained by determining by a weighing process the lifting force experienced by a closed bulb in an atmoshere of the gas in question. A further simplification is obtained by determining the pressure which the gas in question must have in order to have the same specific weight as dry, carbon dioxide-free air at the same temperature and atmospheric pressure. If the air and an argon-nitrogen mixture have the same specific weight at the same temperature then the ratio of their pressures is a direct measure of the composition of the argon-nitrogen mixture. It is hereby assumed that Boyle's law is strictly valid, which is permissible in this case. If the measurements are to be very accurate, and if one

is working with easily condensible vapours, it may be necessary to take into account deviations from the laws for perfect gases.

It was finally found possible to simplify the weighing without too great a loss in accuracy by using a spring scale instead of an ordinary balance with a swinging beam.

In *fig. 1* the main details of the apparatus are shown. *a* is a column containing gas whose specific weight is to be determined. In this column hangs a spiral spring *b*, which carries the bulb *c*. The extension of the spring is a measure of the weight of the bulb diminished by the upward pressure of the gas in question. This pressure is equal to the specific weight of the gas multiplied by the volume of the bulb.

In order to read off accurately the extension of the spring a microscope *d* is used with a horizontal cross hair. With the microscope one observes a horizontal piece of wire fastened to the spring and the pressure of the argon-nitrogen mixture can be adjusted until this wire coincides with the cross hair of the microscope.

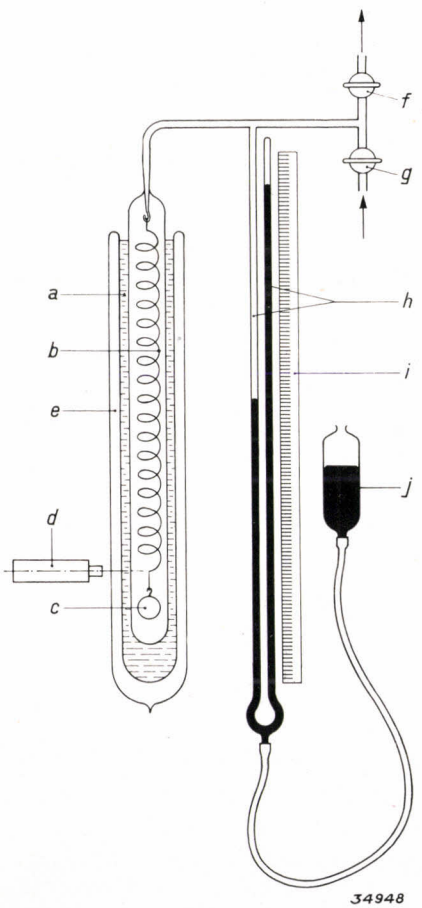

Fig. 1. Apparatus with spring scale for the measurement of the specific weight of gas mixtures. *a* tube which is filled with the gas *via* the stopcock *g*; *b* spring (molybdenum wire); *c* bulb, upon which the gas exerts an upward pressure proportional to the specific weight; *d* microscope with cross hair for observation of the position of the spring; *e* Dewar jar filled with water to keep the temperature of the gas constant: *f* exhaust tap connected with vacuum pump; *h* tubes of a manometer for observing the pressure of the mixture measured; *j* mercury reservoir which can be raised and lowered in order to change the pressure of the mixture slightly and in that way to make the index on the spring coincide accurately with the cross hair.

In order to maintain a constant temperature in the column *a*, it is surrounded by a water bath in a Dewar jar *e*. The Dewar jar is silvered except for a strip in front of the microscope. The column can be evacuated through the stop cock *f*, and the gas to be examined may be admitted through *g*. The pressure is read off from the mercury manometer *h* with scale *i*. By moving the reservoir *j* up and down the pressure can be slightly varied with *f* and *g* closed.

The spring was originally made of quartz since this material is particularly suitable due to its small elastic inertia and its chemical stability [2]).

Later, when it was discovered that molybdenum could also be used, its use was adopted since the great brittleness of the quartz was found to be a disadvantage. The spring must of course be extremely flexible in order to have sufficient sensitivity. For the same reason it is desirable to make the volume of the bulb as large as possible. On the other hand the bulb may not be too heavy since otherwise the flexible spring would be loaded beyond its limit of elasticity. The molybdenum wire used has a thickness of 0.12 mm and is wound with a low pitch 17 turns around a mandrel 28 mm in diameter. The sensitivity amounts to about 1 mm extension for a load of 1 mg. The bulb weighs about 300 mg and thus produces an extension of 300 mm. This extension does not exceed the limit of elasticity. The volume of the bulb is about 15 cc. The upward pressure of atmospheric air (760 mm and 20° C) on the bulb is thus about 18 mg. 1 mm variation in pressure thus gives a variation in upward pressure of 18/760 = 0.02 mg, corresponding with a displacement of 0.02 mm of the mark on the spring. This displacement can just be observed through the microscope and thus corresponds approximately with the limit of accuracy of the apparatus. The same limit is also given by the accuracy with which the gas pressure may be read. Since 1 mm Hg is about 0.13 per cent of the total pressure (~1 atmosphere), and since a change in the composition of the mixture by 1 per cent corresponds to a change in pressure of 0.4 per cent, it is clear that the composition of an argon-nitrogen mixture can be determined with an accuracy of about 0.3 per cent.

[2]) Philips techn. Rev. **1**, 126, 1936.

In order actually to attain this accuracy it is very important that the spring should be free of elastic inertia and that the bulb should not be appreciably deformed upon variations in pressure. This has been studied in numerous test measurements. Within the limit of observation of the apparatus no error was found. The temperature sensitivity is of course very great, even more than 1/273 per °C, probably because the elasticity of the molybdenum decreases with increasing temperature. Thanks to the water jacket and the Dewar jar, however, the temperature remains sufficiently constant so that the temperature effect is not disturbing.

A great advantage of the spring scale over a beam balance is that it is practically aperiodic. If the equilibrium is disturbed, due to increase in pressure for instance, the scale is seen to execute several vibrations with a period of about $^1/_2$ sec; within a few seconds, however, the movement is so strongly damped that it cannot be observed even with the microscope. The vibration of the mercury in the manometer usually lasts longer than that of the spring.

The total length of time needed for a measurement is about 5 minutes. Great skill is not required of the operator. The same amount of time must be allowed for the preceding calibration of the apparatus with dry air free of carbon dioxide. Calibration, however, needs in general only be carried out once for a whole series of measurements.

It is obvious that other gas mixtures than argon-nitrogen can also be investigated with the spring scale. If for example mixtures containing hydrogen are measured, the specific weight of the gas in question may be considerably smaller than that of air at 1 atmosphere. In that case, in order to make the comparison with air, the gas mixture being measured would have to be put under a pressure of several atmospheres, which is undesirable in connection with the lightness of the construction of the bulb. In such a case therefore it is advisable to admit air to a pressure of less than 1 atmosphere; this means that the microscope must be lowered slightly.

Analysis of argon-nitrogen mixtures by the determination of the vapour tension

Since liquid oxygen is produced in large quantities in the Philips rare gas plant, it is always possible to realize the temperature of the boiling point of oxygen, namely —183° C. The boiling point of argon lies directly below that of oxygen, namely at —185° C. If argon is brought to the temperature of boiling oxygen, its vapour tension is slightly greater than 1 atmosphere. It is actually found that condensation only occurs at a pressure of 1050 mm. With increasing proportion of nitrogen in an argon-nitrogen mixture the vapour tension increases. Pure nitrogen has a vapour tension of 3.6 atmospheres at the temperature of boiling oxygen.

If it is desired to determine the composition of a gas mixture by finding out at what pressure the mixture begins to condense, it must be kept in mind that the composition of the product condensed is not in general the same as that of the gas. The less volatile component, in our case argon, shows a tendency to become concentrated in the fluid, while in the gas a decrease in the proportion of argon

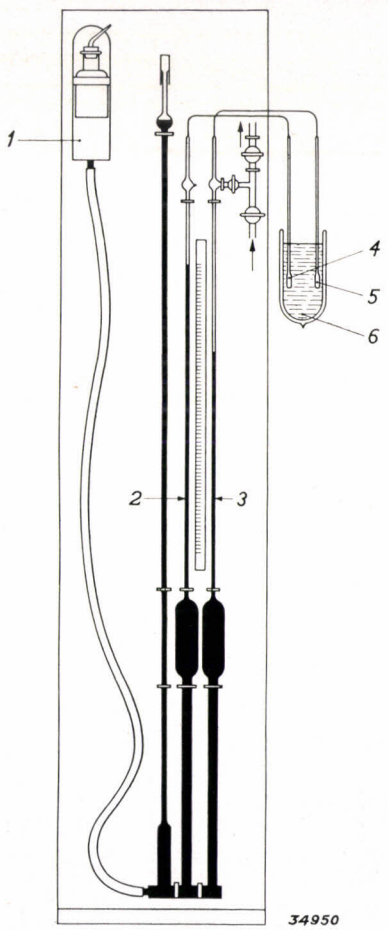

Fig. 2. Apparatus for the determination of the vapour pressure of argon-nitrogen mixtures. By lowering the mercury reservoir *1*, the mercury is allowed to flow out of tubes *2* and *3*. Tube *2* is permanently filled with pure argon, while tube *3* is filled with the mixture under consideration *via* the stopcocks. After the stopcocks have been closed the mercury reservoir is raised again. The wider portions of tubes *2* and *3* are thereby filled with mercury and the gas displaced is driven through narrow capillaries into tubes *4* and *5*, respectively, which are immersed in liquid oxygen (Dewar jar *6*).
Since the gases in these tubes condense, the position of the mercury column in tubes *2* and *3* indicates the vapour pressure of pure argon and of the gas under consideration, respectively. The scale is calibrated in per cent of nitrogen. In tube *2* the mercury column must therefore stand at zero, which forms a check on the purity of the boiling oxygen in the Dewar jar.

occurs. Only when the condensation is nearly complete, can the composition of the fluid be said to correspond to the original composition of the gas.

This is the principle upon which is based the determination of the composition of argon-nitrogen mixtures by means of the apparatus shown in *fig. 2*. The measurement is begun by lowering the mercury reservoir *4* so that the mercury column *3* runs empty and the widened part of the column is filled with the mixture to be measured. When the stopcocks are now closed and the mercury container again raised, the gas mixture is almost completely condensed in tube *6* which is immersed in boiling oxygen. The height assumed by the mercury column is a measure of the vapour pressure of the mixture.

In *fig. 3* the vapour pressure of the argon-nitrogen mixture is given as a function of the composition. According as one considers the abscissa as the composition of the fluid or the vapour, the upper or the lower curve is obtained. We are concerned with the first case, and thus observe that the vapour pressure increases almost linearly with the concentration of nitrogen. At about 10 per cent nitrogen the accuracy of the apparatus is about 0.3 per cent. For larger contents in nitrogen the apparatus cannot be used because the vapour pressure becomes too high. Moreover, the equilibrium between the fluid phase and the gas phase, which are joined only through a narrow capillary, becomes established with more and more difficulty as the difference in composition between the two phases becomes greater. This difference increases with the concentration of the nitrogen which therefore must not practically be greater than 25 per cent.

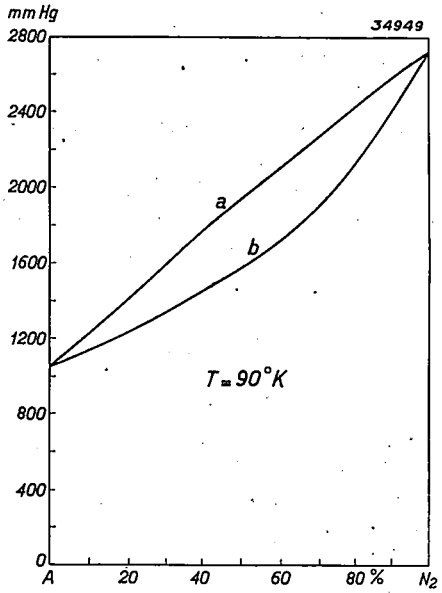

Fig. 3. Vapour pressure of argon-nitrogen mixtures as a function of the composition *a* of the liquid, *b* of the gas.

The great advantage of the apparatus is that it works very rapidly. One determination takes only about 2 minutes, and after some practice can be carried out by any one.

ABSTRACTS OF RECENT SCIENTIFIC PUBLICATIONS OF THE N.V. PHILIPS' GLOEILAMPENFABRIEKEN

1447: H. C. Hamaker: Adsorption of iodine vapour by powders (Rec. Trav. Chim. Pays Bas **58**, 903-916, July-Aug. 1939).

According to a method developed by J. H. de Boer samples of powders which had been heated in a vacuum were exposed to iodine vapour. The iodine was adsorbed on the surface of the powder. The amount adsorbed is determined by a simple chemical titration. The necessary precautions, as well as the degree of reproducibility of these processes is described in great detail. Surface reactions and the influence of grinding in a ball mill can be studied by means of the corresponding changes in adsorption.

1448: E. J. W. Verwey: Electronic conduction of magnetite (Fe_3O_4), and its transition point at low temperatures (Nature, London, **144**, 327-328, Aug. 1939).

The electronic conduction is determined for different oxides of iron of the Fe_3O_4 type. This is important from a theoretical standpoint, since Fe_3O_4 is an abnormally good semi-conductor, possesses a remarkable crystal structure in which there is probably a statistical distribution between tri and bivalent iron ions at equivalent lattice positions, and in addition seems to have a transition point in the neighbourhood of 120° K.

1449: J. D. Fast: The appearance of two new branches of metallurgy as a result of the development of the electric lamp industry (Metaalbewerking **6**, 116-120, 132-139, 145-150, 159-162, 174-176, 189-192 and 203-205, June-Sept. 1939). Original in Netherlands language.

Two branches of metallurgy have appeared as a result of the need felt by the developing electric lamp industry of being able to manufacture wire out of the metals with high melting points. In these articles a survey is given of the history of their development and the most important applications. For the contents of the articles the reader may be referred to Philips techn. Rev. **3**, 353, 1938 and **4**, 321, 1939.

1450: A. H. W. Aten jr.: Artificial radioactive substances as indicator (Chem. Wbl. **36**, 607-609, Sept. 1939). Original in Netherlands language.

In this lecture given before the Nederlandsche Natuur- en Geneeskundig Congres (April 1939), it was explianed how it is possible to follow certain atoms in their course through the body by adding small quantities of artificial radioactive substances. It is for example possible to study the way in which substances containing phosphorus distribute themselves throughout animal organisms.

1451-1453: J. M. Stevels: Cold flames. (Chem. Wbl.) **36**, 638-642, 654-657, 657-663, Sept. 1939). Original in Netherlands language.

This is a review of theory and practical research on flames such as occur in gases at very low pressure. These flames differ from ordinary ones by the absence of an ignition temperature. In order to keep such a so-called cold flame cold, it is necessary to remove the heat developed by the reactions occurring so rapidly that the temperature does not rise appreciably. A cold flame is a very suitable medium for the investigation of reaction velocities, and also of the nature of the chemical bond in general, as is discussed at length in the last article.

1454: J. Boeke and H. van Suchtelen: Direct rapid chemical Analysis with the mercury dropping electrode. (Z.Elektrochem. **45**, 753-756, Oct. 1939). Original in the German language.

Compare Philips techn. Rev. **4**, 231, 1939 for the contents of this article.

VOL. 5 No. 4 APRIL 1940

Philips Technical Review

DEALING WITH TECHNICAL PROBLEMS
RELATING TO THE PRODUCTS, PROCESSES AND INVESTIGATIONS OF
N.V. PHILIPS' GLOEILAMPENFABRIEKEN

EDITED BY THE RESEARCH LABORATORY OF N.V. PHILIPS' GLOEILAMPENFABRIEKEN, EINDHOVEN, HOLLAND

BLACK-OUT BY THE FILTER METHOD

by E. L. J. MATTHEWS and J. A. M. van LIEMPT. 535.345.6 : 628.972 : 355.585

By installing an indoor illumination system with yellow light and colouring the window-panes green a satisfactory black-out illumination can be obtained. The interior illumination is invisible at night to an observer in the air, while about 25 per cent of the daylight is able to pass through the windows whose colour is not unpleasant for the eye.

For the purposes of air raid precautions private dwellings, and in general localities where an adequate illumination is required only at certain spots, can be provided with a satisfactory "black-out illumination" with the help of "Protector" lamps, as was explained in a previous number of this periodical [1]). If, however, it is a question of making the illumination in large factory buildings, offices, shops or other buildings, where a fairly high intensity of illumination is required over the whole floor space and is to be made invisible from the outside, the problem is encountered of providing shutters or other means of cutting off the light from huge window surfaces. Such provision is not only expensive but is also open to the serious objection that the screening devices must be opened and shut daily, while the problem of ventilation is difficult to solve.

A much more elegant solution is offered by the filter method. The glass is covered with a coating of paint or coloured cellophane which transmits practically none of the light from the part of the spectrum emitted by the lamps which provide the interior illumination. This principle is illustrated by *fig. 1*, where curve *A* represents for example the spectral composition of the artificial illumination and curve *B* the spectral transmission of the coloured layer which is used to cover the glass. The coloured coating, however, transmits enough daylight to make artificial illumination unnecessary in the daytime, and it is only necessary to use artificial lighting somewhat longer at twilight. If circumstances permit, the colour of the filtered daylight can be made less pronounced for instance by leaving a small part of the window space uncoloured and screening this at night with shutters. It will be clear that in these considerations it is assumed that it is possible to avoid the radiation of light of any other colour in the rooms in question, such as that of hand lamps, open fires and welding arcs.

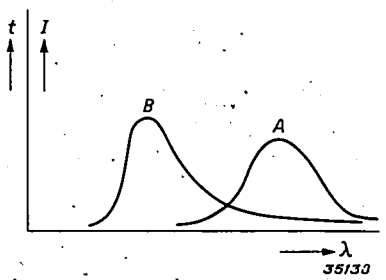

Fig. 1. For a practical black-out illumination by the filter method, curve *A* of the spectral distribution of intensity *I* of the artificial illumination, and curve *B* of spectral transmissibility *t* of the coloured windows must overlap as little as possible.

For practical purposes such a wartime illumination can be achieved with the help of lamps which radiate chiefly yellow light and if necessary by suppressing any light of shorter wave lengths. As a coating which is practically opaque for this light, use was formerly made of a type of paint which transmits well only a narrow spectral region in the blue and strongly absorbs the other components of daylight. The screening toward the outside was indeed adequate, but the effect in the daytime was anything but satisfactory. If the blue paint is applied sufficiently thick, it transmits only 4 to 5 per cent of the daylight, so that the interior illumination is insufficient and, due to the blue colour, depressing.

It has been determined experimentally that much

[1]) Philips techn. Rev. 4, 15, 1939.

more satisfactory results can be obtained by making the windows green in a suitable way instead of blue. It is much more pleasant to work in the green filtered daylight than in the blue, while it will appear from further considerations that sufficient screening of the yellow interior illumination can still be procured with a higher transmissibility for daylight.

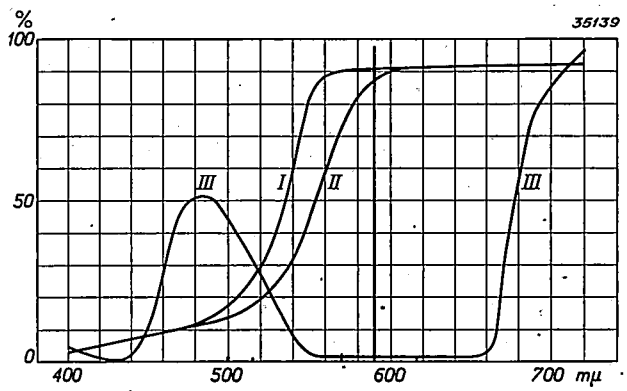

Fig. 2. Spectral transmissibility of orange "Selectiva" glass in the cold state (*I*), and at operating temperature of sodium lamps (*II*). Curve *III* gives the spectral transmissibility of clear glass covered with a green coating (paint *A* in the following) in a layer of such thickness that a total of 25 per cent of daylight is transmitted. In addition the position and relative intensity of the spectral lines of the unfiltered sodium light are also indicated.

In order to obtain this yellow artificial illumination, incandescent lamps may be used with a coloured bulb, of orange "Selectiva" glass for example, or of sodium lamps, which if desired may also be provided with an orange "Selectiva" vacuum jacket in order to remove the green and blue components which may still occur to some extent in the light of sodium lamps. The light of these orange Selectiva lamps is not unpleasant to work under, while an additional great advantage is that orange Selectiva glass is a coloured glass. With these lamps therefore there are no difficulties due to scaling off, or to lack of fastness of colour or stability toward heat, which may occur when a lamp of ordinary glass is covered with a layer of lacquer. Moreover, it will be difficult to find a suitable lacquer of the right colour.

Fig. 2 shows the variation of transmissibility of orange Selectiva glass in the cold state (*I*), and at the operating temperature of the lamp (*II*), with the wave length, while *III* shows this variation for an appropriate kind of green paint. Furthermore the relative spectral composition of natural unfiltered sodium light is represented, from which it may be seen that sodium light possesses practically no intensity, especially after passing through Selectiva glass in the spectral region which is well transmitted by the green paint. These sources of light and this paint therefore form together a suitable combination for wartime illumination. We shall now examine how the permissible level of artificial illumination and the corresponding transmissibility of the windows to be blacked out can be determined in practical cases. We must however first know the permissible brightness seen from the outside of the windows at night.

Permissible brightness of the windows

The permissible brightness of the light openings depends upon the solid angle within which the observer sees the illuminated surface. We begin with the relation already indicated by Bouma in this periodical (*fig. 3*) between this angle and the intensity of illumination E_0 produced on the eye of the observer by the radiating surfaces (assumed circular) in order to be seen from a perpendicular direction. These data may also be applied to windows surfaces which are not too elongated in form. It may be seen that for small angles of vision it is only a question of the total light intensity, while for large angles of vision it is only the brightness that is important. The values given here, however, refer to observations made in the laboratory and according to Bouma the intensities of illumination which just escape notice on a starlight night are found by multiplying the values from fig. 3 by a factor 100.

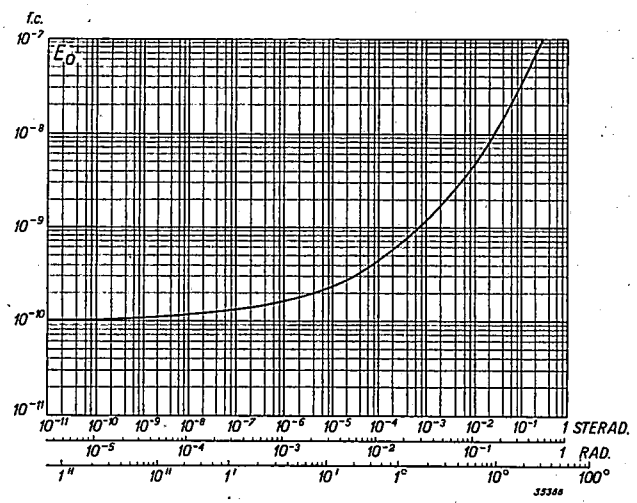

Fig. 3. Intensity of illumination E which circular radiating surfaces must produce on the eye of the observer in order to be visible in a perpendicular direction, as a function of the angle within which they are seen.

With the help of these data the relation represented in *fig. 4* between the permissible brightness B for horizontal windows vertically under the aeroplane and the area of their surface is found for different flying altitudes. For non-horizontal windows

these values for the permissible brightness may be multiplied by a factor K, greater than unity.

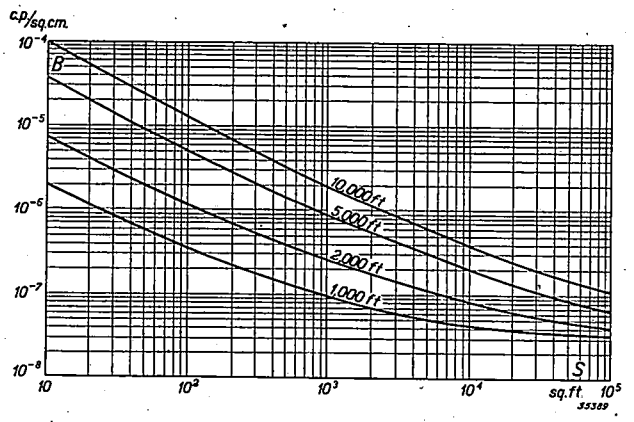

Fig. 4. The maximum permissible brightness B in c.p./sq.cm for horizontal windows with a surface area of S sq.ft is shown for different flying altitudes.

On the basis of the situation sketched in *fig. 5* we shall try to find the direction of vision making the angle α with the horizontal plane at which the greatest intensity of illumination is produced on the eye of an observer flying at a given altitude h above the earth in the vertical plane perpendicular to the window. From this the above-mentioned factor K can be calculated. The windows V make an angle β with the horizontal, and we shall assume that they radiate diffusely according to Lambert's law with a luminous intensity I perpendicular to their surface. If the observer is at a distance r at an angle α with the horizontal, he receives an intensity of illumination:

$$E = \frac{I}{r^2} \cos(\alpha + \beta - 90°) = \frac{I}{r^2} \sin(\alpha + \beta) \quad . \quad . \quad . \quad (1)$$

Since the altitude $h = r \sin \alpha$, this becomes:

$$E = \frac{I}{h^2} \sin^2 \alpha \sin(\alpha + \beta) \quad . \quad . \quad . \quad . \quad . \quad . \quad . \quad . \quad . \quad . \quad . \quad (2)$$

The most dangerous situation is that where α has a value such that this expression reaches a maximum. This occurs at:

$$\operatorname{tg} \alpha = \frac{3 + \sqrt{9 + 8 \operatorname{tg}^2 \beta}}{2 \operatorname{tg} \beta} \quad . \quad . \quad . \quad . \quad . \quad . \quad . \quad . \quad . \quad . \quad . \quad (3)$$

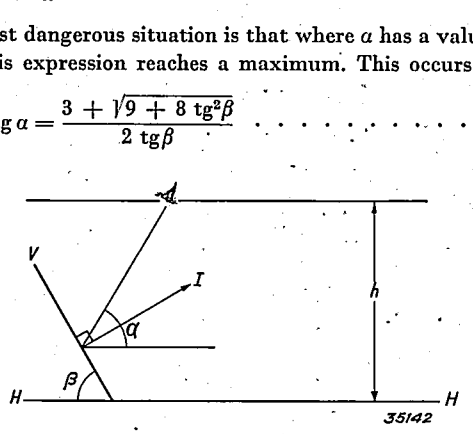

Fig. 5. The illuminated windows V make an angle β with the horizontal plane H. Their maximum luminous intensity is I. At an altitude h the window V is observed under an angle α with the horizontal plane by an observer flying in a vertical plane perpendicular to the window.

The direction α with the horizontal, in which the greatest intensity of illumination occurs on the eye, is represented in *fig. 6* as a function of the angle β which the windows make with the horizontal. With vertical windows the most dangerous direction of vision is at an angle β of nearly 55°.

The factor K, by which the value for the permissible brightness to be read off in fig. 4 in the case of non-horizontal windows may still be multiplied, is according to formula (2), now given by:

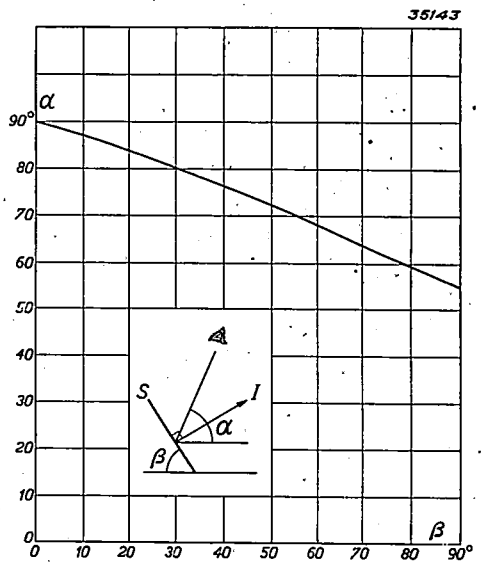

Fig. 6. The direction α with the horizontal plane, at which the greatest intensity of illumination strikes the eye, as a function of the angle β between the plane S of the window and the horizontal plane.

$$K = \frac{1}{\sin^2 \alpha \sin(\alpha + \beta)}, \quad . \quad . \quad . \quad . \quad . \quad . \quad . \quad . \quad . \quad . \quad . \quad (4)$$

where for the sake of security in the most unfavourable case the value of α which follows from formula (3) must be substituted. In *fig. 7* factor K is plotted as a function of the slope β of the windows.

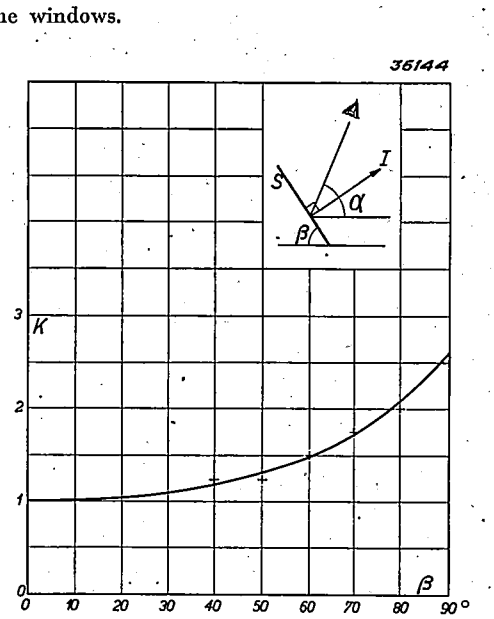

Fig. 7. For windows which make an angle β with the horizontal plane, the permissible intensity of illumination calculated for horizontal windows may be multiplied by a factor K. Several rough values of K which may be used in practice are indicated in the figure by crosses.

For several values of the slope β (fig. 5) of the windows the following values of K may be used in practice:

β	0°	30°	40°	50°	60°	70°	80°	90°
K	1	1,1	1,2	1,25	1,5	1,75	2	2,5

From now on we shall limit ourselves to a consideration of a flying altitude of 2 000 ft. If for some reason it is necessary to take other altitudes into consideration, it is only necessary to multiply the brightness found for 2 000 ft by a factor H which may be deduced from fig. 4. For the sake of simplicity this factor H is drawn in *fig. 8* as a function of the window area for several flying altitudes. It may clearly be seen that for very large surfaces it is only a question of their brightness, so that the flying altitude is of little importance.

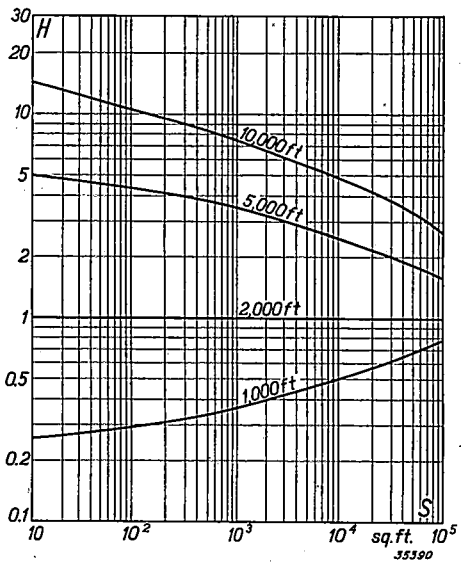

Fig. 8. For several altitudes the factor H is given as a function of window surface area S. H is the factor by which a permissible brightness calculated for an altitude of 2000 ft must be multiplied.

Level of illumination and transmissibility of the windows

From the brightness which is permissible for the light openings according to the foregoing considerations we shall now deduce the level of illumination which the interior artificial illumination may produce without being seen from the outside. With a given window area it is then a question whether or not this can be covered with a coloured coating of such a thickness that the necessary artificial illumination is sufficiently blacked out at night without the transmissibility for daylight becoming too low.

The degree to which the different spectral components of daylight are absorbed by the green layer varies very much, and therefore the transmissibility t for yellow light and that t_d for daylight for different thicknesses of paint are not simply proportional to each other. The relation between t and t_d (both expressed in %) has been measured for different kinds of paint. In *figs. 9* and *10* such paint-characteristics are reproduced for two different types of paint A and B. Curves *1* and *2* are for filtered and unfiltered sodium light respectively, and *3* is for the light of incandescent lamps in bulbs of orange Selectiva glass.

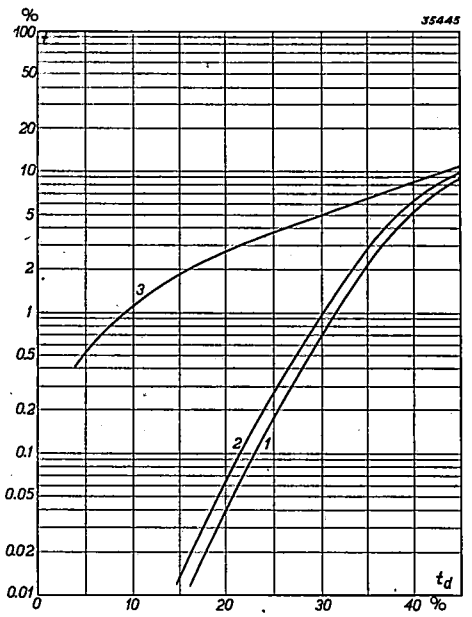

Fig. 9. For a given kind of paint A the transmissibility t for yellow light is represented as a function of the transmissibility t_d for daylight. Curves *1* and *2* are for filtered and unfiltered sodium light respectively. Curve *3* refers to the light of electric lamps fitted with orange Selectiva glass bulbs.

With a given transmissibility for daylight a combination of paint and kind of light is more suitable, the less yellow light is transmitted, *i.e.* the lower the characteristic. If for example with filtered sodium lighting (curve *1*) a daylight transmissibility of 25 per cent is required, it is found that upon use of paint A the transmissibility for the artificial light is about 0.18 per cent, while with paint B it is about 3.5 per cent. In combination with sodium light therefore paint A is much better than paint B. If artificial illumination with orange incandescent lamps is used the two kinds of paint are found to have the same transmissibility of nearly 2 per cent for the yellow light, with a daylight transmissibility of 15 per cent; for greater values of t_d paint A is better than B, but at smaller values of t_d paint B is better.

If a daylight transmissibility of about 25 per cent is required, as will usually be necessary for workshops and similar localities, sodium illumination together with paint A is the most suitable

combination. If a daylight transmissibility of less than 15 per cent is adequate, as for example is usually the case in entrance halls and stairways, the combination of filtered incandescent light and paint B may well be used.

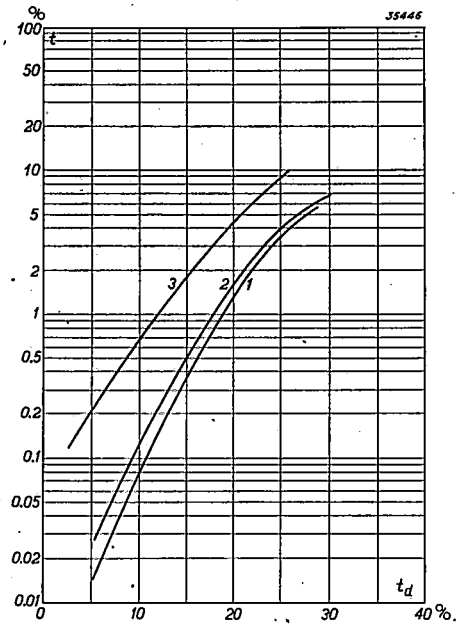

Fig. 10. Paint characteristics similar to those in fig. 9 for another paint (B).

In order to be able to deal with practical cases by means of our graphs it is first necessary to define more precisely what values must be taken for the different quantities occurring in them. For the area of the illuminated window surface S, which occurs in fig. 4, in the case of a roof or wall with many windows separated by dark strips one must take the total surface observed from the direction of the aeroplane, while as brightness the average brightness over this total surface may be taken.

In fig. 4 the brightness B permissible on the outside is given for every total window surface area. If one deduces from this the intensities of illumination E which may be permissible for the interior artificial illumination, the transmissibility t for the yellow light used, determined by the paint characteristic of fig. 9 or 10, is not of itself sufficient, but the proportionality factor between the intensity of illumination inside and the brightness of the light openings should also be known. Different cases may occur according as the glass of the window is diffusing or clear. With clear glass one sees through the window the illuminated background of the room whereby it is of course assumed that the light source itself is invisible. If this background has an illumination intensity of E_g, and if the reflectivity of the background is ϱ per cent, while t is the transmissibility expressed in per cent of the yellow artificial light following from fig. 9 or 10, the brightness observed through the window becomes:

$$B_g = 1.076 \cdot 10^{-7} \frac{t_g \varrho E_g}{\pi} \quad \cdots \quad (5)$$

With a diffusing glass pane the brightness on the outside is:

$$B_r = 1.076 \cdot 10^{-5} \frac{t_g E_r}{\pi}, \quad \cdots \quad (6)$$

where E_r represents the intensity of illumination on the inside of the windows. Depending on the shape of the room and the nature of the lighting system, there will be a definite relation between this E_r and the intensity of illumination E_g of the background, which may be represented by:

$$E_g = \frac{a E_r}{100} \quad \cdots \quad (7)$$

where a represents a constant factor expressed in per cent. The brightness for the diffusing glass may therefore be expressed as follows in terms of the intensity of illumination of the background:

$$B_r = 1.076 \cdot 10^{-7} \frac{t_g a E_g}{\pi} \quad \cdots \quad (8)$$

If we now compare formula (8) with formula (5) we see that for the case where $a < \varrho$ diffusing glass is preferable, when $a > \varrho$, however, clear glass is better.

For a normal background one may in general let ϱ equal 30 to 35 per cent, and with an ordinary indoor illumination without good shade fixtures clear glass windows will usually be preferred. The sharp reflections which may occur on the pieces of work are in this case neglected, but they are usually too small in size to be able to draw the attention of an observer from the air. In the case of frosted glass windows this difficulty does not arise, since in that case the surface of the window acts as a secondary light source. In factories in which many white objects are present (white paper in printing establishments, light coloured textiles in textile mills), one must count on a higher coefficient of reflection of 60 to 70 per cent, and in such cases diffusing glass will be preferable, especially when the light sources are so shaded that they produce no direct illumination on the windows.

Diagrams

In order to be able in a simple way to obtain an idea of the levels of illumination which may be permitted in the room in question in combination

with the desired values for daylight transmissibility, diagrams may be used which give a direct relation between the permissible intensity of illumination E, the daylight transmissibility t_d and the window surface area S, while all auxiliary quantities are eliminated.

In *fig. 11* such a diagram is given for filtered sodium light in combination with paint A (*i.e.* corresponding to curve *1* in fig. 9). In this diagram from the diagram may be permitted. If the windows are diffusing only about 0.3 of the intensity which would follow from the diagram must be allowed on the inside of the windows. From this diagram one may also read off immediately the maximum window surface area which can be blacked out satisfactorily in this way, if given minimum requirements are made not only for the daylight transmissibility but also for the level of artificial illumination.

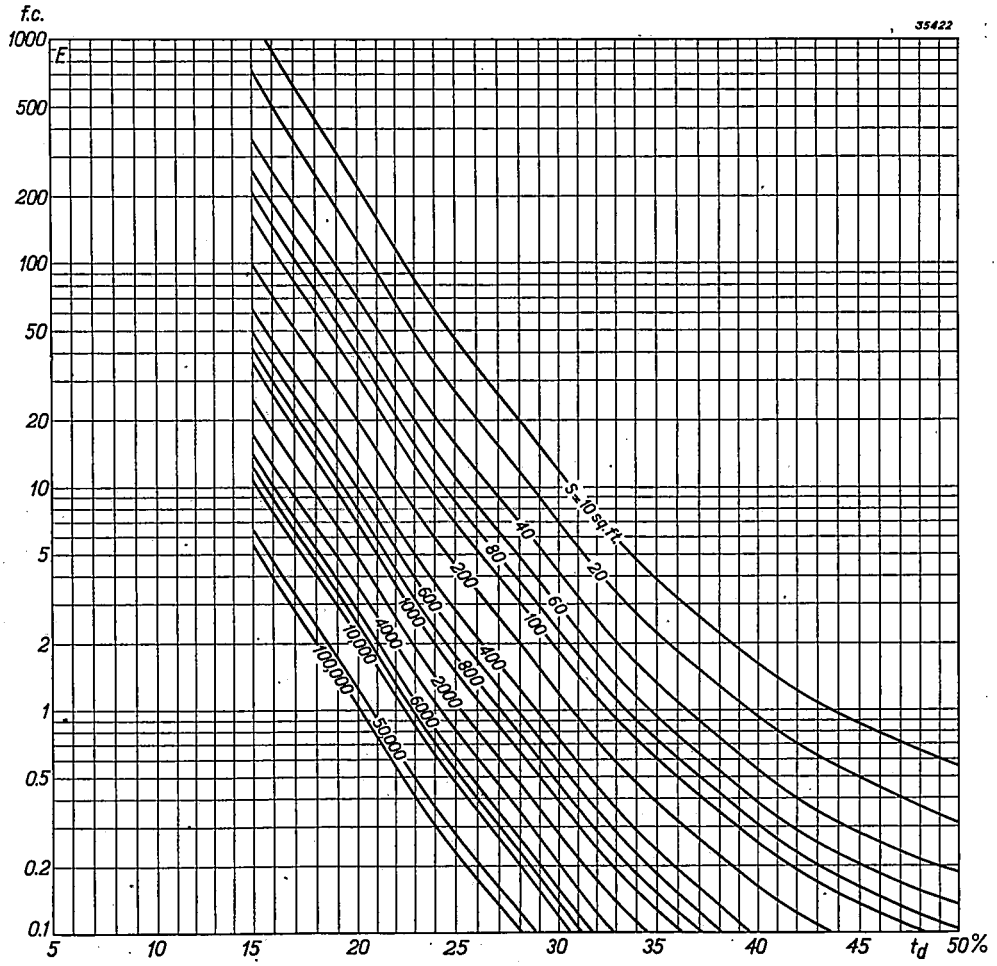

Fig. 11. By means of this graphical representation the relation is determined which exists when filtered sodium light is used in combination with paint A between the daylight transmissibility t_d, the permissible intensity of illumination E with horizontal, clear glass panes, and the area S of the window surface which must be blacked out, for a flying altitude h of 2 000 ft.

therefore one may immediately read off the combination of daylight transmissibility and intensity of artificial illumination with which horizontally placed windows with a given area may be blacked out satisfactorily in this way. According to the foregoing, it is advisable in printing establishments and other industries where the average background is light in colour to allow only half the intensity of illumination which would follow from the diagram. If the windows are vertical an intensity of illumination which is 2.5 as great as what would follow

Fig. 12 refers to filtered incandescent light in combination with paint B (*i.e.* corresponding to curve *3* of fig. 10). It may be seen that good results may be obtained if the window surfaces are not too large, and if a moderate daylight transmissibility is considered satisfactory.

With diagrams such as those in figs. 11 and 12 it is possible to answer various questions. If a room with a given window surface area S must be provided with wartime illumination, it may be asked for example how much one would lose in

permissible daylight transmissibility if more artificial light should be demanded. Fig. 11 immediately supplies the following answer to this question. If for example approximately a 30 per cent more intense artificial illumination were desired, this would mean a decrease of the daylight transmissibility of only one per cent from 26 per cent to 25 per cent for instance.

The manner in which this diagram may be used in practice will be illustrated in the following by means of some simple examples.

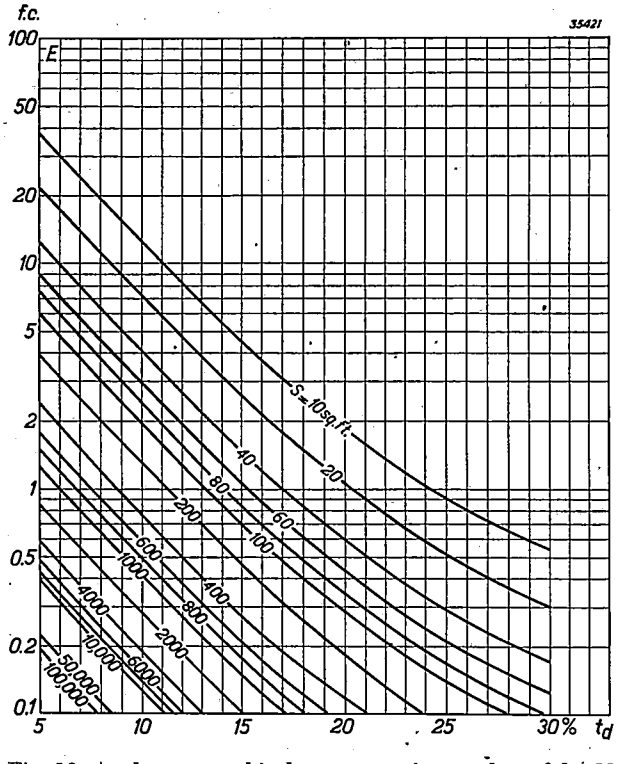

Fig. 12. Analogous graphical representation to that of fig. 11; here, however, for the light of orange Selectiva glass lamps in combination with paint *B*.

Practical examples

In a workshop with a vertical window surface area of 100 sq.ft a wartime illumination system of sodium lamps in orange Selectiva vacuum jackets is installed, while the diffusing panes are to be covered with paint *A* in such a way that they still transmit 25 per cent of the daylight. From fig. 11 the intensity of illumination may be found which the sodium lamps may produce on the inside surface of the frosted glass. For horizontal clear glass windows we find that the permissible intensity on the piece of work would be 7 ft.c. For vertical windows this may be multiplied by 2.5, while in order to obtain the intensity of illumination on the inner side of the diffusing glass windows this result must still be multiplied by 0.3. The result is the following:

$$0.3 \times 2.5 \times 7 = 5.25 \text{ ft.c.}$$

If a much higher horizontal intensity of illumination were desired, and an illumination of 20 ft.c. on the inside of the windows were unavoidable, it is equivalent to $E = \frac{20}{2.5 \times 0.3} = 27$ ft.c in fig. 11, where for a surface of 100 sq.ft. a daylight transmissibility of approximately 21 per cent is found. The question then is whether, for the case in question, this is sufficient.

As a second example we shall consider the case of a roof with a surface of 6 000 sq.ft, 40 per cent of which consists of diffusing glass, and which makes an angle of 70° with the horizontal. It is desired to retain 25 per cent of the daylight, and filtered sodium light is to be used in combination with paint *A*. In fig. 11 *E* is found to be about 0.61 ft.c. The permissible intensity of the illumination on the inside of the diffusing windows, which only occupy 0.4 of the total surface area, may be taken 2.5 as high, and must, moreover, due to the 70° slope, be multiplied by a factor 1.75, and due to being diffusing by a factor 0.3, so that the result would be about 0.8 ft.c. By screening off all direct illumination it must therefore be tried to keep the intensity of illumination on the inside of the windows below 0.8 ft.c. If this is impossible, part of the windows must be covered by blinds, and the others fitted out by the filter method. If in this case it were only necessary to guarantee invisibility for a flying altitude of at least 5 000 ft. then according to fig. 8 the intensity of illumination could be 2.7 times higher, *i.e.* 2.16 ft.c.

THE HUM DUE TO THE MAGNETIC FIELD OF THE FILAMENTS IN TRANSMITTING VALVES

by K. POSTHUMUS.

621.396.822 : 621.396.615.1

When the filament of a directly heated electron tube is fed with alternating current, a periodic change in the rhythm of the mains frequency occurs in the properties of the tube. In particular the anode current will exhibit a periodic fluctuation which gives rise to hum. In the case of transmitting valves the most important cause of hum is the periodically changing magnetic field of the filaments. The influence of the magnetic field is discussed theoretically in this article. The results are tested by comparing them with the results of measurements carried out on the transmitting valve, type TS 20/30. In conclusion a theoretical and experimental study is given of attempts to decrease hum by dividing the filament system into a number of parts which are fed with alternating currents of different phase.

When the filaments of directly heated electron tubes are heated with alternating current in order to simplify the connections, the properties of the tube will in general exhibit a periodic fluctuation in the rhythm of the A.C. voltage. This is understandable, since different quantities which influence the operation of the tube vary periodically. The following properties are chief among these:

a) the temperature of the filament,
b) the voltage along the filament,
c) the magnetic field of the filament.

With small electron tubes, such as ordinary radio amplifier valves, the filaments are so thin that upon direct heating with alternating current their temperature fluctuations would assume values far beyond those permissible. Indirectly heated cathodes are therefore used, which have a much larger heat capacity. Moreover in this case the filament is shielded by a nickel tube by which the fluctuations mentioned under b) are also avoided. By winding the filament bifilarly the fluctuations mentioned under c) can be made practically harmless.

In the case of large transmitting valves, for instance water-cooled transmitting valves for high power, the filaments are in general so thick that their temperature scarcely fluctuates at all when they are heated with alternating current. The variations in the voltage along the filament and those of the magnetic field of the filament, however, may cause fairly considerable fluctuation of the anode current, so that the high-frequency anode alternating current experiences a modulation which is later observed as hum in the reception. The influence of the magnetic field of the filament is usually the greater of the two causes of hum, and this will be discussed in some detail in this article.

If we wish to study mathematically the influence of the magnetic field on the motion of the electrons, we must make several simplifying assumptions about the geometric configuration of the valve. In the case of water-cooled transmitting valves a number of filaments are arranged to form a cylindrical shell, while around this at a certain distance is a second cylinder (the control grid) which has a different potential from that of the filaments.

We shall consider both cylindrical surfaces as equipotential surfaces, and assume that the inner cylinder is uniformly covered with emitting wires. The problem is then reduced to that of two concentric cylinders between which electrons move under the influence of a radial electric field and a magnetic field perpendicular to the electric field and to the axis of the cylinder. We shall simplify the problem still further by taking plane electrodes instead of the cylindrical electrodes (see *fig. 1*).

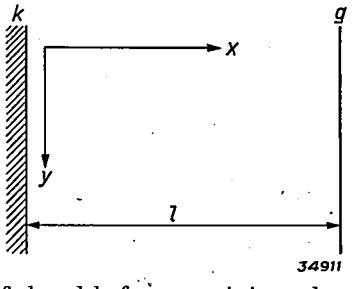

Fig. 1. Simplified model of a transmitting valve for the calculation of the influence of the magnetic field due to the heating current, *k* plane cathode surface, *g* plane grid surface at a distance *l* from the cathode. The magnetic field is perpendicular to the plane of the drawing.

In the following the anode current of the model, so obtained and differing so much from the actual transmitting valves, will be calculated as a function of the magnetic field. We shall then ascertain how conclusions can be drawn from the results about the behaviour of valves actually constructed, and to what degree the results are confirmed experimentally.

Statement of the problem

We imagine the cathode of fig. 1 to be extended infinitely in all directions of the y-z plane, while the electrons move in the x direction with the initial velocity zero. The magnetic field H varies in the z direction and is assumed to be dependent only on x.

The electrons which leave the cathode are accelerated in the x direction by the fall in electric potential V. The value of the field is determined not only by the potentials of the various electrodes, but also by the space charge of the electrons situated between cathode and control grid. This space charge, which is proportional to the current, exerts a repelling action on the following electrons, which are just about to leave the cathode, in other words, it lowers the field strength at the surface of the filament. At a certain value of the current the electric field at the surface of the filament vanishes, and this value is the current which actually prevails. If a still larger number of electrons per second should be emitted than that which corresponds to this current, the electric field would become negative, and would drive back just enough of the electrons to bring the current back to the limiting value mentioned.

Due to the presence of the magnetic field the electrons will describe curved paths, and will therefore be unable to leave the filament as quickly as would otherwise be the case. The space charge is thus increased, and will therefore cause the electric field at the cathode surface to vanish at a smaller limiting value of the anode current.

This decrease in the anode current due to the magnetic field forms the object of our calculations.

The equations of motion of an electron

If $-e$ is the charge and m the mass of an electron, the motion of the electron satisfies the following equations:

$$e\frac{\mathrm{d}V}{\mathrm{d}x} - H(x)\, e\frac{\mathrm{d}y}{\mathrm{d}t} = m\frac{\mathrm{d}^2x}{\mathrm{d}t^2} \quad \cdots \quad (1)$$

$$H(x)\, e\frac{\mathrm{d}x}{\mathrm{d}t} = m\frac{\mathrm{d}^2y}{\mathrm{d}t^2} \quad \cdots \quad (2)$$

In a previous article in this periodical [1]), in explaining the operation of the magnetron, the solution of these equations was dicussed for the case in which the electric field, $E = -\mathrm{d}V/\mathrm{d}x$, is constant throughout the whole of space. In our case, in which the potential is influenced by the space charge, the method of solution there given is however unsuitable and we must find another.

If we multiply (1) by $\mathrm{d}x/\mathrm{d}t$, and (2) by $\mathrm{d}y/\mathrm{d}t$ we can eliminate $H(x)$ by adding the two equations. One then obtains the following:

$$e\frac{\mathrm{d}V}{\mathrm{d}t} = m\left(\frac{\mathrm{d}x}{\mathrm{d}t}\frac{\mathrm{d}^2x}{\mathrm{d}t^2} + \frac{\mathrm{d}y}{\mathrm{d}t}\frac{\mathrm{d}^2y}{\mathrm{d}t^2}\right),$$

from which it follows that:

$$\tfrac{1}{2}\, m\left[\left(\frac{\mathrm{d}x}{\mathrm{d}t}\right)^2 + \left(\frac{\mathrm{d}y}{\mathrm{d}t}\right)^2\right] = e\, V(x) \quad \cdots \quad (3)$$

This already takes into account the condition that at the surface of the filament ($V = 0$) the x component as well as the y component of the velocity disappears. Equation (3) is nothing else than the law of conservation of energy, and expresses the fact that the magnetic field does no work.

In order to carry the integration farther we must know $V(x)$ as a function of the coordinate. $V(x)$ is equal to zero at the surface of the cathode ($x = 0$), and has a certain effective value V_e in the grid plane ($x = l$). The variation in the space between grid and cathode is determined by the differential equation.

$$\frac{\mathrm{d}^2V}{\mathrm{d}x^2} = 4\pi\varrho, \quad \cdots \quad (4)$$

where ϱ is the density of the space charge. Between the space charge ϱ, the local velocity $\mathrm{d}x/\mathrm{d}t$ of the electrons and the current i the following relation exists:

$$i = \varrho(x)\frac{\mathrm{d}x}{\mathrm{d}t} \quad \cdots \quad (5)$$

The current i indicated in equation (5) is the so-called "convection current" which is caused by the motion of charged particles. Since the magnetic field changes relatively slowly (compared with the transit time of the electrons) we may consider the situation as practically stationary. The convection current then corresponds to the total current and is therefore not a function of x.

The calculation of the anode current

From equations (4) and (5) it follows that:

$$\frac{\mathrm{d}^2V}{\mathrm{d}x^2} = \frac{4\pi i}{\dfrac{\mathrm{d}x}{\mathrm{d}t}} \quad \cdots \quad (6)$$

This equation may be integrated if $\mathrm{d}x/\mathrm{d}t$ is known as a function of x. We first calculate from equation (2):

$$m\frac{\mathrm{d}y}{\mathrm{d}t} = e\int_0^x H(x)\,\mathrm{d}x,$$

[1]) Philips techn. Rev. 4, 189, 1939.

having made use of the fact that for $x = 0$ dy/dt disappears. The integral on the right we shall call $F(x)$ in the following. With the help of equation (3) we now find that:

$$\frac{dx}{dt} = \sqrt{2\frac{e}{m}V - \left[\frac{e}{m}F(x)\right]^2}$$

and thus by substituting in (6):

$$\frac{d^2V}{dx^2} = \frac{4\pi i}{\sqrt{2\frac{e}{m}V - \left[\frac{e}{m}F(x)\right]^2}} \quad \ldots \quad (7)$$

In order to solve this differential equation we must make a special choice of the function F, that is, of the magnetic field H. In practice the variation of the magnetic field may be very different according as the currents through the different filaments are all in the same direction, or alternately in opposite directions, or follow some other rule. We shall consider a number of different cases, and investigate whether it is possible to draw a general conclusion from them.

1. *No magnetic field*

If the magnetic field may be neglected, and thus if $F(x) = 0$, equation (7) passes over into the well known differential equation of Langmuir which may be solved by setting

$$V = k \cdot x^{4/3} \quad \ldots \ldots \quad (8)$$

This can easily be tested by differentiating equation (8) twice, and substituting d^2V/dx^2 and V in differential equation (7). One then finds that this equation is satisfied if the coefficient k has a definite value, namely:

$$k = \left(\frac{9\pi i}{\sqrt{2e/m}}\right)^{2/3} \quad \ldots \ldots \quad (9)$$

The solution of the differential equation thus found satisfies the above-mentioned condition that the field-strength $-dV/dx$ equals zero at the surface of the cathode ($x = 0$). The current corresponding to this is therefore the desired anode current. By filling in the above value of k in equation (8) one finds:

$$18\pi i\frac{e}{m} = \frac{\left(\frac{2e}{m}V\right)^{3/2}}{x^2}.$$

V is here the potential at the point x which may be chosen arbitrarily. When x is taken equal to l then $V = V_e$, and one obtains:

$$18\pi i\frac{e}{m} = \frac{\left(\frac{2e}{m}V_e\right)^{3/2}}{l^2} \quad \ldots \ldots \quad (10)$$

From this relation the current i is known, if the distance l and the potential difference V_e in the plane of the grid are given.

We shall now examine how this current changes due to the presence of the magnetic field of the filament.

2. *Weak magnetic field*

The differential equation may be solved for a fairly general form of the magnetic field, which must however satisfy the condition that H depends only on x, when the restriction is introduced that the magnetic field is weak, and thus that F is always small. In that case we may substitute for the square root occurring in differential equation (7) a development in a series to obtain a good approximation. The influence of the magnetic field on the variation of the potential may then be represented by a small correction in the variation of potential between the electrodes calculated above for $H = 0$. Instead of equation (8) therefore we write:

$$V = \left(\frac{9\pi i}{\sqrt{\frac{2e}{m}}}\right)^{2/3} x^{4/3} + w(x) \quad \ldots \ldots \quad (11)$$

and when the correction term w is known, we may deduce from this equation the manner in which the current i varies with the magnetic field which determines the term w. In order to determine w equation (11) must be differentiated twice, and the quantity d^2V/dx^2 so obtained, as well as V must be substituted in the original differential equation (7). When in the resulting expression, the square root is expanded into a series, of which only the first two terms are considered, a simple linear differential equation of the second order is obtained for w, namely:

$$\frac{d^2w}{dx^2} + \frac{2}{9}\frac{w}{x^2} = \frac{1}{9}\frac{e}{m}\left(\frac{F(x)}{x}\right)^2.$$

This equation is easily solved. The "homogeneous solution" may for example first be determined, which occurs when the right-hand member is equal to zero, and then the right-hand member may be considered by the so-called method of "variation of the constants". The result of this calculation, which we shall not give in detail [2]), is:

[2]) For the intermediate calculations see Philips Transm. News. No. 1, 1940, where the calculations are published in a considerably more detailed form. In addition to the case of plane electrodes the case of cylindrical electrodes is also dealt with.

$$w=\frac{x^{2/3}}{3}\int_0^x \xi^{-5/3}\frac{e}{m}\left[F(\xi)\right]^2 \mathrm{d}\,\xi-\frac{x^{1/3}}{3}\int_0^x \xi^{-4/3}\frac{e}{m}\left[F(\xi)\right]^2 \mathrm{d}\xi \tag{12}$$

When the function $w(x)$ so obtained is substituted in equation (11), and the resulting equation is again solved for the current, we find that the current is altered by the presence of the magnetic field.

In order to obtain comprehensible results we choose for the variation of the magnetic field the special form:

$$H(x) = H(x/l)^n,$$

where n must be a negative power since the magnetic field becomes weaker with increasing value of x. Without indication of place H indicates here and in the following the field strength in the grid-place $(H(l))$.

The function $F(\xi)$ which appears in (12) now becomes:

$$F(\xi) = \int_0^\xi H(x)dx = \frac{H}{n+1}\,\xi^{n+1}.$$

For this form of $F(\xi)$ the integration in equation (12) can immediately be performed. The expression for w so obtained is substituted in equation (12). When the resulting equation is solved for the anode current we obtain:

$$\left.\begin{aligned} 18\,\pi\, i\,\frac{e}{m} &= \left(\frac{2e}{m}V_e\right)^{3/2}\left[\frac{1}{l^2}-\frac{1}{6}\,\frac{e\,H^2}{m\,V_e\,N}\right], \\ \text{where}\quad N &= \left(n+1\right)^2\left(2\,n+\frac{5}{3}\right)\left(2\,n+\frac{4}{3}\right). \end{aligned}\right\} \tag{13}$$

This is the final result. It may be seen that the magnetic field acts to lower the anode current, and this lowering is proportional to the square of the magnetic field and inversely proportional to the effective grid voltage. This is of course only a first approximation, and it may be expected that higher powers of H will appear with strong magnetic fields.

Discussion of the results

Further consideration of the calculation shows that the result given in equation (13) is only reliable for values of n which are not more negative than $-1/2$. For a number of values of n between zero and $-1/2$ the variation of the anode current as a function of the magnetic field in the plane of the grid as calculated according to equation (13) is shown in *fig. 2* (dotted lines). The parameters of the six curves give the exponent n in the above formula for the field strength.

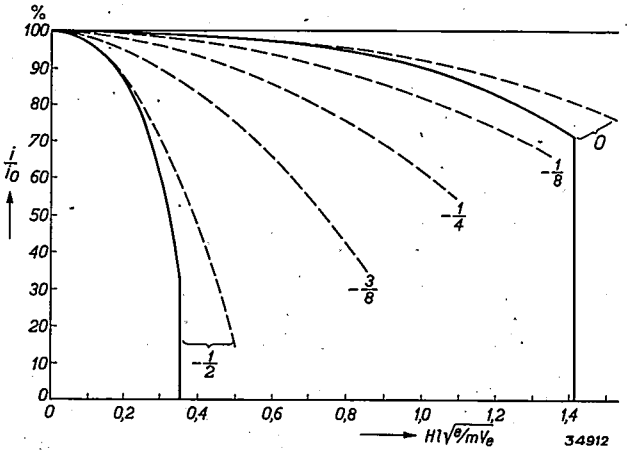

Fig. 2. Variation of the anode current in per cent of the maximum value as a function of the magnetic field strength in the grid plane l (expressed by the dimensionless quantity $H/\sqrt{e/mV_e}$). The parameters indicate the value of the exponent n in the expression for the variation of the magnetic field: $H(x) = H/(x/l^n)$. Continuous curves: $n = 0$ and $n = -1/2$. Broken line curves: variation calculated in a first approximation (equation (13)) for $n = 0, -1/8, -1/4, -3/8, -1/2$.

When the variations of the anode current as a function of the filament current (*i.e.* as a function of the magnetic field) are examined with the help of an oscillograph, it is found that the parabolic curves given in fig. 2 correspond very well with actuality if the decrease in the anode current is not more than about 25 per cent. The further decrease in the anode current with increasing filament current, and thus with increasing field, takes place more rapidly than is to be expected from the calculation.

In order to find out to what extent this discrepancy can be explained theoretically an attempt was also made to find exact solutions for equation (7) in addition to the above approximation. This is possible for $n = 0$, *i.e.* with a homogeneous magnetic field and for $n = -1/2$, *i.e.* for $H(x) = H/\sqrt{x/l}$. The calculation, which we shall not discuss here, leads to the continuous curves of fig. 2. If these are compared with the broken line curves corresponding to the same value of n, a good agreement is actually found at low fields H, while the current at high fields decreases more rapidly and suddenly disappears entirely at a definite maximum field strength.

The exact calculated curves for $n = 0$ and $n = -1/2$ are very similar. This similarity becomes more pronounced when instead of the current, the percentage decrease of current is used as ordinate,

and as abscissa, instead of the field strength, the ratio H/H_m, when H_m is the critical field which causes the anode current to disappear suddenly. In *fig. 3* the curves for $n = 0$ and $n = -1/2$ are shown for these new coordinates. It may be seen that the variation is practically proportional for all field strengths, and that the curve for $n = -1/2$ is a factor 2.4 higher than the curve for $n = 0$.

The good agreement between the two curves, which refer to two very different field distributions, makes it probable that the variation of the decrease in current as a function of H/H_m indicated by this curve may be assumed to hold for every field distribution except for a factor. This circumstance makes it possible to apply the results found on the very much simplified model to actually constructed transmitting valves with some chance of success, as will presently be done in drawing our practical conclusions.

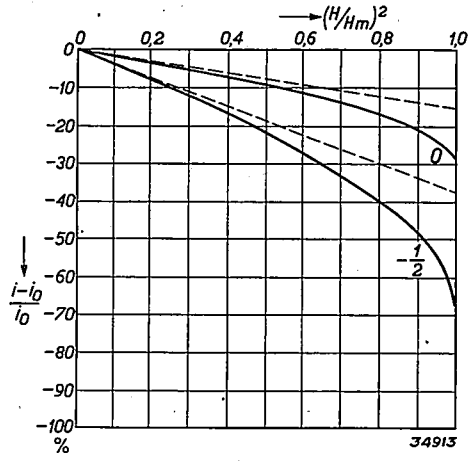

Fig. 3. Percentage decrease of the anode current as a function of H/H_m for $n = 0$ and $n = -1/2$. H_m is the value of the field at which the anode current suddenly disappears. The curves have practically the same shape, with the difference that the lowering at $n = -1/2$ is a factor 2.4 greater than that at $n = 0$.

The "hum" of transmitting valves

In *fig. 4* the accurately calculated variation (continuous line) of the anode current as a function of H/H_m is again plotted for a field distribution:

$$H(x) = \frac{H}{\sqrt{x/l}}.$$

The percentage decrease of the anode current as a function of H/H_m can be very well approximated by the following series:

$$\frac{i_0 - i}{i_0} = 0{,}375\left(\frac{H}{H_m}\right)^2 + 0{,}12\left(\frac{H}{H_m}\right)^4 + 0{,}18\left(\frac{H}{H_m}\right)^{26}$$

which gives the points in the figure. If we assume that this formula is valid, except for a factor, for any given distribution of the magnetic field between the plane of the cathode and that of the grid, we find the following general formula for the

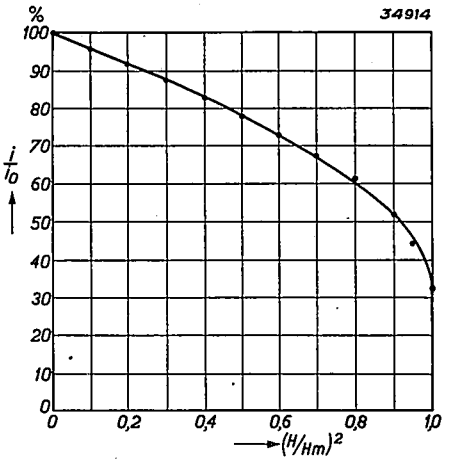

Fig. 4. Variation of the anode current in per cent of the maximum value as a function of H/H_m for a field distribution $H(x) = H/\sqrt{x}$. The curve may be represented by:

$$i = i_0\ (1 - 0.375\ (H/H_m)^2 - 0.12\ (H/H_m)^4 - 0.18\ (H/H_m)^{26}.$$

anode current as a function of the effective grid voltage and the magnetic field:

$$\left.\begin{aligned} \frac{e}{m}\pi i &= \frac{1}{18\,l^2}\left(2\,\frac{e}{m}\,V_e\right)^{3/2}\left[1 - p\,G\left(\frac{H}{H_m}\right)\right], \\ \text{where} \quad G\left(\frac{H}{H_m}\right) &= 0{,}375\left(\frac{H}{H_m}\right)^2 + 0{,}12\left(\frac{H}{H_m}\right)^4 + 0{,}18\left(\frac{H}{H_m}\right)^{26}. \end{aligned}\right\} \quad (14)$$

p is here a factor which depends upon the distribution of the magnetic field. For the above-mentioned field $H(x) = H/\sqrt{x/l}$, $p = 1$, for a homogeneous field $p = 1/2.4 \sim 0.4$.

If p is known, it is possible with the help of equation (14) to calculate how the anode current varies when a transmitting valve is fed with sinusoidal alternating current. Since the quantity H in equation (14) is proportional to the filament current, the anode current i will be composed of a D.C. component and a ripple whose fundamental frequency is equal to twice the mains frequency. In addition the ripple also contains higher harmonics which come from the terms with $(H/H_m)^4$ and $(H/H_m)^{26}$.

The calculation is not difficult but rather complicated [3]) and leads to formulae which are not very clear. We shall therefore confine ourselves to a general discussion of the results.

---

[3]) See the article cited in note [2]).

Hum as a function of the effective anode current

The variation of the hum as a function of the effective anode current can be comprehended qualitatively on the basis of equation (13), in which the anode current is represented in first approximation as a function of the effective potential V_e and the magnetic field H in the plane of the grid. This equation has the following character:

$$i = A\, V_e^{3/2} - B\, V^{1/2}\, H^2,$$

where A and B are constants which are determined by the construction of the transmitting valve.

With a sinusoidally alternating heating current, $H(l)$ is also sinusoidal. If ν is the mains frequency and H_0 the amplitude of the sinusoidal vibration, then:

$$H^2 = H_0^2 \sin^2 2\,\pi\,\nu\,t = H_0^2\,(1/2 - 1/2 \cos 4\,\pi\,\nu\,t)$$

and therefore

$$i = \underbrace{A\, V_e^{3/2} - 1/2\, B\, H^2\, V_e^{1/2}}_{i_g} - \underbrace{1/2\, B\, H^2\, V_e^{1/2} \cos 4\,\pi\,\nu\,t}_{i_w} \quad \cdots\cdots (15)$$

It may be seen that the anode current is composed of a D.C. component i_g which in first approximation is proportional to the three halves power of the effective grid voltage, and an A.C. component which increases with the square root of the grid voltage and is thus proportional to the cube root of the anode direct current.

The effective value of this A.C. component is called the hum current. We are however usually more interested in the so-called hum modulation, which is defined as the ratio between the hum current and the anode direct current. It follows from equation (15) that the hum modulation — at least for sufficiently small values of the field H_0 — is inversely proportional to the effective grid voltage or to the two thirds power of the anode direct current.

In *fig. 5* the hum current and hum percentage calculated by means of equation (14) are plotted as functions of the effective grid voltage. Three values of the parameter p have been chosen, namely 0.5, 1 and 1.5. $p = 0.5$ corresponds to a magnetic field which decreases only slightly with increasing value of x ($p = 0.4$ for the homogeneous field); $p = 1$ corresponds to the case of a field distribution according to $H/\sqrt{x/l}$, while $p = 1.5$ relates to the case where the field decreases even more rapidly with increasing distance from the cathode. In agreement with the above qualitative discussion the hum current is found to be proportional to $i_g^{1/3}$, while the hum percentage is proportional to $i_g^{-2/3}$. Only at very low effective grid voltages, at which the hum percentages become significantly large, do deviations plainly occur.

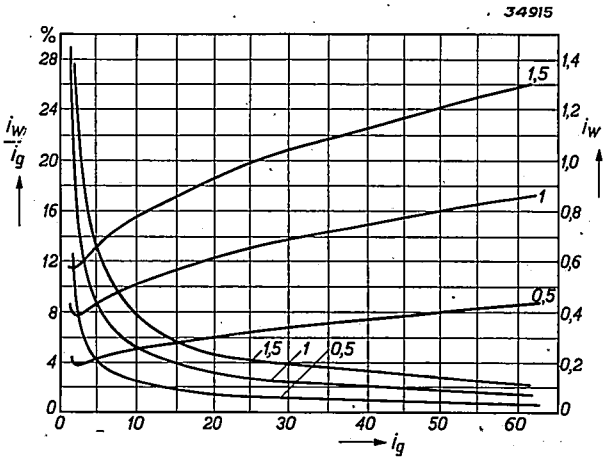

Fig. 5. Effective value of the hum current i_w (arbitrary units) and the hum percentage i_w/i_g, as functions of the effective anode direct current (arbitrary units). The three curves are calculated according to equation (14) with the parameters $p = 0.5$, $p = 1$ and $p = 1.5$.

The results were tested by measurements of the hum of a transmitting valve (type TA 20/23) as a function of the effective grid potential. The points measured are indicated in fig. 6, while the smooth curves in this figure were calculated theoretically with $p = 1.5$. It may be seen that good agreement is obtained. From the large value of p it follows that the magnetic field decreases more rapidly than $H/\sqrt{x/l}$ with increasing distance from the cathode.

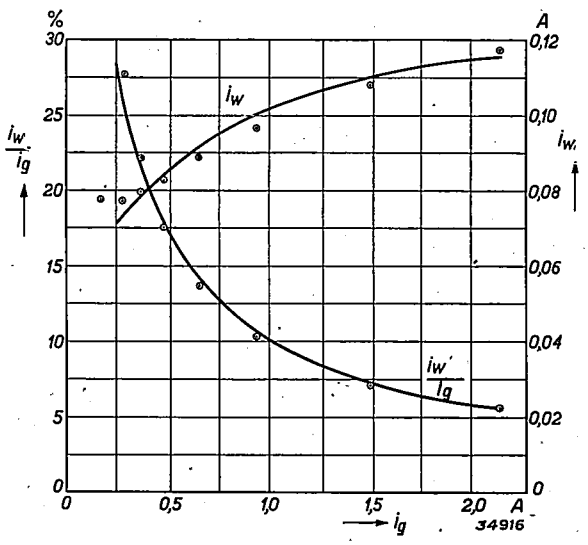

Fig. 6. Hum current i_w and hum percentage i_w/i_g of the transmitting valve type TA 20/30 as functions of the anode current. Circles: measured points, continuous lines: curves calculated with $p = 1.5$.

It is clear that with a valve of the type mentioned hum percentages of from 10 to 30 percent occur, so that one might conclude that the application of A.C. supply with such a valve would be entirely impossible. Upon closer consideration of the mechanism for the generation of the oscillations, however, it is found that the hum percentage of the signal transmitted is at least a factor 10 smaller than that of the valve itself.

Method of combatting hum

An obvious method of decreasing the hum is by dividing the filament system of the valve into a member of equal parts, and connecting these parts to the alternating current at different phases. If the hum current were proportional to $(H/H_m)^2$, as is the case in the first approximation, the use of two phases differing by 90° would already be enough to neutralize the hum entirely. The square of the field contains, in addition to a constant term, only the second harmonic of the mains frequency. This has a phase difference in the two halves of the filament system of $2\times 90° = 180°$, so that the two contributions to the anode current from the two halves of the cathode fluctuate in opposite phases, and the total anode current remains constant.

Due to the term $(H/H_m)^4$, however, a fourth harmonic, in addition to the second harmonic of the mains frequency, also occurs, which cannot be compensated by a division of the system into two halves. Practically, however, this term is of little significance; with a ratio H/H_m of 0.7 it would have only 1/30 of the amplitude of the fundamental frequency, and with smaller amplitudes its influence is much smaller. The last term $(H/H_m)^{26}$ may be entirely disregarded.

If the filament system is divided into three equal parts fed with the three phases of a pure multiphase current, the fourth harmonic will also be eliminated. The mutual difference in phase is 120°, and $4\times 120°$ coincides again with 120°. If the term $(H/H_m)^{26}$ is left out of consideration, therefore, the hum should disappear entirely.

Comparative tests were carried out on several valves of different power between the hum on connection with one phase and that on connection with two phases differing by 90°. The connection with three phases led to structural complications in connection with the condition that transmitting valves must also be able to be fed with direct current. The improvement achieved amounted in one case approximately to a factor $4^1/_2$, in another case to a factor of about 10. The theoretical improvement which, even in the case of the highest hum modulation investigated and where the term $(H/H_m)^4$ is still significant, should have amounted to a factor of more than 30, was thus far from being realized. This may probably be ascribed to the fact that the two halves of the filament which are connected to the different phases are never exactly equal, due to slight asymmetry in the construction, so that the fundamental frequency of the hum is never entirely compensated.

Fig. 7 shows a transmitting valve whose filament can be fed with alternating current of two phases. The two halves of the filament system are provided with separate connecting wires, so that the filament has four connections instead of two.

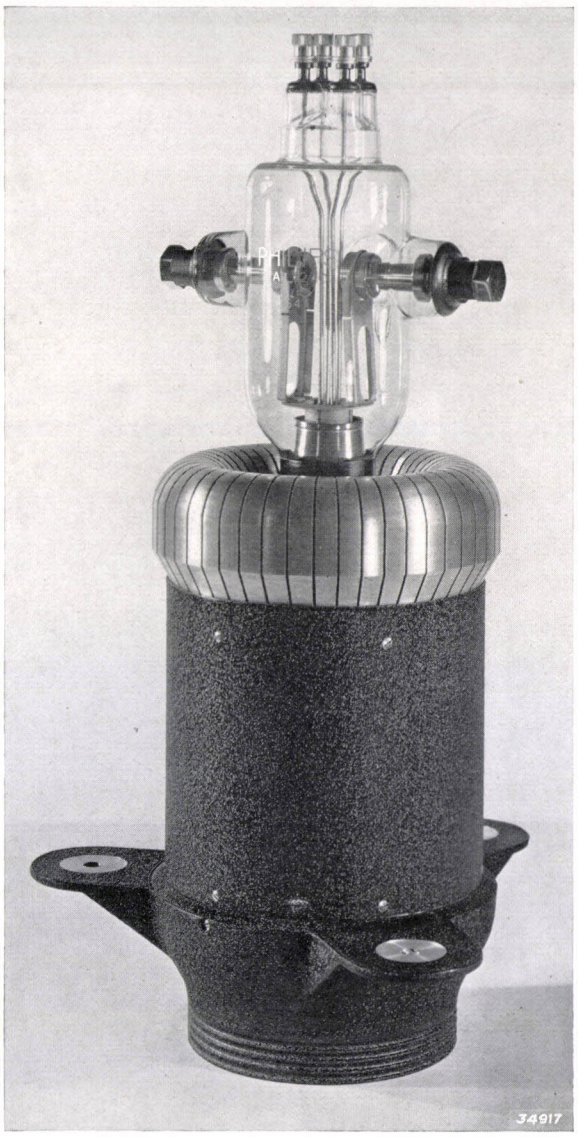

Fig. 7. The transmitting triode type TAL 12/10 (12 kV, 10 kW) with four connecting wires for the filament which is heated with two-phase alternating current.

The valve is a triode which is cooled with compressed air [4]), and which has a power output of 10 kW at an anode voltage of 12 kV. In addition to this two other valves have been developed with two-phase filament systems; a water-cooled triode of 12 kV, 35 kW, and a watercooled pentode of 12 kV, 20 kW.

[4]) On transmitting valves cooled with compressed air, see Philips techn. Rev. 4, 121, 1939.

STEREOPHONIC SOUND REPRODUCTION

by K. de BOER.

534.76 : 534.86

In the ordinary electrical methods of sound reproduction, the perception of direction, which is an essential part of hearing, is lost. After a short survey of the principles of localized hearing the article describes the way in which sound reproduction with retention of the perception of direction, *i.e.* stereophonic reproduction, could be realized. An arrangement which might be used in cinemas is described. It is found to be practically impossible to reproduce the differences of both intensity and time, which are responsible for directional hearing, in the correct relation from the point of view of the hearer. In order to examine the deviations from the "correct" perception of direction which may occur, an investigation has been carried out on the cooperation of time and intensity differences. The results of this investigation are given briefly. In conclusion several practical factors are mentioned in connection with stereophonic reproduction.

An essential part of our perception of sound is a space impression as to the origin of the sound. When for some reason or other the perception of direction from which a sound comes is lacking we often experience an uncomfortable feeling, a feeling of disquietude. This is quite understandable when the hearing function is considered from the teleological point of view. The original function of our sense of hearing may be considered to be that of warning us against danger. This is in agreement with the fact that although we possess eyelids we have no "earlids", in other words there is no provision for temporary suspension of hearing at will, since danger may always be lurking. A warning of danger may be given by the rustling of bushes in the woods, or by the hooting of a claxon at a street crossing, it can however only be useful to the hearer when his ear also perceives from what direction the danger comes, and to some extent also how close it is.

Sounds which have nothing to do with any danger are also customarily associated with a position in space. If there are several sources of sound, such as the different speakers in a play, we distinguish between them by means of directional hearing, and we take it for granted that the acoustic and the visual perceptions agree. In the same way our impressions in listening to a concert performed by a large orchestra are very much influenced by the fact that we hear the sound from the separate instruments coming from different directions, and can identify them not only by their timbre but also by the direction from which the sound comes. This faculty of being able to identify a particular sound when it is accompanied by a large number of other sounds is itself a very important result of directional hearing. We are able to concentrate our attention on the sound from a certain direction, and in this way to put into the background of our consciousness sounds from other directions which are disturbing or undesired at the moment [1]).

All these phenomena in our sence of hearing are nullified in the ordinary electro-acoustic methods of sound amplification and transmission now in use. When we listen at home to a radio broadcast of a concert we hear all the instruments from one direction only — the direction of the loud speaker. The plastic element of the orchestral music is lost. In listening to a radio play the hearer must depend mainly on differences in timbre (and possibly in intensity) in order to distinguish among the different voices. If several persons speak at the same time, or if there are extraneous sounds, it may become very fatiguing for the listener to concentrate his attention on one of the voices without the support of differences in direction. This fact must be taken into account by the director of the play. In sound reproduction in the cinema the lack of a directional effect may also be felt. One

[1]) This has already been pointed out in the article: Improving defective hearing, Philips techn. Rev. 4, 316, 1939.

sees a player move across the screen for example, his voice however continues to be heard from the same direction, namely that of the loud speaker set up behind the screen. Bearing in mind that in the development of the film industry there is a continual striving toward a greater degree of "naturalness", it is clear why attemps are made to make the illusion more perfect by making it possible in reproduction to distinguish by ear the different positions of the source of sound in the original recording. In this article we shall discuss the possibility of such a stereophonic reproduction. For this purpose we shall first examine the principles of localized hearing.

Principles of localized hearing

For localizing a source of sound with respect to an observer three coordinates are needed: the distance, the direction in the horizontal plane (azimuth) and the angle to this plane (height). There is little to say on the latter point: we have practically no direct perception of this factor. The impression that a sound comes from above is gained mainly by tilting the head, and thus this perception is reduced to that of a direction in the "horizontal" plane.

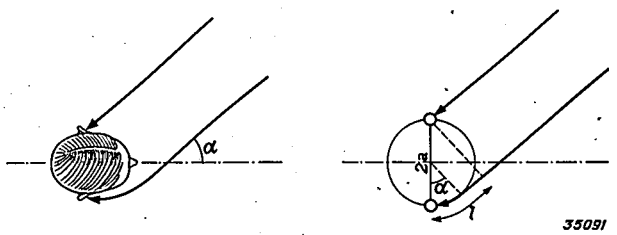

Fig. 1. Sound coming from a direction which makes an angle α with the vertical bisecting plane of the head reaches the two ears with a time difference of $t = l/c$ (c is velocity of sound). The wave which bends around the head is also weakened.

The perception of distance has not yet been entirely explained theoretically in every case [2]). In enclosed spaces it is explained by a variation in the relation between the direct sound (which reached the observer without reflection) and the echo or reverberation. When the distance of the source of sound changes the intensity of the direct sound varies, while that of the reverberation remains approximately constant. This distinguishing feature for distance is not impaired in ordinary electro-acoustic transmission, and thus provides the director of a studio program with the possibility of retaining a certain plastic effect in the reproduction.

By far the most important feature in localized hearing is the perception of direction in the horizontal plane. This depends upon the collaboration of both ears. (*Fig. 1*). If the source of sound is situated in the perpendicular plane bisecting the line joining the two ears, the latter receive exactly the same impressions. When however the sound comes from a direction α, it first reaches one ear, and only after a certain length of time the other, while moreover due to bending around the head of the observer it is somewhat weakened. Our centre of hearing is extraordinarily sensitive to these differences in time and intensity, which, led by experience, it interprets as angular deviations from the bisecting plane.

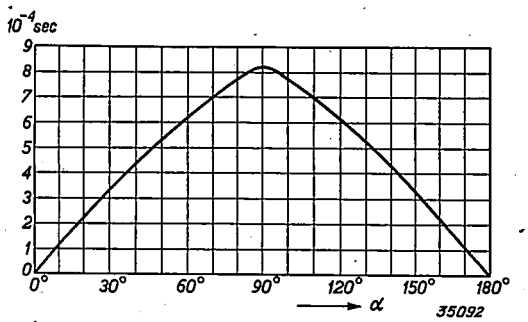

Fig. 2. Time difference t as a function of the angle α.

As to the differences in time, they can easily be calculated from the difference in distance covered l (see fig. 1) and the velocity of sound. If for the sake of simplicity the head is considered to be a sphere with the radius a, then $l = a\,(a + \sin a)$. It has been found experimentally that an angular deviation of only 3° from the bisecting plane can already be observed, which with a distance between the ears of about 20 cm corresponds to a difference in time of 3×10^{-5} sec. In *fig. 2* the time difference is plotted as a function of the angle α [3]).

The differences in intensity at the two ears due to the bending are not so easy to calculate. They have been determined experimentally by Sivian and White [4]), whose results are given in *fig. 3* for several different frequencies. The fact that the

[2]) See in this connection: C. v. Békésy, Akust. Z. **3**, 21, 1938.

[3]) The following is an interesting test of the sensitivity of the sense of hearing to time differences. The two ends of a piece of rubber tubing (gas tubing for example) are held to the ears. The tube is then tapped at any spot. The result is a clear impression of direction which depends upon the spot which was tapped. The spot which must be tapped in order to obtain the impression "straight ahead" can be determined accurately to within a few mm. See J. L. v. Soest and P. J. Groot, Physica, **9**, 111, 1939.

[4]) L. J. Sivian and I. D. White, J. Acoust. Soc. Amer. **4**, 288, 1933. The curves here used are borrowed from J. C. Steinberg and W. B. Snow, Elect. Eng. **53**, 12, 1934.

differences in intensity must also depend upon the frequency of the sound is obvious: the sound waves are only affected by an obstacle when the dimensions of the latter are of the same order of magnitude as the wave length of the sound. If the wave length is much greater than the diameter of the head, the latter does not "cast a shadow".

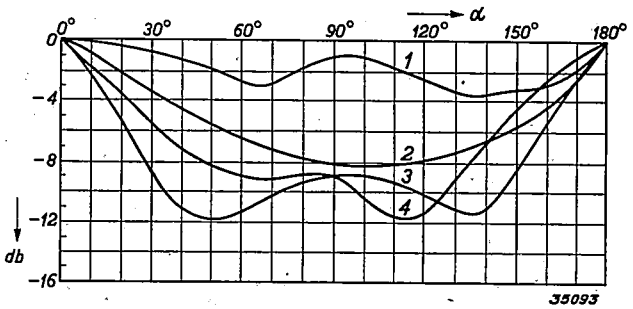

Fig. 3. Intensity difference (in db) between the sound at the right and left ear as a function of the angle α, according to measurements by Sivian and White. In curves *1*, *2*, *3*, *4* the sound consisted of tones of 300, 500, 1 100 and 2 240 c/sec, respectively.

With tones lower than about 400 c/sec (wave length 110 cm) the difference in intensity is practically zero at all angles. If the wave length is much smaller than the head, absolute shielding takes place. With tones higher than about 10 000 c/sec (wave length 3 cm) the difference in intensity already reaches a maximum at a very small value of the angle α, and then no longer varies with α. Perception of direction by means of differences in intensity is most efficient with tones of about 1 000 - 2 000 c/sec, *i.e.* in the same frequency range in which the threshold of hearing is lowest. Considered therefore from the above-mentioned teleological point of view, one might say that the maximum of sensitivity of the ear is adapted to the size of the head.

We are not in general concerned with pure tones, but with sounds of a certain spectral complexity. For our purpose, stereophonic reproduction, speech is especially important. The average distribution of intensity of speech over the whole frequency spectrum is shown in *fig. 4*. With the help of this

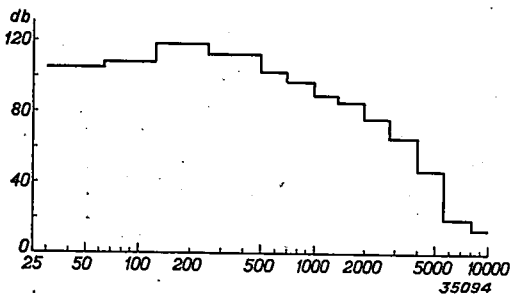

Fig. 4. Speech spectrum. The intensity (in db) per unit of frequency interval is plotted as a function of the frequency in c/sec.

curve and the curves of fig. 3 the differences in intensity can be calculated of the sound occurring at each ear when a speaker is heard from different directions. The result is given in *fig. 5*. It may be seen that for angles between 0 and 50° the intensity difference in decibels increases practically linearly with the angle. The maximum intensity difference amounts to about 7 db. At the above-mentioned angle $\alpha = 3°$ which may be considered as the threshold value of sensitivity to direction, the intensity difference is only about $^1/_2$ db.

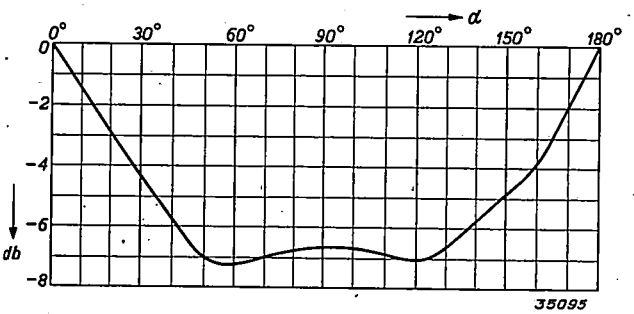

Fig. 5. Average intensity difference (in db) at the right and left ear as a function of the angle α upon hearing speech.

The dependence of the bending on frequency also results in a change of timbre. If for a certain direction of the source of sound (angle α) we plot the relative attenuation at one ear as a function of the frequency, we obtain the curves of *fig. 6*. The sound may be said to pass as it were through a filter in bending around the head, the filter having a frequency characteristic which may be very different for different angles α, as may be seen from fig. 6.

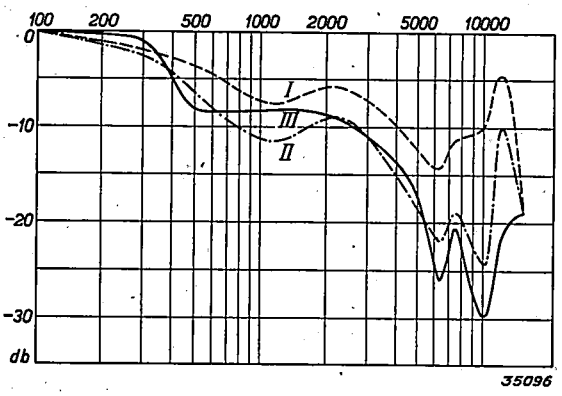

Fig. 6. Frequency characteristic of the bending around the head. Curves *I*, *II*, *III* refer to a source of sound at angles α 30, 60 and 90°, respectively.

Thus for different directions of the source of sound there appear differences in the quality of the sound which may also contribute to the perception of direction [5]).

[5]) With the help of these differences in quality a judgment of direction is also possible to a certain extent with the use of only one ear.

Stereophonic reproduction

In order to retain the impression of direction in electrical transmission of sound, the sound must be delivered to the two ears of the listener with the correct relative time and intensity differences. This may be realized in a relatively simple manner by setting up in the recording room in the place of the absent listener an "artificial head" with two microphones in the positions of the ears. Each microphone, *via* its own amplifier and transmission line (channel), supplies one of two head phones at the ears of the listener. This solution of the problem has already been discussed in this periodical in the description of a hearing apparatus for a deaf person [6]). The artificial head there used is shown once more in *fig. 7*.

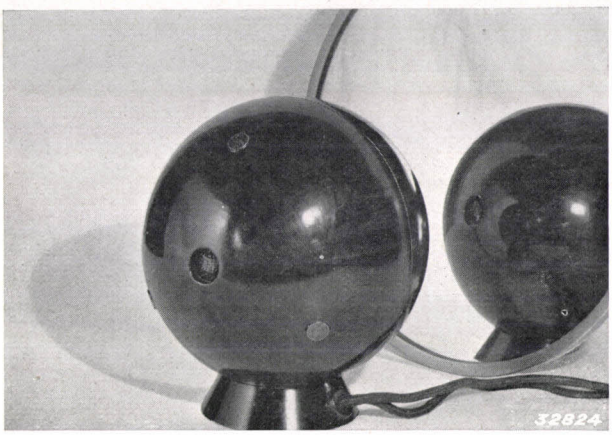

Fig. 7. A sphere with a diameter of about 22 cm may be used as an "artificial head". The microphones are situated at the extremities of a horizontal diameter.

We shall not expatiate upon the fact that two channels are needed for such transmission. This necessity will not present insoluble difficulties in many cases. In sound film for example, where the transmission line between the place of recording and that of reproduction is replaced by a sound track on a film, it is possible to make two sound tracks instead of one on the film, each of which corresponds to the sound for one ear. More objectionable however is the requirement that, on the principle mentioned every member of the audience in the cinema hall would have to wear a set of head phones. It would be preferable to use two common "telephones" for the whole auditorium, *i.e.* two loud speakers, one at each side. When this is done, however, there is immediately a deviation from the proposed principle in so far as both ears now receive sound from both loud speakers. In spite of this fact it has been found possible by experiment to obtain a fairly good stereophonic effect in this way. The factors concerned will be discussed in the following.

[6]) See the article cited in footnote [1]).

Differences in intensity and time in reproduction with two loud speakers

Fig. 8a shows an arrangement which can be used practically in a cinema. The two loud speakers

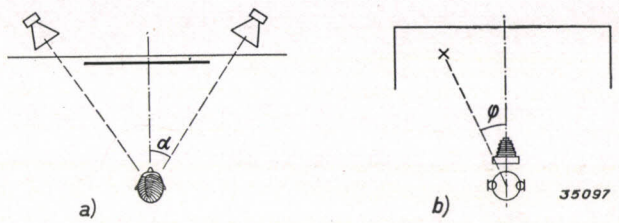

Fig. 8. a) Arrangement for stereophonic reproduction in a cinema. Two loud speakers stand at either side of the screen. A listener at a given distance from the middle of the screen sees the line joining the two loud speakers within an angle of 2α.
b) Arrangement of the artificial head in the studio. The perpendicular bisecting planes of camera and artificial head coincide. The speaker stands for example in the direction φ.

are set up on either side of the screen, the reason for this will be given later. We shall consider the hearer to be situated in front of the screen in the middle, in the plane of symmetry of the arrangement. The artificial head is placed in an analogous position in the recording studio, *i.e.* in such a position that the vertical bisecting planes of artificial head and camera, respectively, coincide with each other, see fig. 8*b*. At a given position of the speaker (angle α) the intensities at the two "ears" of the artificial head differ by a factor p, which can be read off in fig. 5. The same ratio p also holds for the sound intensities which the two loud speakers in fig. 8*a* provide at the position of the listener. Let us assume that the left ear of the listener, looking straight ahead of him, receives an intensity I from the left-hand loud speaker. Then the right-hand loud speaker gives to the right ear an intensity of only pI. In addition however the right ear also receives an intensity qI from the left-hand loud speaker, where q is the attenuation factor which corresponds to the angle α of the direction of the loud speaker according to fig. 5. In the same way the left ear receives an intensity qpI from the right-hand loud speaker. Altogether, therefore, the left ear receives the intensity $I + pqI$, and the right ear the intensity $pI + qI$. The actual ratio between the intensities at the two ears of the listener is therefore not p, but

$$P = \frac{p+q}{1+pq} \quad \cdots\cdots \quad (1)$$

In this equation p varies with the position of the speaker in the recording studio, while q is a parameter which depends upon the relative positions of the listener and the loud speakers. If $q = 0$, *i.e.* if each ear of the listener did not receive any sound from the "wrong" loud speaker, then $P = p$. This case, however, in which the intensity ratio p is exactly retained, cannot be realized with loud speakers, since according to fig. 6 q can never be made smaller than 0.2 (corresponding to an attenuation of 7 db). In the other extreme case where $q = 1$ *i.e.* when each loud speaker has the same effect for each ear, P becomes equal to unity according to equation (1), and there is no difference of intensity at the ears of the listener. For all the intermediate values of the parameter q, P is always greater than p, as a glance at *fig. 9* will show. *The difference in intensity at the ears of the listener is therefore always less than that at the "ears" of the artificial head.*

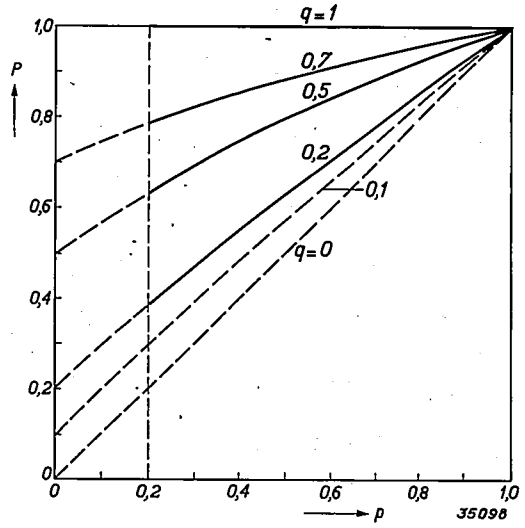

Fig. 9. The ratio P between the intensity of the sound at the right ear and that at the left ear of the listener (fig. 8*a*) as a function of the ratio p at the microphones of the artificial head (fig. 8*b*). The intensity ratio q between the sound contributions which one loud speaker makes to each ear enters as a parameter. q depends upon α, *i.e.* upon the relative positions of listener and loud speakers; it may however according to fig. 5 never be less than about 0.2. It may be seen, that P is always greater than p, *i.e.* the intensity difference is always smaller for the listener than for the artificial head.

Let us now consider the differences in time. In the case of the position of the speaker in the studio as represented in fig. 8*b* the left-hand microphone of the artificial head receives the sound slightly earlier than the right-hand one. The difference amounts t sec. [7]) The left ear of the listener (fig. 8*a*) will then also receive the sound from the left-hand loud speaker t sec earlier than the right ear receives the sound of the right-hand loud speaker. But a moment later (T sec) both ears receive the sound (weaker by a factor q) from the "wrong" loud speaker, and in this case the right-hand ear is served t sec earlier. This is represented schematically in *fig. 10*. It may be seen that both

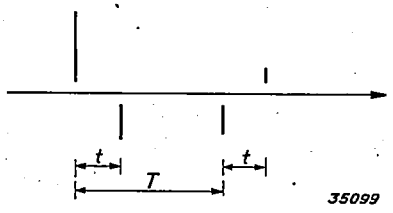

Fig. 10. Above the time axis, the moments of arrival of the sound contributions at the left ear, below the time axis, the same for the right ear. The time difference t corresponds to the angle φ, (fig. 8*b*), the difference T to the angle α (fig. 8*a*). The length of the vertical lines indicates approximately the intensities which the four contributions to the sound may assume.

ears perceive a time difference of t sec between the sound contributions I and $p\,I$, respectively, and that this whole impression is repeated, weakened by a factor q and with reversed time difference, T sec later as a kind of echo. This echo causes a slight vagueness in the directional effect, but it may be neglected in our considerations, especially when $T > t$, which is usually the case.

The result is that the listener perceives an intensity difference P and a time difference t, while, if he stood at the position of the artificial head, he would perceive a (greater) intensity difference p and an (equal) time difference t. As a perception of what direction will the listener now interpret the differences P and t?

No direct answer to this question is possible, since the combination P, t never occurs in "natural" directional hearing as learned from experience. With a given direction with respect to the head there corresponds not only a given intensity difference, but also a definite, unambiguous time difference. It might be supposed that the ear is so accustomed to this unambiguousness, that combinations deviating therefrom would only cause a feeling of confusion. This is fortunately not the case, as will be shown in the following.

The cooperation of intensity and time differences

In order to be able to understand the cooperation of intensity and time differences the following ex-

[7]) For the following considerations it is essential that the reproduction of speech should always be kept in mind. If listening tests are carried out with pure tones or in general with tones having a periodic vibrational form, one can no longer speak unambiguously of a "time of arrival". It is actually found possible in such cases to cause serious confusion of the impression of direction.

periments were carried out in this laboratory. The two loud speakers were set up behind a screen as in *fig. 11*, while on a horizontally placed wooden bar in front of the screen a scale was marked off.

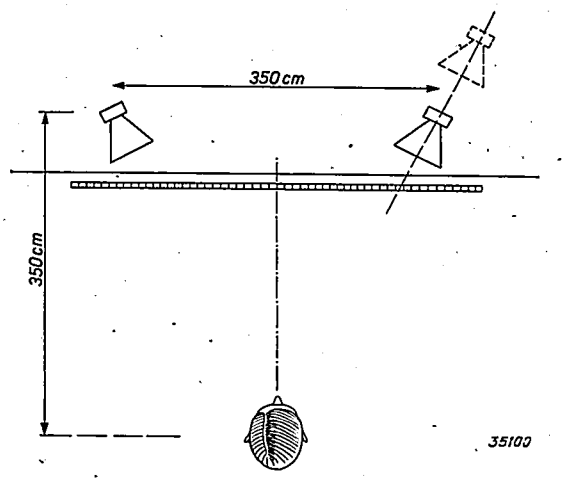

Fig. 11. Arrangement of the loud speakers in the experiments concerning the cooperation of time and intensity differences.

a) Differences in intensity were caused in the sound of the loud speakers. This was done by regulating the volume of one loud speaker with a calibrated potentiometer, while both of them were reproducung the same gramophone record. The listener was then found to receive a fairly sharp impression of direction, and could localize the fictitious source, the "sound image", on the scale with a reproducibility of a few centimeters. In *fig. 12* the angular rotation of the "sound image" so obtained is plotted as a function of the ratio of intensities (in db). At the same time the angle is given (broken line curve) which should correspond to each difference in intensity according to fig. 5. It may be seen that a difference in intensity alone always causes a perception of the angle which is 10 per cent less than that which occurs in natural directional hearing, where the "added" time difference is also present.

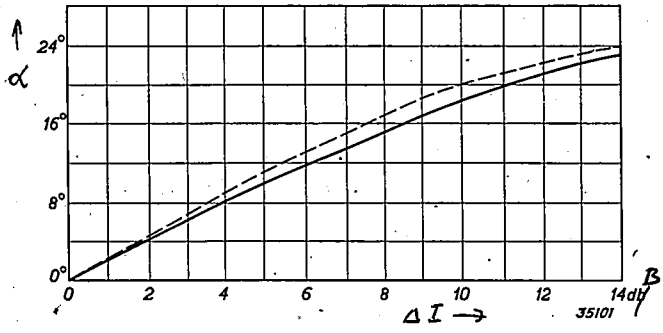

Fig. 12. Angular rotation of the "sound image" away from the middle position when only intensity differences are applied. The broken line curve gives the angles in the case of natural directional hearing, where the intensity difference is always accompanied by an "added" time difference.

b) In the following experiment time differences alone were investigated. These were caused in the sound of the two loud speakers, which were again reproducing the same gramophone record, by shifting one of the loud speakers along the line joining loud speaker and listener. The volume of the sound was so adjusted that the intensities of the two loud speakers always remained the same for the listener. Again it was found that the listener obtained a certain impression of direction, which has been plotted in *fig. 13* as a function of the time difference. The broken line curve indicates the angle which, according to fig. 2, would be observed in natural directional hearing (thus in collaboration with the added difference in intensity). It is interesting to note that the sense of hearing is able to localize a sound when the time differences are greater than ever occur in natural directional hearing, and which time differences therefore, the ear can never actually have "learned" to interpret as indicating direction. For the rest the curves show qualitatively (at least for the range of angles investigated in the experiments) that the possibility of normal perception of direction of sound depends mainly upon differences in intensity, as was already indicated by fig. 12.

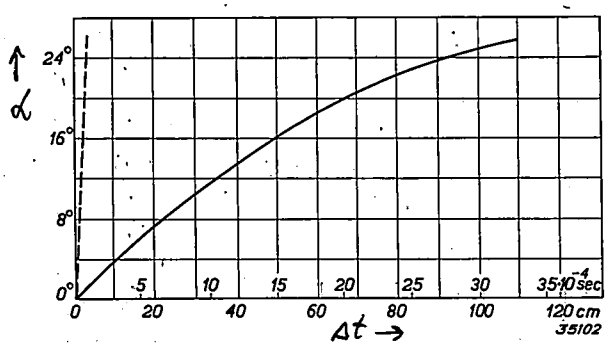

Fig. 13. Like fig. 12 but with time differences alone. The broken line curve refers again to natural directional hearing. The differences in length of path are also indicated on the abscissa. It is remarkable that localization is found to be possible even with differences in length of path which are much greater than the distance between the ears.

c) If differences in intensity and time occur simultaneously, it is found that the angle observed can always be calculated from the data of figs. 12 and 13, in the following way. As a function of the time difference the intensity difference is plotted which would cause the same angular rotation of the "sound image". We then obtain a practically linear relation (see *fig. 14*). As a result every time difference may be expressed unambiguously as an equivalent intensity difference, and *vice versa*. If we now add this equivalent intensity difference to that already present, and find in fig. 12 the angle

corresponding to the total intensity difference, it is found to agree, within the limits of error of the measurement, with the experimentally determined angular rotation of the "sound image" [8]).

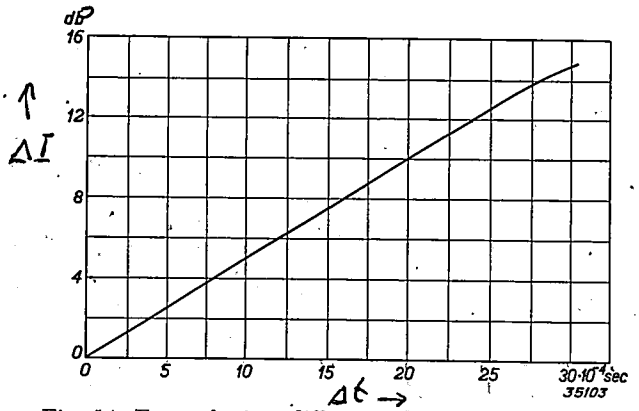

Fig. 14. For each time difference the intensity difference is plotted which causes the same angular rotation of the "sound image".

This additivity must of course also hold for normal directional hearing, where not only any difference in time and intensity are combined, but in which a time difference is "added" to every intensity difference. If we convert the added time differences according to fig. 14 into equivalent intensity differences, and add these to the actual intensity differences, the total always gives the angle actually observed, within the limits of error of the measurement. This is shown in *fig. 15*.

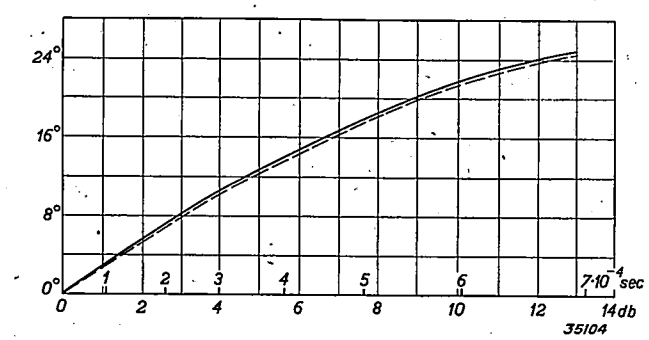

Fig. 15. Perception of angle in normal directional hearing (full line curve), in which an added time difference (indicated on the abscissa) occurs for each intensity difference. By conversion into an equivalent total intensity difference with the help of fig. 14, and then finding the corresponding angle in fig. 12, the broken line curve is obtained, which agrees satisfactorily with the full line curve.

The position of the "sound image"

With the data of figs. 12 and 14 it is now possible to answer the above proposed question as to the directional impression which will occur with any combination P, t of intensity and time differences.

[8]) In the same way of course the intensity difference can be converted according to fig. 14 into an equivalent time difference, and the total angle may then be read off in fig. 13.

If we allow the speaker in fig. 8*b* to move over a given traject in front of the artificial head, then for every position we can calculate the differences P and t, and from them the position at which the listener in fig. 8*a* will preceive the "sound image" to be situated. In *fig. 16* the relation so obtained between the original angle and that observed is given for a particular arrangement. As long as the speaker remains within an angle of about 120° a satisfactorily linear "focussing" of the movement of the source of sound is obtained on the screen [9]).

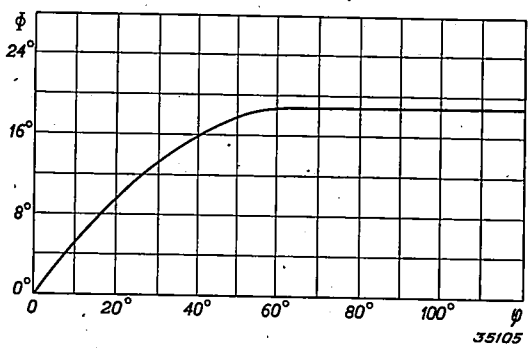

Fig. 16. Angular rotation Φ of the "sound image" as a function of the angle φ of the speaker with respect to the artificial head (fig. 8*b*).

Until now we have always assumed the listener to be situated at a definite place in the plane of symmetry of the loud speakers. In a cinema, however, a large area is actually occupied by the audience. It is clear that for different positions the perception of direction in stereophonic reproduction will be quite different. According to the method applied above, we could calculate the stereophonic effect for each seat. In order however to obtain a general idea, we have carried out a number of listening tests, the results of which are given in *fig. 17* and *fig. 18*. For three places *2*, *3*, *4*, which are indicated in fig. 17, fig. 18 shows how the "sound image" moves, if, for the listener at place *1*, it shifts over a given distance of the screen. For seats more to one side the "focussing" shrinks, the "sound image" moves a shorter distance than the speaker in front of the artifical head. In the shaded region in fig. 17 the "focussing" has shrunk so much that the listeners in these seats observe practically no stereophonic effect at all. By the arrangement of the loud speakers at opposite sides of the screen with the greatest possible distance between them (to make the factor q in equation (1) small), the shaded region of fig. 17 is restricted as much as possible.

[9]) In the above it has always been assumed that the listener looks straight ahead. If he turns his head, then the condition must be satisfied, that the "sound image" remains stationary on the screen. This is found to be the case to a sufficiently close approximation.

In order not to make the intensity differences confused, it is advisable that the sound radiation of the loud speakers should be constant within the angle at which the loud speaker faces the audience. Outside this angle the loud speakers should radiate as little sound as possible, since this sound reaches the audience after one or more reflections in the form of reverberation, by which the sharpness of the sound image is unfavourably affected.

The two amplifiers and loud speakers which are used in reproduction may not differ in quality of reproduction. Otherwise there is a tendency for the listener to interpret the differences in quality as an indication of direction (see above), *i.e.* to concentrate his attention in the direction of the better loud speaker.

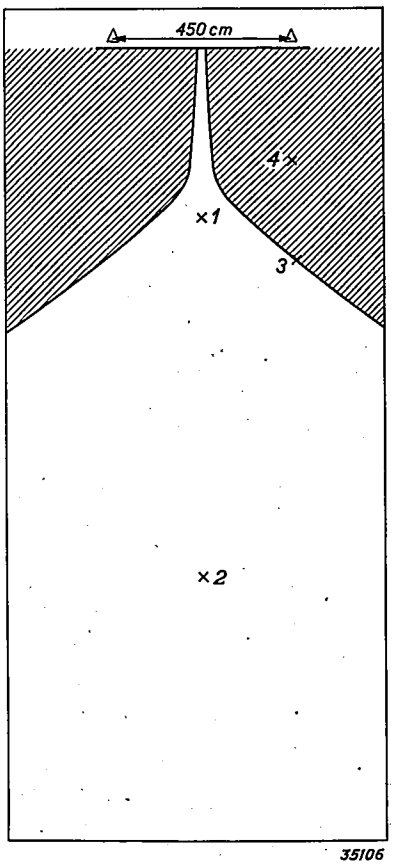

Fig. 17. In the seats situated in the shaded regions the listener observes a maximum displacement of the "sound image" over only half the width of the screen, so that the stereophonic effect is not sufficient here.

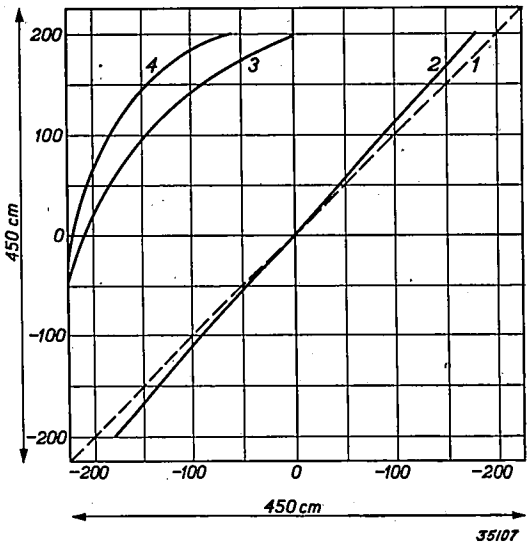

Fig. 18. If the "sound image" for the listener at place *1* (fig. 17) is displaced over the whole length of the screen (450 cm, indicated as abscisse), the listeners at the places *2*, *3*, *4*, in fig. 17 only observe the displacement of the "sound image" indicated as ordinates in the figure.

In sound reproduction in cinemas use is at present commonly made of separate loud speakers for the high and low frequency ranges (above and below about 300 c/sec, respectively). We have already seen that tones with frequencies below 300 c/sec are practically incapable of arousing any perception of direction. Therefore for stereophonic reproduction it is only necessary to set up two loud speakers for the high tones at either side of the screen, while the low tones can be reproduced by a single loud speaker placed at any desired position, for instance behind the middle of the screen.

THE REPRODUCTION OF HIGH AND LOW TONES IN RADIO RECEIVING SETS

by V. COHEN HENRIQUEZ. 621.396.667: 621.396.645.37

In this article the question is considered as to what is the best frequency characteristic for a receiving set when account must be taken of side-band interferences caused by transmitters with frequencies which are very close to that to which the set is tuned. Since the intensity of these interferences may differ very widely, it is desirable to make the characteristic adjustable. It is described in detail how, by means of variable inverse feed-back, it is possible to obtain the desired adjustability of the frequency characteristic.

Introduction

If there were only the electromagnetic field of a single transmitting station present at the receiving aerial, speech and music could be transmitted practically undistorted. The actual situation, however, is that in general a large number of transmitters are in operation at the same time, and their wave lengths are so chosen that two successive carrier waves have an average frequency difference of 9 000 c/sec. When the amplitude of the vibration transmitted is modulated in the rhythm of a sound vibration, then in addition to the carrier wave there are numerous other waves (the so-called side bands), whose frequencies occupy a region which has a width on either side of the carrier-wave frequency equal to the maximum frequency occurring in the sound. When two adjacent transmitters are modulated with sound frequencies higher than 4 500 c/sec, the frequency regions used for the two transmissions will overlap each other (*fig. 1*), so that it is impossible to receive all the frequencies of one transmission without interference by the other. If, for example, the interfering transmitter is modulated with a frequency of 6 000 c/sec, a wave occurs whose frequency differs by only 3 000 c/sec from the desired carrier wave, and which will be heard as a tone of 3 000 c/sec [1]). In general it may be stated that a modulation of the interfering transmitter with a frequency ν is heard as a tone of the frequency 9 000-ν, which results in the well-known crackling effect (side-band splash), usually accompanied by a continuous whistle of 9 000 c/sec from the interfering carrier wave itself.

The side-band interference and the whistle can be practically eliminated by changing the reproduction characteristic of the set in some way or other so that the reception of high tones, especially that of 9 000 c/sec is sufficiently weakened. It is true that the quality of reproduction of the desired transmission is hereby affected, but it is found nevertheless that by a suitable weakening of the reproduction of the high tones a result can be achieved which, in the presence of the interfering transmitter, is judged to be better than an absolutely faithful reproduction.

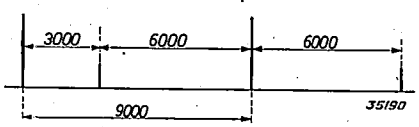

Fig. 1. The carrier waves of two adjacent transmitters have a frequency difference of 9 000 c/sec. If the carrier wave of the interfering transmitter is modulated with a signal of 6 000 c/sec a differential frequency of 3 000 c/sec occurs between one of the interfering sidebands and the carrier wave to which the set is tuned.

The reproduction of low frequencies is also subject to restrictions which have their basis in aesthetic requirements. The loud speaker must be housed in a receiving set whose cabinet may not be too large. If one applies to the loud speaker a current of constant effective value and steadily decreasing frequency, the sound pressure produced in the room will fall suddenly when the frequency falls below the resonance frequency of the radio cabinet. This latter is higher, the smaller the cabinet, and amounts to about 200 c/sec. At the resonance frequency itself there is a peak of sound pressure. The irregular shape of the loud speaker characteristic can be compensated within certain limits in the electrical part of the apparatus. It is however impossible as well as unnecessary to stretch the frequency band reproduced to frequencies lower than about 50 c/sec.

In this article we shall study the shape of characteristic which forms the most satisfactory compromise, and the method by which this characteristic is realized in modern radio receiving sets.

[1]) The low-frequency vibrations, which occur in the detection of the high-frequency signal, have frequencies equal to the differential frequencies between all the vibrations present in the high-frequency signal. If the signal of one frequency (the carrier wave) is appreciably stronger than all the others, practically only differential frequencies between carrier wave and the rest of the signals (side bands) occur. These give rise to the desired low-frequency signal and sometimes to side-band interference. They must not be confused with the sound of the adjacent transmitter which occurs when not only a side-band but also the carrier wave of the adjacent transmitter acts with considerable intensity on the detector.

Choice of reproduction characteristic

The most satisfactory form of frequency characteristic may vary very much according to the nature of the transmission and the relative strength of the interfering transmitters. In speech, for example, frequencies above 4 000 c/sec are almost entirely absent, so that the frequency characteristic might be allowed to fall to zero above 4 000 c/sec without too unfavourable effects on the reproduction. Only modulation frequencies of the interfering transmitter above 9 000 — 4 000 = 5 000 c/sec would then produce side-band interference, and this limitation may be enough to eliminate side-band interference.

In transmission of music the combatting of side-band interference without seriously impairing the quality of the reproduction is much more difficult. It is true that in this case also the frequencies above about 4 000 c/sec can be weakened without too unfavourable effects on the quality of the reproduction, but a complete suppression of these frequencies is certainly undesirable. One must therefore not proceed farther with the weakening of the reproduction of certain frequencies than is absolutely neccssary for the suppression of the interferences at those frequencies. In speech as well as in music the largest part of the intensity is radiated at frequencies from 200 to 1 000 c/sec, at higher frequencies the intensity decreases rapidly per unit of frequency interval. In the case of side-band interference, where the intensity distribution of the interfering transmission is reflected with reversed frequency scale (9 000-ν), the intensity will increase with increasing frequency, so that the reproduction must be more and more weakened with increasing frequency in order to keep it free of interference.

In a given case for example we find that the above mentioned compromise is represented by curve *a* of *fig. 2*. The side-band interference with this reproduction characteristic was equally intense for all the high frequencies which are reproduced in a partially weakened form, and this intensity was just below the threshold value of the ear. As may be seen the low frequencies are also weakened. This is found desirable in order not to disturb the balance between high and low tones by the weakening of the high tones alone.

If the intensity of the interfering transmitter becomes fifty times lower, the high frequencies then need less weakening. The amplification can then be kept constant over a larger region. Only those frequencies which had originally to be weakened more than fifty times in order to keep the corresponding interferences below the threshold value, must now still be weakened. Because of the fact that the high tones are less weakened, the low tones can now be better reproduced without the timbre becoming too low, so that we now obtain curve *b* which provides a considerably better reproduction than curve *a*.

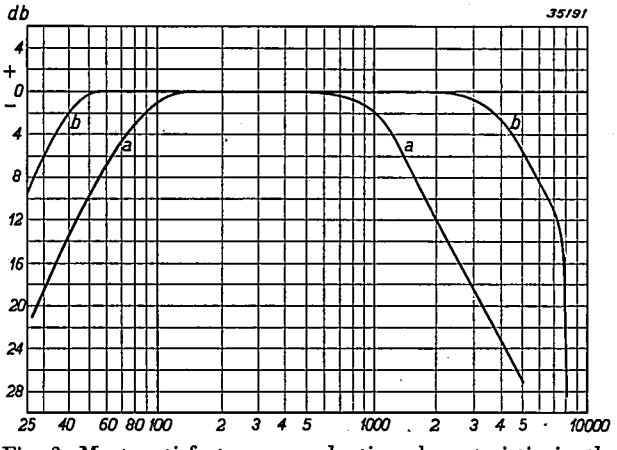

Fig. 2. Most satisfactory reproduction characteristic in the presence of side-band interferences. Toward high frequencies the amplification decreases in such a way that the remaining side-band interferences lie just below the threshold value in every frequency interval. Toward low frequencies the characteristic is also allowed to fall in order to compensate to some extent for the lowering in timbre which occurs due to the cutting off of the high frequencies.
a) Empirically found characteristic in the presence of strong side-band interference. b) Characteristic which can be derived therefrom if the interfering transmitter is 100 times weaker.

It has been found by experiment that the average slope which the curves in fig. 2 must have at high frequencies, in order to keep the side-band interferences just below the threshold value in all frequency regions, must be —3. This means that the amplification for high frequencies must be inversely proportional to the third power of the frequency.

The desired frequency characteristic is therefore horizontal up to a given limiting frequency, and then falls with the third power of the frequency [2]). In order to eliminate the continuous whistle of 9 000 c/sec, caused by the carrier wave of the interfering transmitter, together with the side-band interferences, it is furthermore necessary to weaken at least 30 dB more at these frequencies than is necessary for the suppression of the side-band interferences.

Consequences for the frequency characteristic of the different parts of the receiver

By the total frequency characteristic of a re-

[2]) It is found that the transition from the flat portion to the sloping portion of the characteristic may not take place too rapidly (see fig. 2), because otherwise the reproduction becomes somewhat harsh.

ceiver we mean the relation between the effective sound pressure and the effective input voltage of the corresponding sideband, represented as a function of the frequency. In the case of a superheterodyne receiver this frequency characteristic is the product of the high-frequency characteristic, the middle-frequency characteristic, the low-frequency characteristic and the reproduction characteristic of the loud speaker. Each of these four factors depends upon the frequency, and in principle it is a matter of indifference which factor is influenced by special means to obtain the desired characteristic [3]). Usually the reproduction characteristic is influenced in the high-frequency as well as in the low-frequency part by filters, the last of which has an adjustable band width. A so-called "tone regulator" is also introduced in the low-frequency part to make it possible to regulate the reproduction of the high tones.

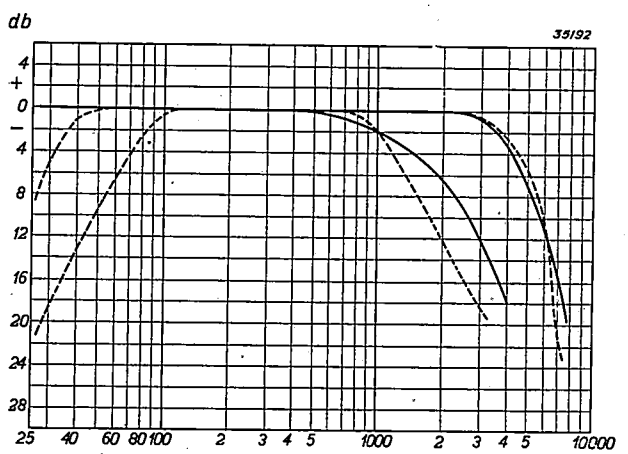

Fig. 3. a) Full lines: reproduction characteristic of the high and middle-frequency part of a receiver at the widest and narrowest position of the variable band filter. Broken lines: desired reproduction characteristics (figs. 2*a* and *b*).

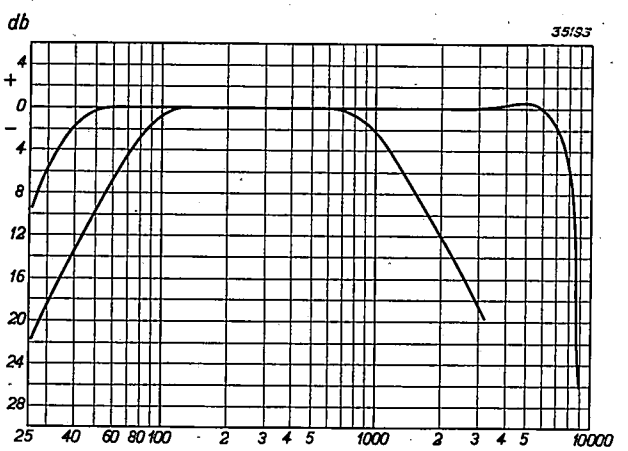

b) Reproduction characteristics which the low-frequency part of the set together with the loud speaker should have in order to obtain the desired characteristics for the whole apparatus at the widest position of the band filter.

In *fig. 3a* the full lines give the reproduction characteristic of the high and middle frequency part for a superheterodyne receiver of the usual type. The two curves refer to the two extreme adjustments of the band width. It may be seen that at high frequencies the curves show some similarity with the desired characteristics according to fig. 2 (broken line curve). The curved section between the constant and the descending part of the curve is however more gradual than is necessary or desirable.

In order to gain improvement in this respect one may try to compensate the difference between the characteristic obtained and that desired in the low-frequency part of the apparatus. It is advisable for this purpose to adjust the band filter to the greatest band width, and make the low-frequency reproduction characteristic variable [4]). The desired shape is represented in fig. 3*b*; it should therefore be obtained by means of low-frequency amplifiers and loud speaker together.

The reproduction characteristic of a loud speaker of good quality changes only very gradually in the region of high frequencies, so that in a qualitative discussion of the total reproduction characteristic it needs not be taken into account. At low frequencies, however, as stated above, greater irregularities occur which may be ascribed to a resonance of the air in the cabinet of the loud speaker.

Fig. 4 shows an example of a loud speaker characteristic. The sensitivity of the loud speaker, *i.e.* the ratio between the sound pressure obtained and the current through the coil, is about constant for frequencies above 400 c/sec. Between 400 and 200 c/sec it rises, and at 200 c/sec it reaches a maximum due to the resonance of the volume of air in the cabinet. At 60 c/sec a second maximum occurs due to the characteristic resonance of the vibrating loud speaker coil. The shape of the characteristic for lower frequencies is of little importance for the quality of reproduction.

In order to compensate the irregularities of shape in the low frequencies and to obtain the frequency

[3]) This is not entirely a matter of indifference, because in no case may two carrier waves act with appreciable intensity on the detector (see footnote [1])). Moreover, due to the curvature of the valve characteristics, undesired effects occur when two transmitters are present simultaneously in appreciable intensity. For example, the carrier wave of the transmitter to which the set is tuned may undergo a modulation in the rhythm of the modulation of an interfering transmitter (cross modulation). In that case the interfering transmitter can no longer be made inaudible, even if the carrier wave and side bands of the interfering transmitter are entirely eliminated further along in the set.

[4]) In the case of unusually strong interferences the band width can still always be made smaller.

characteristic drawn in figs. 2*a* and *b* throughout the whole range of frequencies, the low-frequency

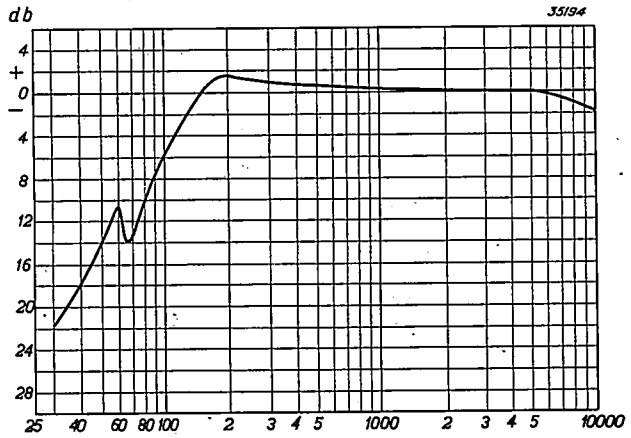

Fig. 4. Reproduction characteristic of a loud speaker (sound pressure as a function of the frequency with constant current). The first maximum is due to the resonance of the loud-speaker coil, the second, weak maximum is due to a resonance of the volume of air in the cabinet.

characteristic must have a shape like that shown in *fig. 5*. Since the reproduction characteristic of the loud speaker decreases below 900 c/sec with decreasing frequency more rapidly than is desirable for the total frequency characteristic, the sensitivity of the amplifier must in that region increase with decreasing frequency. This course is interrupted by a minimum at 70 c/sec, corresponding to the above-mentioned resonance of the loud speaker. The rapidity of the increase must change with the intensity with which the low tones must be reproduced, and the latter as stated above runs parallel with the intensity of reproduction of the high tones. The two curves, as in fig. 2, correspond

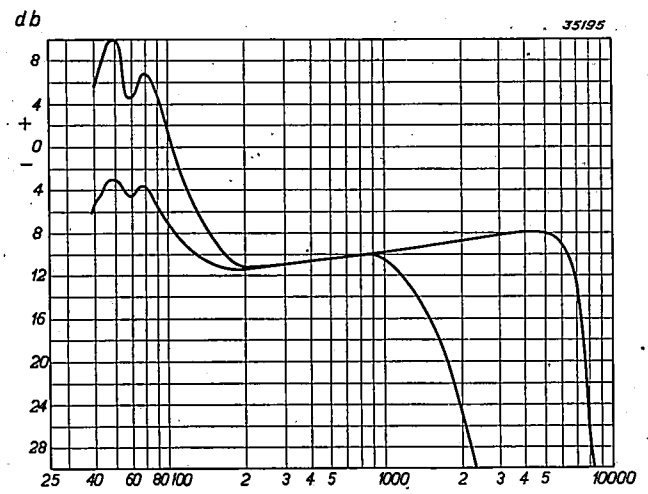

Fig. 5. Frequency characteristic (relation between output current and input voltage), which the low-frequency part of the set should have in order, together with the loud speaker, to provide the characteristic given in fig. 3*b*. The upper and lower curves of the figure correspond to the upper and lower curves respectively of fig. 3*b*.

to the chosen compromise for the cases of a very weak and a very strong interference, respectively, by a transmitter in the adjacent frequency band.

Practical realization of the desired frequency characteristic

A commonly used method of producing a variable weakening of the high tones in the low frequency part of a receiver, consists in bridging the primary terminals of the loud speaker transformer by a condenser with a variable resistance in series. This method is, however, unsuitable for our purpose. When the maximum weakening of the high tones is not applied, and when therefore the variable resistance is not made equal to zero, the impedance of the *R-C* circuit does not approach zero with increasing frequency, but retains a finite limiting value. This means that the weakening obtained in this way does not increase to an unlimited extent with increasing frequency, but also reaches a limiting value. In *fig. 6* the frequency characteris-

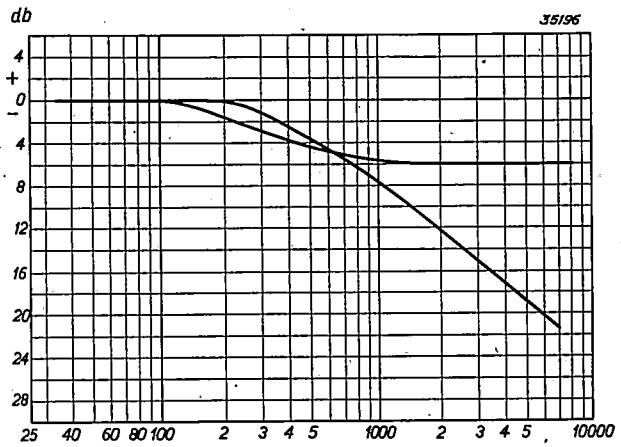

Fig. 6. Frequency characteristic of a low-frequency amplifier when an *R-C* circuit is connected across the input terminals of the loud-speaker transformer as a "tone-regulator", for $R = 0$ and for the maximum value of R. The curves show little similarity with the desired curves of fig. 5.

tics are given which may be achieved at different values of the series resistance, and it may be seen that they do not correspond at all to our requirements (fig. 5). If, instead of the resistance, the capacity should be made variable, less unsatisfactory frequency characteristics could be obtained. We shall not go into this matter here, since a solution which is practically simpler can be found in the application of variable inverse feed-back.

Variable inverse feed-back

It has already been shown in this periodical [5]) that many properties of a receiving set can be varied

[5]) "Inverse feed-back" Philips techn. Rev. 2, 289, 1937.

within wide limits by the use of inverse feed-back. In particular inverse feed-back makes it possible to give the frequency characteristic of an amplifier almost any desired form, by varying the strength of the feed-back as a function of the frequency in a suitable manner.

The amplification μ of an inverse feed-back amplifier has repeatedly been given in this periodical [6]), and is:

$$\mu = \frac{a}{1 + a\beta},$$

where a is the amplification without inverse feed-back and β is the part of the output voltage which is conducted back to the input side. If the inverse feed-back is so arranged that β increases rapidly and in a regulable manner with increasing frequency the desired shape of frequency characteristic can be obtained. As an example, *fig. 7* shows the

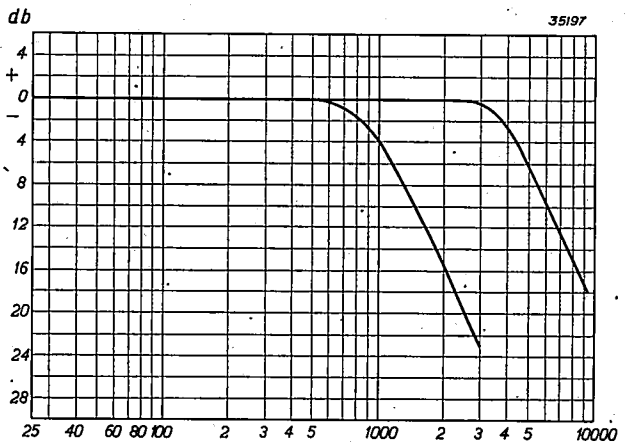

Fig. 7. Frequency characteristic of an inverse feed-back amplifier with an inverse feed-back factor for two values of a. The curves show some similarity with those of fig. 5.

variation of the amplification for an inverse feed-back factor:

$$\beta = a\,\omega^3.$$

The frequency characteristic is then given by:

$$\mu = \frac{a}{1 + a\,a\,\omega^3};$$

This is plotted in fig. 7 for two values of a and has about the desired form, although the finer details of fig. 5 are still lacking.

A possibility of obtaining the desired regulable increase in the inverse feed-back factor as a function of the frequency is given by the arrangement represented in a simplified form in *fig. 8* of a low-frequency amplifier. The voltage from the output side is conducted *via* two channels to the cathode connection of the first amplifier valve (and farther to earth). This takes place from the secondary side of the loud speaker transformer *via* Z_1 and Z_2 and from the primary side of the loud speaker transformer *via* C, R, L, Z_2.

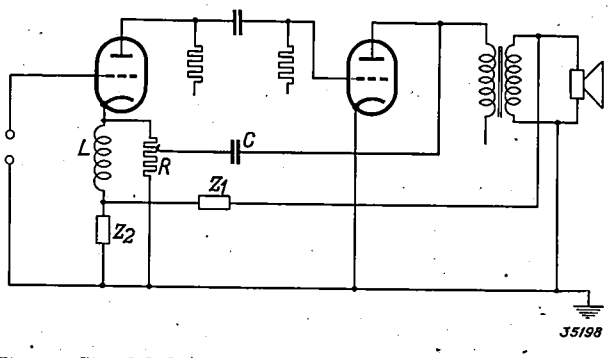

Fig. 8. Simplified connections of a low-frequency amplifier of two stages with variable inverse feed-back, whose intensity increases approximately in the desired manner with increasing frequency.

Although the voltage at the primary side is much greater, at low frequencies only the inverse feed-back of the secondary side is effective, because the condenser C passes practically no current. The inverse feed-back voltage of the secondary is divided between the impedances Z_1 and Z_2, which are so chosen that the strength of inverse feed-back gradually decreases with increasing frequency. The inverse feed-back along the second branch is, however, always more effective with increasing frequency. There are two reasons for this. In the first place at a constant amplitude of the input voltage the voltage at the primary side of the transformer increases with increasing frequency, due to its spreading selfinduction and the increasing impedance of the loudspeaker. In the second place a larger and larger part of the feed-back voltage acts on L, since the impedance of C decreases and that of L increases. The result of the described variation of the inverse feed-back along the two branches is that with increasing frequency a slight increase in amplification is obtained which is followed by a rapid fall. This agrees with the desired characteristic according to fig. 5.

In order to make the variation regulable at high frequencies the resistance R is provided with a sliding contact. When the contact is at the lowest point the feed-back current through C flows directly to earth, so that there is no inverse feed-back. When the contact is at the highest point the inverse feed-back is at a maximum; practically the whole current flows through L and Z_2 since the impedance of this connection to earth is small with respect to R. Thus

[6]) Philips techn. Rev. **1**, 264, 1936 and footnote [5]).

by moving the contact the degree of inverse feed-back can be regulated continuously.

In *fig. 9* may be seen the complete connections

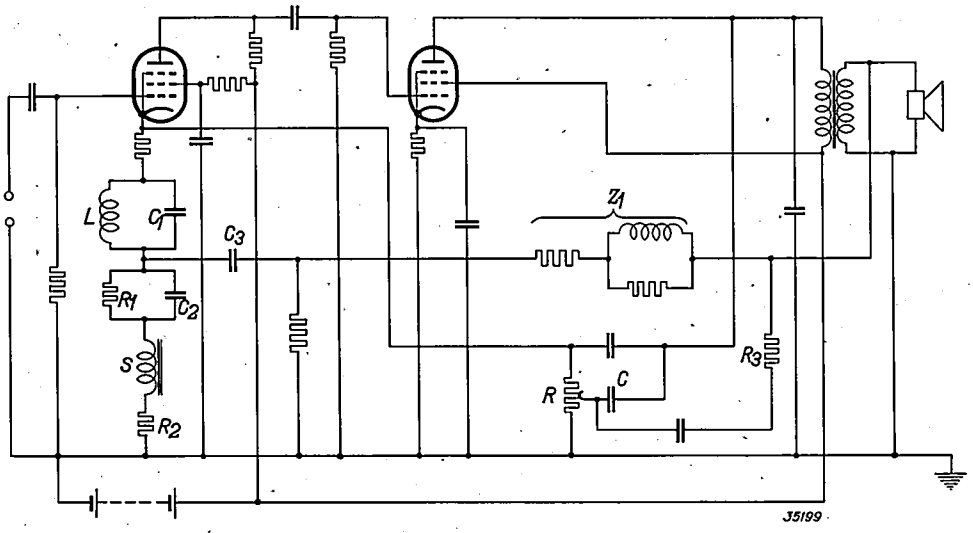

Fig. 9. Complete connections of the variable inverse feedback. In contrast to the simplified connections of fig. 8, these connections also give the desired shape of frequency characteristic (fig. 5) at low frequencies, and moreover provide that at 9 000 c/sec the reception as a whole is less suppressed.

of the low-frequency amplifier whose principle is sketched in fig. 8. The connections contain a number of elements which have not yet been mentioned and which serve to give the reproduction characteristic the desired shape in the finer details. The self-induction L is replaced by a blocking circuit LC_1, which is tuned to a frequency of 9 000 c/sec. At this frequency therefore the inverse feed-back becomes very intense, so that the amplification of this frequency is subject to the desired extra weakening.

The capacity C_2, together with the capacity C_3 and the choke S, provide for the desired shape of reproduction characteristic at very low frequencies [7]). C_2 is so chosen that at 50 c/sec a series resonance of C_2 and S occurs. At this frequency therefore there is only the impedance R_2 left in the cathode connections, and this is relatively small so that only slight inverse feed-back occurs and the amplification has a maximum.

For frequencies above 50 c/sec the connection in series of S and C_2 has an impedance of an inductive nature. At a definite frequency, which lies just above the resonance of the cabinet, series resonance occurs between this inductive impedance and the capacity of C_3. The feed-back voltage then becomes very large and the amplification thus has a minimum which compensates the maximum caused by the resonance of the cabinet. The resistance R_2 serves to damp the series resonance and thereby to adapt it to the character of the fairly well damped resonance of the cabinet. Finally, by means of the resistance R_3 provision is made that the adjustable part of the inverse feed-back is also effective at low frequencies. By this means the low tones are also weakened in increasing degree with increasing weakening of the high tones, which as we have seen is desirable.

In *fig. 10* the frequency characteristic obtained is given for the extreme positions of the tone regulator. A comparison with the curves of fig. 5 shows how closely the desired goal has been achieved.

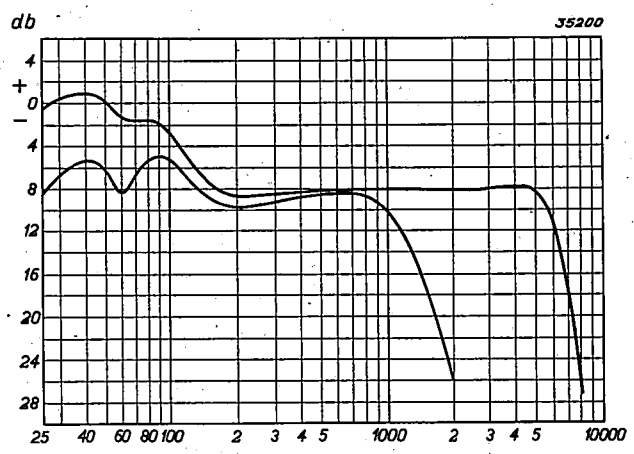

Fig. 10. Frequency characteristic of an amplifier with connections according to fig. 9, for the extreme positions of the variable inverse feed-back. The desired shape of fig. 5 is very closely approached.

[7]) The resistance R_1 serves in the usual way to give the cathode a positive D.C. voltage with respect to earth, so that the control grid takes on a negative bias with respect to the cathode. For our considerations the resistance plays no part, since its value is large compared with the impedance of C_2.

THE SWAGING OF TUNGSTEN RODS

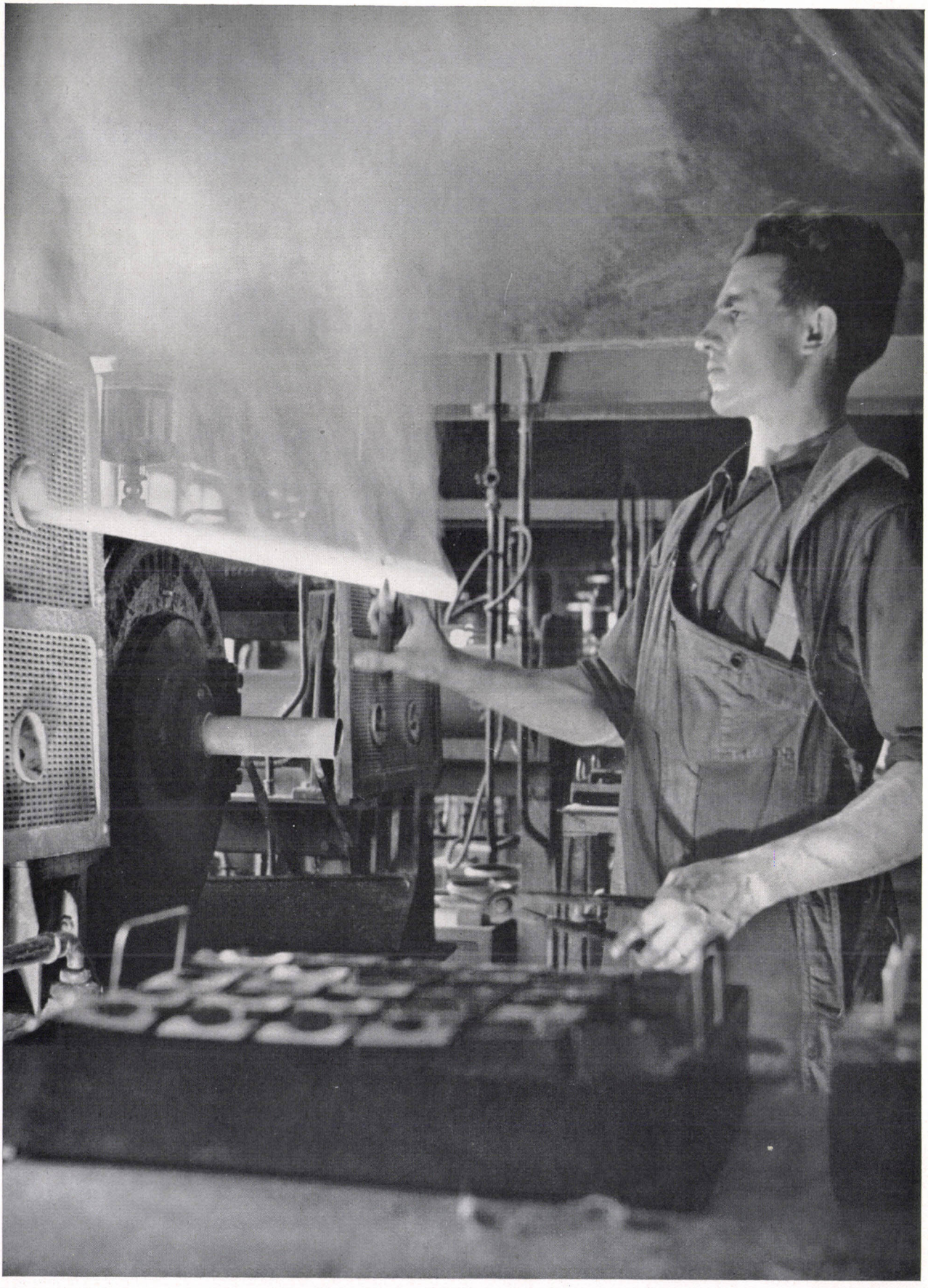

The sintered rods are heated in the electric furnace and gradually introduced into the swaging machine. In this way their diameter is reduced and their length increased.

ABSTRACTS OF RECENT SCIENTIFIC PUBLICATIONS OF THE N.V. PHILIPS' GLOEILAMPENFABRIEKEN

1455: J. H. Gisolf: The dielectric losses of irradiated zinc sulphide phosphors (Physica **6**, 918-928, Oct. 1939).

The changes in dielectric constant and dielectric losses were measured for zinc manganese sulphide upon irradiation with electromagnetic waves of various separate frequency regions between 10^3 and 1.5×10^7 c/sec. Upon irradiation with the long wave absorption bands of the manganese ion itself, no change is found in the dielectric properties, so that the luminescence thereby occurring is indeed caused only by excitation and ionization of the separate atoms. Upon irradiation with frequencies at which the crystal lattice may begin to oscillate, the dielectric properties do however change considerably. With oscillations slower than 1 000 c/sec such great space charges occur in the crystal that the counter fields thereby generated compensate the externally applied fields so completely that the losses are immeasurably small. In the long wave tails of the crystal absorption the appearance of phosphorescence phenomena must also be taken into account, so that the losses depend upon the frequency in a complex manner. In the ultraviolet region of the crystal absorption an absorption coefficient of about 5×10^4 is calculated at a wave length of 3 100 Å from the measurements of the dielectric losses.

1456: J. H. de Boer and H. Bruining: Secondary electron emission. VI. The influence of externally adsorbed ions and atoms on the secondary emission of metal (Physica **6**, 941-950, Oct. 1939).

When a metal surface is covered with electropositive atoms (barium on molybdenum for example) to different degrees, secondary and photoelectric emission are both found to reach a maximum at the same degree of covering σ_m. The increase of secondary emission is therefore caused by a fall in the work function. The secondary emission is proportional to the degree of covering at small values of the latter, while the photoelectric emission then varies exponentially with the same. This difference is a result of the fact that the secondary electrons emitted have a much greater energy than the photo-electrons. With slow primary electrons a selective secondary emission from the adsorbed atoms can be observed.

1457: M. J. O. Strutt and A. van der Ziel: On the electric space charge between parallel electrodes taking into consideration the initial velocity and the velocity distribution (Physica **6**, 977-996, Oct. 1939). Original in the German language.

The following assumptions form the basis of theoretical considerations of the space charge between plane parallel plates (the screen grid and anode of a radio valve, for instance). There is no secondary emission. No electrons return to the space between screen grid and anode when they have once left it. Only stationary states are dealt with, while anode and screen grid have positive potentials. The velocity distribution of the electrons which enter the space in question through the screen grid is given. Since no exact solution of the differential equations can be found, they are solved numerically. The most important difference between these solutions and earlier results in which no account was taken of the velocity distribution of the entering electrons consists in the fact that the regions of the characteristic with double values become smaller with increasing spreading in the electron velocities. For the simple case of the diode Langmuir's well-known formula is obtained as a first approximation.

1458: K. F. Niessen: Curieconstant and Curietemperature of nickel alloys. (Physica **6**, 1011-1033, Oct. 1939). Original in the German language.

For nickel alloys the Curie constant and Curie temperature according to Slater's theory are considered as functions of the percentage of the metal added, particularly for the case of small amounts of this metal. In alloys of nickel with copper and zinc, electrons from the third band of the nickel as well as from that of the added metal are probably missing, while in alloys with polyvalent elements they are only missing from the nickel band.

1459: J. H. Gisolf and F. Kröger: On the proportionality of the luminescence of zinc sulphide phosphors to the irradiation at low intensities (Physica **6**, 1101-1111, Oct. 1939).

Zinc sulphide phosphors which emit several bands next to one another are found to show considerable deviations from the so obvious propor-

tionality between the intensity of the emission bands and that of the irradiation. Because of this the colour changes appreciably with the intensity of irradiation. If it is assumed that the bands in question, not only in the form of fluorescence but also in that of phosphorescence, are exited by the same absorption process, the above phenomena are a result of the competition between fluorescence and phophorescence. The influence of temperature is discussed, and the phenomena are expressed in formulae.

1460: A. J. Heins van der Ven: Output stage distortion. Some measurement on different types of output valves (Wirel. Eng. **16**, 383-390 and 444-452, Aug. and Sept. 1939).

The disturbing effect of distortion in radio reception is discussed, together with an apparatus by which this distortion can be investigated. Measurements are described which were carried out on a circuit consisting of a pre-amplifier and different types of output valves. Modern output pentodes are found to prevent overloading in *fortissimo* passages better than triodes. Without inverse feed back the distortion in a pentode is indeed greater than in a triode, but with a power output of $^1/_3$ of the anode dissipation (*i.e.* the maximum output of a triode) it still remains below the permissible limit of 5 per cent. The greater distortion is not a result of a greater amount of third harmonic but of an extra second harmonic.

With output pentodes the distortion can be considerably reduced with inverse feed back, without causing the sensitivity to fall to a uselessly low level as would be the case with triodes. In addition to the use of push-pull connections which are not discussed in this article, the output pentode is therefore the best type of valve to use when high requirements are made of the quality of reproduction. In conclusion the behaviour of output tetrodes is also discussed. It is roughly analogous to that of pentodes. Tetrodes are, however, more sensitive to the value and the phase angle of the loading impedance than are pentodes.

1461: W. M. Hogendoorn: Ordering and testing castings. (Gieterij **13**, 142-144, Oct. 1939). Original in the Netherlands language.

In this lecture for foundry technicians the requirements are explained which can and must be made of castings in general. It is advisable to give specifications of the desired casting beforehand, in order to prevent later fruitless discussions and to force the foundry to raise the standards of reproducibility and quality of its products. Reliable measurements of the quality of a casting should be made on a part of the casting itself and not on test rods especially cast for this purpose.

1462: J. M. Stevels: New aspects on the cohesion of simple compounds. III (Rec. Trav. chim. Pays Bas **58**, 931-940, Sept.-Oct. 1939).

It is shown that the boiling points of all the halogen derivatives of methane can be calculated as the sum of the contributions of the three effects known as the London, the Keesom and the Debye effects. The three effects are studied to a higher approximation than formerly. It is found that a small correction is sometimes necessary in the old formula for the London effect. The formula for the Keesom effect seems to be correct in all cases. It may now be understood why the formula for the Debye effect does not hold so well according to the investigations of van Arkel and Snoek. In this connection the large distribution of the Debye and Keesom effects to the boiling points of the fluorine derivatives of ethane and ethene can also be understood. In combination with the refraction effect it is now also possible to predict the trend in the boiling points of isomers of the same type. No deviations can be found in the values given in the literature.

1463: J. D. Fast: The transition point diagram of the zirconium-titanium system (Rec. trav. chim. Pays Bas **58**, 973-983, Sept. Oct. 1939).

Both the hexagonal and the regular forms of titanium and zirconium may be mixed to give a homogeneous phase in all proportions. The temperature of the transition from the hexagonal closely-packed form to the cubic body-centred form is lowered by mixing. The minimum in the transition point diagram lies at an atomic ratio of 1 : 1 and a temperature of 545 °C. With this composition the transition thus takes place at a temperature more than 300° lower than that for the pure components. The transition point was determined anew for pure titanium, and the value found was 885° $\pm$ 10 °C. In the melting point diagram there is also a minimum at about 1575 °C and at an atomic ratio of 2 : 1 for titanium with respect to zirconium.

1464: J. H. de Boer and J. D. Fast: The diffusion of hydrogen through iron at room temperature (Rec. Trav. chim. Pays Bas **58**, 984-993, Sept.-Oct. 1939). (Original in German).

When one side of an iron plate is brought into contact with aqueous solutions containing a certain concentration of hydrogen ion, diffusion of the hydrogen through the iron takes place in all cases in which the solution dissolves the iron and frees hydrogen. No diffusion occurs if the hydrogen ion concentration is too low to cause such a development of nascent hydrogen. This shows that the hydrogen atoms which are formed by the chemical reaction are able to penetrate into the iron, but that the hydrogen ions in the solution are not able to do so. In agreement with this, it is found that hydrogen atoms which are formed by a hot tungsten wire in hydrogen are able to penetrate rapidly into iron plates even at room temperature, and may diffuse through the iron. In this way it is possible to evacuate an iron vessel containing hydrogen. Since the hydrogen can only diffuse through the iron from the side where it is dissociated into atoms, it will accummulate on the other side of the iron wall, and the diffusion takes place in opposition to any given hydrogen pressure.

1465: M. J. C. Strutt and A. van der Ziel: Short wave wide band amplification (El. Nachr. Technik **16**, 229-240, Sept. 1939) (Original in German).

The conditions for selectivity which the frequency characteristics of a television receiver must satisfy are compiled on the basis of the frequency spectra of the transmitters in Berlin, Paris, London and New York. The principle is given of a scheme in which vision and sound are separated from the very beginning and in which the high-frequency amplification of the vision is accomplished with the help of simple oscillation circuits as coupling elements in three stages between aerial and rectifier. Cascade amplification with identical and non-identical tuned circuits is dealt with quantitatively. It is found that the selectivity is insufficient in the first case, while in the second case the necessary conditions can be satisfied. Furthermore the changes in the input capacity and resistance are discussed and a method of eliminating them is indicated. Finally the data about noise are given and the smallest input signals which can be received without interference are deduced therefrom.

1466*: J. A. M. van Liempt and W. van Wijk: The rapid gas micro-analysis of mixtures of rare gas and nitrogen (Rev. Trav. chim. Pays Bas **58**, 964-972, Sept. Oct. 1939) (Original in German).

An arrangement is described with which it is possible to determine the composition of mixtures of rare gas and nitrogen in 10 minutes with an accuracy of 0.2% in the nitrogen content. The minimum quantity of gas needed is about 1 cc at 1 atmosphere. The analysis is carried out by means of absorption of the nitrogen by liquid lithium.

1467: E. J. W. Verwey: On the electrical double layer and the stability of emulsions (Chem. Wbl. **36**, 800-803, Dec. 1939) (Original in the Netherlands language).

The significance is discussed of the electrical double layer on the surface of particles for the stability of hydrophobic colloids and emulsions. Various reasons are given why an emulsion cannot be stabilized by the electrical double layer of its own liquid particles, while hydrophobic sols of solid particles can be stabilized by their own electrical double layer. The action of an emulgator which stabilizes an emulsion is based upon the occurrence on the surface of the liquid drops of a state like that already familiar in the case of the electrical double layer at a solid wall, where the whole potential drop occurs in the dispersing medium. Theoretical considerations of the variation of the electrical potential at an interface between two liquids are given in **1471.**

1468: F. A. Kröger: Solid solutions in the ternary system ZnS-CdS-MnS. (Z. Kristallogr. A **102**, 132-135, Nov. 1939).

The ternary phase diagram is discussed of zinc-cadmium-manganese sulphide at 900 °C. The disintegration which occurs in this system is found not to be caused by differences in the lattice constants, but by the difference in the type of bond of manganese sulphide compared with zinc cadmium sulphide.

*) An adequate number of reprints for the purpose of distribution is not available of those publications marked with an asterisk. Reprints of other publications may be obtained on application to the Natuurkundig Laboratorium, N.V. Philips' Gloeilampenfabrieken, Eindhoven (Holland), Kastanjelaan.

Contents of Philips transmitting News. Vol. VI. No. 3/4, December 1939:

K. Posthumus and C. A. Gehrels: Some typical phenomena relative to ultra short wave amplifier circuits.

Long wave telegraphy transmitter type KSVC 20/12.

P. Zijlstra: Some theoretical considerations on the Philips short wave radio beacon.

VOL. 5 No. 5 MAY 1940

Philips Technical Review

DEALING WITH TECHNICAL PROBLEMS
RELATING TO THE PRODUCTS, PROCESSES AND INVESTIGATIONS OF
N.V. PHILIPS' GLOEILAMPENFABRIEKEN

EDITED BY THE RESEARCH LABORATORY OF N.V. PHILIPS' GLOEILAMPENFABRIEKEN, EINDHOVEN, HOLLAND

THE DISTRIBUTION OF THE LIGHT REFLECTED BY DIFFERENT CEILING AND WALL MATERIALS

by Joh. JANSEN.

535.242.44 : 628.93

With indirect illumination, especially from coves along the walls, it is not only the total reflectivity of the surface of the ceiling which is important, but also the distribution of the reflected light in all directions. The chief types of reflection may be related to the usual qualitative characterization of the surface as "dull" or "shiny", "rough" or "smooth". In order to replace this qualitative indication by quantitative information, measurements of the above-mentioned distribution have been carried out on a series of materials at different angles of incidence. A number of results of measurements are given and explained.

The reflectivity of a surface is usually indicated by the coefficient of reflection, *i.e.* the portion of the incident light which is reflected. Besides this total reflectivity, however, in many cases the distribution of the reflected light in different directions also plays an important part. This is especially true when the directions of incidence and reflection make large angles with the normal to the surface. It has for example already been explained in this periodical how the quality of a street lighting system is influenced by this factor [1]). Another striking example is encountered in flood lighting for advertising or decorative purposes. If it were desired to illuminate the front of a white marble building in the usual way by placing searchlights near the foot of the building and directing them obliquely upwards on to the building, it would be found that the desired effect was not attained. The marble surface has, however, a satisfactory reflectivity as is shown by the fact that it appears snow white in the daytime. The explanation is obvious. The marble surface reflects the light specularly to a large extent. When the light falls from above, as is the case in the daytime, it is reflected mainly downward, toward the observer. The light which is projected very obliquely from below upon the building is however reflected chiefly skywards. The general conclusion is that smooth surfaces like marble, polished stone and glass are unsuitable for flood lighting, while rough surfaces, on the other hand, like brick, stucco and the like are very well suited for this kind of illumination.

In the case of indoor illumination also, particularly with indirect lighting, the distribution of the light reflected from the materials may be very important: *Fig. 1* shows a diagram of the ordinary

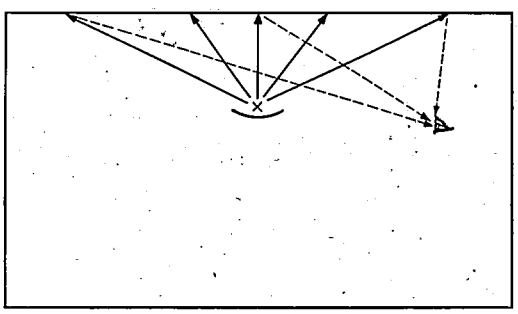

35277

Fig. 1. Indirect illumination with a lamp below the centre of the ceiling.

method of indirect lighting where the source of light hangs below the centre of the ceiling, and radiates its light only toward the ceiling which then as "secondary light source" illuminates the whole room by reflection. It is clear that different parts of the ceiling receive the light at different angles to the normal, some of which are very large, and that an observer sees the different parts from still different directions, some of which diverge very much from the normal. The occurrence of these great variations in angles of incidence and reflection explains

[1]) J. Bergmans, The brightness of road surfaces under artificial illumination, Philips techn. Rev. 3, 313, 1938.

why the type of reflection of the material of the ceiling in different directions absolutely determines the quality of the illumination. These considerations hold even more strictly when the light sources are

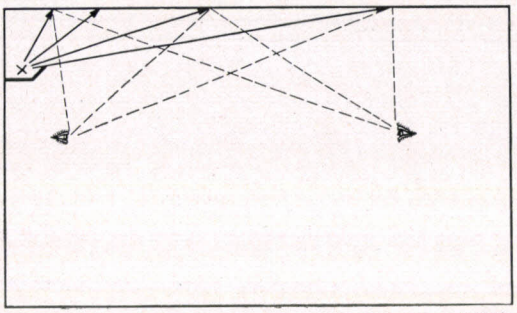

Fig. 2. Indirect illumination with lamps in a cove along the wall. Larger angles of incidence of the light occur here than in the arrangement of fig. 1.

not situated in the centre of the room but along the walls in coves (*fig. 2*). In this case the variations in the angle of incidence are even greater. This type of arrangement is being applied more and more in recent times, since the lack of fixtures hanging from the ceiling promotes a clear view of the room, particularly in long offices [2]) (*fig. 3*).

There has been until now practically no collection of data on the distribution of light reflected by materials of ceiling and walls [3]). Investigations on this subject have been undertaken by the Philips Consulting Bureau on Illumination, and we shall here give some of the results. First, however, we shall give a more general discussion of indirect illumination and the influence exerted by the reflective properties of the ceiling.

Fig. 3. Illumination of a long narrow office room by means of coves along a side wall. The absence of lighting fixtures hanging from the ceiling makes possible a clear view of the whole room.

[2]) The fact that in this arrangement the lamps must only radiate light in a relatively small solid angle is no objection thanks to the technical devices such as silver reflectors, "Cornalux" lamps, etc.

[3]) Measurements of this kind have indeed been carried out on various kinds of building stones for outside walls in connection with the above-mentioned question of floodlighting: F. Benford, Gen. El. Rev. **8**, 424, 1928.

Qualitative characterization of reflection

The aims of indirect illumination may be outlined as follows:

1) In order to avoid glare it is desirable to remove the light sources with their intense brightness from the field of vision of the user.

2) In order to avoid unpleasant contrasts and shadows it is desired that surfaces other than the working surface should be given an adequate and uniform brightness. The surfaces to be considered are walls and ceiling.

3) An adequate intensity of illumination is desired on the working surface. It is desirable that the power to be installed should not be excessively great.

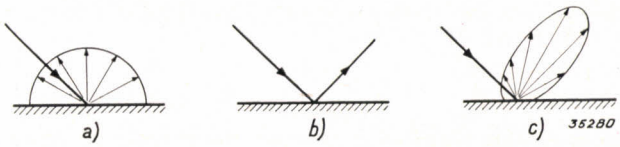

Fig. 4. Distribution of the brightness over all directions with different forms of reflection.

a) Absolutely diffuse reflection according to Lambert's law; the brightness is equally high in all directions.

b) Specular reflection; the brightness is zero in all directions except where the angle of reflection is equal to the angle of incidence. In this direction the brightness is equal to that of the light source.

c) Mixed reflection; the brightness exhibits a more or less pronounced maximum in the direction of specular reflection.

The first requirement is satisfied by the arrangements of figs. 1 and 2 if the sources of light are not below eye level. For point 3) the first requirement is of course a light colour and a high reflectivity of the ceiling. If we now consider a given spot on the ceiling then, according to point 2), it is desired that we should see this spot equally bright from every position in the room. The reflection of the ceiling material should therefore satisfy Lambert's law (entirely diffuse reflection), see the brightness curve *fig. 4a*. For the sake of contrast the distribution of brightness with specular reflection is shown in fig. 4*b*. In practical cases one is usually concerned with intermediate forms of these two extreme cases, a more or less directed reflection (mixed reflection) with for instance a brightness curve like that given in fig. 4*c*.

While in the ideal case of fig. 4*a* a variation in the angle of incidence has no effect on the distribution of brightness, in the case of the more or less directed reflection of fig. 4*c* such an effect must certainly be taken into account. Particularly with large angles of incidence (greater than 45°, for instance) such as occur in a system like that of fig. 2, considerable differences may be expected in this respect, in the sense that with increasing angle of incidence specular reflection will become more and more dominant. This is detrimental not only to the second of the above-mentioned aims, but also to the first and third, because the very bright mirror image of the light source upon the ceiling may be disturbing, and the specularly reflected light can in general only contribute to the effective illumination after several reflections and thus in a considerably attenuated form.

A surface which reflects diffusely we shall call dull, a surface with specular reflection shiny. In addition to this distinction which is based upon the microstructure of the surface, there is also a distinction based upon the macro-structure which is important for reflection phenomena, and which we shall indicate by the terms "rough" and "smooth". A rough surface consists of grains visible to the naked eye which can cast pronounced shadows like miniature hills. On a smooth surface the grains are so small as to be below the limit of visibility. If the light falls perpendicularly on a rough surface, there will be no shadows, with oblique incidence, however, the irregularities cast visible shadows from a given angle (corresponding to the slope of the miniature hills) onwards, and these shadows may give the ceiling a granular appearance (*fig. 5*). The dependence of the reflection on direction in indirect illumination due to the oblique position of the reflecting surfaces will be manifested in a different way than if all the surfaces were horizontal, while a decrease in the total reflectivity may be expected due to the repeated reflection of light between the miniature hills. This last effect becomes even clearer when the rough surface has a fibrous structure, in which case light is captured in the depression of the surface. We shall encounter an example of such a surface later in this article.

Fig. 5. The effect of shadows of the irregularities of a rough surface.

It is obvious that a smooth surface may be either dull or shiny. But a rough surface may also have both properties. By applying an enamel lacquer to a rough base a shiny rough may easily be obtained. Specular reflection is obtained, but in a different direction for each point. Such a "broken reflection" may in the main correspond to a form of mixed reflection.

Quantitative determination of the distribution of the reflected light

In order to replace this qualitative description of the behaviour of various reflecting surfaces by quantitative data, the measuring apparatus shown in *fig. 6* was constructed. By a lamp L and a lens O_1

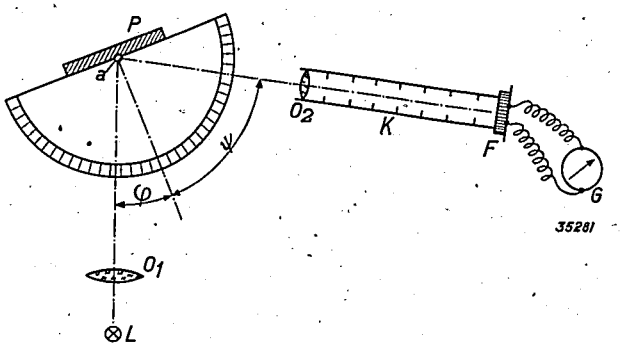

Fig. 6. Apparatus for the measurement of the distribution of the reflected light in different directions. By the light source L and the lens O_1 a circular light spot of uniform intensity is projected upon the test plate P. By turning the plate around the axis a the angle of incidence φ is regulated. The light reflected in a direction Ψ is concentrated by lens O_2 on the photoelement F, whose photocurrent is read from a galvanometer G. The tube K, blackened on the inside, prevents any extraneous or scattered light from reaching the photoelement. The angle Ψ is adjusted by turning the measuring arm.

a light spot of about 6 cm in diameter is projected upon the test plate to be investigated. The intensity of illumination is approximately constant within the circumference of the light spot. The test plate is fastened to a shaft so that it can be rotated. On the same shaft is an arm about 1.50 m long to which is attached a lens O_2 which concentrates the light reflected from the test plate on a photoelectric element (a selenium photocell). The photocurrent generated in the latter is measured directly with a galvanometer and provides a measure of the brightness of the test plate in the direction of observation [4]). In order to obtain comparable results the measured brightnesses are in every case recal-

[4]) The image of the test plate formed by lens O_2 always covered the whole opening of the photoelement, even at the largest angles of observation. The apparent surface, the reflected light flux of which contributes to the excitation of the photocurrent, is therefore constant, *i.e.* the photocurrent is proportional to the brightness of the test plate.

culated for the case where the test plate as a secondary light source radiates a total light flux of 1 lumen per sq.m.

By rotating the test plate and measuring arm the angles of incidence (φ) and of reflection (Ψ) of the light can be regulated. In the measurements the values of the parameter φ of 0°, 30° and 60° were chosen as a rule, while Ψ was varied between +70° and —70° (*fig.* 7). The direction of incidence, the

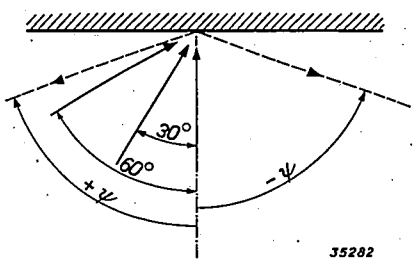

Fig. 7. The angle of incidence φ was set equal to 0°, 30° and 60° successively for all measurements. The angle of reflection Ψ with respect to the normal to the surface investigated is considered positive toward the side of the incident light and was varied between +70° and —70°.

normal to the test plate and the direction of observation always lay in one plane. For the complete calculation of an indirect lighting system the reflection in other planes besides the plane of incidence must of course also be measured. For our present purpose of characterizing different materials, however, the indicated measurements will suffice.

A series of white surfaces which may be used as material for covering ceiling and walls were investigated with the apparatus. As far as possible the same kinds of paint were used on the different surfaces, but were applied by different methods, brushed out smooth or sprayed. The results obtained from six samples are given in *fig. 8a-f.* In addition to the description of the materials used, the total reflectivity (with normal incidence of the light [5]) and the classification according to the qualitative properties given above, two photographs are given of each surface which were taken in such a way that the peculiarities of the surface are presented "in a correct light".

Results of measurements

The samples *a*, *b* and *c* demonstrate the difference between dull and shiny. All three samples were smooth (free of visible irregularities). In the case of sample *a* (dull) the curves which indicate the distribution of brightness are practically circular. This means that, observed in the direction of the light ($\Psi \approx \varphi$) and in the opposite direction ($\Psi \approx -\varphi$), there is little difference. This surface more than all the others investigated most closely approaches the ideal case of reflection according to Lambert's law; the slight deviations at the largest angles are caused by a few local irregularities, accumulations of paint particles, which may be seen as shadow points in the second photograph taken obliquely. The surfaces of samples *b* and especially *c* were not dull but shiny (finished with cellulose lacquer and japan lacquer, respectively). The curves exhibit extremely sharp peaks at $\Psi \approx -\varphi$. The brightnesses in these directions were ten or twenty times higher than in other directions of Ψ. In the photographs also this strongly directed reflection (specular reflection of the light source) may be seen, although because of the limited contrast which can be attained in copying the actual effect is not truly reproduced. For the rest, the brightness in other directions Ψ corresponds approximately to that measured with sample *a*. The light flux at the peaks of the diagrams *b* and *c* is therefore small, and, as far as the efficiency of the illumination is concerned, of little significance [6]). The strong contrasts may however lead to glare.

The other three samples, *d*, *e* and *f* illustrate the effect of a rough surface structure. The test plate *d* was of the same materials as *a* but was tamped, which treatment results in a surface with irregularities about 0.5 mm in height. The diagram shows that the distribution of the reflection over different directions now deviates very much from the circular form. Especially at large values of the angle of incidence φ a considerably greater brightness is observed in the direction of the light ($\Psi \approx \varphi$) than in the opposite direction ($\Psi \approx \varphi$). At $\varphi = 60°$ for instance the two values of the brightness are in the ratio of 2.2 : 1, and at larger angles the ratio increases rapidly. This effect is easily understood from a consideration of fig. 5. With illumination at angles of $\varphi = 45°$, for example, the slopes of the miniature hills which face the source of light are favourable for reflection. Looking in a direction with the light these slopes are clearly seen and the shadow sides are invisible; against

[5]) At other angles of incidence the total reflectivity might have a different value. In the case of the samples investigated, however, the difference for the three parameter values $\varphi = 0°$, 30° and 60° was found to be only very slight (maximum 4%).

[6]) One must not be misled by the fact that the peaks occupy a large part of the area of the diagrams: the area enclosed by these brightness curves has no simple physical significance in particular, this area is not by any means a measure of the total reflected light flux.

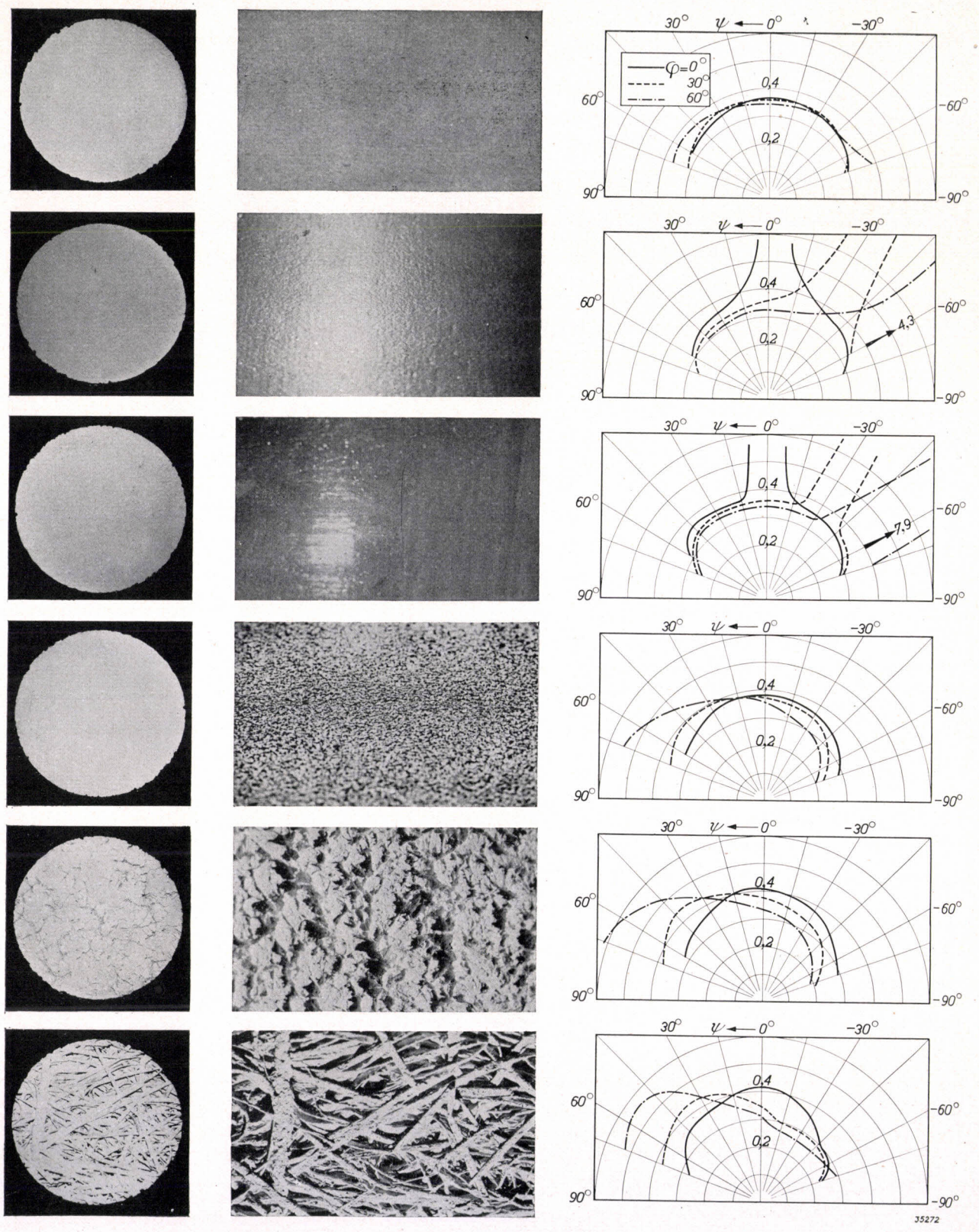

Fig. 8. Photographs and measured brightness distribution of six white surfaces. In the case of the first photograph the angle of incidence φ of the light was always 0°, the angle of observation Ψ = 10-15°. In the second photograph for the samples *a*—*d*, φ = 60°, Ψ = 60°, for samples *e* and *f*, φ = 0°, Ψ = 60°. In the diagrams the brightness is plotted in cp/sq m. which would be observed if a total of 1 lumen of reflected light were radiated per sq.m of the test plate.

a) One coat of priming colour and one coat of size colour; smooth and dull; total reflectivity 86.5% (see note [5]).
b) Two coats of priming colour and one of cellulose lacquer; smooth and fairly shiny; total reflectivity 80%.
c) Two coats of priming colour and one of japan lacquer; smooth and very shiny; total reflectivity 79%.
d) One coat of priming colour and two of size colour tamped; rough (irregularities of 0.5 mm) and dull; total reflectivity 88.5%.
e) Size colour very coarsely tamped; very rough (irregularities of 3 mm) and dull; total reflectivity 82.5%.
f) Size colour on coarse wood fibre board; very rough and dull; total reflectivity 52%.

the light on the other hand one sees only the dark slopes away from the light source and the average brightness observed is therefore much lower.

It must be noted in this connection that wall coverings of the sort *d* (in the form of whitewash or wallpaper) are very common, and that the above-mentioned large angles of observation and incidence are also very important in practical cases (see fig. 2). The consequence is, as the second photograph of sample *d* shows, that the surface appears for a large part covered with shadows. Samples *e* and *f* have a still rougher surface and consequently exhibit the same effect to an even greater degree. In the case of the very irregular fibrous structure of sample *f*, the low reflectivity must moreover be noted (loss of light in the fairly deep crevices of the surface), as well as the irregular shape of the curve representing the distribution of brightness. (This last fact indicates that the cross section of the beam of light which was used for the measurements may here no longer be considered large compared with the irregularities in the structure of the surface being investigated).

Besides the well known fact that with indirect illumination a shiny ceiling must be avoided, the above results show that with a moderately rough structure the ceiling exhibits a maximum brightness in just the opposite direction to that in which the maximum occurs in specular reflection and that with arrangements like the cove systems given in figs. 2 and 3, where angles up to 70 and 80° occur, this effect must be kept clearly in mind. If with such large angles one does not wish to see any disturbing shadows on ceiling and walls, and wishes to attain a satisfactory illuminating efficiency, the surface must be finished as smooth as possible.

This requirement cannot always be satisfied in a simple way. If for example it is required that the ceiling should serve not only as a reflecting plane for the indirect lighting, but that it should also possess sound damping characteristics, we are met with a dilemma; whether to cover the ceiling with a rough or a smooth material. The first is favourable for sound damping and the second is desired for the reflection of light. Which point of view will dominate, or what compromise should be accepted will depend upon circumstances.

When a certain material has been chosen for ceiling and walls, it is possible with the help of brightness curves like those given here, to calculate the effect which may be expected from indirect lighting by means of light sources in certain positions. We hope to be able to discuss this subject at some future time.

ELECTRON TRAJECTORIES IN MULTIGRID VALVES

by J. L. H. JONKER.

537.545.2 : 621.396.694

In the case of tetrodes and pentodes the anode current increases rapidly with increasing anode voltage, and reaches a saturation value at an anode voltage of 20 to 40 volts. It is desirable to make the anode voltage at which saturation occurs as low as possible. For this purpose care must be taken that the electrons are not too much deflected by the wires of the various grids. The deflection of electrons by grid wires and the influence of this deflection on the I_a-V_a characteristic of tetrodes and pentodes is examined theoretically and experimentally in this article. In conclusion the measures are discussed, which can be employed for the purpose of keeping the deflections small.

The properties of transmitting and receiving valves have repeatedly been discussed in this periodical on the basis of diagrams which represent the anode current as a function of the anode voltage, with the control grid voltage as a parameter. In particular the connection has been studied between the maximum output which can be produced under given circumstances and the shape of the I_a-V_a characteristic [1]). Furthermore various installations have been described which were designed for the rapid recording of I_a-V_a characteristics of transmitting and receiving valves. In this article we shall discuss the I_a-V_a characteristics, especially those of multigrid valves, from a more theoretical point of view, and we shall devote special attention to the trajectories of the electrons in the neighbourhood of the grids.

For the sake of orientation the I_a-V_a diagrams of a tetrode and a pentode are again given in *fig. 1*. It may be seen that for a given value of the control grid voltage the anode current at first increases rapidly with increasing anode voltage, and at 20 to 40 volts it has already practically reached its maximum value. In the case of the tetrode the first rapid increase in the anode current is followed by a slight kink due to secondary electrons emitted by the anode which reach the screen grid. In the case of the pentode this kink is absent, since the secondary electrons are driven back by a suppressor grid introduced between screen grid and anode, the wires of which are usually at cathode potential. The secondary electrons in this case therefore return to the anode.

In practical cases where tetrodes and pentodes are used, the object generally is to be able to vary the anode current as widely as possible by a variation of the voltage of the control grid. Since the loading impedance is always included in the anode circuit, changes in the anode voltage naturally also

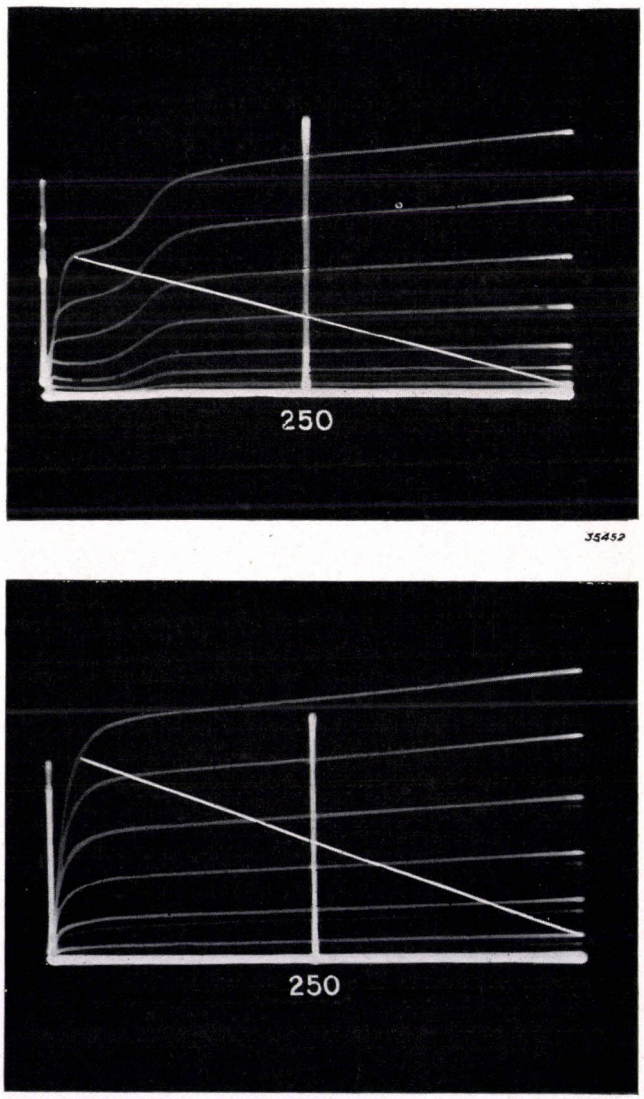

a)

b)

Fig. 1. I_a-V_a characteristics of a tetrode and a pentode. At high anode voltages the anode current is practically independent of the anode voltage. At a certain anode voltage the characteristics of the tetrode exhibit a kink which is caused by secondary emission from the anode.

[1]) For instance in the article: Five electrode transmitting valves, Philips techn. Rev. **2**, 257, 1937.

[2]) In the articles:
Applications of cathode ray tubes, Philips techn. Rev. **3**, 339, 1938;
Recording the characteristics of transmitting valves, Philips techn. Rev. **4**, 56, 1939;
Testing amplifier output valves by means of the cathode, Philips techn. Rev. **5**, 61, 1940.

occur due to this cause, and these changes might affect the variations in the anode current undesirably. As long as the minimum value of the varying anode voltage does not become too low, and the valve continues to operate in the region where the I_a-V_a characteristics is horizontal, the influence of the anode voltage variations on the anode current will only be slight. If, however, the minimum of the anode voltage becomes so low that the neighbourhood of the kink (in the case of the tetrode) or the knee (in the case of the pentode) is approached, the anode current will then increase only very little more, and may even begin to decrease. The curve which represents the anode alternating current as a function of the time for a sinusoidal grid alternating current in this way assumes a very irregular form at the peaks, which may lead to serious distortion.

In order to experience as little difficulty as possible from this disturbance, attempts are made to construct the valves in such a way, that the anode current characteristics remain horizontal to very low anode voltages, and then finally fall at a sharp angle to zero. For this purpose, in systems with cylindrical electrodes, it is necessary in the first place to provide for an accurately centred arrangement [3]), in order that the electrons shall be accelerated and retarded only in radial directions. If this aim were fully achieved the electrons would all attain sufficient kinetic energy, due to the accelerating action of the screen grid, to move counter to the retarding field of suppressor grid and anode at every positive value of the anode voltage, and reach the anode, so that the anode current would reach its maximum value at any given low anode voltage.

Actually, however, the characteristics by no means ever reach this ideal, even with the most careful assembly. The anode voltage at which the anode current reaches its maximum value is always found to amount to 10 per cent or more of the screen grid voltage. It may be concluded from this that, in addition to asymmetry of the assembly, there must be other factors, which have a depressing action on the radial component of the velocity of the electrons.

It has been found that this decrease in radial velocity may be ascribed chiefly to the deflection of the electrons by the wires of the grid.

Due to this deflection the motion of the electrons, which would otherwise be truly radial, is given a tangential component. Since the total velocity does not change (at every point it is given by the value of the potential), the radial component of the velocity of the deflected electrons is smaller than that of the non-deflected electrons. At low anode voltages the electrons which are most strongly deflected, and which therefore move the slowest in radial directions, will be unable to reach the anode against the retarding field of suppressor grid and anode, and it is to this fact that the decrease in anode current with decreasing anode voltage must be mainly ascribed.

In order to test this hypothesis quantitatively, and in addition to investigate to what degree the I_a-V_a characteristics of a pentode can be influenced by structural means, the deflection phenomena of electrons in pentodes have been investigated theoretically and experimentally. By „experimental" investigation we mean here not only measurements carried out on test valves made especially for this purpose, but also a study of the motion of the electrons with the help of models in which the variation of potential in a system is imitated by means of a rubber membrane stretched in a certain way, and the electrons are represented by steel balls rolling across the rubber membrane [4]). We shall begin with a description of the deflection by a positive grid (screen grid), which has also been analyzed theoretically, and will then consider the deflection of the electrons by the control grid and the suppressor grid.

Deflection of electrons by a positive grid

When an electron leaves the cathode with zero velocity it will at first be accelerated by a positive grid in a radial direction, or, when the electrodes are plane, in a direction perpendicular to the cathode. We shall call this direction "radial" in the future for the sake of simplicity. In the neighbourhood of the grid wires, however, the field is no longer truly radial but also contains a tangential component which gives the electron a lateral deflection. The magnitude of this deflection varies according to whether the electron passes midway between two grid wires or closer to one of them. This is illustrated clearly in *fig. 2*, where the electron trajectories are recorded with the help of a rubber membrane for the case of a positive grid, behind which is situated the anode, which is also positive but at a considerably lower potential. The manner in which the deflection which the electrons undergo upon passing the grid varies between two grid wires is clearly shown. It is also clear that the most strongly deflected elec-

[3]) An example of this is given in the last article referred to in footnote [2]).

[4]) This method is described in detail in Philips techn. Rev. 2, 338, 1937.

trons are unable to reach the anode, so that the anode current is smaller than the electron current which passes through the slits of the screen grid.

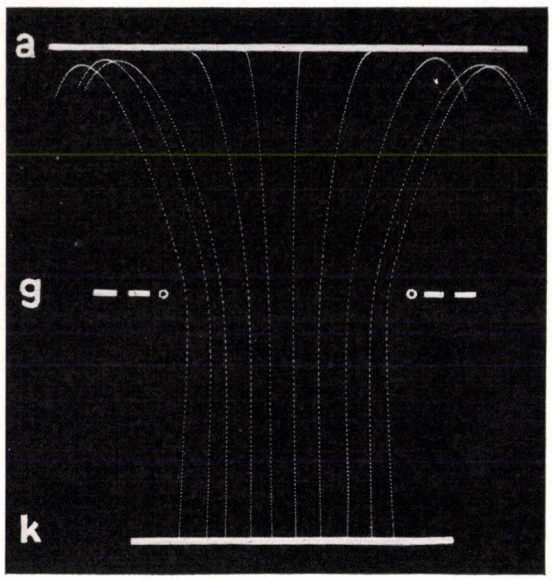

Fig. 2. Electron trajectories between two rods of a plane positive grid followed by an anode plate which is slightly negative. The pictures were obtained by intermittent illumination (50 c/sec) and photographing of balls rolling over a stretched rubber membrane. It may be seen that the strongly deflected electrons do not move as far counter to the anode potential as do the less deflected electrons.

If the anode voltage were gradually increased, the non-deflected electrons would reach the anode first (namely as soon as $V_a > 0$) and only at a considerably higher voltage would all the electrons reach the anode.

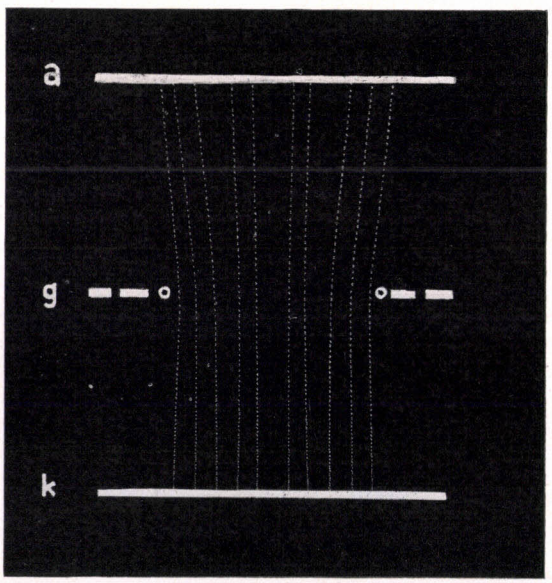

Fig. 3. Electron trajectories between two rods of a plane positive grid followed by an anode at the same potential. This figure is more suitable than fig. 2 for determining the angles of deflection.

In order to be able to measure the angles of deflection of the different trajectories easily it is desirable to choose the circumstances so that the trajectories are straight lines behind the positive grid. This can be achieved simply by giving the anode the same potential as the grid. *Fig. 3* shows the electron trajectories obtained in this way, while in *fig. 4* the results are given which may be deduced from that figure, namely the angle of deflection as a function of the point at which the electron passes the positive grid.

It is immediately obvious that the tangent of the angle of deflection is almost directly proportional to the coordinate x, which indicates at what distance from the middle of the slit between two grid wires the electron traverses the plane of the grid.

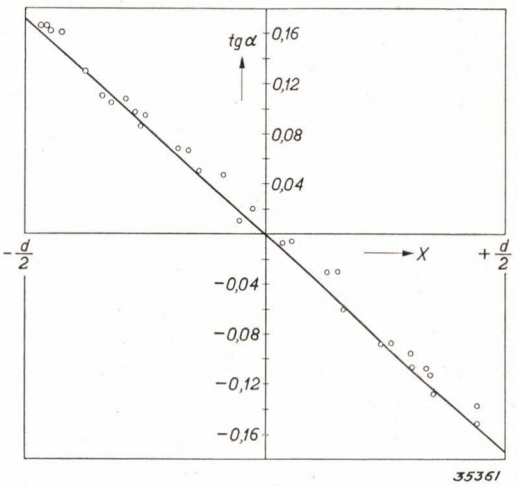

Fig. 4. Tangent of the angle of deflection as a function of the point relative to two grid wires where the electron traverses the grid. Midway between two wires ($x = 0$) no deflection occurs, to the left and right of the middle point the electrons are deflected in opposite directions through an angle whose tangent is proportional to the distance from the middle.

If the maximum angle of deflection α_m for electrons which pass the grid wires as close as possible ($x = d/2$) is known, then by using this relation, the anode current I_a can immediately be calculated which will occur at a given value of V_a when a homogeneous beam of electrons corresponding to a current I_a passes between the grid wires. As may be seen from fig. 2 all the electrons cannot reach the anode at a low anode voltage, but only those whose angle of deflection does not exceed a certain value which we shall call α_0. A certain value of the coordinate x_0 corresponds to this angle α_0, and consequently a certain current, which is given by the following [5]):

[5]) Since the theoretical considerations hold only for small angles, we may in qualitative discussions neglect the difference between the angle itself and its functions sin α and tan α.

$$\frac{I_a}{I_k} = \frac{x_0}{d/2} = \frac{\tan \alpha_0}{\tan \alpha_m} \sim \frac{\alpha_0}{\alpha_m} \quad \ldots \quad (1)$$

α_0 depends upon the grid voltage V_g and the anode voltage V_a. If the anode voltage is equal to zero (cathode potential), then only those electrons can reach the anode which are entirely undeflected. α_0 thus becomes equal to zero, and the same holds for the anode current. With increasing anode voltage α_0 becomes steadily larger, and finally reaches the value α_m, which means that all the electrons which pass through the slits of the screen grid also reach the anode.

What is the relation between α_0, V_a and V_g? The electrons which pass through the slits of the screen grid (potential V_g) have a velocity v which is determined by $^1/_2\, mv^2 = eV_g$ where m is the mass and e the charge of an electron. From this it follows that:

$$v = \sqrt{2\frac{e}{m}V_g}.$$

For electrons which are deflected through an angle α_0 the radial velocity v_r is smaller than v and equal to $v \cos \alpha_0$. Their kinetic energy in a radial direction is therefore

$$^1/_2\, mv_r^2 = {}^1/_2\, m \frac{2e}{m} V_g \cos^2 \alpha_0' = e\, V_g \cos^2 \alpha_0.$$

These electrons which are deflected through an angle α_0 will just be able to reach the anode when their kinetic energy in a radial direction corresponds to the potential difference between grid and anode, thus when:

$$e\, V_g \cos^2 \alpha_0 = e(V_g - V_a), \text{ or}$$
$$V_a = V_g\,(1 - \cos^2 \alpha_0) = V_g \sin^2 \alpha_0.$$

For small angles of deflection we find from this

$$\alpha_0 \sim \sin \alpha_0 = \sqrt{\frac{V_a}{V_g}},$$

and by substituting this value of α_0 in equation (1) for the anode current we find:

$$\frac{I_a}{I_k} = \frac{1}{\alpha_m}\sqrt{\frac{V_a}{V_g}} \quad \ldots \quad (2)$$

The result is therefore that the anode current I_a at a given screen grid voltage V_g is proportional to the square root of the anode voltage V_a. This is of course only valid for low anode voltages, for which $\alpha < \alpha_m$. When $\alpha_0 = \alpha_m$, in other words when

$$V_a = V_g \alpha_m^2,$$

all electrons reach the anode; the I_a-V_a characteristic has a kink, and then continues horizontally with increasing anode voltage.

Before applying the theoretical conclusions to the usual types of construction for practical use, we shall first consider the value of the maximum angle of deflection α_m.

Calculations have been carried out by Below [6]) on the maximum angle of deflection α_m. He considered the electron trajectories in the neighbourhood of a plane grid for the case when the grid potential is high compared with the fluctuations in potential within the region around the grid where the deflection occurs, so that it is permissible to assume that all the electrons pass the plane of grid with the same velocity.

As a result of his calculations follows in the first place the linear relation between the position where the electron passes the grid and the deflection, as was found experimentally in fig. 4. For the maximum angle of deflection he also obtained the following relation:

$$\tan \alpha_m = \frac{\pi \gamma}{V_g}, \quad \ldots \quad (3)$$

where γ is the charge per cm of grid wire.

The charge is determined by the capacity and the potential difference between the grid and the adjacent electrodes, which we have called cathode and anode for the sake of simplicity. The capacities can be calculated approximately by considering the grids as cylindrical or plane electrodes with a certain effective potential. The charge found in this way must then be recalculated per cm of the grid wire. For this purpose the total length l of the grid wire is calculated from the pitch and the radius of the grid, and the charge is then divided by l. The result of these calculations, which we shall not describe in detail, is the following for the case of cylindrical electrodes:

$$\tan \alpha_m = \frac{d}{4 r_g V_g}\left(\frac{V_g - V_k}{\ln \frac{r_g}{r_k}} + \frac{V_g - V_a}{\ln \frac{r_a}{r_g}}\right), \quad (4)$$

where d is the distance between successive wires of the control grid, and r_k, r_g and r_a are the radii of cathode, grid and anode, respectively. For the case of plane electrodes the formula becomes:

$$\tan \alpha_m = \frac{d}{4 V_g}\left(\frac{V_g - V_k}{a_{gk}} + \frac{V_g - V_a}{a_{ga}}\right), \quad (5)$$

where a_{gk} and a_{ga} represent the distances between

[6]) F. Below, Z. Fernmeldetechn. 9, 113-136, 1928.

the grid and the cathode and the grid and the anode respectively. Together with equation (2) equations (4) and (5) give the anode current as a function of the anode voltage and the grid voltage.

Equation (5) can be tested experimentally by measuring the maximum deflection for a number of different electrode configurations by means of a rubber membrane, and comparing the result with the calculation. This check gives quite satisfactory results. The measured deflections are found to agree within 8 per cent with the calculated deflections, as follows from *table I* where a number of cases are summed up. Since there are certain errors in the method of measurement with a rubber membrane [7]), and also since Below's theory is exact only for small angles of deflection, a better agreement could not be expected.

Table I. Deflection of electrons by a positive grid between two electrodes at zero potential.

	Dimensions of the model (cm)				tan a_m	
	a_{ga}	a_{gk}	d	diametre of grid bars	measured	calculated
I	10	10	10	1,0	0,180	0,179
II	20	20	20	1,9	0,188 0,182*	0,177
III	20	20	20	1,0	0,150 0,170	0,158
IV	10	30	10	1,0	0,188 0,183	0,199
V	10	30	5	1,0	0,107 0,123	0,114

* Two measurements being made for the models II—V.

Having shown in this way that the deflection of electrons by the screen grid can be calculated with sufficient accuracy, it would seem obvious that the I_a-V_a characteristics of existing valves can be calculated with the help of the formulae found, and that means of making the shape of these characteristics as satisfactory as possible can be considered. This would indeed be possible if the screen grid were the only electrode which causes a deflection of electrons. In the case of electronic valves of practical importance, however, in addition to the screen grid there is always a control grid and often a suppressor grid also, and these grids may also cause a deflection of the electrons which is found in practice not to be small compared with the deflections caused by the screen grid.

These additional deflections of the electrons by suppressor and control grid cause the anode current to reach its maximum value with increasing anode voltage later than would follow from the theory discussed in the foregoing. Moreover, due to these extra deflections, the shape of the I_a-V_a curve is very much altered in the neighbourhood of the knee. In order to deal with this in detail we shall first investigate the deflection of electrons at the control grid and suppressor grid, respectively, particularly for the simple case where the wires of these grids are at cathode potential.

In the case of the suppressor grid this is practically always the case. The wires of the control grid, on the other hand, usually have a negative potential; zero potential only occurs as a maximum value. Since we are in the first place interested in the shape of the I_a-V_a characteristic at low anode voltages, it is just this maximum control grid voltage with which we are concerned; on the load line the lowest anode voltage corresponds to the highest control grid voltage (see fig. 1).

Deflection of electrons by a grid at zero potential

In the case of a grid at zero potential situated in the neighbourhood of another electrode at a high potential (the screen grid) the condition is no longer fulfilled that the fluctuations in potential in the plane of the grid shall be small compared with the average potential which determines the velocity of the electrons. The velocity of the electrons which reach the slit between two grid wires can no longer be considered independent of the position, but is now considerably greater at the middle of the slit than in the neighbourhood of the grid wire. This is shown clearly in the shape of the electron trajectories as found with the help of the stretched rubber membrane (see *fig. 5*). If the conditions of the above discussed theory were satisfied, then at every point on the grid the tangent of the angle of deflection would be proportional to the distance between that point and the middle of the slit. But in that case the deflection would be opposite in direction to that with a grid at a high potential, so that the electrons would be focussed to a point. Since, however, contrary to the theoretical assumption, the electrons move slower and slower with increasing distance from the middle, so that the deflection is greater than demanded by the theory, the focal distance for electrons on the

[7]) See the article referred to in footnote [4]).

edges of the slit is shorter than for those at the middle of the slit. In optical language, the slit between two grid wires forms a cylindrical lens with a positive spherical aberration.

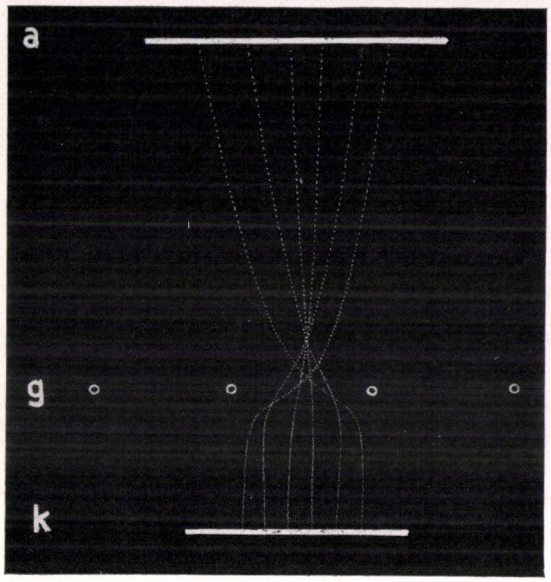

Fig. 5. Trajectories of electrons at the moment of passing a grid at zero potential. The deflection is in the opposite direction to that in fig. 2: the beam of electrons is not spread, but focussed.

Since the angle of deflection of the sharply curved electron trajectories in the neighbourhood of the control grid is difficult to determine from the figure, the angle of deflection α of the electron at the anode is measured instead, and this deflection differs only by a constant factor from the control grid deflection. For the same reason the coordinate x was not determined in the plane of the grid but in the plane of the cathode.

If $\tan \alpha$ is once more plotted as a function of x, then on the basis of the experiments with the rubber membrane the curve given in *fig. 6a* is obtained. Over one half the width of the slit on either side of the middle the curve is practically a straight line, but closer to the grid wires the deflection increases more rapidly than proportional to the distance from the centre line. Close to the grid wire the deflection begins again to decrease because the first deflection is so great that the electrons come under the influence of the adjacent grid wire and are deflected in the opposite direction.

The straight line *b* in fig. 6 represents the deflection which is calculated theoretically on the assumption (actually an incorrect one) that the variations of the potential in the plane of the grid are small compared with the effective grid potential. By combining equations (2) and (5) the following formula is obtained for the angle of deflection α:

$$\tan \alpha = \frac{2x}{d} \frac{d}{4V_{g1}} \left(\frac{V_{g1}-V_k}{a_{g1k}} + \frac{V_{g1}-V_{g2}}{a_{g1g2}} \right), \quad (6)$$

The agreement of the lines calculated with (6) and the curve deduced from the measurements is rather better than might be expected taking into account the rough considerations used; the decrease in the experimental deviation for great values of x has an important influence on this result.

As this formula can be applied with space discharge grids, as well as with secundary emission grids, the deviation phenomena for any grid in tetrodes or pentodes can be described with formula of similar shape.

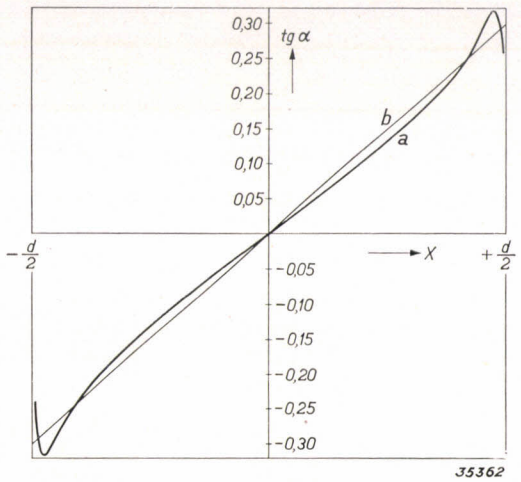

Fig. 6. Tangent of the angle of deflection of electrons which pass a grid at zero potential as a function of the distance between the starting point of the electron and the line half way between two grid wires, α is the angle at which the deflected electrons reach the anode.
a) Experimentally determined curve;
b) Curve calculated on the assumption of a constant potential in the grid plane equal to the average grid voltage.

I_a-V_a characteristics of tetrodes and pentodes

After having accounted for the deviating properties of the individual grids of a tetrode or a pentode, we now can indicate the partition of electrons for different angles of deviation, if these electrons have passed all the grids of a tetrode or a pentode. From this angular partition the I_a-V_a characteristic of the tube can be calculated in a similar manner as used in the given considerations for the angular partition of electrons reflected at the screening grid. With very small anode voltages, in which we are interested here, this picture will agree with the facts, however, this is not the case with greater anode voltages *i.a.* because we neglected the electrons which after having passed the screening grids, are partially lost for the anode current, by

direct reflection on the wires of the space discharge grid.

The cooperation of these deviations in the different grids may occur in various manners. If *e.g.* two successive grids have the same pitch, the electrons which are deviated by the first grid cannot be distributed uniformly over the openings of the next grid, it therefore matters, if the wires of the second grid are placed in line with the wires of the first grid, or if they have a displacement of half the pitch with respect to those of the first one. In the following the first case shall be considered more in detail.

For the present, however, we assume that the grids are unequal in pitch, and therefore that the lateral components of the velocity which are due to the deflection at the three grids may be added together according to the laws of chance.

The tangential component of velocity which is imparted to the electron in the plane of each grid is equal to the total velocity in the plane of the grid multiplied by the sine of the angle of deflection. In this manner one finds with the aid of form. (5) and (6) for the tangential changes in velocity, which the electrons undergo in each of the three grids of a pentode the following:

$$\left.\begin{aligned} v_1 &= \sqrt{\frac{e}{2m}}\, x_1 \frac{1}{\sqrt{V_{g1}}}\left(\frac{V_{g1}-V_k}{a_{g1k}} + \frac{V_{g1}-V_{g2}}{a_{g1g2}}\right), \\ v_2 &= \sqrt{\frac{e}{2m}}\, x_2 \frac{1}{\sqrt{V_{g2}}}\left(\frac{V_{g2}-V_{g1}}{a_{g1g2}} + \frac{V_{g2}-V_{g3}}{a_{g2g3}}\right), \\ v_3 &= \sqrt{\frac{e}{2m}}\, x_3 \frac{1}{\sqrt{V_{g3}}}\left(\frac{V_{g3}-V_{g2}}{a_{g2g3}} + \frac{V_{g3}-V_a}{a_{g3a}}\right). \end{aligned}\right\} \quad (7)$$

x_1, x_2 and x_3 are here the chance position coordinates in each grid, and they may vary from zero to half the pitch. V_{g1}, V_{g2} and V_{g3} are the average potentials in the three grid planes, as in the foregoing. The total tangential component of the velocity behind the suppressor grid is $v_1 + v_2 + v_3$.

If the three expressions in equation (7) are compared it is seen that with normal dimensions of an output pentode they may have about the same order of magnitude. It is therefore quite incorrect to consider only the scattering by the screen grid, for instance, as is sometimes done.

The way in which the three tangential components must be added together is shown in *fig.* 7. It is thereby assumed that $v_1 > v_2 > v_3$. Such an assumption does not detract from the general validity of the analysis, since the total deflection in the approximation in question is independent of the order in which the grids are traversed.

If only the first grid is traversed, all the tangential velocities between $-v_{1\max}$ and $+v_{1\max}$ are present to the same extent in the scattered beam, as indicated in fig. 7*a* (the subscript *max* is omitted in the figure). The diagram has the simple form of a rectangle.

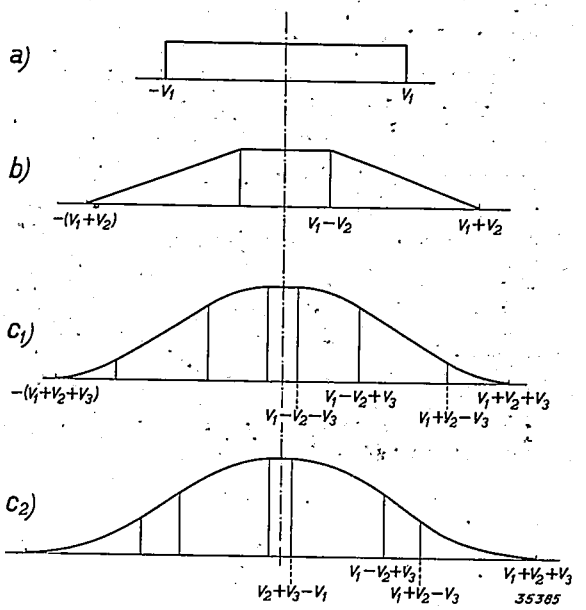

Fig. 7. Distribution of the tangential velocities in a beam of electrons which is scattered by one, two or three grids.

If the beam is scattered by a single grid all tangential velocities between two maximum values $+v_1$ and $-v_1$ occur to the same extent; the distribution of velocities is given by a rectangular diagram (curve *a*).

If the scattered beam is then again scattered by a second grid, the number of electrons per unit of velocity interval is given for every velocity v by the area of curve *a*) between $v-v_2$ and $v+v_2$, where v_2 indicates the maximum tangential velocity imparted to the electron by the deflection at the second grid, which is assumed to be smaller than v_1. In this way the trapezium-shaped curve *b*) is obtained.

If the beam is then scattered once more by a third grid, curve *c*) is obtained, in which the ordinate for every velocity v is given by the area of curve *b*) between $v-v_3$ and $v+v_3$. As to the shape of the curve, a distinction must be made between $v_3 < v_1 - v_2$ (curve c_1) and $v_3 > v_1 - v_2$ (curve c_2). Both curves are composed of parabolic and straight sections. The difference lies in the fact that the middle portion of curve c_1 is horizontal, while in the case of c_2 it is part of a parabola whose curvature is twice as great as that of the other parabolic sections.

If in addition to the first grid the second grid is also traversed, a diagram like that of fig. 7*b* is obtained. All the electrons which have tangential velocities between $v-v_{2\max}$ and $v+v_{2\max}$ after deflection by the first grid now contribute equally to every total tangential velocity v. The number of these electrons can be found by considering the area of the first diagram between $v-v_2$ and $v+v_2$. A trapezium-shaped diagram is obtained as explained in the text under the figure.

If in the same way the scattering by the third

grid is also considered the kinks in the trapezium figure disappear; the diagram becomes a smooth curve composed of straight sections and parabolic curves. As may be seen in fig. 7c two cases must be distinguished: namely $v_1—v_2—v_3 > 0$ and $v_1—v_2—v_3 < 0$. In the first case the upper part of the diagram contains a straight section, while in the second case it is parabolic. The shape of the whole curve already shows a certain similarity with the Gauss curve for the distribution of chance fluctuations, and with an increasing number of grids it would soon approach Gauss curve.

After having determined in this way the distribution curve of the tangential velocities for one, two and three grids, we can calculate the I_a-V_a characteristic for each of these cases. It must be kept in mind that at every anode voltage V_a those electrons reach the anode whose tangential velocity after traversing all the grids is smaller than a certain maximum value v_0, which is given by:

$$^1/_2\ m\ v_0^2 = e\ V_a.$$

In *figs. 8a, b* and *c* the characteristics are reproduced which are calculated in this way for the cases of 1, 2 and 3 grids. The case of one grid, as already stated, has no great practical importance; the case of two grids may, at a very low voltage, at which no appreciable secondary emission occurs, be compared with the characteristic of the tetrode, while the diagram for three grids — also only at very low voltages — corresponds to the case of the pentode.

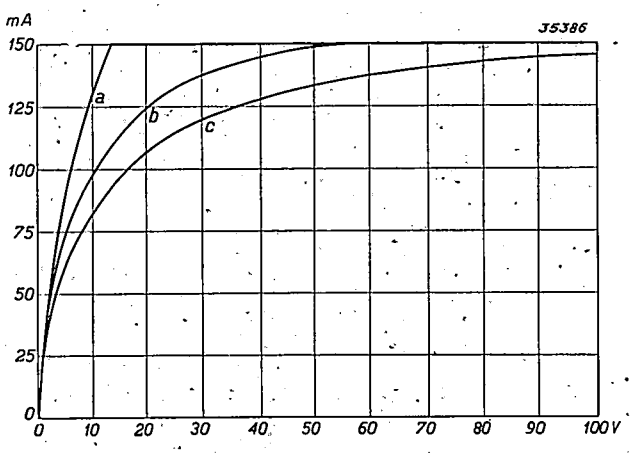

Fig. 8. I_a-V_a characteristics calculated for electron beams which are scattered according to the velocity diagrams of figs. 7*a*, *b* and c_2.

Conclusions as to the construction of tetrodes and pentodes

In order that the anode current may reach its saturation value at the lowest possible anode voltage, it is desirable to make the deflections experienced by the electrons at the grid wires as small as possible. Several conclusions as to the construction of the various grids may be drawn from this requirement.

The control grid

Just as in the case of every grid so with the control grid is the maximum deflection which may occur according to equation (7) proportional to the pitch. It is therefore advisable to make the pitch of the grid small. Since this is done for other reasons also in valves with a steep slope, it is understandable that such valves also have a favourable I_a-V_a characteristic, which fact is manifested in a high value of the ratio between the maximum useful output and the anode dissipation.

If the control grid voltage is strongly negative the electrons cannot pass the grid at any arbitrary spot, but only in a narrow region in the middle of the slits, where the potential in the grid plane is still positive. It is obvious that the deflection of the electrons is hereby weakened, since the deflecting forces are weakest in the middle of the slits. In confirmation of this it is often observed that the knee becomes sharper and sharper with increasing negative control grid voltage.

The screen grid

In the case of the screen grid it would seem better not to make the pitch too low since then the current consumption would become too great. The question arises, however, as mentioned above, whether a decrease in the deflections cannot also be obtained by placing the wires of the screen grid in line with the wires of the control grid.

With satisfactory mutual relations between the pitch and the distance between control grid and screen grid this may indeed bring about an improvement. The electrons are focussed by the control grid, and when the focus does not lie at too great a distance from the screen grid the electrons will tend to pass through the middle of the slits of the screen grid where the deflection is weak. At the same time the screen grid current is hereby diminished and consequently the noise [8]).

Fig. 9 shows the electron trajectories, recorded on a model, through a negative and a positive grid whose wires are placed directly behind one another. As may be seen the deflections which the electrons experience in the two grid planes are not

[8]) This is further explained in: Noise in amplifiers contributed by the valves, Philips techn. Rev. 2, 329, 1937.

independent of each other: those electrons which are most strongly deflected at the control grid also experience the greatest deflection at the

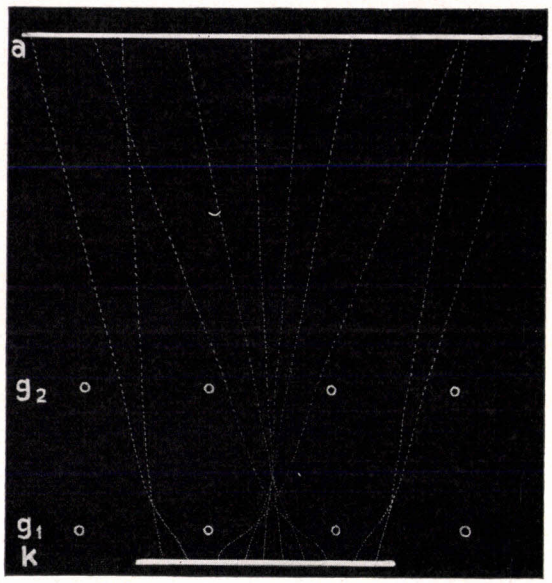

Fig. 9. Electron trajectories for a negative and a positive grid whose wires are situated directly behind each other. The deflection of an electron by the second grid is proportional to the deflection which it has already undergone at the first grid.

screen grid. The deflecting effect of the screen grid in this case may be described by saying that every deflection which the electron undergoes at the control grid must be multiplied by a certain factor. The distribution of the tangential velocities thus remains essentially that of a single grid, so that the I_a-V_a characteristic in this case will have the shape of fig. 8*a* and exhibit a sharp kink. Such a characteristic is indeed found in the case of tetrodes when the wires of control and screen grid are placed directly behind each other.

The suppressor grid

The deflection by the suppressor grid is determined by the third member of equation (7), namely:

$$v_3 = \sqrt{\frac{e}{2m}}\, x_3 \frac{1}{\sqrt{V_{g3}}} \left(\frac{V_{g3} - V_{g2}}{a_{g2g3}} + \frac{V_{g3} - V_a}{a_{g3a}} \right) . \quad (8)$$

As may be seen this expression is composed of two terms which have opposite signs at low anode voltage ($V_a < V_{g3}$). The first term is negative, the second positive. It is obvious that the position and potential of the suppressor grid can be so chosen that the two terms cancel each other. Since in the case in question both V_{g3} and V_a have fairly low values, while the screen grid voltage V_{g2} is high, the numerator of the negative term will be considerably larger than that of the positive term. In order to make the two terms equal in absolute value, the same relation must hold for the denominators, and this means, that the distance a_{ga} between the suppressor grid and the anode must be chosen considerably smaller than that between suppressor and screen grid.

Just as in the case of the control grid and the screen grid, one might in the case of the suppressor grid also attempt to diminish the deflections by making the pitch of the grid low. This device, however, does not produce the desired result. As we

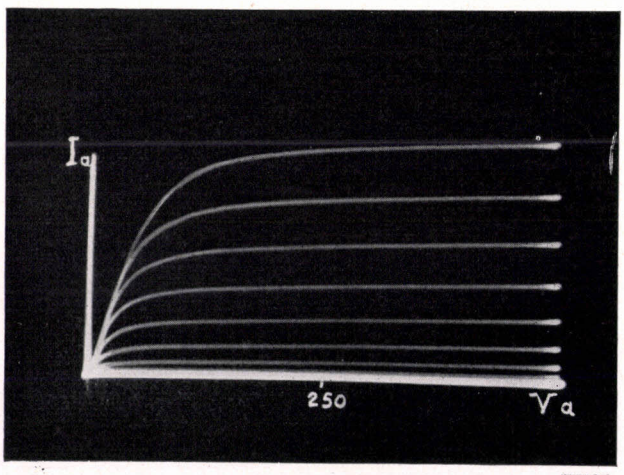

a

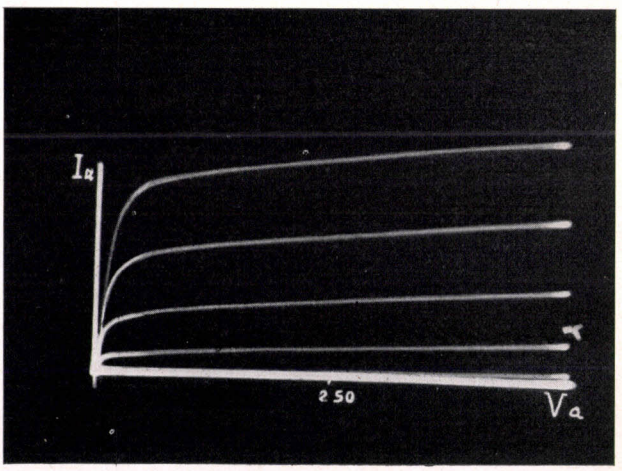

b

Fig. 10. I_a-V_a characteristics of two output pentodes.
a) Earlier type with low slope.
b) Modern type with steep slope, in which the deflections of the electrons have been kept as small as possible by various means. The practically horizontal rectilinear part of the characteristic begins at a much lower anode voltage.

have seen, for a compensation of the two deflection terms it is necessary that the effective suppressor grid potential V_g should lie between those of the screen grid and the anode, because only in that case do the two terms of equation (8) have opposite signs. Since the grid wires themselves are at cathode potential, which is lower than the desired value of the effective potential, it is necessary that the effect of the anode and screen grid should be sufficiently felt between the wires of the grid. Therefore it is of advantage to make the pitch large and to try to keep the deflection small by a suitable choice of the position of the suppressor grid as in the case above.

In *fig. 10* the I_a-V_a characteristics of an earlier and a modern type of pentode (amplifier output valve) are reproduced, from which it may be seen that the flat part of the characteristic could be extended to considerably lower anode voltages. The improvement is obtained mainly be decreasing the pitch of the control grid and by suitable placing of the suppressor grid. The position of the knee in the diagram has been shifted from about 40 volts to about 20 volts.

MICROPHONES

by J. de BOER.

621.395.61

An explanation is given of the different ways in which sound vibrations may be converted in a microphone into vibrations of a membrane, ribbon or plate, which possesses one degree of freedom, and how these vibrations can in turn excite an alternating EMF in an electrical circuit. The considerations provide a basis for the division of microphones into different types. In conclusion several types of microphones are described.

The name microphone was originally used by C. Wheatstone to denote an instrument which served to make very weak sounds audible to the human ear, and which was therefore what we now call a stethoscope. Now, however, the name microphone is used exclusively for instruments which convert air vibrations into electrical AC voltages. The early development of microphones took place during the years 1876 and 1877. At that time Alexander Graham Bell (1876) was laying the foundations of modern telephony. In his work he used a microphone which worked on the electromagnetic principle. One year later (1877) both Thomas Edison and Berliner were granted patents for a much more sensitive microphone, whose action depended upon the variable resistance of powdered carbon. Since that time the further development of the microphone has gone hand in hand with the development of reproduction and recording of sound.

The various kinds of microphones have one feature in common, namely they all first convert the motion of the air particles into motion of a membrane, ribbon or plate. This motion leads to the excitation of an electrical AC voltage, so that the following sequence is always involved:

motion of air → motion of membrane → EMF.

In a sound field the total air pressure can be divided into the normal pressure P of the atmosphere, which is constant, and a varying term $p_\sim$ due to the sound vibrations, the so-called sound pressure.

The following requirement is made of a good microphone. The amplitude of the EMF excited by the sound pressure must be directly proportional to the amplitude of the sound pressure for every frequency $\omega/2\pi$ in the frequency range to be reproduced and the proportionality factor must be independent of the frequency. The amplitudes occurring are usually small enough to satisfy the first condition. In this article it will be explained how it is possible to make the proportionality factor indepent of the frequency.

In the first place we shall discuss the conversion of the motion of the membrane into an EMF, which involves the classification of microphones according to their electrical behaviour. We shall then deal with the different devices for the conversion of the air vibrations into motion of the membrane. This involves an acoustic classification of microphones. Finally the different useful combinations of electrical and acoustic characteristics and several models of different types of microphones will be described.

Electrical classification of microphones

EMF is dependent upon the deviation of the membrane.

In the classic *carbon microphones* (*fig. 1*) a deviation $x_\sim$ of a membrane M causes a change in the transition resistance between grains of

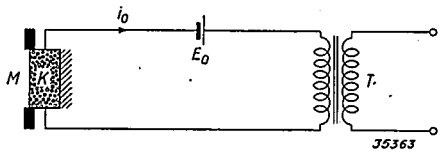

Fig. 1. Electrical circuit of a carbon microphone. M membrane, K grains of carbon, E_0 constant EMF, T transformer from which the alternating voltage of the microphone can be taken.

carbon which are enclosed in a container K. For sufficiently small deviations of the membrane the change in resistance ΔR is proportional to the deviation:

$$\Delta R = Cx_\sim \quad . \quad . \quad . \quad . \quad . \quad . \quad . \quad (1)$$

where the proportionality factor C does not depend upon the frequency. The constant EMF E_0 applied to the microphone circuit gives a current $i_0 = E_0/R_0$ when the total resistance of the circuit is R_0. The small change in resistance ΔR of the microphone is therefore equivalent to an alternating EMF in the microphone circuit:

$$E_\sim = i_0 \Delta R = C\frac{E_0}{R_0}x_\sim \quad . \quad . \quad . \quad (2)$$

The relation between the EMF $E_\sim$ and the deviation $x_\sim$ of the membrane is thus independent of the frequency.

When a *piëzoelectric crystal plate* is stretched or compressed, electrical charges occur upon the side surfaces. If such a crystal C (*fig. 2*) is introduced between a rigid wall and a membrane which is set in motion by sound vibrations, an EMF $E_\sim$ is excited in the crystal which is proportional to the deviation $x_\sim$ of the membrane.

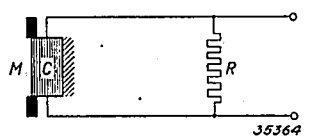

Fig. 2. Diagram of a piëzoelectric crystal, R resistance from which the microphone voltage generated can be taken.

This alternating EMF in turn can be made to excite an alternating current in an electric circuit.

In the case of the *condensator microphone* the moving membrane forms one of the plates of a condenser (*fig. 3*). The motion of the membrane causes changes in the capacity of the condenser. When opposite charges have been put on the plates of the condenser over a resistance R by means of an electric battery, the changes in capacity lead to changes in voltage between the two plates, which in this case also have the same relation for all frequencies with respect to the deviations of the membrane.

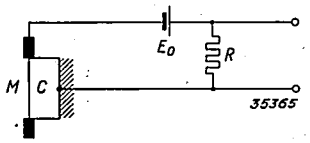

Fig. 3. Diagram of a condenser microphone. M membrane which forms a condenser C with the rigid wall. E_0 constant EMF, R resistance over which the alternating voltage of the microphone can be taken off.

For these three types of microphones the EMF generated is proportional to the deviation of the membrane, no matter how high the frequency. For satisfactory functioning of these microphones, therefore, it is only required that this deviation is proportional to the sound pressure for all frequencies. We shall discuss in the following the degree to which this requirement can be satisfied.

EMF depends upon the velocity of the membrane

In the case of an *electrodynamic microphone*, a membrane, ribbon or plate which is set in motion by the air vibrations is either itself electrically conducting or bears a conductor upon it. This conductor is placed in a constant magnetic field (*fig. 4*) and included in an electric circuit. Due to

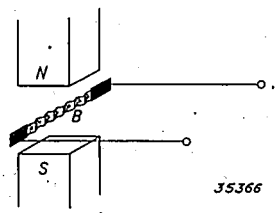

Fig. 4. Diagram of an electrodynamic microphone. N north pole, S south pole of a permanent magnet. B vibrating metal ribbon included in the circuit.

the motion of the conductor in the magnetic field the number of lines of force enclosed within the electric circuit changes:

$$N = N_0 + Cx_\sim = N_0 + Cx_0 \cos \omega t \quad . \quad (3)$$

where C is a constant and $\omega/2\pi$ the frequency. According to the law of induction, an EMF is hereby excited in this circuit, which is equal to the decrease per unit of time in the number of lines of force enclosed:

$$E_\sim = -\frac{dN}{dt} = -C\dot{x}_\sim = C\omega x_0 \sin \omega t, \quad . \quad . \quad (4)$$

where $x_\sim$ represents the derivative of the deviation with respect to time, *i.e.* the velocity of the membrane.

A small piece of soft iron which completes the magnetic circuit of a permanent magnet is fastened to the vibrating membrane of an *electromagnetic microphone* (*fig. 5*). Due to the motion of the

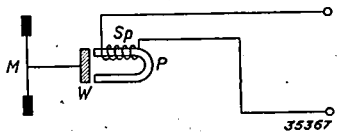

Fig. 5. Diagram of an electromagnetic microphone. *M* membrane to which a piece of soft iron is fastened which vibrates in the field of a permanent magnet *P* which is surrounded by a coil *Sp*.

membrane a varying magnetic field occurs which generates an EMF in a stationary electric coil surrounding the magnet and forming part of an electrical circuit. The situation in the case of such an electromagnetic microphone is quite similar to that in the case of an electrodynamic microphone, and in both cases an EMF occurs which is proportional to the velocity, the proportionality factor being is independent of the frequency. In order to obtain satisfactory reproduction for all frequencies with microphones which function on the electrodynamic or electromagnetic principle, the ratio between the velocity of the moving system and the sound pressure should therefore be independent of the frequency.

Acoustic classification of microphones

Pressure microphones

If one side only of the membrane *M* of the microphone is exposed to the variable sound pressure $p_\sim$ (*fig. 6*), one speaks of a pressure microphone.

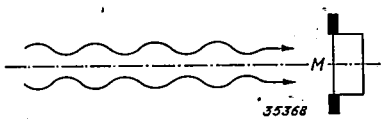

Fig. 6. Pressure microphone with moving membrane *M* placed in a plane sound wave.

In this case the force $K_\sim$ which the air vibrations exert upon the surface S of the membrane is equal to the product of this area and the sound pressure:

$$K_\sim = Sp_\sim = Sp_0 \cos \omega t \quad . \quad . \quad . \quad (5)$$

When the mass of the membrane is m, the frictional resistance r and the stiffness s, the equation of motion of this membrane assumes the following form:

$$m\,x_\sim + r\,\dot{x}_\sim + s\,x_\sim = K_\sim = Sp_0 \cdot \cos \omega t \quad . \quad (6)$$

where $\ddot{x}_\sim$ represents the acceleration.

In such a moving system with one degree of freedom the greatest deviation for a given amplitude of the external force occurs when the frequency of the force is equal to the resonance frequency:

$$\frac{\omega_0}{2\pi} = \frac{1}{2\pi}\sqrt{\frac{s}{m}} \quad . \quad . \quad . \quad . \quad . \quad . \quad (7)$$

The way in which the amplitude of the vibrating system varies with the frequency differs very much according to whether the frequency in question is sufficiently far above or below the resonance frequency or in its vicinity. In these three different frequency regions each of the three terms in the left-hand member of equation (6) in turn plays the most important part, so that one may use the following approximations of equation (6) for the three regions:

$$\omega \gg \omega_0\text{: } m\ddot{x}_\sim = Sp_0 \cos \omega t; \quad . \quad . \quad . \quad (8)$$

$$\omega \approx \omega_0\text{: } r\dot{x}_\sim = Sp_0 \cos \omega t; \quad . \quad . \quad . \quad (9)$$

$$\omega \ll w_0\text{: } sx_\sim = Sp_0 \cos \omega t; \quad . \quad . \quad . \quad (10)$$

In the neighbourhood of the resonance frequency, therefore, the sound pressure determines the velocity of the motion of the membran; for higher and lower frequencies the sound pressure determines the acceleration *viz.* the deviation.

In the case of carbon, piëzoelectric and condenser microphones, as we have already mentioned, the EMF depends upon the deviation of the membrane. As to the acoustic part of these microphones, care must therefore be taken that the ratio between the deviation and the sound pressure is independent of the frequency, *i.e.* equation (10) must be valid. These types of microphone must therefore be constructed as pressure microphones, and care must be taken that the resonance frequency for these systems with a single degree of freedom is made so high that the frequency region to be reproduced falls below it. If the resonance frequency should still lie in the region of the highest tones to be reproduced, a disturbing resonance will occur unless care is taken to make the damping sufficiently severe.

In the frequency region above the resonance frequency the ratio between the acceleration, ($\ddot{x}_\sim = \omega^2 x_\sim$) and the sound pressure is constant, according to equation (8). For the three types of microphone mentioned the amplitude of the EMF generated in the microphone circuit varies for high frequencies according to p_0/ω^2. The sensitivity thus decreases rapidly for high frequencies, as may clearly be seen from the resonance curve given in *fig. 7*.

A microphone working on the electrodynamic or electromagnetic principle will, according to equation (4), reproduce sound satisfactorily if the relation between the velocity of the membrane and the pressure does not depend upon the frequency. A pressure microphone may therefore only be used in these two types in the frequency region for which equation (9) is valid, *i.e.* in the vicinity of the resonance frequency. By making the mechanical damping large, provision may indeed be made that the frequency region in which the reproduction may be considered satisfactory becomes fairly wide, but the sensitivity then usually becomes too low, so that such a solution remains inadequate. If for certain reasons it is nevertheless desired to construct a pressure microphone according to the electrodynamic principle, it is advisable, in order to improve the reproduction of tones above and below this resonance frequency, to pass from the system with a single degree of freedom, which has only one resonance frequency to a system with several degrees of freedom which give rise to several successive resonance frequencies (*fig. 8*). Provision may indeed be made in this way that the sensitivity of the microphone remains practically constant over a wider frequency range, but the reproduction, especially of speech, is of poorer quality due to the maxima indicate the position of the resonance frequencies in the sensitivity curve of fig. 8. We shall therefore not consider such microphones further in this article, and consider only microphones with one degree of freedom.

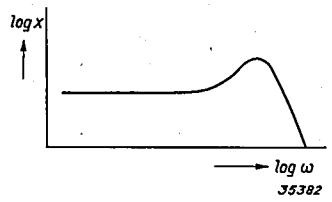

Fig. 7. Resonance curve of a membrane with one degree of freedom; the logarithm of the deviation x as a function of the logarithm of the frequency.

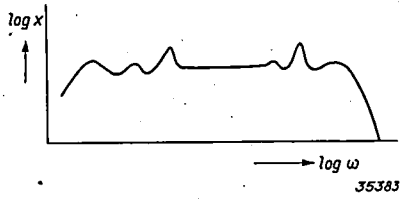

Fig. 8. Resonance curve of a system with more than one degree of freedom.

The sound pressure at a point does not depend upon the position of the surface element upon which one wishes to measure its effect. Therefore the action of a pressure microphone will not depend upon the position of the vibrating membrane with respect to the direction of propagation of the sound waves. A pressure microphone is therefore equally sensitive from all directions, so that the polar linear direction diagram of the sensitivity of this microphone is a circle. If the dimensions of the microphone are not small with respect to the wave length of the sound, the microphone itself distorts the sound so that deviations from this simple picture of the situation occur [1]).

Pressure-gradient microphones

If both sides of a membrane or a vibrating plate can be reached by the sound waves (*fig. 9*),

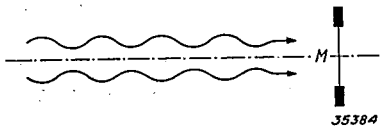

Fig. 9. Pressure-gradient microphone with a moving membrane M both sides of which are exposed to the air vibrations.

the latter will arrive at the front and rear sides with a certain phase difference. If the sound pressure on the front of the membrane amounts, for instance, to

$$p_1 = p_o \cos \omega t \quad . \quad . \quad . \quad . \quad . \quad . \quad . \quad (11)$$

and if the waves must cover a distance which is l cm longer in order to reach the other side, then for a wave length λ the sound pressure on the rear side of the membrane becomes

$$p_2 = p_o \cos (\omega t - 2 \pi l/\lambda) = p_o \cos (\omega t - kl) \quad . \quad (12)$$

where $k = 2\pi/\lambda = \omega/c$, c representing the velocity of sound. If the membrane has an area S, a force $K_\sim$ acts upon it which is the product of this surface and the difference in pressure p_1—p_2:

$$K_\sim = S\,(p_1 - p_2) = Sp_o\,[\cos \omega t - \cos (\omega t - kl)] \quad (13)$$

Since this force is proportional to the pressure gradient, *i.e.* to the fall in pressure per unit of length, such microphones are called pressure-gradient microphones.

If the dimensions of the microphones are small compared to the wave length, *i.e.* if $l \ll \lambda$ or $kl \ll 2\pi$, the force becomes:

$$K_\sim \approx - Sp_o\, kl \sin \omega t \quad . \quad . \quad . \quad . \quad (14)$$

At a certain value p_o of the sound pressure the amplitude of the force acting on the membrane of a pressure-gradient microphone increases proportionally with k, *i.e.* proportionally with the fre-

[1]) *Cf.*: Philips techn. Rev. 4, 144, 1939.

quency. The equation of motion for the membrane becomes:

$$m\ddot{x}_{\sim} + r\dot{x}_{\sim} + sx_{\sim} = K_{\sim} = -Cp_0\,\omega \sin \omega t \ldots (15)$$

which may be simplified in the following way for the frequency regions indicated:

$$\omega \gg \omega_0 = \sqrt{\frac{s}{m}} : m\ddot{x}_{\sim} = -Cp_0\,\omega \sin \omega t; \quad . \; . \quad (16)$$

$$\omega \approx \omega_0 \quad : r\dot{x}_{\sim} = -Cp_0\,\omega \sin \omega t; \quad . \; . \quad (17)$$

$$\omega \ll \omega_0 \quad : sx_{\sim} = -Cp_0\,\omega \sin \omega t. \quad . \; . \quad (18)$$

By integration of (19) and (17) the following expressions are obtained:

$$mx_{\sim} = Cp_0 \cos \omega t, \; . \; . \; . \; . \; . \quad (16')$$

$$rx_{\sim} = Cp_0 \cos \omega t, \; . \; . \; . \; . \; . \quad (17')$$

which are valid for $\omega \gg \omega_0$ and for $\omega \approx \omega_0$ respectively. From formula (16 and 16') it may be seen that for frequencies sufficiently far above the resonance frequency the ratio of the velocity of the membrane to the sound pressure becomes independent of the frequency. This is exactly what is required of a good electrodynamic (or electromagnetic) microphone, since in that case the ratio between the EMF excited and the velocity of the membrane is independent of the frequency. When a pressure-gradient microphone acting on the electrodynamic principle is used, very good reproduction can therefore be obtained for alle frequencies above the region of resonance.

If one desired to construct a pressure-gradient microphone on the principle of the carbon, piëzoelectric or condenser microphones, it could only be used for frequencies in the neighbourhood of the resonance, since the deviation only in that region is proportional to the sound pressure.

The gradient of the sound pressure depends upon the direction in which it is considered. Therefore in the case of a pressure-gradient microphone the induced EMF will depend upon the position of the membrane with respect to the direction of propagation of the sound waves. If in *fig. 10* we indicate the front and rear sides of the membrane by the points V and A, for which points the largest possible difference of path l for the sound exists, then the difference of path when the membrane is turned through an angle α with respect to the direction of propagation of the waves becomes equal to $l \cos \alpha$. In formulae (12) and (14) l must then be replaced by $l \cos \alpha$, so that the induced EMF will also be proportional to $\cos \alpha$. If this EMF is plotted in a polar diagram as a function of the angle α, a directional diagram is obtained which consists of two circles touching each other (*fig. 11*).

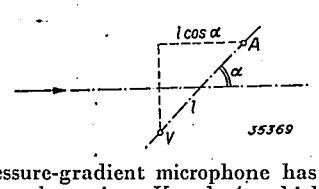

Fig. 10. A pressure-gradient microphone has the maximum sensitivity when the points V and A, which represent the front and rear sides of the membr ne, lie one behind the other in the direction of incidence of the sound, so that the difference in path is l for a plane sound wave. At an angle α this difference is only $l \cos \alpha$.

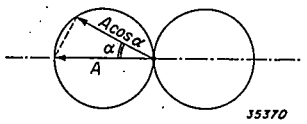

Fig. 11. The polar diagram of the sensitivity of a pressure-gradient microphone consists of two circles touching each other. At an angle α the sensitivity it is $A \cos \alpha$.

If the membrane is perpendicular to its position of greatest sensitivity, no EMF at all is induced, since the sound waves reach both sides of the membrane simultaneously and no difference in pressure occurs. Microphones with such a direction diagram may very well be used in rooms in which there is much noise and reverberation [2]) since this undesired sound in general arrives at the membrane with the same intensity from all directions while the sound to be amplified comes from a definite direction.

Combination of pressure and pressure-gradient microphone

If a pressure and a pressure-gradient microphone are connected electrically in series, a microphone is obtained whose EMF becomes equal to the sum of the EMF's of the two microphones. If for instance the EMF E_1 is generated in the pressure microphone and E_1 in the pressure-gradient microphone at its optimum position, then at any given position of the latter (at an angle α) the total EMF is:

$$E = E_1 (1 + \cos \alpha) \; . \; . \; . \; . \; . \quad (19)$$

The polar direction diagram then becomes a so-called cardioid (*fig.12*). For $\alpha = 0°$ the sensitivity, is greatest, while in the opposite direction ($\alpha = 180°$) the sensitivity would be zero since the pressure and pressure-gradient microphones give exactly equal and opposite EMF's with such orientation. Advantage may be taken of this characteristic when it is desired to reproduce the sound from a given direction while suppressing that from another direction.

[2]) *Cf.*: Philips techn. Rev. 3, 221, 1938.

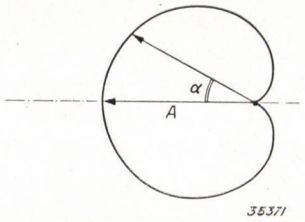

Fig. 12. The polar diagram of the sensitivity of a combination of a pressure and a pressure-gradient microphone having the same maximum sensitivity is a cardioid.

Technical models

After this general discussion we shall now deal briefly with four types of microphones constructed by Philips.

Carbon microphone

Carbon microphones may very well be used for the recording of the spoken word. While it is true that with very high sound pressures the magnitude of the contact surfaces between the grains is not proportional to the pressure exerted, so that the sound will be distorted, nevertheless carbon microphones have the advantage that they produce a much larger EMF than other kinds of microphones. A much smaller amplification is therefore needed with a carbon microphone, which makes it peculiarly suitable for simple applications.

The sensitivity of carbon microphones is higher, the larger the grains of carbon which is contains. The quality of the sound, however, diminishes at the same time, since the noise also increases with the size of the grains. Furthermore the carbon packs together somewhat in use, so that the sensitivity decreases with time. This can be prevented by tapping the microphone lightly.

Fig. 13. Carbon microphone, type 4225, special model for reporters. The microphone can be hung in the buttonhole of the coat.

An interesting use of the carbon microphone type 4225 is the reporter's microphone shown in *fig. 13*, which can be worn in the buttonhole. The relative sensitivity expressed as sound energy in db is shown in *fig. 14* as a function of the frequency,

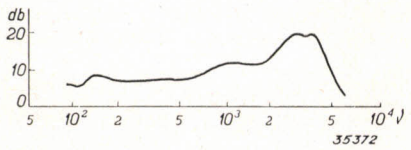

Fig. 14. Relative sensitivity of the carbon microphone, type 4225, expressed in db, as a function of the frequency.

from which it may be seen that the resonance frequency lies at about 3000 c/sec, while the sensitivity decreases rapidly with increasing frequency above 5000 c/sec. In *fig. 15* the dependence of the relative sensitivity in db on the direction is plotted in horizontal coordinates for frequencies of 1000 and 5000 c/sec, respectively. It may be seen (curve *a*) that the sensitivity at 1000 c/sec varies very little with the direction, so that the ideal pressure microphone is very closely approached. At higher frequencies, however, a much greater dependence on direction appears, as may clearly be seen in fig. 15*b*. This is a result of the fact that for frequencies of about 5000 c/sec the dimensions of the microphone are no longer small compared with the wave length.

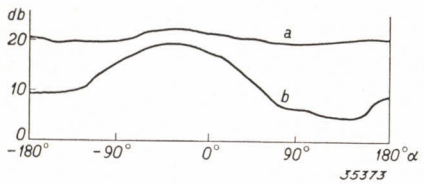

Fig. 15. Relative sensitivity of the carbon microphone, type 4225, as a function of the direction from which the sound is incident; *a*) at 1000 c/sec; *b*) at 5000 c/sec.

Crystal microphone

In the diagram of fig. 2 the air vibrations are transmitted by means of a membrane to a piëzoelectric crystal, Rochelle salt ($NaKC_4O_6$, $4H_2O$) for example. In crystal microphones constructed in this way care must be taken that the sensitivity for high frequencies does not vary irregularly with the frequency due to resonances in the driving mechanism. This has indeed been done in the crystal microphone type 9529, which is used for exemple in the table model of the so-called acorn microphone shown in *fig. 16*. The following point must, however, be kept in mind in connection with this

Fig. 16. Acorn model of a crystal, type 9 529, provided with a table standard. (height about 9 cm)

microphone. If a thin crystal plate of Rochelle salt is stretched in the direction of its length (*fig. 17a*) the two sides of the plate take on opposite charges, so that when it is used as a membrane (*fig. 17b*) and thus bent so that the two sides are stretched and compressed respectively they will then assume the same polarity. If two crystal plates are stuck together in such a way that their polarities are opposite (fig. 17*c*), a plate is obtained which assumes opposite charges on its two free sides upon bending [3]). Two such "bimorphous" crystal plates are mounted together in the manner shown in fig. 17*d*. Each of these plates experiences the effect of the sound pressure on the outer side only, so that the result is a pressure microphone.

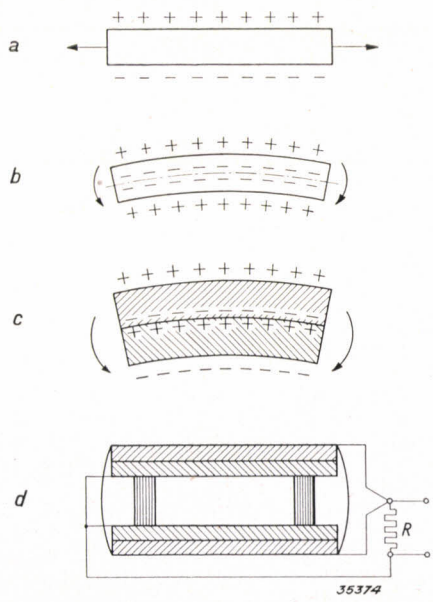

Fig. 17.*a*) If a piëzoelectric crystal plate is stretched opposite electric charges appear on its side surfaces. When compressed the charges are reversed.
b) Upon bending, the electric charges on the two sides have the same sign, which is opposite to that in the neutral layer whose length is not changed.
c) If two piëzoelectric crystal plates are fastened together with opposite orientation, the result is a so-called bimorphons crystal, which upon being bent assumes opposite charges on its two free surfaces.
d) The piëzoelectric crystal used in the crystal microphone, type 9 529, consist of two bimorphons crystals, one side only of which is exposed to the pressure of the air vibrations.

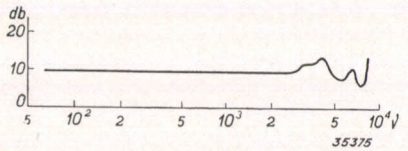

Fig. 18. Relative sensitivity of the crystal microphone, type 9 529, expressed in db, as a function of the frequency.

In *figs. 18* and *19* it is shown how the relative sensitivity in db depends, respectively, upon the frequency and the direction from which the sound strikes the microphone. For frequencies up to 5 000 c/sec the sensitivity is found to be practically independent of the direction, and above that frequency only slightly dependent on the direction.

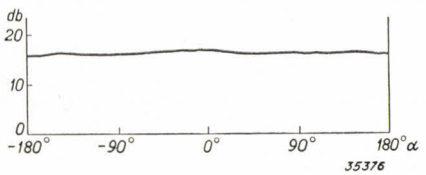

Fig. 19. Relative sensitivity of the crystal microphone as a function of the direction at 5 000 c/sec.

This is because of the small dimensions of the piëzoelectric crystal. The resonance frequency lies in the vicinity of 4 000 to 5 000 c/sec and presents no difficulties. In order to provide that not only the EMF $E_{\sim}$ generated, but also the terminals voltage $V_{\sim}$ shall depend only slightly upon the frequency, the external resistance R which completes the electrical circuit of the microphone must be made larger than the internal impedance of the microphone. Since the crystal behaves as a capacity C, the terminals voltage becomes therefore:

$$V_{\sim} = \frac{E_{\sim}}{\sqrt{1 + 1/\omega^2\, C^2\, R^2}} \quad \cdots \quad (20)$$

This expression is only independent of the frequency when $\omega\, CR \gg 1$, *i.e.* for sufficiently high

[3]) According to patents of the Brush Crystal Company, Cleveland, Ohio.

frequencies, and increases linearly with the frequency when $\omega CR \ll 1$. If the microphone capacity is, for instance, $C = 2\,000$ $\mu\mu$F, and the external resistance $R = 1$ MΩ, at a frequency of about 80 c/sec the absolute value of ωCR will be approximately unity, so that $V = 0.72\,E$. Above 100 c/sec the terminals voltage does not change very much more with the frequency.

In the technical construction of these microphones care is taken that the microphone is well protected against the entry of moisture since the Rochelle salt crystals are not unaffected by water. Furthermore the microphone may not become too warm. If the Rochelle salt reaches a temperature above 55° C it loses its water of crystallization which is responsible for the piëzoelectric properties. When the temperature is lowered the water of crystallization does not recombine. The limit of 55° C is fortunately so high that it is never reached under normal conditions.

Ribbon microphone

In the table model of the ribbon microphone type 9 522 shown in *fig. 20*, a corrugated aluminium ribbon several microns thick is stretched between the pole pieces of a permanent magnet. The air vibrations exert their pressure on both sides of the ribbon which thus acts as a pressure-gradient microphone. Due to the motion of the ribbon in a magnetic field an EMF is excited in the circuit in which the ribbon is included, so that the microphone is of the electrodynamic type. According to the foregoing considerations, for a pressure-gradient microphone of the electrodynamic type the reproduction will be practically independent of the frequency when operating above the resonance frequency; formula (16′). In the case of this ribbon microphone the resonance frequency lies at about 50 c/sec, which is sufficiently low to ensure a practically constant sensitivity for the frequencies of speech and music.

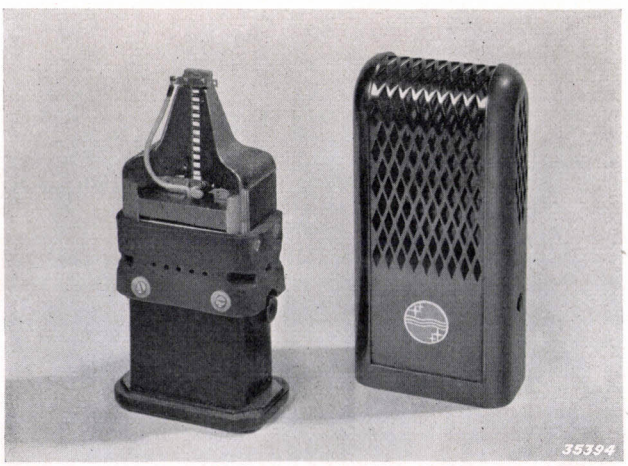

Fig. 20. Ribbon microphone, type 9 522, opened (about 20 cm high and 9 cm broad).

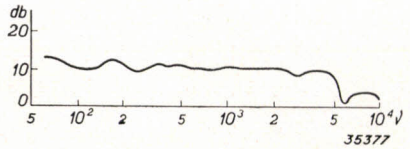

Fig. 21. Relative sensitivity of the ribbon microphone, type 9 522, expressed in db, as a function of the frequency.

It may be seen from *fig. 21* that the relative sensitivity of the ribbon microphone changes only slightly for the frequencies from 100 to 5 000 c/sec, while at 5 000 c/sec it begins to decrease. This may be explained as follows. The sensitivity of the microphone is given by the approximation formula (14). If, however, the product $kl = 2\pi\nu l/c$ becomes of the order of magnitude of 2π, (14) no longer holds and the succeeding terms of the series in the precise formule (13) must also be taken into account. From further considerations [4]) it is found that the sensitivity of the microphone will be practically independent of the frequency up to that frequency for which $kl = \pi$, *i.e.* where the product of k and the width $a = l/\pi$ of the pole piece is about unity. Now $k = 2\pi\nu/c = 2\pi\nu/34\,000$, so that with a width of the pole pieces of about one cm we may expect that the sensitivity will change little up to a frequency of 5 000 c/sec. For higher frequencies the sensitivity then decreases quite rapidly as may be seen in fig. 21. If it were desired that the sensitivity should decrease only at a higher frequency, this may be accomplished by making the pole pieces smaller, but under otherwise similar conditions this takes place, according to equation (14) at the cost of the magnitude of the sensitivity.

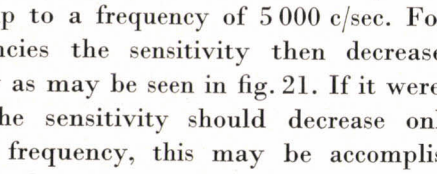

Fig. 22. Relative sensitivity of the ribbon microphone, type 9 522, as a function of the direction at 5 000 c/sec.

In *fig. 22* may be seen the manner in which the relative sensitivity of the ribbon microphone at 5 000 c/sec depends upon the direction from which the sound comes; for lower frequencies the dependence is practically the same. As must be expected

[4]) J. de Boer, Physica, **5**, 545, 1938.

in the case of a pressure-gradient microphone, the sensitivity to sound from directions perpendicular to that of greatest sensitivity is practically zero.

Coil microphone

In conclusion we shall describe a second type of pressure-gradient microphone of the electrodynamic type. In order to obtain a larger EMF the conductor which moves in a magnetic field consists of an electric coil in this case. *Fig. 23*

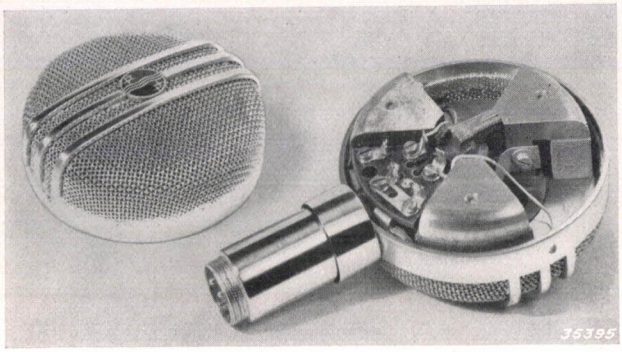

Fig. 23. Coil microphone, type 9 528, opened, rear view with back of magnetic circuit (cross section in fig. 24); diameter about 9 cm.

shows a coil microphone, the rear side of which has been opened. In the diagram of the cross section (*fig. 24*) it is shown how the coil (*Sp*) is wound upon a paper cap fastened to the membrane. The coil moves in a ring-shaped magnetic field; in the photograph the edge of the paper cap may be seen lying in the ring-shaped air gap.

Furthermore in fig. 23 it may be seen that the magnetic circuit is not closed over the entire circumference of the ring, but only over three parts by means of pieces of magnet steel *M*. The outer ring and the inner ring which form the north and south poles are made of soft iron. If the magnet steel had the form of a complete cylindrical shell, as is the case in the magnetic system of a loud speaker, the total number of lines of force cut by the vibrating coil, and thus also the EMF excited in the latter, would be larger. In spite of this that form is not chosen, in order to prevent the formation by the magnetic system of a resonating cylindrical space behind the membrane (open organ pipe), which leads to irregularities in the dependence of the sensitivity upon the frequency.

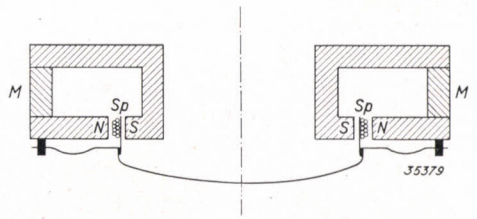

Fig. 24. Cross section of coil microphone. The coil *Sp* is wound on a paper cap the edge of which can be seen in fig. 25 in the air gap between the two poles. *N* north pole, *S* south pole. *M* are the three pieces of magnet steel, which provide the magnetomotive force for the soft iron ciruit.

By making the fastening of the membrane very flexible care is taken that the resonance frequency will lie below 100 c/sec. From this frequency, according to *fig. 25*, the relative sensitivity is found to depend little upon the frequency, up to about 5 000 c/sec. The magnitude of the sensitivity is such that with a sound pressure of 1 dyne/cm^2 and an output impedance of the microphone of 500 Ω a voltage of 0.9 mV is obtained.

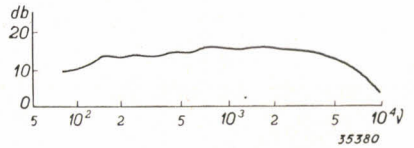

Fig. 25. Relative sensitivity of the coil microphone, type 9 528, expressed in db, as a function of the frequency.

The manner in which the relative sensitivity depends upon the direction from which the sound comes is shown in *fig. 26*. At a frequency of 500 c/sec, the sensitivity for directions perpendicular to that of greatest sensitivity is indeed approximately zero (fig. 26*a*) as is to be expected from a pressure-gradient microphone; for higher frequencies the minima are less pronounced (fig. 26*b*).

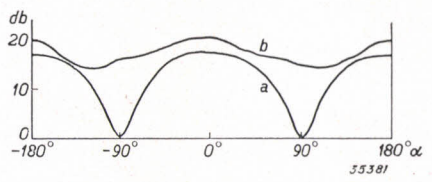

Fig. 26. Relative sensitivity of the coil microphone as a function of the direction. *a*) at 500 c/sec; *b*) at 5 000 c/sec.

THE ACCURACY OF MEASUREMENTS OF FIELD STRENGTH

by J. D. VEEGENS and J. J. ZAALBERG van ZELST. 621.317.42 : 621.396.81

A discussion is given of the main factors which affect the accuracy of measurements of the field of radio transmitters. A description is given of the way in which these factors are taken into consideration in the construction of the Philips recording field-strength meter. With this instrument it is found possible to measure the field strength with sufficient accuracy.

The strenght of the field of a radio transmitter is a quantity which is very important in transmitting and receiving technology, and which must therefore be known in many cases. In measurements for scientific purposes and also in certain cases such as the testing of transmitting and receiving installations which must precisely fulfill certain requirements as to efficiency, radiation or sensitivity, an accuracy of to within 1 per cent or less will be required. In most practical cases, however, it is unnecessary to measure the field strength with such great accuracy. Due to the influence of local or atmospheric conditions the field strength may vary so much that it will often serve no useful purpose to measure more accurately than to within 10 to 20 per cent.

The purpose of this article is to discuss the chief factors which affect the accuracy of measurements of field strength, and to indicate the method used in the construction and perfecting of the Philips recording field-strength meter [1]) of keeping the inaccuracies within satisfactory limits. It will be found that these inaccuracies are introduced during the calibration of the instrument, which process may be carried out at any desired moment by the user. For the calibration a concentrated EMF is introduced into the aerial circuit in place of the divided EMF which the field of a transmitter would induce therein. In the following it will be shown how care must be taken that the resistance through which this calibration EMF is introduced into the aerial circuit is practically free of induction, and that the voltage of the calibration oscillator is sufficiently sinusoidal. The influence will further be studied of the introduction of the calibration EMF into one of the windings of the loop aerial, while in conclusion the influence will be discussed of the capacities between the different supply connections and the windings. Before dealing with these points we shall first give a short discussion of the arrangement of the field-strength meter.

[1]) A detailed description of this apparatus (type GM 4 010) has already been given in this periodical: M. Ziegler, A recording field-strength meter of high sensitivity, Philips techn. Rev. 2, 216, 1937.

The principle of the field-strength meter

The essential components of a field-strength meter are an aerial and a "voltmeter" for high-frequency AC voltages. The field whose strength is to be measured induces an EMF in the aerial, which is proportional to the field strength and also depends upon the form of the aerial. It is desirable that the relation between the field strength to be measured and the EMF excited thereby shall not depend upon the surroundings to any great extent. This can be realized with the help of a loop aerial, which moreover has the advantage of being less sensitive to interfering fields, since it receives only a small range of frequencies and its reception is directional. In order to cover a wide frequency range different loop aerials can be used. The EMF which is excited in the loop aerial causes between the terminals of the "voltmeter" a voltage difference which is a measure of the field strength.

The "voltmeter" consists of an amplifier with several tuned circuits by which the signal to be measured is amplified selectively, so that transmitters of a different frequency have no disturbing effect. The amplified signal is further rectified and conducted to an indicating instrument. The "voltmeter" also contains an attenuator with which it is possible to pass over to different measuring ranges for very divergent field strengths.

The calibration of the field-strength meter as a source of error

In technical manufacture it is practically impossible to make the properties of a loop aerial and the sensitivity of the voltmeter sufficiently constant. The properties of the aerial depend upon frequency, temperature and the degree of moisture of the air. The sensitivity of the voltmeter depends not only upon the frequency and the temperature of the surroundings, etc., but also upon the supply voltages of the amplifier. In order to eliminate this effect it is a practical necessity to be able to calibrate the instrument absolutely at any desired moment. In order to do this the whole field-strength meter might be placed in a radiation field of known

intensity, as is indeed done in special cases, in spite of the difficulties involved. In practice, however, it is impossible to apply such a "standard field" for every measurement which is carried out with the field-strength meter.

The customary method of calibration therefore is that of applying a known concentrated EMF to the aerial (substitution method), and *it is this method of calibration which forms the chief source of errors in field-strength meters*. If great accuracy is required in this method, it is not sufficient to know exactly the EMF generated, but one must also be certain that, within the desired limits of accuracy, this EMF will cause the same indication on the voltmeter as an equally great EMF induced by the external field. As will appear from the following this condition is not generally satisfied.

The application of a known calibration EMF

The calibration EMF is obtained by passing a current of known strength i_0 and variable frequency ν over a resistance ϱ which is connected in series with the aerial. In the substitution scheme of *fig. 1a* the total impedance of the aerial with the network connected with it is called Z. As to currents and voltages in the impedance Z this arrangement is absolutely equivalent to that of fig. 1*b*. In both cases a current $i_0\,\varrho/(\varrho + Z)$ flows through Z. The accuracy with which the calibration EMF E_0 is known thus depends exclusively upon that with which ϱ and i_0 are determined.

In order not to decrease the sensitivity of the field meter unnecessarily the calibration resistance ϱ, which is introduced into the loop circuit, must have a low value. In the Philips field-strength meter a value of about 0.1 ohm has been chosen. It is advisable for practical reasons that the same calibration EMF be obtained at the same value of i_0 for alle frequencies up to 30 megacycles per sec (*i.e.* a wave length of 10 m). This means that the influence of skin effect and selfinduction on the magnitude of the impedance of ϱ must be negligible. In the Philips field-strength meter a type of construction has been employed for this calibration resistance such that up to 50 megacycles per sec the impedance deviates less than 1 per cent from the DC value. This result is achieved by stretching 15 chrome nickel wires of a diameter 25 μ and a length 1 mm parallel to each other between two parallel copper discs (*fig. 2*).

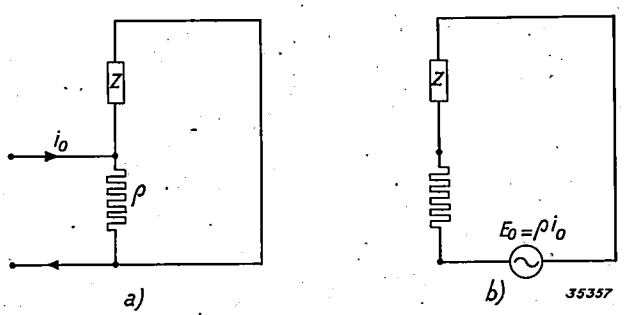

Fig. 1. Equivalent diagrams for the aerial with the network connected with it (total impedance Z) when fed with a calibration current i_0 for a calibration resistance ϱ, and with a calibration EMF E_0, in series with the calibration resistance, respectively.

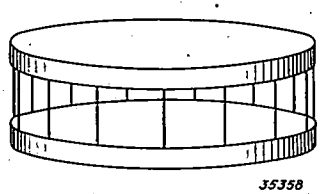

Fig. 2. Induction-free resistance consisting of two circular copper discs between the edges of which fifteen thin chrome-nickel wires are stretched.

The calibration current i_0 is provided by the calibration oscillator and contains a certain proportion of harmonics which might give rise to inaccuracies. The current is, however, measured by means of a thermocouple and a millivoltmeter, so that the influence of the different harmonics on the indication of the meter is manifested only in the form of correction terms which are related to each other as the squares of their amplitudes and not as the amplitudes themselves. The significance of this may be seen from the following example. If the amplitude of one of the harmonics is 10 per cent of that of the fundamental, and if we indicate the effective value of the fundamental component by i_0 and therefore that of the harmonics by 0.1 i_0, the indication of the millivoltmeter corresponds to a current of the magnitude:

$$\sqrt{i_0^2 + (0.1\,i_0)^2} \approx 1.005\,i_0$$

With a thermocouple the error is therefore only 0.5 %, while with a peak current meter in that case the error may amount to 10 per cent in both directions. The calibration oscillator may therefore easily be so constructed that the error in the magnitude of the calibration current may be neglected when it is measured thermally.

Influence of the asymmetry of the aerial circuit

By means of the field of a radio transmitter an EMF is excited in a loop which is small with respect to the wave length [2]). The EMF is proportional

[2]) Since in the case of the Philips field-strength meter the dimensions of the loop aerial are always small compared with the wave length of the field of radiation, it is unnecessary to consider the deviations which might occur if the substitution method were applied to aerials of larger dimensions.

to the intensity of the field and to the surface and number of windings of the loop. Since, however, a loop aerial as a whole also possesses capacity with respect to earth, without special precautions an EMF will also be induced in the aerial which depends upon the position of the loop with respect to the earth and to objects in its neighbourhood. The influence of this effect, the so-called aerial effect, can be avoided by arranging the aerial circuit so that it is absolutely symmetrical with respect to earth. To satisfy this condition a loop aerial can be used, which consists of two similar windings. As may be seen in *fig. 3*, however, the calibration resistance ϱ is introduced into one of the windings, thus causing an asymmetry in the aerial circuit. This resistance is, however, so small that the asymmetry which it causes in the aerial circuit is too slight to cause an appreciable aerial effect, but the calibration voltage is not introduced into the loop circuit symmetrically with respect to earth. If the voltage over the whole loop circuit were measured, it would be a matter of indifference where the EMF were introduced, but, as indicated clearly in fig. 3, the voltmeter V acts over only one of the two windings of the aerial. As a matter of fact this simplifies the construction and a calculation, which we are giving below, shows that is only involves a small error.

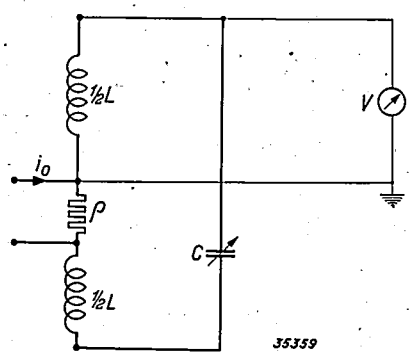

Fig. 3. The loop aerial consists of two symmetrical parts. The voltmeter V indicates the voltage on one of the two halves, which is a measure of the field strength around the aerial. The self-induction of the aerial is L, the tuning condenser C, calibration current i_0, calibration resistance ϱ.

Due to the resonance into which the loop circuit is brought, a calibration EMF E_0 applied *via* ϱ causes a much greater voltage Q_0E_0 over the winding of the loop to which the voltmeter V is connected. An EMF E induced by a transmitter in the loop circuit gives a voltage QE on the voltmeter. In general Q is not equal to Q_0. The relative error due to the asymmetrical introduction into the aerial circuit of the calibration voltage is now given by the relation $(Q - Q_0)/Q_0$. The larger the factors Q and Q_0, *i.e.* the higher the voltage over the coil with respect to that over the calibration resistance the less difference it will make whether or not the calibration voltage is included in the measurement by the voltmeter. On the basis of the simple diagram of fig. 3 in which further resistance in series or in parallel with the self-induction may be allowed, it may be calculated as a first approximation that $Q - Q_0 < 1/(8Q_0)$. The relative error thus becomes smaller than $1/(8\ Q_0^2)$. In the case of the loop aerials which are provided with the Philips field-strength meter for use in different frequency regions, the values of Q_0 lie between 20 and 150, so that in these cases the error may be neglected.

If high field strengths, greater than 50 mV/m, for instance, were to be measured, a high voltage might occur at the terminals of the "voltmeter". Such voltages, however, should be avoided because the amplifier valves would then operate outside their range of linearity, and there would no longer be a linear relation between the voltage supplied and the indication of the instrument. It would be better in such a case to introduce more resistance into the loop circuit. By giving the loop circuit a higher resistance, however, the factors Q_0 and Q are diminished, and it may indeed be necessary in that case to take into account the error due to asymmetry.

Influence of capacities between the different supply lines and windings

In fig. 3 only a very schematic representation is given of the actual aerial circuit. In *fig. 4* it may be seen that the loop aerial is placed at a distance of about 20 cm above the metal case in which are situated not only the voltmeter and the calibration oscillator but also the resistance ϱ and the condenser C. This distance is necessary in order that the metal case may not be able to disturb the field around the aerial. The presence of the lines which connect the aerial with the instrument, gives rise to considerable capacities between other parts of the aerial circuit as well as between the windings of the loop.

In order to discover the effect of these capacities upon the accuracy of the calibration method, further experiments were carried out with the field-strength meter. Each capacity in turn was artificially increased by known amounts, and in each the ratio Q/Q_0 was measured under the thus altered conditions. It is then found to be permissible in practical cases to assume that the capacities

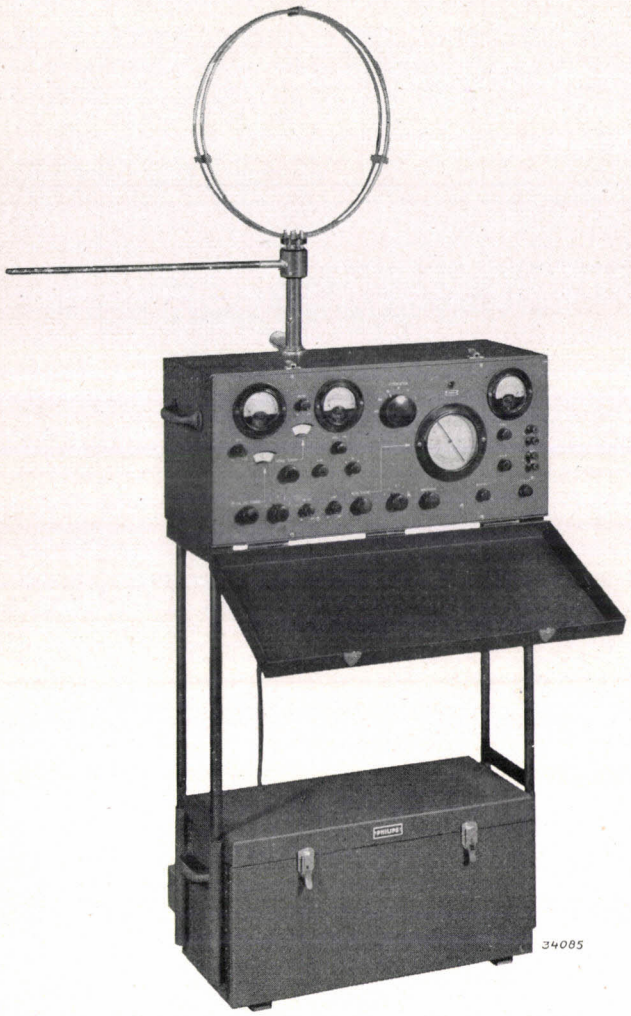

Fig. 4. The Philips recording field-strength meter type GM 4010. Since the metal case in which the instrument is housed distorts the field in its immediate vicinity the loop aerial must be set up sufficiently far away from it.

between the connections, and for loops with two windings the capacity between the two windings also, are concentrated. In this way it becomes possible in the case of a loop aerial with two windings to carry out the calculations on the basis of the substitute diagram given in *fig. 5*. The capacity between the two windings of the loop aerial is represented by k. The six different capacities between the four supply lines, taken two at a time, are a_1, a_2, b_1, b_2, d and e. The capacity of the voltmeter V is hereby included in a_2. Here also, as in the case where the coupling capacities were neglected, it makes a difference in the voltage on the voltmeter V whether the EMF due to the field is induced divided over the whole aerial, or introduced in a concentrated form at a point of symmetry. If we again indicate the factors by which the voltage is increased by Q and Q_0, and if these are not too small, we find the following for the relative error:

$$\frac{Q-Q_0}{Q_0} \approx \frac{\omega^2 L}{4}(a_1 + a_2 - b_1 - b_2 - k), \quad . \quad (1)$$

where ω represents the angular frequency and L the total self-induction of the loop circuit. The errors found experimentally agree very well with this expression.

It may be concluded from the above that for a given loop the relative error will disappear if provision is made, by the addition of certain capacities, that

$$a_1 + a_2 - b_1 - b_2 - k = 0 \quad . \quad . \quad . \quad (2)$$

In order furthermore to avoid the aerial effect, these correction capacities are so chosen that they also bring about symmetry with respect to earth, thus: $a_1 = a_2$ and $b_1 = b_2$. According to the formulae the capacity d which is in parallel with the resistance ϱ has no appreciable effect on the accuracy. The capacity e is already compensated automatically in the tuning condenser C.

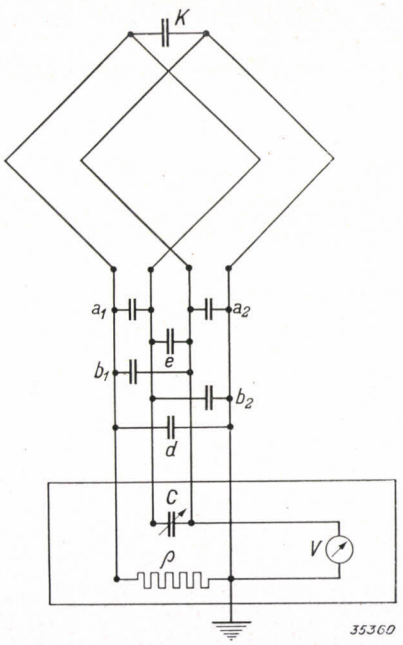

Fig. 5. Equivalent diagram for a loop aerial consisting of two windings. C tuning condenser, ϱ calibration resistance, a_1, a_2, b_1, b_2, d and e are the six capacities between the four supply lines taken two at a time. The capacity between the two windings is represented by k.

Loop aerial with more than two windings

With the Philips field-strength meter for use in the frequency region from 4 to 25 megacycles per sec (*i.e.* 75 to 12 m wave length), there are four different loop aerials, (*fig. 6*) each of which consists of two windings. The foregoing discussion may therefore be applied. If one desires to obtain a sufficiently large EMF at low frequencies without using loop aerials of very large dimensions, it is necessary to choose loops with a larger number of windings.

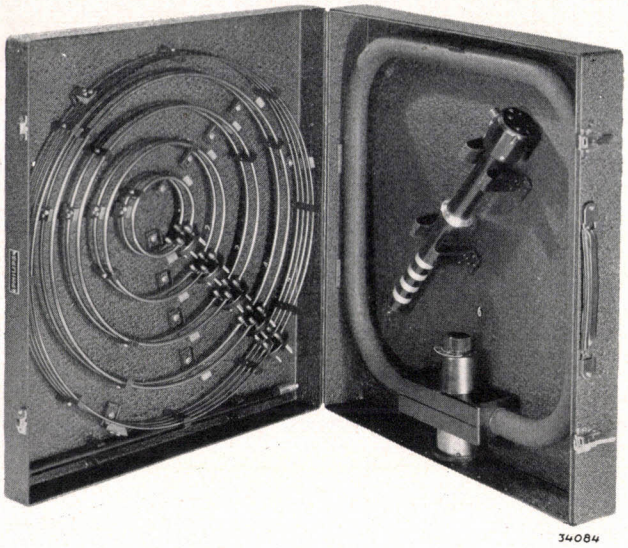

Fig. 6. The case containing the loop aerials provided with the Philips field-strength meter. In the left-hand section may be seen four double loops, which cover the frequency range from 4 to 25 megacycles per sec, as well as a loop consisting of four windings intended for 1,7 to 4 megacycles per sec. In the right-hand section is the loop aerial consisting of a large number of windings which may be connected in four different ways in series and in parallel with each other. This variable aerial serves the frequency range from 0,15 to 1,7 megacycles per sec.

The frequency region from 1.7 to 4 megacycles per sec is covered by a loop aerial with 4 windings, while finally for frequencies from 0.15 to 1.7 megacycles per sec (*i.e.* wave lengths from 2 km to 180 m) a loop aerial can be used which consists of a large number of windings connected in 4 different ways in series and in parallel with each other (fig. 5). Since according to the experiments the capacities for loops with more than two windings may not be considered concentrated, formula (1) cannot be applied to such cases. Since the situation is too complicated for simple calculation, it is better to determine the corrections experimentally, namely by comparison with a loop aerial with two windings whose errors are compensated in the manner here given. This has actually been done with the variable loop aerial which is a feature of the latest type of Philips field-strength meter. In the case of this aerial the corrections are indicated graphically as a function of the frequency.

Accuracy of measurement of the Philips field-strength meter

If we assume that the incidental errors in the results of the measurements which may arise in the setting, reading etc. are eliminated by repeating the measurement a sufficient number of times, there then still remain several other systematic errors besides those already mentioned which we shall here discuss.

The "effective height" of the loop aerial, that is the proportionally factor between the EMF generated and the field strength, is accurately known to within only 0.5 per cent. The inaccuracies in the circuit which provides for the rectification and amplification, and in the instrument which serves as indicator for the field-strength meter, together cause an error in the results of 2 per cent at the most. The attenuator which is used for passing over from one measuring range of the voltmeter to another may be the source of an inaccuracy of 0.5 per cent.

For the sake of comparison a summary of the magnitude of the errors already discussed is given in the following. The occurrence of the aerial effect may cause an error of 1 per cent. Due to the dependence of the calibration resistance ϱ on the frequency a maximum error of 1 per cent may be introduced. The occurrence of higher harmonics in the calibration current i_0 and the error in the instrument with which the latter is measured give an inaccuracy of 1 per cent in the results. Due to the incomplete compensation of the error caused by the mutual capacities (a_1, b_1, etc.) an inaccuracy of 1 per cent at the highest is caused.

If all the errors mentioned here should act in the same direction there would be a maximum error of 7 per cent. In general, however, these errors will not all act in the same direction, nor will they all assume maximum values at the same moment. Therefore one may in practical cases assume that an accuracy to within 4 per cent is obtained.

From the foregoing summary it is also clear that the fundamental errors adherent in measurements with this field-strength meter are of the same order of magnitude as the errors pertaining to the amplifier tubes and indicating instrument used. It is possible that the accuracy of the field-strength meter might be further enhanced by the use of precision meters. The practical utility of the method for measurements on the spot would, however, thereby be lost.

ABSTRACTS OF RECENT SCIENTIFIC PUBLICATIONS OF THE N.V. PHILIPS' GLOEILAMPENFABRIEKEN

1469: F. A. Kröger: Note on the wurtzitesphalerite transition of zincsulphide (Z. Kristallogr. A **102**, 136-137, Nov. 1939) (Original in English language).

Zincsulphide occurs in two enantiotropic modifications with a transition point at 1020 ±5 °C. The velocity of transformation depends very much on the temperature and the dimensions of the crystals.

1470: A. Bouwers: The indirect radiograph (Radiology **33**, 357-362, Sept. 1939) (Original in English language).

The indirect radiograph obtained by means of a reduced picture of the screen image with a lens is compared with the direct image. With approximately equal contrasts the lack of sharpness of the indirect image is found to be approximately proportional to the cube root of the ratio between the intensity of the direct image and that of the reduced image. Since this ratio is inversely proportional to the square of the aperture, the relative aperture must be made as large as is possible without the reproduction faults becoming too large. If a tube with a rotating anode is used for the indirect image and one with a stationary anode for the direct image, the photographic quality of the indirect image is just as good as that of the direct image. In conclusion it is described how with a rotating anode exposures can best be made of the dimensions 24×32 mm, those of the ordinary miniature camera.

1471: E. J. W. Verwey and K. F. Niessen: The electrical double layer at the interface of two liquids. (Phil. Mag. **28**, 435-446, Oct. 1939) (Original in English language).

The variation of the potential is studied in the neighbourhood of an interface between two liquids, about which a small amount of electrolyte is distributed. The total potential difference due to the fact that one liquid has an excess of positive ions and the other an equal excess of negative ions is divided into two parts which are situated on either side of the interface. The largest part of the potential drop occurs in the liquid for which the product of ion concentration and dielectric constant is the larger. In general this product will have very different values for two substances, and if the total potential difference is not too great, it occurs almost entirely in the phase for which this product is the smaller. This does not, however, mean that the decrease in the density of charges on both sides of the interface need be very different. For larger total potential differences the partition of the potential drop between the two phases is somewhat less unequal, while for very large potential differences it approaches equality. For chemical applications of these considerations *cf.* **1467.**

1472*: M. J. O. Strutt: Modern short wave receiving technique (245 pages, Springer Berlin 1939) (German language).

Problems are discussed in this book which occur in the reception of radio waves of wave lengths from 50 to 0.2 m. The problems connected with receiving aerials and with the connection between aerial and receiving set are dealt with. Reliable methods of measuring currents, voltages and impedances at these short wave lengths are indicated. The problems are discussed which occur in the design of valves for amplification, mixing and rectifying voltages and currents at such high frequencies. In conclusion the important factors in the construction of complete receiving sets are discussed. The main text is kept as free as possible of mathematical analysis, which are, however, collected in an appendix for the sake of completeness.

1473: C. J. Bakker: Het splitsen van zware atoomkernen door neutronen. (The fision of nuclei of heavy atomes by neutrons). (Ned. T. Natuurk. **6**, 333-345, Dec. 1939).

In this address to the Netherlands Physical Society (Sept. 1939) a survey is given of the results obtained by the bombardment of nuclei of heavy atoms with neutrons. Hahn and Straßmann discovered in Jan. 1939 that uranium can be broken up in this way into radioactive isotopes of barium and lanthanum, and that no so-called transurania are obtained, as was formerly assumed. An investigation in the Philips laboratory has shown that the primary process of fision of uranium takes place in different ways. Furthermore analogous results were obtained with thorium. *Cf.* in this connection: **1410** and **1420.**

---

*) An adequate number of reprints for the purpose of distribution is not available of those publications marked with an asterisk. Reprints of other publications may be obtained on application to the Natuurkundig Laboratorium, N.V. Philips' Gloeilampenfabrieken, Eindhoven (Holland), Kastanjelaan.

1474*: H. Bremmer: Geometrisch optische benadering van de golfvergelijking (Geometrical optical approximation of the wave equation) (Handelingen 27e Ned. natuurk. en geneesk. Congres te Nijmegen, pp. 88-91, April 1939).

In this address before the Natuurk. en geneesk. Congres the well-known approximation formula of Wentzel, Kramers and Brillonin for the solution of a wave equation was derived in a new way. In the special case of one dimension an exact solution can be given in the form of a series, each term of which can be interpreted physically, and the first term of which is the well-known W.K.B. approximation.

1475*: F. A. Heyn: Het breken van uranium en thorium-kernen onder neutronen-bombardement (The breaking up of uranium and thorium nuclei upon neutron bombardment). (Handelingen 27e Ned. natuurk. en geneesk. Congres te Nijmegen, pp. 110-112, April 1939).

When uranium or thorium nuclei are bombarded with neutrons, among other products the radioactive rare gases krypton and xenon occur. The reactions of these rare gases are discussed in this paper (see also **1410**). Several reaction schemes are indicated.

1476*: J. F. Schouten: Het gebruik van de Fourieranalyse bij de interpretatie der onscherpe afbeelding. (The use of Fourier analysis in the interpretation of out-of-focus images). (Handelingen Ned. natuurk. en geneesk. Congres, pp. 110-119, April 1939).

It is shown in this paper that to a certain degree the exact form of an object can be deduced from an out-of-focus image by making use of a theorem of Fourier analysis. An example is the reconstruction of the exact shape of a spectral line from the poorly defined image which occurs due to the finite width of the slit. A semi-electrical arrangement is demonstrated with which the true line form can immediately be obtained from the apparent one and can be made visible on a cathode-ray oscillograph.

1477*: J. H. van der Tuuk: Metingen in verband met de diepte-scherpte aan röntgenstralen voor spanningen tot 1 millioen volt (Measurements in connection with the depth of focus on X-rays for voltages up to 1 million volts). (Handelingen Ned. natuurk. en geneesk. Congres, pp. 198-201, 1939).

For the contents of this address the reader is referred to Philips techn. Rev. 4, 153, 1939.

1478: A. Bouwers: La production des rayonnements pénétrants. (Acta Univ. int. contra cancrum, Paris 4, 245-253, 1939). (Original in French language.)

Penetrating rays which may be used for the purposes of therapy are:

a) photons (x and γ-rays)
b) neutrons
c) electrons (β-rays).

β and γ-rays have natural sources while x-rays and neutrons are obtained artificially. Neutrons can be obtained by allowing natural γ-rays to act upon beryllium, for instance, or by accelerating the atom nuclei of helium or heavy hydrogen sufficiently and allowing them to act upon a plate of suitable material. The acceleration may be direct or successive.

Hard x-rays are produced with the help of generators on the electrostatic or on the cascade principle. A generator with sealed x-ray tube for 1 million volts is described. An important problem is the protection against undesired radiation. For x and γ-rays the methods are well-known. For neutrons materials containing much hydrogen can best be used, such as water or paraffin, and combining these with a thin layer of a substance containing boron (boric acid for instance).

1479*: J. H. van der Tuuk: Recente metingen aan harde röntgenstralen (Recent measurements on hard x-rays). (Ned. T. Geneesk. **83**, 5815-5819, Dec. 1939).

In this address before the Netherlands society for electrology and röntgenology a discussion is given of the degree to which differences could occur in biological action between x-rays of various hardnesses and between x-rays and neutrons. The production of neutrons and of very hard x-rays is discussed. In conclusion a detailed study is made of the physical properties of very hard x-rays, see also **1477***.

1480: A. Bouwers and J. H. van der Tuuk: Further experiments with x-ray tubes for high voltages up to one million volts. (Brit. T. Radiol. **12**, 658-666, Dec. 1939). (Original in the English language.)

An improved sealed x-ray tube for voltages to one million volts is described. If a filter of 2.5 mm

of copper is used, the radiation of 800 kV DC voltage and a tube current of 1 mA amounts to about 14 röntgen/min at a distance of 1 m from the focus. The half-value thickness of the radiation may with this tube amount to 103 mm copper or 4.2 mm lead. The thickness of the lead screen by which the intensity of the radiation is reduced to below the tolerance dose, amounts at 1 million volts and 1 mA to 9 cm for the primary radiation, for the radiation scattered in the body irradiated to only a few mm. Furthermore, the nature of the radiation 10 and 20 cm under the surface of the skin is investigated with the help of a water phantom. In conclusion the intensity and the hardness of the radiation in the direction of the incident electrons is measured and found to be considerably greater than in a direction perpendicular to this.

1481*: M. J. O. Strutt and K. S. Knol: Measurements of currents and voltages down to a wavelength of 30 centimeters. (Proc. Inst. Rad. Eng. **27**, 783-789, Dec. 1939).

This is an English version of an article originally written in German which was reviewed under **1430.**

1482: J. M. Stevels: De berekening van de kookpunten van eenvoudige verbindingen (The calculation of the boiling points of simple compounds). (Natuurwet. T. **21**, 256-262, 1939).

In this article a summary is given of the method by which the boiling points of simple organic compounds can be calculated from three different contributions to the cohesion of the compound. For the contents refer to **1407, 1408** and **1462.**

1483: W. de Groot: De internationale temperatuurschaal voor temperaturen boven 1000 °C. (The international temperature scale for temperatures above 1000 °C). (Ned. T. Natuurk. **7**, 34-48, Jan. 1940).

A critical discussion is given of the principle upon which is based the international temperature scale above 1063 °C, as defined by optical pyrometry. The accuracy of the measurements is discussed and a lisest of fixed points on the temperature scale, such as have been determined recently in different laboratories, is given. A further study is made of the uncertainty in the constant c_2 of the radiation formula of Planck.

1484: F. A. Kröger: Luminescence and absorption of zincsulphide, cadmiumsulphide and their solid solutions (Physica, **7**, 1-12, Jan. 1940). (Original in the English language.)

In the case of ZnS, CdS and ZnS-CdS solid solutions a new emission is found at a temperature of —180 °C. The emission bands found consists of at least five parts, lying at equal intervals: the boundary of the emission bands at the short wave end coincides with the boundary of the fundamental absorption bands at the long wave end.

The emission bands were thus explained as combination frequencies due to the transition of one electron with a vibration. With the help of these emission bands an several new absorption measurements it has been established that in the series of ZnS-CdS solid solutions the edge of the fundamental absorption region is continuously displaced from ZnS to CdS.

ZnO exhibits an emission and an absorption in the ultraviolet which are quite similar to those of ZnS and CdS.

VOL. 5 No. 6 JUNE 1940

Philips Technical Review

DEALING WITH TECHNICAL PROBLEMS
RELATING TO THE PRODUCTS, PROCESSES AND INVESTIGATIONS OF
N.V. PHILIPS' GLOEILAMPENFABRIEKEN

EDITED BY THE RESEARCH LABORATORY OF N.V. PHILIPS' GLOEILAMPENFABRIEKEN, EINDHOVEN, HOLLAND

THE USE OF X-RAYS AND CATHODE RAYS IN CHEMICAL AND METALLOGRAPHIC INVESTIGATIONS *)

by W. G. BURGERS.

539.26:539.72

Diffraction diagrams taken with X-rays or electron beams are capable of supplying information about the identity and essential characteristics of the structure of a material. After a brief statement of the fundamentals of the interpretation of such diagrams, the possibilities of the application of diffraction research in chemical and metallographic work are illustrated by means of a series of examples.

Introduction

One of the most powerful aids in the examination of the structure of matter is the refraction (diffraction) experienced by X-rays in passing through the matter. This phenomenon, like the diffraction of electron rays, which according to the insight of modern physics may in many respects be considered as a wave phenomenon analogous to X-rays, gives insight into the arrangement of the atoms (or molecules, as the case may be) in crystals. The information gained in this way may on the one hand be brought into connection with the nature of the binding forces between the atoms, and on the other hand with the properties of the crystal complexes built up therefrom.

In general, diffraction investigations can only produce such results in the hands of investigators who are completely at home in the crystallographic foundations of structure analysis and who have specialized in this subject. On the other hand, however — and this lends the method of diffraction analysis its great *practical* significance — many chemical and metallographic problems can be studied by this method and a solution can be reached without a deep knowledge of crystallography being required. This possibility is based upon the fact that in principle diffraction analysis of a substance gives data not only about the crystallographic structure, but also about the crystalline state in which the substance exists and upon which many of its properties are found to depend, as well as about its chemical composition. As one of the characteristics of the crystalline state may be considered the fact as to whether the substance is built up of large or small crystal blocks, and further the state of perfection of the crystal blocks and their position in a given material. Changes in the crystallographic structure of compounds or alloys can often also be ascertained and related to changes in their properties, without it being necessary to call in the aid of crystallography proper.

Before illustrating the significance of these possibilities by means of several concrete examples, we shall first explain briefly how the information mentioned is obtained from the diffraction phenomena.

Foundations for the interpretation of diffraction diagrams

Spot photographs

The atoms of which a crystal is built up are, in an "ideal" crystal, arranged in a regular way upon groups of parallel planes which groups intersect each other (*fig. 1*) and are called crystal lattice planes. In each group two successive planes are at a definite distance apart. For a given crystal all these lattice plane distances are fixed, as also the angles between the various intersecting groups of planes.

If a beam of X-rays or electrons falls upon a crystal, the rays are scattered in all directions by

*) Editor's note: In the following article, with the consent of Prof. W. G. Burgers, we give the main content of the address delivered by him upon his acceptance of a professorship at the Technische Hoogeschool in Delft on January 15th 1940. Of the possibilities of application here reviewed, a number have already been dealt with in the first and second volumes of this periodical.

the atoms. Due to interference the scattered rays neutralize each other in general, except in very definite directions. Fortunately for our power of imagination these directions may be described as those in which the primary beam of rays would be reflected if the lattice planes were mirrors.

For the formation of such a spot pattern the external boundary of the crystal is a matter of indifference to a certain extent. Thus if a substance is irradiated which consists of a collection of larger or smaller crystalline fragments with irregular boundaries, each of these so-called crystallites will

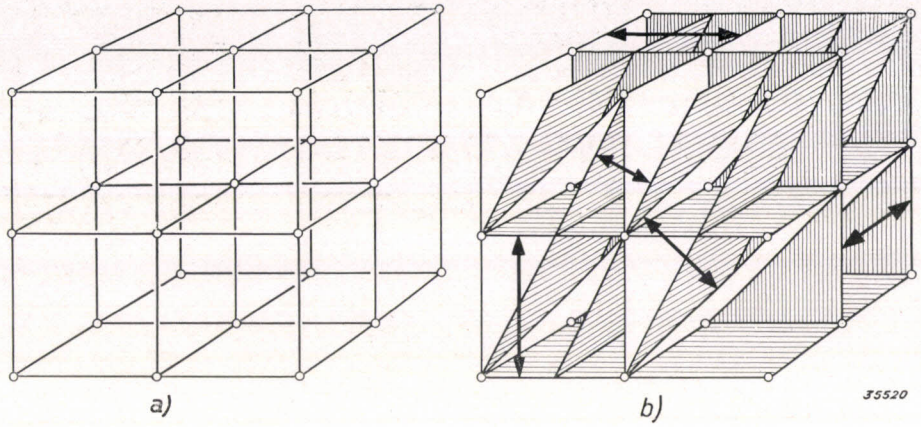

Fig. 1. The atoms are regularly arranged in a crystal according to a lattice, a simple type of which is here represented (*a*). The atoms in such a lattice may be imagined as arranged upon groups of mutually parallel planes which intersect each other at definite angles. Several planes of five of these groups (there are of course many more) are shown here (*b*), with the corresponding lattice plane distances.

Upon a photographic film placed around the crystal, therefore, in addition to a central spot produced by the unscattered rays of the primary beam, a very definite pattern of spots will be formed. Such a so-called Laue photograph is shown in *fig. 2*. From this pattern, on the basis of the above-mentioned simple mirror relation, the position of all the crystal lattice planes with respect to the direction of radiation can be derived. In this way, therefore, the crystal lattice can be analyzed, or — what is more important at the present moment — the position of the lattice (expressed crystallographically: the position of the crystal axes) can be ascertained.

Fig. 2. Spot pattern obtained by the diffraction of a beam of X-rays through a single crystal (Laue photograph).

give rise to a spot diagram. In the case of most ordinary materials the individual crystallites are so small that the beam of X-rays [1]), which may have a diameter of $^1/_2$ mm for example, falls upon several at once. The diffraction diagram then exhibits a superposition as it were of a number of separate spot patterns. If the position of the crystallites in the substance under examination is entirely random as far as the orientation of their crystal lattices is concerned, then the spots are distributed more or less uniformly over the whole photograph as may be seen in *fig. 3a*. If, however, the crystallites have definite preferred positions, that is if the substance shows a texture, then the spots are collected in definite groups, each of which corresponds to crystal lattice planes of the same "kind" belonging to the different, approximately similarly oriented crystallites. Fig. 3*b* is an example of such a photograph. The mean position of the crystallites with respect to the boundary of the substance, *i.e.* the crystallographic character of the texture, can again be ascertained by means of the above-mentioned simple mirror relation between spot and lattice plane.

The smaller the crystallites in the substance, the greater the number which will be struck simul-

[1]) For the sake of brevity we shall here and in the following speak only of X-rays. Electron rays can also generally be understood.

taneously by the X-ray beam, and therefore the greater the number of spots on the photograph. At the same time the intensity of every spot decreases in general with the size of the reflecting crystal lattice plane. Information about the size of the crystallites can thus be deducted from the spot diagram. This is illustrated by a comparison of fig. 3*a* and *c* which show the contrast between a fine and a coarse crystalline substance.

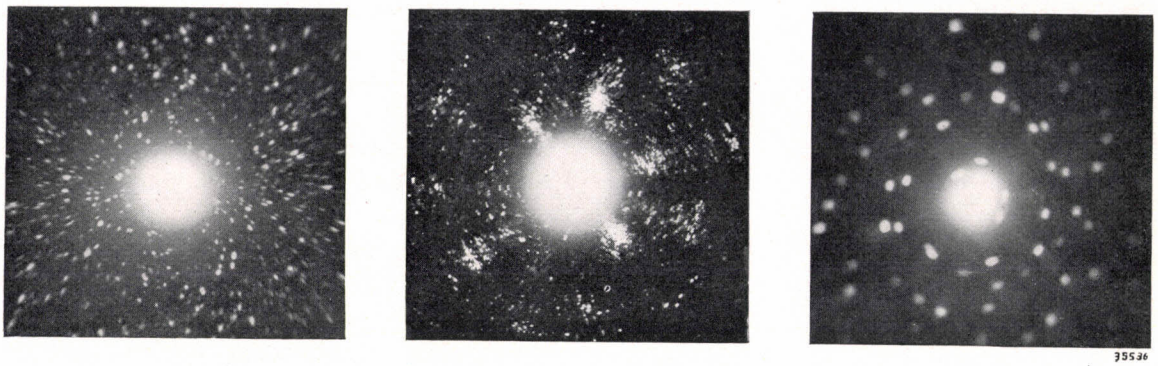

Fig. 3. Spot photographs. Upon simultaneous radiation of a number of crystallites a superposition of all the spot patterns is obtained. With random positions of the crystallites the spots are spread over the whole photograph (*a*), when there are preferred positions the spots are collected into groups (*b*). While in (*a*) 20 to 30 crystallites are irradiated at the same time (fine crystalline substance), in (*c*) there were only a few (coarse crystalline substance).

The crystallites of which a substance consists are themselves often built up of small regions which are not absolutely parallel but join each other at a small angle (*fig. 4*). This is true of every crystal to a certain extent, due to irregularities in the process of growth. The phenomenon occurs much more pronounced in plastically deformed crystals, where, due to the sliding of parts of the crystal along one another, rotation and bending of crystal lattice planes by 10° or more may occur. Just as a circular spot is stretched out to a line or otherwise upon reflection in a curved mirror (familiar to every one from the distorting mirrors at fairs, etc.), in the same way the reflection of X-rays at the curved lattice planes of such an imperfect crystal will give rise to elongated spots on the photograph (see *fig. 5*), whose length and position can give us some information about the nature of the *crystal defect.*

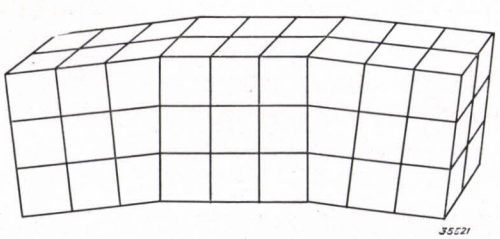

Fig. 4. Imperfect crystal built up of small contiguous lattice zones lying at small angles to each other. The lattice planes of the crystal are bent, as it were.

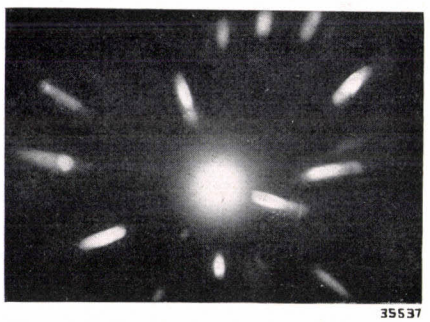

Fig. 5. Spot diagram of an imperfect crystal.

Circle diagram

In the foregoing it is tacitly assumed that every lattice plane, no matter at what angle the X-rays are incident, can reflect the X-rays. This is, however, not always true. The "reflection" of an X-ray takes place at a whole group of mutually parallel lattice planes at once (*fig. 6*). If the reflected ray is to possess an observable intensity, all these reflections must reinforce each other by interference, *i.e.* the difference in length of the path of rays reflected at different planes of the group must be a multiple (n) of the wave length (λ). From this follows the condition

$$2\,d \sin \Theta = n \cdot \lambda, \quad . \quad . \quad . \quad . \quad . \quad . \quad (1)$$

$$n = 1, 2, 3, \ldots,$$

where d is the lattice plane distance characteristic of the lattice plane, and Θ is the angle between lattice plane and X-ray beam. If the beam of X-rays is polychromatic, *i.e.* if it contains rays of a whole

range of wave lengths, then for each combination d, Θ, *i.e.* for every lattice plane present, there are rays whose wave length satisfies equation (1), so that every plane gives rise to a spot on the diffraction

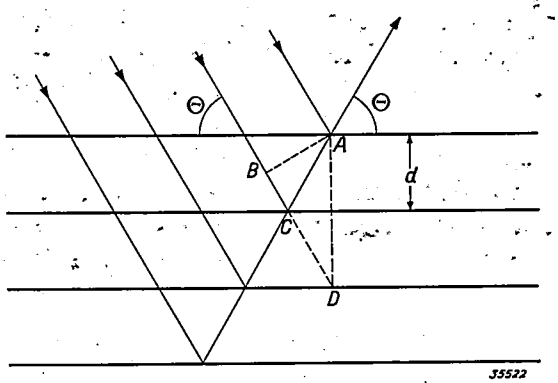

Fig. 6. The refraction of the X-rays may be considered as a reflection at the lattice planes in which all the planes of one group work together. In order that the reflected ray may not disappear due to interference, the difference in traject $BC + AC$ must be an integral multiple (n) of the wave length λ. Since $CD = CA$ the difference of traject is equal to the side BD of the right triangle DBA where $DA = 2d$ and the angle $BAD = \theta$. Formula (1) follows from this.

photograph. In this way we obtain the spot diagrams discussed above. If, however, the X-ray beam is monochromatic, *i.e.* if all the rays have the same wave length λ, reflection at a given kind of lattice plane can only occur when the angle Θ at which the X-rays strike the lattice plane fits the given combination d, λ. Therefore if the monochromatic X-ray beam strikes a single crystal, many fewer or even no spots at all will appear on the photograph. If the X-ray beam simultaneously strikes a large number of crystallites in which the lattice plane under consideration is in each case at a different angle to the beam, all those crystallites will contribute to the reflection in which this angle satisfies equation (1). Reflected X-rays can therefore only occur at angles of 2 Θ with respect to the beam, where Θ is given by equation (1). The scattered X-rays therefore all lie on a number of cones having apex angles of 4 Θ, see *fig.* 7, which intercept the photographic film in a series of concentric circles or rings. In the case of sufficiently finely crystallized preparations the spots lie so close together on these circles that they give the impression of continuous rings.

Since each circle corresponds to a definite lattice plane distance, and, as already mentioned, a very definite group of lattice plane distances belongs to a given crystal, the circle system is characteristic of the crystal lattice under consideration, and in general it is different for every substance. In this way the monochromatic diffraction photograph may be used simply for the identification of a substance, either element or compound. In the presence of different kinds of crystals (different phases) in the same preparation the different ring systems corresponding to them occur at the same time in the diffraction diagram, so that they make possible an analysis of the mixture.

At the same time, however, the circle diagram is able to provide other valuable information. Because of the fact that the diameters of the rings (angles Θ) are directly connected with the lattice plane distances (d) a slight change in those distances will manifest itself in a corresponding change in the ring diameters, and thus in a shifting of the rings. Such changes in the lattice dimensions may occur for example due to elastic strain or by the taking up of substances in solid solution.

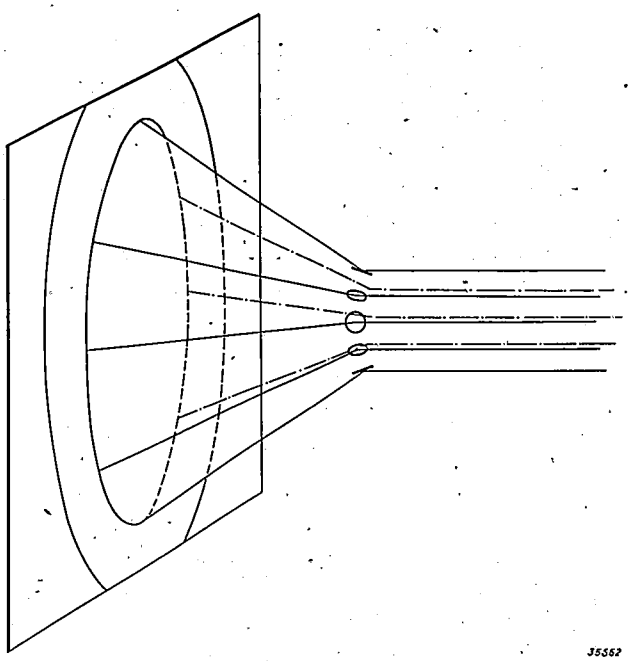

Fig. 7. The formation of circle diagrams. In a polycrystalline substance upon which a monochromatic X-radiation falls, only those crystallites are active as "reflectors" in which the lattice planes are at angles Θ to the beam according to equation (1). The rays reflected at a particular type of lattice plane therefore all lie on a cone with the apex angle 4Θ.

Finally the circle diagram like the spot diagram is able to provide data about the size and degree of perfection of the crystallites, and about the occurrence of preferential orientations. Only when a very large number of crystallites is struck by the beam will the circles appear continuous, as stated above, (*fig. 8a*); when the number is smaller, *i.e.* when the crystallites are larger, every ring is resolved into a number of spots (fig. 8*b*), whose number and definition permit an estimation of the size of the crystals. In the presence of texture, the

spots are again collected into definite groups, *i.e.* the intensity of the diffraction rings varies along the circumference (fig. 8*c*). The intensity of the

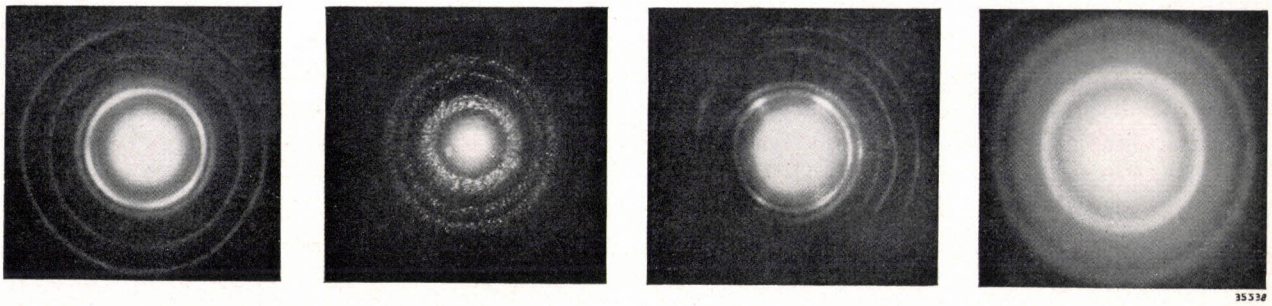

a) *b*) *c*) *d*)

Fig. 8. Circle diagrams: *a*) rings continuous and sharp; *b*) rings decomposed into points: presence of larger crystallites; *c*) rings with varying intensity along their circumference: presence of texture; *d*) rings not sharp: crystal defects.

diffraction lines and in some cases their definition can also be influenced by crystal flaws (fig. 8*d*), according to whether the flaws are spread over many or few atoms.

A lack of definition in the diffraction diagram may also occur due to a quite different cause, namely when the number of atoms collaborating in the scattering is very small. In such cases the investigation with electron beams offers a welcome supplementary method.

Diffraction of electron beams

Fundamentally the same considerations are valid for electron beams as were given above for X-rays; they are therefore to provide similar information about the state and the chemical character of a crystalline substance. Due, however, to their much stronger reaction with the atoms, electron beams give a clear diffraction picture with much smaller amounts of substance than are required for the refraction of X-rays, and consequently, with the same amounts of substance, electron beams give much sharper pictures. On the other hand the penetration of electron rays is very slight for the same reason, so that the information obtained with their help relates only to the state of the substance in very thin layers, a few atoms thick.

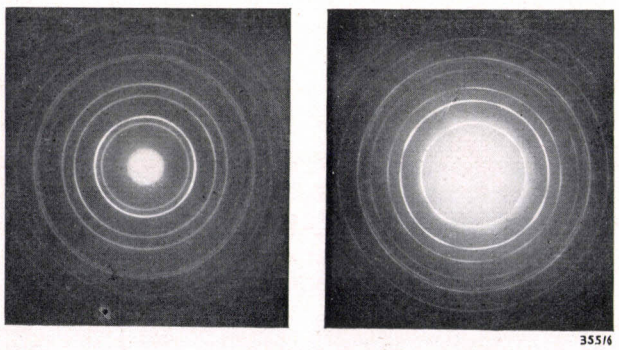

a) *b*)

Fig. 9. Electron diffraction diagrams: *a*) of an extremely thin gold foil, *b*) of aluminium foil with obvious texture.

In *fig. 9a* the electron diffraction picture is given of an extremely thin gold foil (obtained by etching away). The great sharpness of the rings is striking. Fig. 9*b* shows a similar diagram of an aluminium foil, in which it may be concluded from the variations in intensity around the circumference that there is a texture.

Possibilites of practical application

We shall now illustrate by a number of examples the different possibilities of application of diffraction analysis which follow from the foregoing. These applications may be divided into two main groups. In the first group the problem is that of the nature or composition of a substance, in the second, of the crystalline state in which it exists.

Nature and composition of a substance

Identification of a compound

The simplest application is that for the identification of a compound. For example, by characterizing the ring diagram of each compound by giving the angles of refraction and intensities of the three strongest lines [2]), a kind of table for determination can be obtained. Such tables have been made by Hanawalt, Rinn and Frevel [3]), among

[2]) If it is only a question of the diameter of the rings (and not for instance of the variation in intensity around their circumferences) it is sufficient to photograph a narrow strip passing through the centre of the system. Instead of complete circles one then obtains a number of more or less curved lines on the photograph.

[3]) J. D. Hanawalt, H. W. Rinn and L. K. Frevel, Ind. Eng. Chem. **10**, 457, 1938.

others, for a relatively large number of compounds (1 000). Due to all kinds of factors, however, such as differences in the crystalline state of the samples used, changes in intensity, etc. may occur which make the use of the tables difficult if not impossible. In general therefore it is better to compare the diagram obtained from the unknown substance with self-made diagrams of comparison substances. In the case of investigations in a given laboratory the choice of comparison substances to be considered will usually be limited to a relatively small number of repeatedly occurring substances of which a collection of diagrams can be prepared in advance.

As an example of an identification on these lines we may mention a case of an organic compound, namely an osazone obtained by Meuwissen and Noyons [4]) in their investigations of the occurrence of vitamine C in urine. The X-ray diagram of this compound was found to be identical with that of the osazone of ascorbic acid (vitamine C) and quite different from the X-ray diagram of the osazone of reductinic acid (see *fig. 10*) which is built up chemically in an analogous way to a certain extent. This result confirmed their assumption that vitamine C occurs in normal urine.

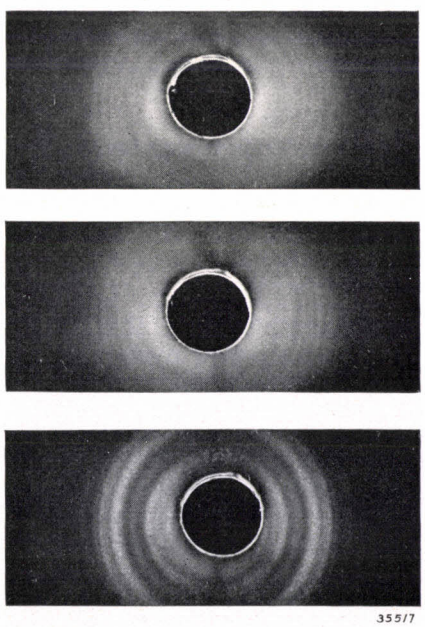

Fig. 10. Comparison of the diffraction patterns of the osazone *a*) of the product isolated from urine, *b*) of ascorbic acid (vitamine C) and *c*) of reductinic acid.

It is particularly in organic chemistry where the identification by means of diffraction diagrams is still only little used, that this method, in addition to identification by determination of melting point or other methods, deserves more attention. Only a small amount of material is needed for making the diffraction diagram, ten milligrams for instance. The X-ray diagram, filed with the sample investigated, may also be of use later on, in order for example to ascertain any change or decomposition of the substance. Isomers (if crystalline) can also be distinguished from each other in this way in spite of their identical chemical composition. The diagrams of ortho- and paradioxybenzene for instance differ plainly from each other.

If the amount of a preparation available is smaller than that mentioned as necessary for making an X-ray diagram, an examination with electron rays — as explained above — may offer a solution. By this method it was found possible to obtain an excellent line diagram with only a few crystal needles of the acetate of a provitamine D obtained from an animalic product by Boer, Reerink and van Wijk [5]). The ring system was practically identical with that which was obtained from the acetate of synthetic 7-dehydrocholesterol. (Upon continued investigation it was found that ergosterol acetate, which is related in atomic composition, gives only a slightly different diagram, so that in this case the diffraction test could not provide absolute proof of the identity of the synthetic and the natural product. This identity was, however, established by another method.)

Analysis of a mixture

If the material to be examined consists of a mixture of different substances, the diagram, as previously mentioned, exhibits the lines belonging to the various components of the mixture, and from it therefore, again by comparison with known diagrams, the composition of the mixture can be deduced qualitatively, and to a certain extent quantitatively also, by estimating the relative intensities. The significance of the analysis obtained in this way is that it gives us the compounds and not, like purely chemical analysis, the atomic composition. By this method, for example, it was possible to find out whether thorium oxide, which is added to the original tungsten oxide in the preparation of metallic tungsten for electric lamps, is present as such in the metallic tungsten after the reduction process or has also been reduced to the metal — a question which was of great practical importance in connection with recrystallization phenomena in the filament [6]). Another practical

[4]) T. Meuwissen and E. Noyons, Acta brevia Neerlandica, **8**, 85, 1938.

[5]) A. G. Boer, E. H. Reerink, A. van Wijk and J. van Niekerk, Proc. Roy. Acad. Amsterdam **39**, 622, 1936.

[6]) Z. anorg. allg. Chem. **193**, 144, 1930; see also Philips techn. Rev. **1**, 188, 1936.

example is furnished by the investigations carried out at the Agricultural High School in Wageningen on the composition of clay minerals [7]). In the case of just such complicated compounds (silicates) where the chemical analysis gives only little information about the actual structure, the diffraction method may be particularly useful.

Investigation of solid solutions

The possibility of identification also renders X-ray analysis a valuable tool in the study of reactions in the solid state, which are otherwise approached only with difficulty. If the reaction products form new phases they can be recognized by their line systems; if, however, they are taken up in solid solution in the original phase, an expansion or contraction of the crystal lattice is the result, which is manifested in a gradual shift of the original lines. The change in lattice-plane distances can be calculated from this shift, and the approximate quantitative composition of the solid solution can often be deduced [8]). In metallurgical laboratories the determination of phase limits is being carried out in this manner to an increasing extent.

As an example of a reaction in which a new phase as well as a solid solution could occur we may mention here the research on tantalum carbide wires [9]), which might be used as filaments in vacuum lamps. Such wires, which are made by heating carbon filaments in tantalum halide vapour, were found to exhibit great differences in electrical resistance and in rate of evaporation (blackening of the bulb). Chemical analysis is difficult because of the insolubility of the carbide, and moreover it destroys the test filament. With X-ray diffraction pictures on the other hand it was easy to ascertain that the less suitable wires contained the carbide Ta_2C in addition to the carbide TaC, while in some cases the metal itself was present in solid solution in the carbide. The remedy for the latter evil was simple; by subsequent heating of the wires in an atmosphere of methane the excess of tantalum was converted into the carbide TaC.

The absorption of gases in metals may also be studied to some extent with the help of diffraction analysis. A good example of this occurred in an investigation by de Boer and Fast [10]) on the mobility of oxygen in zirconium under the influence of an electric field. The metal is able to take up a large quantity of oxygen in solid solution (up to 40 atom per cent). The dimensions of the crystal lattice as well as the electrical resistance increase with the oxygen content. If a direct current was sent for some time through a zirconium wire containing oxygen, the resistance of the section of wire in the neighbourhood of the positive pole was found to increase considerably — visible directly by the lighter glowing of this section — while the resistance near the negative pole decreased at the same time. This phenomenon must, according to the investigators mentioned, be ascribed to the fact that the oxygen moveds toward the anode through the zirconium lattice, probably as a negative ion. under the influence of the electric field, and there increases the concentration of oxygen. The diffraction diagrams of the parts of the wire in the neighbourhood of the poles did indeed indicate an increase in the lattice distances at the anode and a decrease at the cathode, in agreement with the above-mentioned interpretation of the phenomenon as an "electrolysis in the solid state".

Finally the possibility of the investigation of diffusion processes in solid substances may be mentioned in this connection. Due to the limited depth of penetration of the X-rays used in diffraction analysis, the information which the diffraction diagrams provide about the composition relate only to the outermost layer of the substance examined, which is 10 or 20 microns thick, for example. If the surface layer is removed by etching and a new X-ray diagram is made, any deviation in the composition of the surface layer, caused by diffusion can be brought to light. With electron rays even much thinner surface layers (oxide films, for instance) can be determined and identified in this way.

Crystalline state

While the applications of diffraction analysis mentioned until now may be considered more or less as supplementary to analyses carried out by purely chemical methods, it is quite a different matter with the applications in which the character of the crystalline state is in question. It should be stated in advance that the knowledge of the crystalline state, i.e. of the size and state of perfection of the crystallites, their orientation, etc. may be of great importance, since a large number of the properties of materials, such as electrical conductivity, photochemical behaviour, chemical activity, cohesion, can be considerably influenced even by relatively slight changes in the crystalline state.

[7]) C. H. Edelman, F. A. van Baren, J. Ch. L. Favejee and H. J. Hardon, Mededeelingen van de Landbouwhoogeschool te Wageningen **43** (1939), Verhandeling 4-6.

[8]) See for example Philips techn. Rev. **1**, 220, 1936.

[9]) See Philips techn. Rev. **1**, 253, 1936.

[10]) J. H. de Boer and J. D. Fast, Rec. Trav. chim. Pays Bas **59**, 161, 1940.

The determination of such a correlation implies not only an increase of knowledge but it may often also be of practical significance when the properties in question are themselves difficult to measure, or when, as in manufacturing processes, they can only be revealed after the process has already proceeded too far.

Size and state of perfection of the crystallites

Of the many cases where information is required about the size and state of perfection of the crystallites, we shall in the first place mention the investigation of the chemical activity of various substances. Hoffmann and co-workers [11]) found that preparations of carbon and soot were most active when they consisted of very small crystallites or of crystallites with a very much distorted lattice. Such pieces of information are able to serve as guides in the preparation of these materials for technical use.

In the case of another substance of quite a different nature, namely butter, attempts were made to obtain information from the X-ray diagram about the state of the crystallized component, in the hope of being able to find a relationship between differences in solidity of kinds of butter prepared in different ways and differences in the size of the butter-fat crystals, which were to be expected on the basis of other considerations. Although our preliminary tests gave no clear answer to the question [12]), in principle it does not seem impossible that more extended investigations of this nature may be of value in the study of questions in the chemistry of foodstuffs.

Orientation of the crystallites

Layers of metal or salt deposited by evaporation, or sputtering or electrolytically often exhibit an anisotropy in their properties. This is found to be connected with the fact that the crystallites are oriented in definite preferential directions, which can be studied by means of diffraction analysis. Such a texture can be shown for example in the case of nickel layers electrolytically deposited [13]), where on the one hand certain properties such as adhesion and brilliance are found to be correlated with the texture, while on the other hand the occurrence and nature of the texture are found to depend in a complex manner on the thickness of the layer and the condition under which the electrolysis was carried out, such as current density, size of the electrolysis vessel, stirring, etc.

Another interesting example of X-ray analysis of texture is the investigation of the orientation of the cellulose crystallites in the wood of violins of different sound quality [14]). It was found here that while in all cases examined the belly of the violin exhibited a pronounced texture as shown by the X-ray diagram, such a texture in the back of the violin occurred only in the case of the less good violins; in the better class instruments it was practically absent (*fig. 11*).

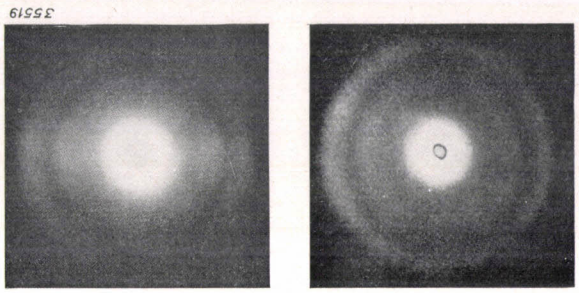

a) *b*)

Fig. 11. In the back of violins of poor sound quality the cellulose crystallites show evidence of texture (*a*), which is absent in the case of violins of good quality (*b*). (From Lark-Horowitz and Caldwell, Naturwiss. **22**, 450, 1934).

An orientation of the crystallites also occurs regularly in the working of metals. The crystallites in drawn wire and rolled sheet always assume certain preferential positions; by heat treatment following the working, in which new crystals are formed by recrystallization, these preferential positions can be entirely modified. The texture leads to an anisotropy in the properties of the metal which may be either desired or undesired for the purpose in view. A good example of a desired anisotropy obtained by working is that of the rolled nickel-iron strip for cores of loading-coils, diffraction diagrams of which are reproduced in *fig. 12* and explained in the text under the figure [15]). An undesired anisotropy is often encountered in the punching of caps and sockets out of rolled sheet-iron. It leads to the formation of a lip [16]). The determination of these textures by X-ray methods and of their crystallographic nature may be very valuable for the sake of the indications it gives as to desirable alterations in the process of working.

[11]) U. Hofmann and D. Wilm, Z. Elektrochem. **42**, 504, 1936.

[12]) W. van Dam and W. G. Burgers, J. Dairy Sci. **18**, 45, 1935.

[13]) See Philips techn. Rev. **1**, 95, 1936.

[14]) K. Lark-Horowitz and W. I. Caldwell, Naturwiss. **22**, 450, 1934.

[15]) For a more detailed discussion see Philips techn. Rev. **2**, 93, 1937.

[16]) Philips techn. Rev. **2**, 158, 1937.

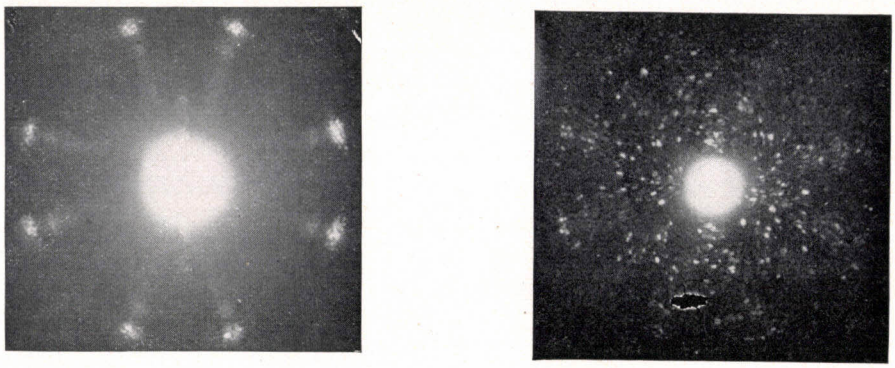

a) *b*)

Fig. 12. Cores for loading coils are made of nickel-iron strip with strongly anisotropic magnetic properties. The desired anisotropy is obtained by rolling and recrystallization, which results in a pronounced texture. By means of X-ray photographs the process can be controlled at an intermediate stage of the treatment to find out whether (*a*) or not (*b*) the required texture has been attained.

Lattice distortions in metals

The pronounced property of metallic crystals of being deformed plastically also involves the fact that not only the orientation but also the internal state of the crystallites may undergo great changes during working and heat treatment, *i.e.* lattice distortions occur in and among the crystallites. These distortions differ from the above-mentioned crystal defects in that they are accompanied by internal tensions in the deformed metal which are in turn of influence on many practically important properties such as electrical resistance, mechanical hardness, magnetizability, etc. Such lattice distortions and conditions of strain also occur in the separation of one component out of a supersaturated solid solution.

The investigation of lattice distortions by means of the broadening and changes in intensity of the lines or spots in diffraction diagrams is a particularly good sphere of application in which the diffraction method may not only serve in routine control tests (for instance, for the presence of internal strains) but where it can also contribute to the knowledge of phenomena which have not yet been explained scientifically. An interesting and technically important example of this are the recent investigations [17]) of the differences between so-called cold-hardened and warm-hardened copper-aluminium alloys. The metal aluminium can take up several per cent of copper in solid solution at 500 °C; at 200 °C it cannot take up more than a few tenths of a per cent. By quickly cooling an alloy which has been saturated at a high temperature to room temperature, however, the homogeneous state is, as it were, fixed. The alloy is now mechanically soft. The hardness, however, is found to increase slowly again, to a maximum value which is reached in the course of several days (socalled ageing, cold hardening). If the alloy, after having reached its maximum hardness, is heated for instance to 200 °C, a decrease in hardness at first takes place, and after longer heating a new state of hardness occurs (warm hardening). These phenomena can now be correlated with the occurrence of lattice distortions resulting from the diffusion processes which initiate the separation of the excess copper atoms present. Diffraction diagrams of single crystals of the alloy immediately after the rapid cooling from the high temperature exhibit, in addition to well-defined points, some poorly defined stripes also which increase in clearness and definition during the ensuing ageing [17]). Closer analysis of these stripes showed that they must be ascribed to the appearance of small plate-like aggregates of copper atoms, several atoms thick at the most, along the sides of the tubes of the crystal lattice, and it must be assumed that this beginning of aggregation is already accompanied by an increase in hardness. Upon heating to 200 °C a disappearance of the stripes in the diffraction diagram, together with the decrease in hardness, occurs at first. The aggregates thus redissolve. The increase in hardness upon longer heating is again accompanied by the reappearance of the stripes which now, however, are much sharper, and thus indicate the formation of considerably larger copper aggregates. After still longer heat treatment the stripes break up into sharp points, from which it may be concluded that the plate-like aggregates grow to still larger complexes.

[17]) G. D. Preston, Phil. Mag. **26**, 855, 1938; A. Guinier, Thèses, Paris 1939.

With this example we wished to illustrate how differences in technological properties of alloys teated in different ways can be reduced to differences in internal structure. In doing this we have wandered somewhat from the validity of the thesis which was stated at the beginning of this paper: that the diffraction method can be successfully applied, even without a deeper knowledge of the crystallographic foundations of the science of structure. We hope, nevertheless, that it will have appeared from the series of applications here summed up that the sphere in which our thesis holds is sufficiently extensive to insure diffraction analysis an important position among the research methods with technical application.

TECHNICAL PHOTOMETRY OF GAS-DISCHARGE LAMPS

by P. J. ORANJE.

535.24 : 621.327.4

In order to control the manufacture of gas-discharge lamps an apparatus was designed which makes it possible to carry out measurements on gas-discharge lamps in a reliable, rapid and inexpensive manner with an accuracy of 3 per cent in the light flux. The apparatus consists of 18 photometers which can be read from a central point. The time necessary to heat up the gas-discharge lamp in the photometer can be used to measure lamps in other photometers.

When it is a question of measuring large numbers of sources of coloured light daily in the control of the manufacture of gas-discharge lamps, in addition to the problems which occur in the photometry of sources of coloured light in general [1]), there are also practical difficulties. After an explanation of these points we shall in this article discuss how the light flux of gas-discharge lamps is determined in a technical way in the control laboratory of the Philips factories.

[1]) See: Physical Photometry, Philips techn. Rev. **4**, 260, 1939; The Photometry of Metal vapour lamps, Philips techn. Rev. **1**, 120, 1936.

Statement of the problem

In contrast to a research laboratory a control laboratory in general carries out measurements on only a limited number of types of lamps. As a rule, however, a large number of lamps of the same type must be measured successively. The light flux of these lamps must be known under conditions such as occur in practical use. One does not deter-

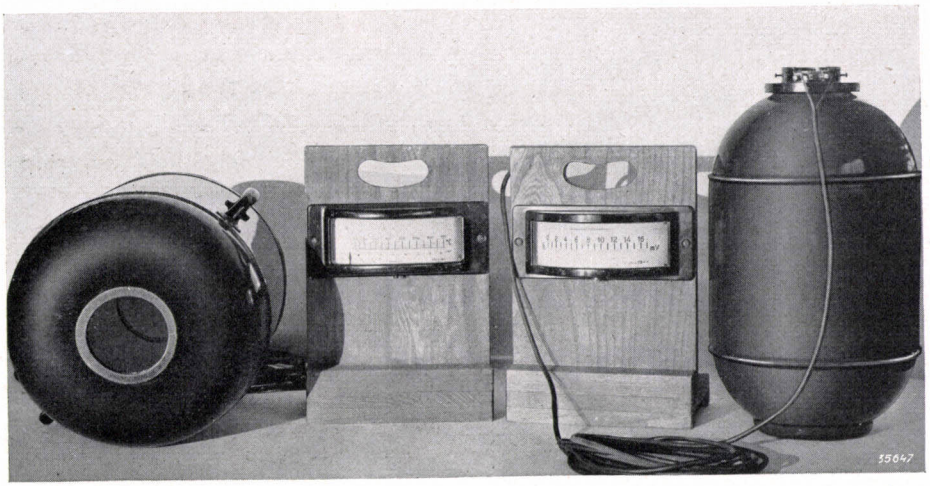

Fig. 1. Two small portable integrating spheres, photographed in different positions.

mine therefore (as is often done in scientific research) the light flux for a definite current or for a definite power of the lamp, but the light flux which occurs when the lamp is connected to a certain, accurately known apparatus in series on a main of a certain voltage, and when it has been in operation long enough to have reached the state occurring in permanent operation. This heating time for gas-discharge lamps may amount to from 15 to 30 min.

It is chiefly this long time for heating up which is experienced as a difficulty in control measurements of gas-discharge lamps. If the lamp is allowed to burn in the photometer during the whole time of heating up, the photometer is "occupied" much longer for every measurement than is necessary for the measurement itself. If, however, the lamp is not inside the photometer while heating up, then for every measurement either the lamp to be measured must be moved to the photometer or the photometer to the lamp, which involves difficulties which will be explained in the following.

Against the moving of the lamp the following points may be advanced:

1) Shocks, which easily occur during the transportation of the lamp, may cause the light flux of some kinds of gas-discharge lamps to change. Particularly in the case of sodium lamps a displacement of the liquid sodium in the lamp may lead to a permanent change in the light flux.

2) Some gas-discharge lamps (especially mercury lamps) do not reignite immediately after an interruption of the supply voltage, so that the current may not be interrupted during the transport from the rack where the lamp burns to the measuring table. This involves great complication of the installation with much chance of poor contacts, wear and tear, etc.

The objections to the moving of the photometer to the lamp are more serious than those to the moving of the lamp to the photometer:

1) In connection with the requirement that the measurement must take place rapidly, it is desirable that an objective measurement with the help of a light-sensitive element should be carried out. This means, however, that the apparatus contains very delicate components. Due to shocks or jars the

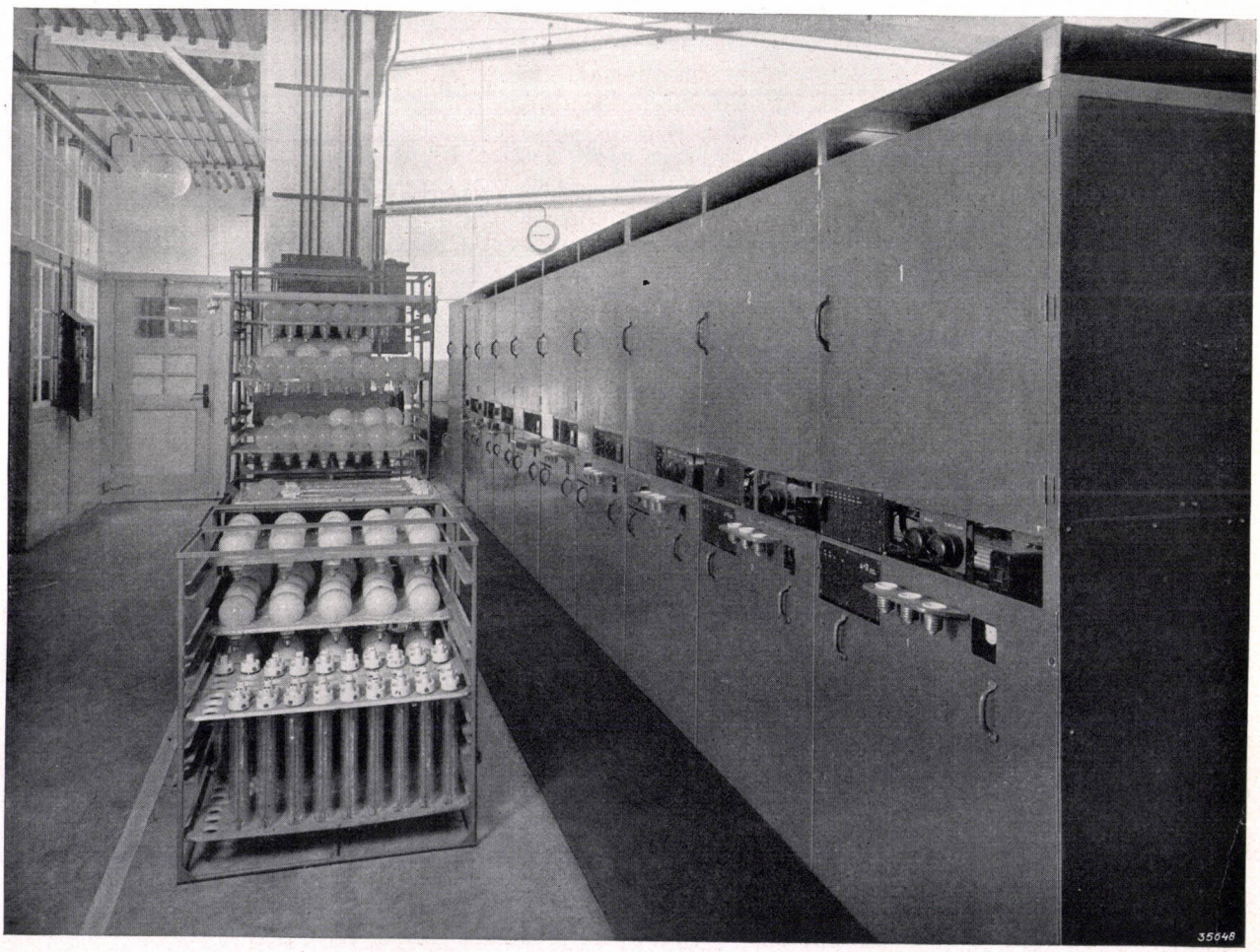

Fig. 2. Row of nine photometer chambers intended for routine measurements of gas-discharge lamps. The whole installation consists of two such rows.

element can be slightly displaced or damaged, the contacts may also suffer, etc.

2) The sphere of a transportable photometer must be small (see *fig. 1*). This means that the result is no true measure of the light flux, but also depends upon the light distribution of the lamp, so that for instance slight deviations in the shape of the lamp or socket, imperfect centering of the lamp, etc. may have considerable influence on the results of the measurement. Moreover during the measurement the small sphere becomes appreciably warm, which may have a noticeable effect upon the reflective properties of the internal surface and upon the sensitivity of the photo-element. Experience has shown that, due to these influences, even with daily calibration it is practically impossible to reach a greater accuracy than about 8 per cent with a portable photometer sphere.

In order to avoid the objections mentioned, in the installation to be described below a large number of photometers were set up side by side, so that the lamp can heat up in the photometer sphere itself, and neither the measuring apparatus nor the lamp need be moved. In order to facilitate the measurement the installation was so arranged that the results can be read off at a central point. Before proceeding with the technical execution of the installation we shall first discuss how the problems which are inherent in heterochromic photometry were solved in this special case.

Principle of the photometric method employed

As stated, the light flux of the lamp to be measured is determined with the help of an integrating photometer. In this photometer is a screen whose brightness is measured by means of a photo-element. The ratio between this brightness and the light flux of the lamp to be measured is determined by calibrating the photometer with a standard lamp with known light flux.

If the spectral composition of the light of the comparison lamp deviates from that of the gas-discharge lamps to be measured, the ratio of the photocurrents which are obtained with these two lamps is only a measure of the ratio of the light fluxes when the spectral sensitivity curve of the light sensitive element corresponds to the international eye-sensitivity curve. Two measures are therefore taken.

Firstly a highly sensitive element is used whose spectral sensitivity is to some extent adapted to that of the eye [2]). Secondly the deviations, which occur due to the fact that the correspondence between the spectral sensitivity of the photo-element and of the eye is not perfect, — together with other errors which may occur in the measurement with a photometer sphere — are considerably reduced by using the installation only for the comparison of lamps of the same type. The colour adaptation of the photo-element need therefore only be carried so far that the colour differences between individual gas-discharge lamps of the same sort do not cause any noticeable error.

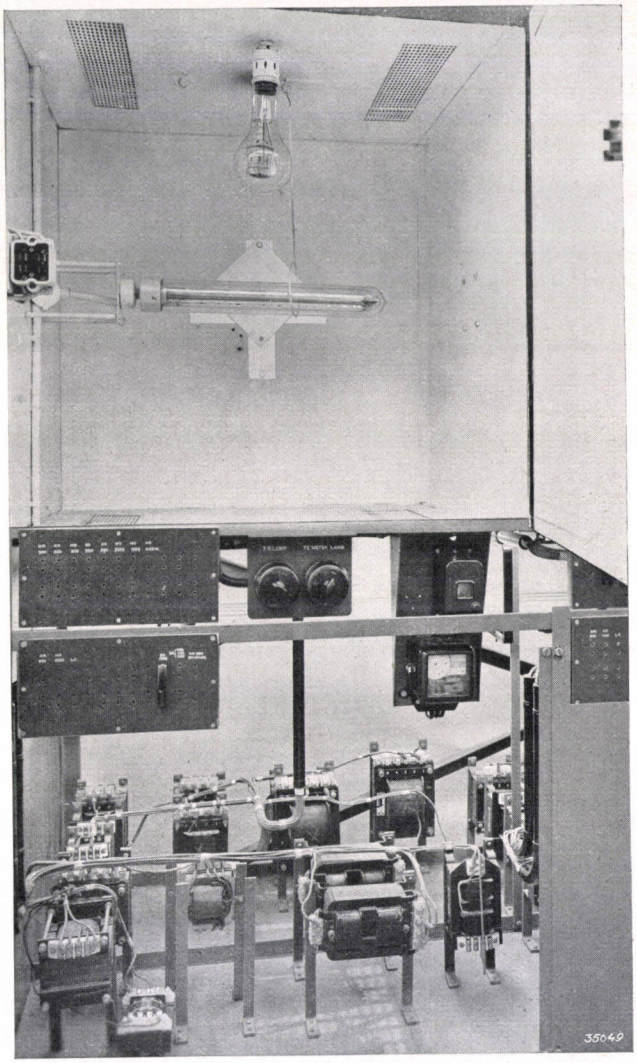

Fig. 3. An opened photometer-chamber. Through the bulb of the electric lamp may be seen a socket, to the left on the wall a second socket for the gas-discharge lamp to be measured. The latter contains a sodium lamp. Below the chamber to the left the switchboard by which various apparatus may be connected in series; in this case the apparatus for the sodium lamp SO 1000. In the middle the switches for the electric lamp and lamp to be measured, on the right the time relay. Below the various series of apparatus for different types of gas-discharge lamps.

[2]) According to Dresler such a photo-element can be realized by a selenium barrier-layer cell and several filters placed side by side slightly overlapping in front of the cell. By changing the regions which are covered by one or more filters, the spectral distribution of the sensitivity can be given the desired character. See for instance A. Dresler, Das Licht **3**, 41, 1933; J. Rieck, Das Licht **7**, 115, 137 and 157, 1937.

Construction of the installation

The installation is composed of 18 integrating photometers. For the sake of simplicity they are not spherical as is common, but cubic (edge 0.9 m) and placed in two rows of 9 "back to back". *Fig. 2* gives a view of the installation. The part below the switches contains a number of accurately known apparatus to be connected in series, while the part above the switches forms the photometer chamber proper. In *fig. 3* one of the photometers may be seen open. On the upper surface of the photometer chamber there is an electric lamp which serves for control of the photometer, which process will be discussed later. Behind this lamp and on one of the side walls two lamp sockets are mounted and connected in parallel, so that it is possible to let the lamp to be measured burn either in a horizontal or a vertical position. Between these lamp sockets and the supply mains, by means of a special plug-in contact in the switchboard below the photometer, any one of the above mentioned apparatus can be connected in series. Upon shutting the door the circuit in which the lamp is included is closed, while the contacts are always free of tension when the door is open.

In the upper and lower planes of the photometer strips of perforated metal have been set in. At the back of the chamber is the photo-element, which is shielded in the usual way from direct light.

By means of two rotating switches all the connections of every photometer can be switched over to the central measuring table which is shown in *fig. 4*. One exception is the connection for the current of the photo-element. In order to avoid disturbances which may easily occur at the very low voltages

Fig. 4. Measuring table of the installation. The vertically placed instruments measure the mains voltage and the current (when a transformer is used, primary and secondary separately). The instruments placed obliquely on the table measure the total power. The left-hand horizontal meter measures the photo-current, the right-hand one the voltage on the contacts of the lamp. To the right on the table may be seen the handles of the rotating switches, each of which serves part of the photometer cabinets. To the left on the table a series of switches for the photo-elements of the different photometer chambers. Above the meters are the neon lamps which glow when the heating time of the corresponding lamp has ended.

of barrier-layer photo-elements, this connection is by means of a separate cable to a separate switchboard on the measuring table.

When the door of the photometer is shut a time relay (see fig. 3, to the right below the photometer) is switched on, and after a previously chosen length of time it lights a numbered neon lamp on the measuring table. This is the sign to the operator that the lamp has burned long enough for the measurements to begin. On the other hand the operator at the measuring table can signal back to the person working at the photometer that the lamp has been measured.

A measurement proceeds as follows. A calibrated lamp of the type to be tested is first placed in the photometer. The time relay is set at the necessary heating time, and the door is shut. As soon as the neon lamp of the photometer chamber in question ignites at the measuring table, the operator there determines the photo-current, then switches off the gas-discharge lamp and switches on the electric lamp and again determines the photo-current. From the relation between these two photo-currents the apparent light flux of the electric lamp can be calculated.

After this calibration of the photometer chamber the calibrated gas-discharge lamp is replaced by the similar gas-discharge lamp which is to be measured, and this is measured with the electric lamp as standard lamp. The installation is best operated by two persons: one changes the lamps and the other does the measurement.

The light flux of the electric lamp found will in general differ slightly from the true light flux, because the colour adaptation of the photocell is not perfect. This is, however, of no importance since the error is exactly compensated when the electric lamp is subsequently used as standard lamp for the measurement of a series of gas-discharge lamps of the same type. In principle the electric lamp could be omitted and the gas-discharge lamp compared directly with the calibrated model. The introduction of the electric lamp, however, has the advantage that this light source, which is permanently available, very constant and rapidly put into action, makes it easy by means of occasional checks, to take into account any change in the sensitivity of the photometer, so that the calibration of the photometer need not be repeated for several weeks at a time.

As already stated, thanks to the fact that comparative measurements are carried out exclusively on a single type of lamp, the influence of numerous sources of error (selective reflection of the inner wall, irregular distribution of the light radiation in different directions, difference between the sensitivity curve of photo-element and the eye, casting of shadows by the lamp, etc.) is reduced to a minimum. The accuracy attained, which may be estimated to be within 3 per cent, may indeed be considered high for routine measurements.

The capacity of the installation depends upon the nature of the lamps to be measured and is determined chiefly by the time for heating. For example about 75 HP-lamps (small air-cooled mercury lamps) can be measured per hour, while for sodium lamps the number is much smaller, since sodium lamps must cool in the photometer after the measurement until the sodium has solidified.

VIEW OF A PART OF THE INDUSTRIAL PLANT OF N.V. PHILIPS' GLOEILAMPENFABRIEKEN, EINDHOVEN

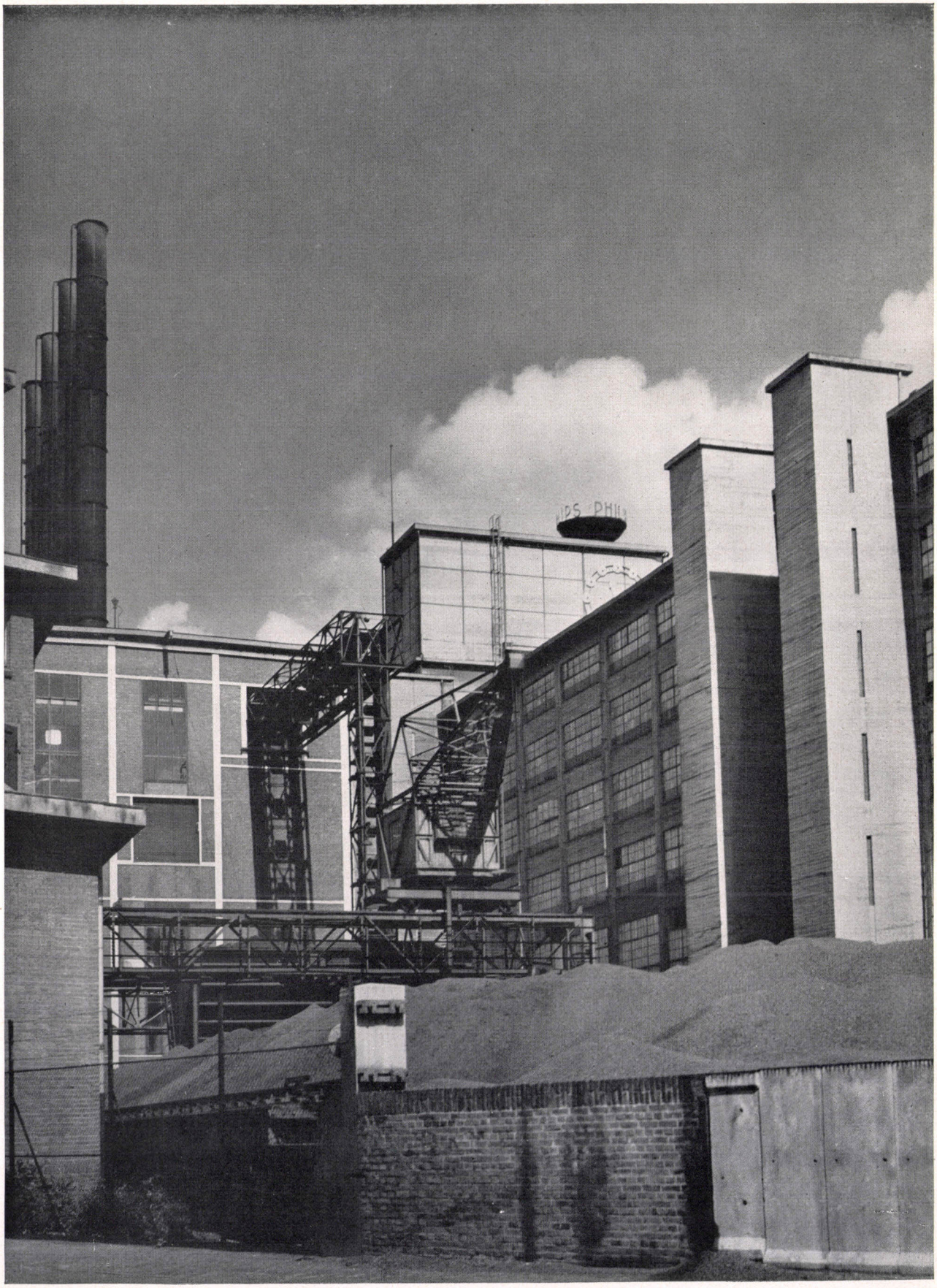

A NEW PUSH-PULL AMPLIFIER VALVE FOR DECIMETRE WAVES

by M. J. O. STRUTT and A. van der ZIEL.

537.543:621.385

For the reception of signals with wave lengths shorter than 1 metre electronic valves are needed with very low input and output damping, steep slope and low noise resistance. The socalled acorn pentode satisfies the first requirement but fails to satisfy the last two. In order to satisfy these last requirements electrode systems with larger dimensions must be used. At frequencies above 10^8 cycles/sec., however, such systems possess too great input and output damping. It is shown in this article that the imput and output damping of such systems can be considerably lowered by connecting two systems in a push-pull circuit in a suitable way. After an explanation of the construction and properties of the push-pull amplifier valve EFF 50 developed on this principle, the possibilities of its employment are dealt with. In particular a discussion is given of the results which can be obtained upon application of this valve in amplifying and mixing stages.

Methods of measurement have been developed in this laboratory in recent years by which currents, voltages and impedances at very high frequencies (up to about $1.5 \cdot 10^9$ c/s. corresponding to a wave length of 20 cm) can be accurately determined. These measurements have in the first place been applied to electronic valves in order to investigate the behaviour of these valves in detail [1]). On the basis of the insight obtained, new valves have been developed which give better results at very high frequencies than those used until now. After an explanation of the limitations in the application of the existing electron valves the construction and properties of one of these new types of valves, namely the push-pull amplifier valve EFF 50, is discussed in detail.

The function of an electron valve

The electron valve serves in general to amplify the incoming signal and to transmit it in some form or other to the following stage. In the case of a high-frequency amplifier, for instance, the requirement is that the character of the voltage transmitted shall be a faithful enlarged image of the incoming voltage within a certain frequency region. In the case of a mixing stage, on the other hand, it is desired that the modulation of the transmitted voltage shall have the same character as the modulation of the input voltage, while the character of the voltage itself is quite different; the latter has, namely, a much lower frequency than the input signal.

In addition to the quantitative requirement of a satisfactory enlargement of the amplitudes, there is the qualitative requirement that the desired relation between output voltage and input voltage shall be realized as fully as possible. According to whether the amplitude of the input voltage is very large or very small, two kinds of deviations may here occur. At very great amplitudes due to the curvature of the valve characteristics, the relation between input and output voltage, or between input and output modulation, deviates from true proportionality, or, in other words, distortion occurs. The relation is thus indeed unambiguous, but does not have the desired form. At very small amplitudes the reserve is true: the above mentioned distortion does not occur, but the relation between input and output voltage is no longer absolutely sharp: with a fixed input voltage the output voltage may still exhibit certain fluctuations, which are caused by incidental phenomena in the valve. If these fluctuations are of the same order of magnitude as the signal voltage obtained at the output, there can no longer be the least question of a relation between input and output voltage. These fluctuations, which are usually called noise, thus set a lower limit to the input voltage at which the valve can be used [2]). Since this limit is found to be of essential significance for the usefulness of a receiving installation, we arrive at the conclusion that, as far as the function of an electronic valve is concerned, *the valve must amplify as much as possible and give as little noise as possible.*

In the following we shall see how far valves of ordinary construction are capable of fulfilling this function.

Specification of the requirements made of electronic valves

The amplification of an electronic valve can be expressed quantitatively by four quantities which connect the output voltage and current with the input voltage and current. This is done by

[1]) M. J. O. Strutt: Moderne Kurzwellen-Empfangstechnik, Verlag Springer 1939; Moderne Mehrgitter-Elektronenröhren, 2nd edition, Verlag Springer 1940.

[2]) The factors which determine the noise of a receiving set were dealt with in detail in a previous article (M. Ziegler, Philips techn. Rev. 3, 189, 1938).

means of the equations:

$$\left.\begin{aligned} i_a &= A\,v_g + B\,v_a \\ i_g &= C\,v_g + D\,v_a \end{aligned}\right\} \quad \ldots\ldots\ldots \quad (1)$$

which have been given and discussed previously in this periodical [3]). A, B, C and D are in general complex quantities depending upon the frequency: they are called the characteristic admittances of an amplifier valve. The admittance A is nothing other than the slope of the valve, B is the output admittance, C the input admittance and D the reaction admittance. If the admittances are known, the amplifying properties of the valve can be calculated in every connection. The noise properties are however not given thereby, and must be considered separately.

The most efficient way of characterizing the noise of an electronic valve is by the introduction of the concept of noise resistance. The definition of noise resistance is based upon the fact that a "noise voltage" appears in every resistance, *i.e.* that at its extremities certain voltage fluctuations occur due to the thermal motion of the electrons in the interior of the resistance. In effective magnitude these fluctuations are proportional to the square root of the resistance value and the temperature. By the noise resistance R of an electronic valve is understood that resistance whose voltage fluctuations (at room temperature) are of the same magnitude as those voltage fluctuations which would have to be introduced between grid and cathode of an electronic valve in order to cause the anode current to fluctuate as much as actually occurs due to the noise of the valve.

If we now return to the function of the electronic valve, it may be seen immediately from the above that it is desirable to make the slope A as steep as possible and the noise resistance R as small as possible. In order to understand the influence of the output admittance B and the input admittance C, we must consider the connection in which the valve is used. From equation (1), however, it follows immediately that the real parts of these admittances give rise to energy losses at the output and input ends, which is undesired in principle, so that it is important to make these admittances as small as possible.

Special cases

We shall confine ourselves here to the special case of high-frequency amplification, making a distinction between

1) the high-frequency amplifier stage of a cascade amplifier (two identical stages following one another), and
2) the high-frequency amplifier stage of a superheterodyne receiver (which is followed by a mixing stage).

We may begin by dealing with both together with reference to the scheme represented in *fig. 1*. The input and output circuits are formed by tuned oscillation circuits with the impedances Z_1 and Z_2. In parallel with Z_1 is the input impedance $1/C_1$. In parallel with Z_2 is the output impedance $1/B$ and, *via* the transformer T, the input impedance $1/C_2$ of the following stage. Although $1/Z_1$, $1/Z_2$, C_1, B and C_2 are in general complex, we shall in the following always confine ourselves to the real parts, since by correct tuning of the circuits the imaginary parts can always be made to compensate each other.

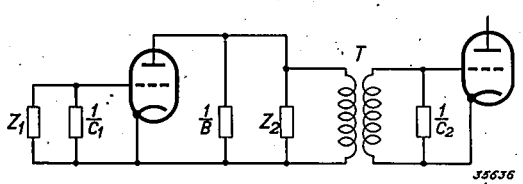

Fig. 1. Diagrammatic representation of a high-frequency amplifier stage connected to a second stage *via* a transformer T. Z_1 and Z_2 are the impedances of the input and output circuits, respectively, of the first stage; C_1 and C_2 are the input admittances of the first and second amplifier valves, respectively, B is the output admittance of the first amplifier valve.

If the amplification, *i.e.* the relation between the output voltage E_u and the input voltage E_i of the given circuit, is calculated for a transformation ratio n, one finds:

$$\frac{E_u}{E_i} = \frac{A\,n}{n^2 C_2 + \dfrac{1}{Z_2} + B}.$$

This expression as a function of n has a maximum for $n^2 = (B + 1/Z_2)/C_2$, and the maximum amplification amounts to:

$$\frac{E_u}{E_i} = \frac{A}{2\sqrt{\left(B + \dfrac{1}{Z_2}\right) C_2}} \quad \ldots\ldots \quad (2)$$

It is often possible to make $Z_2 \gg 1/B$. On this condition:

$$\frac{E_u}{E_i} = \frac{A}{2\sqrt{BC_2}}.$$

If $2\sqrt{BC} > A$, the ratio E_u/E_i becomes less than unity, and there is therefore no longer any ampli-

3) See in this connection the article by M. J. O. Strutt, and A. van der Ziel, Philips techn. Rev. 3, 103, 1938.

fication possible. If a given amplification is desired, for instance by a factor v, the condition

$$\sqrt{BC_2} < A/2\,v \quad \ldots\ldots \quad (3);$$

holds for the input and output admittances, and it may therefore be seen that the two admittances may not exceed a certain magnitude.

As to the noise, it is more difficult to reach a numerical formulation of the requirements made. These requirements depend of course entirely upon the intensity of the available input signal. We may, however, state that a decrease in the noise of electronic valves is only of importance as long as this disturbance is not weak compared with the noise due to other sources. Besides the electronic valves it may be seen in the figure that there are other sources of noise, namely the impedances Z_1, $1/C_1$, $1/B$, Z_2 and $1/C_2$.

Let us first consider the noise from the first amplifier valve and the first oscillation circuit. In fig. 1 we see that between grid and cathode of the first valve the impedances Z_1 and $1/C_1$ are in parallel with each other, thus at the same spot as the imaginary noise resistance R. From this it follows that the noise from this noise resistance R must be small compared with the noise of the two impedances Z_1 and $1/C_1$ connected in parallel. If this condition is satisfied, the contribution of the first valve to the noise is small compared to that of the other sources of noise mentioned. This requirement thus indicates an upper limit for the noise resistance R. If we now consider first the case where $1/C_1$ is large compared with Z_1 our requirement amounts to

$$R \ll Z_1.$$

When, however, Z_1 is large compared with $1/C_1$ one would expect as condition

$$R \ll \frac{1}{C_1}$$

From a more detailed consideration it is found that in the last condition C_1 must be replaced by C_e, *i.e.* by that part of the input admittance which is due to the transit time of the electrons. The calculation, which we shall not reproduce here, shows that the product RC_e is a measure of the maximum value of the ratio between signal voltage and noise voltage which can be obtained by adapting the first stage to a given aerial. The larger this product, the less useful the valve.

Until now we have given the requirements for making the noise due to the first valve as small as possible compared with the noise from the input circuit. If we now make the requirement that the noise properties so obtained shall suffer as little disadvantage as possible from the following stages, it is found that a lower limit must be set to the amplification of the first stage. We must now make a distinction between the cases (1) and (2) mentioned above.

In case 1) (cascade amplification) the input resistance and noise resistance of the second valve are about as large as those of the first valve, the same is thus true of the fluctuations which occur in the second stage.

When we represent the total fluctuations of valve plus circuit of each stage by a noise resistance R_t, the noise resistance which, connected to the input of the first stage, represents the noise of both stages together, amounts to:

$$R_t + \frac{R_t}{v^2},$$

where v is the amplification. If v has the value 3, for example, the total noise resistance at the input of the first stage becomes only about 10 per cent greater due to the presence of the second stage, and the equivalent voltage fluctuations become only 5 per cent greater, since these fluctuations are proportional to the square root of the noise resistance. In cascade amplification, therefore, an amplification of 3 must be considered as sufficient in connection with the noise.

In the case of a mixing valve in the second stage, the total noise resistance of this stage is generally considerably greater than with a high-frequency amplifier valve in the second stage, for instance, a factor 10 greater. If the requirement is again made that the influence of the second stage on the noise shall be appreciably less than that of the first stage, the amplification must be made considerably higher, 5 to 10 times instead of 3 times.

Limitations of electronic valves at high frequencies

In the foregoing we have stated the requirements which must be met by the admittances of an electronic valve if it is to fulfil its function. Passing on to higher frequencies it becomes more and more difficult to fulfil this requirement.

As has been explained in detail in the article quoted about the behaviour of electronic valves, while the slope A remains unchanged, at least in absolute value, up to very high frequencies, both the input and the output admittances (we refer always to the real parts) increase steadily with increasing frequency, usually proportional to the square of the frequency. The result is that the left-hand side of equation (3) becomes steadily

larger with increasing frequency, so that the equation no longer holds for valves of ordinary construction for frequencies above about 10^8 cycles/sec.

The cause of the undesired increase in input and output admittance lies, as explained in the article referred to, in two phenomena:

1) the finite transit time of the electrons between the electrodes in the valve;
2) the self-inductions and mutual inductions of the connecting wires of the various electrodes.

If it is desired to keep the input and output admittances small at high frequencies, therefore, it is necessary to combat these two phenomena.

The acorn pentode

A very obvious method of decreasing the inductive effects and the transit times is to diminish the dimensions of the valve. The result of the technical development which took place in this direction several years ago is the so-called acorn pentode, whose admittances are given in *fig. 2* as functions of the frequency.

The acorn pentode may be used for amplification purposes up to about 2×10^8 c/s. (1.5 m). At this frequency the input admittance C is 1/4 000 Ω, the output admittance B = 1/10 000 Ω and the slope A = 1.4 mA/V. With the help of equation (3) it may be calculated that at this frequency an amplification is possible by a factor

$$v = A/2\sqrt{BC} = 4.6.$$

If, in agreement with experience, it is assumed that the admittances increase with the square of the frequency, then for the case of cascade amplification ($v = 3$) an upper limit of about $2.5 \cdot 10^8$ c/s. (1.2 m) can be calculated.

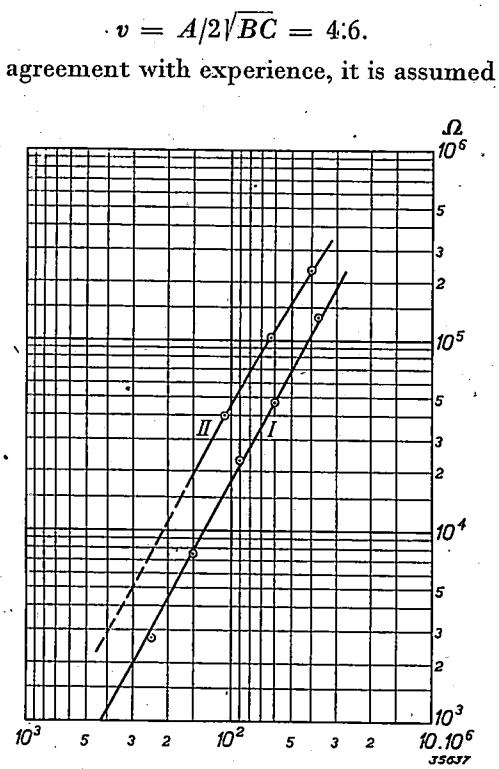

Fig. 2. Input resistance (curve *I*) and output resistance (curve *II*) of the acorn pentode 4 672 as function of the frequency in c/s.

The noise resistance of the acorn pentode amounts to about 8 000 ohms [4]). The product RC_e at $2 \cdot 10^8$ c/s is thus about 2, which may be considered tolerable. With increasing frequency, however, this product rapidly increases, so that as far as noise is concerned the application of the acorn pentode is subject to about the same limitations as set by the amplification.

A further reduction of the dimensions of the valve, which theoretically would mean an improvement, is at present not yet possible technically. Moreover it is very much a question whether the expected improvement would be realized. It is essential that the decrease in size of the valve should not result in a decrease in steepness of slope. Theoretically this requirement could be fulfilled, since the slope is entirely determined by the relations between the dimensions. Actually, however, there are a number of effects which, with decreasing dimensions, have an unfavorable influence upon the slope of a valve, so that the ratio $A/\sqrt{BC}$ will increase little or perhaps not at all upon further reduction of the dimensions. In the present position of technology the acorn pentode must be considered as the most satisfactory compromise as far as the dimensions of the valve are concerned, so that it will not be possible to develop a valve in this direction which is suitable for the amplification of higher frequencies than $2 \cdot 10^8$ c/s.

On the principles discussed above we shall now point out a new line of development which will carry us farther than the line employed until now of decreasing all the dimensions.

A new type of high-frequency amplifier valve

As we have seen, for frequencies higher than 2×10^8 c/s, 1.5 m) it is desirable to have a valve with a steeper slope and a lower noise resistance than the acorn pentode. Valves with steep slope can be constructed by applying various devices. One of these is the enlargement of the surface of the cathode while keeping the distance between the electrodes in the valve constant. This method is analogous to the connection in parallel of a number of elec-

[4]) It must be noted here that the noise of a valve is actually somewhat stronger than is indicated by the above-mentioned noise resistance. With the high frequencies in question the intensity of the noise of the valve is a function of the impedance between grid and cathode. The above-mentioned value of 8 000 Ω holds for a very small value of this impedance.

trode systems. It therefore also leads to a decrease in input and output resistance so that no advantage is gained. When this method is eliminated there remains as second possibility the method used in the acorn pentode, namely by decreasing the distance between control grid and cathode, using at the same time a thinner grid wire and a lower pitch. In this case the input and output resistance need not become smaller. Starting with electronic valves of ordinary construction we have applied this second device. The distance between grid and cathode was reduced to 90 μ, and the slope thereby obtained amounts in the normal adjustment of the valve to 11 mA/V at an anode current of 10 mA.

An increase on the slope of a valve involves automatically a lowering of the noise resistance. The greater the slope the smaller the amplitude of the grid A.C. voltage necessary to cause a given fluctuation of the current. In the construction of the new high-frequency amplifier valve, however, an attempt was made to combat noise even more fully by decreasing the noise A.C. itself. This could be done be keeping the screen grid current low.

The fluctuations of the anode current in a pentode are caused partly by the fact that the electron current emitted by the cathode itself fluctuates, and for an important part also they are caused by the fluctuations of the current distribution between screen grid and anode [5]). The latter fluctuations may be kept small by providing that the screen grid current itself amount to only a small percentage of the total cathode current. In this respect an improvement was obtained in the construction in question by taking thinner screen grid wires and making the pitch of the screen grid greater than is usual in ordinary high-frequency amplifier valves. This has indeed as result that the screen grid fulfils its shielding function less effectively, but it is just the amplification at very high frequencies which is found to suffer no serious disadvantage from this.

The screen grid has the function of shielding the anode from the control, in order that a change in the anode voltage may have no influence on the anode current (high output resistance) and on the control grid voltage (small reaction).

In a valve of ordinary construction the output resistance is of the order of 10^6 Ω at low frequencies. No advantage could be taken of such a high output resistance in the case of the amplification of very high frequencies, since the resistance of the tuned circuits connected in parallel amounts only to several thousand Ω. As to the static output resistance, therefore, there is no objection to making the shielding between control grid and anode less effective than is usual in valves intended for lower frequencies.

The same result is reached as far as reaction is concerned. The reaction can be described by a capacity C_{ag} between control grid and anode, and is kept as small as possible by the screen grid. At high frequencies, however, the reaction is found to be caused to a large extent, not by the capacity between control grid and anode, but by the mutual capacities, self-inductions and mutual inductions of the various connections of the electrodes. The effect of this additional source has in many cases a greater absolute value and a sign opposite to that of the effect of the capacity C_{ag}. In these cases an increase of C_{ag} is immediately permissible and it even leads to a decrease in the total reaction.

By the decrease of the screen grid current, together with the increase in the slope, the noise resistance was reduced to 600 Ω, thus to about 1/13 of the value of the noise resistance of the acorn pentode. For the smallest input voltage to be amplified, which is proportional to the square root of the noise resistance, this means a gain by a factor 3.5.

As to the amplification, the improvement is even more important compared with the acorn pentode. The slope has increased from 1.4 to 11, thus by a factor 8, and when unput and output impedance are kept constant the same is true of the amplification.

The performance at high frequencies with the above-described construction is, however, not to be considered satisfactory. While the influence of the transit times will indeed be only relatively slight thanks to the short distance between control grid and anode, the inductive and capacitive effects of the connection wires are no smaller than in ordinary electronic valves, and these may have the well-known damping effect on the input and output circuit.

It has been found by measurements and calculations that this damping in the case of valves with steep slopes is mainly due to inductive effects of the cathode connections (inside and outside the valve) and is proportional to the slope. Since we are here concerned with a valve of very steep slope it is therefore necessary to combat the influence of the inductive effects of the cathode connections.

The push-pull amplifier valve EFF 50

The elimination of the inductive effects of the cathode connections is found to be possible by a special application of the push-pull principle. Two identical electrode systems fused together into a single bulb are provided as shown in *fig. 3a* with a common cathode connection. The voltage biases of

[5]) See in this connection the article by M. Ziegler, Philips techn. Rev. 2, 329, 1937. In that article the phenomena which give rise to the noise in receiving valves are discussed in detail. From the discussion given the following formula can be derived for the noise resistance of a pentode:

$$R = \frac{4\,000}{S_a}\left[1 + 5\,\frac{I_{g2}}{S_a}\left(\frac{I_a}{I_{g2} + I_a}\right)\right]\ \Omega,$$

where the value of the slope S_a must be substituted in mA/V and the anode current I_a and the screen grid current I_{g2} in mA.

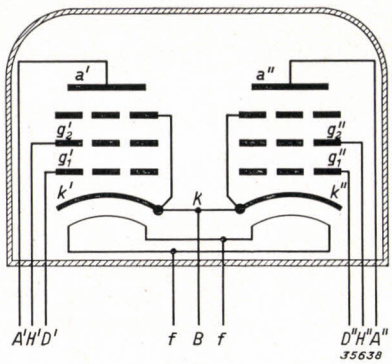

Fig. 3 a) Diagram of the electrode arrangement of the push-pull amplifier valve EFF 50. Two identical pentode systems with a common cathode connection B_k and indirect heating (ff) are mounted in an all-glass bulb.

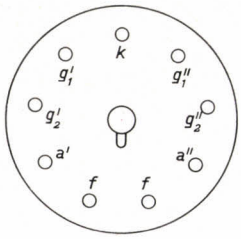

b) Arrangement of the electrode pins in the base of the push-pull amplifier valve EFF 50.

corresponding electrodes are chosen equal, while the A.C. voltage of the control grid is supplied in opposite phase to the two halves of the system. The anode A.C.'s of the two halves of the system will then exactly cancel each other in part B^k of the cathode connection, so that inductive effects can only occur in the section $k'kk''$ of the cathode connection, which can be kept very short.

The input voltage acts over the terminals $D'D''$; the resistance between these terminals may therefore be considered the input resistance. The input resistance is obviously twice as high as that of a single system. Moreover, due to the employment of the push-pull principle by which the connection wire B^k is rendered ineffective, the input resistance of each separate system is increased by a factor of about 2.5, so that a total increase of the input resistance by a factor 5 is obtained. The remaining part of the input damping must be ascribed chiefly to the transit time of the electrons between cathode and control grid. The output resistance between A' and A'', which is affected to a smaller degree by the transit times of the electrons, amounts to even more than five times that of a single valve; it amounts, for instance, to ten times.

Another advantage of the push-pull principle is that the input and output capacities of the whole valve amount to only half of the capacities of each system separately, which makes these capacities not appreciably greater than in the acorn pentode.

Construction of the push-pull valve

A form has been chosen for the construction of the push-pull valve which is also used for modern receiving valves for ordinary broadcasting wave lengths, namely the so-called all-glass construction which has previously been described in this periodical [6]). This may be seen in *fig. 4* together with several developmental models of different construction.

[6]) See the article: A new principle of construction for radio valves, Philips techn. Rev. **4**, 162, 1939.

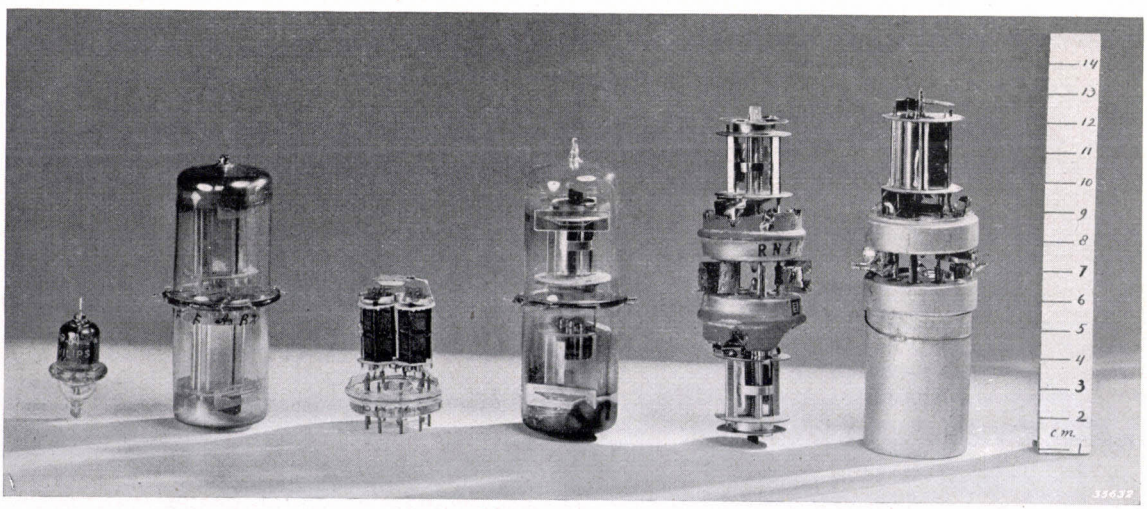

Fig. 4. Acorn pentode 4 672 (left) and a number of developmental models of the push-pull amplifier valve EFF 50. In the case of the first four of these models (second, fourth, fifth and sixth from the left) the systems are assembled end to end; in the final model (third from left) the systems are side by side. The two systems are surrounded not only by a glass bulb, but also by a common gauze cage which has been removed in order to show the assembly to better advantage. To the right a centimetre scale.

The connecting leads of the electrodes in the all-glass construction are all led out through a flat base plate. As may be seen in fig. 3*a* the push-pull valve has nine connections, the arrangement of the nine pins in the base is shown in fig. 3*b*.

The connecting pins which are fused into the glass base are often made of chrome-iron for reasons connected with glass technology. Due to the high magnetic permeability of this material considerable skin effect occurs at frequencies of the order of 10^8 c/s and higher, so that the resistance at these frequencies becomes several hundred times the resistance for direct current. A decrease of the resistance can be obtained by covering the surface of the pins with a non-magnetic material, such as copper or silver.

It is important to keep the resistance of the pins low, because this resistance contributes to the input and output damping. If, for example, we consider the input end, the admittance between the connecting pins is given by the substitution scheme sketched in *fig. 5*, where r_s represents the resistances and L_s the self-inductions of the grid connections, while C_{kg} stands for the capacity between control grid and cathode in each system. The real part of the admittance of this circuit is:

$$\frac{1}{R_p} = \frac{r_s \omega^2 C_{kg}^2}{2\,(1-\omega^2 L_s C_{kg})^2}$$

and thus gives rise to a damping which is proportional to r_s and to the square of the frequency (r_s also increases with the frequency and is approximately proportional to $\sqrt{\omega}$).

Measurements carried out on valves with pins of copper-covered wire indicated that R_p was still larger than 10 000 Ω at a frequency of 3×10^8 c/s.

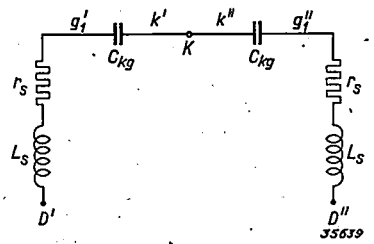

Fig. 5. Substitution diagram for the admittance between the connection terminals of the two control grids.

Application of the push-pull amplifier valve for high-frequency amplification

In the application of the push-pull valve for the amplification of high-frequency signals, various cases can be distinguished, such as the amplification of a carrier wave with a very broad modulation band (television) and the amplification of a carrier wave modulated with sound. Although the new push-pull valve also offers certain advantages for the first mentioned application, we shall confine ourselves to the second, which is at the moment the most important in the wave region below 2 m.

In *fig. 6* a diagram is given showing the principle of the amplifier. The input signal is induced in the coil S_p of a tuned oscillation circuit, whose extremities are connected to the grid connection pins D' and D'' of the push-pull valve [7]). The condenser C_1 we shall for the time being leave out of consideration, as well as several other components whose functions will be discussed later.

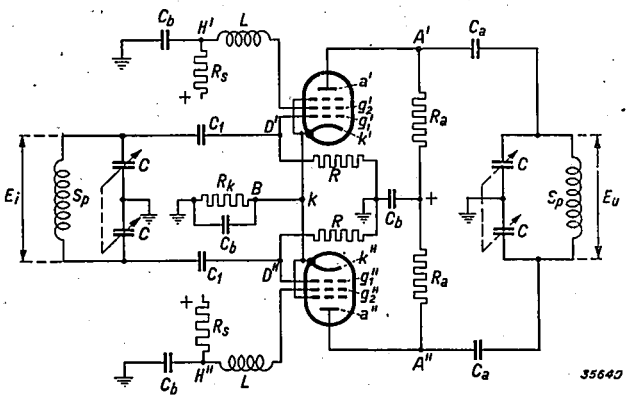

Fig. 6. Connections of a high-frequency amplifier with push-pull valve. The input voltage is applied to the two control grids in opposite phase; the output voltage is taken off from the two anodes in opposite phase. The self-inductions L serve to diminish the input damping, while by a suitable choice of the condenser C_1 and C_a the amplification E_u/E_i can be affected. S_p self-induction, with C, C tuned to the frequency of the A.C. voltage to be amplified; R_k cathode resistance, bridged by a block condenser C_b in order to obtain a negative control grid voltage; R grid leakage resistance; R_s supply resistances for the screen grids; R_a supply resistances for the anodes.

The D.C. voltages for the screen grids and anodes are taken from a positive voltage source via the resistances R_s and R_a, respectively. The anode A.C. passes, via the anode terminals A' and A'', to the tuned output circuit giving the output voltage E_u on the latter.

If S is the slope of the valve, the following formula is found for the amplification of the stage:

$$\frac{E_u}{E_i} = {}^1/_2\, S Z_u \quad \ldots\ldots\ldots \quad (4),$$

where Z_u is the impedance between the anodes. The value of Z_u depends upon the output impedance of the push-pull amplifier valve, upon the impedance of the oscillation circuit $Sp\ C\ C$ and on the input impedance of the next stage in the circuit. Here again we must make a distinction between cascade amplification and superheterodyne amplification.

If in the case of cascade amplification we go as far as frequencies higher than $3 \cdot 10^8$ c/s. the

[7]) The input circuit S_pCC may be considered as a symbol for some kind of aerial circuit, for instance for a dipole combined with a transmission line of suitable length. In any case it is advisable to employ a connection which is symmetrical with respect to earth. By this means it is possible with the help of a dipole to obtain an input voltage twice as great as in the ordinary input connection which is earthed at one end, and where often therefore only half of a dipole can be employed.

imput impedance of the following stage becomes so low, even with a valve of the type EFF 50, that it is a serious obstacle to obtaining satisfactory amplification. It is found, however, that this damping can be eliminated to a large extent by including a self-induction in the screen connection. The A.C. voltage of the screen grid thereby generated produces, via the capacity between screen grid and control grid, a current in the control grid circuit which is opposite in phase to the control grid voltage, so that the real part of the input admittance is reduced [8]).

When the second stage is a mixing stage, care must also be taken that its input admittance is sufficiently high. Two diodes in push-pull connection

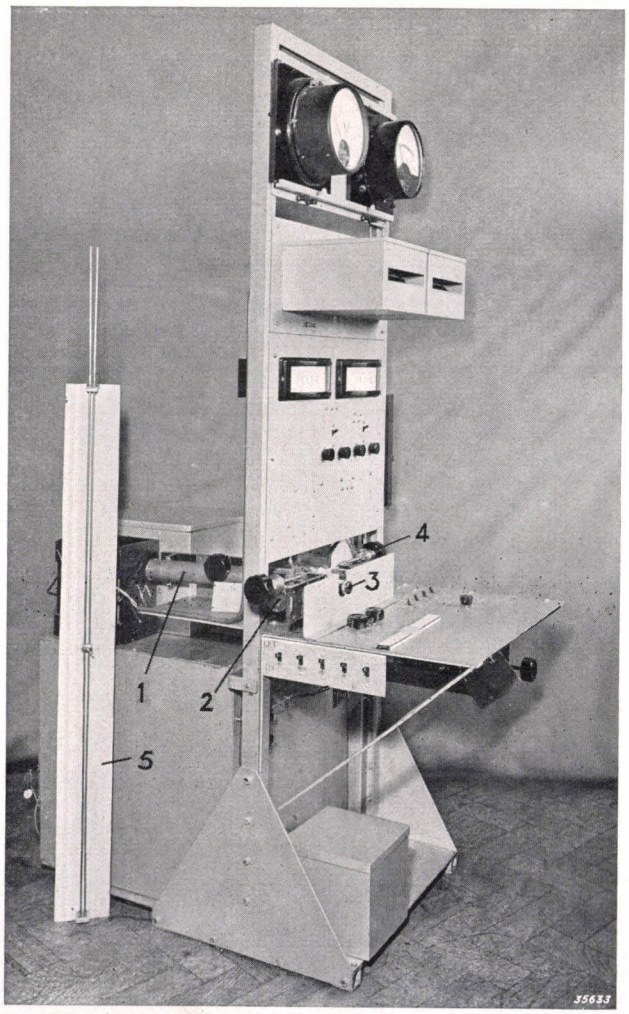

Fig. 7. Installation for the measurement of input and output admittance as well as amplification of push-pull valves at frequencies up to $6 \cdot 10^8$ c/s (50 cm). The meters at the top indicate the control grid voltages and the anode and screen grid currents. Underneath are two micro-ammeters, belonging to the diode voltmeters for the input A.C. voltages of the two control grids with respect to the cathode; below these, two similar micro-ammeters for the output end. *1* oscillator, *2* tunable input circuit consisting of two Lecher conductors with earthed covering; *3* valve to be measured; *4* tunable output circuit, *5* wave meter.

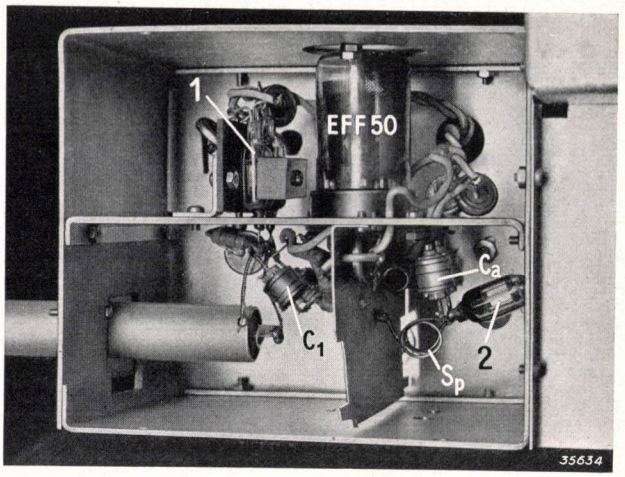

Fig. 8. Simple arrangement for the measurement of the amplification of push-pull valves in a circuit according to fig. 6 at a frequency of $3 \cdot 10^8$ c/s. *1* diodes for the measurement of the input A.C. voltage. *2* diodes for the measurement of the output A.C. voltage. The other symbols in the figure correspond to those of fig. 6.

may for instance be used as mixing stage, or one EFF 50 in a connection which will shortly be discussed. In both cases at a frequency of 3×10^8 c/s. a value of Z_u of about 3 000 Ω can be obtained. Since at this frequency the slope corresponds approximately to its static value of 11 mA/V, the amplification $v = {}^1/_2 \times 11 \times 10^{-3} \times 3\,000 = 16.5$.

In testing this result experimentally a complication occurred which we shall discuss in detail, because it involves a point which may also be important in the practical application of the valve. If we consider fig. 6 we see that the input voltage as well as the output voltage is measured at the extremities of a coil. In the above calculation we have assumed that these voltages correspond to the voltages between the control grids g_1', g_1'' and between the anodes $a'a''$, respectively. For frequencies like those in question this is, however, not true, since the connecting wires of the coil to the grids (or anodes) possess considerable self-induction. This has already been pointed out in the discussion of the influence which the resistance of the grid connection pins has on the input damping, and we may use the substitute circuit, fig. 5, there derived in order to calculate the relation between the voltage E_i across the coil and the true input voltage E_i' between the control grids. If the series resistance r_s

[8]) In principle the application of this method is not limited to the push-pull amplifier valve, but offers a possibility of eliminating the input damping in the case of any amplifier valve. In practice, however, this method has the objection for most valves that the self-induction needed for a satisfactory lowering of the input damping is 20 to 30 times as great as with the push-pull valve EFF 50. Self-inductions of this order of magnitude, at the frequencies of decimetre waves, exhibit resonance phenomena which give rise to undesired effects.

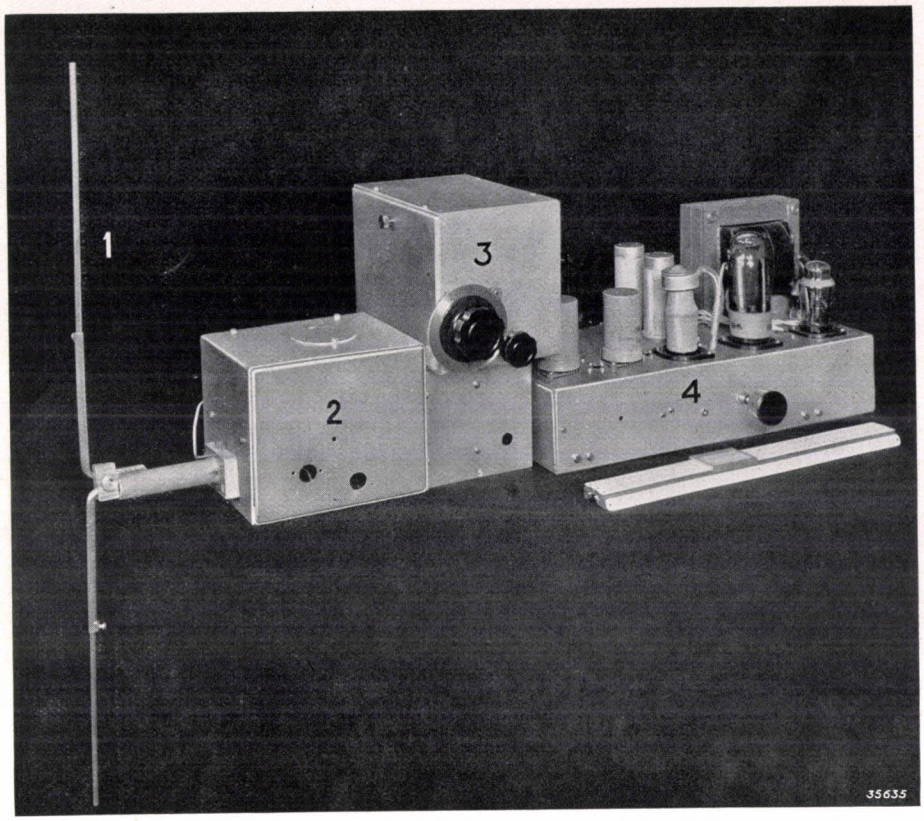

Fig. 9. Complete receiver for signals with a frequency of about $3 \cdot 10^8$ c/s. *1* dipole aerial; *2* box containing the circuit of fig. 6; *3* mixing stage; *4* intermediate and low-frequency part. To give some idea of the dimensions a slide rule about 25 cm long may be seen to the right.

is hereby neglected, we find for sufficiently large values of C_1:

$$\frac{E_i}{E_{i'}} = 1 - \omega^2 L_s C_{kg}$$

and an analogous relation holds for the output end. It may be seen that the voltage at the extremities of the coil is in general smaller than the voltage between the electrodes.

As to the measurement of the amplification, the condensers C_1 and C_a were so chosen that in the input as well in the output circuit, at the frequency for which the amplification was being investigated, series resonance occurred between these capacities and the self-inductions of the connecting wires (about $4 \cdot 10^{-8}$ henries), so that the total impedance of the connection between the coil and the electrodes is zero. In that case E_i and E_u corresponds to the actual input and output voltages, respectively, so that equation (4) can be tested. The measurements were carried out with the help of apparatus especially developed for that purpose (see *figs. 7, 8* and *9* with the text under the figures), and gave the theoretically expected results at frequencies of $3 \cdot 10^8$ c/s. It may be concluded from this that, within the limits of the experimental error, which may be taken as about 5%, the slope of the valve does not change up to frequencies of $3 \cdot 10^8$ c/s. As stated, at a frequency of $3 \cdot 10^8$ c/s, an amplification by a factor 16.5 is obtained when an output circuit with an impedance of 3 000 Ω is used. At a frequency of $5 \cdot 10^8$ c/s (60 cm wave length) the amplification might still amount to 8 under certain circumstances. These figures, which by no means represent an upper limit since impedances higher than 3 000 Ω can also be realized, are appreciably larger than what can be attained with the help of the acorn pentode.

As for noise also, the push-pull amplifier valve is appreciably better than the acorn pentode. At a frequency of $3 \cdot 10^8$ c/s the electron part of the input admittance for the push-pull amplifier valve is $C_e = 1/600\ \Omega^{-1}$, while the noise resistance $R = 1\,200\ \Omega$, both values calculated between g_1' and g_1'' (see figs. *3a* and *6*). The acorn pentode, on the other hand, has at the same frequency an input admittance of $1/2\,000\ \Omega^{-1}$, almost entirely due to the transit times of the electrons, and a noise resistance of 8 000 Ω. The product RC_e, which, as already mentioned, determines the noise prop-

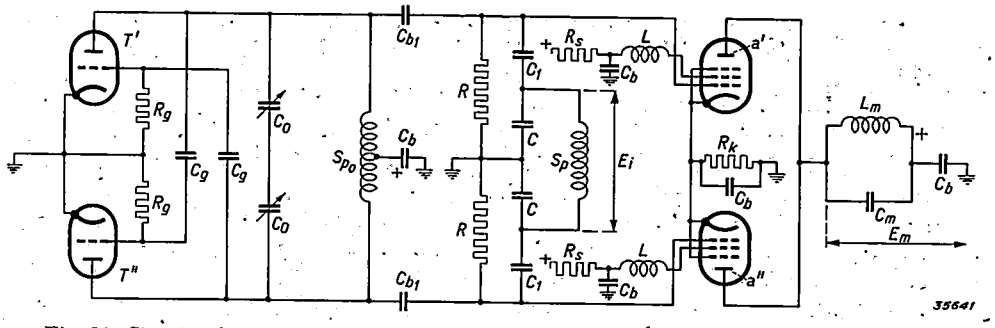

Fig. 10. Circuit of a mixing stage with the help of the push-pull amplifier valve EFF 50. The input voltage E_i is applied to the two control grids in opposite phase. The same is done via the small capacities C_{b_1} with the oscillator voltage generated by the triodes T' and T''. The necessary oscillator voltage is of the order of 1 V, while the necessary negative bias is 2 V higher than the oscillator voltage. The intermediate-frequency output voltage E_m is taken from the two anodes in the same phase with the help of the intermediate frequency circuit L_mC_m . R_g grid leakage resistances of the triodes; C_g grid condensers of the triodes; $C_0C_0Sp_0$ oscillator circuit. The other symbols correspond to those of fig. 6.

erties of a valve [9]), therefore, in the case of the acorn pentode, in spite of its lower input admittance, is twice as unfavourable as in the case of the push-pull amplifier valve.

For the practical application of the push-pull amplifier valve it is very important to know whether or not any slight differences between the two halves of the valve which may occur during manufacture, are detrimental to the performance of the whole valve. This was investigated experimentally with the help of the measuring arrangement shown above. It was found that large differences in the anode currents (for instance 5 mA in one half and 15 mA in the other) cause the amplification, the input resistance and the output resistance to change by several per cent at the most.

This good performance may also be explained theoretically. Since at the high frequencies of decimetre waves the capacitive impedances between cathode, control grid and anode are small compared with the internal resistance of the valve, the anode A.C. in the two halves of the system will be exactly in opposite phase, if care is only taken that the external impedance of both systems with respect to earth is the same, and that the anode A.C. voltage varies exactly in opposite phase in the two systems. Both conditions can be satisfied by providing that the two halves of the coil S_p (fig. 6) are sufficiently strongly coupled with each other.

Although slight asymmetries have little unfavourable effect on the amplification of the valve, it remains nevertheless undesirable that one half of the valve should give much more direct current than the other half. This can be prevented by a suitable choice of the supply resistances of each of the screen grids (see fig. 6).

[9]) As we have seen the input resistance can be made very large by the introduction of a self-induction in the screen grid connection, and at first glance it might be supposed that a favourable influence might be exerted hereby on the ratio between signal and noise. This is found, however, not to be the case. Closer investigation shows that the ratio between signal voltage and noise voltage does not become better by the application of this device.

Application of the push-pull amplifier valve in mixing stages

In receiving sets it is also possible to use the valve EFF 50 as a mixing valve. Several different connections have been tried out for this purpose. One of these is shown in *fig. 10*. Several of the desirable properties of the valve, namely the slight noise resistance, the steep slope and the possibility of obtaining a high input resistance are also useful in this application. With the scheme of fig. 10, with suitably chosen voltages for each half of the valve, a so-called conversion slope of 2.8 mA/V can be obtained. This conversion slope indicates the ratio between the amplitude of the intermediate-frequency signal in the anode current and the amplitude of the high-frequency signal on the control grid. The amplification (intermediate-frequency output voltage divided by high-frequency input voltage) is, in the scheme shown, equal to the product of the conversion slope of one half of the valve and the impedance of the output circuit for the intermediate frequency used.

If the mixing stage is connected behind a high-frequency amplifier stage, it is desirable to make the input resistance of the mixing stage high by the use of self-inductions in the screen grid circuit, as was already explained.

The noise resistance of the push-pull amplifier valve when used in a mixing stage amounts to about 5 000 Ω between the input terminals, which may be considered unusually low. If the input resistance of the valve is increased to improve the amplification of the first stage, the noise of course also becomes stronger.

EXPERIMENTS WITH STEREOPHONIC RECORDS

by K. de BOER.

534.76:534.85

In the previously discussed method of stereophonic reproduction two channels must be available for the transmission. When such a reproduction is to be recorded in the form of "stereophonic records" two sound tracks must be traced on the gramophone record which can be scanned simultaneously by two pickups. In the arrangement for practical purposes, in addition to the differences in intensity and time which determine the position of the "sound image", there are additional time differences which result in a gradual or oscillating shift of the sound image. The measures and tolerances are discussed by which these shifts can be kept within the desired limits.

Introduction

In the method of stereophonic reproduction (reproduction which retains a sense of the positions of the various sources of sound), which was recently discussed in this periodical [1]), the sound is intercepted at two places in the recording room, conducted along two separate channels and reproduced in the receiving room at two places. The two microphones for the interception may for instance be placed on either side of a sphere ("artificial head"). The reproduction may take place either with two head phones or with two loud speakers which are set up in the manner indicated in *fig. 1*.

In the article mentioned we showed that with such an arrangement good stereophonic reproduction is possible. The practical consequences of the requirement that two channels (amplifiers + transmission lines) must be used we did not discuss there. According to the nature of the application of stereophonic reproduction, this requirement is accompanied by entirely different problems — different as to character and degree of importance. In the case of cinemas, one of the most important spheres of application for stereophonic reproduction, the creation of a second channel, which in this case would consist of a second sound-track on the film, will offer no fundamental difficulties. In broadcasting the problem is more difficult: two separate channels in the form of two transmitters working on different wave lengths for a single programme will hardly be found available. It may perhaps be found possible to use the side bands on either side of one carrier wave as separate channels. Another possibility of application which we should like to mention is in making an orchestra plastically audible in different rooms of a restaurant or the like at the same time. In this case for the second channel only an extra amplifier and 20 or 30 metres of cable are needed.

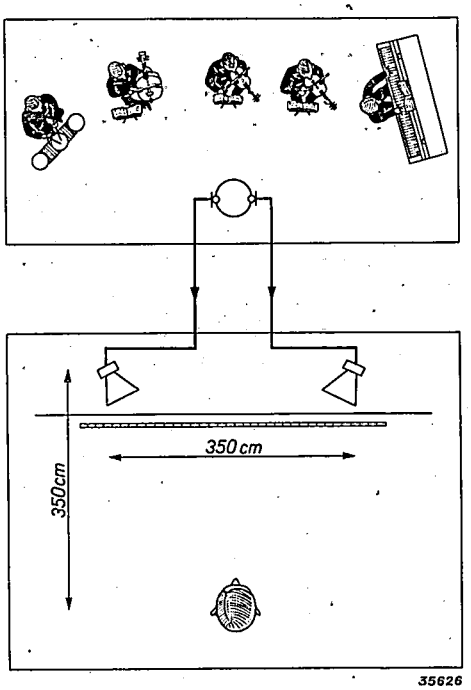

Fig. 1. Scheme of a stereophonic sound transmission. In the recording room (above) are two microphones on either side of a sphere ("artificial head"); two channels to the reproduction room (below); here two loud speakers at left and right in front of the listener. In our experiments the dimensions indicated were used as a rule. On the scale in front of the loud speakers the sound image can be definitely located to within a few centimeters.

For the purpose of experimenting with arrangements for stereophonic reproduction, as well as for its practical use in general, recorded stereophonic music and speech is needed. With this need in view, experiments have been carried out in this laboratory on the recording of stereophonic sound on gramophone records. In the case of such "stereophone records" each of the two contributions to the sound which the microphones receive must be recorded in a separate groove on the disc. One method would be to cut one track on each side of the disc, and upon reproduction to scan both sides simultaneously with two pickups. In order to make this possible the disc would have to be sufficiently stiff, and moreover this method would necessitate the development of entirely new gramophone mechanisms. A

[1]) Philips techn. Rev. 5, 107, 1940 (April).

simpler method is to divide the surface of the disc into two zones, the innermost of which contains one sound track and the outer the other. Such records can easily be made with the apparatus for sound recording [2]) described in this periodical, by mounting two sound track cutters side by side on the transport shaft. Each cutter is then fed from one of the microphones. In *fig. 2* this arrangement is shown.

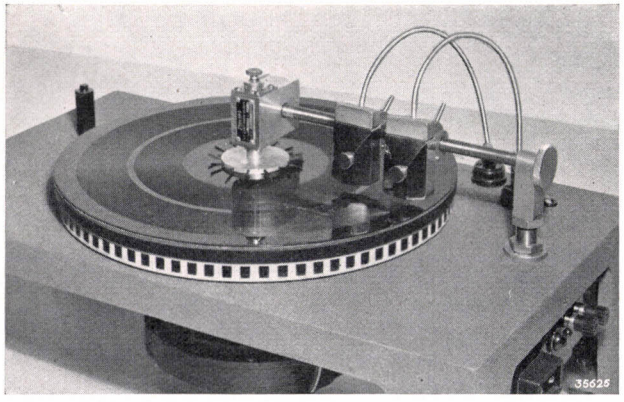

Fig. 2. Apparatus for sound recording on discs, designed for stereophonic recording. Two sound track cutters are mounted on the transport shaft, each of which is fed from one of the two microphones and which cut a sound track in the inner and outer zones, respectively, of the disc.

In the article already referred to [1]) it is explained that the perception of direction is based upon slight differences in the intensity and moments of arrival of the two sound contributions which are received by the two ears. These differences in intensity and time must be faithfully recorded in the two sound tracks on the sterephone record and must be reproduced upon playing the record with equal fidelity. Due to various causes extra time differences occur between the two sound contributions when the record is played, so that the position of the source of sound observed by the listener (the "sound image") experiences a displacement. It will perhaps be interesting to discuss in somewhat more detail the peculiar difficulties connected with this phenomenon, particularly because of the fact that they form a good illustration of the peculiarities of stereophonic reproduction.

Movement of the scanning needle

In recording, the sound cutter is moved by the transport shaft over the disc in a straight line which coincides with a radius of the disc [3]).

[2]) K. de Boer and A. Th. van Urk, A simple apparatus for sound recording, Philips techn. Rev. **4**, 106, 1939.

[3]) Actually, for practical reasons, the needle is made to move on a line which passes several mm away from the axis of the disc. The influence of this on the results in the following discussion may, however, be neglected.

In reproduction, on the other hand, the pickup is fastened to the end of a rotating arm and thus describes an arc of a circle on the disc. This is unavoidable if the lifetime of the disc is to be sufficiently long. In reproduction the spiral grooves of the sound track itself must furnish the guidance for the radial displacement of the needle point, and in order to limit wear and tear of the grooves it is desirable that they should need to exert only an extremely small force on the needle. Guidance of the needle in a straight line, either by means of a rail or one of the jointed constructions for this purpose, familiar in cinema technology, would, however, always be accompanied by fairly large forces of friction — when the play in the position of the pickup is limited to the required degree.

Due to the fact that in reproduction the needle describes a different path on the disc than in the recording, time differences occur. The arm of the pickup is adjusted for both sound tracks so that the needles stand exactly on the straight line of the recording at the beginning and end of the sound track; see *fig. 3*. It may be seen that during the

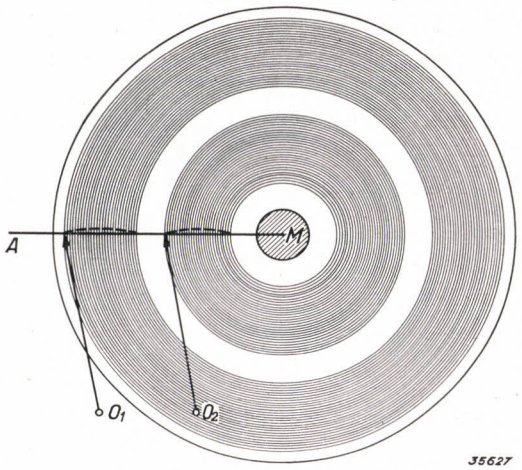

Fig. 3. Stereophone record with sound track in two zones. During recording the two needles moved along the straight line AM, upon reproduction they describe the two arcs of a circle around the pivots O_1 and O_2 of the pickup arms.

playing of the record the two sound contributions experience first a gradually increasing and then a decreasing retardation. This would cause no shift in the sound image if the retardation were equal for both sound contributions. This is, however, not the case, although the deviation of the needle is the same on both tracks (fig. 3), due to the difference in speed of the disc at different distances from the centre, the same time differences do not correspond to these equal deviations.

The relative time difference occurring in the two sound contributions can easily be calculated. In the

coordinate system x, y of *fig. 4*, we let the mean radius of the two zones equal L and l, respectively, the width of the zones $2d$ and the length of the arms on which the pick-ups are fastened P and p,

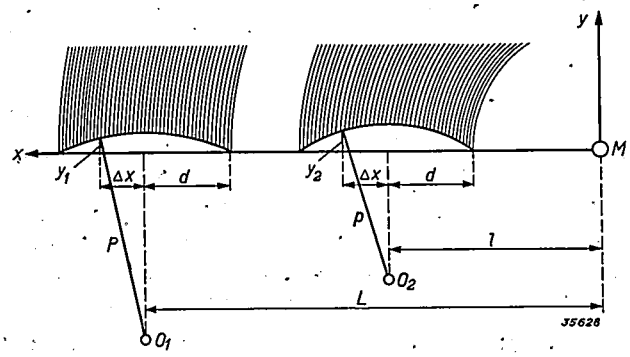

Fig. 4. Geometrical configuration of the paths of the needles in recording and reproduction for the calculation of the relative time differences occurring between the two sound contributions.

respectively. Between the shift Δx of the needle from the middle of the zone and its deviation y_1 or y_2 respectively from the straight recording line, the following relation exists:

$$\Delta x^2 + (y_1 + \sqrt{P^2 - d^2})^2 = P^2,$$
$$\Delta x^2 + (y_2 + \sqrt{p^2 - d^2})^2 = p^2.$$

For sufficiently large values of P and p this can be simplified to

$$y_1 = \frac{d^2 - \Delta x^2}{2P}; y_2 = \frac{d^2 - \Delta x^2}{2p} \quad \ldots \quad (1)$$

The speed of the disc at Δx is:

$$\left.\begin{array}{l} \text{in the outer zone } v_1 = 2\pi n(L + \Delta x), \\ \text{in the inner zone } v_2 = 2\pi n\ (l + \Delta x), \end{array}\right\} \quad (2)$$

where n is the number of revolutions per second of the disc. The retardation of the sound at point Δx is

$$\Delta t_1 = \frac{y_1}{v_1} \text{ resp. } \Delta t_2 = \frac{y_2}{v_2}, \quad \ldots \quad (3)$$

thus the relative difference in time, after substituting values from (1) and (2) is:

$$\Delta t = \Delta t_1 - \Delta t_2 = \frac{d^2 - \Delta x^2}{4\pi n}\left[\frac{1}{P(L + \Delta x)} - \frac{1}{p\ (l + \Delta x)}\right].$$

This expression has a maximum in the neighbourhood of $\Delta x = 0$ (about the middle of the zones). For this point

$$\Delta t_0 = \frac{d^2}{4\pi n}\left(\frac{1}{PL} - \frac{1}{pl}\right) \quad \ldots \quad (4)$$

In our experiments we have always worked with the following dimensions, suitable for practical use. $L = 12.45$ cm, $l = 7.35$ cm, $d = 1.85$ cm; n is ordinarily 78/60 r.p.s. If in the first instance we take for P and p the usual length of 20 cm, then

$$\Delta t_0 = 5.8 \cdot 10^{-4} \text{ sec.}$$

We have seen in the article so often referred to [1]) that the angular displacements of the sound image, which are caused by various simultaneous intensity and time differences are additive, and especially that between the time differences and the rotations caused thereby the relation shown in *fig. 5* exists. When the original sound image in the arrangement shown in fig. 1 was situated exactly in the middle of the scale, then according to fig. 5*a* shift of 46 cm corresponds to the calculated time difference Δt_0. If for example the gramophone record is of a piece of music played by a small orchestra, the middle instrument would be heard as if moved nearly half a meter from his original position halfway through the performance. This is of course very undesirable. It has, however, been found that a shift of not more than 20 cm may be considered permissible, which means a time difference of 2.4×10^{-4} sec.

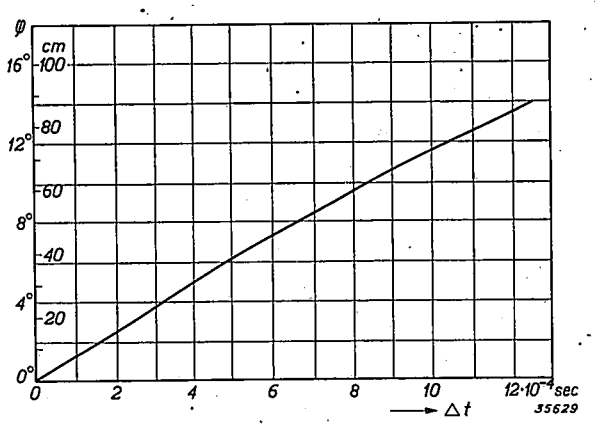

Fig. 5. Angular rotation φ (or shift) of the sound image which is caused by a time difference Δt.

The time difference Δt_0 could be limited to this value by making the equal arms P and p sufficiently long. It follows from equation (4) that Δt_0 is inversely proportional to this length. In our case P and p would have to be made $20 \cdot 5.8/2.4 = 48$ cm long, so that a rather awkward construction would result. A better method is to make the arms P and p of unequal lengths, such that

$$PL = p\,l \quad \ldots \quad (5)$$

Then according to equation (4) $\Delta t_0 = 0$. The relative time difference between the two sound contributions therefore disappears not only at the beginning and end of the sound track but also in the middle: The time difference which can occur

at other intermediate times can be calculated to be $0.4 \cdot 10^{-4}$ sec. at the most. The maximum shift of sound image corresponding to this is about 4 cm and therefore quite harmless.

For the above mentioned dimensions equation (5) becomes

$$P = 0.59\, p$$

If the arm P for the outer zone is made 20 cm long, then p must be 34 cm long. In *fig. 6* a photograph of such an arrangement may be seen.

Fig. 6. Arrangement for playing stereophonic records. The arm of the outer pickup is shorter than that of the inner pickup according to a definite relation (equation (5)).

Placing the needles on the record

Another possible cause of extra time differences between the two sound contributions are small errors made in setting the two needles on the disc. They should be set upon corresponding points in the two sound tracks. In order to be able to do this a small radial scratch is made with each cutter beside the sound track at the beginning and end of the recording. Upon reproduction, by adjusting the length of the pick-up arms care must be taken that the needles stand in these scratches. Suppose a deviation of $\pm\varepsilon$ to occur in this setting (*fig.* 7). During the playing of the whole record this deviation will remain unchanged. The time difference between the two sound contributions, assuming the most unfavourable case when $y_1 = \varepsilon$ and $y_2 = -\varepsilon$, is according to equation (3):

$$\Delta t = \varepsilon \left(\frac{1}{v_1} + \frac{1}{v_2}\right) \cdot$$

Thus after substituting from equation (2)

$$\Delta t = \frac{\varepsilon}{2\pi n} \left(\frac{1}{L + \Delta x} + \frac{1}{l + \Delta x}\right) \cdot$$

It is obvious that during the playing of the record (Δx varies from $+d$ through zero to $-d$) this expression does not pass through a maximum, but increases gradually from an initial value Δt_a to a final value Δt_e. We may imagine the time difference to be composed of a constant part Δt_a and a part which increases from zero to $\Delta t_{\max} = \Delta t_e - \Delta t_a$. The angular displacement of the sound image due to the constant part Δt_a (the time difference at the beginning of the record) may be neglected. This difference can, thanks to the above-mentioned additivity, simply be compensated by introducing a constant intensity difference between the two sound contributions, by means of the volume controls of the two amplifiers, such that an equal and opposite shift of the sound image is obtained. There thus remains the steadily increasing part of the time difference, which causes a gradually increasing shift of the sound image during the playing of the record. At the end of the record the time difference is:

$$\Delta t_{\max} = \frac{\varepsilon}{2\pi n} \left[\left(\frac{1}{L-d} + \frac{1}{l-d}\right) - \left(\frac{1}{L+d} + \frac{1}{l+d}\right)\right] \cdot$$

Substituting the above indicated numerical values for n, L, l and d gives:

$$\Delta t_{\max} = 0.012 \cdot \varepsilon.$$

If we now demand that the final shift of the sound image shall be not more than 20 cm, *i.e.* that $\Delta t_{\max} = 2.4 \times 10^{-4}$ sec., the value of ε which follows is 0.2 mm. This is therefore the maximum error which may be made in setting each needle on the record.

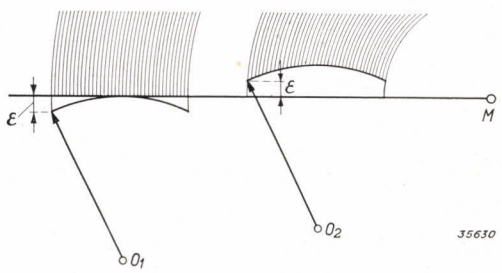

Fig. 7. In setting the needles upon corresponding points on the two sound tracks a slight error ε may occur.

Eccentricity of the gramophone axis

When the hole in the middle of the gramophone record is somewhat larger than the axis of the turntable, the record may be slightly excentric. In ordinary reproduction this has no other consequence than a slight, generally not disturbing rising and falling of the tones. In the case of stereophonic reproduction, however, a new effect occurs, namely an oscillation of the sound image at a frequency n (number of revolutions of the disc). This may be explained as follows. In *fig. 8* the record, which is

placed eccentrically upon the axis, is drawn in two extreme positions. It is of no concern whether this is for recording or reproduction, and we shall only assume for the sake of simplicity that in one of the two processes the record will be exactly centred

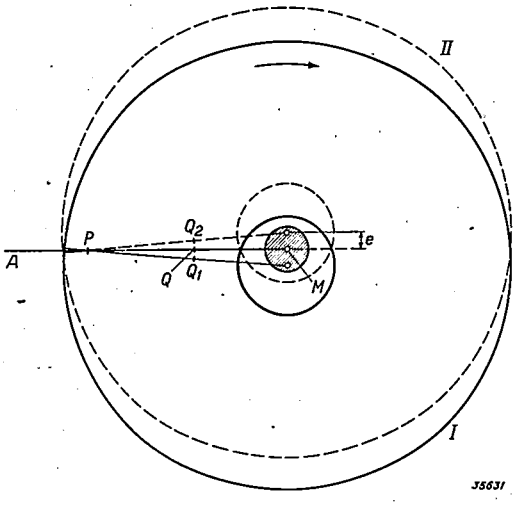

Fig. 8. The axis of the turn table lies in the hole of the disc with an excentricity e. For the sake of simplicity we assume the needles to move along the line AM in recording and playing. At a given moment, for instance, they are at P and Q. In position I of the record the inner pickup should actually be at Q_1, in position II of the record at Q_2. The sound of the inner zone in reproduction is therefore periodically slightly behind and ahead, respectively, of that of the outer zone.

and that the needles run exactly along the radial line AM in recording as well as reproduction. Imagine now that the record is in position I and that the outer pick-up is at point P. The corresponding point in the inner zone is Q_1; the needle in this zone is, however, at Q, and the sound contribution of the inner zone is therefore somewhat behind. After half a revolution the record is in position II and when the outer pick-up is at P the inner one should be at Q_2, while actually it is at Q, and thus the sound contribution of the inner zone is ahead. The result is a time difference between the two sound contributions changing its sign periodically, and thus an oscillation of the sound image about an intermediate position.

Experience has shown that such an oscillation when the frequency is greater than $^1/_3$ c/s, is interpreted as a lack of definition of the sound image, which has a width about equal to twice the amplitude of the motion back and forth. The effect is not disturbing when this amplitude is not greater than about 5 cm, thus the maximum time difference $\Delta t < 0.6 \times 10^{-4}$ sec. From this the permissible eccentricity of the axis can easily be calculated. It follows from fig. 8 that the amplitude of the deviation in position between the two needles amounts to

$$^1/_1\, Q_1 Q_2 = \frac{L - l}{L + \Delta x} \cdot e,$$

where e is the eccentricity (distance between the centres of axis and disc) and the other symbols are the same as above. According to equations (3) and (2) the time difference

$$\Delta t = {}^1/_2 \frac{Q_1 Q_2}{v_2} = \frac{(L - l)\, e}{2\pi n\, (L + \Delta x)\, (l + \Delta x)}.$$

Δt reaches its greatest value at $\Delta x = -d$ (at the end of the record). With the already given numerical values one finds

$$\Delta t_{\max} = 0.0107 \cdot e,$$

thus the permissible eccentricity

$$e = \frac{0.6 \cdot 10^{-4}}{0.0107} = 0.006 \text{ cm}.$$

Since the eccentricity can at the most be equal to half the difference in the diameters of the axis and of the hole in the disc, the lack of definition of the sound image is certainly kept within the desired limits when the tolerance for the diameter of the hole is made 0.1 mm. By a suitable construction of the axis of the turn table it is also possible entirely to suppress the eccentricity and therefore the oscillation of the sound image.

ABSTRACTS OF RECENT SCIENTIFIC PUBLICATIONS OF THE N.V. PHILIPS' GLOEILAMPENFABRIEKEN

1485: F. A. Kröger: Luminescence and absorption of solid solutions in the ternary system ZnS-CdS-MnS (Physica 7, 92-100, Jan. 1940).

The system of solid solutions ZnS-CdS-MnS exhibits a fundamental absorption region and a system of bands. The latter are characteristic of manganese and practically independent of the composition of the solid solutions. The fundamental absorption region consists of two absorption bands. The first band is found in ZnS and CdS, the second in MnS.

At room temperarure all ternary solid solutions exhibit emission in a band which is to be ascribed to the lattice. The wave length of the maximum of these bands depends upon the composition of the solid solutions and changes from blue for pure ZnS to infra red with pure CdS.

At —150° C, in addition to the emission bands described, others are present which are characteristic of manganese.

Unheated ZnS-MnS solid solutions obtained by coprecipitation exhibit photoluminescence in the same emission bands as are observed with phosphors prepared at high temperatures.

1486: F. M. Penning and J. H. A. Moubis: Cathode sputtering in a magnetic field (Proc. Kon. Ned. Akad. Wet. 43, 41-56, Jan. 1940).

The sputtering of a metal surface is the result of the freeing of one or more metal atoms by the collision of an ion against the surface. The elementary process can be characterized by the coefficient ϑ_o (V_p), which indicates how many metal atoms are freed by one ion of a given energy V_p (including those which return). For a direct measurement of ϑ_o (V_p) it is necessary that the gas pressure be very low, so that the ions shall not be retarded by collisions with gas atoms and that sputtered metal atoms may not return to the metal surface. Measurements at such low pressures are possible in a self-sustaining gas discharge, if a magnetic field of a certain direction and strength is used with a suitable electrode arrangement. From measurements made, using this device, a value of ϑ_o of 1.7 was found for argon ions and copper, and for argon ions and aluminium a value of 0.7 (both for an ion energy of 500 volts). Preliminary measurements were also carried out for argon and hydrogen ions with nickel and silver. For $500 < V_p < 1400$ volts ϑ_o was found to be about proportional to V_p, so that a definite energy V_p/ϑ_o is necessary to free one atom. The minimum energy necessary for freeing an atom is the atomic heat of evaporation W. We may therefore define the efficiency of sputtering as $\varepsilon = W/(V_p/\vartheta_o)$. This ε is found to be of the order of one per cent and less, in agreement with previous determinations.

1487: J. F. Schouten: Diffraction of light by sound film of the variable width type (Physica 7, 101-121, Feb. 1940).

Upon the diffraction of light by strips of sound film diffraction patterns are obtained which may be considered as two dimensional Fourier analyses of the strip of film. With purely sinusoidal modulation the distribution of intensity in the pattern contains all the Bessel functions of whole order. On a line in the spectrum parallel to the length of the film the spectrum gives the exact Fourier analysis of the sound modulated on the film. Comparison with ordinary optical gratings brings out various properties which are discussed. The broadening of the lines which occurs may be ascribed to the finite length of the film. In conclusion the possibilities for the application of these phenomena are briefly discussed.

1488: M. J. O. Strutt and K. S. Knol: Resistance measurements of iron wire in the frequency region from 10^7 to 3×18^8 c/sec (Physica 7, 145-154, Feb. 1940). (Original in German).

The resistances of iron wire have previously been determined in the region from 10^6 to 10^7 c/s. in order to investigate certain anomalies found by others in this region. In this investigation no anomalies were discovered. The measurements described give an extension to 3×10^8 c/s. Three wires of 20-40 microns were used. The method of measurement and the results are described at room temperature as well as at the temperature of liquid oxygen (—183° C). The measurements at room temperature again brought no anomalies to light; the measurements at —183° C exhibited a gradual decrease in the permeability with increasing frequency. With the help of Maxwell's theory it is shown that at room temperature the same change of permeability would be expected at a frequency 5 or 6 times as high. In conclusion the possible causes of this phenomenon are discussed.

1489: J. van Slooten: Input capacitance of a triode oscillator (Wireless Eng. **17**, 13-15, Jan. 1940).

It is shown in a general way that the input capacitance of a triode oscillator with grid condenser and leakage resistance decreases with increasing anode voltage. The value of this change in capacity is calculated and found to be in agreement with the experiments.

1490: H. C. Hamaker and E. J. C. Verwey: The role of the forces between the particles in electrode position and other phenomena (Trans. Far. Soc. **36**, 180-185, Jan. 1940).

The investigation of the formation of a covering layer by electrophoresis from suspensions in organic media exhibited a parallelism between this deposition of a layer and the formation of a sediment by settling. This leads to the assumption that electrodeposition is only a mechanical problem in which the electrical nature of the phenomenon is of secondary importance. The electrical field only provides the force which drives the particles to the electrode and presses them against it.

Assuming this to be the case, the process of deposition is analyzed with the help of potential curves. Two kinds of curves can be used to describe the phenomenon. The formation of a covering layer is discussed in detail in these two cases. They should lead to slightly different properties of the layer, but in the case of the suspension investigated the differences observed are not sufficiently pronounced to distinguish between the theoretical possibilities.

1491: H. C. Hamaker: The influence of particle size on the physical behaviour of colloidal systems (Trans. Far. Soc. **36**, 186-192, Jan. 1940).

It is generally assumed that the difference between suspensions and colloidal solutions is only a difference in size of particle. The size of particle is, to be sure, a very important factor. Many properties of a sol depend upon the relation between forces of different natures which act upon the particles. Each of these forces will change independently with the particle size, so that their relation will depend to a large extent upon this size. The different forces which play a part in the deposition of a layer and their dependence on particle size are discussed and on the basis of the discussion the behaviour of colloidal systems under the influence of gravity and in a centrifuge is dealt with. It may be expected that observation of the properties of a precipitate obtained by centrifuging will be able to furnish valuable information about the potential curves which hold for sols.

1492: E. J. W. Verwey: Electrical double layer and stability of emulsions (Trans. Far. Soc. **36**, 192-203, Jan. 1940).

A discussion is given of the reason why a stable emulsion can never be obtained without an emulsifier. It is assumed that the boundary surface potential occurs due to the ion distribution equilibrium of electrolytes in the two liquid systems. Since the charge on both sides of the double layer has an extension which is determined by thermal movement, the electrokinetic potential is already lowered thereby. Moreover, this extension usually is so great that the double layer cannot be formed completely in concentrated emulsions or with small droplets. In the case of a double layer, emulsifiers restore the necessary conditions which must exist at the boundary of the liquid and the solid substance in order to obtain the necessary high value of the potential.

1493: H. C. Hamaker: Formation of a deposit by electrophoresis (Trans. Far. Soc. **36**, 279-287, Jan. 1940).

It is possible to form a deposit of the suspended material by electrophoresis from certain organic liquids. This phenomenon is discussed from the experimental point of view. With certain limitations the quantity deposited is proportional to the time, the surface of the electrode, the electric field and the concentration.

At low voltages, short times and too low concentrations, deviations from this simple law are observed. The deviations observed can be understood from theoretical considerations. In conclusion a simple method is indicated of studying the density of the layers, and observations are recorded which were obtained by this method.

VOL. 5 No. 7 JULY 1940

Philips Technical Review

DEALING WITH TECHNICAL PROBLEMS
RELATING TO THE PRODUCTS, PROCESSES AND INVESTIGATIONS OF
N.V. PHILIPS' GLOEILAMPENFABRIEKEN

EDITED BY THE RESEARCH LABORATORY OF N.V. PHILIPS' GLOEILAMPENFABRIEKEN, EINDHOVEN, HOLLAND

OUTPUT AND DISTORTION OF OUTPUT AMPLIFIER VALVES UNDER DIFFERENT LOADS

by A. J. HEINS van der VEN.

621.396.645.331.018.7

Since the impedance of a loud speaker varies considerably with the frequency, it is not sufficient to know the power delivered by an output valve at a given distortion for the optimum loading resistance only. The influence of the magnitude and the phase angle of the loading impedance on the output, especially that of output pentodes, forms the subject of this article. The significance is discussed of the curves measured for the reproduction. The behaviour of the output pentode is compared with that of the output triode and tetrode. In conclusion the influence of inverse feed-back is demonstrated by means of two diagrams.

The power which can be delivered by an output amplifier valve, a pentode for instance with a given distortion, depends very much upon the impedance with which the valve is loaded. This can easily be understood by considering the idealized I_a-V_a diagram of a pentode, *fig. 1*. When the valve is loaded with a resistance R_a, the momentary values v_a and i_a of the anode voltage and current, respectively, lie on a line drawn through the operating point I_a, V_a with the slope $-1/R_a$ with respect to the V_a axis, as explained in an earlier article [1]): the load line. The amplitude described on this load line (for example, end points A and B on line a) depends upon the magnitude of the grid A.C. voltage, and the output is proportional to the area of the shaded triangle. As long as the grid A.C. voltage is sufficiently small, the vibration along the load gives a faithful representation of this. On line a, however, which corresponds to a low loading resistance, the amplitude of the anode alternating current permissible without distortion may not become larger than the value I_a of the anode direct current. In the same way, on line c for a high loading resistance the amplitude of the anode A.C. voltage may not become larger than the anode D.C. voltage V_a. If the grid voltage varies more than corresponds to these limits, which may be read off in the diagram, the tops of the curves for anode current and voltage would be cut off considerably, *i.e.* there would be strong distortion. The distortionless output is thus limited at low loading resistances by the anode current and, as appears from the corresponding triangle, it is given by $^1/_2\ I_a{}^2R_a$; with high loading resistance the output is limited by the anode voltage, and given by $^1/_2\ V_a{}^2/R_a$. From fig. 1 it may at once be seen that the largest possible value of the output is obtained when $R_a = V_a/I_a$: both anode A.C. voltage and current then have their maximum

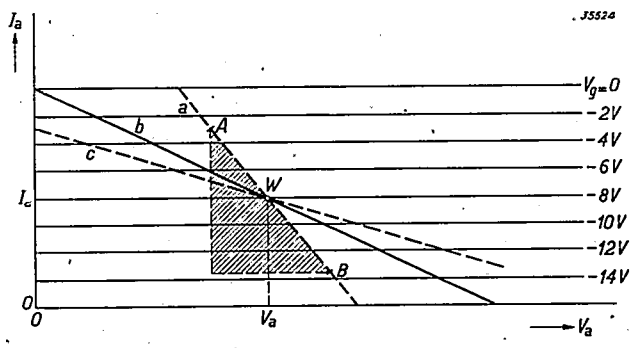

Fig. 1. I_a-V_a diagrams of an idealized pentode. The lines a and c are load lines for a low and a high loading resistance R_a, respectively. The amplitude AB along the load line is determined by the grid A.C. voltage, the shaded triangle gives the output. The reproduction is free of distortion as long as the amplitude of the anode A.C. (on line a) does not become greater than the anode D.C. I_a, or the anode D.C. voltage V_a, respectively. The output at different loading resistances is hereby limited. The limit lies highest for the "optimum" loading resistance $R_a = V_a/I_a$, line b.

[1]) A. J. Heins van der Ven, Testing amplifier output valves by means of the cathode ray tube. Philips techn. Rev. 5, 61, 1940. Figs. 3 and 12 have already been given in that article. We assume in every case here that the output valve operates in a class A amplifier connection, *i.e.* that the operating point is so chosen that the anode current never becomes zero at the normal grid voltage amplitudes.

values, and the output amounts to $^1/_2\ V_a\ I_a$. This loading resistance is called the optimum resistance, R_{opt}. For $R_a < R_{opt}$, according to the above, the maximum output is proportional to R_a, for $R_a > R_{opt}$, it is inversely proportional to R_a. In *fig. 2* this relation between output and loading resistance is represented graphically.

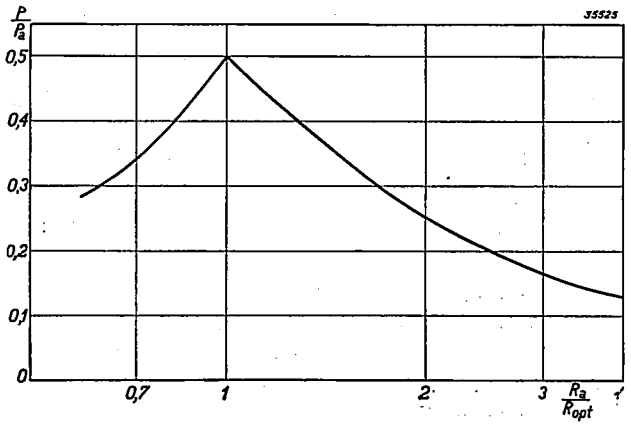

Fig. 2. For the ideal pentode the distortionless output is a maximum of $P = {}^1/_2\ I_a{}^2 R_a$ at loading resistances R_a smaller than the optimum R_{opt}, and the maximum $P = {}^1/_2\ V_a{}^2/R_a$ for $R_a > R_{opt}$. When $R_a = R_{opt} = V_a/I_a$ the limit is $P = {}^1/_2\ I_a V_a = {}^1/_2\ P_a$.

In order to characterize an output valve one often makes use of the power which the valve can deliver at a given distortion in the above-mentioned optimal loading resistance $R_{opt} = V_a/I_a$. In most practical cases, however, the output valve is not loaded with the optimal resistance, but with one

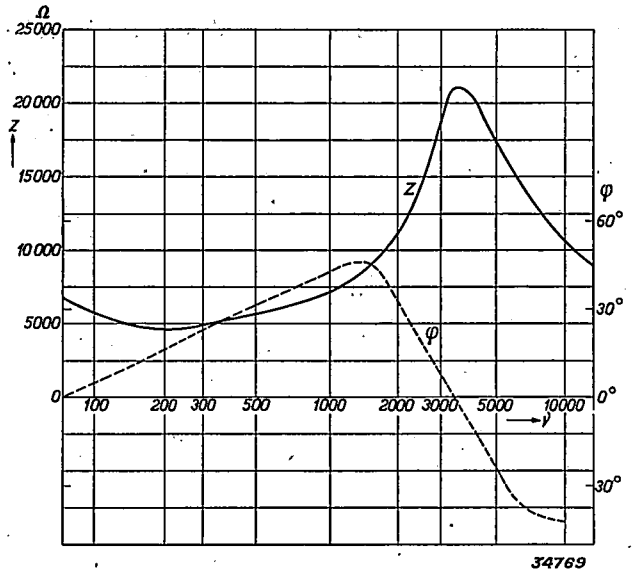

Fig. 3. Quantity Z and phase angle φ of the impedance of a normal loud speaker as a function of the frequency ν in c/s. As customary in receiving sets, in parallel with the primary winding of the loud speaker transformer there is a condenser of 2 000 $\mu\mu$F, which is responsible for the fall in the impedance at $\nu > 3\,000$ c/s. At 1 000 c/s Z is about equal to the optimal loading impedance of the output pentode EL3 (7 000 ohms), while at 3 000 c/s Z has increased to about three times this value.

or more loud speakers whose impedance varies as a rule very much with the frequency and moreover exhibits a certain phase angle. As an example the magnitude and phase angle of the impedance is given in *fig. 3* of a normal type of loud speaker as a function of the frequency. Considering this fact, it is important in judging an output valve to know the relation between output and distortion also at loads other than the optimum.

For the case of an ideal pentode we have already found the curves of fig. 2 for this purpose. These curves divide the surface of the whole diagram into two zones: at points below the limiting line there is no distortion, while the opposite is true at points above the line. In the case of an actual pentode there is no such sharp transition. The I_a-V_a diagram in this case differs from that of the ideal case in that the different characteristics (V_g = constant) are not at equal distances from each other, so that distortion already occurs before the above-mentioned limits can be reached. In *fig. 4*

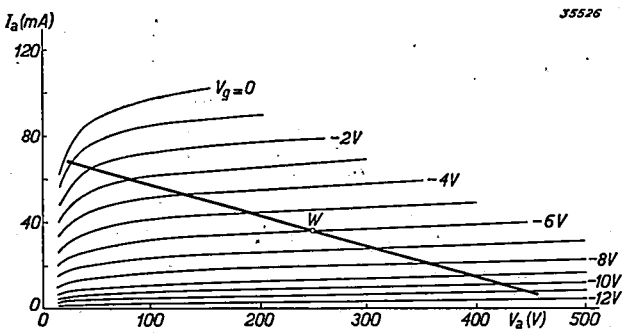

Fig. 4. In the case of an actual pentode — in contrast to that of an ideal pentode — there is already a distortion at outputs below the limit given in fig. 2. This is caused by the fact that the successive characteristics cut off sections of unequal lengths on the load line, as a result of which harmonics occur in the anode A.C. and A.C. voltage.

it may be seen that the sections which the successive characteristics intercept on the load line gradually become shorter, the farther away from the operating point one proceeds in both directions. This means that, with a purely sinusoidal grid A.C. voltage, harmonics occur in the anode A.C. voltage and current. This distortion might be investigated as a function of the amplitude along the load line (*i.e.* of the output), by measuring the sections intercepted on the load line. In practice, however, this method is too elaborate and too inaccurate. It is better to measure the quantities in question, output and distortion, directly. Several results of such measurements, chiefly on output pentodes, will be given and discussed in this article. First, however, we shall examine briefly the question of the quantitative measure which is used for the

distortion and the magnitude of the latter which is permissible in practical cases.

Definition and permissible value of the distortion factor

As a measure of the distortion of an alternating current the "distortion factor" D is usually employed. This is defined as follows:

$$D = \sqrt{\frac{i_2^2 + i_3^2 + i_4^2 + \cdots}{i_1^2}} \quad \ldots \quad (1)$$

i_1 is here the purely sinusoidal current supplied as input signal, and $i_2, i_3, i_4, \ldots$ the currents of the different harmonics occurring in the output signal. The denominator is sometimes written $i_1^2 + i_2^2 + i_3^2 + \ldots$ instead of i_1^2. In practical cases where D is usually less than 10 per cent this makes no great difference.

If the factor D is used as a measure of the distortion, the quality of the reproduction must be better the smaller the value of D. This is in general in agreement with experience. There are, however, cases where the reproduction is very poor while only a small distortion can be measured. This is in particular the case when phenomena with a discontinuous character occur. When, for instance, a grid A.C. voltage which becomes positive for an instant at its peaks is supplied to the output valve of an amplifier, a grid current begins to flow at those instants. This sudden load on the preceding stage may, when it has not been taken into account, cause a distortion which is much more disturbing than would be concluded from the distortion factor measured.

In working with the factor D, therefore, one must first be sure that no discontinuous phenomena occur. In a complete receiving set it will sometimes be difficult to find this out without special means. In a simple low-frequency amplifier care must only be taken that no grid current flows in any of the valves and that the grid A.C. voltages do not assume such a value that the anode voltage remains zero during part of the period (see above).

How large may the factor D become? From the results obtained by different investigators [2]) it appears that it is usually sufficient for good reproduction if the distortion factor is smaller than 5 per cent. In a few very special cases the requirement may be made that the distortion factor should not amount to more than 1 to 1.5 per cent [3]), while for carrier-wave telephony for scientific investigations and calibrations (tone generators) the distortion may only amount to fractions of one per cent.

Influence of the magnitude of the loading resistance

In *fig. 5* the relation between output distortion and load is represented graphically for the output pentode EL3. The curves show the output at a given distortion as a function of the loading resistance. (It is assumed for the present that the latter has the phase angle $\varphi = 0°$).

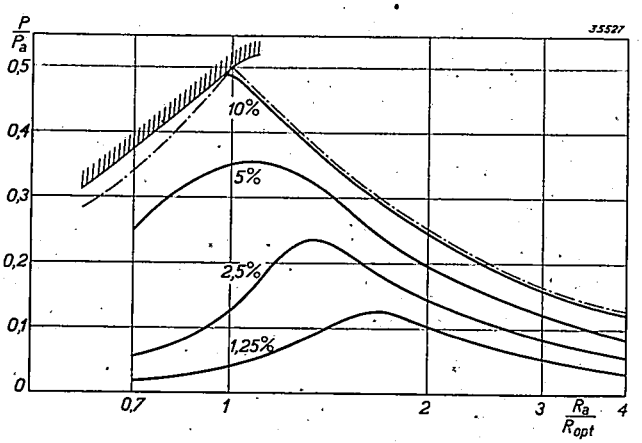

Fig. 5. The output P of the output pentode EL3 as a function of the loading resistance R_a with the distortion factor D as parameter. The unnamed quantities P/P_a and R_a/R_{opt} are plotted (the permissible value of $P_a = I_a \cdot V_a$ is 9 watts in this case; R_{opt} = optimal load, in this case 7 000 ohms). The broken lines indicate the limits for the distortionless output of an ideal pentode (fig. 2). In the case of the shaded line grid current begins to flow.

In order to make the diagram more easily comparable with similar diagrams of other valves, the output P and the loading resistance R_a are not themselves plotted, but P is referred to the power $P_a = I_a V_a$, which is converted into heat at the anode without grid A.C. voltage being supplied to the valve and R_a to the already mentioned optimum loading resistance R_{opt}, as is indicated in fig. 2. Ordinates and abscissae are therefore the unnamed ratios P/P_a and R_a/R_{opt}, respectively. The curve with the parameter value of $D = 5$ per cent represents the above-mentioned limit for "good quality", while in addition the curves for $D = 1.25$, 2.5 and 10 per cent are given.

The limiting curves of fig. 2 are also indicated by broken lines in the figure. These are valid for an idealized pentode. By means of these curves an idea is given of the degree to which the valve considered approaches the ideal case.

If such a high grid A.C. voltage is supplied to the valve that the limiting line drawn is exceeded, a region is entered in which the disturbing character of the distortion is no longer determined by D,

[2]) For instance: F. Massa, Proc. Inst. Rad. Eng. **21**, 682, 1933, and H. von Braunmühl and W. Weber, Akust. Z. **2**, 135, 1937.

[3]) H. G. Beljers, T. Ned. Radiogenootschap **6**, 115, 1934.

since the anode current and voltage are cut off more or less discontinuously. Upon further increase of the amplitude of the grid A.C. voltage, the latter finally becomes positive at its peaks and grid current flows. The limit of this region is indicated in fig. 5 by the shaded line.

The reproduction of speech and music; comparison of pentode and triode

What conclusions may now be drawn from fig. 5 as to the reproduction with the output pentode considered? When the listener desires to increase the volume of the reproduction and does this by ear, he will proceed only so far that no disturbing distortion occurs in any frequency region in the case of music and speech. The average level which is reached in this way will depend upon the height of the peaks occurring in the music or speech and on their distribution over the frequencies. Suppose that the loud speaker has the impedance curve represented in fig. 3. A certain value of the loading resistance then corresponds to each frequency (we shall neglect the phase angle of the impedance in these considerations), thus at each loading resistance in the diagram of fig. 5 the average level must lie as far below the theoretical limiting line or below the line with the greatest permissible distortion as is required by the peaks occurring here. The value of R_a (the frequency) at which this restriction is most serious will depend upon the frequency spectrum of the sound reproduced and on the position of the line for the permissible distortion.

The average level may then in general be set higher, the higher the positions of the lines D = constant, and in particular, the higher the limiting line where discontinuous phenomena begin to occur. With the optimum load this limit lies at about $P/P_a = 0.5$ for the valve EL 3, see fig. 5. When it is kept in mind that an average level of 0.2 watt already represents a very considerable volume of sound, and that the line $P/P_a = 0.022$ corresponds to this in the 9 watt pentode mentioned, it will be seen that there is still a very wide margin for the peaks.

For the sake of comparison a similar diagram is given in *fig. 6* for the output triode AD1 (combined with a valve EF6 as pre-amplifier valve). In this case the output at loading resistances greater than the optimum is sharply limited by the occurrence of grid currents (thus not so much by the distortion factor). The limit lies at about the same level as the curve $D = 5$ per cent for the output pentode considered (fig. 5); for the optimum load especially it lies at $P/P_a = 0.32$, thus considerably lower than the theoretical limit with the pentode. The difference in the way in which the output is limited offers an important practical advantage in the use of the pentode. Assume that the sound has been adjusted to the correct permissible volume by ear. In the case of the pentode, the ear has for instance used the curve $D = 5$ per cent as criterion and this was not exceeded at the greatest intensity observed during the adjustment. If afterwards the intensity becomes greater, the sound is indeed somewhat more strongly distorted, but there is still a gradual transition to the level at which discontinuous phenomena and the accompanying very disturbing distortion occur. In the case of the triode on the other hand, in making the adjustment, the ear has already been compelled to make use of the criterion that no grid currents began to flow at the greatest intensity observed. If in this case the intensity becomes greater still, for instance in *fortissimo* passages of the music, a sudden very unpleasant distortion may result.

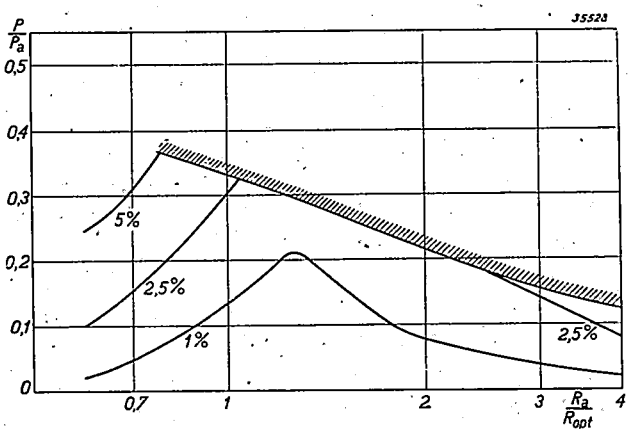

Fig. 6. Diagram similar to that of fig. 3 for the output triode AD 1 (combined with the pre-amplifier valve EF 6). The output is sharply limited by the occurrence of grid currents. The limit for $R_a = R_{opt}$ lies lower than with the output pentode.

Comparison of output pentode and tetrode

The fact, that in fig. 5 in the region $R > R_{opt}$ the curves run more or less parallel to the limiting line on which the amplitude v_a of the anode A.C. voltage has the maximum value V_a, indicated that when D = constant here, v_a is also approximately constant, *i.e.* that the distortion is here mainly determined by the anode A.C. voltage and less by the magnitude of the loading impedance. In *fig. 7* where v_a is plotted as a function of R_a/R_{opt} for different values of D, this is expressed much more clearly. On the basis of the I_a-V_a diagram this behaviour is easily understood: if in fig. 4 the slope of the load line is slightly changed, from the optimum to larger values of R_a, the amplitude which can be described along the load line without touch-

ing zones of greatly deviating density of V_g curves, remains unaltered in the first approximation. A comparison of the pentode with a tetrode is interesting in this respect. As was briefly indicated in the article cited [1]), in tetrodes (in the modern types too, which more nearly resemble pentodes) the secondary emission from the anode to the screen grid cannot be entirely suppressed. This

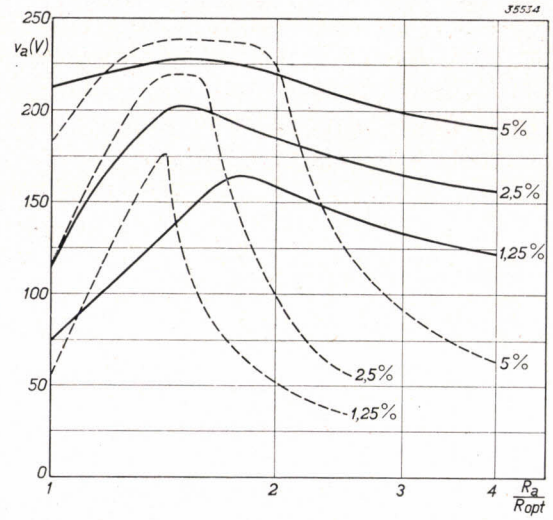

Fig. 7. In the region where $R_a > R_{opt}$ the distortion of an output pentode is mainly determined by the anode A.C. voltage v_a. The v_a curves here drawn for constant distortion therefore have a fairly long section practically parallel to the R_a axis. The broken line curves refer to an output tetrode which obviously behaves quite differently.

causes kinks in the I_a-V_a curves, see, for instance, *fig. 8*. If in such a diagram the load line for $R_a = R_{opt}$ is drawn it is seen that, upon a rotation of the line (increase of R_a), the sections of the line cut off by the V_g curves may rapidly become very unequal, see *fig. 9*. The distortion then increases very rapidly with R_a with equal amplitude along the line (amplitude v_a), or conversely for a given distortion the amplitude v_a of the anode A.C. voltage must become very much smaller. The broken line curves in fig. 7 show this clearly.

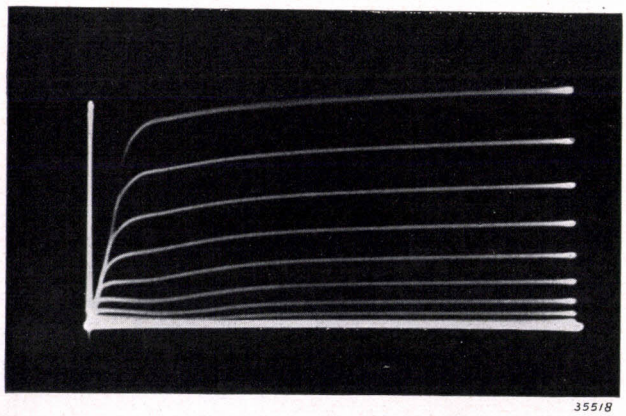

Fig. 8. I_a-V_a diagram of a tetrode.

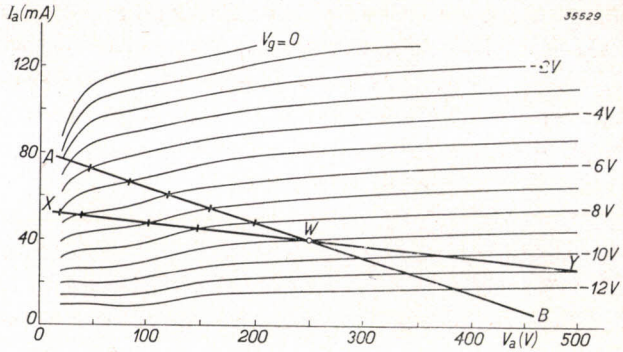

Fig. 9. Load lines for $R_a = R_{opt}$ (line AB) and for $R_a = 3 \cdot R_{opt}$ (line XY) in the I_a-V_a diagram of an output tetrode. The line AB is divided into almost equal sections by the successive curves for V_g = const. and therefore anode current and voltage vary practically linearly (at least according to an only slightly curved line) with the grid A.C. voltage. In the case of line XY, however, the sections cut off are very unequal in length: starting from the operating point W in the direction WX there is first a long section, then a much shorter one, then again a longer one and finally a short one again; the anode current and voltage here vary very irregularly with the grid A.C. voltage and a large distortion results.

Influence of the angle of the loading impedance

In the foregoing it has always been assumed that the loading impedance is a pure resistance, so that between the anode current and voltage there was no phase shift (straight load line). From the curve of fig. 3, however, it was found that in practice a phase shift must in fact be considered. If the phase shift φ is given different values successively, and in each case the output is measured as a function of the quantity Z with the distortion D as a parameter, a diagram like fig. 5 is again obtained, in which now, however, each curve for D = constant disintegrates into a set of curves for different values of φ.

Such a curve is given in *fig. 10*. The measurements are again carried out on the output pentode EL3,

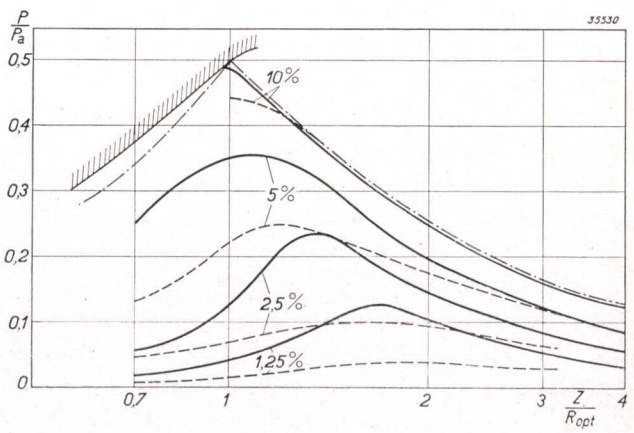

Fig. 10. Output of the output pentode EL3 as a function of the loading impedance Z. For each value of the distortion D a load with a phase angle $\varphi = 0°$ (full lines) and with a phase angle $\varphi = 45°$ (broken lines) is investigated. The phase shift between anode current and voltage is found to have an unfavourable effect on the output.

in which a self-induction and resistance in series was included in the circuit, while the distortion of the current in this circuit was measured. The phase shift amounted to $\varphi = 45°$ (dotted-line curves) and $\varphi = 0°$ (full-line curves), respectively. The latter curves are thus the same as in fig. 5. Not the true output $^1/_2\, i_a\, v_a \cos \varphi$, but the apparent output $^1/_2\, i_a\, v_a$ is plotted. For this reason the ideal limiting curve is the same for all values of φ, and in the curves obtained the influence of the valve properties only is expressed (not that of the work factor).

The figure shows that in the presence of a phase shift the output with a given distortion is considerably diminished. This may be explained as follows. The distortion may be chiefly ascribed to a second and third harmonic in the anode A.C., and we have already seen above that the occurrence of such is reflected in the inequality of the sections which the successive characteristics V_g = const. in the I_a-V_a diagram cut off on the load line. If the shortening of the sections takes place in the same way on both sides of the operating point, as is approximately the case with a straight load line with a slope close to the optimum, then the anode A.C. remains symmetrical, *i.e.* it contains no second harmonic. In *fig. 11* where the distortion due to the second and third harmonic, as well as the total distortion, is plotted as a function of the loading resistance, it may clearly be seen that due to this disappearance of the second harmonic

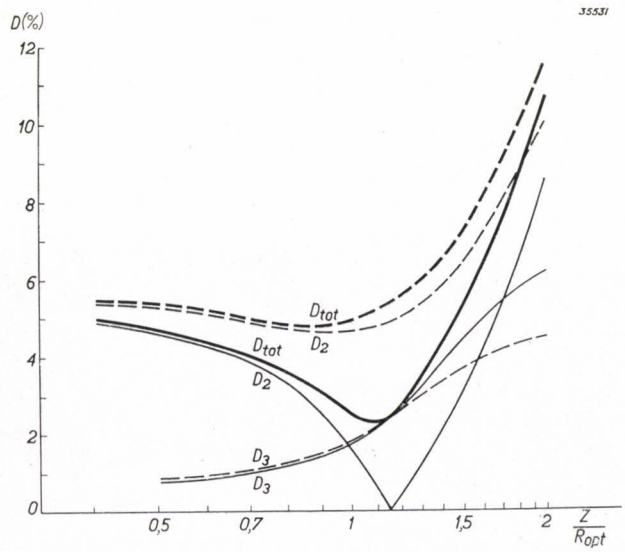

Fig. 11. The distortion factor of the output pentode EL3 is measured as a function of the magnitude of the loading impedance with constant grid A.C. voltage. The total distortion D_{tot} as well as the separate distortions D_2 and D_3, due to the second and third harmonics, respectively, are measured. The full line curves refer to the case where the loading impedance has the phase angle $\varphi = 0°$: in the neighbourhood of $Z = R_{opt}$ the second harmonic disappears. The broken line curves are valid for $\varphi = 45°$; in this case D_2 is never equal to zero, D_{tot} is therefore always greater than for $\varphi = 0°$.

in the neighbourhood of the optimal load the total distortion also reaches a minimum at this point. If the load is not a pure resistance, but the loading impedance has a certain phase angle, then the load line is not straight but elliptical (see *fig. 12*; without distortion it would be a true ellipse). Independent of the slope of the axis of this ellipse (magnitude of Z) the regions where the points of intersection with the characteristics begin to lie close together are always situated on parts of the ellipse which do not lie symmetrically with respect to the operating point. In this case therefore the second harmonic, and thus also the total distortion, always retain an appreciable value (fig. 11 broken-line curves). The curves which show the output at constant distortion will therefore be lower than in the case without phase shift.

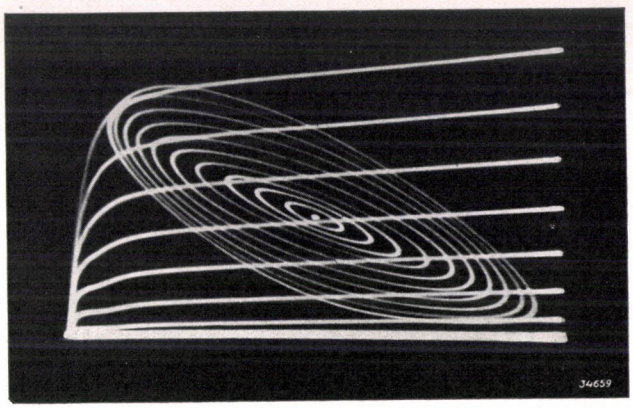

Fig. 12. With a phase shift between the anode current and voltage the load line in the I_a-V_a diagram (with sinusoidal grid A.C. voltage) becomes a more or less distorted ellipse about the operating point; the slope of the axis of the ellipse is given by the magnitude of Z, the loading impedance. In this case the amplitude of the grid voltage was varied by equal intervals.

Inverse feed-back

By the application of inverse feed-back, as repeatedly discussed in this periodical [4]), distortion of the reproduction can be decreased. This means that in figs. 5 and 10 the curves D = const. are all shifted to higher outputs. At the same time, however, it may be seen that the influence of the phase angle is eliminated to a considerable extent, so that the curves for $\varphi = 45°$ are much less unfavourable compared with those for $\varphi = 0°$. Even with the slight inverse feed-back which is obtained by omitting the condenser usually connected in parallel with the cathode resistance of the output valve, this may clearly be seen, as shown in *fig. 13*. About half of the amplification of the output stage is sacrificed in this inverse feed-back.

[4]) See for example, B. D. H. Tellegen, Philips techn. Rev. **2**, 289, 1937.

A more usual form of inverse feed-back is that in which a voltage is conducted from the loud speaker or anode circuit of the output valve back to the grid of the pre-amplifier valve. This feed-back may be made proportional to the loud speaker current (current inverse feed-back) or to the loud speaker voltage (voltage inverse feed-back), by taking it off from a resistance either in series or in parallel with the loud speaker. *Fig. 14* gives the distortion diagram of the valve EL3 combined with the pre-amplifier valve EBC3 with the application of a "fourfold" voltage inverse feed-back. By this is meant that the amplification is reduced to $^1/_4$ of its value without inverse feed-back. It may be seen that with this relatively weak inverse feedback the output at a given distortion has become considerably greater, while at the same time a phase shift now no longer has any practical effect. The remaining difference in output at $\varphi = 0°$ and $\varphi = 45°$ with this voltage inverse feedback even has an opposite sign to that in the case of no feed-back.

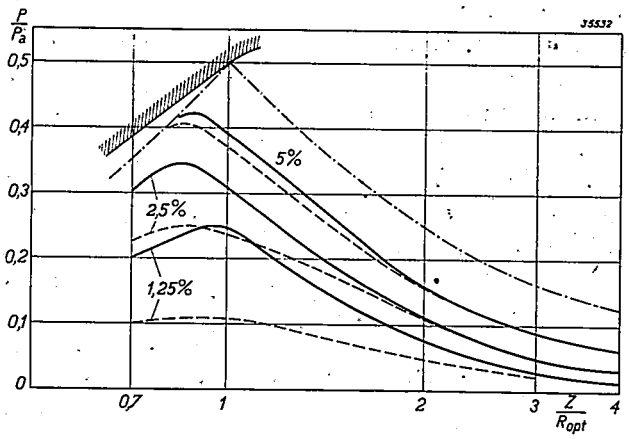

Fig. 13. Diagram similar to that of fig. 10 for the same output valve upon application of very slight inverse feed-back. The curves for a given distortion are higher than without inverse feed-back and the influence of the phase angle is less.

If, as in this case, no account need be taken of the influence of a phase shift, conclusions may be drawn directly from the above considerations about the adaptation to each other of loud speaker and output valve. The most important frequency region, *i.e.* that in which the most important contribution to the total sound intensity is delivered, lies in general in the neighbourhood of 1 000 c/s. Care should therefore be taken that the absolute value of the loud speaker impedance corresponds as nearly as possible in this frequency region to the optimal loading resistance of the output pentode. As may be seen, therefore, the loud speaker with the impedance curve given in fig. 3 is well adapted to the pentode EL3 whose optimum loading resistance is 7 000 ohms.

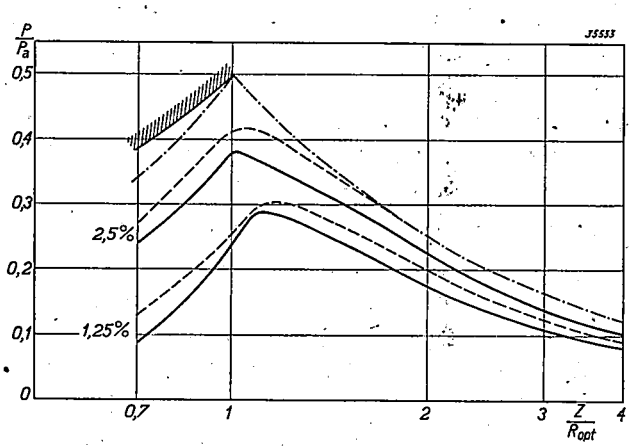

Fig. 14. Diagram similar to that of figs. 10 and 13 with the application of fourfold voltage inverse feed-back. The curves lie still higher than in fig. 13, and the difference for $\varphi = 0°$ and $\varphi = 45°$ has even changed its sign.

A PERMANENT MAGNET WHICH CAN LIFT 3 500 TIMES ITS OWN WEIGHT

by J. L. SNOEK.

621.318.22 : 669.15.018.58

The ratio between the lifting power and the weight of a magnet forms a better measure of the quality of the magnet steel than the lifting power alone. By the application of modern magnet steels a ratio of 3 500 has successfully been achieved. In this article the factors are discussed which must be considered in the construction of a magnet in order to make the ratio of lifting power to weight as large as possible.

In the early period of the development of permanent magnets and at the time when natural permanent magnets were scarcely exceeded in strength by artificial ones, a common test of the strength of a magnet was the measurement of its lifting power. One still finds in musea, besides natural magnets of reinforced magnetic iron ore, heavy magnets of carbon steel which are capable of lifting considerable loads. Considerations of technical advantage were scarcely taken into account in the making of such magnets; it was only a question of the demonstration of an interesting natural force which was rendered as large as possible by suitable means.

At the present time these demonstrations have lost much of their attraction, since it is commonly known that magnets of any desired lifting power could be made by increasing the dimensions of the magnet steel sufficiently. As to this increase, the technical possibilities are now practically unlimited, in any case an attempt to reach the limit of possibility would exceed the scope of a simple demonstration.

The question of the ratio between the maximum load which a permanent magnet can lift and the weight of the piece of magnet steel used is quite different. It will immediately be understood that this ratio provides a better criterion of the performance of the magnet steel than the size of the load lifted as such. Instead of making the load which a magnet can lift larger and larger, it is of more advantage to try to make the weight of the magnet which will lift a given load smaller and smaller. An example of such a demonstration which was given before the Natuur- en Geneeskundig Congres in Nijmegen in April 1939, is reproduced in *fig. 1*. An old magnet of 10 kg together with the maximum load it can lift (15 kg) was suspended from a modern permanent magnet with a suitable armature. The magnet steel of the latter magnet did not weigh more than 100 g.

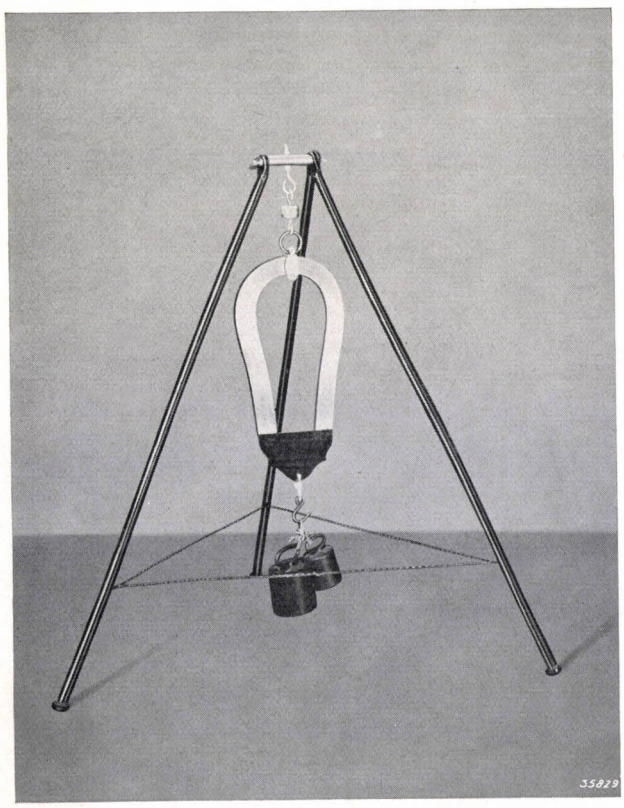

Fig. 1. Demonstration of the progress in the construction of magnets by improvement in the magnet steel. An old magnet of 10 kg (for which we owe thanks to Prof. Dr. A. D. Fokker of the Teylerstichting at Haarlem) with its maximum load (15 kg) hangs from a modern loud-speaker magnet, the steel of which weighs only 100 g.

Strictly speaking the ratio between lifting power and weight is also no pure measure of the qualities of a magnet steel, but is found itself to depend upon the absolute dimensions with a given shape and properties of the magnetic material. The force with which the armature of a magnet is held, with given inductions in the iron circuit, is proportional to the surface of contact between armature and magnet. Since the inductions which occur in the material are not changed upon proportional changes in the dimensions, we see that the lifting power is proportional to the square of the dimensions, while the weight increases with the cube of the dimensions.

The ratio would therefore be more favourable the smaller the dimensions are kept. There is, however, a technical limit to the reduction of the dimensions, due to the accuracy with which the connected parts of the magnetic circuit can be worked. If for instance the ground surfaces are not absolutely plane and smooth, there is an air gap between the parts which has a certain magnetic resistance. If moreover a kind of iron with a permeability of $\mu = 4\,000$ is used for the pole pieces, the resistance of an air gap of 1 micron corresponds to that of 4 mm of soft iron, and it is therefore very difficult to make the dimensions of the iron circuit smaller than, for example, 1 cm without the induction being so much lowered due to the transition resistance in the air gap, that the ratio between lifting power and weight also begins to become smaller.

At definite dimensions of the magnet, therefore, the ratio between lifting power and weight will reach a value which cannot practically be exceeded, and which in turn is determined in the first instance by the quality of the magnet steel.

By the application of modern types of magnet steel it has been found possible to construct a magnet which can lift 3 500 times its own weight (see *fig. 2*). The kind of steel used is "Ticonal" 3.8 with a remanence of 12 000 gauss and a coercive force of 550 oersted. The pole pieces consist of an alloy of 50 per cent cobalt and 50 per cent iron. This alloy has a higher magnetic saturation than pure iron, and at a field strength of only 5 oersted it reaches an induction of 19 000 gauss. The surface of contact between the armature and the pole pieces amounts to only 0.1 sq.cm; the lifting power is 1.65 kg. Since the magnet steel used — a cube of edge 4 mm — weighs only 0.47 g, a ratio of 3 500 is achieved.

It will perhaps be of interest to learn how this tiny magnet was designed.

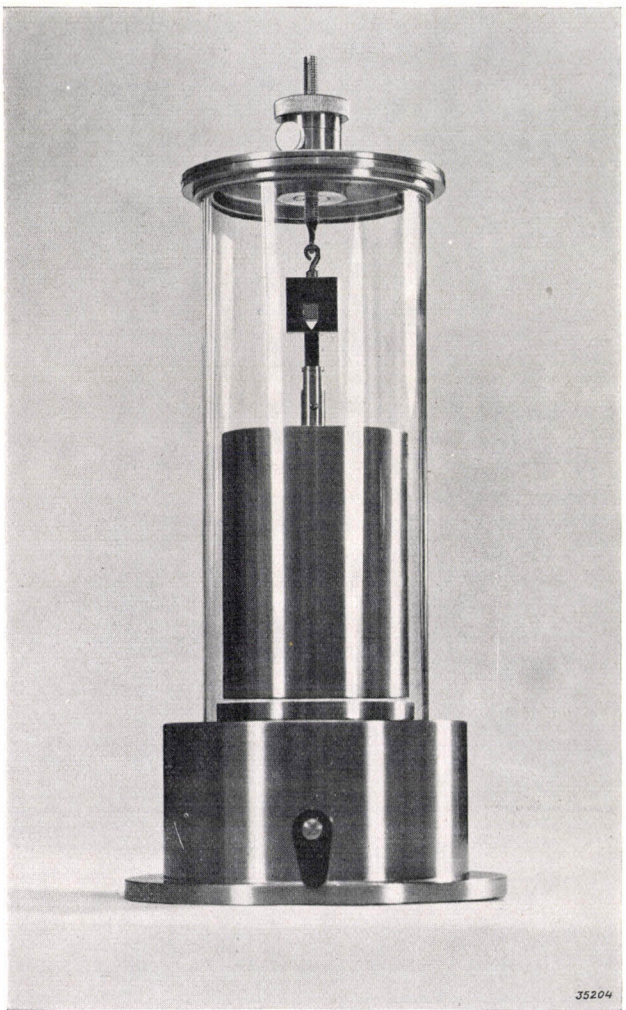

Fig. 2. A magnet which can lift 1.65 kg and the steel of which weighs only 0.47 g.

Construction of the magnet

The lifting power of a magnet is given by

$$K = \frac{1}{8\pi} \int B_n^2 \, df,$$

where B_n is the component of the magnetic induction which is perpendicular to the surface of contact between magnet and armature, and df is an element of this surface. If S is the area of the surface, then in the case of a homogeneous induction

$$K = \frac{1}{8\pi} B_n^2 \cdot S = \frac{1}{8\pi} \frac{\Phi^2}{S},$$

where Φ is the flux of the magnet. From this formula it follows that with a given magnetic flux it is advantageous to constrict the bundle of lines of force as much as possible at the position of the surface of contact.

In order to make the surface S small it is desirable to use for the pole pieces and the armature a material which has a very high magnetic saturation. As stated, an alloy of cobalt and iron was employed whose magnetic saturation is 15 per cent higher than that of pure iron. By carefully annealing the material, magnetization nearly to saturation can be achieved in a field of several oersted.

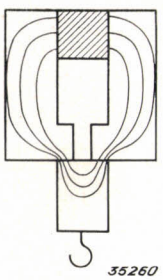

Fig. 3. Principle of the construction of a magnet with great lifting power. The magnet steel is shaded.

In *fig. 3* the principle of the construction is shown. The magnetically hard material is shaded while the soft material is left white. The surface of contact between the pole pieces and the armature is made as small as possible; it must, however, remain large enough to cause practically the whole flux to pass through the armature and not through the air gap between the pole pieces. This air gap may not be made arbitrarily wide, but must be so narrow that the magnet retains its full strength upon pulling off the armature [1]).

When the dimensions of the air gap and the surface of contact of the armature are determined, the optimum dimensions of the magnet steel can also be determined. The cross section must be sufficiently large to magnetize the armature to the optimum value, while the length must be so great that the remanence of the magnet upon pulling away the armature does not fall too suddenly. These two requirements, however, as well as the above mentioned factors concerning the proportions of air gap and surface of contact, cannot be expressed directly in formulae so that it is impossible to calculate the optimum dimensions. It is better to determine them experimentally.

Fig. 4 shows how this is done. Two rectangular pieces of cobalt-iron 4 mm thick were separated by a copper foil 0.1 mm thick. These pieces were clamped in a frame of V2A steel, and the whole

[1]) If L is the length of the magnetically hard material and l the width of the air gap, then upon pulling away the armature there occurs in the steel a demagnetizing field $H_i = Bl/L$. (See A. Th. van Urk, Philips techn. Rev. **5**, 29, 1940). l must be made so small that this field causes practically no decrease in the remanence.

soldered together with solder having a high melting point to give a strong unit.

A groove was then cut as shown in fig. 4*b*. The most favourable apex angle of the V-shaped groove was studied experimentally and amounts to about 60°.

The upper part of the groove, in which the magnet steel will be inserted later, was temporarily closed with a suitable piece of V2A steel in order to be able to heat it without deformation.

The magnet steel is now introduced (fig. 4*c*), and when in position magnetized by holding it in the field of an electromagnet. The V2A steel is then ground away from the lower side, and determinations of the force of attraction for armatures of different shapes are begun. With a sufficiently great length of air gap (copper foil) this is at first only slight. By grinding off thicker and thicker layers from the under side (if necessary with heat treatment between successive grinding processes in order to remove tensions) the length of air gap at which the attractive force is a maximum can be determined experimentally. Fig. 4*d* gives the form finally reached.

As may be seen from the figure, the piece of magnet steel bears absolutely no load. The cube which is ground beautifully smooth, is so loose in the groove that it can le pushed away with a pencil. Nevertheless it is of course responsible for the flux which causes the force between the pole pieces and the armature.

The ratio obtained of 3 500 between lifting power and weight would have been considered unattainable several years ago. The experiments which were carried out in the development of the magnet described, however, confirm the impression that the result obtained by no means represents an upper limit, and that twice this ratio could be reached if the experiments were continued [2]). Although the construction and the material of the pole pieces contribute very much to the attainment of this favourable result, it may nevertheless be said that the progress which has become possible in recent years is mainly to be ascribed to the improvement in magnet steel. A simple estimation shows that with equal care in construction with a carbon steel less than one tenth of the ratio would be reached which is obtained with the modern steel.

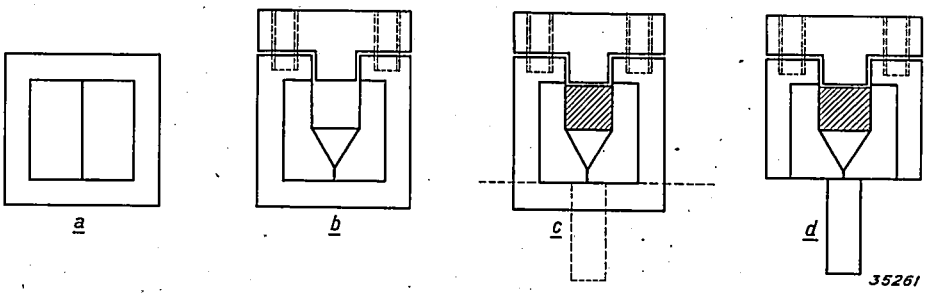

Fig. 4. Construction of the magnet shown in fig. 2.
a) Two pieces of cobalt-iron, separated by a copper foil, are soldered into a frame of V2A steel.
b) A groove is cut in the piece, which will later contain the magnet steel. The groove is temporarily closed with a small piece of V2A steel and the whole is heated to free it of tensions.
c) The piece of magnet steel is inserted. The whole is magnetized in the field of an electromagnet, and with different armatures the force of attraction is determined which is obtained after grinding away the lower part of the frame of V2A steel.
d) More and more material is ground away on the lower side until the lifting power has reached a maximum.

[2]) In the meantime a ratio of 5 000 was obtained with another construction. The absolute lifting-power, too, in this case was considerably increased *viz.* 65 kg with a weight of magnet-steel of only 13 g.

THE USE OF SELENIUM VALVES IN RECTIFIERS

by D. M. DUINKER.

621.314.634

Due to the danger of breakdown or overheating, the voltage and current, respectively, on a blocking-layer valve are limited. In this article these limits are derived by means of the dynamic characteristics of the valves, with special reference to the selenium valves manufactured by Philips. The allowable peak voltage in the blocking period amounts to 35 volts. From this follows the permissible transformer voltage in various rectifier connections. The allowable direct current can be read off from a graph for different form factors; it amounts to 4.4 to 6.6 amp. for selenium valves of 90 cm² effective surface with cooling plates. The connection of valves in series and in parallel is discussed. From the properties of the valves (counter EMF and resistance) the external characteristic of the rectifier can be derived. This is explained by means of examples and one practical example is treated numerically.

The construction and operation of blocking-layer valves, in particular the selenium valves manufactured by Philips, has already been dealt with in this periodical [1]). Since these valves, compared with mercury-cathode valves and hot-cathode valves, have the advantage that they need no attention at all when in operation and are always ready for use, they are particularly suitable in rectifiers for the supply of telephone mains and other signaling arrangements. In addition to this, in rectifiers for all other purposes such as the charging of accumulator batteries, galvanic chromium plating, etc. blocking-layer valves are being more and more commonly used.

In designing a rectifier one begins with the requirement that it shall be able to give a certain current and voltage. The number of valves, necessary for taking care of this, is determined by the maximum voltage and current values permissible for one valve. In the following we shall consider the selenium valve in this respect, and, more generally, its application in different rectifier connections.

In order to make clear the restrictions set to the voltage and current of a blocking-layer valve, we must recall the construction of such valves. They are built up of a semi-conductor and a metal, between which there is a thin insulating or blocking layer (*fig. 1*). Such a combination has the property that an electric current experiences a greater resistance in the direction from the metal to the semi-conductor ("blocking direction") than in the opposite direction ("transmitting direction"). In the case of selenium valves a layer of selenium deposited on a metal base plate is used as semi-conductor. By a heat treatment the blocking layer is formed on the free surface of the selenium; upon this, as metal, an alloy is finally spread which must have a lower melting point than selenium. One or more connecting wires are soldered to the metal layer, while a second contact is connected to the base plate.

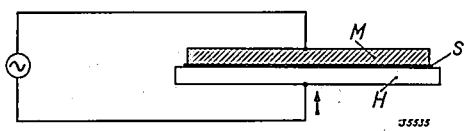

Fig. 1. Diagram of a blocking-layer valve. *M* metal, *S* insulator (blocking layer, with a thickness of the order of magnitude of 10^{-5} cm), *H* semi-conductor. The arrow indicates the transmitting direction.

The limits of the load on the valve are now determined by the fact that with too high a voltage a breakdown of the blocking layer occurs, while with too high a current too great heating, and thus fusion of the alloy used occurs. Although neither of these two phenomena need make the valve immediately useless, it will nevertheless be clear that they should be avoided as far as possible.

The current-voltage characteristic

The limits mentioned for the current and voltage will be derived in the following with the help of the current-voltage characteristic of the valve, the principle of which is illustrated in *fig. 2*. In the ideal case the resistance in the transmitting direction is zero and in the blocking direction infinite, *i.e.* the ideal characteristic coincides with the upper vertical and left-hand horizontal coordinate axes. Actually a small current also flows in the blocking direction; this "leakage current", however, increases at first very slowly, but from a certain voltage on, very rapidly with increasing voltage, which indicates that with a slight further increase of the voltage breakdown will occur. This voltage may be taken as the permissible limiting value. In the transmitting direction also the characteristic deviates from the ideal, due to the fact that the resistance

[1]) W. Ch. van Geel, Blocking layer rectifiers, Philips techn. Rev. 4, 100, 1939. In this article we shall use the term "rectifier" for a complete arrangement and shall indicate the rectifying element of the circuit by the term "valve".

does not become exactly zero. The energy consequently lost as heat in the valve causes the above-mentioned rise in temperature which increases

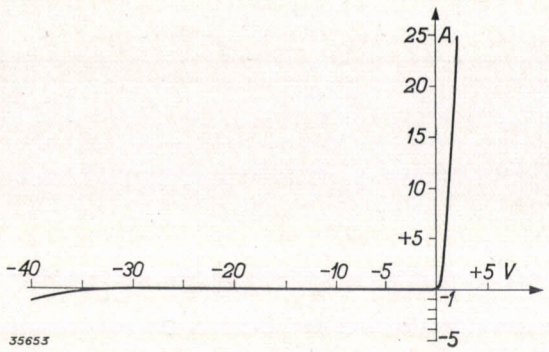

Fig. 2. Current-voltage characteristic of a selenium valve. In the ideal case the characteristic coincides with the left-hand and upper vertical coordinates.

with the current. If the relation between the losses in the valve and the rise in temperature is known (determined by the cooling), the permissible losses can be determined, and from that, by a method to be discussed later, the permissible current can be determined with the help of the current-voltage characteristic.

We have continually spoken of "the" characteristic, and one might thus be inclined to think of a relation obtained by the successive application of different voltages and measurement of the current in each case. The current values given by such a "static" characteristic may, however, differ appreciably from those occurring during operation. Upon application of a voltage in the blocking direction the current reaches a final value [2]) only slowly, which value — aside from its being reproducible only with difficulty — will certainly not correspond to the momentary value occurring upon the application of a rapidly alternating voltage. The characteristic for the transmitting direction will also be different with static measurement than during operation of the valve, when transmitting and blocking states alternate with each other. It is therefore necessary to record the characteristics of valves under conditions as far as possible like normal operating conditions. The most suitable method for this is with the cathode-ray oscillograph, by means of which the desired "dynamic" characteristic (relation between the momentary values [3]) of current and voltage) can be made directly visible. The connections used for this are given in *fig. 3*. It must here be noted that it is not possible to record the characteristic for blocking and transmitting directions simultaneously. If the deviations from the ideal case, with which we are here concerned, are to be made visible on a reasonable scale, a small scale for the voltage and a large one for the current are needed for the blocking direction, where the voltages are high and the currents low, and for the transmission direction, just the opposite. It is therefore desirable for practical reasons to record the two parts of the characteristic separately. The way in which this is done is explained in the text under fig. 3.

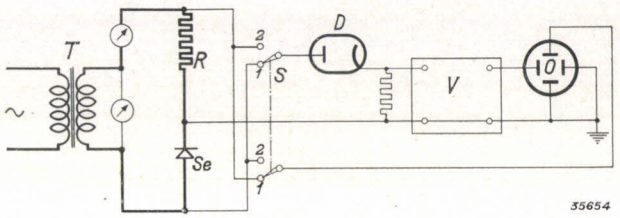

Fig. 3. Connections for recording the dynamic characteristic of selenium valves. The valve *Se* is fed from the transformer *T* and loaded with the (induction-free) resistance *R*. Blocking and transmitting characteristics cannot be recorded at the same time, since quite different scales are required. For the transmitting characteristic the switch *S* is set at *1*. The voltage on *R* is hereby conducted to the plates for vertical deflection of the cathode ray oscillograph *O*, so that the vertical deflection is proportional to the valve current. The valve voltage, after the diode *D* has suppressed the high voltage peaks in the blocking direction, is amplified with the amplifier *V* and applied to the plates for horizontal deflection. For the blocking characteristic *S* is set in position *2*. The (high) blocking voltage on *Se* now acts directly on the plates for vertical deflection, the voltage decay along *R* is conducted to *V via* the diode *D*. The diode now transmits only the low voltage on the resistance *R*, which is caused by the leakage current; the horizontal deflection is thus proportional to the leakage current. By connecting several valves (six, for instance) in series, a five to tenfold amplification in *V* is sufficient for obtaining a reasonable size of image. The average characteristic of the six valves is then measured.

Permissible voltage

In *fig. 4* two characteristics recorded for a Philips selenium valve for the blocking direction are shown,

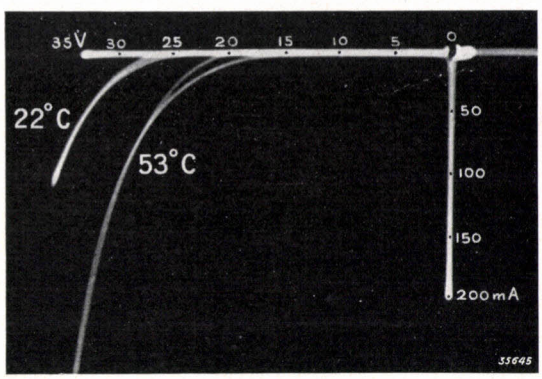

Fig. 4. Blocking characteristic of a selenium valve with an effective surface of 90 cm², at different temperatures.

[2]) See the article cited in footnote [1]).

[3]) It is clear that this relation must depend to a certain extent upon the frequency of the A.C. voltage used for the measurement, because at sufficiently low frequencies it must gradually take over the form of the static characteristic. The characteristics used in this article refer to frequencies of about 50 c/s.

as obtained at different temperatures of the valve. At the higher temperature the "leakage resistance" is found to decrease. The voltage, however, at which the leakage current begins to increase very rapidly, and above which therefore there is danger of breakdown of the blocking layer, is found to be about the same for all temperatures; it amounts to about 35 to 40 volts. The peak value of the alternating voltage on the valve may therefore be raised to about 35 volts, which may be considered a very high value for blocking-layer valves.

not be exceeded, it is advisable to make the limit for the nominal transformer voltage lower by a factor equal to the ratio of the highest mains current occurring to the nominal mains current.

If the desired D.C. voltage demands the application of higher A.C. voltages e, recourse must be had to the connection in series of a number, s, for instance, of valves. If these valves all had exactly the same blocking characteristic, the same blocking voltage would act on all the valves, since the same leakage current flows through them all. Actually,

Table I

	A	B	C	D	E	F
1	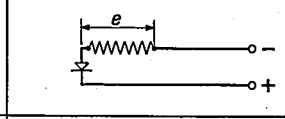	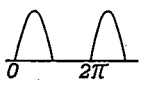	$2\sqrt{2}$	$n=$ 1	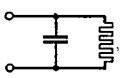	$f=$ 2 à 2,5
2	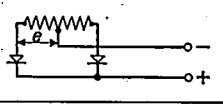	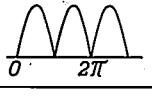	$2\sqrt{2}$	2	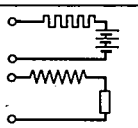	ca.2 ca.$\sqrt{2}$
3	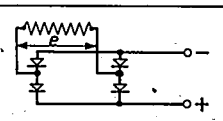	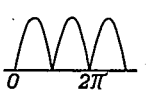	$\sqrt{2}$	2	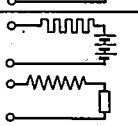	ca.2 ca.$\sqrt{2}$
4	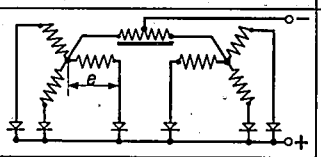	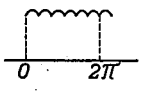	$2\sqrt{2}$	6		$\sqrt{3}$
5	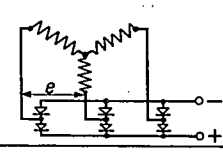	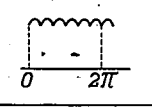	$\sqrt{2}$	3		$\sqrt{3}$

35669

In column A several customary rectifier connections are given: *1* is the simplest, single-phase connection, *2* the two-phase star connection, *3* the three-phase Grätz connection (by which the A.C. voltage is rectified in both halves of the period), *4* a six-phase rectifier with a so-called interphase transformer, *5* the three-phase Grätz connection. Column B shows the form of the rectified voltage. Column C gives the ratio between the peak voltage which acts on one valve at no-load and the effective transformer voltage (e). Columns D-F are only spoken of later on in this article. D gives the number of contributions to the current which come together at each connection terminal, which can easily be counted in the sketches of column A, column E gives several commonly occurring types of loading, F the rough values of the form factor f of the valves hereby occurring. With a larger number of phases, as in the connections *4* and *5*, the form factor does not depend so closely on the load.

From the permissible peak value, the voltage which may be applied to the valves in different rectifier connections can now be deduced. In *Table I* the relation is given for a number of ordinary rectifier connections (column A), between the peak voltage on each valve and the effective transformer voltage e (column C; for the meaning of e see the diagrams). From this it follows that for the connections *1*, *2* and *4* the permissible voltage $e = 12.5$ volts, and for connections *3* and *5* $e = 25$ volts. Since the permissible peak value of 35 volts must

however, there is always a certain divergence in the properties of the valves, so that the total blocking voltage will be divided more or less unevenly among the valves connected in series. In order to be able to keep this irregularity within narrow limits, the valves are sorted into groups after manufacture: in each group the leakage current, measured with a given voltage applied, exhibits a given maximum deviation from a mean value, characteristic of the group. By connecting in series valves of the same group only, in the most un-

favourable case one of the s valves will only have to carry a voltage about 18 per cent higher than the total voltage divided by s. This voltage must remain below the permissible value of 12.5 and 25 volts, respectively. The permissible transformer voltage e which may safely be applied to the s valves connected in series is thus $0.85 \cdot s \cdot 12.5$ volts (or $0.85 \cdot s \cdot 25$ volts).

One peculiarity must be noted when a selenium valve is used alternately at different voltages. The blocking characteristic is not unchangeable, but varies according to the magnitude of the mean blocking voltage. The lower the latter the smaller the leakage resistance [4]). The variation takes place very slowly upon lowering the voltage (the change is only noticeable after several days); upon increasing the voltage, on the other hand, it takes place relatively quickly (in a few minutes). The result is that a valve which has operated for days at a low voltage (for instance at less than $^1/_4$ of the maximum permissible voltage), and is then suddenly connected to a much higher voltage, exhibits temporarily an abnormally high leakage current. After a few minutes, however, the characteristic has become adapted, and the leakage current has sunk to the ordinary value.

Permissible current

In order to find the limit of the direct current which a valve can give, we must, as already mentioned, examine the losses in the valve. The losses are made up of two parts: the loss w_d caused by the resistance experienced by the current in the transmitting direction (effective current); and the loss w_s caused by the flow of leakage current in the blocking state. The blocking loss w_s is found to amount to only 5 to 10 per cent of the transmitting loss w_d in normal use. We shall therefore first examine only the latter.

Losses in the transmitting direction

The power ω_d dissipated in the valve can be calculated at each moment as the product of current i and voltage v_d. The average wattage loss $\overline{w_d}$ is found by integrating w_d over one period T of the supply A.C. voltage and dividing the result by T:

$$\overline{w_d} = \frac{1}{T} \int_0^T i \cdot v_d \, dt \quad . \quad . \quad . \quad . \quad (1)$$

v_d is given as a function of i by the dynamic characteristic for the transmitting direction, which is shown in *fig. 5* recorded for three different temperatures. For a given temperature and not too low

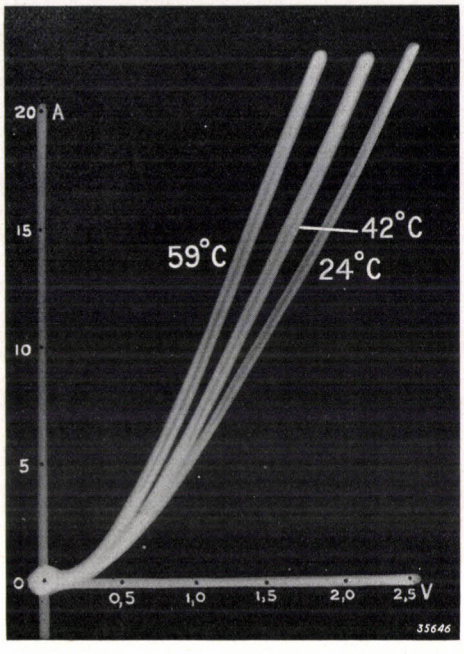

Fig. 5. Transmitting characteristic of a selenium valve (90 cm² effective surface) at different temperatures.

currents, the characteristic can be sufficiently accurately represented by:

$$v_d = v_0 + i \cdot r, \quad . \quad . \quad . \quad . \quad . \quad (2)$$

where the quantities v_0 and r, which are independent of the current, may be considered as "counter EMF" and resistance of the valve, respectively. *Fig. 6* shows how v_0 and r are determined from the characteristic recorded with the oscillograph; in the example given $v_0 = 0.9$ volt, $r = 0.07$ ohm (this value holds for a selenium valve of about 90 cm² effective surface; v_0 is independent of this surface, r inversely proportional to it).

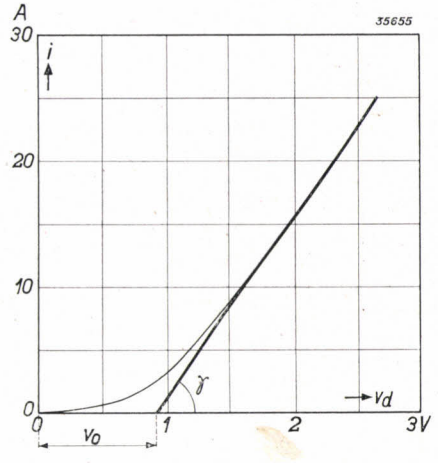

Fig. 6. The transmitting characteristic for not too small current amplitudes is approximately a straight line: the valve has, as it were, a counter EMF v_0 and a resistance r ($= \cot \gamma$).

[4]) Such a phenomenon also occurs in the case of electrolytic condensers. See W. Ch. van Geel and A. Claassen, Philips techn. Rev. **2**, 65, 1937.

From (1) and (2) it follows that:

$$\overline{w_d} = v_0 \cdot \frac{1}{T}\int_0^T i \, dt + r \cdot \frac{1}{T}\int_0^T i^2 \, dt = v_0 i + r i^2_{\text{eff}} \quad (3)$$

Here i is the average value, i_{eff} the effective value of the current rectified by the valve. Equation (3) may also be written in a somewhat simpler form by introducing the ratio between i_{eff} and i, the so-called "form factor", f, which may to some degree be considered as characteristic of the form of the current [5]):

$$\overline{w_d} = v_0 i + r f^2 i^2 \quad . \quad . \quad . \quad . \quad (4)$$

In *fig.* 7 this ratio between wattage loss and direct current is represented graphically for different form factors f. For v_0 and r the values of the example in fig. 6 are here taken.

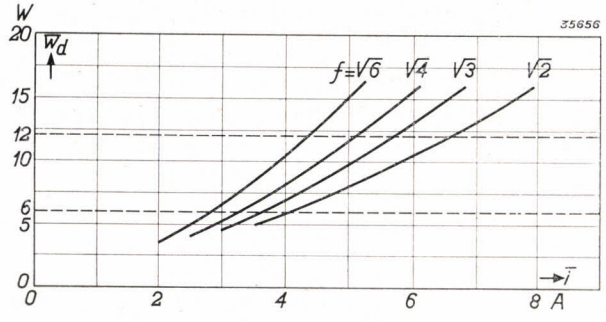

Fig. 7. Wattage loss $\overline{w_d}$ in the transmitting direction as a function of the mean direct current $\bar{i}$, calculated according to formula (4) for different values of the form factor f as parameter.

Permissible dissipation in the valve

What now is the value of the direct current i with which the valve may be loaded? In order to discover this we must know the relation between the losses in the valve and the rise in temperature which they cause. This relation, which naturally depends upon the method of cooling the valve, has been determined experimentally and is given in *fig.* 8 for valves *a*) without special provision for cooling, and *b*) with cooling plates (see *fig.* 9). The permissible temperature of the valves has been determined to be 65 °C with a reasonable margin

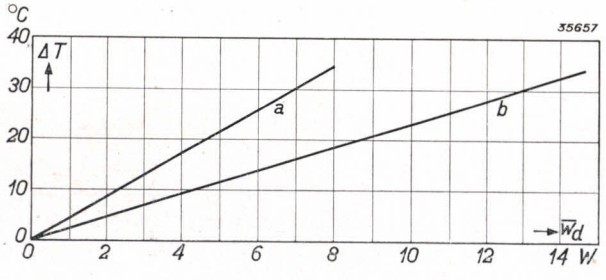

Fig. 8. Rise in temperature ΔT of a selenium valve (90 cm² effective surface) mounted in the ordinary way, as a function of the energy dissipated; *a*) without cooling plates, *b*) with cooling plates (aluminium, 20 × 20 cm, 2 cm thick).

[5]) The form factor is always larger than unity and usually lies between 1.4 and 2.5; for flattened curves it is lower than for pointed ones.

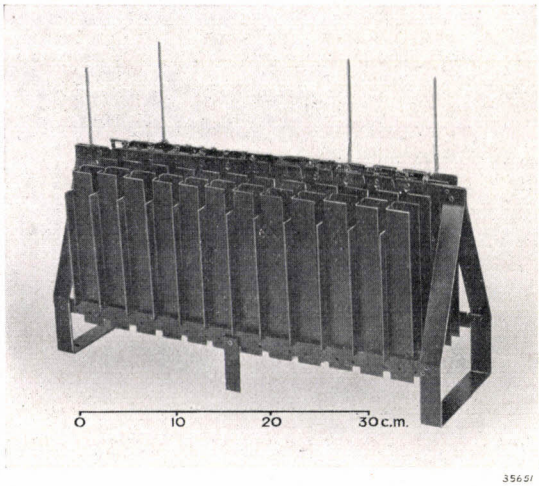

Fig. 9*a*. Valves (with cooling plates) of a Grätz rectifier according to table I, 3. Where each valve stands in the diagram there is a group of three selenium valves (90 cm² surface) in series; thus $s = 3$, $p = 1$. With this rectifier 21 cells of a lead accumulator in series can be charged with a maximum charging current of 10 amp.

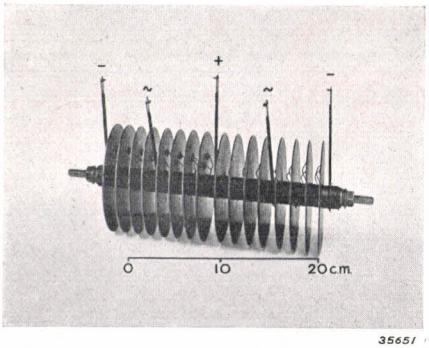

Fig. 9*b*. Valves (without cooling plates) of a similar Grätz rectifier; here, however, $s = 4$, $p = 1$. 28 lead cells in series can be charged with a maximum current of 6.5 amp.

of safety. With an arrangement such that the air flowing along the valves has not been pre-heated by any other source of heat, a maximum initial temperature of 35 °C in non-tropical countries may be assumed, so that the rise in temperature due to the losses may amount to 30° C. According to fig. 8 this corresponds to a loss of 13 watts without cooling plates. From these limits for the permissible loss $\overline{w_{d_{\max}}}$, the permissible direct current $\bar{i}$ through the valve may be found with different forms of current (form factors f) by finding the point of intersection of the curves drawn in fig. 7 with the line $\overline{w_d} = \overline{w_{d_{\max}}}$ (this line actually lies somewhat lower than 7 and 13 watts, respectively, as we shall see in the following).

The values of v_0 and r by which the shape of the curves in fig. 7 is determined, still depend very much upon the temperature, as was indeed to be concluded from the appreciable difference between the three characteristics of fig. 5. Because of this dependence on temperature — in *fig. 10* the limits are given between which may lie the values of v_0 and r, which are quite different for different valves — the curves of fig. 7 are actually valid only for one temperature, which would have to be provided for the valve artificially by making different cooling conditions for every value of $\bar{i}$. The method described of determining the permissible value of $\bar{i}$, gives the correct result when the curves are drawn specially for the temperature 65 °C. This temperature is just reached with a dissipation $\overline{w_d}_{\max}$ with the cooling conditions present when the valve is in use.

The values of v_0 and r chosen for fig. 7 are somewhat larger than ever occur at 65 °C (see fig. 10). At smaller values of v_0 and r according to (4), $\overline{w_d}$ will only reach the value $\overline{w_d}_{\max}$ at a larger value of $\bar{i}$. The permissible direct current values at $\overline{w_d}_{\max}$ read off from fig. 7 are therefore on the safe side.

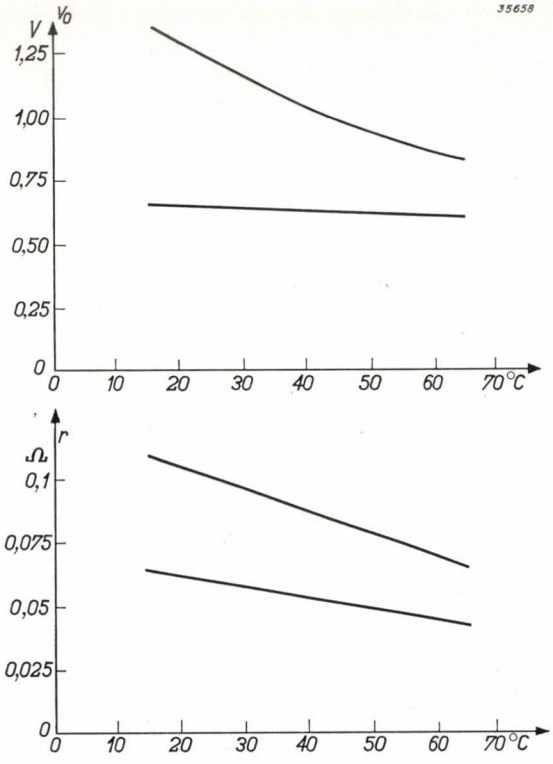

Fig. 10. Counter EMF v_0 and resistance r of selenium valves as a function of the temperature. The values of r are for 90 cm² effective surface (v_0 is independent of the surface). The two curves indicate approximately the extreme values occurring.

Losses in the blocking direction

A correction must now be introduced into these considerations because of the energy loss w_s due to the leakage current. An equation similar to (1) holds in this case:

$$\bar{w}_s = \frac{1}{T}\int_0^T i_l \cdot v_s \, dt, \quad . \quad . \quad . \quad . \quad (5)$$

where i_l is the leakage current and v_s the blocking voltage. The variation of i_l as a function of v_s is given by the blocking characteristic (fig. 4). It is not as easy to express this in a formula as was the case with the transmitting characteristic. It is therefore simpler to plot the momentary values $w_s = i_l v_s$ as a function of the time and to integrate graphically or planimetrically.

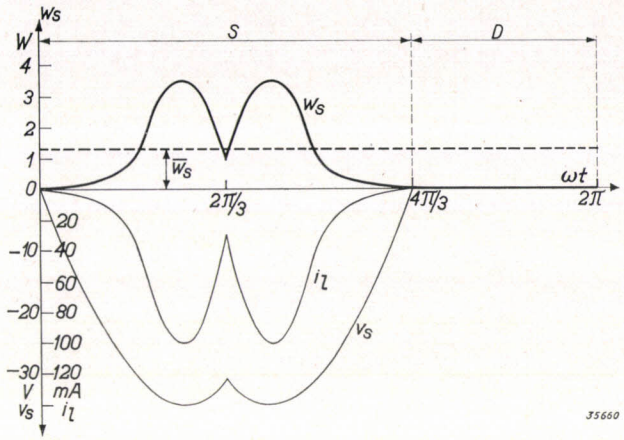

Fig. 11. Variation of the blocking voltage v_s on a valve in the three-phase Grätz connection (5 in table I). With the help of the blocking characteristic (fig. 4) the variation of the leakage current i_l may be calculated from this, and by multiplication of v_s with i_l the variation of the energy dissipated w_s can be constructed; $\bar{w}_s$ is the mean value of this wattage loss, S blocking interval, D transmitting interval.

If we first consider the no-load state, the blocking voltage v_s is given at every moment by the no-load voltage of the transformer. The variation of v_s is thus known for every connection. In *fig. 11*, for example, the variation of v_s is given for the connection 5 in table I (so-called three-phase Grätz connection). With the help of the leakage current with time, i_l can be constructed from this. The variation of i_l can of course also be recorded directly, with the help of an oscillograph (*fig. 12*). By multiplying the momentary values of v_s and i_l by each other, the variation of the blocking loss

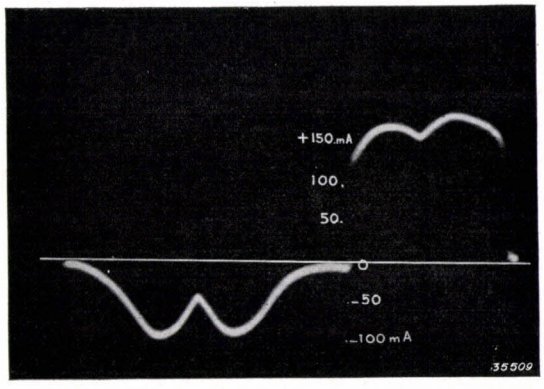

Fig. 12. Oscillogram of the leakage current for the case dealt with in fig. 11. The current agrees satisfactorily with that indicated in fig. 11.

$\overline{w_s}$ may be found (see fig. 11), the average value of which, $\overline{w_s}$, may be determined by integration. In the example of fig. 11 at $e = 25$ volts (the maximum permissible voltage) $\overline{w_s} = 1.3$ watts. In the case where $e = 21$ volts one finds only $\overline{w_s} = 0.6$ watt. The great difference may easily be understood from the rapidly accelerated growth of the leakage current at the highest permissible voltages (fig. 4).

When the rectifier is loaded the blocking loss is less than with no load, due to the voltage loss caused in the valves when they are just in the transmitting period, and sometimes in impedances connected in front of the valves (we shall return to this later) by the loading current in the transformer. We are therefore perfectly safe if we calculate a value of, for instance, 1 watt for the blocking losses $\overline{w_s}$ during operation. By subtracting this energy from the permissible dissipation found from fig. 8, we finally obtain for the permissible loss in the transmitting direction, at a maximum air temperature of 35 °C, $\overline{w_d} = 12$ watts (with cooling plates) and 6 watts (without cooling plates).

The direct current obtainable

With these values of $\overline{w_d}_{\max}$ we now find in fig. 7 as permissible direct current $\overline{i}_{\max}$ for a valve of 90 cm² surface, according to the form factor f ($\sqrt{6} > f > \sqrt{2}$), a value between 4.4 and 6.6 amp. (with cooling plates) and between 2.8 and 4.1 amp. (without cooling plates). The total average current $\overline{I}$ which a rectifier in one of the connections of table I can give is found by multiplying $\overline{i}_{\max}$ by the number of contributions to the current n which come together at the positive or negative terminal of the external connection. This number, which can easily be counted in the sketches of column A, is given in column D of table I. In column F are given several approximate values of the form factor f in the connection in question and with the type of load sketched in column E.

If a direct current $\overline{I} > n\,\overline{i}_{\max}$ is required, then in the place of every valve in the connection used p valves must be connected in parallel. Just as when the valves are connected in series, the irregularity in the distribution of the current among the p valves must here also be taken into account. Here also the irregularity is limited by sorting the valves after manufacture into groups in which the voltage loss v_d measured at a given current i deviates by a few per cent at the most from a mean value. When valves of the same group only are connected in parallel, in the most unfavourable case one of the p valves has to take up a current about 18 per cent higher than the total current divided by p. By making this equal to the permissible maximum it is found that the current obtainable with p valves amounts to $0.85 \cdot p \cdot \overline{i}_{\max}$.

It must still be noted that the permissible direct current derived from fig. 7 is for selenium valves in continuous operation. With intermittent loading higher values are permissible, since the limitation is only a question of temperature. The heat capacity of the valve is then also of influence.

The above-mentioned phenomenon of a temporarily diminished "leakage resistance" upon switching a selenium valve to a high voltage after a long period of operation at a low voltage is also accompanied by a temporary increase in the blocking loss. In such a case therefore it is advisable, in order to prevent overheating, to wait a few minutes before changing over to full current load.

The external characteristic of rectifiers

We have shown in the foregoing, how, from the maximum permissible blocking voltage, the transformer voltage is derived to which a given arrangement of valves can be connected. How high must the transformer voltage be chosen to obtain the required D.C. voltage? To find this the voltage loss in the whole circuit, particularly that in the valves themselves, must be taken into account. This voltage loss, and with it the D.C. voltage obtained, varies with the rectified current (equation (2)). For many applications it will be important to know the relation between the D.C. voltage delivered and the direct current produced. This relation, the so-called external characteristic, may be affected by the connection in series of suitable impedances, and adapted to the purpose for which the rectifier is used.

We shall explain some of these points by means of a few examples.

Three-phase Grätz connection

In the rectifier connection *fig. 13a* (No. 5 of table I) the three coupled voltages of a three-phase main are rectified in both the positive and negative half of a period, so that a D.C. voltage with a six-phase ripple occurs at the output terminals (fig. 13*b*). Each of the six sine tops has a maximum at $e_0 = e\sqrt{2}$ and a width $\pi/3$, so that the average D.C. voltage becomes:

$$\overline{U}_0 = 6 \cdot \frac{1}{2\pi} \int_{\pi/3}^{2\pi/3} e_0 \sin \omega t \, \mathrm{d}(\omega t) = \frac{3}{\pi} e_0 \,. \quad (6)$$

This expression holds for the case where the possible counter EMF of the load is never greater than U_0 at any moment. If it were greater, the valve just about to come into action would be in the

blocking state instead of in the transmitting state, and we would not be able to integrate over the whole sine peak. If we exclude this case, *i.e.* if the counter EMF is always smaller than $e_0 \sin \pi/3$, it would follow from (6) that the D.C. voltage is independent of the current $\bar{I}$. No account is here taken of the internal voltage loss in the valves, however. (The voltage loss in the transformer may here be neglected).

In the position of every valve in fig. 13*a* there may be a group of p branches in parallel each having s valves in series. Since equation (2) is valid for each valve, it is easy to see that the relation between the momentary value of the voltage v and the current i through such a group is given by:

$$v = s\left(v_0 + i\frac{r}{p}\right), \quad \ldots\ldots \quad (7)$$

where v_0 and r are the average counter EMF and approximation formula (2) and (7) used for the dynamic transmitting characteristic of the valves can only be applied with sufficiently high current, for instance $i > 7$ amp. in the figure (more generally with a current density greater than about 80 mA/cm²). With smaller currents the voltage loss in the valve is smaller than that given by the formulae, and consequently the external characteristic in fig. 13*c* will also deviate from a straight line according to (8) at small loads, and will vary according to the broken-line curve.

Single-phase Grätz connection

For charging accumulator batteries the simpler Grätz connection *fig. 14a* is often used (No. 3 in table I), with which a single-phase alternating current is rectified in both halves of the period. The rectified voltage (fig. 14*b*) here consists of two

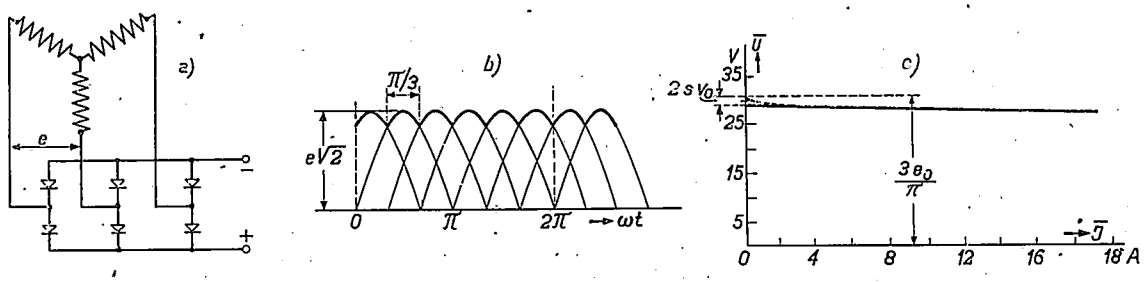

Fig. 13. *a*) Rectifier in three-phase Grätz connection (5 in table I).
b) The D.C. voltage delivered consists of the tops of six sine curves with maxima $e_0 = e\sqrt{2}$, and $\pi/3$ in width. The lowest value of the voltage occurring is $e_0 \sin \pi/3$.
c) External characteristic: mean D.C. voltage $\bar{U}$ as a function of the mean direct current $\bar{I}$ given. For the valves it is assumed that $v_0 = 0.6$ volt and $r = 0.05$ ohm. Transformer voltage $e = 22.5$ volts.

resistance of one valve. In the connections of fig. 13*a* the direct current always flows through two valve groups in series and there causes a voltage loss $\Delta U = 2\,s\,(v_0 + I\,r/p)$. The average D.C. voltage is thus actually:

$$\bar{U} = \frac{1}{2\pi}\int_0^{2\pi} (e \sin \omega t - \Delta U)\, \mathrm{d}(\omega t) =$$

$$= \bar{U}_0 - 2s\left(v_0 + \frac{r}{p}\bar{I}\right) = \left(\frac{3}{\pi}e_0 + 2\,sv_0\right) - 2\frac{s}{p}r\bar{I} \quad (8)$$

In fig. 13*c* this relation is represented. The rectifier behaves, as far as direct current and D.C. voltage delivered are concerned, like a source of voltage with the EMF $3e_0/\pi - 2\,sv_0$, and the internal resistance $2\,sr/p$ (when we neglect the resistance of transformer and connections).

Fig. 13*c* is drawn to scale for the case where $p = 1$, $s = 1$, $v_0 = 0.6$ volt, $r = 0.05$ ohm, $e = 25$ volts. As could be seen from fig. 6, however, the half sine curves $e_0 \sin \omega t$. In this case, due to the fact that the voltage periodically falls back to zero, we have just the case which was excluded in the first example, namely that due to the counter EMF U_t in the circuit, the charging current can only flow as long as $e_0 \sin \omega t > U_t$. If R_t is the total resistance of the circuit the momentary value of the current is given by:

$$I = \frac{e_0 \sin \omega t - U_t}{R_t} \quad \ldots\ldots \quad (9)$$

The average value of the charging current is found by integration:

$$\bar{I} = 2 \cdot \frac{1}{2\pi}\int_{\alpha}^{\pi-\alpha} I\, \mathrm{d}(\omega t),$$

where α indicates the moment when I becomes zero, thus $\sin \alpha = U_t/e_0$.

The essential difference from the first example

is therefore that the limits of integration depend upon the method of loading (the counter EMF U_t). Integration gives:

$$\overline{I} = \frac{2e_0}{\pi R_t}\left(\sqrt{1-\left(\frac{U_t}{e_0}\right)^2} - \frac{U_t}{e_0}\cos^{-1}\frac{U_t}{e_0}\right) \quad . \quad (10)$$

The relation thus found between $\overline{I}$ and U_t, the charging characteristic of the rectifier, is graphically represented in fig. 14*c*; in order to make the curve generally valid the unnamed numbers $\overline{I}\,\pi\,R_t/2e_0$ and U_t/e_0 are plotted.

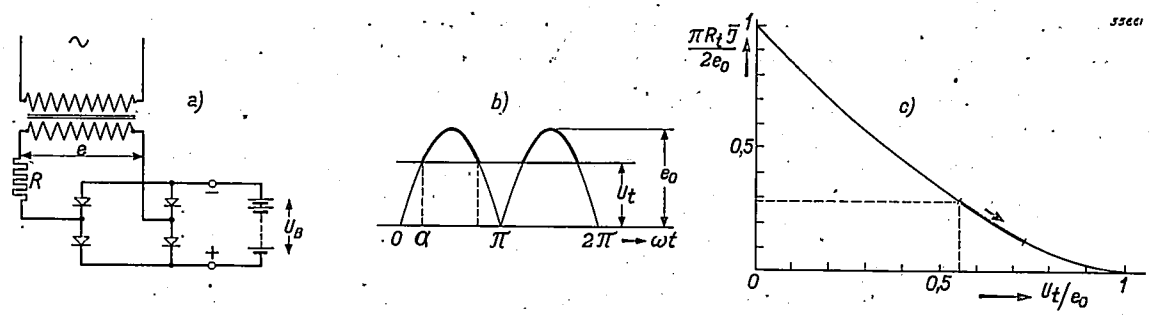

Fig. 14. *a*) Charging rectifier in single-phase Grätz connection (3 in table I). The series resistance R, by which the charging current is reduced to the desired value, can be situated either on the alternating current side (as here indicated) or on the direct current side. The former connection has the advantage that in operation the full transformer voltage $e_0 \sin \omega t$ does not act as blocking voltage on the valves, but only that voltage diminished by the voltage loss in R. This also makes the leakage current smaller.
b) Variation of the rectified voltage. Charging current is delivered only at moments when $e_0 \sin \omega t$ is larger than the counter EMF U_t in the circuit (this is mainly the voltage of the battery to be charged).
c) Charging characteristic (relation between average charging current $\overline{I}$ and counter EMF U_t (battery voltage). The quantities $\overline{I}\,\pi\,R_s/2e_0$ and U_t/e_0 are plotted. If it is required that with an increase in the counter EMF in the ratio 2.7 : 2.0 a decrease in the charging current to one half shall take place, the part of the characteristic indicated by a heavy line must be used, with an abscissa of 0.56 and an ordinate of 0.28 at the beginning. The required value of e_0 and R_t can be calculated from this.

What value must now be chosen for the transformer voltage (e_0) and the circuit resistance (R_t) in order to have the charging proceed as desired? The counter EMF U_t consists chiefly of the battery voltage U_B, which increases gradually during charging (with lead accumulators from about 2.0 to 2.7 volts per cell), so that according to fig. 14*c* the charging current falls. Now it is desirable on the one hand to begin with a high charging current in order to keep short the total time necessary for charging, while on the other hand it is desirable that toward the end of the process of charging, the current is automatically — *i.e.* without it being necessary to change e_0 and R_t — so decreased that the accumulator plates are not injured by excess gas development. In practice it is found that both requirements can be met when the initial and final currents are in the ratio 2 : 1. It follows from the charging characteristic that for this to be true, with a ratio 2.7 : 2.0 between the counter EMF at the end and that at the beginning, the abscissa at the beginning must be

$$U_t/e_0 = 0.56 \quad . \quad . \quad . \quad . \quad . \quad . \quad (11)$$

and the ordinate:

$$\pi R_t\,\overline{I}/2e_0 = 0.28 \quad . \quad . \quad . \quad . \quad . \quad (12)$$

Now we have seen in the first example discussed (equation (8)) that the valves give a counter EMF $2\,sv_0$ (the charging current passes through two valve groups in series each time) which is added to the battery voltage U_B; therefore

$$U_t = U_B + 2\,sv_0 \quad . \quad . \quad . \quad . \quad . \quad (13)$$

Furthermore the internal resistance of the two groups of valves is $2\,sr/p$, therefore

$$R_t = R + 2\,sr/p \quad , \quad . \quad . \quad . \quad . \quad . \quad (14)$$

when R is the remaining circuit resistance, *i.e.* the series resistance plus the resistance of the transformer, the connections, etc.

With the help of equations (11) to (14) and the required charging current, e_0 and R_t can now be calculated. Assume that a battery of 24 lead cells in series must be charged with a rectifier for which $p = 1$ and $s = 4$; for the selenium valves, v_0 may be 0.6 volt and $r = 0.05$ ohm. The charging current $\overline{I}$ must be 10 amp. at the beginning and 5 amp. at the end. Equation (13) gives $U_t = 24.2 + 8 \cdot 0.6 = 52.8$ volts. From this with equation (11): $e = e_0/\sqrt{2} = 52.8/0.56 \cdot \sqrt{2} \approx 67$ *volts*. Furthermore equation (12) gives: $R_t = 0.28 \cdot 2 \cdot 67 \cdot \sqrt{2}/\pi \cdot 10 = 1.69$ ohms. Finally with the help of equation (14)

one finds: $R = 1.69 - 8 \cdot 0.05 \approx 1.3$ *ohms*. If the internal resistance of the transformer, etc. is subtracted from this, the resistance is obtained which must be connected in series.

If we apply to this numerical example the consideration about the permissible voltage on the valve, we see that the rectifier was generously proportioned in this respect. The blocking voltage e acts on $s = 4$ selenium valves in series; according to the above discussion e may here reach the value $0.85 \times 4 \times 25 = 85$ volts. With the value of 67 volts to be chosen there is a generous margin of safety for mains voltage fluctuations. As to the current in this example where $p = 1$ and $f \approx 2$ (see table I), the current per valve group with cooling plates may amount to about 5.1 amp., (fig. 7), the total direct current $\overline{I}$, therefore, to 10.2 amp. (because $n = 2$, see table I). The desired initial charging current of 10 amp. is therefore just permissible.

From these examples it will be clear how the properties of the selenium valves are taken into account in designing a rectifier.

MEASUREMENT OF PHASE ANGLES WITH THE HELP OF THE CATHODE RAY TUBE

by W. NIJENHUIS.

621.317.3:621.385.832

Various methods are used for the measurement of phase angles between two voltages. Several of these methods are discussed briefly. A new method is then described which permits rapid and easy measurement, which covers the whole region from 0 to 360° and with which an accuracy of 2° can be attained. In this method the phase difference is measured by the difference in position of a luminous semi-circle on the screen of a cathode ray tube. The manner is described in which the circular motion of the fluorescent spot and the sharp limitation of the semi-circle, required for reading off the results, is obtained. The apparatus constructed in the Philips laboratory can be used for voltages of 6 mV to 3 V and for frequencies from 100 to 100 000 c/s. In conclusion a few sources of possible error in measurement are discussed.

In many alternating current problems phase angles, either between current and voltage in an impedance or between input and output voltages in the case of quadripoles, etc., play an important part. In high current technology the significance of the phase angle in the form of the work factor is well known. As to low current technology, we may refer to telephony, where phase shifts caused by transmission lines may affect the intelligibility (phase distortion [1])); to television where the video-frequency signals must be transmitted strictly true to phase; and finally to radio and amplifier technology where phase problems are continually to be dealt with. An instructive and less generally familiar example of such a problem is discussed in the present number of this periodical [2]), namely the influence of the phase angle of a loud-speaker impedance on distortion and output of an output amplifier valve.

How are such phase angles measured? As long as it is a question of determining the phase angle of a complex impedance, bridge connections can be used with which the real and imaginary parts of the impedance can be measured separately. For the more general case where the phase of a given alternating current or A.C. voltage is required with respect to another current or voltage there are numerous methods. We shall here describe a method worked out in this laboratory which makes use of a cathode ray tube. For a better understanding, however, it is first desirable to give a brief survey of several other methods used until now, in which a cathode ray tube was also used.

Various methods of measurement

A very simple determination of phase shifts is made possible by the use of an electron switch [3]). By this means the variation with time of two voltages (or currents) can be made visible simultaneously on the screen of a cathode ray oscillograph (*fig. 1*), so that the relative phase shift — difference in time between corresponding points — can be measured directly. The accuracy is in this case naturally limited. The error may amount for instance to from 5 to 10°.

Other methods work with Lissajous figures: the two voltages are applied to the two sets of deflection plates of a cathode ray tube. If the frequencies of

[1]) See for instance Philips techn. Rev. 4, 20, 1939.

[2]) A. J. Heins van der Ven, Philips techn. Rev. 5, 193, 1940.

[3]) Philips techn. Rev. 4, 267, 1939.

the two voltages, assumed to be purely sinusoidal are in a simple ratio — only in that case may we speak of a constant relative phase shift — a stationary Lissajous figure appears on the screen;

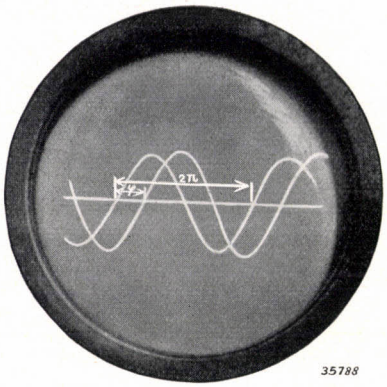

Fig. 1. With the help of an electron switch the variation with time of two quantities, for instance two voltages, can be shown simultaneously on the screen of a cathode ray oscillograph, so that the relative shift φ can be measured directly.

in the simplest case, when the two voltages have the same frequency, it is an ellipse. From the form of the ellipse the phase angle can be deduced (*fig. 2a*). In practice use may be made of a stencil upon which a series of ellipses for different phase angles is drawn (fig. 2*b*); this stencil is laid on the fluorescent screen, and the required phase angle is found by interpolation. The accuracy of this method, however, is not very high. Moreover it covers a measuring region of only 180°, since the ellipses are repeated for larger angles. Instead of applying the two voltages directly to the deflection plates, the method can be made more sensitive by first deriving from one of them a voltage with a frequency eight times as great (see fig. 3). This is done, however, at the expense of the size of the measuring region. The Lissajous figure produced repeats the same series

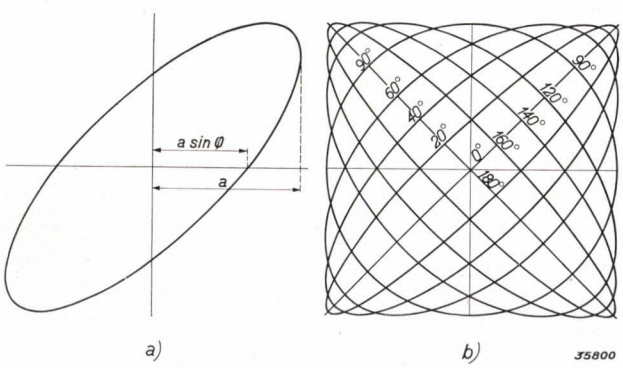

Fig. 2. *a*) From the shape of the ellipse which occurs on the screen with a phase shift φ of the two deflecting voltages of a cathode ray tube, the angle φ can be derived.
b) With the help of a stencil on which a series of ellipses are drawn the angle φ can be determined by interpolation.

of shapes every $180/8 = 22^1/_2°$, so that the method can only be used when it is a question of a small range of angles.

An interesting possibility of measuring a phase angle is offered by a cathode ray tube in which the two directions of deflection of the electron beam are not always perpendicular, but can be adjusted to any desired angle. Such a tube can be realized by using for deflection two magnet coils placed against the neck of the tube (as is customary in television tubes [4])), one of which coils can be rotated through an angle α, which can be read off with respect to the other. If a current $i_0 \cos \omega t$ flows through the first coil, and through the second a current $i_0 \cos (\omega t + \varphi)$, in general an ellipse appears on the screen, whose character depends upon φ and the angle α, and which for $\alpha = \pi + \varphi$ passes over into a circle. The required angle φ is thus found as the (positive or negative) supplement of the angle α at which the movable magnet coil must be set in order to obtain a true circle on the fluorescent screen. This criterion permits quite a sharp setting, so that a measurement of φ is possible with an accuracy of a few degrees. The ranges of distinguishable angles is here also only 180° (because φ and $-\varphi$ lead to the same angle α).

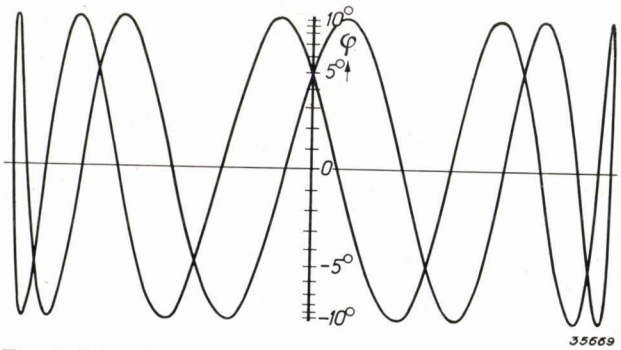

Fig. 3. Lissajous figure obtained by the deflecting voltage sin 8 ωt and sin $(\omega t - \varphi)$; the angle φ can be read off on the scale. In this case $\varphi = 5°$.

Principles of the new method

Just as in the last method described, in the method worked out in this laboratory the phase difference is also directly visible as an angle, but in contrast to the above-described method the measuring range extends over all angles from 0 to 360°. The principle of the method is as follows (see the diagram of *fig. 4*).

To the two sets of deflection plates of an ordinary cathode ray tube two auxiliary voltages are applied which have the same frequency as the two given voltages whose phase difference is to be measured. Care is taken that the two auxiliary voltages have

[4]) See Philips techn. Rev. **4**, 342, 1939, fig. 12.

equal amplitudes and differ 90° in phase, so that the fluorescent spot describes a circle on the screen.

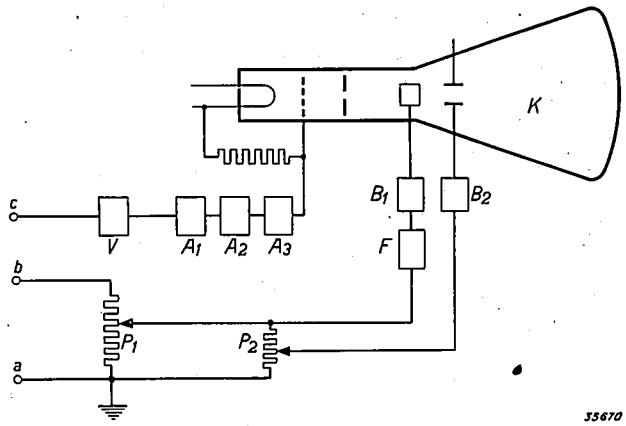

Fig. 4. Diagram of the new phase meter here described. An auxiliary voltage applied at *b* with the same frequency as the voltages to be compared is fed *via* two push-pull amplifiers B_1, B_2 to the two sets of deflection plates of a cathode ray tube *K*. By rotating the phase of one of the deflecting voltages 90° in the stage *F* and regulating the amplitudes with the potentiometers P_1 and P_2 the fluorescent spot is made to describe a circle. The voltages to be compared, applied successively to *c*, are fed *via* a regulatory amplifier *V* and three cut-off stages $A_{1,2,3}$, which are discussed in the text, to the regulatory electrode of the cathode ray tube, so that the beam current is modulated synchronously with the revolving light spot. The difference in position of the semi-circle on the fluorescent screen gives the phase difference of the voltages being compared.

One of the given voltages is now applied to the regulatory electrode (the grid) of the cathode ray tube. The beam current is hereby modulated in the same frequency as that of the deflecting voltages, *i.e.* the fluorescent spot is intense on one half of the circle traced and weak or invisible on the other half. The position of the greatest and of the smallest intensity, *i.e.* the position of the semi-circle (*fig. 5*) which is thus produced [5]), depends upon the phase of the modulating voltage with respect to the deflecting voltages. The same is repeated with the second given voltage. From the difference between the two positions of the semi-circle the required phase angle can be deduced.

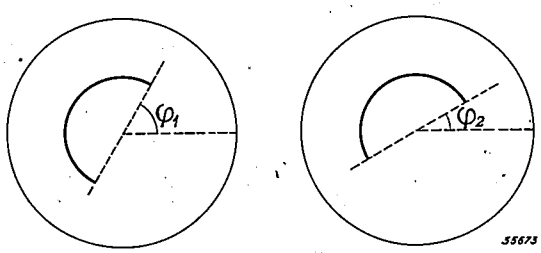

Fig. 5. Semi-circle on the fluorescent screen. If for one of the voltages this is at an angle φ_1 and for the other at the angle φ_2, the phase angle between the two voltages is $\varphi = \varphi_1 - \varphi_2$.

[5]) A similar principle is applied in the apparatus of Balth. van der Pol and C. C. J. Addink (Philips techn. Rev. 4, 205, 1939) for the rapid and accurate measurement of frequencies. Whether or not the semi-circle remains stationary is a very sharp criterion of the equality of the frequencies of the deflecting and modulating voltage.

Practical application

Obtaining the circle

In order to obtain the circular motion of the fluorescent spot the same source of voltage is used as that from which the voltages whose phase is to be compared are taken. The voltage is on the one hand conducted to one set of deflection plates *via* a potentiometer and a push-pull amplifier [6]) and on the other hand it is rotated 90° in phase in a phase-rotating stage and conducted to the other set of deflection plates *via* a second push-pull amplifier. The connections of the phase-rotating stage are shown in principle in *fig. 6a*. As may be seen from the accompanying vector diagram (fig. 6*b*), a voltage is obtained between the terminals *3* and *4* whose phase with respect to the given input voltage (*1-2*) can be changed by variation of *R*.

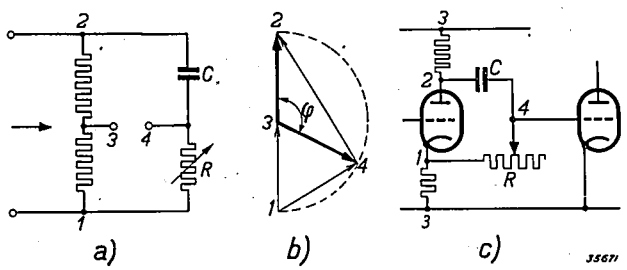

Fig. 6. *a*) Diagram illustrating the principle of the phase-rotating stage. For each frequency *R* is made equal to $1/\omega C$.
b) Corresponding vector diagram. By variation of *R* the voltage between *3* and *4* is rotated in phase, without changing the amplitude.

By making $R = 1/\omega C$ the desired phase shift of 90° is obtained for the given frequency ω. Moreover, in order to obtain a circle, the amplitude of the deflection voltage with rotated phase must always be equal to that with non-rotated phase. According to the vector diagram the connections of fig. 6 have the property that the amplitude of the rotated voltage (*3-4*) is not affected by the variation of the phase, which very much facilitates resetting to obtain a circle upon passing to another frequency.

The vector diagram — and thus the property mentioned — is only valid when no current is taken off between the terminals *3* and *4*. This is here approximately the case since the voltage *3-4* is fed to the grid of an amplifier valve. For practical reasons the connections are in reality made as represented in fig. 6*c*.

The modulated voltage

In order to be able to determine the position

[6]) The use of push-pull amplification is necessary in order to obtain a sharp image on the screen and in order to limit as far possible the distortion of the deflection voltages which would cause a deviation from true circular form.

of the semi-circle on the fluorescent screen easily, it must break off sharply at the ends. This means that the voltage which modulates the intensity of the fluorescent spot must be very steep at the zero points. This is easily obtained with sufficient amplification of the (sinusoidal) voltage; at the same time, however, the cathode ray tube would be overloaded by the large amplitude of the regulatory voltage. This can be avoided simply by cutting off the peaks of the voltage: the originally sinusoidal voltage then has the shape of a "square sine" (*fig. 7*), and the curve representing the variation of the light intensity around the circumference of the circle on the fluorescent screen then has the same form.

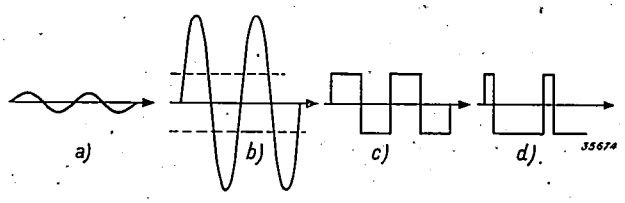

Fig. 7. The fronts of the sinusoidal voltage given (*a*) can be made sufficiently steep (*b*) by amplification, while at the same time the high peaks occurring are cut off at the level of the dotted line, so that a "square sine" (*c*) is obtained. If the levels given by the dotted lines are not symmetrical an asymmetrical "square sine" (*d*) occurs.

The connections given in *fig. 8a* (which serve at the same time for the desired amplification) serve to cut off the voltages. A sinusoidal A.C. voltage with large amplitude is applied to the terminals *1-3*. Whenever the voltage falls so far in the negative direction that the grid voltage v_g drops below the cut-off voltage v_m of the valve (fig. 8*b*) the anode current i_a remains zero until $v_g > v_m$ again. In this way the negative sine peaks are suppressed. Whenever the voltage in the positive direction increases so far that the grid potential becomes higher than the cathode potential, grid current begins to flow. The accompanying voltage decay over the resistance r makes the potential at *2* (the grid voltage) remain behind that at *1*; and with a sufficiently large value of r, the potential at *2* can never rise higher than the cathode potential, so that the anode current will already have the desired form.

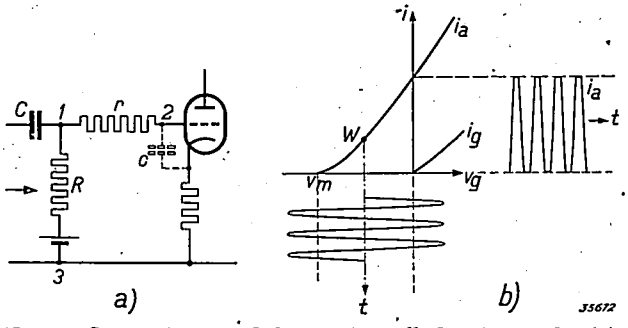

Fig. 8. Connections used for cutting off the sine peaks (*a*). If the voltage fed to *1-3* falls below the cut-off voltage v_m of the amplifier valve (*b*), the anode current i_a remains zero. If the voltage rises so that the potential at *2* reaches the cathode potential, grid current flows, and due to the voltage drop $i_g \cdot r$, the potential of *2* remains below that at *1*. With sufficiently high value of r the anode current will vary according to the desired "square sine" form.

In this connection the following must be noted. The zero level of the voltage applied, *i.e.* the operating point of the valve (*W* in fig. 8*b*) must lie halfway between the two constant levels (cut-off voltage and cathode potential) where the sine peaks are cut off. With an asymmetrical position of the zero level an asymmetrical "square sine" would occur (fig. 7*d*), and both ends of the semi-circle on the screen would be slightly lengthened or shortened. While it is true that the chord which joins the ends of the arc of the circle remains parallel to the original diameter so that the measurement is not unfavourably influenced with slight asymmetry, nevertheless with greater asymmetry the measurement would become very inaccurate. In the grid bias required for the correct position of the operating point the voltage decay $i_g \cdot R$ which is caused by the grid current i_g over the leakage resistance R must also be taken into account. The part of the grid bias which serves to compensate for this voltage drop is represented in fig. 8*a* by the battery shown in series with R.

With a given grid bias the correct position of the operating point is thus obtained only when the grid current has a certain mean value $\bar{i}_g$. The value of $\bar{i}_g$, however, depends closely upon the height of the sine peaks which must be cut off by the whole arrangement. If the connections are arranged for a given height of these peaks, *i.e.* for a given amplitude of the voltages whose phases are to be compared, and if a voltage with another amplitude is then fed to *1-3*, a discrepant i_g value occurs, the compensation of the voltage drop $\bar{i}_g R$ is not correct, and the operating point of the valve shifts until the positive voltage peaks projecting above cathode potential cause an $\bar{i}_g$ of the correct value. In order to avoid this shift, and the accompanying lengthening or shortening of the arc, the voltages to be compared must first be brought (at least approximately) to the constant amplitude for which the grid bias is calculated. We have done this by first feeding the voltages to an amplifier with automatic volume control which gives a practically constant output voltage with an input voltage between 6 mV and 3 V (maximum deviations 10 per cent).

Frequency region

It is stated above that with sufficiently high

resistance r (fig. 8*a*) the potential at point *2* no longer increases to any extent as soon as grid current begins to flow. In practice, however, it is found impossible to give the resistance r such a high value as would be required for this. The cutting off of the sine peaks is therefore not complete, so that the anode current of the valve varies about as shown in *fig. 9b*. In order to make the remaining reduced sine peaks disappear and to obtain a true "square sine", two more stages like the one shown are connected behind the stage in fig. 8*a*.

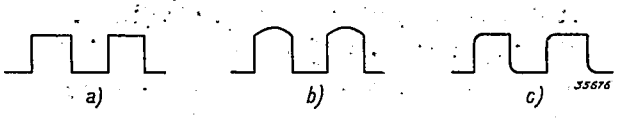

Fig. 9. If the resistance r in fig. 8*a* is not sufficiently high to cut off the sine peaks completely, instead of a "square sine" (*a*) we obtain a voltage variation which still has sine peaks, like curve (*b*). These are eliminated in the following cut-off stages. If an ideal "square sine" is applied to *1-3* of the last cut-off stage, then at point *2* due to the resistance r and the grid capacity c (fig. 8*a*), the potential cannot jump suddenly, and a rounding off of the curve is the result (curve *c*).

Let us now consider the last of these three stages. The voltage fed to this stage has almost the form of the "square sine"; the potential at point *1* therefore would at certain moments (corresponding to the beginning of the semi-circle visible on the screen) jump discontinuously from zero to a given value. Then, however, the potential of the grid (point *2*) varies as a function of the time according to $1 - \exp(-t/rc)$, where c is the unavoidable grid capacity of the valve (indicated in fig. 8*a* by a dotted line). In fig. 9*c* this variation is shown. The round corner which makes the beginning of the semi-circle poorly defined can be described by a relaxation time proportional to rc. For satisfactory reading this relaxation time must amount to not more than a certain fraction, for instance $^1/_{100}$, of the whole period (circumference of the circle). From this it follows that the highest frequency at which satisfactory results can be obtained is inversely proportional to r. Naturally r cannot be made indefinitely small, since then the whole effect of the cut-off stage in question would become illusory. At the value of r chosen by us the rounding of the corners is not disturbing up to frequencies of about 100 000 c/s.

At the low-frequency end the frequency region in which the phase can be measured is limited due to a similar cause. If we again consider the last of the three cut-off stages, and again assume that in the one before the last an ideal "square sine" has been obtained, then due to the finite size of the coupling condenser C and the leakage resistance R in fig. 8*a* the variation of potential at point *1* will take on the form of *fig. 10b* (thin lines): the decrease of potential after each jump can be described by a relaxation time proportional to RC. As long as this time is large with respect to the period, the decrease is not disturbing, since the sine peaks are in any case cut off in the last stage according to the dotted line. At very low frequencies, however, the voltage represented in fig. 10*c* is obtained, which no longer gives a sharply ending semi-circle.

The lower frequency limit can be lowered by increasing R and C. In our case, where it was not particularly a question of low frequencies, the proportions were such that the lower frequency lay at about 100 c/s.

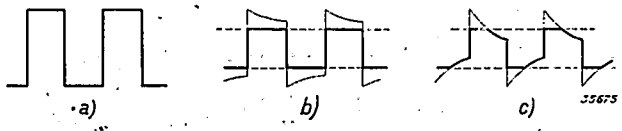

Fig. 10. If a "square sine" voltage (*a*) is supplied to the circuit of fig. 8*a*, the voltage at *1-3* varies according to (*b*) due to the limited size of R and C. As long as the downward sloping parts are cut off (*b*) this decay is not disturbing. At low frequencies, however, (*b*) gradually passes over to forms like (*c*) which cannot be used.

The apparatus as constructed

In *fig. 11* a photograph is given of the apparatus as constructed in this laboratory. The phase meter is mounted together with a tone generator which serves as voltage source for many measurements. Other details are given in the text under the figure. A celluloid plate which can be rotated with the help of a ring is placed directly over the screen. On this plate a set of parallel lines and a number of concentric circles are drawn (*fig. 12*). The latter serve for facilitating regulation of the circle which is obtained by adjusting the phase and amplitudes of the deflection voltages. When the circle has been obtained and given a suitable size [7]) (potentiometer P_1 in the diagram of fig. 4), the two voltages between which the phase angle is to be determined are fed in turn to the cut-off apparatus. By turning the ring with the celluloid plate so that the extremities of the semi-circle obtained fall upon one of the parallel straight lines the angle can be read off on a scale around the ring with an accuracy of $^1/_2°$.

By this method it is particularly easy to study the behaviour of filters. If the phase rotation is required which an input voltage of a given frequency undergoes in the different filter cells, the

[7]) A suitable size is for instance a diameter of 8 cm. With the acceleration voltage of 2 000 V of the cathode ray here used — this high voltage is desirable in order to obtain a sufficiently high intensity of the image for measurement in a room which is not darkened — deflection voltages of about 200 V (peak value) are necessary.

filter and the circle apparatus of the phase meter are supplied from the tone generator with the desired frequency, and the voltage behind each cell is successively tapped off and fed to the cut-off apparatus of the phase meter. In this way a series of semicircles is obtained in which the gradually increasing phase rotation is clearly demonstrated.

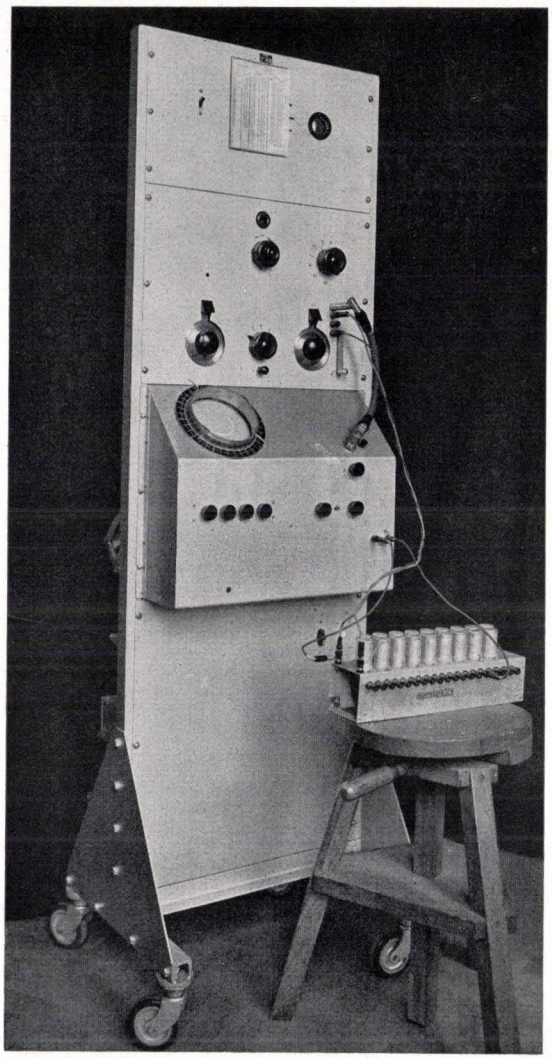

Fig. 11. The phase meter is mounted together with a tone generator (above) on one frame. To the left may be seen the screen of the cathode ray tube which is placed obliquely for easy reading. With the seven knobs below, the shape, size, position, sharpness and intensity of the circle on the screen are adjusted. To the right in front of the apparatus is a filter connected for measurement.

Accuracy of measurement

It is clear that with a differential measurement any possible phase rotations in the regulatory amplifier and the cut-off connections of the phase meter have no effect on the results, when this rotation is the same for both the voltages to be compared. Since these voltages have the same frequency, they can only be distinguished by their amplitude (and

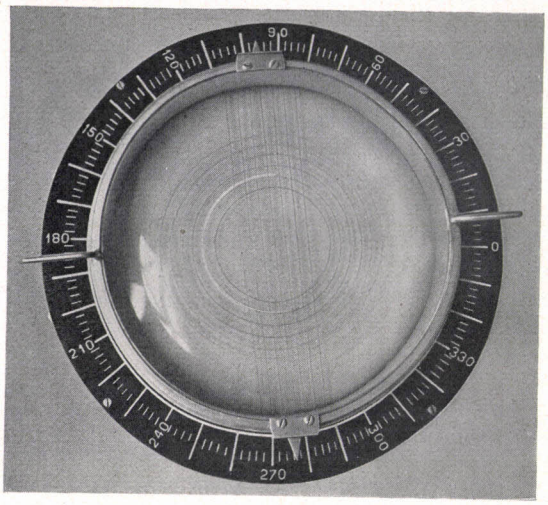

Fig. 12. Close-up of the fluorescent screen and of the celluloid plate over it which can be rotated by means of a ring. On the plate is a set of parallel lines and concentric circles. The ring bears a scale of angles.

their phase). In control measurements at 100 000 c/s. it has been found that in the whole range of amplitudes in which the measurement is possible, the phase rotation varies not more than 1° (see *fig. 13*).

Another possible source of error which we shall consider is a slight deviation of the image obtained on the screen from a true circle. The lighting up and dying out of the revolving light spot takes place at given moments t, and in our measurements we assume that ωt (aside from a multiple of 2π) is equal to the angle α at which the guiding ray of the light spot stands at the moment t. This is correct only as long as the spot traces a circle with constant velocity. Suppose that in adjusting the circle we had truely sinusoidal deflection voltages which were shifted exactly 90° in phase, but that in making the amplitudes equal we have made a slight error.

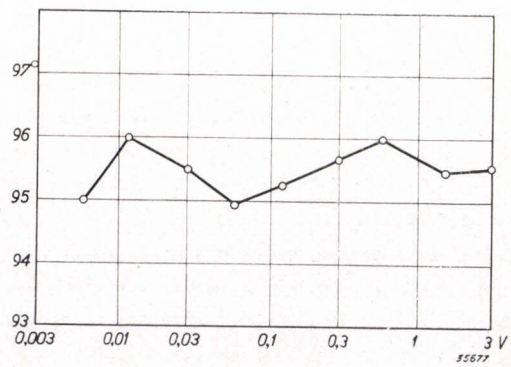

Fig. 13. For comparative phase measurements a phase rotation in the cut-off apparatus presents no difficulty when this rotation is independent of the amplitude. It is found that this requirement is satisfied for amplitudes between 6 mV and 3 V with an accuracy of 1°.

Let the horizontal deflection be

$$x = \cos \omega t$$

and the vertical: $y = (1 + \varepsilon) \sin \omega t$.

The angle α read off at moment t is given by:

$$\tan \alpha = y/x = (1 + \varepsilon) \tan \omega t$$

There is now a slight difference between α and ωt, which may be expressed approximately by:

$$\alpha - \omega t \approx \tan(\alpha - \omega t) = \frac{\tan \alpha - \tan \omega t}{1 + \tan \alpha \tan \omega t} =$$

$$= \frac{\varepsilon \tan \omega t}{1 + (1 + \varepsilon) \tan^2 \omega t} \approx \frac{\varepsilon}{2} \sin 2\omega t.$$

The error in the phase angle read off is therefore $\varepsilon/2$ at the most. This can be understood more easily by considering the length r of the guiding ray of the light spot. This length is

$$r = \sqrt{x^2 + y^2} =$$

$$= \sqrt{1 + (2\varepsilon + \varepsilon^2) \cos^2 \omega t} \approx 1 + \varepsilon \cos^2 \omega t,$$

while with a perfect circle ($\varepsilon = 0$) r would equal one in the scale chosen. The maximum radial deviation from the circle of the figure obtained (ellipse) is thus ε, and it may be stated that the maximum error in the phase angle measured is one half the maximum deviation from circularity. If for instance the radius is 4 cm and the greatest radial deviation is 1 mm (this accuracy is easily attained), then $\varepsilon = 0.025$ and thus the possible error in the phase angle is 0.012, *i.e.* about $^3/_4°$. For other possible causes of deviations from the true circle, (harmonics, phase shift not exactly 90°) a similar estimation is found. Taking these considerations into account, the possible error in the comparative measurements described, in the frequency region 100 - 100 000 c/s and in the amplitude region 6 mV - 3 V, can be set at about 2°. The accuracy is the same for all angles between 0 and 360°.

An important property of the phase meter described, which we wish to point out in conclusion, is its slight sensitivity to interferences. Interfering voltages, if they are of a different frequency from the one examined, have no effect at all on the measurement, which is contrary to the case of almost all other methods. The hum voltage of 50 c/s. for instance, which often appears as interfering voltage, only makes the circumference line of the circle somewhat wider without changing its position. Interferences of the same frequency as the one being examined, for instance due to induction in the connections of the phase meter, must of course here also be avoided as in every method of phase measurement, since they affect the quantity to be measured itself.

TECHNICAL TEMPERATURE MEASUREMENT WITH THERMO-ELEMENTS

536.53

Nowadays in the preparation or working of almost every technically used alloy, the alloy is subjected to a carefully worked-out heat treatment, which has the purpose of influencing in a certain direction the mechanical, magnetic or other properties of the material. Such a heat treatment consists of heating the metal successively for definite times to definite, more or less accurately prescribed temperatures. The methods by which this is done will not be considered here, but we shall concentrate our attention on the problem of how these temperatures are controlled.

Since it is here a question of fairly high temperatures in general, for instance in the neighbourhood of 500 or 1000 °C, and since a rapid and simple measurement is required for such technical purposes, the thermo-element is the most suitable device. The thermo-voltage between the two contact metals whose junction has been brought to the temperature to be determined is measured by means of a galvanometer which need not be especially sensitive, since at temperatures of 500 °C for instance, with suitably chosen contact metals (for example chromel-alumel), thermo-voltages of 20 mV and more are obtained. The measuring instrument can be made of a registering type so that a continual control is possible of the whole heat treatment.

What is determined in such a thermo-electric measurement is in fact not a temperature, but a temperature difference. There must in any case always be a closed circuit, *i.e.* the two contact metals join not only at the welded junction but also at a second spot (indirectly perhaps, *via* one or more intermediate metals, see below). At this second "cold" junction there is an opposing EMF which depends upon the temperature of this point. The EMF measured is the difference between the two EMF's and therefore depends upon the difference in temperature of the two points of contact. If the indicating instrument is to be calibrated directly

in temperature units, *the second contact must be kept at a definite constant temperature.*

How can this condition be satisfied? The air temperature is far from sufficiently constant, since in many cases the temperature must be determined to within a few degrees. In a laboratory it is customary to create a constant temperature artificially by means of melting ice; for routine measurements, however, this method would be too expensive. Instead of this use can be made of the fact that running water from the mains has a temperature which varies only slightly summer and winter. A still simpler method is obtained when one realizes the reason for the fact just mentioned: the pipe system of the water mains lies mainly underground and the water takes on the temperature of the ground through which it flows. This ground temperature is more or less constant (independent of the air temperature). An obvious solution is therefore to keep the cold contact of the thermoelements at the desired constant temperature by putting it at some depth underground. This method is actually followed in the Philips factories.

It is clear that the upper layer of soil will follow the temperature fluctuations of the air to a certain extent, or rather, to a certain depth. In order to discover at what depth the ground temperature no longer varies with time to any extent, the temperature of the soil at various depths on the grounds of this laboratory has been measured during a long time. For this purpose a series of narrow pipes of different lengths were driven into the ground. An ordinary mercury thermometer mounted in a copper block was lowered to the bottom of every pipe. Thanks to the large heat capacity of the copper block no appreciable error could occur during the daily pulling up and reading of the thermometers. In *fig. 1* the variation of temperature at 0.5 m, 2 m and 4 m depth measured in this way is given, while the region over which the air temperature varied is shaded. It is clear from the figure that the variations of the ground temperature become smaller with increasing depth, and moreover — an interesting and for the rest well-known phenomenon —, that the half-yearly temperature maxima and minima exhibit a certain shift, increasing with the depth, with respect to the temperature at the surface. This phase shift, which is a result of the delayed penetration of the sun's warmth due to the poor heat conduction of the soil, already amounts to about three months at a depth of 4 m. From experiments of other investigators it has been found that at a depth of about 8 m the phase shift is half a year, so that at that depth the highest temperature appears in December and the lowest in June.

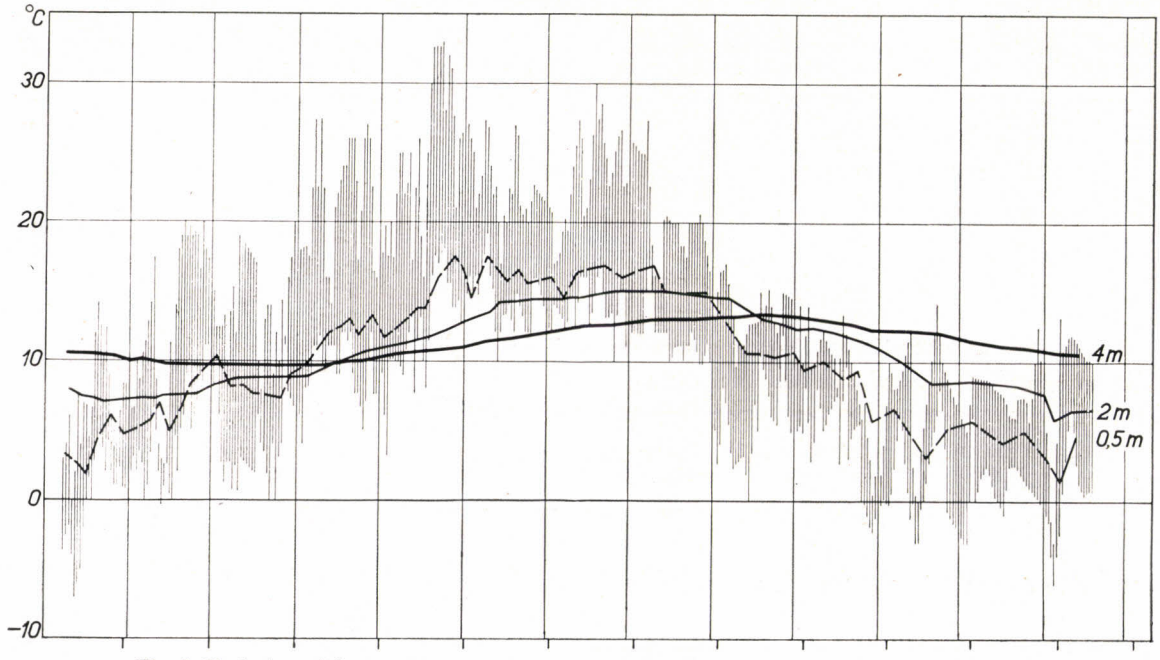

Fig. 1. Variation of the temperature of the ground at different depths during one year. For the sake of comparison the region between the maximum and minimum temperatures of the air, measured daily, is shaded. With increasing depth the amplitude of the yearly temperature fluctuation becomes smaller, while at the same time it exhibits a phase shift.

We are mainly interested in the maximum temperature variations, which are plotted in *fig. 2* as a

function of the depth. The broken line curve represents measurements by Tait in Edinburgh, which were carried out in quite a different type of soil. The conclusion to be drawn from the results of the measurements is that in general a depth

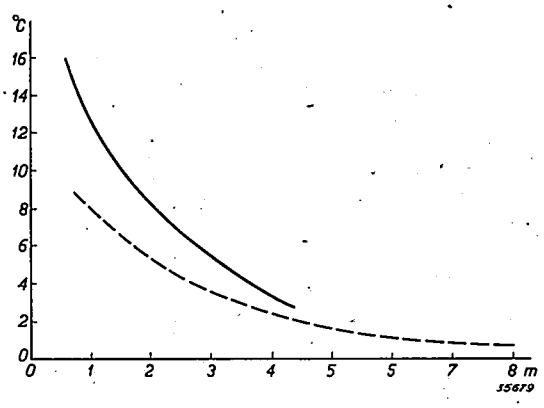

Fig. 2. The maximum temperature difference occurring during a year as a function of the depth. The full-line curve refers to measurements carried out in Eindhoven (sand ground), the broken-line curve gives the result of measurements by Tait (Edinburgh, porphyry rock).

of 4 m is enough, with if necessary a positive correction in the months March to May and a negative correction in the months September and October of 2° in the calibration of the thermo-elements. Under buildings the temperature variations are still smaller than in the measurements here described out of doors.

In the practical application of the method a less pleasant consequence is the fact that the wires of the thermo-element would have to be very long in order to place the cold junction at the required depth in the ground. This is particularly unpleasant when the measurement of the EMF is not done by a compensation method as is in general the case with technical measurements. The alloys used for the thermo-element often have a fairly high specific resistance, so that with long lengths of wire the indication of the galvanometer becomes appreciably different from what it would be if only the resistance of the galvanometer were included in the circuit. The chromel-alumel elements, for instance, have a resistance of 0.23 ohm per metre length of the pair of wires with a thickness of wire of 2.3 mm.

Improvement can be achieved by the use of a socalled compensation connection. The latter consists of two metals which have a smaller electrical resistance than the contact metals of the thermo-element, and which are thermo-electrically equivalent to the latter, *i.e.* they give the same thermo-EMF without. however, needing to have the same great resistance to heat. In *fig. 3* is shown how the compensation connection is made. If we indicate the thermo-EMF between any two metals P and Q whose contact point has the temperature τ by E^{τ}_{PQ} (which then equals $-E^{\tau}_{QP}$), then the total thermo-EMF in the circuit of fig. 3 is:

$$E = E^{t}_{AB} + E^{x}_{BC} + E^{\Theta}_{CD} + E^{x}_{DA}, \quad . \quad . \quad (1)$$

where t is the temperature to be determined, Θ the constant temperature of the ground and x the unknown and varying air temperature of the points of connection of the compensation connection. Since, when $t = \Theta = x$, the total thermo-EMF is zero, then

$$E^{x}_{AB} + E^{x}_{BC} + E^{x}_{CD} + E^{x}_{DA} = 0.$$

Thus equation (1) becomes

$$E = E^{t}_{AB} - E^{\Theta}_{DC} + \left(E^{x}_{DC} - E^{x}_{AB}\right) \quad . \quad (2)$$

Therefore, except for a constant, the desired thermo-EMF E^{t}_{AB} is actually measured when the expression in parenthesis, which varies with x, disappears for all air temperatures x to be considered, *i.e.* when in this region the pair of metals DC is thermo-electrically equivalent to AB.

The chromel-alumel elements give, in the temperature region in which x may lie, *i.e.* between about 0 and 50 °C, a thermo-EMF of 0.0406 mV/°C. The combination constantan-copper can here be used as an easily conducting compensation connection. For a certain kind of constantan wire (the properties of constantan vary slightly according to the source), combined with normal electrolytic copper wire, we found a thermo-EMF of 0.0410 mV/°C, which corresponds very well with the value for chromel-alumel. The resistance of the compensation connection with a wire thickness of 2.5 mm amounted to about 0.1 ohm per m, and is therefore about $2^1/_2$ times as small as that of the chromel-alumel wires.

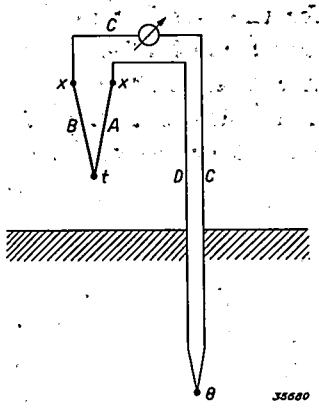

Fig. 3. In order not to be compelled to make the wires AB of the thermo-element very long, a compensation connection o two (thermo-electrically equivalent) metals C and D is joined to it, whose junction is given the constant ground temperature Θ. t is the temperature to be determined, x the air temperature of the connecting points of the compensation connection.

VOL. 5 No. 8 AUGUST 1940

Philips Technical Review

DEALING WITH TECHNICAL PROBLEMS
RELATING TO THE PRODUCTS, PROCESSES AND INVESTIGATIONS OF
N.V. PHILIPS' GLOEILAMPENFABRIEKEN

EDITED BY THE RESEARCH LABORATORY OF N.V. PHILIPS' GLOEILAMPENFABRIEKEN, EINDHOVEN, HOLLAND

METALS AS GETTERS

by J. D. FAST.

621.528 : 546.431 + 546.831

In order to obtain the required high vacuum in radio valves, X-ray tubes, etc. and especially in order to maintain the vacuum after sealing off, use is made of metals which take up gases and hold them fast. Barium and zirconium in particular are used for this purpose. The properties upon which the action of these getters is based is discussed. In the case of barium and related metals it is a question of a chemical corrosion of the metal with the formation of a new phase, whereby the essential point is that the corrosion is always progressive (in contrast to what is desired in the case of corrosion-resistant metals), due to the fact that no dense surface layer of reaction products is formed. In the case of zirconium the action as getter is based upon the remarkably high solvent capacity of the metal for most gases encountered. In conclusion several details about the application of the getters mentioned are discussed.

Introduction

In the manufacture of electric lamps, radio valves, X-ray tubes, etc. the removal of air and other undesired gases from the bulbs or tubes is an important process. The evacuation by means of high-vacuum pumps is generally not sufficient, especially because the walls and electrodes of the tubes always contain all kinds of gases, such as oxygen, nitrogen, hydrogen, etc. as such, or in the form of decomposable compounds, and during operation these gases, due partly to the heating of the tube, may be freed and thus destroy the vacuum.

This is combatted during manufacture by heating the valves on the pumps to such a temperature that the gases present in the walls, etc. are freed as far as possible. Nevertheless, the possibility always remains that small quantities of gas will be freed during operation. In order to render this gas harmless, "getters" are employed. Getters are substances which are introduced at suitable spots in the tubes to be evacuated, and which, like the walls and electrodes, are able to take up gases, but with this difference, that the gases are so firmly held by the getter that they can no longer be freed under the conditions prevailing during operation, which is after all the essential point. The getter thus acts, as it were, like a high-vacuum pump permanently connected with the tube. At the same time it makes it possible to shorten the pumping time in manufacture and to obtain lower gas pressures than is possible with ordinary high-vacuum pumps.

The oldest getter, and one that is still used in incandescent lamps, is phosphorus. For radio valves and X-ray tubes this substance cannot be used, because much higher vacua are required in these cases (phosphorus has a relatively high vapour pressure). In the latter cases, metals are used as getters, nowadays especially barium and zirconium. In this article we shall explain why just these two metals are especially suitable as getters. There will also be an opportunity of going somewhat deeper into the processes which take place upon the action of gases on metals in general.

The chemical corrosion of metals by gases. Barium as getter

The requirement that the metal which is to be used as getter must be able to bind quickly and completely the above-mentioned gases, such as oxygen, nitrogen, etc. may also be expressed by saying that the metal must be easily attacked or corroded by these gases. The getters are, therefore, as it were, the antipodes of the corrosion-resistant metals so important technically [1]). This contrast will be elaborated in the following.

[1]) We are here considering only corrosion by gases and not by liquids.

In order to be easily corroded by the gases mentioned, the getter must in the first place fulfil the chemical requirement of possessing great affinity to oxygen, nitrogen, hydrogen, etc. As a measure of this affinity, in most cases, and as an approximation, the heat of formation of the metal-gas compounds may be taken. If we take for instance the reaction with oxygen, then the requirement is that the oxide of the metal which is to be used as getter must have a large heat of formation. There are, however, various metals, such as aluminium, tantalum, etc. which satisfy this requirement, but which are nevertheless very stable in an atmosphere of oxygen. A great affinity to the different gases is therefore not sufficient to insure the satisfactory action of a metal as a getter.

If we consider the example mentioned, the corrosion of a metal by oxygen, somewhat more closely, it is found that in general the oxide is formed as a solid film on the surface of the metal. If this film is dense and coherent, further oxidation involves a diffusion of one of the reacting substances (or both of them) through the layer. At room temperature such a transport of material in the solid state scarcely takes place at all, the reaction therefore practically comes to a stop after the formation of a thin film of oxide. A dense coherent oxide film thus protects the metal against further oxidation.

If, however, the oxide layer formed possesses pores and cracks, the gas can reach the underlying metal by these paths without a diffusion in the solid state being necessary. In this case therefore the oxidation is able to progress, the oxide layer grows with time.

According to a rule proposed by Pilling and Bedworth [2]) a coherent oxide layer is formed when the volume of the oxide is greater than that of the metal oxidized. If the volume of the oxide is smaller, pores and cracks appear in the layer [3]). Also when other non-metals than oxygen act on a metal, dense or porous surface layers are formed according to the metal attacked, and the above-mentioned rule seems to hold here also. A striking phenomenon, for example, is the immediate violent reaction of potassium with bromine, while sodium, which is chemically so closely related to potassium, can be kept in contact with bromine for years. The volume of potassium bromide is smaller than that of potassium, the volume of sodium bromide is greater than that of sodium.

From the above a further condition which a metal must satisfy in order to be considered as a getter follows directly. No dense protective layers must be formed on the metal, so that the taking up of gas from the surrounding atmosphere can continue uninterrupted. This requirement is particularly important in connection with the metal oxide, since oxygen is one of the most dangerous contaminations in high-vacuum tubes, and a dense layer of oxide prevents the corrosion by other gases. In agreement with the rule of Pilling and Bedworth, therefore, getters must be sought among the metals whose oxide has a smaller volume than the metal. The alkali metals and the alkaline earth metals belong to this group. The former cannot usually be used since getters for radio valves and X-ray tubes must have a fairly high melting point in connection with the conditions of operation and manufacture. Moreover, the vapour tension of the alkali metals (except lithium) is too high. The choice is limited therefore to the alkaline earth metals, which are in fact commonly used as getters. Since the chemical activity of the alkaline earth metals increases in the order: magnesium, calcium, strontium, barium, it is clear that barium is especially suitable as getter.

Before continuing with the subject of getters we should like to complete the above discussion by contrasting them with the corrosion resistant metals.

Conditions for corrosion-resistance

Corrosion resistance can evidently be expected in the cases of the metals upon which dense coherent layers are formed by the action of gases (in addition to the precious metals such as gold, etc.). Since the protective action of such a layer is based upon the fact that the reacting substances are forced to diffuse through the coherent layer, the resistance to corrosion is greater, the lower the velocity of diffusion through the layer. This property must therefore be considered more closely.

As a matter of fact it is remarkable that diffusion takes place at all. Diffusion of course requires a concentration gradient, which means that the metal and gas atoms in the compound forming the surface layer must be present in variable proportions, thus in general in proportions which deviate from the exact stoichiometric composition. Such deviations are indeed possible. Most chemical compounds have a certain range in the system of their components (homogeneity range) within which the atomic proportions can change continuously without a new phase being formed. The excess of one of the components compared with the stoichiometric amount is then, as it were, in solid solution in the compound. If it is a question of a binary compound of the form AB, which contains an excess of the component B, this deviation from the stoichiometric composition may occur in three different ways

[2]) N. B. Pilling and R. E. Bedworth, J. Inst. Metals, **29**, 529, 1923.

[3]) The phenomenon recalls the "craquelé" of the pottery maker's art, in which two layers of coloured glaze are applied one over the other to the object. The upper layer shrinks more than the other upon cooling, and thus exhibits numerous tiny cracks through which the colour of the underlayer becomes visible.

which are represented diagrammatically in *fig. 1*. In the compounds in question, of a metal and a non-metal, the components A and B are usually present in the form of oppositely charged ions. In this case, due to the strong repulsion between similar particles, only types *I* and *II* of fig. 1 need be considered:

I) the points of the lattice AB are all occupied and the excess of particles B present are situated between these points;

II) part of the particles A are missing from the lattice AB, so that holes of atomic dimensions are formed.

In the first type diffusion takes place by the particles B diffusing particles are ions, while electrical neutrality is maintained during the diffusion by the diffusion of a corresponding number of electrons. The positive metal ions, due to their small size, are much more mobile than the negative ions. By a consideration of the contributions made by the motion through the lattice of ions and electrons, respectively, to the total electrical conductivity of the metal-gas compound, this theoretical representation could also be confirmed quantitatively [4]).

In addition to the conditions mentioned for high corrosion resistance — homogeneity range of the metal-gas compound small and involving an excess of the metal — which follow

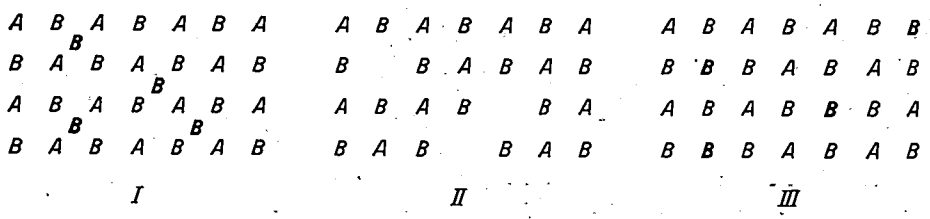

Fig. 1. When a compound AB contains an excess of the component B in solid solution there are three possibilities:
I) The excess particles B are situated at random spots between the points of the normal lattice AB.
II) In the lattice AB, there are here and there unoccupied points where A particles are missing from the stoichiometric composition.
III) In the lattice AB A particles are here and there replaced by B particles. (The representation is borrowed from C. Wagner and W. Schottky, Z. phys. Chem. B **11**, 163, 1930).

jumping from one intermediate lattice position to the one next to it, and thus moving from regions with large excess of B to regions with small excess of B. In the second type particles A can jump from hole to hole, and in this way diffuse through the layer. The last method of diffusion always takes place relatively rapidly, so that it is more favourable for corrosion resistance when the metal-gas compound can only have lattice defects of type *I*. Furthermore, the diffusion velocity under otherwise similar conditions is greater, the greater the possible difference in concentration of the excess particles B in the layer. Therefore it is desirable that the compound AB should have only a very small homogeneity range.

It may be mentioned in passing that type *I* usually occurs when the soluble component B present in excess is the metal; type *II*, when A is the metal. This is simply because the (positive) metal ions are usually considerably smaller than the (negative) non-metallic ions, and can therefore fit more easily into the spaces between the normally occupied lattice points. From this it may be seen that in both the diffusion mechanisms described the metal is the component which diffuses through the layer. This may seem strange since one is inclined to assume that if anything is to penetrate through the surface layer it ought to be the gas. In the cases investigated until now (the investigations have extended over the last ten years), however, it has been found that the metal actually diffuses through the metal-gas compound to the outside. If, for example, a copper wire is oxidized through and through at a suitable pressure and temperature, it is found to have become hollow. Another very convincing proof is the corrosion of silver by sulphur described by Wagner, which is illustrated in *fig. 2* and explained in the text beneath the figure. An explanation of the fact that it is always the metal which diffuses (thus in a lattice of type *I* particles B, in type *II* particles A), is furnished by the assumption that the

from the requirement of a low velocity of diffusion, and which therefore must also be manifested, according to the above, in a very low ionic or electronic conductivity of the compound, there are other more or less obvious requirements. The compound must have only a low vapour tension and must possess great hardness so that the protecting layer will not be volatilized or easily broken through upon mechanical injury. It is indeed found that the oxides of the metals commonly used in corrosion-resistant alloys, such as chromium and aluminium, are distinguished by just these properties.

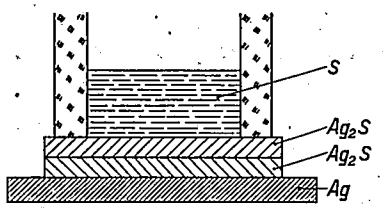

Fig. 2. A silver plate and two plates of pressed silver sulphide (Ag_2S) are pressed together, while at 220° C liquid sulphur is allowed to act upon the uppermost Ag_2S plate. A silver sulphide growth is seen to be formed upon this plate which becomes heavier, while the silver plate is found to decrease in weight correspondingly. The middle plate of Ag_2S does not change its weight. Therefore silver diffuses through the silver sulphide to the sulphur. (C. Wagner, Z. phys. Chem. B **21**, 25, 1933).

The solution of gases in metals. Zirconium as a getter

While the above discussion of the "getting" of

[4]) C. Wagner, Z. phys. Chem., B **21**, 25, 1933; **32**, 447, 1936; **40**, 455, 1938.

gases will have made it clear why barium is a suitable getter, the same cannot be said of the second metal mentioned in the introduction, zirconium. Zirconium oxide has a greater volume than the metal — the condition for the formation of a protective oxide layer — and it otherwise satisfies practically all the requirements which have just been mentioned for a corrosion-resistant metal. Below 200° C zirconium is indeed one of the best corrosion-resistant metals. At high temperature, however, a new phenomenon appears, which in our discussion has not yet been taken into account: the oxide is dissolved in the zirconium.

This effect could be neglected in the foregoing since the solubility of, for instance, oxygen or nitrogen in most metals is very small. Up untill quite recently the greatest of such solubilities known were those of oxygen in silver and of nitrogen in iron; in both cases the solubility at room temperature is less than 0.01 atoms per cent. In recent years, however, it could be shown [5]) that there are several metals which can take up many atoms per cent of oxygen and nitrogen in solid solution, and that this is especially so with zirconium. In this case also the phenomena have been studied in the greatest detail. Oxygen particularly is extremely soluble in zirconium. Even a sample with the composition 60 at. % Zr + 40 at. % 0 was found by X-ray analysis to form only one phase (with a hexagonal lattice). For nitrogen the limit of solubility lies at about 20 atoms per cent of N.

The taking up of oxygen or nitrogen atoms in the zirconium lattice (which is found to take place in the interstices of the lattice) may occur directly from the gas phase or from a layer of zirconium oxide or nitride which has been formed on the surface of the metal. In order that the layer should rapidly disappear completely, the great solubility is, however, not sufficient; the atoms taken up must also be able to diffuse easily from the outside to the inside of the zirconium lattice, in order to make room for new ones. This velocity of diffusion is found to be extremely small at low temperatures [6]). This is the reason why the oxide or nitride layer on zirconium remains intact and protects the metal from further "corrosion". At higher temperatures, on the other hand, above 1 000° C, for instance, the oxygen and nitrogen atoms (or ions) diffuse very easily through the zirconium lattice, so that homogeneous solutions are obtained and the metal surface is continually restored as long as the limit of solubility is not reached.

In order that, in spite of their great mobility in the metal lattice, the oxygen and nitrogen atoms shall not leave it, the energy level of the gas in the metal must lie considerably lower than outside the metal, *i.e.* the gas must be held bound in the metal by strong chemical forces. This is actually the case in zirconium. If the other metals related to zirconium in the fourth main group of the periodic system of the elements are examined, it is found that the chemical activity increases in the order: titanium, zirconium, hafnium, thorium. Just as in the case of the alkaline earth metals one would expect to find the best getter qualities in the last metal of this series. It has, however, been found that the unusually high solvent capacity occurs only in the case of the first three. Since hafnium is very expensive and differs in properties only slightly from zirconium, zirconium has been chosen from this group for use as a getter.

In addition to oxygen and nitrogen, other gases also, especially hydrogen, are taken up in large quantities by zirconium in solid solution. While for the taking up of all other gases the most favourable temperature of the zirconium is the highest possible, this is not so with hydrogen. For this gas there is a definite, optimum temperature zone between 300 and 400° C. In order to understand this we must observe the process of solution from a different angle for a moment.

At a definite constant temperature T_1 the amount of gas c, which a metal can contain in solid solution, at first increases with the pressure p of the gas in

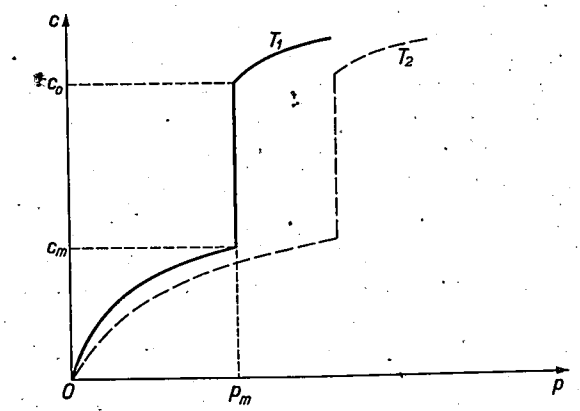

Fig. 3. The amount of gas c dissolved in a metal at constant temperature T_1 at first increases with the pressure p. At the limit of solubility c_m the equilibrium pressure of the solution is p_m. Then, while the pressure remains constant, a metal-gas compound begins to be formed. When all the metal is converted into this new phase (amount of gas taken up c_0), upon further increase in pressure the gas content in the compound can in general still increase (range of homogeneity).

[5]) J. H. de Boer and J. D. Fast, Rec. trav. chim. Pays Bas **55**, 459, 1936; J. D. Fast, Metallwirtschaft, **17**, 641, 1938.

[6]) Actually it is not a question of the diffusion alone, but also of the passing of the atoms of the gas through the boundary surface of the metal, for which, as for diffusion, a certain activation energy is necessary.

the surrounding atmosphere, usually [7]) proportionally with $\sqrt{p}$ (see *fig. 3*). At a certain pressure p_m the limit of solubility c_m is reached, *i.e.* the gas no longer dissolves, but in addition to the metallic phase a new phase (a metal-gas compound) begins to be formed, and the pressure remains constant until all the metal has been converted into the metal-gas compound. At a higher temperature T_2 the equilibrium pressures in the cases in question are higher for all values of c. With a given solution, therefore, the amount of gas dissolved can be decreased not only by decreasing the gas pressure at constant temperature, but also by increasing the temperature at constant pressure.

As an example let us consider the solution of oxygen in silver. At a temperature of 200° C a limit of solubility is found of 0.016 at. % at a pressure $p_m = 1.74$ atm. For 500° C the corresponding values are 0.17 at. % and $p_m = 386$ atm. Since these pressures can easily be realized experimentally, it is thus possible to cause the oxygen content of silver to increase or decrease at will within the limit of solubility. In the case of the solution of oxygen and nitrogen in zirconium, on the other hand, the values p_m and, *a fortiori*, the equilibrium pressures, at gas contents below the solubility limit, are found to be so small ($<10^{-6}$ mm Hg) that they cannot be attained even with the best high-vacuum pumps, and this is even true at temperatures of for instance 1500° C. From this it follows, on the one hand, that upon employment of a sufficient amount of zirconium as getter in oxygen or nitrogen, the gases will be taken up except for infinitesimally small amounts, and on the other hand, that afterwards the gases once taken up cannot be driven out of the zirconium with all the existing means at our disposal!

It will now be clear that it was unnecessary to speak of equilibrium pressures of the solid solution when discussing the action of zirconium as a getter for oxygen and nitrogen. In the case of hydrogen, however, the equilibrium pressures of the solution in zirconium can only be neglected at low temperatures. At temperatures above about 400° C they may already lie higher than the pressures which are considered permissible in high-vacuum tubes. The hydrogen taken up at a lower temperature from the evacuated tube would then be partially given off again. On the other hand, with increasing temperature, just as in the case of oxygen and nitrogen, the velocity with which hydrogen is taken up by the zirconium becomes steadily greater. The most favourable compromise seems to lie in the temperature range mentioned, 300—400° C.

[7]) Namely, when the molecules in the gas phase consist of two atoms and the gas dissolves in the metal phase in atomic form.

The method of application of barium and zirconium as getters

Thanks to the property that at room temperature zirconium does not act as a getter, because of the oxide and nitride layers formed (on the contrary it is particularly corrosion-resistant), no special measures need be taken while introducing zirconium into the high-vacuum tube. Barium, however, which also acts as a getter at lower temperatures, and which is therefore very unstable in air, must be protected by, for instance, enclosing it in a jacket of copper or nickel when it is introduced into the tube. After the tube has been evacuated to a certain pressure, the barium is freed in vapour form by heating, and condenses as a mirror on the glass wall of the tube. Upon evaporation the barium already takes up greedily any gas left in the tube, so that the tube is evacuated much more quickly to a lower final pressure than is possible with a pump. This action is also obtained with magnesium (the least active of the alkaline earth metals), and magnesium was formerly used for this purpose on a large scale; since, however, magnesium when in the solid state takes up practically no more gases, it does not entirely fulfil the function of a getter as outlined in the introduction.

In certain cases the manner of introducing the barium encounters the objection that the metal may also condense on spots, where its presence is undesired. Moreover, the presence of the metallic mirror has an unfavourable influence on the heat radiation through the glass, which is serious especially in certain types of transmitting valves. These objections are avoided by using zirconium. This metal can be applied as a thin layer on one of the electrodes or support wires or it may be in the form of a separate rod or plate in the tube. Care must only be taken that part of the zirconium remains at a relatively low temperature (400° C for instance) during operation, in order to bind the hydrogen, while another part must assume much higher temperatures in order to take up the oxygen, nitrogen, etc. rapidly. At the same time the spot where the getter is applied must be chosen so that it can easily be reached by the gas atoms freed at another spot which are to be bound. This latter action can be very much promoted by bringing the getter to an electric potential such that any gaseous ions formed will be drawn towards it.

A NEW FITTING FOR ROAD LIGHTING

by J. BERGMANS and W. L. VERVEST.

683.854: 628.971.6

The advantages of mirror reflectors for road lighting are only fully enjoyed when an attempt is made to make the distribution of brightness over the surface of the road as uniform as possible for all conditions of the road surface (dry, damp, wet). It is known that uniform illumination is not necessary, and even undesired for this purpose. An examination is made of a new light distribution in which not only the reflecting properties of the dry roadsurface are considered but also those of a damp or wet surface. It is also shown that this new light-distribution of the road lighting fitting is also more satisfactory as far as glare is concerned than the light-distribution which corresponds to a uniform brightness on a dry road only. A description is given of the fitting ZE 30 developed on this basis, which is not only suitable for mounting on poles but also for suspension on cross wires. In conclusion photographs and visibility measurements of an installed system are given.

Introduction

In the lighting of roads and highways the aim is to provide sufficient brightness for the eye of the roaduser on a long narrow strip, with a relatively small number of light points. In order to prevent wastage of luminous flux in the strips of ground lying beside the road or on the house fronts, it is logical to choose the light distribution of the light source in such a way that the luminous flux is directed mainly on to the surface of the road. This is more important the higher the light sources are mounted, according to the tendency of modern road lighting. Mirror reflectors and other fittings for directed light, by means of which the light distribution can be very considerably influenced, will therefore be more suitable for the purpose than fittings with diffusely transmitting or reflecting surfaces where the light distribution is less under control, so that when, for instance, the light sources are high it is impossible to prevent the house fronts from being disturbingly brightly illuminated.

One may therefore reasonably expect that for road lighting the best solution is a fitting with specular reflection. Nevertheless, in practice objections have been encountered to the use of mirrors or refractors, namely the following:

1. On damp and wet pavements a poor distribution of brightness was obtained.
2. The reflectors caused more glare.
3. The illumination on both sides of the street, for instance that of the house fronts, was often insufficient.

In the following it will be shown that these objections are not fundamental to mirror reflectors, but that in the design of the most appropriate light distribution the reflecting properties of damp or wet road surfaces are not duely taken into account.

Brightness distribution on the road surface

It has long been known, and it has been confirmed by recent investigations [1]) that for good observation on the road it is advisable to make the distribution of brightness as uniform as possible. In order to obtain this uniform distribution of brightness a uniform distribution of the illumination is, however, by no means the prevailing condition. This may be expressed in another way by remarking that the light distribution of the fitting must be corrected for the reflecting properties of the road surface. We have, however, found in publications only examples for this correction with dry roads and we emphasize that, as far as we know, these corrections for wet roadsurfaces are wanting.

To give an impression of the difference in brightness distribution, which happens to occur, when a definite installation changes over from dry to damp, we mention that certain points of the road surface will get a brightness 10 to 20 times higher and other points 3 times lower.

It is therefore clear that after correcting the fitting for a dry road surface large differences in brightness will occur, if the roadsurfaces is damp or wet.

We shall see, that if in computing the light distribution the reflecting properties of the damp road surface are also taken into account lighting installations can be made with give perfect results under all weathering conditions.

Glare with fittings using specular reflecting or refracting surfaces.

In the observation of the relatively low bright-

[1]) See P. J. Bouma. Measurements carried out on road lighting systems already installed, Philips techn. Rev. 4, 292, 1939; Peri, Rilievi sperimentali sulla illuminagione di strade. Communication to the 43rd annual meeting of the A.E.I. in Turin, Sept. 1939.

[2]) This is dealt with in more detail on page 98 of J. Bergmans: Light reflection by road surfaces, dissertation, Delft 1938.

nesses on the road, the sensitivity of the eye to contrast plays an important part. The glaring effect of a light source can therefore best be judged by determining the decrease in sensitivity to contrast which results from the glare. As has already been discussed in this periodical [3]), this glare depends in the first place upon the illumination on the eye by the glaring light source, and upon the angle between the direction of incidence of the disturbing light and the direction of view.

When in practice it has been observed that a mirror reflector gives rise to more glare than a diffusing fitting, the cause must be sought in the greater illumination received by the eye, in the case of the mirror, from a direction which makes only a small angle with the direction in which the objects were observed.

If in designing the light distribution of a fitting not only the reflecting properties of the dry road surface are considered but also the properties of the surface being damp, a smaller amount light will be radiated in directions making small angles with the direction of view. This results in light distributions, which are much more satisfactory from the point of view of glare. In order to demonstrate this we must, however, first consider more closely the reflective properties of ordinary road surfaces.

Brightness coefficients of the average road surface

As has already been explained in this periodical [4]) the reflective properties of a road surface can be represented with the help of the so-called brightness coefficient q. By the brightness coefficient is meant the ratio for a given point, of the observed brightness and the illumination, which is a function of the direction of illumination and of vision.

The value of q for a given point is determined not only by this combination of directions, it is also dependent on the nature of the road surface, and moreover, it changes very much with the degree of moisture on the surface. It therefore seems very doubtful at first glance whether it is possible, by measurements of the brightness coefficient under different circumstances, to arrive at a kind of average reflection characteristic of a road surface, which could form the basis for the calculation of a lighting fitting of general utility, and thus not based upon a special road surface and a certain state of moisture on that surface.

In practice, however, this is actually found to be possible. If for one definite combination of directions of illumination and observation the individual values of q are measured for different types of road surface, it is found that in the dry state they differ by a factor 4 and in the damp [5]) state by a factor 9. If now for a given combination of directions we determine the geometric average of these values of q, then the individual q values will only deviate by a factor of 2 from the average in the dry state. In the same way we determine the geometric average for the damp state. In this case the individual q values will only deviate by a factor 3 from that average. By this process one thus obtains two sets of q values, which are representative of the average dry road surface and the average damp road surface.

The factors 2 and 3 between the brightness coefficients of various road surfaces with the same combination of directions are small compared with the ratios between the brightness coefficients which may occur for the same road surface for different combinations of directions of illumination and observation, which are of the order of 1000. We may therefore say that the brightness coefficient changes mainly with the direction of illumination and observation, and only to a lesser degree with the nature of the road surface, so that the introduction of the above-mentioned average road surface is justifiable.

Fig. 1a and *b* give a diagram of the reflective properties of the average road surface just introduced. We assume that the road is lighted from a point 10 m vertically above L, and that the observer (height of eye 1.5 m) stands at A, 150 m from L. For each point on the road surface the combination of direction of illumination and observation is then determined, so that we can note the corresponding q values calculated as the geometric average of our measurements on different road surfaces. The curves of fig. 1*a* connect points with the same value of q in the dry state and fig. 1*b* gives similar "iso-q" curves for the damp state of the average road surface. Both states of the surface differ very much in the nature of their reflection from completely diffusely reflecting surfaces; a much stonger reflection occurs in certain directions. The average reflection coefficient of very bright road surfaces [6]) is a maximum of about

[3]) See P. J. Bouma, The problem of glare in highway lighting, Philips techn. Rev. 1, 225, 1936.

[4]) J. Bergmans:, The brightness of road surfaces under artificial illumination. Philips techn. Rev. 3, 313, 1938.

[5]) More detailed specification of the damp but not yet inundated state was given in the author's dissertation (see footnote [2]) on pages 81 and 82. See also the first article cited in footnote [1]).

[6]) The highest diffuse reflection coefficient which was measured in an elaborate investigation of about 40 different road surfaces was 29 per cent. See in this connection and in connection with the definition of the "average" reflection coefficient, the article cited in footnote[1]) pages 296 and 297.

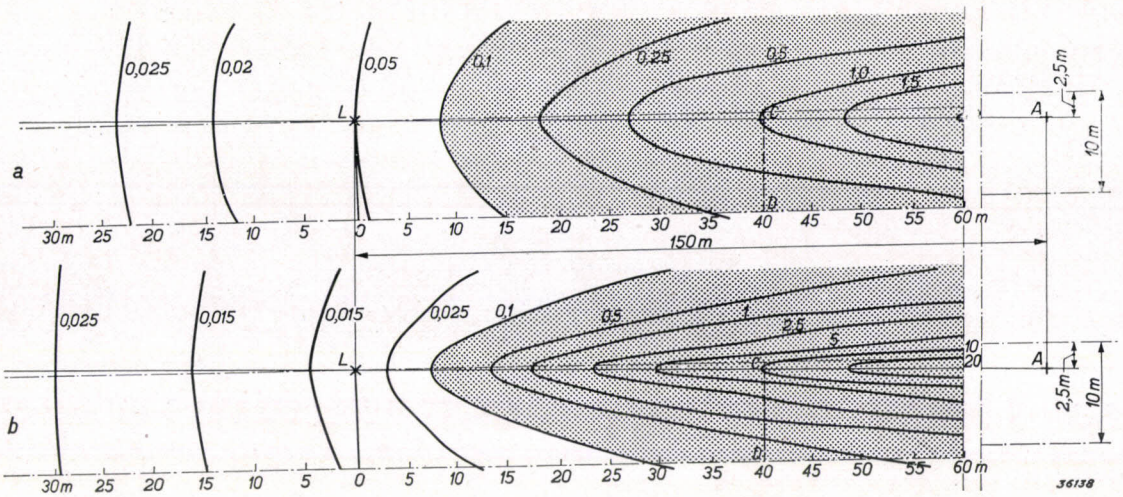

Fig. 1. A road 10 m wide is illuminated by a light source suspended 10 m above L on the curb. At a distance of 150 m from L the observer A stands 2.5 m from the curb above which the source hangs. For an average road surface lines are drawn through points with the same brightness coefficient expressed in c.p./m² brightness per lux illumination; *a*) for the dry state, *b*) for the damp state of the road surface.

$\varrho = 30$ per cent. If we assume a completely diffuse reflection, in which of course q = constant, then this would correspond to a q value of 0.1, because

$$q = \frac{B}{E} = \frac{\varrho E/\pi}{E} = \frac{1}{\pi}\varrho = \frac{0{,}3}{3{,}14} \approx 0{,}1.$$

The part of the road where the brightness coefficients of the average road surface are actually higher than 0.1 is shaded in fig. 1*a* and *b*. It may be seen that this is the case on a very large part of the road surface. In the case of the average dry road (fig. 1*a*) local regions occur with a q value 15 times as high, while the damp road (fig. 1*b*) exhibits q values at certain places more than 200 times as high. There are, however, also places (on the non-shaded part of fig. 1*a* and *b*) where the value of q both in the damp and the dry state is about five times as small as with the diffuse comparison surface.

From this comparison it may therefore be seen how extremely important it is in the construction of fittings to take into account the actual reflection properties of the road surfaces.

Chosen distribution of the luminous flux over the road surface

As indicated above, in order to obtain the best results as to visibility the fitting must provide a light distribution such that the brightness of the road surface is as uniform as possible. The q values may serve as a guide. By definition q is the quotient of brightness and illumination, *so that in order to attain uniform brightness the illumination at every point of the road surface must be inversely proportional to the value of q.*

Since a road lighting fitting must be able to be used not only when the road is dry but also when it is damp, a compromise must be found between the light distributions which would follow from figs. 1*a* and *b* for the two conditions. In order to show how this is done we shall deal with a definite example. We assume that the light source is suspended vertically above the edge of the 10 m wide road (see fig. 1*a* and *b*), and we consider the transverse cross section CD which is 40 m, *i.e.* a distance equal to four times the suspension height of the light points, away from L. The variation of the brightness coefficient over this cross section, which can be read off in fig. 1*a* and *b*, is given separately in *fig. 2* (q_d and q_v, respectively). It may be seen that the brightness coefficient of the point D, *i.e.*

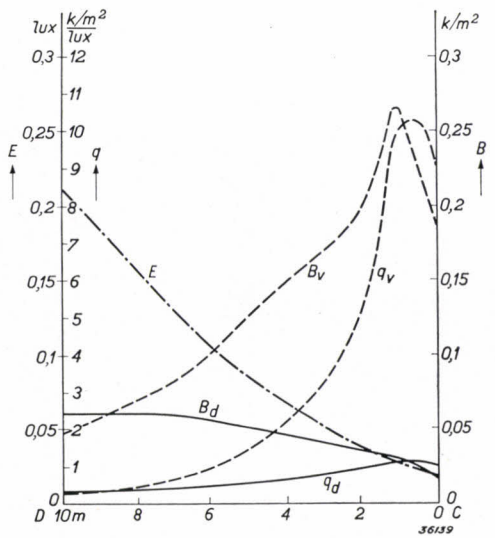

Fig. 2. Variation of the brightness coefficient q, the illumination E and the brightness B along the line CD of fig. 1 for a dry road surface (full lines) and for a damp surface (broken lines).

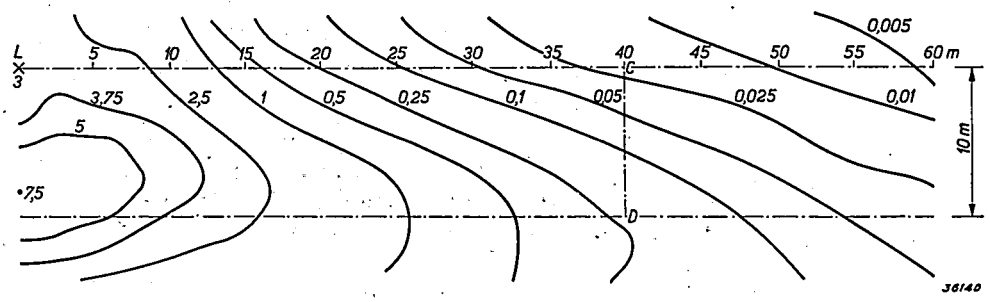

Fig. 3. A fitting of the type ZE 30 provided with a mercury lamp type 125 W MB/V is situated 10 m above point L on the edge of a 10 m wide road. With a total luminous flux of 5 000 lm of the lamp the values of the illumination given in lux are obtained on the pavement. Iso-lux curves are drawn on the surface of the road, from which it may be seen that the opposite side of the road is much more strongly illuminated than the side where the fitting hangs, *cf.* for example points C and D 40 m from the source.

on the opposite side of the road, for dry and damp states has practically the same value, namely about 0.3; at point C, on the same side of the road as the light source, the brightness coefficients for dry and damp states are very different, about 3 and 30 times as great as on the opposite side of the road, respectively.

If the points on the line CD are illuminated uniformly, which is approximately the case with most fittings now in use, curves q_d and q_v also give the variation of the brightness, and the brightness at C would exhibit a pronounced maximum. This is then manifested in the appearance of narrow, very bright streaks on the road surface which may be extremely disturbing for observation, since a small obstacle, a pedestrian or cyclist for example, standing next to such a streak is not observed at all.

From the foregoing, the remedy will be obvious: the light must be emitted chiefly toward the opposite side of the road, so that the illumination of point D is greater than at C by a factor 10. The effect of the greater brightness coefficient at C is then compensated in the most satisfactory way. With a dry road surface the brightness at D is then about 3 times as great, and with a damp surface about 3 times as small as at C, and these are brightness differences which may be considered permissible. We are thus faced with the remarkable fact that the brightness which is caused on the opposite side of the road in the dry state is greater than the brightness on the side where the light source itself stands.

The practical realization of this conception has led to the construction of a new fitting equipped with specular reflecting surfaces which will be described in the following.

Fig. 3 gives the distribution of the illumination over the road surface when the new fitting is used, and shows that the illumination on the opposite side of the road is indeed many times as

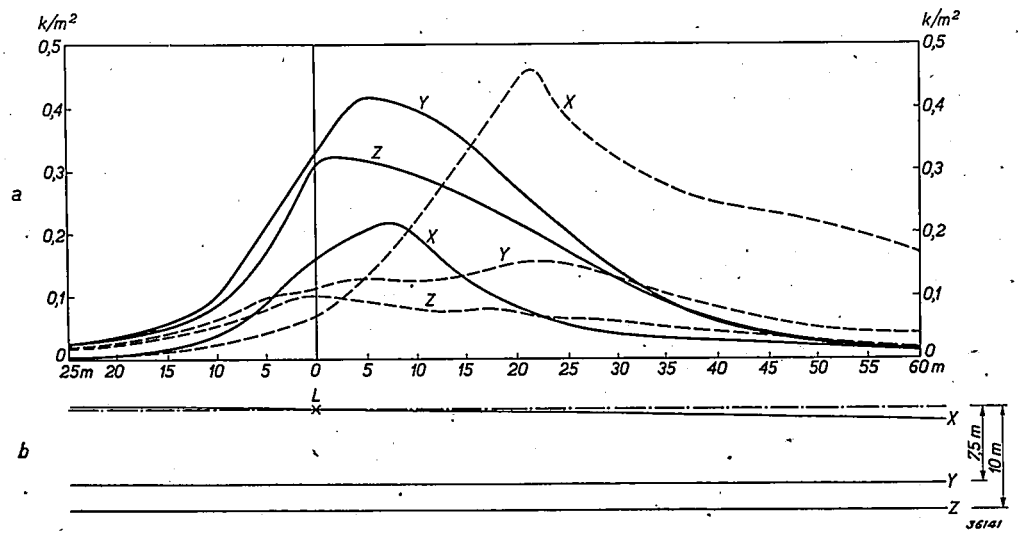

Fig. 4. Variation of the brightness (a) on the road along three different lines x, y and z which are indicated in (b). Line x is the line joining L with the observer A. Line z is the opposite edge of the road and y is parallel to it and 2.5 m away from it; y is thus the centre line of the opposite traffic lane. The full-line curves refer to the dry state, the broken-line curves give the variation of brightness for the damp state.

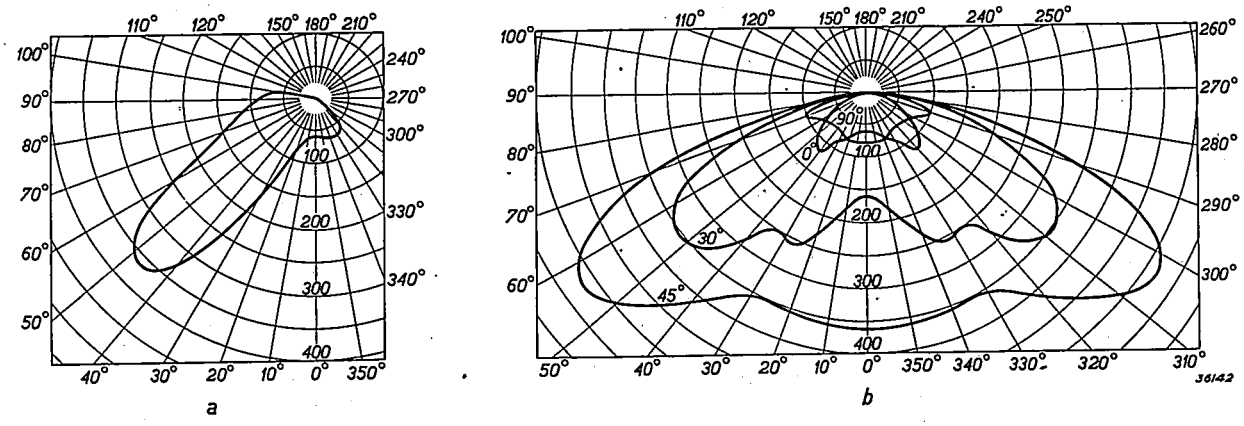

Fig. 5. Distribution of luminous intensity with the fitting type ZE 30 provided with a mercury lamp type 125 W MB/V.
a) Distribution in the vertical plane perpendicular to the axis of the street.
b) Light distribution in four planes indicated in fig. 6.

great as on the side where the source of light hangs.

In *fig. 4a* it is shown how the brightness on the street varies along three different lines x, y and z, specified in fig. 4*b*. Line x is the line joining L with the observer A. Line z is the edge of the road on the opposite side, and y is parallel to it and 2.5 m from it, *i.e.* it marks the middle of the opposite traffic lane. The full-line curves in fig. 4*a* refer to the dry state, while the broken-line curves give the variation of brightness for the damp state of the road surface.

It may be seen from these curves that the remarkable effect which was described above for the transverse cross section CD, holds not only for that particular place, but that for a whole strip of the roadway the brightness in the dry state on the opposite side of the road is higher than on the side where the light sources are suspended. In this way the bright streak on the road surface is made as broad as is practically possible.

Distribution of the luminous intensity of the new fitting

The light distribution which has been given to the new fitting ZE 30 may be seen in *fig. 5*. The light distribution of a fitting is ordinarily given by drawing the polar light distribution curve for several veetical planes passing through the source. When the light distribution in these planes varies only slightly, there is not much objection to this method. With a fitting which has a very unsymmetrical light distribution, such as the one here described, great difficulties are however encountered, because the points of the road surface for which the illumination can then be calculated, are distributed very unevenly over the roadway. We have therefore chosen a different method of representation, in addition to the polar light distribution curve of the plane perpendicular to the direction of traffic and we have measured similar curves (see fig. 5*a*) and drawn them for planes which are derived from the vertical plane parallel to the direction of the road by rotating it about a horizontal line passing through the light source (see the curves of fig. 5*b* and the indication of the measuring planes in *fig. 6*). When these curves are used, then the points for which the illumination on the road can be computed are distributed much more logically over the surface, while from such a representation, the question, which is for instance important in the problem of glare, can be answered as to how the candle-power varies for an observer moving normally along the road, *i.e.* along the direction of the length of the road.

It is striking how little light is emitted by the fitting in the vertical plane (0°) parallel to the axis of the road. Especially at small angles with the horizontal a very limited luminous intensity in this plane, due to the high value of q, gives the best results for attaining the correct brightness distribution over the road surface.

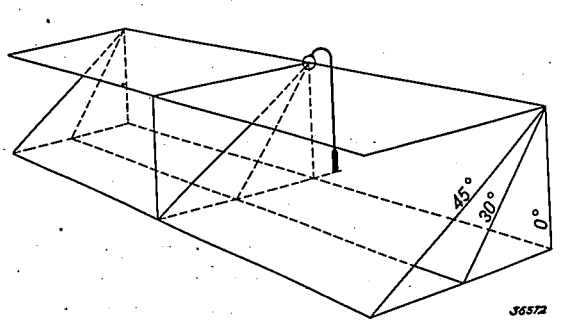

Fig. 6. Sketch in perspective of the planes for which the light distributions in fig. 5 are drawn.

Due to the low candle power in this direction the disturbance by the light from the source is also a minimum. The two requirements of the greatest possible uniformity of brightness, also in the damp state, and that of low glare are therefore not mutually exclusive, but on the contrary can be realized at the same time.

An important point to which attention must still be called is that the luminous intensity in each of the curves of fig. 5*b* passes very gradually from the highest value to the very small value in the horizontal direction. The nature of this transition is of great significance for the distribution of brightness in the perspective of the road. When instead of the curve chosen by us, there was a sharp cut off at 70 or 80°, as often occurs with other fittings, then this cutting off would be manifested on the road surface as an annoying stripe. As may be seen in fig. 1*a* and *b* especially in the damp state, the brightness coefficient on the line joining L and A increases very sharply with increasing distance from L when the distance from L is greater than the distance corresponding to an angle of emission of 70°. This results in the fact that with many fittings the brightest spot in the damp state lies at a point on the above-mentioned line between 70 and 80°. If all light radiation is suddenly cut off at greater angles, a very disturbing brightness distribution occurs on the road surface. With the very gradual cutting off which is shown in the curves of fig. 5*b*, this phenomenon need not be feared.

Finally we wish to call attention to the radiation in the horizontal plane (90°). The light emitted in this direction is not incident on the road itself, but illuminates the houses standing on the road, so that the road is not as it were isolated, and police patrol service is made easier. From the nature of the case the illumination of the house fronts may and must be lower than that of the road. Too low an illumination, however, may be detrimental to the safety of those who leave a house and enter the road, since they are not promptly observed by the traffic on the road. If the house fronts are illuminated with light sources which are all mounted on the same side of the road, a much too local illumination of a few houses is obtained, while the others remain too dark. If this is prevented by specially directing the light toward the more distant houses, the latter cause disturbing shadows so that the desired effect is not reached. By illuminating the house fronts from the opposite side, on the other hand, good results can be obtained.

Position of the fitting with respect to the surface of the road

In figs. 1*a*, 1*b* and 3 we have indicated the edges of the road with dash-dot lines in such a way that the light source was situated just above the edges. This does not mean, however, that the fitting could not be used satisfactorily suspended on wires over broad roads. In this case also care must be taken for as uniform possible brightness over as broad as possible strips of the road surface, and for this special purpose the new fitting is suitably constructed. In order to illuminate the house fronts also, the fittings must be so hung that they always radiate from the outside of the road towards the middle.

In order that the fitting shall be in the proper position with respect to the surface of the road, it must if necessary be fastened to the suspension wire by means of a flexible line coupling device (*fig.* 7).

Due to the twisting of the suspension wire a small amount of swing about a horizontal axis perpendicular to the direction of the traffic will be retained. Such a swing, which is unusually annoying in fittings with a sharp cut-off, is undisturbing in the case of the new fitting due to the "gradual cut-off" of the light.

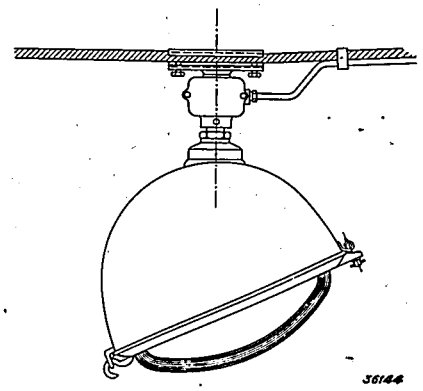

Fig. 7. The fitting can be fastened with a clamp arrangement so firmly to the suspension wire that it can only swing about a horizontal axis perpendicular to the direction of the street. The swinging about this axis, namely about the suspension wire, which occurs in windy weather, is not disturbing.

Construction of the new fitting

Care has been taken in the construction that the glass parts, mirror and cover, each in its frame, can be easily introduced into the housing when it is assembled, and that at the same time they can be removed from the fitting in a simple manner in order to be cleaned. In both cases the system has been used with a hook on one side and a screw for fastening on the other (see *fig.* 8). Not only the screw which holds the mirror fast (at C),

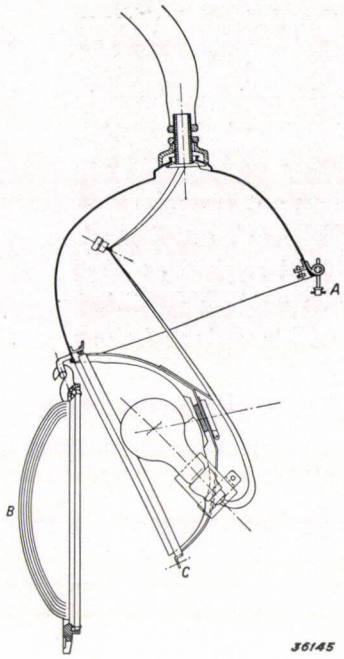

Fig. 8. Fitting ZE 30 shown opened. The cover glass and the mirror, both fastened in their steel frames are hooked on at one side. The fitting is closed by screwing tight the frame of the cover glass at the other side.

but also the nut *A* with which the cover glass *B* is fastened, cannot be lost, and are so constructed that if they are loosened by vibration, the parts are still held together.

In *fig. 9* a diagram is given of the paths of the rays in the reflector. Mercury lamps as well as ordinary incandescent lamps may be used. In order to obtain about the same light distribution in both cases it was necessary to choose a different position for the mercury lamps. (75 W or 125 W MB/V) from that for the ordinary incandescent lamps. In fig. 9 the position of the incandescent lamps is indicated by *G* and that of the mercury lamps by *K*. This is carried out technically so that there are two spring clamps (fig. 8) in the frame of the mirror for holding the cylinder in which the lamp holder is fastened. One spring clamp serves for the incandescent lamp and the other for the mercury lamp. It is also indicated on the fitting cylinder at what height each lamp must be set in order to obtain the desired result.

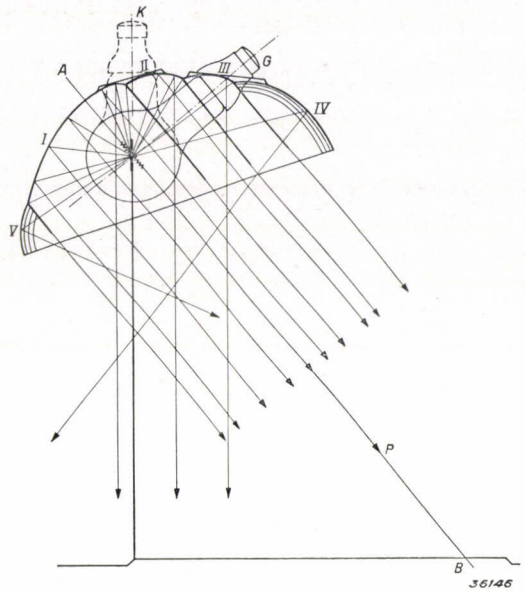

Fig. 9. The silvered glass mirror of the fitting ZE 30 consists of segments *I-V*. The largest part of the light is reflected in the direction *APB*. The correct position of the electric lamps with respect to the mirror is indicated by *G*, that of the mercury lamps 75 W or 125 W MB/V by *K*.

Fig. 10 is a photograph of the fitting and of each of the main components: housing, mirror frame and covering glass. In the photograph of the mirror

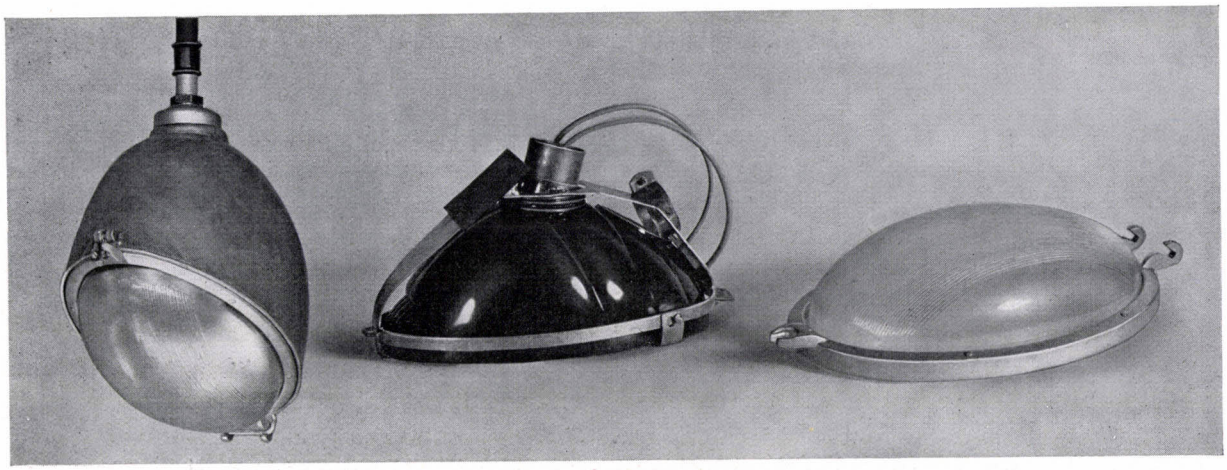

a) b) c)

Fig. 10. *a*) Fitting ZE 30 suspended ready for operation (height of the complete fitting about 40 cm);
b) mirror frame;
c) cover glass.

Fig. 11. Road provided with ZE 30 fittings in which are mercury lamps 125 W MB/V (5000 lm). Height of suspension of the light sources 9 m, spacing 34 m. All the sources are on the same side of the street above the curb. Width of street curb to curb 12 m. Dry road surface. Above is a series of density standards for the determination of the brightness of every point on the road surface; see the article cited in footnote [1]).

frame it may be seen that the mirror is made fast by means of a large coiled spring and that no screws are used for this purpose.

The silvered glass mirror is provided with a special protecting layer of fired enamel. The silver layer is thus situated between two glasslike surfaces, in front the glass body of the mirror and on the back the layer of enamel. This provides sufficient protection of the silver layer not only against effects of temperature, but also against those of the atmosphere. Such mirrors are also resistant to the effects of sea air, so that the fitting can be used without danger close to the sea.

In *figs. 11* and *12* two parts of a street are shown which is illuminated with the fitting ZE 30. The light sources are set up on only one side of the road. This arrangement, which is much less favourable than one on both sides or over the middle of the road, offers great advantages in judging the fitting. From a photograph it is impossible to see from which source of light a given spot on the road surface is illuminated. When, however, the light sources are only situated on one side of the road, and considerable brightness is observed in the photograph on the other side of the road, it is certain that this is due to the good qualities of the fitting.

The road shown in figs. 11 and 12 is 12 m wide from curb to curb. The light sources are suspended at a height of 9 m above one curb at intervals of 34 m. Mercury lamps type 125 W MB/V were used which give a luminous flux of 5 000 lumens. Power installed 3.8 kW per km. The road surface consists of granite blocks.

The photographs show clearly that even with this unfavourable ratio of width of road to height of suspension (12 m to 9 m) the entire surface of the road, damp as well as dry is sufficiently uniformly bright. The fronts of the houses on the opposite side of the road are also clearly visible.

For measurements of visibility a distinction must be made between the values which are observed when one stands on the half of the road upon which the light sources are situated and those on the other side. For the two cases, which correspond to the two directions of the traffic, we have determined the smallest observable contrast, namely at the most favourable spot (Z) and the least favourable spot (z) in the field of vision. These measurements were carried out in dry as well as damp weather.

Fig. 12. The same installation as in fig. 11 with damp road surface.

The results are the following [7]):

		dry	damp
Observation on the side of the light sources	Z	31.9	39
	z	38.2	15
Observation on the opposite side	Z	30.4	34.2
	z	39.2	50

The above values for a road lighted on only one side of such a width and with such a low power installed, may be considered very satisfactory, and they show especially that the decrease in visibility upon transition from dry to damp is very slight.

[6]) Similar measurements on numerous other road surfaces are discussed in the article cited in footnote [1]).

AN ELECTRODYNAMIC PICK-UP FOR THE INVESTIGATION OF MECHANICAL VIBRATIONS

by J. SEVERS.

621.317.351 : 621-752

In the case of the Philips vibration pick-up GM 5 520 the mechanical vibrations of the object investigated are converted electrodynamically into an electrical alternating current voltage, whose variations can be made visible on the screen of a cathode ray oscillograph. The construction of the pick-up, particularly as concerns the choice of characteristic frequency, the damping and the sensitivity required, are here briefly discussed. The interpretation of the velocity and deviation oscillograms obtained, and the method for quantitative measurement of vibration are then dealt with. When the oscillograph GM 3 156 is used, the vibration to be investigated can be shown with an enlargement of 3 500 times at frequencies down to 10 c/s. In conclusion a discussion is given of the way in which the pick-up can be applied to the vibrating object, and several examples of its use are dealt with.

In the last decades increasing attention has been devoted to the mechanical vibrations which occur at all kinds of spots on technical objects, and which may be undesired for various reasons. In the case of parts of engines or structural parts, for instance of motors, aeroplanes, bridges, etc. it is the destructive effect of the vibrations, in other cases, such as in ships, vehicles and buildings, it is the annoyance of the vibrations to human beings which makes it necessary to combat them.

Before they can be combatted they must be known. How are mechanical vibrations investigated? Various instruments have long existed for this purpose which enlarge mechanically or optically the generally very small deviations occurring upon vibration to values which can be read off directly or recorded if desired. A more modern method is to bring about the enlargement not mechanically or optically, but electrically. In this way, thanks to the highly developed amplifier technique, it is easily possible to investigate vibrations with relatively high frequencies and low amplitudes, while at the same time the possibility is offered of constructing handy, transportable apparatus, which, unlike most of the older apparatus, is not confined to a given method of arrangement nor to a definite direction of the vibrations.

Use is made of these possibilities in the Philips vibration pick-up GM 5 520, which we shall describe in this article.

The method of converting the motion

The enlargement is obtained in the case of the electric vibration pick-up by converting the varying deviation of the vibrating object into a varying electrical voltage, which can then be amplified at will, and whose variations, made visible on the screen of a cathode ray oscillograph, form a picture of the variation of the deviation to be measured. In the Philips vibration pick-up the conversion of the mechanical vibrations into an A.C. voltage is carried out on the electrodynamic principle: a magnet whose lines of force cut the windings of a coil is allowed to follow the movements of the vibrating

object. It is obvious that it is here necessary that the coil should not follow the movements of the vibrating object, since only with a relative displacement of magnet and coil will a voltage be generated. This involves a fundamental problem which we shall first examine in more detail.

It is a very general rule that the deviation of a point on the vibrating object can never be measured except by the relative displacement of that point with respect to a second point whose motion is known. The simplest thing is to choose for the second point a fixed point which does not take part in the vibrational movement. This is, however, impossible in many cases. It is only necessary to think of the vibrations which occur during earthquakes: no fixed point outside the earth's surface is available, and points on the earth's crust which do not share in the vibration, or to only a small degree, are too far away to be used for the measurement. In the vibrations of ships, bridges, etc., and in general in the vibrations of large masses at low frequencies (several c/s), the same difficulty is usually encountered.

For such cases one may choose as point of comparison the position of a mass which is connected by means of a spring to the vibrating object (*fig. 1*). If m is the mass, c the stiffness of the

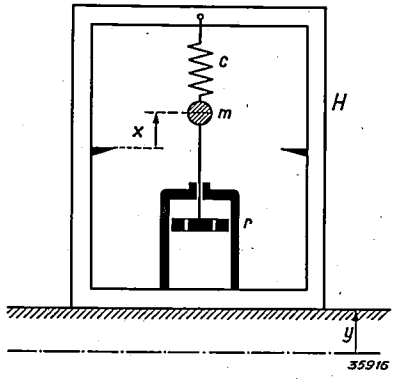

Fig. 1. Diagram showing the principle of a vibration pick-up in which no use is made of a fixed point outside the vibrating object. The relative deviation x of the mass m with respect to the housing H is measured, and furnishes a measure for the absolute deviation y of the housing (*i.e.* of the vibrating object).

spring, r the coefficient of damping prevailing, then the following differential equation holds for the relative displacement x of the mass with respect to the vibrating object:

$$m\frac{d^2(x-y)}{dt^2}+r\frac{dx}{dt}+cx=0 \quad . \quad . \quad . \quad (1)$$

In this equation y is the required deviation of the object investigated, while x can be measured directly. With the sinusoidal vibration

$$y=y_0\cos\omega t$$

in the stationary state x becomes

$$x=x_0\cos(\omega t-\varphi), \quad . \quad . \quad . \quad . \quad . \quad . \quad (2)$$

where

$$x_0=y_0\frac{(\omega/\omega_0)^2}{\sqrt{4D^2(\omega/\omega_0)^2+(1-(\omega/\omega_0)^2)^2}} \quad . \quad . \quad (3)$$

and

$$\operatorname{tg}\varphi=\frac{2D\,\omega/\omega_0}{1-(\omega/\omega_0)^2} \quad . \quad . \quad . \quad . \quad . \quad (4)$$

In these expressions $\omega_0=\sqrt{c/m}=2\pi$ times the resonance frequency of the undamped vibrating system and $D=r/2\,\omega_0 m$, the so-called damping factor.

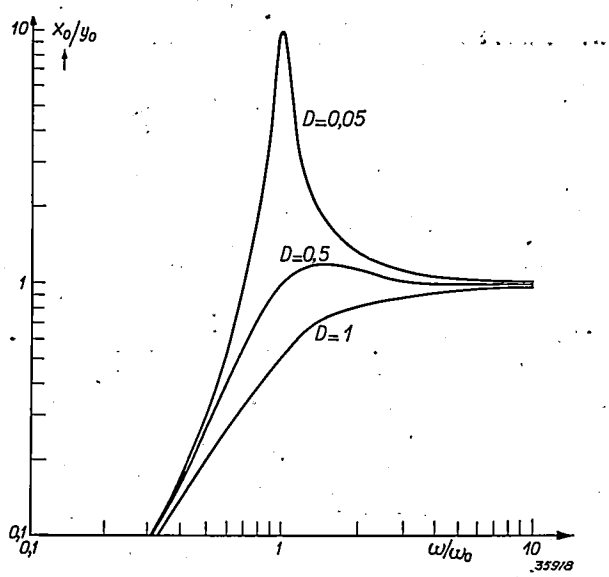

Fig. 2. Frequency characteristics of a pick-up on the principle of fig. 1, for different values of the damping factor D. At frequencies $\omega/2\pi$, which are far enough above the resonance frequency $\omega_0/2\pi$, the relative amplitude x_0 to be measured is practically equal to the absolute amplitude y_0 of the object.

In *fig. 2* the ratio x_0/y_0 given by (3) is plotted as a function of the frequency for different values of the damping factor D. It may be seen that at frequencies sufficiently far above the resonance frequency $\omega_0/2\pi$, the ratio x_0/y_0 is constant and equal to unity: the mass m, due to its inertia, then remains practically at rest and thus behaves as if it were fastened to a fixed point outside the vibrating object [1]).

[1]) The considerations given here are valid for all cases in which vibrations must be recorded and reproduced, thus also for microphone, gramophone pick-up, etc. A comparison with the laryngophone which was described in this periodical 5, 6, 1940, is particularly instructive. In that case also the "direct" and the "indirect" method of driving were compared and, as in this case, the indirect method was chosen. In that case, however, it was a question of the quadratic variation of the ratio x_0/y_0 as a function of the frequency, which is obtained at frequencies below the resonance frequency.

In the technical application of a vibration pick-up one is often concerned with rotating engines whose speed generally lies between 120 and 3 000 r.p.m. The fundamental frequencies of the expected vibrations may therefore be very low (several c/s). It is therefore desirable that the flat part of the frequency characteristic of fig. 2 should extend as far as possible toward the low frequencies. For this purpose the vibration pick-up must have as low a characteristic frequency as possible, and it is advisible to choose a value $D \approx 0.5$ for the damping factor.

Construction of the vibration pick-up

The principle illustrated diagrammatically in fig. 1 is realized in the following way in the Philips vibration pick-up (see *fig. 3*). The mass m is formed

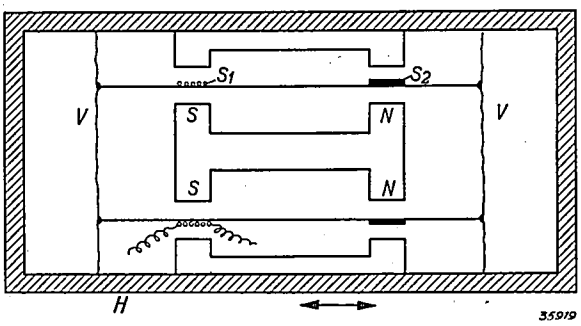

Fig. 3. Cross section of the electrodynamic vibration pick-up (very much simplified). The coils S_1 and S_2 move in the ring-shaped air gaps of a magnetic circuit which is excited by a permanent magnet. These coils are connected with each other and hung on two membranous springs V. S_1 provides the output voltage, S_2 (a copper ring) the desired damping force.

mainly by two coils S_1 and S_2 fastened to each other, which are suspended in a cylindrical housing by means of two membranous springs. The housing shares in the movement of the vibrating object. The coils can move in two ringshaped air gaps of a permanent magnet fastened to the housing. The coil S_1 provides the desired output voltage; the coil S_2 consists of a closed ring, and the current induced in this ring gives rise to the desired damping force (second term of equation (1)).

In making the design it was kept in mind that the vibration pick-up should be able to be used in any desired position. When the pick-up is turned from the horizontal to the vertical position the coils will be displaced over a distance x_m which is given by

$$c\, x_m = m\, g,$$

(g is the acceleration due to gravity), and thus

$$x_m = g/\omega_0^2 \quad \ldots\ldots\ldots \quad (5)$$

For a linear relation between voltage and deviation, the coils must always intersect the same magnetic flux and therefore too great a variation from the position of rest of the coils would obviously lead to very uneconomical constructions. It follows from equation (5) that a lower limit is thereby prescribed for the characteristic frequency ω_0 to be chosen. The pick-up here described was constructed for a maximum throw of the coils of 3.75 mm, while it was required to be able to measure vibration amplitudes up to 2 mm. The permissible variation x_m from the position of rest is thus 1.75 mm, so that according to (5) $\omega_0/2\pi$ could be made equal to 12 c/s.

While the ratio c/m is determined in this way, further consideration shows that the total mass m of the moving system must be made as small as possible. It may easily be deduced that the damping coefficient r (equation (1)) is proportional to the volume v of the damping ring and to the square of the field strength H_2 in the air gap [2]). Thus the damping factor D becomes

$$D = \frac{r}{2\,\omega_0 m} \sim \frac{H_2^2 v}{m} \quad \ldots\ldots \quad (6)$$

Since, except for a certain factor given by the required play of the ring in the gap, v is equal to the volume of the air gap, $H^2{}_2 v$ is actually the total magnetic energy, and therefore proportional to the quantity of magnet steel. In order to obtain the desired damping factor D therefore ($D \approx 0.5$), when ω_0 is once chosen, less magnet steel is necessary the smaller m is. Now a limitation of the quantity of magnet steel needed is very much desired, not only for economic reasons, but also to keep the whole vibration pick-up as small and light as possible, so that the movement of the object being investigated cannot be affected by the application of the pick-up. Obviously a type of magnet steel will be chosen which has the highest possible magnetic energy per cubic centimetre.

A limit is set to the reduction in size of the pick-up mainly by the requirements relating to the sensitivity demanded. The voltage induced in the

[2]) If l is the length of the coil (circumference of the ring) in cm, H the field in gauss, then the induced voltage in volts is

$$e = 10^{-8}\, l \cdot H \cdot \mathrm{d}x/\mathrm{d}t.$$

This causes a current $i = e/R$ (R is the electrical resistance of the ring) and hereby a retarding force

$$K = 0{,}1 \cdot H \cdot i \cdot l = 0{,}1 \cdot H \cdot l \cdot e/R.$$

By filling in e and $R = \varrho \cdot l/q$ (ϱ = the specific resistance, q the diameter of the ring) one obtains

$$K = \frac{10^{-9} \cdot H^2 \cdot v}{\varrho} \cdot \frac{\mathrm{d}x}{\mathrm{d}t} = r\,\frac{\mathrm{d}x}{\mathrm{d}t}.$$

coil S_1 is

$$e = l \cdot H_1 \cdot \frac{dx}{dt} \cdot 10^{-8} \text{ volts}, \quad . \quad . \quad . \quad . \quad (7)$$

where l (cm) is the length of wire and H_1 (gauss) the field strength in the gap in which coil S_1 moves. In order to obtain a given sensitivity $e/dx/dt$ with a minimum amount of magnet steel (magnetic energy $H_1^2 v_1$), the volume v_1 of the air gap, and thus that of the coil, will be made as small as possible, and the length of wire l as great as possible. This means a thin wire and many windings. Attempts in this direction are, however, limited by the requirements that the wire must be able to be wound without difficulty, and that the self-induction of the coil (which is proportional to the diameter of the coil and to the square of the number of turns) must be kept so low that the resonance between the self-induction of the coil and the characteristic capacity of the coil plus the capacity of the connecting cable will lie far enough above the frequency region in which the measurements are being done. In this way one is bound to a given coil volume which cannot be reduced, and thereby not only is the amount of magnet steel required to obtain the field H_1 prescribed, but, because of the contribution of the voltage coil to the mass m in equation (6), the amount of steel necessary for the field H_2 in which the damping ring moves is also prescribed to a certain extent.

If m is made as small as possible, then for a given characteristic frequency, c must also become small, *i.e.* the springs must be very weak in the direction of vibration. In a direction perpendicular to this, however, they must be very stiff in order to guarantee a satisfactory centred motion of the coils in the ringshaped air gaps. This is achieved by the use of membranous springs with which a relatively slight lateral play of the coils in the air gaps suffices. Nevertheless, this play is again a reason why the whole system cannot be made too small. With a proportional reduction in size of all the other dimensions the ineffectual part of the volume of the gap becomes more and more important.

The oscillogram obtained

The EMF e excited in the coil S_1 is proportional to the velocity dx/dt at which the coil moves. If therefore we apply the voltage of the coil directly to a cathode ray oscillograph, we obtain an image of the momentary values of the vibration velocity. Such a velocity oscillogram is indeed often used in the investigation of vibrations of acoustic frequencies, since the velocity provides a better measure of the sound caused by such vibrations than the deviation. In general, however, the mechanical engineer will be more interested in the deviation itself. A voltage proportional to the deviation x is obtained by applying the voltage e of the coil to the simple circuit shown in *fig. 4*. If $R \gg 1/\omega C$, then

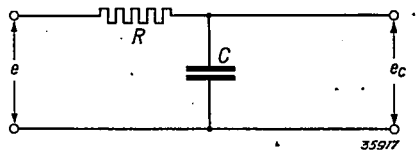

Fig. 4. "Integrating element". If the voltage e (output voltage of the vibration pick-up) is proportional to the velocity dx/dt of the vibrating object, then the voltage e_c is proportional to the deviation x if $R \gg 1/\omega C$. By applying the voltage e_c to a cathode ray oscillograph the form of the vibration in question is made visible on the fluorescent screen.

the current i through the condenser is practically equal to e/R, and the voltage on the condenser becomes:

$$e_c = \frac{1}{C} \int i \, dt = \frac{1}{RC} \int \text{const.} \frac{dx}{dt} \, dt = \text{const.}' \cdot x.$$

The voltage e_c applied to the cathode ray oscillograph thus gives an oscillogram of the deviations.

In the case of purely sinusoidal vibrations the velocity and deviation oscillograms obtained give a correct picture of the motion of the vibrating object. This is, however, not immediately the case when the vibration possesses harmonics, since in that case for faithful reproduction, it is necessary that not only the amplitude relations but also the relative phase differences of the components should be retained. The first requirement is satisfied when all the frequencies occurring fall within the flat part of the characteristic (fig. 2). The second condition means that the phase shift (φ in equation (4) with in

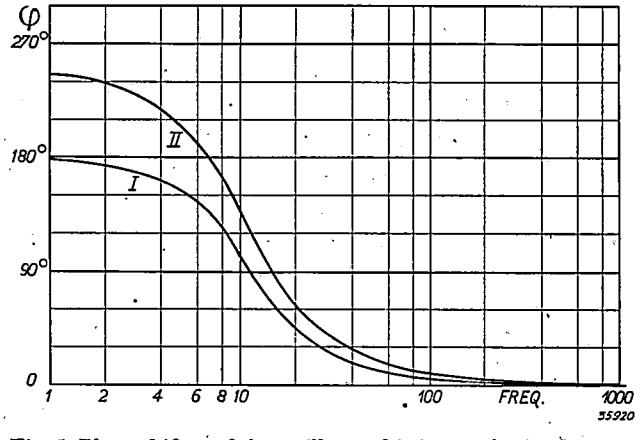

Fig. 5. Phase shift φ of the oscillographic image obtained, compared with the original vibration, as a function of the frequency (c/s). Curve I holds for the velocity oscillogram (φ is here given by equation (4), in which $D = 0.48$ and $\omega_0 = 2\pi \cdot 12$), curve II for the deviation oscillogram.

addition, for the deviation oscillogram, the phase shift in the circuit of fig. 4) must be the same for all frequencies occurring, which is the case only at relatively high frequencies, see *fig. 5*. The influence of phase shifts may not be simply neglected in this case, as is customary in acoustics, since for the destructive action and the disturbing effect it is just the peak values of the deviation, which depend closely upon the phase relation between the harmonics, which are most important. *Fig. 6* illustrates the differences which may occur between the oscillogram and the original vibration. These differences must certainly be taken into account in judging and interpreting the oscillograms.

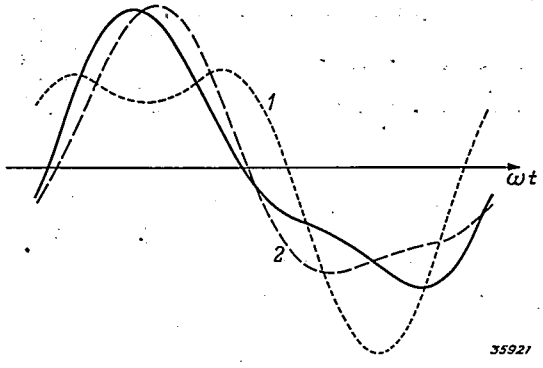

Fig. 6. The housing of the vibration pick-up may vibrate according to the relation: $x = \sin \omega t + 0.3.\ \sin\ (2\omega t - 45°)$: full-line curve. According to the value of ω, the oscillogram obtained with the oscillograph GM 5 520 will deviate more or less from this curve. At $\omega/2\pi = 10$ c/s the broken-line curve *1* is obtained, at $\omega/2\pi = 25$ c/s, the broken-line curve *2*.

Another distortion of the oscillogram might occur due to a deviation from the linearity of the flexibility of the spring assumed in equation (1). With a horizontal direction of motion the flexibility is indeed found not to be perfectly linear, due to an unavoidable very slight sagging of the membranous springs. The effect of this, however, is hardly appreciable: at the highest amplitudes to be measured (in the horizontal direction 3.75 mm, see above) maximum deviations of a few per cent occur in the sine tops.

The method of measurement and the enlargement obtained

In order not only to study the nature of the vibrations but also to determine them quantitatively, the following method is used. While the voltage e_c is applied to the cathode ray oscillograph, the time base is switched off so that a vertical stripe of a definite length appears on the screen. Then instead of e_c, an A.C. voltage is applied to the oscillograph with the help of a potentiometer through which an accurately determined alternating current from the mains flows. The A.C. voltage must be such that a stripe of the same length is obtained. The potentiometer is calibrated directly in microns (vibration amplitude). In the same way, by omitting the integrating element fig. 4, the velocity amplitude can be determined.

The calibration of the potentiometer is only valid for the flat part of the frequency characteristic. For lower frequencies the result must be multiplied by a correction factor derived from the characteristic. Since for different individual vibration pick-ups the characteristics vary somewhat due to an unavoidable slight divergence in the properties of the springs and magnets, etc., upon manufacture the curve of the correction factors of each individual pick-up is recorded and accompanies the pick-up. Actually two correction curves are used, one for the approximately vertical position of the pick-up and one for the approximately horizontal position. The small difference between the two curves may be ascribed to the slight sagging of the membranous springs already mentioned. In *fig. 7* an example of such a correction curve is reproduced. Above about 50 c/s no correction is necessary, for frequencies between about 10 and 50 c/s it is still relatively small, and only at still lower frequencies it is necessary to know the frequency accurately for satisfactory measurement. This can be determined with the oscillograph.

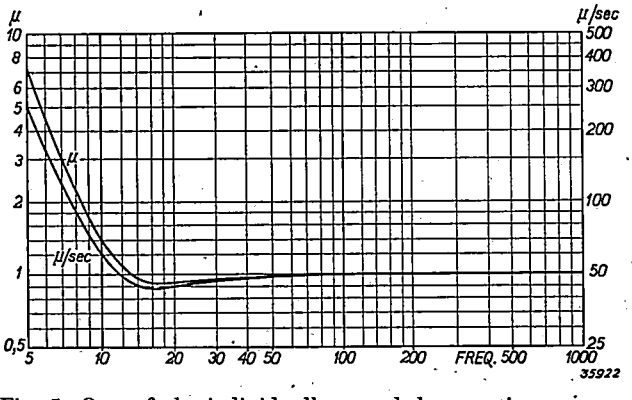

Fig. 7. One of the individually recorded correction curves. This furnishes the factor by which the reading on the calibrated potentiometer must be multiplied for every frequency in order to obtain the true amplitude (left-hand scale) or the velocity amplitude (right-hand scale).

In the method of measurement described it is tacitly assumed that the cathode ray oscillograph is just as sensitive to the frequency of the vibration to be investigated as to that of the comparison voltage (50 c/s). In the case of the cathode ray oscillograph GM 3 152 previously described in this periodical [3]) this is true down to frequencies of about

[3]) Philips techn. Rev. 4, 198, 1939.

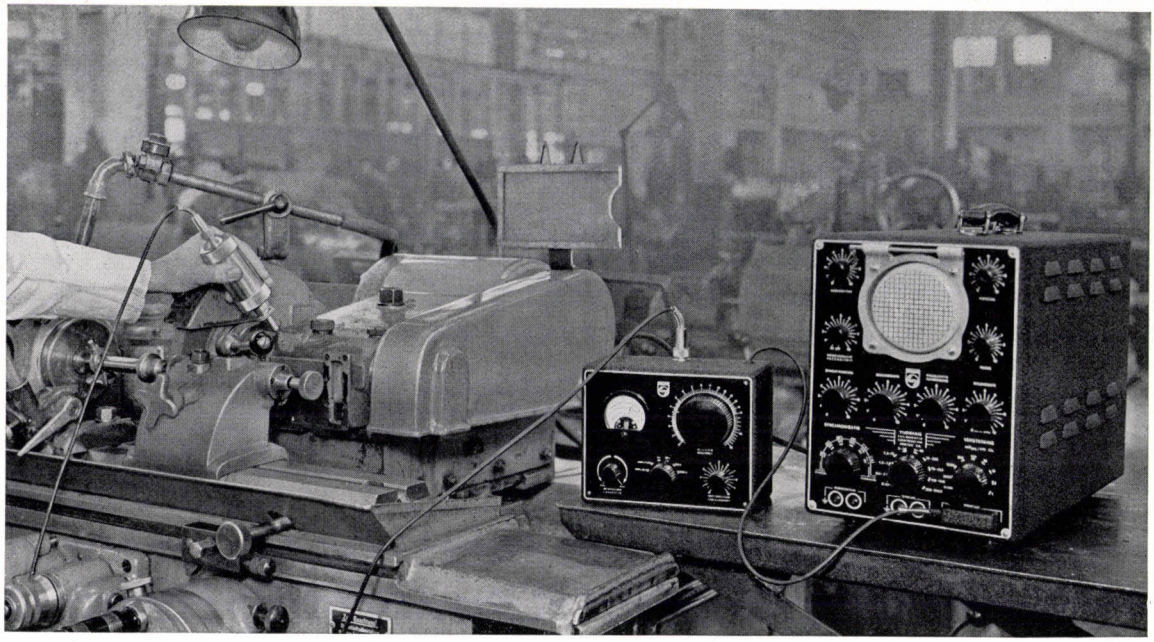

35924

Fig. 8. Complete apparatus for vibration testing with the pick-up GM 5 520. The latter in this case is pressed with a short steel rod against the machine being investigated. (It was here a question of investigating the effect of a lack of balance in a grinding machine on the accuracy of the work). On the right the cathode ray oscillograph GM 3 156 and the box containing the integrating element, the calibrated potentiometer for the determination of the amplitudes and other components.

10 c/s, with the new oscillograph GM 3156, this is true even down to 0.3 c/s.

The vibration pick-up in combination with the integrating element gives, in the flat part of the frequency characteristic, an output voltage of 1 mV (peak value) for an amplitude of 1 micron (and for a velocity amplitude of 50 microns/s). On the screen of the oscillograph GM 3 156 one obtains with this voltage a stripe 7 mm long (double amplitude) when the highest amplification is used. The vibration being investigated is thus delineated with an enlargement of 3 500 times. When the oscillograph GM 3 152 is used the enlargement is smaller by a factor of about 6. The accuracy of reading in the case of the comparative method described may be estimated at about 1 mm in the length of the stripe.

In measurements in the neighbourhood of the resonance frequency the results are slightly affected by the temperature of the vibration pick-up. This effect is based upon the dependence on temperature of the resistance of the damping ring, whereby the damping factor which determines the shape of the frequency characteristic near the resonance may change somewhat. The frequency characteristics are recorded at 20° C. Measurements at 12 c/s then give values about 4 per cent too high with 10° increase in temperature, while toward higher and lower frequencies the temperature effect quickly disappears.

In *fig. 8* a photograph is given of a complete measuring arrangement. In the left-hand box standing beside the cathode ray oscillograph and connected by means of a shielded cable to the vibration pick-up, are the integrating element, the potentiometer, the necessary switches and other components.

The application of the pick-up to the vibrating object

The housing of the vibration pick-up must follow the motion of the vibrating object which is being investigated. When it is a question of low frequencies, below 100 c/s, for example, it is sufficient to press the pick-up against the vibrating surface with the hand. The long axis of the pick-up must be in the direction of vibration, since the pick-up only reacts to the vibration component in its axial direction. Use can also be made of this characteristic in order to discover the direction of vibration if it is not already known. For the case in which the direction of vibration is parallel to the surface against which the pick-up can be pressed there must be sufficient friction between the surface and the housing of the pick-up. For this purpose the housing is provided with two milled rings. (*fig. 9a*).

For the investigation of the movement of various points which may be difficult to reach, a long steel rod can be used, which can be screwed into the pcik-up, and with which the object can be gone over point by point (*fig. 9b*). The long rod is also useful for vibration measurements on electromotors and the like, in order to keep the vibration pick-up at a distance from any stray magnetic fields. Although

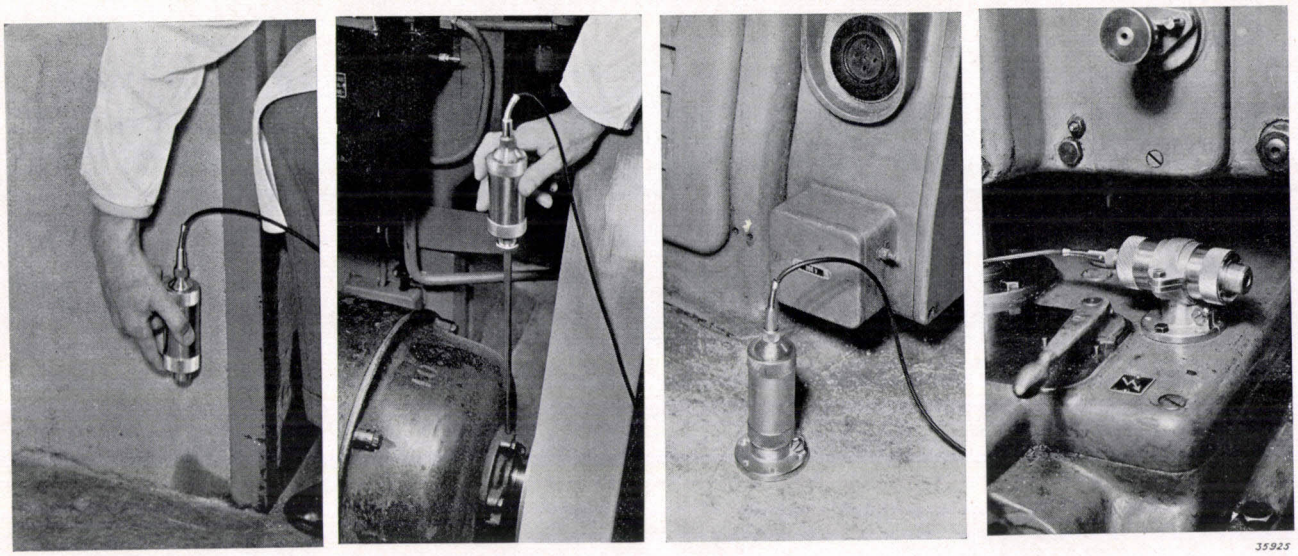

a *b* *c* *d*

Fig. 9 *a-d*. Different methods, in which the vibration pick-up may be fastened to the vibrating object.

the iron case of the pick-up provides satisfactory magnetic protection (the field strength of an external field at the position of the coil becomes about 30 times smaller than it would be without this shielding), nevertheless, due to the large number of windings of the pick-up coil, measuring errors might occur: an external alternating field of 1 gauss in the direction of length of the coil at 50 c/s causes a voltage at the output of the integrating element of $^1/_4$ mV.

For going over the vibrating object point by point it is very advantageous that the pick-up possesses relatively strong damping (damping factor $D = 0.48$). The stationary vibration given by equations (2) to (4) is always preceded by a starting oscillation whenever the pick-up is applied, which dies out proportionally to exp $(-\omega_0 Dt)$. With $\omega_0 = 2\pi \cdot 12$ and $D = 0.48$, it is found that this factor decreases in less than 1/5 sec to 1/1000, so that the oscillogram obtained is almost immediately stationary.

Attention has already been called to the fact that the motion of the vibrating object may not be affected by the addition of the mass of the pick-up. The pick-up here described weighs 580 grams, which weight may usually be entirely neglected in the case of the objects commonly occurring in machine construction and structural work. For the investigation of smaller objects a lighter weight, *i.e.* a still smaller pick-up would be desirable. This would be obtained, however, according to the above considerations, at the expense of the sensitivity of the pick-up.

In investigations which extend over a period of time, such for instance as the balancing of motors or setting up engines so as to be free of vibration, it is easier not to apply the vibration pick-up with the hand each time, but to fasten it to the object. This can be done by means of a base plate (*fig. 9c*) which can, if necessary, be screwed to the vibrating surface and when the pick-up must be parallel to the surface it can be done with a clamp (*fig. 9d*).

Fastening by means of a base plate and screws is particularly suitable when vibrations of higher frequencies are to be investigated. The surface layer of the vibrating object together with the mass of the pick-up forms a vibration system by itself, whose characteristic frequency must lie above the frequency region being investigated if the results are not to be quite incorrect. A soft surface layer or a possible layer of paint or grease may result in a low characteristic frequency: this becomes higher, however, the greater the pressure with which the pick-up is applied to the surface.

In order to investigate in more detail the different methods of fastening, we made use of a massive block which was set vibrating by a powerful loud speaker system, and upon which, in a small cavity, a miniature example of the ordinary vibration pick-up was rigidly fastened. The motion of the block was measured by this means, while the result was compared with that obtained with an ordinary pick-up fastened to the block in different ways. It was found that the combination applied for tangential vibrations: pick-up in clamp, clamp in base plate, with well tightened screws, can be used up to frequencies of 200 c/s. When the steel rod or the milled edges of the housing are used, measure-

ments to about 500 c/s can be made, while in the case in which the pick-up is clamped on to the base plate (fig. 9c) and screwed to the vibrating surface it is certain that the pick-up can faithfully follow vibrations of 1 000 c/s and higher. In all cases a rigid, hard surface of the vibrating object is assumed.

Examples of application

In the above a number of possibilities of application have been mentioned in passing. We shall here discuss two examples in more detail.

The first example [4]) relates to the balancing of a high-speed aggregate. A compressor for coking-oven gases, driven by a steam turbine wheel with 4 800 r.p.m. was mounted on a relatively thin shaft, in order to make the characteristic frequencies of the possible bending vibrations lower than the number of revolutions when in operation. Such a system must be balanced, not only statically, but also dynamically, which is usually done at a relatively low number of revolutions. Due to the thin shaft, however, at the operating speed considerable bending and, with it new lack of balance, can occur, which is not present at low speeds. This could easily be controlled by fastening the vibration pick-up here described to the housing of the turbine, and measuring the vibrations occurring. The dotted-line curve of *fig. 10* was first obtained: the balance obtained at low speed was actually found to be unsatisfactory. By shifting the balancing weights in such a way that the axis experienced as small a bending load as possible, the full-line curve was finally obtained: in normal operation practically no more vibration is present.

As a second example we may mention an investigation of vibration machines for testing the life of lamps. In testing electric lamps as to their resistance to vibration, frames are used which are brought into vibration by a motor with an excentric rotating mass. In order to obtain comparable results it is very important that all the lamp holders in the frames of the different vibration machines should vibrate with the same amplitude, not only in the fundamental frequency

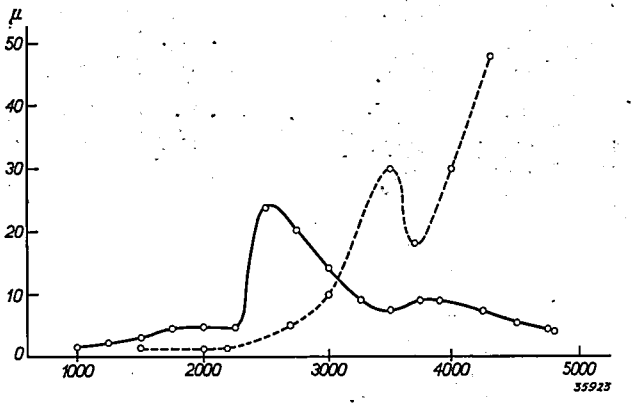

Fig. 10. Vibrations of the housing of a turbo-compressor, as a function of the speed (r.p.m.). In the case of the broken-line curve the balance was inadequate for the operating speed (4 800 r.p.m.), the balancing was thus continued until the full-line curve was obtained (N.V. Werkspoor).

but also in any possible harmonics. With the pick-up described we have studied this for various vibration machines. In the case of one machine the same amplitude of the fundamental frequency was found at all the lamp holders in the frame; it was, however, also found that there was a fairly strong seventh harmonic whose amplitude deviated several per cent in different holders. In the case of another machine the higher harmonic was lacking. It is clear that in judging the lifetime tests such differences must be taken into account. For removing these differences a vibration investigation such as here described furnishes the necessary information.

[4]) We are indebted for the data of this example, which was encountered in the work of the N.V. Werkspoor, to Ir. M. J. Visser of the department for vibration investigation of that company.

ADSORPTION PHENOMENA AT METAL CONTACTS

by J. J. WENT.

541.183.5 : 537.311.4 : 621.3.066.6

The electrical resistance of metal contacts can be divided into two parts, a "convergence resistance", which is determined by internal properties of the contact material, and a "transition resistance", which depends upon the properties of the surface of contact. In this article the transition resistance is studied of clean metal contacts, particularly of molybdenum. By heating the contact surfaces in a vacuum to temperatures of 1 500—1 600° C the transition resistance can be made to disappear completely. A study is made of the way in which the transition resistance of a contact cleaned in this way changes when the surfaces of contact are exposed to oxygen at room temperature and at —160° C. Conclusions may be drawn from the observations about the adsorption phenomena at metal surfaces.

In almost every piece of electrical apparatus there are numerous places where the electrical current must pass from one electrical conductor to another which is pressed against it with a certain pressure. In this transition the electric current in general experiences a resistance of from several thousandths of an ohm to twenty or thirty ohms, depending upon the nature of the contact. In practice it is desirable to make this resistance as small as possible.

In an earlier article in this periodical [1]) a discussion was given of the phenomena which determine the resistance of a contact. The resistance was divided into two components: the convergence resistance R_u which occurs in the interior of the contact materials due to the fact that the current lines of force must be constricted in the very small contact surface, and the transition resistance R_o proper, which occurs at the surface of contact itself. In that case it was chiefly the convergence resistance R_u which was dealt with, and its dependence upon the pressure of contact and the hardness of the material of the contact. In this article we shall consider somewhat more closely the transistion resistance R_0. The investigation of this transition resistance is not only of technical interest, but is, moreover, found to furnish surprising insight into the adsorption phenomena at the surface of the contact material. It is mainly from this point of view that the subject will be treated in what follows.

The method of measurement

In order to be able to measure the transition resistance satisfactorily it is of importance to choose the experimental conditions such that the transition resistance R_0 between the surface of contact is considerably larger than the convergence resistance R_u. This necessity leads to measuring conditions which are exactly opposite to the conditions which are striven for in the practical technical use of contacts. If a is the radius of the surface of contact, assumed to be circular, then the convergence resistance R_u is proportional to $1/a$, as was explained in the article already referred to. The transition resistance on the other hand is inversely proportional to the area of the surface of contact and thus proportional to $1/a^2$. The ratio R_u/R_0, which must be made as small as possible for the investigation in question, is therefore proportional to a. The radius a must therefore be as small as possible, which, for our investigations, also involves the advantage that the absolute value of the resistance is also relatively large, and therefore easy to measure. In the case of technical contacts, on the other hand, every attempt is made to keep the absolute value of the resistance as low as possible, and thus to make the radius a as large as possible.

In order to keep the radius of the surface of contact small, low contact pressures must be used and, moreover, a contact material must be chosen with a relatively great hardness. In this case two molybdenum rods were used as contact pieces, and they were laid crosswise over each other with a contact pressure of a few grams. In order to reduce the ratio R_u/R_0 still more, part of the measurements were done at a low temperature (—160° C). At this temperature the specific resistance of molybdenum, and with it the proportional convergence resistance, is considerably lower than at room temperature, while the transition resistance changes only slightly with the temperature [2]).

Several observations

It was at first ascertained whether it is possible to make the transition resistance disappear completely by cleaning the contact surface thoroughly.

[1]) Philips techn. Rev., 4, 332, 1939.

[2]) *Cf.* R. Holm and W. Meissner, Z. Phys. 74, 715, 1932.

For this purpose the molybdenum rods were placed in a vacuum tube and heated for a long time at a temperature of about 1500° C. The contact resistance measured at room temperature was indeed found to become smaller and smaller and finally to approach a final value which differs only slightly from the theoretically calculated pure convergence resistance. This would mean that the transition resistance has practically disappeared.

A confirmation of this result could be obtained by ascertaining how the contact resistance depends upon the temperature. The contact resistance is composed of the convergence resistance which changes very much with temperature, and the transition resistance which is practically independent of the temperature. As the contribution of the transition resistance becomes smaller, the temperature coefficient of the total contact resistance will therefore have to increase in order finally to reach a value which is equal to that of the specific resistance of the contact material.

This is found experimentally to hold. According as the total contact resistance decreases, its temperature coefficient increases. The ratio $R_{200} : R_{160°}$, which was taken as a measure of the temperature coefficient, finally reaches a value of 2.1, while the ratio of the specific resistances of molybdenum at these temperatures amounts to 2.3. If it is assumed that R_0 is entirely independent of the temperature, it follows from these values that the residual transition temperature at room temperature amounts at the most to 10 per cent of the convergence resistance.

After a perfectly clean contact had been obtained in this way, oxygen at a temperature of —160° C was admitted to the tube in order to find out what effect it has upon the transition temperature. The result is reproduced in *fig. 1*. The transition resistance already exhibits considerable increase at oxygen pressures of the order of 10^{-4} mm, and at a pressure of about 0.01 mm it reaches a saturation value which amounts to about 0.013 ohm with the contact in question. The relation between the resistance and the pressure is easily reversible: when the oxygen is pumped off, the resistance changes according to the same curve as during admittance of the oxygen, and finally disappears entirely. No time lag was observed in reaching the resistance corresponding to each pressure. It may be concluded from this that the contact resistance adapts itself to the oxygen pressure in less than 10 sec. (*i.e.* the time necessary for the measurement).

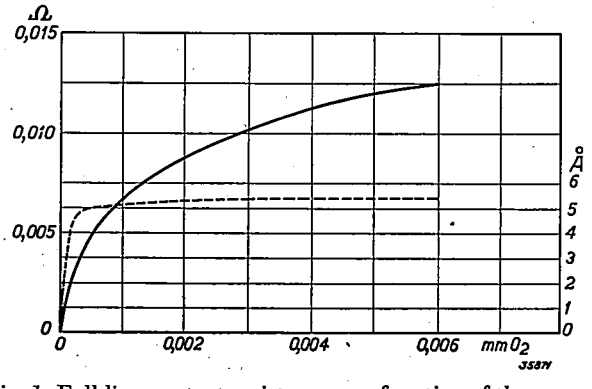

Fig. 1. Full-line: contact resistance as a function of the oxygen pressure for a molybdenum contact at —160 °C. Broken line: the distance between the parts of the contact derived from the above resistance, calculated for a work function of 3.8 volts.

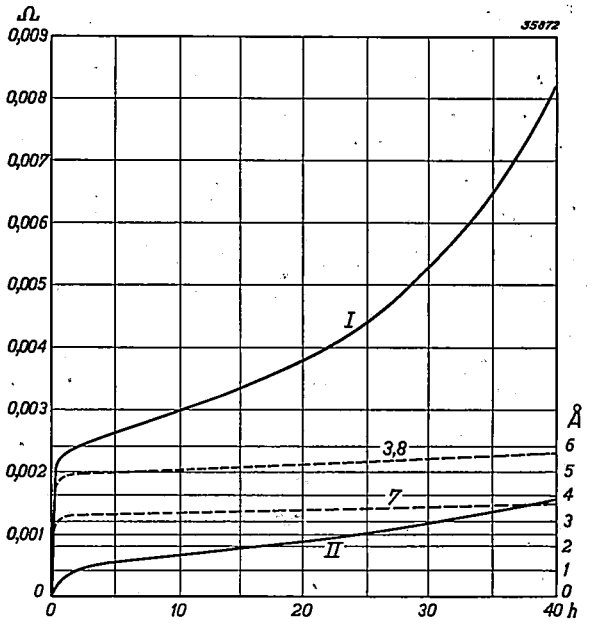

Fig. 2. Curve *I*: variation of the transition resistance of a molybdenum contact as a function of the time, where the contact surfaces are exposed to oxygen at room temperature.

Curve *II*: the part of the contact resistance which remains when the oxygen is pumped off at the time indicated. The curve is recorded by evacuating at certain moments during the exposure to oxygen, carrying out the measurement and then again admitting oxygen.

Broken-line curves: the distance between the contact points calculated from curve *II*, when a work function of 3.8 volts and 7 volts, respectively, is assumed.

If the same experiments are repeated at room temperature, the results are less simple. In the first place the contact resistance is not a function of the pressure alone, but depends very much upon the time during which the contact metals have been exposed to the oxygen (see *fig. 2* curve *I*). Moreover, the relation between oxygen pressure and contact resistance is not reversible: if at a given moment the oxygen is pumped off, a certain resistance persists, which is given by curve *II* of fig. 2. It may be seen that the two curves as functions of the time rise steadily without it being possible to speak of saturation.

Explanation and completion of the observations

The change in the contact resistance upon the admission of oxygen indicates that the metal surfaces are attacked in one way or another by the oxygen. Upon this assumption, in order to understand the difference between the behaviour at low temperature and at room temperature, at least two processes must be assumed to take place: a reversible process which proceeds rapidly, and an irreversible process which only occurs at a higher temperature, and proceeds much more slowly. Both processes are of such a nature that the molybdenum becomes covered with a layer which has a resistance of the order of 10^{-8} to 10^{-9} ohm/cm^2.

For further identification of these processes one must begin with the existing information about the adsorption of gases on metals.

a) Van der Waals adsorption

If a metal surface is exposed to oxygen, it becomes covered with a monomolecular layer of oxygen. The molecules of this oxygen layer are bound to the metal surface by relatively weak forces of attraction, which are always present between molecules, even though the molecules exhibit no chemical activity with respect to each other. These forces are called van der Waals forces, because they are found to be of the same type as those which van der Waals considered reponsible for the condensation of gases.

Although the strength of the van der Waals bond generally amounts to only a few per cent of that of the chemical bond, it is large enough to give rise to a dense covering of the metal with oxygen molecules at an oxygen pressure of less than 0.01 mm. The result is that the two pieces of metal cannot approach each other more closely than to a distance equal to twice the thickness of an oxygen molecule. It is obvious that the electrons passing from one part of the contact to the other will experience a certain resistance in passing through this space.

In order to calculate the magnitude of this resistance, we consider the contact as consisting simply of two pieces of metal situated at a definite distance from each other, and take no account of the fact that the space between these pieces of metal is filled with oxygen. The electrons which must pass from one part of the contact to the other must then leave the metal and enter the empty space, for which a certain φ (work function) is necessary, and they may then enter the second part of the contact, whereby the work function is regained.

Since the kinetic energy of practically all the electrons in the metal is smaller than the work function, it might be expected that the electrons would not be able to leave the metal, so that the contact resistance would be infinitely large. With a distance between the electrodes which is not too small (for instance larger than 10^{-5} cm) this is indeed true. If, however, the distance becomes smaller than 10^{-6} cm, electrons with a kinetic energy smaller than the work fonction also have a

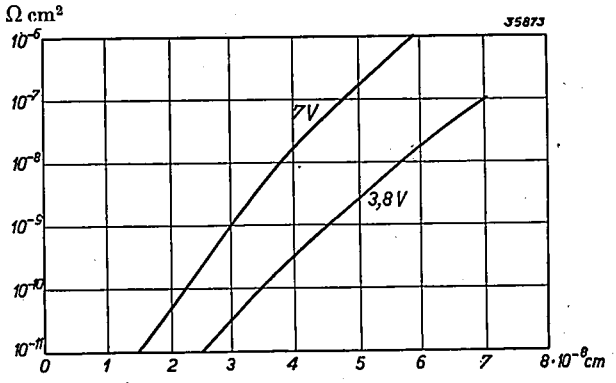

Fig. 3. Relation between the distance between two pieces of metal and the transition resistance for different values of the work function. At a first approximation this relation is expressed by equation (1). The figure gives a closer approximation.

certain chance of passing from one part of the contact to the other. This is a result of the wave nature of matter which makes itself felt when the motion of electrons is considered over distances which are not very large compared with their wave lengths [3]). If on the basis of wave mechanics one calculates the transition resistance of a contact with a surface of contact O, a distance d between the parts of the contact and a work function φ, then as a first approximation one obtains:

$$R_0 = \frac{h^2\, d}{\sqrt{2m\varphi}\, O} \exp\left(\frac{\pi d}{h}\sqrt{2m\varphi}\right), \quad \cdots \quad (1)$$

where h is Planck's constant and m the mass of the electron. In *fig. 3* the relation is shown between R_0, O and d for different values of the work function φ. When it is kept in mind that the surface of contact of contacts is in general only of the order of 10^{-8} cm^2, it may be seen that an appreciable conductivity between two metal surfaces can only occur for distances d between these contacts up to about 10^{-7} cm.

In the case of molybdenum contacts the work function has a value of about 3.8 volts. If one

[3]) A qualitative explanation of this phenomenon was given in this periodical in an article on blocking-layer rectifiers: Philips techn. Rev. 4, 100, 1939.

calculates the distance between the metal surfaces for this value from the transition resistance observed, one finds a variation as a function of the oxygen pressure such as is indicated with a broken line in fig. 1. It is striking that the distance between the metal surfaces seems already to approach its final value at a considerably lower oxygen pressure: between 0.0005 and 0.06 mm oxygen pressure the distance d changes by only 19 per cent, the transition resistance R_0, however, is more than doubled by this change.

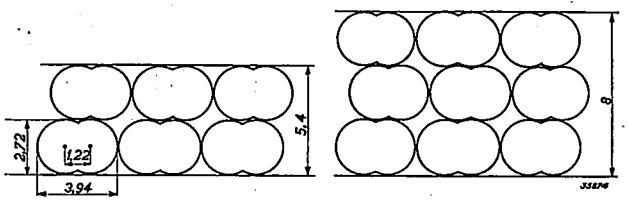

Fig. 4. A distance of 5.4 Å provides space for a double layer of oxygen molecules; a distance of 8 Å provides space for a threefold layer of oxygen molecules.

The final value of the distance d amounts to 5.4 Å. Since the thickness of an oxygen molecule, according to research with the help of electron diffraction, is 2.72 Å, this agrees exactly with what would be expected if each of the parts of the contact were covered with a monomolecular layer of oxygen (see *fig. 4*). A contact resistance about 100 times greater is sometimes observed at high oxygen pressures. This corresponds to a distance $d = 8$ Å. Apparently in these cases one of the parts of the contact is also covered with a second layer of oxygen ($3 \times 2.72 = 8.16$).

b) Activated adsorption

If the contact surfaces are exposed to oxygen at room temperature, as already stated a gradual increase of the contact resistance with time is observed, which upon pumping the oxygen away only gradually disappears again. Apparently the oxygen bound by van der Waals forces passes gradually over into another state in which it adheres much more strongly to the surface, so that the molecules cannot immediately be removed by evacuation.

A phenomenon by comparison with which this behaviour may be explained is known to chemistry under the name of activated adsorption. Molecules which are adsorbed by van der Waals forces are converted by a certain activation process into a state in which the bond is much stronger. In the case of oxygen, for example, it is known that in some cases the adsorbed molecules are split into atoms which are then bound chemically by the underlayer; this chemical combination is indeed much stronger than the bond due to van der Waals forces.

A representation of this process may be given by plotting the binding energy of an oxygen molecule and of the atoms formed from it as a function of the distance between the molecule (or atom) and the surface of the metal [4]). A diagram is obtained such as that shown in *fig. 5*. The potential energy of the adsorbed molecule or atom is plotted vertically. For a definite distance the potential energy has a minimum, and this is at a distance from the wall at which the adsorbed particle is in equilibrium. For the atom this distance is always smaller than for the molecule, since the atom has a smaller diameter. Furthermore the depth of the minimum for the atom is considerably greater, since the chemical bond is much stronger than the bond due to van der Waals forces.

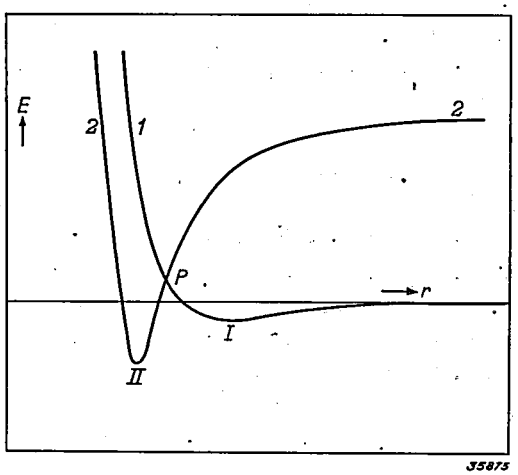

Fig. 5. Potential energy as a function of the distance from the molybdenum surface: *1* for an oxygen molecule, *2* for two oxygen atoms. The atoms are bound more firmly and at a smaller equilibrium distance from the surface than the molecules.

We now see that a molecule will first be found by van der Waals forces and thereby reach the potential minimum *I*. At a sufficiently low temperature it will remain in this minimum. At room temperature, however, the molecules are sufficiently strongly agitated to carry out vibrations, and it may occur that the point P is suddenly exceeded. This means that the molecule can dissociate into atoms without any further addition of energy. The atoms now behave as may be deduced from potential curve *2*, *i.e.* they are chemically bound at a distance given by the position of the potential minimum *II*.

[4]) This view or activated adsorption was first given by J. E. Lennard Jones, Trans. Farady Soc. 28, 333, 1932.

This distance can again be determined by calculating the distance between the parts of the contact from the contact resistance measured. The difficulty is here encountered, however, that the work function φ is not known in the case of activated adsorption. If the molybdenum surface is covered with a layer of molecules, as in the case of adsorption by van der Waals forces, then — as has been done above — it may be assumed that the work function of an electron will not differ appreciably from that of an electron from the clean molybdenum surface, which is 3.8 volts. If, however, the surface is covered with chemically bound oxygen atoms, the latter are negatively charged [5]). The electrons which leave the metal are pushed back by this negative charge and the work function is hereby increased to for instance 6 volts or more.

Since the correct value of the work function is not known, we have calculated d for two values of φ: a value of 3.8 volts, which is certainly too small, and a value of 7 volts, which is very probably too large. The broken-line curves of fig. 2 give the results; these have been derived from curve *II*. It is found that the thickness of the layer of oxygen no longer changes to any extent after 5 hours. With $\varphi = 3.8$ volts a distance of 5.8 Å between the parts of the contact is calculated, while with $\varphi = 7$ volts a distance of 3.8 Å is found. The actual distance is probably less than 5 Å, and in any case less than the distance which prevails with adsorption by van der Waals forces, as was also assumed in drawing the potential curves.

Migration of oxygen molecules over the surface

In the experiments described until now, when oxygen was admitted or pumped off, the parts of the contact were taken apart so that the contact surfaces could easily be reached by the surrounding oxygen molecules. If, however, the perfectly clean contacts are pressed together, and then only oxygen is admitted, it is found that at a low temperature (—160° C) no increase of the resistance occurs at all. At room temperature the resistance begins to increase gradually, much more slowly, however, than when there is direct contact between the oxygen and the molybdenum (see *fig. 6*).

It may be conluded from this that the molecules adsorbed by van der Waals forces remain in position at low temperatures, but at room temperature they migrate over the surface and in doing this penetrate between the surfaces of contact. At the same time the above-described process of activated adsorption takes place, *i.e.* the molecules at a certain moment pass into the dissociated state; the thus formed oxygen atoms are bound chemically and thus their migration interrupted.

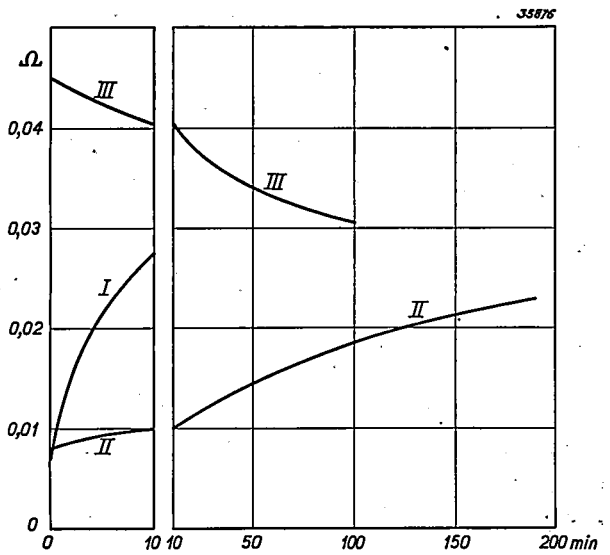

Fig. 6. Curve *I*: variation of the contact resistance as a function of the time, for a molybdenum contact whose parts are exposed at room temperature to oxygen and afterwards pressed together (corresponds to curve *I* of fig. 2).

Curve *II*: same as curve *I* for the case where the parts of the contact remain pressed together all the time, so that they cannot be immediately reached by the oxygen molecules.

Curve *III*: variation of the contact resistance as a function of the time after the oxygen has been pumped off, for a contact whose surfaces were exposed to oxygen and then pressed together, so that the oxygen molecules could not easily escape.

In this way the molybdenum becomes gradually covered with an atomic layer of oxygen, and this also takes place between the surfaces of contact. When this covering is complete, it might be imagined that on the top of the layer of oxygen atoms a layer of oxygen molecules might be formed which also penetrates between the surfaces of contact. This can be studied by finding out how the resistance changes when the oxygen is pumped off. If a layer of oxygen molecules were present, upon decrease in pressure this layer should creep away gradually from between the surface of contact, so that the transition resistance would decrease. If, however, the oxygen layer between the surfaces consists entirely of oxygen atoms, then even at room temperature they will remain in their places, so that the contact resistance upon pumping off the oxygen will not change at all.

This last was actually observed when the parts of the contact were exposed to oxygen for about

[5]) This has been found from investigations of the electron emission of tungsten which is chemically closely related to molybdenum.

three hours while being pressed together. It follows from this that the molecules which creep between the contact surfaces are all split up into atoms. If on the other hand the open contact is exposed to oxygen, it is found that the contact resistance, after closing the contact and pumping off the oxygen, again partially disappears, as curve *III* of fig. 6 shows. With an opened contact, therefore, a layer of molecules is apparently formed on top of the layer of oxygen atoms.

If it is desired to make the transition resistance diappear entirely, the molybdenum must be heated so highly during evacuation that the chemically bound oxygen atoms also evaporate. As was mentioned in the beginning, the melting point of molybdenum is high enough for this to be done: heating to 1500° C gives the desired result.

What exactly happens when this is done cannot be stated with certainty. It seems as if the atomic oxygen layer does not evaporate directly, but is first transferred into a different state. If the molybdenum is heated to a lower temperature, for instance 1100° C, no decrease in the resistance is observed, but, on the contrary, a fairly considerable increase. It is possible that this may be ascribed to the formation of molecules of molybdenum oxide (MoO_3). This oxyde has a considerably higher vapour tension than molybdenum itself, so that upon heating to 1500° C the molecules can evaporate and the surface becomes perfectly clean.

STANDARDIZATION OF ACOUSTIC QUANTITIES

389.6 : 534.6.081.1

In February 1937 [1]) tables were given in this periodical for the sound pressure and the velocities of the air particles at different sound levels, as well as for the frequency of the different musical tones. The remark was there made that it was extremely unfortunate that different standards were used in different countries by different investigators. Since this situation has recently been changed by international regulation, it will perhaps be useful to give the tables once more, brought into agreement with this regulation.

The sound level is indicated in "phons", *i.e.* the number of decibels above a definite threshold value. As threshold value, *i.e.* as the sound intensity to which the level of zero phons is ascribed, the intensity 10^{-16} watts/cm^2 was decided upon at a conference in June 1937 in Paris, called together on the initiative of the C.C.I.F. (Comité Consultatif International Téléphonique). This intensity corresponds to an effective sound pressure of 2×10^{-4} dynes/cm^2. In *table I* the effective values of the sound pressure and of the velocity of the air particles are given for the sound levels from 0 to 120 phons. With the help of the values given for the levels from 60 to 80 phons, increasing by intervals of 1 phon, interpolation can be carried out in the main table, as explained in the accompanying text.

The regulation as to the frequencies of the musical tones was arrived at in May 1939 in London; at a meeting of one of the committees of the I.S.A. (International Federation of Standardizing Asso-

[1]) R. Vermeulen, Octaves and Decibels, Philips techn. Rev. 2, 47, 1937.

ciations) the frequency of A, upon which the tuning of musical instruments is based, was fixed at 440 c/s [2]). In *table II* the frequency of the other tones of the equally tempered scale is given. The last column gives the intervals for one octave.

R. Vermeulen.

[2]) *Cf.* also: Balth. van der Pol and C. C. J. Addink, The pitch of musical instruments and orchestras, Philips techn. Rev. 4, 205, 1939. In this article it is stated that the pitches practically occurring in concerts are very divergent, and that the average of the values of A measured lay just at 440 c/s.

Table I

Level (phons)	Intensity (W/cm²)	Sound pressure		Air velocity	
0	10^{-16}	0,2	Millidyn/cm²	0,05	Mikron/sec
10	10^{-15}	0,63		0,16	
20	10^{-14}	2		0,5	
30	10^{-13}	6,3		1,6	
40	10^{-12}	20		5	
50	10^{-11}	63		16	
60	10^{-10}	0,2	Dyn/cm²	50	cm/sec
70	10^{-9}	0,63		160	
80	10^{-8}	2		0,05	
90	10^{-7}	6,3		0,16	
100	10^{-6}	20		0,5	
110	10^{-5}	63		1,6	
120	10^{-4}	200		5	

Table I (Interpolation)

Level (phons)	Intensity (W/cm²)	Sound pressure		Air velocity	
60	1,0	0,2	Dyn/cm²	50	Mikron/sec
61	1.26	0,22		56	
62	1,58	0,25		63	
63	2,0	0,28		71	
64	2,5	0,32		79	
65	3,2	0,36		89	
66	4,0	0,40		100	
67	5,0	0,45		112	
68	6,3	0,50		126	
69	8,0	0,56		140	
70	10	0,63		158	
71	12,6	0,71		177	
72	15,8	0,80		200	
73	20	0,89		220	
74	25	1,00		250	
75	32	11,2		280	
76	40	12,6		310	
77	50	14		350	
78	63	16		400	
79	80	18		460	
80	100	20		500	

Interpolation: all values are repeated every 20 phons except for a factor of a power of 10. If for instance the sound level is 27 phons, the sound intensity lies between 10^{-14} and 10^{-13} W/cm²; from the more detailed table for the most commonly occurring values between 60 and 80 phons, one finds at $27 + 2.20 = 67$ phons the value 50; thus the result is 5.0×10^{-14} W/cm². In the same way the sound pressure 4.5 millidynes/cm² and the air velocity 1.12 μ/sec. are found.

Table II

Tone \ Octave	C_2-C_1	C_1-C	C-c	c-c^1	c^1-c^2	c^2-c^3	c^3-c^4	c^4-c^5	c^5-c^6	c^6-c^7	Intervalle
c	16,35	32,70	65,41	130,81	261,63	523,25	1046,5	2093,0	4186,0	8372	1,0000
cis=des	17,32	34,65	69,30	138,59	277,18	554,36	1108,7	2217,5	4434,9	8870	1,0595
d	18,35	36,71	73,42	146,83	293,67	587,33	1174,7	2349,3	4698,6	9397	1,1225
dis=es	19,45	38,89	77,78	155,56	311,13	622,26	1244,5	2489,0	4978,0	9956	1,1892
e	20,60	41,20	82,41	164,81	329,63	659,26	1318,5	2637,0	5274,0	10548	1,2599
f	21,83	43,56	87,31	174,61	349,23	698,46	1396,9	2793,8	5587,6	11175	1,3348
fis=ges	23,12	46,25	92,50	185,00	369,99	739,99	1480,0	2960,0	5919,9	11840	1,4142
g	24,50	49,00	98,00	196,00	392,00	783,99	1568,0	3136,0	6271,9	12544	1,4983
gis=as	25,96	51,91	103,83	207,65	415,30	830,61	1661,2	2322,4	6644,9	13290	1,5874
a	27,50	55,00	110,00	220,00	**440,00**	880,00	1760,0	3520,0	7040,0	14080	1,6818
ais=bes	29,14	58,27	116,54	233,08	466,16	932,32	1864,6	3729,3	7458,6	14917	1,7818
b	30,87	61,73	123,47	246,94	493,88	987,76	1975,5	3951,1	7902,1	15804	1,8877
c	32,70	65,41	130,81	261,63	523,25	1046,50	2093,0	4186,0	8372,0	16744	2,0000

VOL. 5 No. 9 SEPTEMBER 1940

Philips Technical Review

DEALING WITH TECHNICAL PROBLEMS
RELATING TO THE PRODUCTS, PROCESSES AND INVESTIGATIONS OF
N.V. PHILIPS' GLOEILAMPENFABRIEKEN

EDITED BY THE RESEARCH LABORATORY OF N.V. PHILIPS' GLOEILAMPENFABRIEKEN, EINDHOVEN, HOLLAND

A CATHODE RAY TUBE WITH POST-ACCELERATION

by J. de GIER.

621.317.755 : 621.317.087

In order to obtain a high scanning speed with a cathode ray tube it is desirable to raise the accelerating voltage for the electrons as high as possible. In the ordinary models this attempt is limited because of the fact that the dimensions of the tube would have to be increased with the voltage and the deflection sensitivity would decrease. These disadvantages are very much reduced when post-acceleration is applied *i.e.* when the electrons are accelerated anew with the help of an extra electrode after they have passed the deflection plates. By this means a considerably higher scanning speed can be attained without it being necessary to increase the dimensions of the tube, while in addition the sensitivity is not so unfavourably affected as when the electrons have already attained their final velocity before they pass the deflection system. In this article the post-acceleration tube DN 9-5 is described which has been developed from the cathode ray tube DN 9-3. The electrode for post-acceleration can be given a voltage of 5 000 volts with respect to the cathode. A maximum scanning speed of 24 km/s. is hereby obtained. A detailed account is given of the way in which the post-acceleration electrode affects the deflection sensitivity of the cathode ray tube and of the way in which the distortions caused by the post-acceleration electrode are combatted.

A very important quantity for the characterization of the performance of a cathode ray tube is the maximum scanning speed, *i.e.* the maximum speed at which the light spot may move on the screen of the cathode ray tube in the case of a phenomenon occurring only once, in order to be visible or to be recorded photographically. In an earlier article in this periodical [1]) an account was given of the electrical tube properties and factors of the photographic process which determine the maximum scanning speed. As to the electrical tube properties, in order to obtain a high scanning speed, provision must be made for a high beam current, a small diameter of the spot and a high speed of the electrons which strike the flourescent screen. In the photographic method, moreover, it is chiefly a question of a large relative aperture of the photographic objective and the greatest possible reduction in size of the photograph.

In order to illustrate the scanning speeds which can be obtained with ordinary types of cathode ray tubes, an investigation may serve which was carried out on the cathode ray tube DN 9-3 (a tube with a screen diameter of 9 cm, which is employed in the cathode ray oscillograph GM 3 152). The accelerating voltage in this case amounted to 1 000 volts, the current in the beam to 20 μA. The oscillogram was a reduction of the image in the ratio 1 : 4, while a lens with an aperture 1 : 2,2 was used, such as is found in many of the miniature cameras at the present time. The film used was Agfa Isopan. It was found that the greatest scanning speed with which an easily visible blackening of the film is obtained amounts to 850 m/s. This means that a phenomenon with a duration of 10^{-5} sec can be represented by a line of 8.5 mm arc length. In many technical applications this will be adequate, but for the investigation of breakdown phenomena, surge voltages, etc., where processes with a duration of 10^{-6} or 10^{-7} sec may occur, considerably higher scanning speeds are required.

The obvious method of solving the difficulties is by trying to increase the scanning speed by choosing more favourable values for the above-mentioned factors which determine the scanning speed. An increase in the scanning speed by a reduction in the diameter of the spot (0.8 mm) is, how-

[1]) J. F. H. Custers: The recording of rapidly occurring electrical phenomena with the aid of the cathode ray tube and the camera, Philips techn. Rev. 2, 148, 1937. On the subject of a new instrument for measuring scanning speeds see: L. Blok, Philips techn. Rev. 3, 216, 1938.

ever, practically impossible, since the constriction of the beam is limited by the mutual repulsion of the electrons. This repulsion is also the cause of the fact that no success is achieved by increasing the beam current; this would result in an increase in the diameter of the spot, which is undesired in connection with the sharpness of the oscillogram and, moreover, has an unfavourable effect on the scanning speed, which is inversely proportional to the spot diameter at a given light intensity.

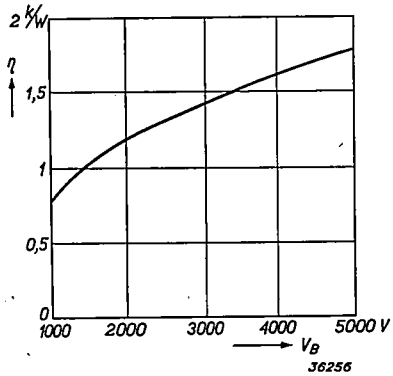

Fig. 1. Efficiency η of the conversion of electrical energy into light (c.p./watt) as a function of the accelerating voltage V_B of the electrons which strike the fluorescent screen.

It is indeed possible to obtain a very appreciable improvement by increasing the accelerating voltage. In the first place, with constant current more power is converted into light, and proportional to this power the maximum scanning speed also increases. In the second place the efficiency of the conversion also becomes greater (see *fig. 1*), so that the amount of light produced with an increase of the voltage from 1 000 to 5 000 volts, for instance, is not five times, but more than ten times as great. In the third place the mutual repulsion of the electrons becomes continually less effective with increasing velocity, so that the light spot on the screen can be reduced in size, which, as we have seen, means an increase in the scanning speed obtained. In the fourth place, in certain cases when there is no particular need of this reduction in spot diameter, it would be possible to increase the current with increasing voltage, whereby the power, and thus also the scanning speed, would increase still more. Practically, an increase of the voltage by a factor 5 means an increase in the maximum scanning speed by 25 or 30 times.

Any considerable increase in the accelerating voltage is, however. not immediately possible in cathode ray tubes of small dimensions such as are used in portable types of cathode ray oscillographs. The insulation of the leads in the tube DN 9-3 is calculated for potential differences of 1 000 or perhaps 1 200 volts. For 2 000 volts the base would have to have dimensions which cannot be considered for a portable instrument. Another, fundamental, objection to the increase in voltage is that the deflection sensitivity of the tube is hereby decreased, since the deflection of the cathode ray by a given deflection voltage is inversely proportional to the accelerating voltage. With an accelerating voltage of 1 000 volts the deflection sensitivity of the tube DN 9-3 is 0.4 mm/volt for the first set of plates and 0.3 mm/volt for the second, and these values must not be decreased too much by the increase in the accelerating voltage.

Principle of the post-acceleration tube

It is possible to overcome the above difficulties by making the acceleration take place in two stages instead of directly. The focussing system forms an electron beam with a velocity corresponding, for instance, to 1 000 volts. This beam passes successively the systems for vertical and horizontal deflection and then undergoes a second acceleration with the help of an electrode at a considerably higher potential, and at such a distance from the other electrodes that the insulation does not present insuperable difficulties. If, in addition, this second acceleration, the so-called post-acceleration of the electron beam, is made to take place in such a way that the direction of the beam remains unchanged, the second objection to the high voltage, decrease in sensitivity, is eliminated.

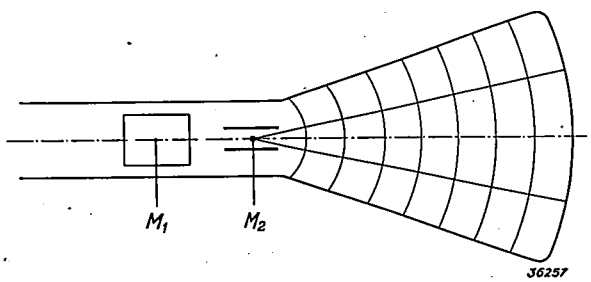

Fig. 2. Principle of the post-acceleration without decrease in the deflection. Behind the deflection system there is an accelerating field whose equipotential surfaces are perpendicular to the trajectories of the electrons.

If we wish to accelerate the electrons which leave the deflection system without changing their direction, we must excite an electric field whose equipotential surfaces are perpendicular to the direction of the beam of the electrons at every point (see *fig. 2*). The cross sections of these equipotential surfaces in the horizontal plane would be circles with the centre M_1, while in the vertical plane they would be circles with the centre M_2.

In order to give the potential field in the whole

space the desired character, it is sufficient to cause the potential at the boundaries of the tube to vary in the correct way. This can be done by covering the walls of the tube with ring-shaped conducting strips, corresponding to the lines of intersection of the equipotential surfaces and the wall of the tube, and bringing these strips to the desired values of the potential (see *fig. 3*). In practice it has been

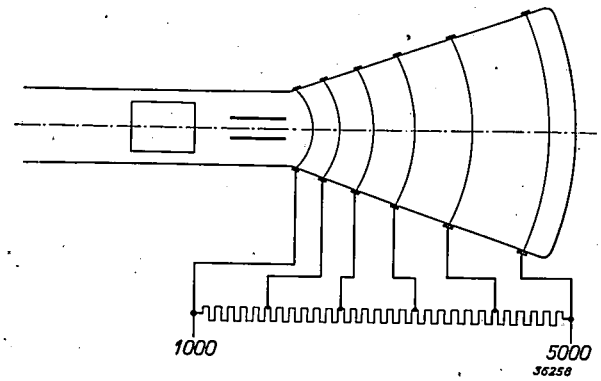

Fig. 3. A given prescribed potential field can be realized by fixing the extreme values of the potential in a suitable manner.

found that such a complicated structure is unnecessary; instead of a large number of narrow strips, two broad coatings can be used: one at 1 000 volts, *i.e.* the potential which determines the speed of the electrons in the deflecting system, and one at 5 000 volts, for instance, which determines the speed at which the electrons impinge on the fluorescent screen.

The principle of this arrangement is shown in *fig. 4*. As may be seen from the equipotential sur-

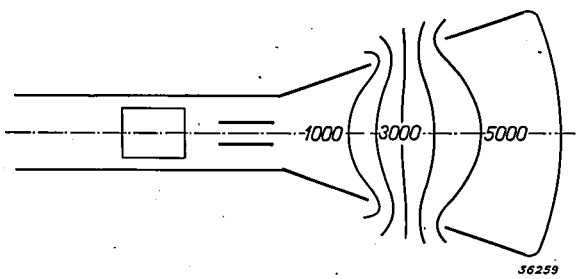

Fig. 4. Principle of the post-acceleration tube. This may be considered as a simplification of fig. 3. The equipotential surfaces do not have exactly the desired form.

faces which hereby occur, the potential field has not exactly the desired character, and it is found that the post-accelerating field also deflects the electron trajectories, so that the sensitivity of the tube decreases slightly with increasing post-acceleration. We shall examine this phenomenon more closely because the attempt to combat it has had some influence on the construction of the new tube.

The lens action of the post-acceleration electrode [2])

In order to describe the motion of an electron in an electrostatic field qualitatively, use can often be made of an analogy between the trajectory of an electron in a potential field and the path of a light ray in a medium with an index of refraction which is in general variable. This analogy is as follows. If an electron at a point at zero potential has the velocity v_0, and if, to every point in space, an index of refraction given by the following is ascribed:

$$n = \sqrt{\frac{v_0^2 + \frac{2e}{m} V}{v_0^2}}, \quad \cdots \quad (1)$$

where V is the potential at the point in question, then a light wave which is emitted in the same direction as the electron follows the same trajectory as the electron [3]).

If we apply this proposition to the space behind the deflection system of the post-acceleration tube, we see that, after passing the deflection system in fig. 4, the electron beam first passes through a number of less strongly negatively refracting planes. To make this clear, the optical system which is formed in this way is given in *fig. 5b*. In this figure the positive and negative refracting surfaces lying close together are indicated by a single surface.

The system already shows some similarity with an optical lens, with this difference, that the index of refraction is greater in the image space than in the lens itself. We may, however, adopt more normal relations by setting the index of refraction in the image space equal to unity once more, and at the same time changing the curvature of the last lens surface so that the refractive properties of the lens remain the same. The lens represented in fig. 5*c* is then obtained, with a convex and a concave surface. The vertical planes H and H' in fig. 5*c* indicate the main planes of the lens and show that the lens must be imagined somewhat closer to the deflection system than the middle of the open space

[2]) The following considerations were first given by W. Rogowski and H. Thiele: Über die Nachbeschleunigung bei Braunschen Röhren, Arch. Elektrot. 33, 411, 1939.

[3]) This proposition can most easily be deduced from the analogy between the so-called principle of least action of Maupertuis:

$\int \sqrt{T}\, ds$ = minimum for the trajectory actually described of a mass point (T kinetic energy, ds element of trajectory)

and the proposition of Fermat for optics:

$\int n\, ds$ = minimum for the path chosen by the light (n index of refraction).

The quantity under the radical sign in equation (1) is, except for a factor, nothing else than the kinetic energy, from which the analogy between electron trajectory and light ray immediately follows.

between the coatings. We shall use this optical picture further in the discussion of the influence of the post-acceleration on the deflection of the beam.

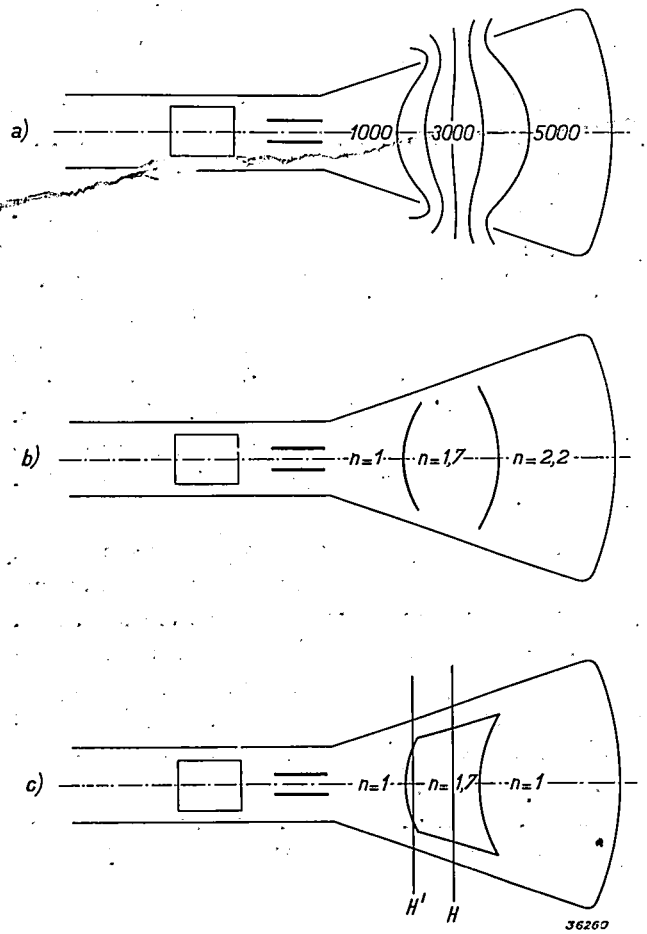

Fig. 5. Lens action of the post-acceleration field.
a) Form of the equipotential surfaces.
b) Lens, which would have the same refracting effect on a light ray as the electric field on the electron trajectories.
c) Lens, derived from b) by reversing for the second surface both the sign of the curvature and the sign of the change in index of refraction, so that the refraction of this surface remains the same. The optical analogy with the potential field thus obtained is a lens in air. H and H' are the main planes of the lens.

It is very important for the sensitivity of the cathode ray tube at what point this lens is situated and how strong it is. *Figs. 6a-f* make this clear. In cases *a* and *b*, which most closely approach the form actually chosen, the lens is quite weak, but still strong enough to cause the deflection of the beam to decrease appreciably. Fig. 6*c* represents a considerably stronger lens. The residual deflection of the beam now becomes very small. It is therefore clear that the decrease in sensitivity upon application of post-acceleration need by no means always be smaller than with a direct acceleration of the electron beam. It may even happen that no sensitivity at all remains (fig. 6*d*), or that the sign of the deflection is reversed by the post-acceleration lens (fig. 6*e*). In the last case it is even possible theoretically to increase the strength of the lens so much that the absolute value of the deflection becomes greater than the original deflection in the absence of post-acceleration (fig. 6*f*). In practical cases the possibilities offered by *e* and *f* cannot be used directly because a very strong deflection of the beam is always accompanied by distortions. We are thus concerned with cases *a*, *b* and *c* where the sensitivity is decreased by the action of the post-acceleration, and we can only try to choose

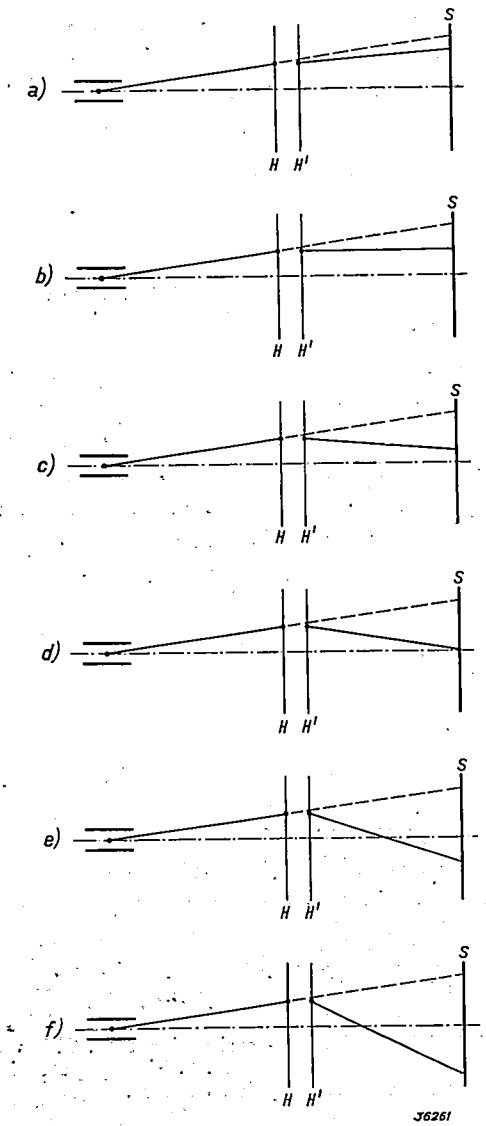

Fig. 6. Influence of the post-acceleration lens on the deflection of the electron beam by the deflection plates.
a) and b) Weak post-acceleration lens. The deflection of the electron beam is only slightly decreased.
c) and d) Strong post-acceleration lens. The deflection of the electron beam is considerably diminished and disappears in the last case entirely.
e) and f) Very strong post-acceleration lens. The deflection of the electron beam has a direction on the screen opposite to that caused by the deflection plates. In the last case the absolute value of the deflection caused by the presence of the post-acceleration lens is increased.

the conditions in such a way that this decrease is as slight as possible.

In the first place the lens itself must be made as weak as possible. The strength of the lens increases with increasing post-acceleration voltage, so that in practical cases this voltage will not be made higher than necessary for the particular phenomenon to be projected on the screen. The absolute value of the voltage is not actually the determining factor for the strength, but the relation between the voltages of the first and last coating. It might therefore be imagined that the lens could be made weaker by increasing the voltage of the first coating. In doing this, however, as already mentioned, one is limited to about 1 000 volts in the case in question due to considerations of a structural nature.

When the voltages of the coatings are chosen, the strength of the lens can still be affected by suitable construction of the electrodes. To make the lens as weak as possible the diameter of the electrodes must be as large as possible. By constructing the electrodes in the form of wall coatings, this condition is satisfied, the diameter of the tube is naturally limited by the size of the oscillograph apparatus. Furthermore, the strength of the lens increases with increasing distance between the coatings and this should therefore be taken as small as possible. A practical limit is set to this by the requirement of sufficient insulation. This point will be considered further in the following.

Finally an attempt may be made to choose the position of the lens in the tube so that its deflecting effect is as small as possible. In this respect a certain amount of variation is found to be possible with a given strength of the lens.

If for a weak lens the magnitude of the deflection finally obtained is calculated as a function of the position of the lens, it is found that the deflection has a minimum when the lens is situated symmetrically with respect to the point halfway between the deflection plates and the point at the centre of the screen. Every displacement from this plane of symmetry thus improves the sensi[illegible] The lens might for example be placed as close as possible to the screen. This displacement is, however, limited by the fact that, as we have seen, the lens is always further away from the screen than the open space between the coatings, which themselves must be applied at not too small a distance from the screen, since otherwise the potential does not attain the desired high value over the whole surface of the non-conducting screen. If one attempts, conversely, to displace the lens as far as possible towards the deflecting system that difficulty does not arise, but the equipotential surfaces of the post-acceleration field are then deformed by the presence of the field of the deflection plates, which is not rotation symmetrical, and the lens exhibits an astigmatism. This difficulty, however, is found not to be unconquerable, so that the second method is to be preferred. In the discussion of the practical construction we shall see how the astigmatism is corrected.

Construction of the post-acceleration tube

Fig. 7 is a photograph of the post-acceleration

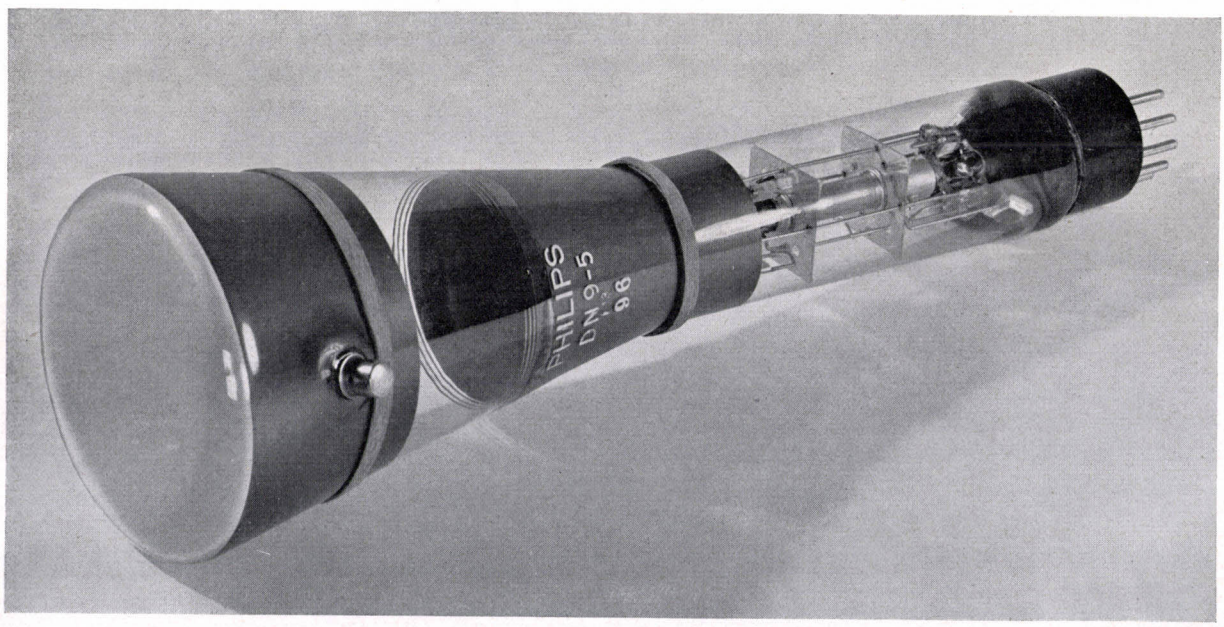

Fig. 7. Photograph of the post-acceleration tube DN 9-5.

tube DN 9-5. Both the external dimensions and the internal electrode system correspond in the main to those of the tube DN 9-3 previously described [4]) of the cathode ray oscillograph GM 3 132. The most important difference is that the conducting coating on the inner wall of the tube is split into two coatings A and B, of which part A as in tube DN 9-3 is connected to the anode of the focussing system, and is at a potential of 1 000 volts with respect to the cathode, while coating B has a separate lead to the outside to which any desired voltage between 1 000 and 5 000 volts can be applied [5]).

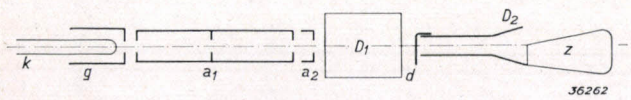

Fig. 8. The internal cathode system of the cathode ray tube DN 9-5 with post-acceleration. k cathode, g regulatory electrode, a_1 focussing anode with voltage of about 275 volts, a_2 post-acceleration anode with voltage of 1000 volts, D_1 and D_2 deflection system, d rods for combatting trapezium distortion, paddles for combatting astigmatism and distortion due to the post-acceleration.

Both coatings consist mainly of a deposit of graphite on the inside of the glass. In order to make the edge of electrode A smoother in order to increase the flashover voltage, at the edge the graphite was replaced by platinum; in addition, in front of this edge lie several ring-shaped stripes of the platinum deposit which are not brought to a definite potential, but are free to become charged. These stripes influence the distribution of potential between the coatings in such a way that the breakdown potential becomes still higher. In this way it was made possible for the voltage on electrode B to be raised to 5 000 volts without danger of flashover between the two coatings.

The internal electrode system of the post-acceleration tube is shown diagrammatically in *fig. 8* while *fig. 9* is a photograph of the system. The electrons which leave the cathode k and pass the regulatory electrode g, then they are accelerated by the tubular anodes a_1 and a_2, the first of which is at an adjustable focussing voltage of about 275 volts and the second at the acceleration voltage of 1 000 volts.

The electron beam which leaves the focussing system passes the two sets of deflection plates D_1 and D_2 which serve for vertical and horizontal deflection, respectively, of the electron beam. The system D_2 has two rods d which serve to eliminate the so-called trapezium distortion which occurs when a non-balanced voltage is applied to the second set of deflection plates [6]).

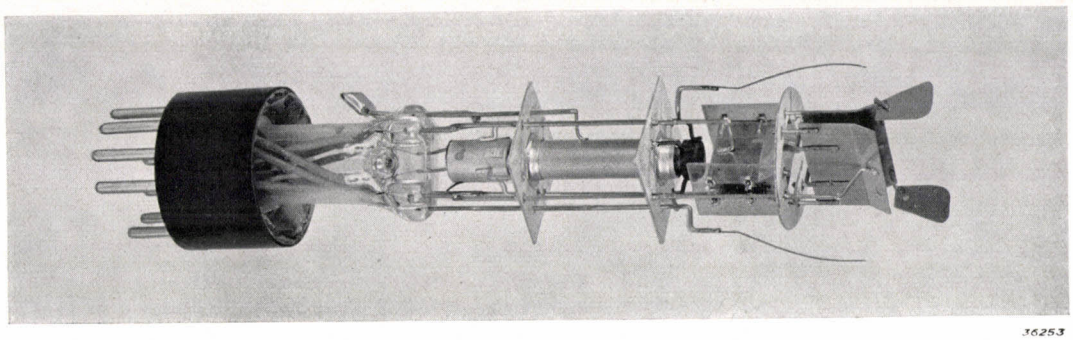

Fig. 9. Photograph of the internal system of the post-acceleration tube.

Due to the post-acceleration two other types of distortion also occur, namely:

1) an astigmatism of the electron beam, which has already been mentioned in connection with the choice of position for the post-acceleration lens;
2) a barrel-shaped deformation of the oscillogram.

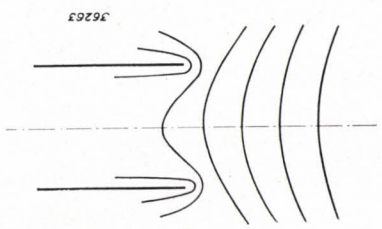

Fig. 10. The equipotential surfaces of the post-acceleration field are compressed, at it were, which leads to astigmatism.

[4]) J. D. Veegens, Philips techn. Rev. **4**, 210, 1939.

[5]) For this purpose the convenient supply apparatus GM 4 198 may be used, which gives an adjustable voltage of from 0 to 5 kV. This supply apparatus is adapted to the measuring apparatus provided with the post-acceleration tube, namely the cathode ray pressure indicator GM 3 154 and the cathode ray oscillograph GM 3 156.

[6]) In the customary application of the cathode ray tube the horizontal deflection is obtained with the help of a saw-tooth generator. In the case of the cathode ray oscillograph GM 3 152 this gives a non-balanced voltage, *i.e.* the potential of one terminal of the generator is constant, while that of the other varies. In order not to obtain trapezium distortion, the terminal which has a variable potential must be connected to the plate bearing the rods.

Both phenomena may be ascribed to the fact that the potential field of the post- acceleration electrode penetrates between the deflection plates and here undergoes a deformation like that sketched in *fig. 10*. The equipotential surfaces are more sharply curved by the set of plates D_2 in the plane of the drawing, thus in the horizontal plane, than in the vertical plane, which means in optical language that a cylindrical lens is placed in front of the actual post-acceleration lens.

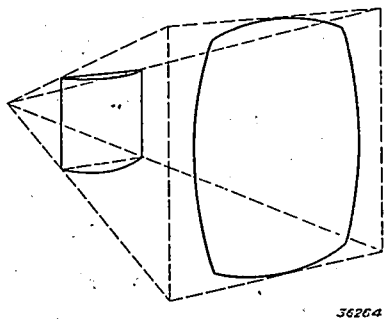

Fig. 11. Action of an astigmatic lens (cylindrical lens). An originally rectangular beam is compressed in one direction and in addition given a barrel-shaped distortion.

This cylindrical lens strengthens the electron lens in the horizontal plane, so that the beam no longer has a focus point on the screen, but a focus line. Moreover, it deforms the oscillogram in the way shown in *fig. 11*: in the first place it decreases the sensitivity of the system in the direction of the time base, and in the second place it leads to a barrel-shaped distortion of the oscillogram.

The astigmatism and the consequent distortion can be combatted by providing a plate of set D_2 with paddle-shaped appendages (see fig. 9 and more clearly *fig. 12*). These paddles provide an extra focussing of the beam in a direction perpendicular to the extra focussing by the set of plates D_2, and thus combat the astigmatism. The paddles are made so large that the astigmatism is just eliminated, the barrel-shaped distortion is then also found to have disappeared.

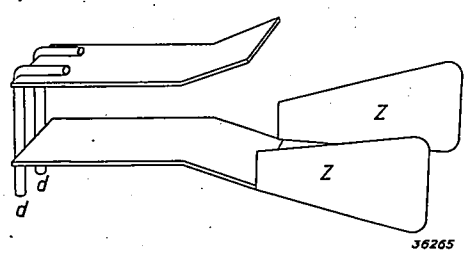

Fig. 12. The second system of deflection plates (D_2) with rods d and paddles z.

Properties of the post-acceleration tube

Focussing voltage

Fig. 13 shows the variation of the focussing voltage with the post-acceleration voltage. As has already been mentioned in the discussion of the

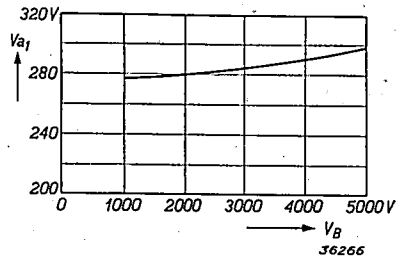

Fig. 13. Variation of the focussing voltage, which must be applied to the anode a_1 to obtain a sharp spot, as a function of the voltage of the post-acceleration electrode with respect to the cathode.

astigmatism, the post-acceleration lens also has a focussing action on the beam. If the tube is switched on without post-acceleration, and then focussed, the focussing voltage of the electrode a_1 must be increased as soon as the post-acceleration is set in action. The strength of the lens a_1-a_2 is hereby made smaller, which is necessary to keep the sum of the lens strengths constant.

Deflection sensitivity

Fig. 14 shows the relation between the deflection sensitivity and the post-acceleration. The voltage

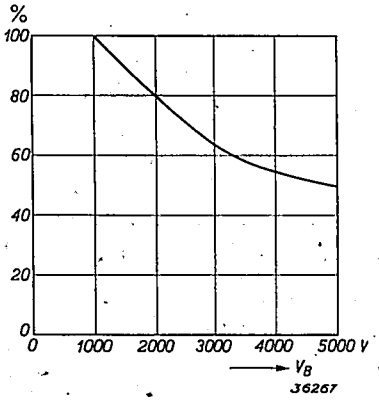

Fig. 14. Relative change in the deflection sensitivity as a function of the voltage of the post-acceleration electrode with respect to the cathode.

of a_2 and the coating A has been kept constant at 1 000 volts, while that of the second covering varies between 1 000 and 5 000 volts. The reduction in sensitivity is greater, the stronger the post-acceleration, as has already been shown.

With post-acceleration with a voltage of 5 000 volts with respect to the cathode the sensitivity amounts to one half of that without post-acceler-

ation. If the same system were allowed to operate without post-acceleration with an anode voltage of 5 000 volts, the sensitivity would be 1/5 of that at 1 000 volts, so that the post-acceleration is 2.5 times more favourable than a direct acceleration of the electron beam, as far as the sensitivity is concerned.

Size of image and definition

The reduction in the deflection sensitivity with increasing post-acceleration is naturally accompanied by a decrease in the maximum size of the image which can be attained without the oscillogram being distorted or cut off by the deflection plates. In designing the tube the primary aim was to give the tube the same sensitivity at a voltage on the screen of 1 000 volts (thus without post-acceleration) as that possessed by the tube DN 9-3. The deflection plates then also have such appropriate dimensions that the whole screen can be covered at 1 000 volts.

With a maximum post-acceleration (5 000 volts with respect to the cathode) this is, however, no longer possible. The largest oscillogram which can be obtained without deformation has dimensions of 40 by 40 mm, while the screen itself has sufficient area for an image 65 by 65 mm. This reduction is size of the image by no means involves a loss of details, however, since the fluorescent spot becomes sharper with increasing voltage. With constant beam current the reduction in size of the spot with increasing voltage on the screen is found to be about as great as the reduction in size of the oscillogram due to the decreased deflection sensitivity.

Scanning speed

Extensive tests have been carried out to determine the maximum scanning speed. Use was here again made of a camera with a lens aperture 1 : 3,2 and Agfa Isopan roll film. If the post-acceleration electrode has a voltage of 5 000 volts with respect to the cathode, then with a fourfold reduction and a beam current of 20 μA the maximum recordable scanning speed is 24 km/s. At a voltage of 1 000 volts one obtains, under otherwise the same conditions, the scanning speed of 850 m/s already mentioned, so that there is a gain of a factor 25.

In laboratory measurements lenses with larger apertures, 1 : 1.5 for instance, will usually be available, and with such lenses a scanning speed of 100 km/s. can be obtained.

In conclusion, here are a few practical hints for the use of the post-acceleration tube.

The post-acceleration voltage must not be connected to the screen as long as the fluorescent spot is stationary. Due to the high power the spot would immediately burn in, which means that at the spot where the screen is struck by electrons of too high energy the sensitivity of the screen for electrons of low energy decreases appreciably. A straight line, also, *i.e.* a deflection with one set of plates offers no security against burning in. If, however, an A.C. voltage acts on both deflection plates then, with a beam current of 5 μA, for instance, the image may be kept continuously on the screen without there being a chance of burning in even at the highest post-acceleration voltage. (This beam current of 5 μA is sufficient to cause an image to appear on the screen which can also easily be seen in a well-lighted room). With short exposures one may go as far as 20 μA. For very rapid phenomena the regulatory electrode will simply be connected to the cathode, whereby a beam current of about 50 μA is obtained. One must then, however, work very quickly in adjusting the definition and desired size of image, since in that extreme case the image may only remain on the screen for a few seconds.

A PHOTOCELL WITH AMPLIFICATION BY MEANS OF SECONDARY EMISSION

by M. C. TEVES.

621.383.2

For the amplification of photocurrents use may well be made of secondary emission. The previously described electron multiplier, which is based on this principle, serves very well in the case of very weak photocurrents which vary at a very high frequency (television), but it is too complicated to be considered for simpler applications such as for sound film. A simpler construction which is suitable for this latter purpose is described in this article. The amplifier part consists of three stages with secondary emission, and, contrary to the case with the electron multiplier, it works entirely electrostatically, so that no external magnetic fields are necessary. About a hundredfold amplification is obtained, and thereby a photoelectric sensitivity of 2 to 3 mA/lm.

In almost all the cases where photocells are used, such as signalling and counting arrangements, sound film apparatus, television transmitting systems, etc. the currents obtained are too weak to be used directly, so that it is practically always necessary to amplify the current. The amplifier circuits familiar in radio technology are the first to be considered for this purpose. In addition it is possible to amplify the photocurrent in the tube itself to a certain extent by means of a rare gas filling, in which every photoelectron can free new electrons by ionization of the gas atoms. A third possibility is the application of secondary emission, *i.e.* the freeing of secondary electrons from an auxiliary anode which is struck by the primary photoelectrons. With a suitable choice of material for the auxiliary anode and of the voltage, every primary electron leads to the emission of 5 or 6 secondary electrons, so that the current can be amplified by a factor 5 or 6. If desired this process can be repeated a number of times, and in this way a very high amplification obtained.

The advantages of amplification by secondary emission over amplification with amplifier valves have already been explained in a previous article in this periodical [1]). They are mainly due to the fact that secondary emission causes no dark current, *i.e.* when the photocurrent is zero the secondary emitting plates also give no current. With an amplifier valve, on the other hand, a certain anode current flows even in the absence of the voltage to be amplified, and this current exhibits certain fluctuations (noise) which may be very disturbing upon amplification of very weak signals. Amplification by means of a gas filling, as far as noise is concerned, is less advantageous than amplification by means of secondary emission. Moreover, it is impossible to attain an amplification of any desired magnitude with the help of a gas filling, and finally, due to the relatively slow motion of the positive ions, the current in the gas exhibits time-lag phenomena [2]) which are manifested in a decrease in the amplification with increasing frequency, and which are already clearly observable at acoustic frequencies.

From these considerations it is found that not only for the amplification of photocurrents with a very high frequency (television), but also for sound film apparatus it may be advantageous to use photocells with amplification by secondary emission. A photocell for the latter purpose with three stages of amplification by secondary emission was developed in this laboratory and forms the subject of this article.

Requirements assumed in the design

The requirements which must be made of a photocell for use in sound film and the like are quite different from those made of the previously described photocell with secondary emission [3]) (electron multiplier). For the tubes there referred to, which are used chiefly in television technology, it is not too important how extensive and complicated the construction is and how great are the pains taken in the setting and adjustment, since there is practically no other available solution which meets the requirement of linear amplification, independent of the frequency and free of noise, of the very weak photocurrents there prevailing, with their intensity fluctuations of very high frequency.

In the case of the sound film, on the other hand, where the necessary amplification can be obtained in many ways, the use of a photocell with secondary emission is only justified when the possible complications resulting from its use are less important than the simplifications which become possible in

[1]) See H. Rinia and C. Dorsman, Television system with Nipkow disc, Philips techn. Rev. **2**, 72, 1937, especially p. 74.

[2]) See A. A. Kruithof, Philips techn. Rev. **4**, 48, 1939.

[3]) See J. L. H. Jonker and M. C. Teves, Philips techn. Rev. **3**, 133, 1938.

other parts of the apparatus due to the greater strength of the photocurrent.

In the first place it is desirable that the necessary voltage of the photocell shall not be higher than the voltage which can be provided by the eliminator of normal sound film amplifiers (500 to 560 volts). Neither must it be necessary for the voltage to be exactly constant and precisely adapted to the cell, so that the cell can for instance be exchanged for a new one without it being necessary to readjust the apparatus. Finally it is desirable that the dimensions of the photocell shall be such that it can be built into a sound head of normal construction.

The limitation of the available voltage means either a limitation of the number of secondary emitting electrodes or a limitation of the available voltage per stage. In either case the amplification factor is limited. The best compromise lies at a voltage of about 150 volts per stage. This gives three stages of amplification by secondary emission, which thus require a voltage of 450 volts. The potential of the final anode must be higher by a certain amount than that of the last secondary emitting plate in order to draw all the electrons emitted by that plate to itself. It need not, however, be chosen higher than 650 volts.

The amplification to be obtained with three stages of secondary emission amounts to about a factor of 100. This means practically that in the construction of the apparatus connected to the photocell at least one amplifier valve can be omitted, while at the same time the noise level and the reproduction of high frequencies will be more satisfactory.

As to the second requirement (lack of sensitivity to fluctuations in the voltage), the previously described construction of the electron multiplier does not furnish a satisfactory solution. In that construction, which is given once more in *fig. 1*, the motion of the electrons is determined by the electric fields of the successive electrodes and by a magnetic field perpendicular to the plane of the figure. In order to obtain the desired electron trajectories this magnetic field must be carefully adjusted as to strength and direction, and since the curvature of the trajectories depends upon the ratio between the intensities of the magnetic and electric fields, the potentials of the electrodes must be kept absolutely constant.

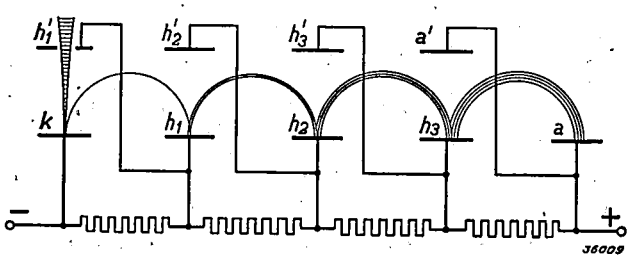

Fig. 1. Electron multiplier with electrostatic and magnetic deflection of the electrons. A light ray causes electrons to be emitted from the cathode k, which free secondary electrons from the auxiliary anodes h_1, h_2, h_3, successively. The electrodes h_1', h_2', h_3' serve to provide the desired electric fields. The magnetic field is perpendicular to the plane of the drawing.

The obvious method of avoiding this difficulty is to use only electrostatic fields for the deflection of the electrons. When this is done the necessary fields can be provided by the electrode system of the cell, so that no external components must be regulated with respect to the cell. Moreover, with sufficiently low initial velocities of the electrons, their trajectories are then entirely determined by the relative values of the potentials of the different electrodes and not by their absolute values, which are then only of importance to the operation of the cell in as far as they influence the amplification factor of the secondary emitting plates.

In recent years a large number of types of electron multiplier systems which work purely electrostatically have been proposed, a few of which were described in the article referred to in footnote [3]). These constructions have, however, certain disadvantages which are explained in the article mentioned, and which make it impossible for any of them to rival the constructions with mixed electrostatic and magnetic deflection of the electrons. In the meantime, however, a new and very simple construction has been proposed [4]), which offers great advantages for our purpose.

Electrode systems with electrostatic focussing

Fig. 2 gives a cross section of the system with the electron trajectories obtained. The system consists of a number of electrodes with successively higher potentials which are so interlocked that the secondary electrons which leave a certain part of one electrode (shaded in the figure) are attracted by the following electrode and strike it within the corresponding region. In this way, in principle, any desired number of stages can be used, care must only be taken, by choosing a suitable shape for the first electrode, that the photoelectrons are actually focussed on the shaded part of the first auxiliary anode.

Beginning with the customary spherical photocathode, this can be done in the manner shown in *fig. 3*. Use is here made of the fact that the electric field between the photocathode and the anode has a focussing effect on the electrons, such that

[4]) V. K. Zworykin and J. A. Rajchman, Electrostatic electron multiplier, Proc. Inst. Radio Eng. 27, 558-566, 1939.

a very much reduced image of the cathode appears on the anode. If an opening is made in the anode all the photoelectrons will pass through it which are

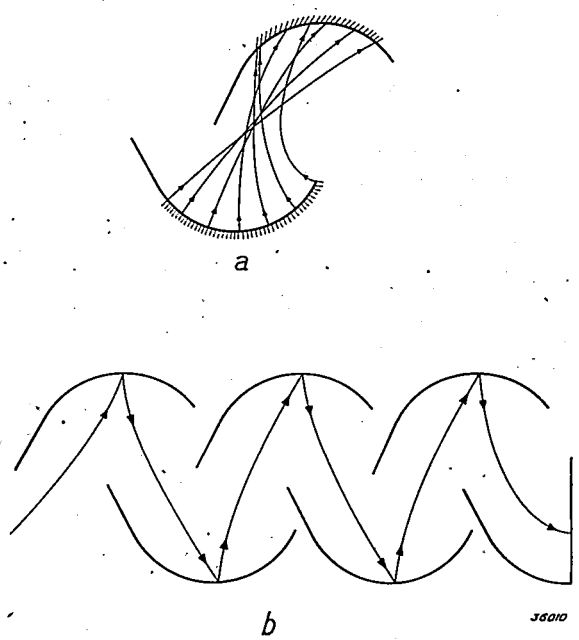

Fig. 2. *a*) Trajectories of the electrons between two successive electrodes of an electron multiplier with purely electrostatic focussing. The electrons which are freed on the shaded region of the lower electrode strike the corresponding shaded region of the upper electrode; the beam is therefore not broadened by passing through the successive stages.
b) Five successive stages of an electron multiplier with electrostatic focussing.

emitted from a certain region of the photocathode, which region is considerably larger than the opening. In this way it is possible to combine the electrons from all parts of the photocathode which are important for direct illumination from the outside into a relatively narrow, homogeneous and well directed beam.

Thanks to this concentration of the electron beam it is possible to make the rest of the photocell, in which the triple amplification by secondary emission takes place, very small. The whole electrode system, consisting of the anode of the photocell, three secondary emitting auxiliary anodes and the final anode, is about 2 cm long, while the diameter of the spherical photocell is 4 cm. The area of the region on the cathode from which the photoelectrons reach the electron multiplier is about 1 cm^2 The light from the outside must therefore be concentrated on this spot. Part of the incident light is reflected by the photocathode on the other parts of the cathode. The photoelectrons freed by this scattered light also go to the anode, they do not, however, pass through the opening. In this way about $^1/_4$ to $^1/_3$ of the emission of the cathode is lost.

Further loss occurs because of the fact that not all the electrons follow the desired path from one secondary emitting electrode to the next. This is due to the fact that in the collision of an electron with the electrode, in addition to secondary electrons with a velocity from 0 to 15 volts (with a maximum in the velocity distribution at about 5 volts), directly reflected electrons also occur which have practically the same energy as the incident electron (150 volts). For these very fast electrons the system is not designed. They will also finally reach the last anode, but may skip one or more electrodes on the way, and therefore contribute less to the amplification of the anode current.

These losses show why the total amplification is less than the product of the amplification factors of the individual stages. If each of the secondary emitting electrodes emits an average of 6 electrons per incident primary electron, then the ratio between the current to the last anode and the current which enters the multiplier would theoretically be $6^3 = 216$, while actually it is about 130; the ratio of the current to the last anode to the total original photocurrent then amounts to about a factor 100.

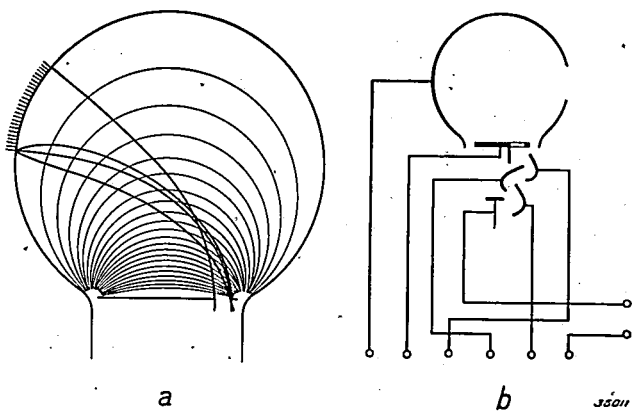

Fig. 3. *a*) Trajectories of the photoelectrons between a spherical photocathode and a plane anode (the thin lines are equipotential lines). The photocathode is projected in reduced size on the anode. The electrons freed from the shaded part of the photocathode pass through the opening of the anode and are multiplied in the succeeding multiplier system.
b) Cross section of the system.

Construction of the photocell

The final construction of the photocell corresponds very closely to the diagram given in fig. 3. The photosensitive layer is deposited directly on the glass of the spherical upper part of the bulb, while the five other electrodes are assembled on a glass pinch which conducts the leads of these electrodes to the base. The connection of the photocathode is led out separately at the top. *Fig. 4* is a photograph of the photocell with the amplifier stages in which

the various electrodes with the exception of the first anode can clearly be seen.

A special problem is the combination in one tube of the photoelectrically sensitive surface and the secondary emitting surfaces. As was previously explained in the description of the electron multiplier [5]), it is advisable to make these surfaces of the same material, since otherwise there is a danger that the surfaces layers will have detrimental effects upon each other while they are being prepared. As a possible solution the use of a silver underlayer covered with caesium oxide and adsorbed caesium was suggested. With such a layer the caesium oxide molecules have a very high secondary emission, while the adsorbed caesium atoms possess a high photoelectric sensitivity.

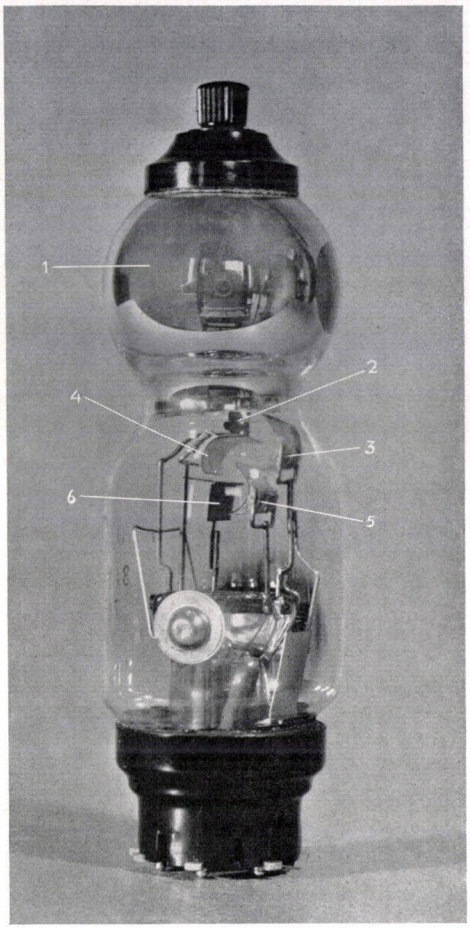

Fig. 4. Photocell with amplification by secondary emission. *1* Internal metallic deposit upon which the photo-electrically sensitive layer is deposited; *2* first anode; *3*, *4*, *5*, secondary emitting auxiliary electrodes; *6* final anode. The current to the final anode is about 100 times as high as the photocurrent and amounts to 2 to 3 mA/lm.

In order to increase to a maximum both the secondary emission and the photoelectric sensitivity, the oxidation of the secondary emitting electrodes would have to be carried farther than that of the photocathode, namely so far, if possible, that all the adsorbed caesium was converted into caesium oxide. Such different treatment of otherwise identical electrodes, however, is accompanied by great difficulties, because there is a tendency for an equilibrium to be established during the preparation, at which equilibrium all the electrodes adsorb the same percentage of caesium. These difficulties have, however, been successfully overcome by treating the secondary emitting electrodes before covering with caesium oxide in such a way that they adsorb practically no caesium, so that when the photocathode and the secondary emitting cathodes are prepared together, no excess of caesium appears on the latter.

In this way we succeeded in combining in one tube a sensitive photocathode (20-30 μA/lm) and an electrode with high secondary emission (multiplication factor about 6 at 150 volts), without it being necessary to follow any other method of procedure in preparing the photocathode than is customary for ordinary photocells.

The choice of the voltages

If a large number of secondary emitting electrodes were to be used one after the other, it would be obvious that the voltage from one electrode to the following should be increased by the same value each time, for instance 150 volts. The voltage of the first anode must by experiment be so chosen that electrons which pass through the hole in this anode are concentrated as well as possible on the first secondary emitting plate of the amplifying system. The voltage of the last anode must be higher than that of all the other electrodes, but is further of no importance.

In our case of only three secondary emission stages, such a short system results that the first and the last electrode influence the field distribution over the whole system, so that the successive stages of amplification by secondary emission are not exactly identical. The best choice of voltage is then found to be slightly different from that according to a geometric series, and must be determined experimentally. This can easily be done by connecting the different electrodes to a potentiometer and changing its adjustment until the maximum current is obtained with constant total voltage and constant illumination of the photocell. The optimum mutual relations between the voltages found in this way is found to be independent of the total

[5]) See the article cited in footnote [3]), p. 136.

voltage, which only determines the amplification. At a total voltage of 635 volts the series of voltage values given in *table I* was found to be the most satisfactory.

Table I

photocathode	0 volts
first anode	25 ,,
first secondary anode	300 ,,
second secondary anode	450 ,,
third secondary anode	580 ,,
last anode	635 ,,

The sensitivity obtained amounts to 2 to 3 mA/lm under the conditions indicated, which means that light fluxes above a few tenths of a millilumen are sufficiently intense to be registered with a single amplifier stage following the photocell. The maximum light fluxes available with sound film amount to about 20 millilumen. These give sufficiently great voltage variations on the output resistance of the photocell to load the output stage of a sound-film amplifier fully. If photocells without amplification or with gas amplification are used, this is impossible, and pre-amplification must be employed, one stage with gas-filled photocells and two with vacuum cells.

Besides this structural advantage the photocell with secondary emission, as already mentioned, also offers advantages in the quality of reproduction. In the reproduction of Philips-Miller film, the sound track of which is of very high quality, the differences between the different kinds of photocells can clearly be heard. The secondary emitting photocell gives practically no distortion or noise. When a gas-filled photocell is used there is appreciable distortion and, moreover, an attenuation of the high tones. Due to the high amplification necessary with the vacuum cell the noise is disturbingly audible; the contribution of the first amplifier valve to the noise is in this case greater than that of the photocell.

X-RAY PHOTOGRAPHY WITH THE CAMERA

by A. BOUWERS and G. C. E. BURGER.

778.33:771.3

While in the customary method of X-ray photography the film is pressed against a fluorescent screen placed in the beam of X-rays (contact photograph), a different method has recently been worked out in which the luminous X-ray image on the fluorescent screen is photographed with a camera. Since by this method the cost of a photograph is very much reduced, and the pictures obtained are not inferior to an ordinary fluoroscope image, the method is very well suited for series work in the detection of tuberculosis. The quality of the camera photograph obtained is compared with that of the contact photograph, and experiments are discussed which were performed in order to test the practical utility of X-ray camera photography. In conclusion the installation used in the Philips Medical Department is described and a short discussion is given of the problem of the danger of exposure to radiation.

In medical X-ray work two methods have long been used side by side: fluoroscopy, in which the X-ray shadow image of the patient is observed on a fluorescent screen, and X-ray photography in which the X-ray picture is recorded on a film which is pressed against the fluorescent screen. Finer details can generally be distinguished in the photograph than in the fluorescope image, so that the doctor can form a sharper diagnosis from a photograph. Sometimes, however, particularly in series examinations of groups of people for the detection of tubercular lung lesions, it is not so much a question of the precise observation of a lesion. as of ascertaining that a lesion is present. In this case therefore fluoroscopy sufficed. This was very fortunate, since lung photographs made in the way described are quite expensive due to the large dimensions of the film required (normally 30 × 40 cm). Moreover, in the work of detection mentioned, fluoroscopy has the advantage that the doctor can project any possible diseased spots in different ways between the shadows of the skeleton in the image by turning the patient slightly in the fixed X-ray beam, and thus runs less chance of failing to detect any lesions hidden behind parts of the skeleton. In order to obtain the same security with the photographic method two or three photographs of each person in different positions would have to be taken, and the objection of expense would become even greater.

For these reasons series examinations for tuberculosis were confined to fluoroscopy, and the advantages which the photographic method offers with respect to objective documentation and the possibility of having a case judged by different doctors were relinquished.

In recent years another photographic method has now been developed [1]) which makes it possible, in detection work also, to profit by the advantages mentioned (documentation, etc.). In this method, so-called X-ray camera photography, the film is not placed at the point where the X-ray picture is formed, but the picture formed on the fluorescent screen is photographed by means of one of the normal miniature cameras at 2.4 × 3.2 cm, for instance. The costs of the photographic material, developing, archive space, etc. are hereby enormously reduced and no longer constitute an objection. This method has been applied for some time on a large scale by the Philips Medical Department for tuberculosis series examination.

The principle of the method is not new. Shortly after the discovery of X-rays, attempts were made to apply the principle, and from the beginning it has formed the basis of all experiments in X-ray cinematography of heart and lungs. The fact that the method did not immediately come into general use may be ascribed to the impossibility of obtaining a satisfactory quality of picture with the means then available. The quality of an X-ray picture depends upon the average density and the definition. It is found, however, as we shall explain later, that the increase in the definition always takes place at the expense of the density and *vice-versa*. While the compromise thus made necessary gave useful results in the case of ordinary X-ray photography ("contact photographs"), with X-ray camera photography the conditions for the compromise are much less favourable due to the loss of light in the photographic transmission, so that it was only the very high-speed lenses with their sharp definition and the sensitive, fine-grained films which have recently been developed for use in miniature photography, as well as the very much improved fluorescent screens, which have made X-ray camera photography practically possible.

We shall examine somewhat more closely the considerations mentioned above, by comparing the

[1]) M. de Abreu, Z. Tuberkulose **80**, 70, 1938.

exposure conditions for the camera photograph and for the contact photograph. In *fig. 1* the two situations are represented schematically. For the contact photograph a film with an emulsion on both sides is used, and fluorescent screens (foils) are pressed against both sides of the film. In the camera photograph the fluorescence image is focussed on the film by a lens at a distance a with a

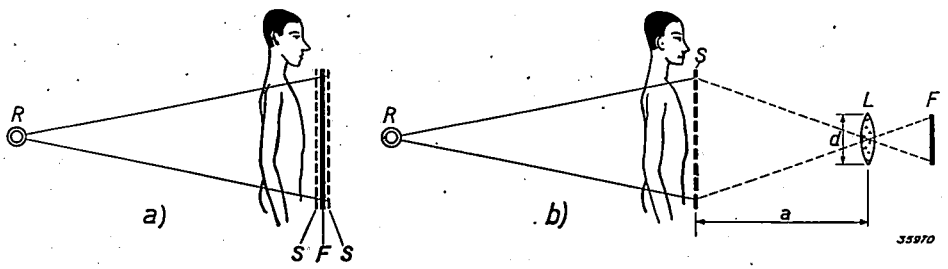

Fig. 1. Diagram of the situation in taking an X-ray contact photograph (a) and camera photograph (b). R source of X-rays (focus), S fluorescent foil or screen, F film, L lens.

diameter d and a focal distance f. While in the first case half of the radiation from each of the two fluorescent screens, or in other words, the total radiation of one screen, contributes to the blackening of the film, in the second case only the fraction captured by the lens is effective. This fraction is

$$k = \frac{\pi d^2/4}{4\pi\, a^2} = \frac{d^2}{16a^2}.$$

The quantity of light per cm² film surface is the deciding factor for the average density obtained, and since the camera photograph is reduced in the ratio a/f [2]), to obtain the same density on the camera photograph a total light radiation would be necessary n times as great as for the contact photograph, where

$$n = \frac{1}{k} \cdot \left(\frac{f}{a}\right)^2 = 16 \left(\frac{f}{d}\right)^2 \quad . \quad . \quad . \quad . \quad (1)$$

If we calculate with a relative aperture of the lens of $d/f = 1 : 1.5$, and this is approximately the maximum attainable practically at present, then according to (1) 36 times as much light is needed for the camera photograph as for the contact photograph [3]).

What are the consequences of this with respect to the definition? In the contact photograph there are three factors which contribute to the lack of sharpness U: that due to motion U_b, caused by the heart beat, the geometrical lack of sharpness U_g (half width of shadow), caused by the finite dimensions of the source of X-rays (the focus) and the foil lack of sharpness U_f, which is due to the grain and the finite thickness of the fluorescent foil. The total lack of sharpness is

$$U = U_b + U_g + U_f \quad . \quad . \quad . \quad . \quad . \quad . \quad (2)$$

U_b is proportional to the exposure time, U_g to the width of the focus, U_f, as shown by tests [4]), to the light yield of the foil. These same three quantities: exposure time, width of focus and light yield, also determine the toal quantity I of the fluorescence light, I is proportional to each of them:

$$I \sim U_b \cdot U_g \cdot U_f \quad . \quad . \quad . \quad . \quad . \quad . \quad . \quad . \quad (3)$$

It is clear that with a given product of three variable quantities, their sum can be a minimum when all three are equal. The conditions for the photography (exposure time, size of focus, kind of fluorescence foil) are thus best chosen so that

$$U_b = U_g = U_f, \quad . \quad . \quad . \quad . \quad . \quad . \quad (4)$$

since in that case the total lack of sharpness U is a minimum, and is

$$U \sim \sqrt[3]{I} \quad . \quad . \quad . \quad . \quad . \quad . \quad . \quad (5)$$

so that the lack of sharpness of the camera photo-

[2]) Strictly speaking this ratio is $a/f - 1$, but as $a/f \gg 1$ we can use a/f for its value.

[3]) In this simplified representation, no account is taken of the light absorption of the lens, which may be quite important particularly in lenses with large relative apertures. In the lenses here used it was about 30 per cent. This loss of light is partly compensated for by other effects. Altogether the ratio of 36 here given will be quite close to the truth. But even if the ratio were wrong by a factor 2, it is found from the following considerations that this has only a slight influence on the final result.

[4]) See A. Bouwers and W. J. Oosterkamp, Fortschr. Röntgenstr. 54, 87, 1936. In the discussion it is assumed that the exposure time is short compared with the period of the heart beat, so that the speed of movement of the particles in the lung is practically constant during the exposure, and that an X-ray tube with rotating anode is used. With a stationary anode the permissible specific focus loading depends also upon the time of loading, so that a more complicated formula takes the place of (3).

graph would be $\sqrt[3]{n}$ times as great as that of the contact photograph, where n is given by equation (1).

With the value of d/f given $\sqrt[3]{n}$ becomes 3.3. Thus a lack of sharpness of 3.3 mm in the camera photograph when it is enlarged to the same dimensions corresponds to a lack of sharpness of 1 mm in the contact photograph.

The ratio can, however, be made more favourable. We began with the assumption that the camera photograph must have the same average density as the contact photograph. Actually, however, there is no reason for trying to obtain the same density in the camera photograph, since it is usually observed by projecting it about life size, and films must be "thinner" for projection. This makes the required amount of light I smaller, and according to (5) the lack of sharpness also. Furthermore miniature films have in general a steeper gradation than the large X-ray films, so that it is possible to work with harder X-rays (which give less contrasty negatives), *i.e.* with higher voltages on the X-ray tube. Since the efficiency of the excitation of the X-rays then rises considerably, a smaller focus is large enough to give the same intensity of X-rays, and the geometrical lack of sharpness thus becomes smaller. Moreover, when the picture quality is chiefly determined by the lack of sharpness, it is advisable to reduce this lack of sharpness still more by slight compromises on other points, for instance by increasing the tube voltage slightly further, and then accepting the reduced contrast which results. In this way the geometrical lack of sharpness is still more reduced. The same effect is obtained by decreasing the distance b between the focus and the fluorescent screen: for the same intensity of X-rays the width of the focus must be chosen so that $h \sim b^2$, and since the half width of shadow is proportional to h/b, for constant intensity this decreases proportionally with b. Of course a greater distortion of the shadow image must in this case also be accepted. Finally it is also advantageous to choose a somewhat longer exposure time than would correspond to condition (4). By this means the lack of sharpness U_g and U_f, which are constant over the whole photograph, are slightly decreased at the expense of a greater lack of sharpness due to motion U_b, which is, however, mainly confined to the neighbourhood of the heart and the large blood vessels. In the other parts of the lung where lesions most often occur there is a slight gain in sharpness.

In the camera photographs which are taken in the series examinations at Philips the usual tube voltage for the contact photograph of 50-70 kV is increased to 80-95 kV (the increased scattered radiations which hereby occur and which would lead to an undesired fogging of the photograph are made harmless by a thin scattered radiation raster); the distance b is reduced from 150 to 85 cm and the exposure time is 0.4-0.6 sec. instead of 0.1 sec. By this means the increase of the resulting lack of sharpness in the camera photograph is reduced to a factor 2. In order to give an idea of the excellence of the quality of the picture obtained in this way, an enlargement of a camera photograph, like thousands which have already been made here, and a reduction of a contact photograph of the same patient are reproduced side by side in *fig. 2*.

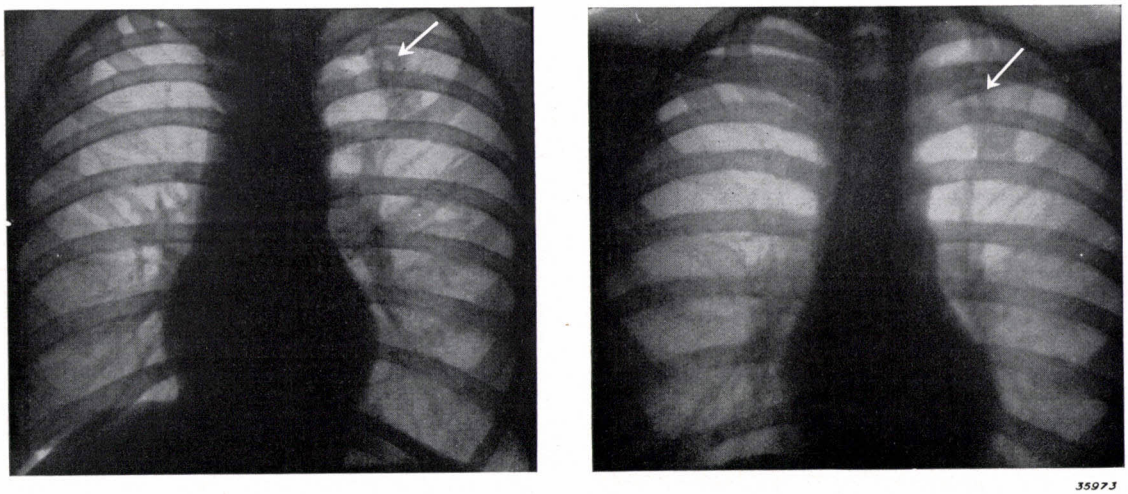

Fig. 2. Left: reduced contact photograph, right: enlarged camera photograph of the lung of the same patient. Under the left hand collar bone (see arrow) there is a small ring shadow which indicates an active tubercular process. This shadow as well as the blood vessels in the lung may also be seen very clearly in the camera photograph.

We have not yet spoken of two more causes of lack of sharpness which occur in the camera photograph: the grain of the film and the lack of sharpness of the lens, *i.e.* the size of the aberration circle in which a point is projected. Here again we encounter the incompatibility between density and sharpness. The grain of the film is larger with greater sensitivity, and the aberration circle of a lens increases with its relative aperture. Due to the great progress in miniature photography, however, with the film used by us with a sensitivity of about 17/10 DIN and with a lens with $d/f = 1 : 1.5$ the lack of sharpness is still small compared with that due to the above mentioned causes. We found a film grain varying from 5 to a maximum of 25 microns, and an aberration circle of our lens of 20-30 μ at the centre of the picture (this is somewhat larger at the edge). The lack of sharpness U may, however, amount to about 2 mm in the picture when brought to normal size, and to about 150 μ in the picture reduced about 13 times.

We shall not discuss the question of whether the X-ray camera photograph, which according to the above is not much inferior to the contact photograph, will not in time be able to replace the latter. The comparison here given, however, leads to the conclusion that camera photography can certainly take the place of the fluoroscopy customary in detection examinations, where less severe requirements are made with respect to the observation of details. Before we proceeded to the introduction of the method in series examinations, we tested its utility in practical cases by means of the following experiments [5]).

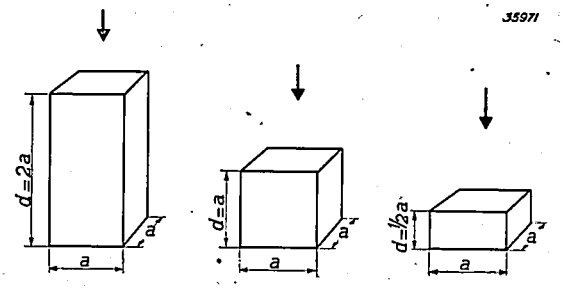

Fig. 3. Shape of the three objects which are used for the visibility tests with phantoms. The arrow indicates the direction of the X-rays.

In the first place the size was determined of the smallest object still just observable in the X-ray picture, by a method previously described in this periodical [6]). The chest of the patient was replaced in these experiments by a "phantom" of "Philite" in which cavities of different dimensions were made to represent the objects to be observed. Since the visibility increases with the contrast, which in turn depends upon the thickness of the object (dimension in the direction of the X-rays) the experiments were always done with three kinds of objects of the form shown in *fig. 3*. If the minimum thickness of the object required for visibility is plotted as a function of the width, the curves given in *fig. 4* are obtained. Fig. 4*a* relates to a normal phantom, fig. 4*b* to one in which unusually much scattered X-radiation occurred and which therefore represents the conditions occurring with stouter patients. It is found from the curves that smaller objects can generally be observed on the camera photograph better than in fluoroscopy, and that the difference in favour of X-ray camera photography is particularly pronounced with stouter patients.

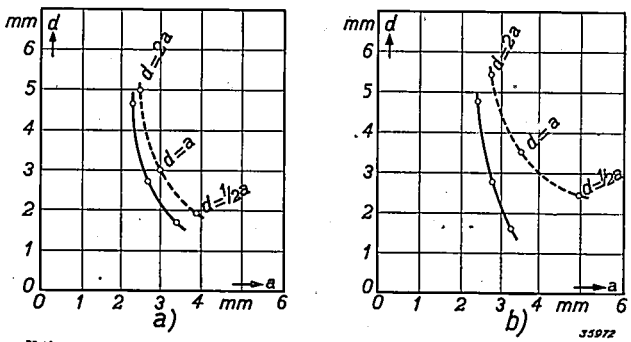

Fig. 4. The smallest object observable in a phantom in the fluorescope image (broken-line curves) and on the camera photograph (full-line curves). The minimum thickness d required for visibility is plotted as a function of the width a. The points measured refer to the three types of object of fig. 3.
a) Phantom corresponding to a normal patient. For the fluoroscopy the normal tube voltage of 54 kV was used.
b) Phantom corresponding to stout patient. Due to the larger quantity of scattered radiation in fluoroscopy as well as in camera photography a so-called scattered radiation raster (Lysholm filter) was used. Moreover, the voltage was raised to 70 kV for the fluoroscopy.

Finally as a crucial experiment a comparison was made of the diagnoses which were made by different doctors independently of each other working according to the three methods of examination in a series of about 200 cases. In *table I* the results of this comparison are given. The cases are divided into three groups according to the seriousness of the lesions found in the lungs. Only in two cases of small inactive lesions did the X-ray camera photograph give less decisive results than the contact photograph and fluoroscopy. In eleven cases of large lesions fluoroscopy furnished less complete information. It must be remarked that for each patient exposures were made in three different directions, namely from back to front, front to back and obliquely through the body. From the last column of the table, in which the number of cases is indicated in which the second and

[5]) G. C. E. Burgers, Handelingen 27e Ned. natuurk. en geneesk. Congres, p. 194, 1939; Maandschr. Kindergeneesk. **9**, 187, 1939.

[6]) B. van Dijk, Several problems of fluoroscopy, Philips techn. Rev. **4**, 114, 1939. More detailed in G. C. E. Burger and B. van Dijk, Fortschr. Röntgenstr. **54**, 492, 1936; **55**, 464, 1937; **58**, 382, 1938.

Table I

Comparison of contact photograph (Co), camera photograph (Ca) and fluoroscopy (Fl)

Category of patients	Number of cases	Satisfactory agreement of all 3 methods	Fl. gives less than Co and Ca	Fl. and Ca. give less than Co	Ca gives less than Co and Fl.	Improvement by additional photographs
Large lesions	94	83	11	—	—	22
Few active lesions	17	17	—	—	—	16
Small inactive or no lesions	81	75	—	4	2	18

third exposure brought additional evidence to light, it is clear how important this is. In series examinations at Philips at least two camera photographs are always made.

The technique of the camera photographs is very simple. The camera is mounted at the end of a light-tight photo tube with the fluorescent screen at the other end (see *fig. 5*) and is permanently focussed on the screen. The focussing is done with the fluorescence light itself, in order to be independent of any chromatic aberration of the lens. The shutter of the camera is superfluous and is therefore

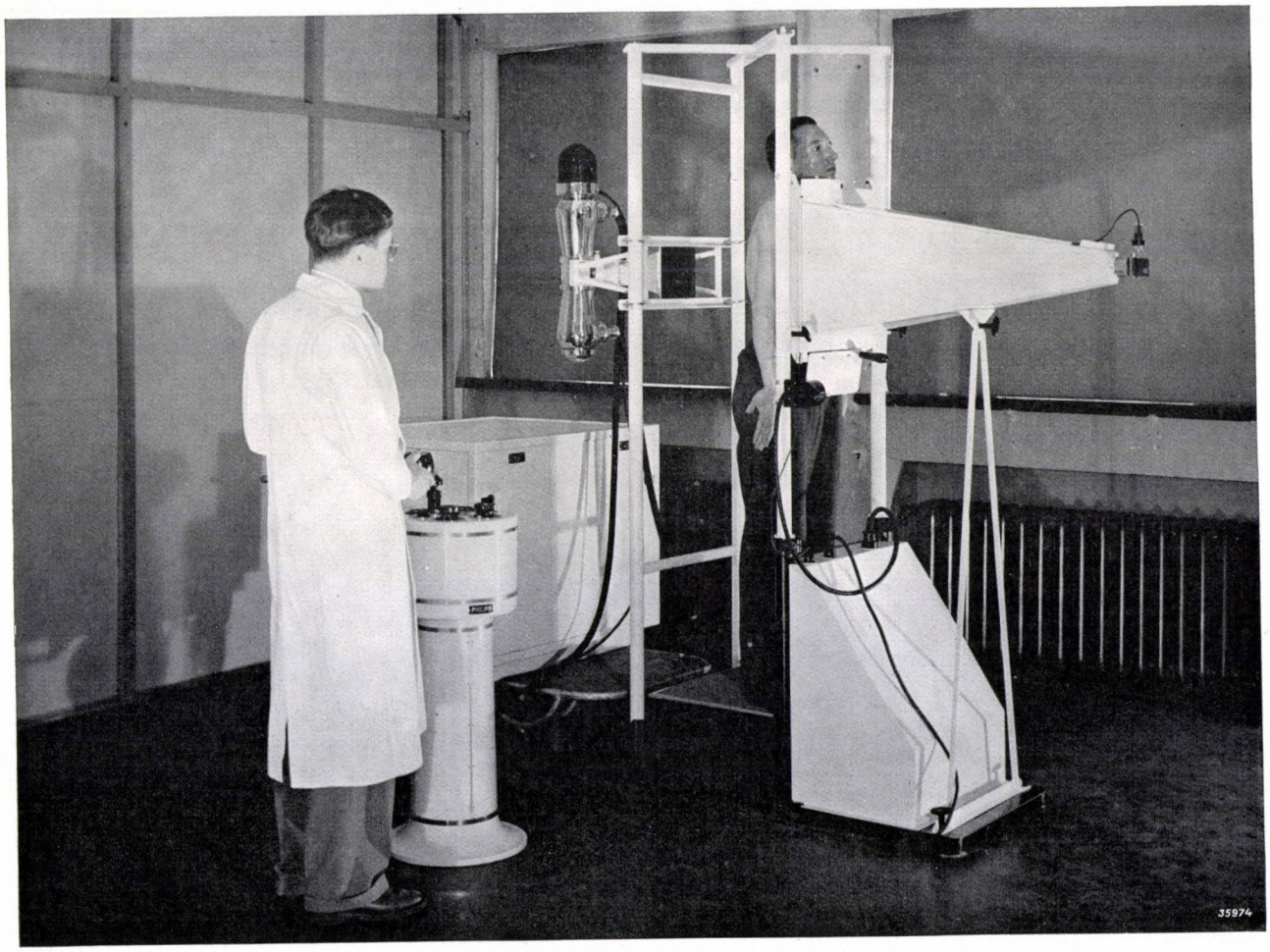

Fig. 5. Apparatus for taking X-ray photographs with a camera. In the middle the X-ray tube in an earthed covering (walls which serve only to cut off scattered X-radiation are here removed). The patient stands upon a platform whose height can be adjusted, with his chest against the fluorescent screen to which a photo tube is connected with a light-tight joint. The camera is mounted at the end of this (extreme right). In the large box on the left is the high voltage generator which is operated from the stand shown in front of it. The person who makes the exposures need only see that the patient is in the right position and switch on the X-ray tube with a hand switch which also operates the film transport.

removed, while the film transport is coupled with the switch which operates the X-ray tube by a simple mechanism. In a box which may be seen to the left on top of the photo tube a card is inserted for every patient, upon which number, name, date and other data are written. The card is photographed on a corner of the X-ray exposure, so that mistakes are impossible.

One question which we should still like to touch upon is the danger from exposure to the rays. The dosage of radiation which the patient receives on his skin in making a camera photograph is 0.6-1.0 röntgen. In X-ray fluoroscopy, which takes about 1 minute, the dose is 2-3 r. If two or three exposures are made of one patient, he does not obtain a larger total dosage than in fluoroscopy. (The dosage is of course considerably larger than the tolerance dosage of 0.2 r per day, which is permissible without injury to the health. Since, however, the fluoroscopy or photography of each patient only takes place at intervals of several months, the dosage of 3r mentioned can do him no harm.) For the operators the situation is much more favourable in the photographic method than in fluoroscopy. While in fluoroscopy the examining doctor must take care not to expose particularly his hands too much to X-radiation, in the photographic method, the person who makes the exposure, and this obviously need not be a doctor, can protect himself completely against the radiation by standing at a proper distance during the exposure, and if desired behind a lead or lead glass screen. In the arrangement used by us, for additional security a lead-covered revolving door was constructed (this was removed in fig. 5). When this door is not closed the X-ray tube cannot be switched on.

A TONE GENERATOR

by L. BLOK.

534.42 : 621.396.615.11

The tone generator GM 2 307, which can be used for the testing of loud speakers, amplifiers, cables, etc., is constructed on the heterodyne principle. The desired low-frequency signal is obtained by applying two oscillations of higher frequencies, one of which is variable, to a mixing valve. The choice of the frequencies is discussed, and it is explained how the frequency characteristic is made flat and how the deformation of the low-frequency signal is made small. The result is a characteristic which is practically flat from 30 to 16 000 c/s and an average deformation of 0.4 per cent with an output of more than 200 mW. At the expense of slightly greater deformation the output can be further increased to a maximum of 1 000 mW. By suitable arrangement of the components the shift of the frequency due to temperature fluctuations is very much restricted; upon heating up, the generator varies by a total of only about 20 c/s. The shift of the zero point of the frequency scale can be corrected in a simple way, and is checked by means of a cathode ray indicator. The influence of fluctuations in the mains voltage on the magnitude of the output voltage is made very small by means of compensation connections. In conclusion the different methods of application of the tone generator are discussed.

For measuring the frequency characteristic and the distortion factor of electro-acoustic installations or parts of such, for instance amplifiers, filters, cables, loud speakers, an instrument is needed which gives a pure sinusoidal voltage with a frequency variable over the whole acoustic frequency range. Such an apparatus, a so-called tone generator, may be realized in principle in very different ways. An oscillation of the desired frequency may for instance be generated mechanically, and then converted into an A.C. voltage by an electrodynamic system. Examples of this are the electrical tuning fork, which is often used for calibrations, and a tone generator described some time ago in this periodical [1]), in which the oscillation was generated by means of a tuned string.

The region within which the frequency can be varied is practically always very limited with such mechanical generators, so that in order to cover the entire range of acoustic importance, *i.e.* about 30-16 000 c/s, a whole series of oscillators would have to be used. In this respect it is easier to excite the desired oscillation with a syren. With an optical syren, which has also been described pre-

[1]) Balth. van der Pol and C. C. J. Addink, Philips techn. Rev. 4, 205, 1939.

viously [2]), sinusoidal oscillations can be produced whose frequency can be varied within wide limits by regulating the rate of revolution of the driving motor. Such an arrangement cannot, however, be considered for measurements on a technical scale, where an apparatus is required which is easy to use and easily transportable.

Satisfactory solutions of the problem are obtained when the oscillations are excited electrically, by means of tuned L-C circuits. But here also the most obvious method, namely of tuning the L-C circuit of an oscillator directly to the required frequency ($f = {}^1/_2\,\pi\sqrt{LC}$), is not practically possible, since very large condensers and coils would then be necessary for the lowest frequencies, while in order to cover the whole frequency range comprising 9 octaves, a whole series of oscillating circuits would again have to be used. Both difficulties are avoided when the heterodyne principle is applied. The oscillation with the desired frequency f is then obtained as a beat between two much higher frequencies f_1 and f_2. The two oscillators for the production of these high frequencies require only small values of C and L, which, moreover, need to be altered only slightly to cause the desired variation of the differential frequency f. The Philips tone generator GM 2 307, which will be described in the following, is constructed on this principle. It must be stated in advance that no attempt was made to satisfy the extreme requirements which may be made for certain laboratory experiments, but that the primary aim was to produce a simple portable apparatus, which is easy to use, permits a reasonable accuracy of measurement and which can be adapted to very divergent conditions of use.

Realisation of the heterodyne principle

In *fig. 1* the apparatus is shown diagrammatically. The two generators G_1 and G_2 provide the signals with the output frequencies f_1 and f_2 respectively. The beat with the differential frequency $f = |f_1 - f_2|$ is obtained in the same way as is customary in radio receiving sets on the heterodyne principle, by applying the two signals to a mixing valve M. The anode current of the mixing valve then contains, in addition to components with the frequencies f_1 and f_2, components with the combination frequencies $f_1 + f_2$ and $|f_1 - f_2|$, as well as combination frequencies of the harmonics, $|mf_1 \pm nf_2|$. The combination frequency $|f_1 - f_2| = f$, with which we are concerned, is singled out by the low-pass filter F and brought to the desired level by the amplifier V. The differential frequency f can be regulated by changing the frequency f_2 of the generator G_2 [3]).

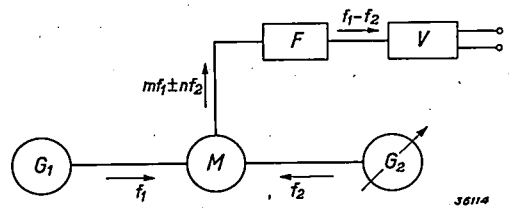

Fig. 1. Diagram showing the principle of the tone generator. G_1 constant, G_2 variable oscillator, M mixing valve, F filter, V amplifier.

While the maximum difference between the frequencies f_1 and f_2 is prescribed by the upper limit of the desired frequency range (16 000 c/s), the absolute sizes of f_1 and f_2 are not yet fixed. The advantage of the application of the heterodyne principle, namely that no large values or variations of C and L are required, however, becomes more pronounced the higher f_1 and f_2 are chosen. There is still another circumstance which makes it advisable to choose the highest possible values for these frequencies. The filter F must attenuate the signals f_1 and f_2, which are much stronger than the desired signal $|f_1 - f_2|$ to levels so low that they may be neglected; this is done more easily the farther apart lie the highest frequency to be used f_{max} and the frequencies f_1 and f_2, *i.e.* the higher f_1 and f_2 are made. The combination frequencies of the harmonics also, for instance $|f_1 - 2f_2|$, $|2f_1 - 3f_2|$, etc., then lie farther from f_{max}, as shown in *fig. 2*, the higher f_1 and f_2 are chosen (the combination frequencies $|2f_1 - 2f_2|$, $|3f_1 - 3f_2|$, are naturally not displaced).

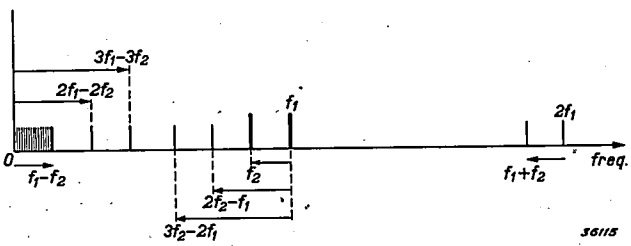

Fig. 2. Position of the original frequencies f_1 and f_2 and of the combination frequencies occurring $|mf_1 \pm nf_2|$.

On the other hand the frequencies f_1 and f_2 may not be raised indefinitely. The requirement must be made that the percentage variations of the oscillator elements necessary for regulating f shall be large with respect to the unavoidable small varia-

[2]) J. F. Schouten, Synthetic sound, Philips techn. Rev. 4, 167, 1939.

[3]) While in radio receiving sets the frequency of the local oscillator is so changed that the "intermediate frequency" obtained as beat with the signal received is constant, in this case it is the "intermediate frequency" which is varied.

tions due to temperature fluctuations, etc., since otherwise the frequency f when finally set might vary very much, which is of course undesired. At oscillator frequencies f_1, f_2 of the order of magnitude of 100 000 c/s, the variation of the frequency can still be kept within permissible limits relatively, while the construction of the filter does not yet offer any particular difficulties.

For setting the frequency zero, the two oscillators must have the same frequency, $f_1 = f_2$. Suppose that it is desired to make f_2 variable; must the differential frequency f then be obtained by raising or by lowering f_2? At first glance this seems a matter of choice; seen from the point of view of the variation of the frequency, however, there is only one answer to the question. The tuning of f_2 takes place in practice with the help of a constant condenser in parallel with a rotating condenser. The latter, which is in general quite sensitive to fluctuations in the humidity of the air, etc., contributes materially to the undesired variation in capacity, which is greater the greater the capacity to which the rotating condenser is adjusted. Now a given capacity variation is relatively most appreciable at a low differential frequency f. It is therefore advisable to arrange the apparatus so that for the lowest frequencies f the rotating condenser of G_2 stands at the smallest capacity, *i.e.* so that the differential frequency f is increased by increasing the capacity, thus by lowering the frequency f_2 of the tuning generator G_2.

On the basis of the above considerations a frequency $f_1 = 100\,000$ c/s was chosen for the constant oscillator, while the frequency f_2 can be varied between 85 000 and 1000 000 c/s, in the tone generator GM 2 307. Moreover, the "constant" oscillator is not absolutely constant, but its frequency can be raised from 100 000 to 101 000 c/s. By this means a fine adjustment of the frequency f is made possible. The two condenser scales are calibrated directly in c/s, the frequency f is found by adding the readings of the two scales; the maximum value of f is thus $15\,000 + 1\,000 = 16\,000$ c/s [4]).

Distortion and frequency characteristic of the tone generator

In order to measure the distortion factor of any transmission element, the input voltage applied to it, *i.e.* the output voltage of the tone generator, must be as free as possible of distortion. Furthermore, it is desirable for recording frequency characteristics, that the tone generator should give the same output voltage for all frequencies, *i.e.* that it should itself have a flat characteristic. In order to make clear how this condition is fulfilled in the tone generator here described we shall examine the process of the "mixing" of the frequencies f_1 and f_2 somewhat more closely.

If the voltage with the frequencies f_1 and f_2 applied to the two control grids of the mixing valve have the amplitudes V_1 and V_2 respectively, the amplitude of the anode A.C. obtained, having the differential frequency $f_1 - f_2$, may be written as follows:

$$I = S_c \cdot V_1 , \quad \ldots\ldots\ldots \quad (1)$$

where the so-called conversion slope S_c depends upon V_2. The voltage V_1 of the constant oscillator is constant, the voltage V_2 of the variable oscillator changes more or less, however, with the frequency desired, so that S_c and with it I, would also change with the frequency. In the case of the mixing valve here used (the triode-hexode ECH 3) the conversion slope is found to change only very little with V_2 for voltages V_2 of the order of magnitude of 25 volts on the third grid. V_2 is thus made to fall in this voltage region.

As for the distortion, care must be taken that the frequencies $2f_1 - 2f_2 = 2f$ and $3f_1 - 3f_2 = 3f$, etc., which may still fall within the transmission region of the filter (F in fig. 1) connected behind the mixing valve, are only represented very weakly in the anode current of the mixing valve. The appearance of these frequencies may be ascribed to two main causes:

1) they are formed by the mixing valve as differential frequencies of the harmonics already present in the grid A.C. voltages applied;
2) they are formed by the mixing valve as higher combination frequencies ($mf_1 \pm n f_2$) of the grid A.C. voltages, even when the latter are purely sinusoidal.

It is clear that to avoid the first effect it is sufficient when only one of the two grid A.C. voltages gives as few harmonics as possible. The second effect is combatted by making the grid voltage V_1 small with respect to the voltage V_2. Both conditions are realized by connecting a low-pass filter F_1 behind the oscillator G_1, see *fig. 3*. The harmonics of f_1 are here eliminated, and at the same time the signal is brought back to the desired low level, about 0.1 volt. Both conditions could of course

[4]) The fact that the fine regulation is obtained by increasing f_1 is contradictory to the principle developed that f must be increased by lowering the oscillator frequency. The rotating condenser in G_1 necessary for the fine regulation of f_1 is, however, much smaller than that in G_2, the shift in its capacity has therefore much less effect, while in this way it is made possible simply to add the readings of the two scales.

have been fulfilled without the filter, by only allowing the oscillator G_1 to oscillate with a very small amplitude, which also makes the distortion small. In that case, however, another cause of distortion would become evident, namely the reaction of the (very high) A.C. voltage V_2 on the oscillator G_1, *via* the capacity between the two control grids. Due to the intermediate filter, which also has an attenuating effect in the opposite direction, the reaction is now limited.

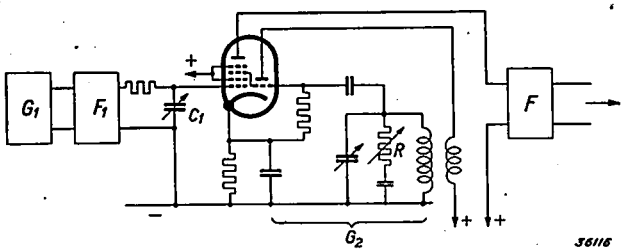

Fig. 3. A few details of the connections of the oscillators G_1, G_2 and of the mixing valve. The filter F_1 removes the harmonics from the signal given by G_1 and weakens it to the desired degree, at the same time preventing a reaction of G_2 on G_1. The condenser C_1 serves for any necessary regulation of the distortion and the output of the tone generator, the variable resistance R serves for a zero point correction of the frequency scale.

The last cell of the filter F_1 is indicated separately in fig. 3. It consists of a connection in series of a resistance and a condenser C_1. The voltage on the latter is the grid A.C. voltage V_1 applied to the mixing valve. The apparatus is now so arranged that the capacity of the condenser C_1 can if desired be slightly lowered, whereupon a larger fraction of the total voltage acts on the elements in series. V_1 then becomes larger and a higher output is obtained, or with a given loading resistance a higher output voltage. While the output of the tone generator usually amounts to somewhat more than 200 mW, it may in this way, if necessary for special measurements, be increased to 1 000 mW. Of course the distortion also increases from the normal value of 0.4 per cent to 1 to 2 per cent. Conversely, when the distortion of 0.4 per cent is still too high for the required purpose, the voltage V_1 can be reduced by increasing the capacity of C_1, and thus the distortion is reduced to a minimum of 0.25 per cent. The output of the tone generator then of course also falls to 100 mW. It would not in any case be possible to proceed in this way to reduce the output much farther, since the signal given by the mixing valve must be heard sufficiently high above the hum and noise level of the amplifier.

The amplifier V, which consists of three stages, works with a strong inverse feed-back, by which an amplification factor independent of the frequency is obtained. Since also the magnitude of the signal given by the mixing valve, as already stated, scarcely depends upon the frequency at all, the frequency characteristic of the tone generator is practically entirely flat (see *fig. 4*). Due to the inverse feed-back the distortion in the amplifier is also kept small. The average values of the final distortion have already been mentioned.

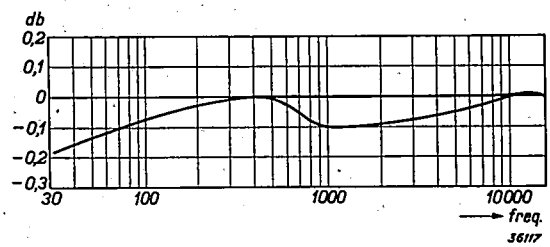

Fig. 4. Frequency characteristic of the tone generator.

The shift of the frequency

Several measures have already been mentioned above, which were intended to limit the shift of the frequency f as much as possible. We shall examine this point somewhat more closely. The main cause of a shift in the frequency is a variation of the temperature, particularly during the heating up after the tone generator has been switched on, which may take several hours before a constant temperature is reached. We may set the relative frequency change, which an oscillator undergoes with a temperature change t, proportional to t, and we call the proportionality factor the temperature coefficient a of the oscillator. In the case of the tone generator the change df of the desired frequency f is given by

$$df = df_1 - df_2,$$

thus

$$df = f_1\, a_1\, t_1 - f_2\, a_2\, t_2, \quad \ldots \quad (2)$$

where a_1, t_1 and a_2, t_2 are the temperature coefficients and the temperature variations of the two oscillators with the frequencies f_1 and f_2, respectively. In general a_1 and a_2 will differ by a certain amount Δa, and in the same way t_1 and t_2 by Δt. Equation (2) thus becomes

$$df = f_1\, a_1\, t_1 - (f_1 - f)(a_1 - \Delta a)(t_1 - \Delta t),$$

or when Δa and Δt are sufficiently small with respect to a and t:

$$df = f\, a_1\, t_1 + f_1\, (a_1\, \Delta t + t_1\, \Delta a) \quad \ldots \quad (3)$$

The first term of this expression signifies an absolute frequency variation which increases with the tone frequency f required. In order to limit this variation the temperature coefficient and the tem-

perature increase of the two oscillators will be made as small as possible. In *fig. 5*, a photograph of the tone generator opened, it is possible to see what measures have been taken to limit the rise in temperature of the oscillators. The supply apparatus section (transformer, rectifier, etc.) in which the most heat is developed is in a separate compartment in the upper half of the apparatus. The coils and condensers which determine the frequencies of the two oscillators are in the lower right and left-hand corners which remain relatively cool, due to the fact that a current of fresh air flows along the walls of the apparatus through the ventilation slits. In this way the temperature increase of the oscillators upon heating up is limited to about 6°. The temperature coefficients α_1 and α_2 amount to about 5×10^{-5} so that the first term of (3) causes a shift of $f \cdot 3 \times 10^{-4}$, *i.e.* at the highest frequencies about 5 c/s. Since the accuracy with which the frequency scales are calibrated and can be read is also limited, and in our case may involve an error of 100 c/s for instance at the highest frequencies (relative accuracy about 1 per cent), it would serve no useful purpose to reduce the shift in question still farther.

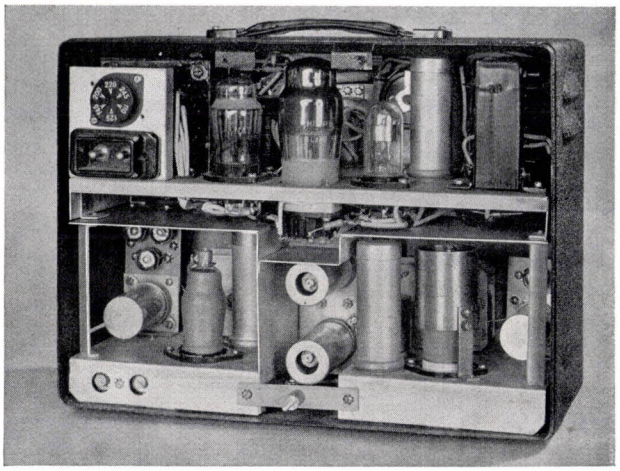

36125

Fig. 5. Position of the components in the tone generator GM 2 307; in the top compartment is the supply apparatus and the amplifier, to the right and left below, the coils and condensers of the oscillators.

The second term of equation (3) is more important. This term expresses an absolute frequency variation which is independent of the desired frequency f. Due to the large value of f_1 (100 000 c/s) the second term is comparable in magnitude with the first term, even at the highest tone frequencies f, and at the low frequencies only the second term is important. To keep this term sufficiently small it is obvious in the first place that f_1 may not be chosen indefinitely high, as was stated at the beginning of this article. Furthermore Δt and Δa should be made as small as possible, *i.e.* the two oscillators should be made to vary in the same way as far as possible. Δt is actually made very small by the symmetrical position in the cabinet [5]) (see fig. 5). In this way the final result is such that within the first 15 min after being switched on the frequency does not shift more than 9 c/s, see *fig. 6*; in the succeeding hour it shifts about another 8 c/s, and in the final state, which is reached after several hours, the total frequency variation is about 20 c/s.

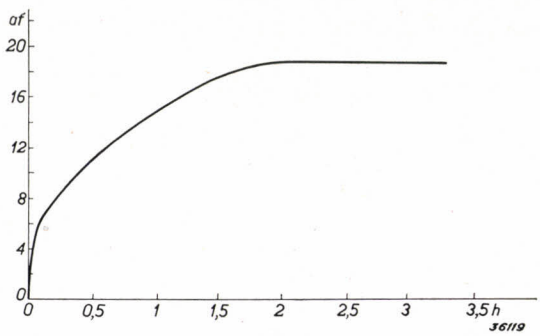

Fig. 6. The shift in frequency of the tone generator during heating up. df in c/s is plotted as a function of the time elapsed since switching on.

In order always to be able to make the calibration of the frequency scales agree with the frequencies actually obtained in spite of the shift (and any possible frequency variations upon fluctuations in the temperature of the surroundings), another small constant condenser, with an adjustable resistance R in series with it, is connected in parallel with the rotating condenser of the oscillator G_2, see fig. 3. By varying R the small condenser is made to contribute more or less to the total capacity, and in this way the frequency f_2 is slightly affected. If the two rotating condensers are set at the zero position of their frequency scales, then by means of this fine regulation f_2 can be made exactly equal to f_1, and thus $f = 0$ exactly. The equality of f_2 and f_1 is ascertained by means of a cathode ray indicator which works in the same way as the optical tuning indicator in radio receiving sets. The first stage of the amplifier consists of an amplifier valve EFM 1. This valve contains, in addition to the electrode system of an ordinary pentode, a fluorescent screen *Fl* (see *fig. 7*), upon which part of the electron current emitted by the cathode impinges. In the path of these electrons there is an electrode *P*

[5]) It is also possible to give Δt and Δa different signs, and thereby to make the second term disappear entirely for a given temperature rise. For the rest of the temperature region, however, it is still desirable to make Δt and Δa small.

connected to the screen grid, which throws a "shadow" on the fluorescent screen, the size of which shadow depends upon the screen grid potential. This is influenced by the A.C. voltage on the control grid of the valve; at sufficiently low frequencies of the control grid voltage, *i.e.* when f_2 has been made equal to f_1 within a few c/s, the shadow on the fluorescent screen is seen to grow larger and smaller periodically. The resistance R is then adjusted so that the flicker becomes steadily slower and the shadow finally becomes stationary, which is a sharp criterion for the equality of f_2 and f_1.

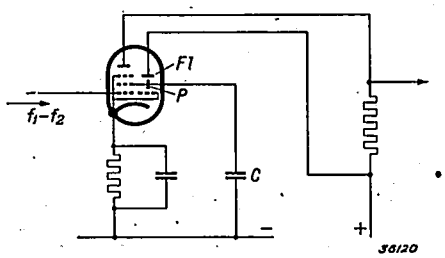

Fig. 7. Connections of the low-frequency pentode EFM 1 which is also arranged as cathode ray indicator. The zero point of the frequency scale is checked by this means.

At higher frequencies (>30 c/s) the screen grid potential may of course no longer increase and decrease with the control grid voltage, since at those frequencies the valve must act as a normal amplifier. A condenser is introduced for this purpose between screen grid and cathode, which forms practically a short circuit for the frequencies mentioned, so that the screen grid potential remains constant.

The shift in the amplitude of the output voltage

For recording frequency characteristics it is desirable that the signal given by the tone generator should remain constant not only in frequency but also in magnitude. The magnitude of the signal is, however, determined by the various plate voltages which may vary considerably due to fluctuations in the mains voltage supply. The temperature variations also during the heating up, etc. may manifest themselves in an undesired way in this respect, since the resistance of the windings of the supply transformer and therefore also the plate voltage hereby changes. In order to limit as far as possible the influence of plate voltage variations on the ouput of the tone generator, we have employed a compensation connection, the principle of which is given in *fig. 8*. The voltage E obtained from the supply apparatus feeds a neon tube L and a loading resistance R_b, which is formed by the mixing valve and the two amplifier valves of the tone generator. The voltage V indicated in the figure serves to supply the valve in the generator G_1 (see fig. 3). It may be seen that $V = V_0 - iR$,

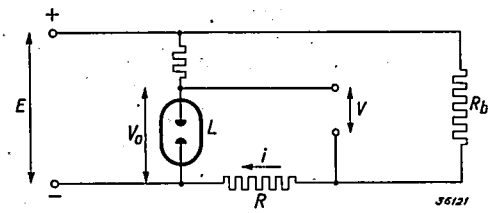

Fig. 8. Compensation connection for obtaining a constant output voltage of the tone generator. E, D.C. voltage given by the supply apparatus, R_b, loading resistance (mixing valve + two amplifier valves). L neon lamp, V plate voltage for the valve in the oscillator G_1 (fig. 3).

where V_0 is the voltage on the neon valve and i is mainly the current through the loading resistance R_b. When E increases, i will increase by the amount Δi; V_0, however, remains practically constant (it increases by the very small amount ΔV_0 for instance). Thus V varies with

$$\Delta V = \Delta V_0 - R \cdot \Delta i .$$

By choosing a suitable value for R, ΔV can be made more or less negative. Thus while the anode voltage of the three valves indicated by R_b rises with increase of E, that of the first valve falls, and it is clear that these two effects can be made to cancel each other exactly by a suitable choice of R, so that the output voltage of the tone generator as a first approximation is independent of the voltage E, and thus independent of the mains voltage and the temperature. The result thus obtained is reproduced in *fig. 9*. It may be seen that, with mains voltage fluctuations of 10 per cent, the signal of the tone generator only varies 1 per cent in intensity.

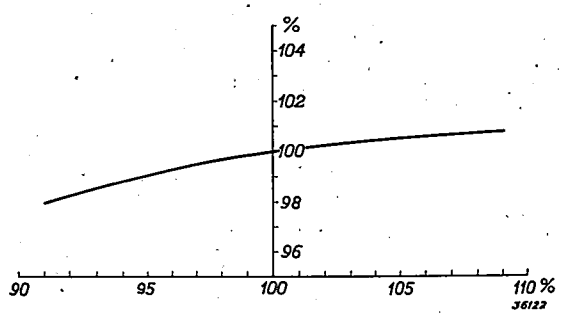

Fig. 9. Shift of the output voltage of the tone generator (vertical axis) upon variations of the mains voltage (horizontal axis).

The use of the tone generator

The voltages which are needed as input voltages in the investigation of different amplifiers may be

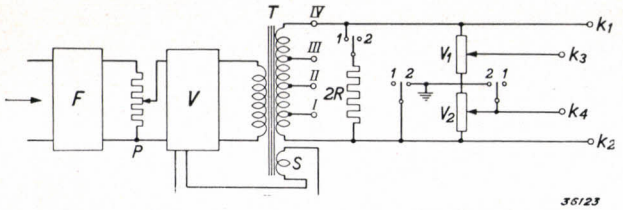

Fig. 10. Connections of the output of the tone generator. With the taps *I-IV* of the output transformer *T* the tone generator can be adapted to loading impedances of 1 000, 500, 250 and 5 ohms. *S* is the winding for inverse feed-back. With the potentiometer *P*, which is calibrated directly in volts for the tap *IV*, the intensity of the signal is regulated. On tap *IV* an attenuator V_1, V_2 can be connected (this case is shown in the figure). At position *1* of the three switches (operated by a single knob) the two equal attenuators V_1 and V_2 are in series, and a balanced voltage which can be regulated in steps of 10 dB is obtained between the terminals k_3 and k_4. At position *2* of the switches V_2 is out of connection and k_4 earthed, so that an unbalanced voltage is obtained. Due to the fact that in position *1* the resistance $2R$ (R is the resistance of one attenuator) is connected in parallel with $V_1 + V_2$, the output transformer is loaded with the same resistance (R) in both positions, so that the voltage which can be measured between k_1 and k_2 remains exactly the same.

very different. Therefore in the tone generator the filtered output voltage of the mixing valve is applied to the amplifier *via* a potentiometer (*fig. 10*). With this potentiometer, which because of its flat frequency characteristic and the slightness of the influence of mains voltage variations, etc., could be calibrated directly in volts, it is possible to set the output voltage given by the tone generator at the desired value. The calibration is valid for adaptation to a loading impedance of 1 000 ohms, the maximum voltage is normally 15 volts in this case. In order to be able to adapt the tone generator approximately to the object being investigated, in the testing of loud speakers, cables, etc., the output transformer is provided with taps for loading impedances of 1 000, 500, 250 and 5 ohms, respectively. The transformer is so constructed that even when the taps are used the frequency characteristic of the tone generator remains practically flat. Furthermore by means of a simple commutation an attenuator can be connected to the output transformer, and with this the signal can be weakened in steps of 10 dB. The attenuator is so constructed that not only a balanced voltage can be obtained for the investigation of push-pull amplifiers, but also an unbalanced voltage, earthed at one side. This is explained in the text under fig. 10. *Fig. 11* is a photograph of the tone generator in which the different knobs for operation of the potentiometer, the attenuator, etc. may be seen.

If higher voltages than 15 volts are needed, as for instance for measuring the deformation of large amplifier valves at full load, or for the investigation of transmitter valves which are used as modulator, the voltage may be taken from the primary winding of the transformer. About 50 volts are then available. By increasing in the manner described (with the condenser G_1, see fig. 3) the output of the tone generator still more at the expense of somewhat greater distortion, a voltage of 125 volts can even be obtained here.

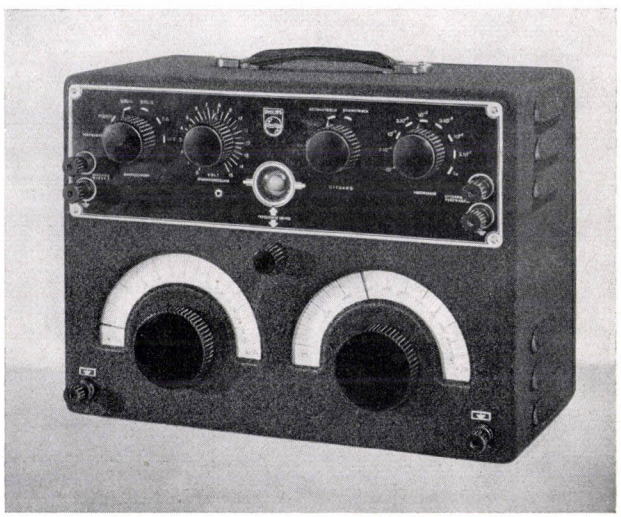

Fig. 11. The tone generator GM 2 307. On the front panel may be seen the knobs of the rotating condensers (below) with the frequency scales from 0 to 1 000 and from 0 to 15 000 c/s. Above in the middle the cathode ray indicator, to the right and left the knobs of potentiometer, attenuator, etc.

SUBJECTIVE PHOTOMETRY

by J. VOOGD.

535.24

Although it is possible at the present time to carry out the measurements in light technology by an objective physical method, subjective photometry still has very great practical importance. On the basis of investigations carried out in this laboratory an attempt is made to discover which subjective method of measurement offers the best guarantee of obtaining correct results in the measurement of gas-discharge lamps. The use of the filter method is recommended with the flicker photometer and a calculated filter transmission. The filter must be so chosen that the spectral composition (not the colour!) of the filtered light of the comparison lamp corresponds as closely as possible to that of the lamp to be measured, while a group of persons must be chosen as observers at the flicker photometer, such that the average curve of eye sensitivity is well matched with the international eye-sensitivity curve (yellow: blue ratio 0.985).

Due to the development of gas-discharge lamps interest in photometry has increased very much [1]). It was found that the results of measurements obtained by visual photometry of these coloured light sources were dependent on the method of measurement used. This fact led, on the one hand, to a new investigation of the basis of visual photometry, while on the other hand it led to attempts to develop objective methods in addition to the visual methods for the determination of the light flux or light intensity of a lamp.

In a previous article in this periodical [2]) an accurate physical photometer was described, which was constructed in this laboratory, and which has since then been found to be absolutely reliable in practical use. In many laboratories, however, the use of an accurate objective photometer has not yet been adopted. The problems of visual or subjective photometry have therefore retained a practical significance in addition to a theoretical one.

In this article we shall deal with the question which visual method of measurement offers the best guarantee of obtaining correct results. We shall in doing this make use of data which have been obtained in this laboratory during recent years.

The foundation of the subjective photometry of coloured light sources (heterochromous photometry) was laid about 30 years ago, mainly by the work of the American Ives. Ives stated that a useful system for heterochromous photometry must satisfy the following laws:

1) the transitive law:
   If $a = b$ and $b = c$, then $a = c$;
2) the additive law:
   If $a = b$, then $a + c = b + c$.

From the investigations carried out by Ives in the first stages of heterochromous photometry, it follows that the results of measurements of every individual observer obey both laws when the work is done under certain photometric conditions. These wellknown conditions of Ives are the following:

1) the field of the photometer must be observed within an angle of 2°,
2) the brightness of the field must amount to about 8×10^{-4} stilb.

If these conditions are fulfilled, it is then, according to Ives, a matter of indifference whether a photometer with adjustment to equal brightness or a flicker photometer is used.

Thanks to the validity of the additive law, under the conditions mentioned above every wave-length interval in the spectrum of the radiation emitted gives a contribution ot the total brightness which is proportional to the intensity of the radiation in that wave-length interval and to a factor which depends upon the wave length, and which is called the relative eye-sensitivity. Different investigators have determined the eye-sensitivity as a function of the wave length for a number of observers. On the basis of the individual eye-sensitivity curves thus collected, which are mutually quite divergent, an attempt was made in 1924 to determine a curve which might be considered as the average curve of human eye-sensitivity. This curve, known as the international eye-sensitivity curve, has since then become of fundamental significance in heterochromous photometry.

By basing heterochromous photometry upon the international eye-sensitivity curve, and also by the acceptance of the new light unit, the photometric units have obtained physical definition. In order to measure the light intensity K of a light source, the following relation must be determined:

$$K = \frac{\int E_1(\lambda)\ V(\lambda)\ \mathrm{d}\lambda}{\int E_2(\lambda)\ V(\lambda)\ \mathrm{d}\lambda} \quad \ldots \quad (1)$$

[1]) The photometry of metal vapour lamps, Philips techn. Rev. 1, 120, 1936; The new unit of light intensity, Philips techn. Rev. 5, 1, 1940.

[2]) Physical Photometry, Philips techn. Rev. 4, 272, 1939.

In this expression $E_1(\lambda)$ is the spectral intensity of the light source to be measured, $E_2(\lambda)$ that of the light source introduced as unit at the wave length λ, and $V(\lambda)$ the international eye-sensitivity at the wave length λ. The integration must be performed over the whole visible spectrum.

Present investigations on the subject of practical visual photometry are for the purpose of finding a method which gives results in agreement with this physical definition. The difficulties thereby experienced are caused by the fact that in the light of later experience it must be doubted whether the foundation of subjective photometry as developed by Ives holds with sufficient accuracy.

Several experiments

When Ives' conditions are satisfied the results of measurement by one observer should be the same when a flicker photometer is used as when a photometer with adjustment to equal brightness is used. This has been tested precisely for several cases.

The light intensity of a gas-discharge lamp was compared with that of a standard lamp whose light had passed through a filter. This filter was so chosen that the colour of the comparison lamp seen through the filter was well matched with that of the gas-discharge lamp. Upon adjustment to equal brightness the accuracy of measurement was not disturbed by the presence of too great a colour difference on the photometer field.

As gas-discharge lamps, a mercury-vapour lamp (HO 1 000) and a sodium lamp (SO 400) were used. In addition the mercury-vapour lamp was also measured through a filter which transmits only the strong green line. For each of these three cases a suitable colour-matching filter was found for the standard lamp. The comparison of the light intensity of the gas-discharge lamp with that of the combination of comparison lamp and colour-matching filter was carried out with different photometers. In the first place we used the Lummer-Brodhun photometers from which the contrast plates had been removed. The field of vison of the photometer is shown in *fig. 1a*. Measurements were also done with the Bechstein photometer with adjustment to equal brightness (also without contrast plates), whose field is shown in fig. 1*b*. Measurements were finally done with a flicker photometer. In all the measurements the area and brightness of the field of vision satisfied Ives' conditions.

From the measurements for one gas-discharge lamp done by one observer we obtained by means of the three photometers, three values of the candle power: K_{LB}, K_B and K_f. These three values should be equal, except for a slight difference due to errors in measurement. In order to indicate to what degree this is true we have used the ratios K_{LB}/K_f and K_B/K_f.

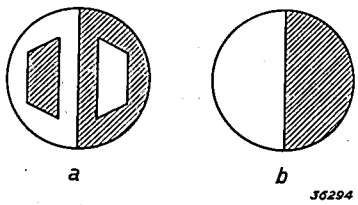

Fig. 1. a) The field of vision of a Lummer-Brodhun photometer.
b) The field of vision of an equal brightness photometer according to Bechstein.
The cross-hatched and non-cross-hatched portions must be adjusted to equal brightness.

In *table I* these ratios are given for each gas-discharge lamp as determined by different observers.

Table I

Observer	Light source					
	Mercury lamp		Mercury lamp through green filter		Sodium lamp	
	K_{LB}/K_F	K_B/K_F	K_{LB}/K_F	K_B/K_F	K_{LB}/K_F	K_B/K_F
I	1.03	1.00	1.03	0.96	0.99	1.00
II	1.08	1.03	1.03	0.94	1.00	1.01
III	1.05	1.04	1.02	0.98	0.97	1.00
IV	0.99	1.01	1.05	0.97	0.98	0.98
V	1.07	1.02	1.00	0.94	0.99	1.00
VI	1.01	0.98	0.93	0.95	0.97	0.98
VII	1.05	0.99	1.03	0.97	1.02	0.98
VIII	1.04	1.02	—	—	—	—
IX	1.02	1.02	1.06	0.98	0.96	1.02
Average	1.04	1.01	1.02	0.96	0.98[5]	0.99[5]

In spite of the differences between the individual observers it may be stated that the ratios K_{LB}/K_F and K_B/K_F differ in some cases systematically from the value 1.00. The most favourable case is that of the sodium lamp, where the results agree quite well for the three photometers. In the case of the mercury lamp the lowest light intensity is measured with the flicker photometer; the light intensity measured with the Bechstein photometer corresponds fairly well with this. With the Lummer-Brodhun photometer, on the other hand, it is clear that a higher light intensity is found.

The situation is still different for the mercury lamp seen through a green filter. According to the flicker photometer the candle power here is 2 per cent lower than according to the Lummer-Brodhun photometer, and 4 per cent higher than according to the Bechstein photometer.

In judging these differences it may be noted that it was to have been expected that differences would occur between the measuring results obtained with the flicker photometer and those obtained with the photometer with adjustment to equal brightness. The criteria of adjustment are of quite different character in these cases. It is remarkable, however, that the two photometers with adjustment to equal brightness should exhibit systematic mutual differences. We have not been able to accertain the cause of this. It is probably significant here that the colour matching, no matter how good it is, can never be perfect. The slight remaining colour difference has a different effect upon the adjustment with the Lummer-Brodhun photometer than on that of the Bechstein photometer. With the Bechstein photometer the colour difference is more clearly observed and the observer remains conscious of the fact that he is adjusting different coloured halves of the photometer field to equal brightness. With the Lummer-Brodhun photometer, on the other hand, this slight colour difference is scarcely noticed during the adjustment. This is probably due to the greater subdivision of the field of vision of this photometer.

From the above described experiments it is found in any case that divergent results can be obtained under Ives' conditions in photometry with different photometers. The question therefore arises as to whether the transitive and additive laws are valid in the measurement with each of these photometers, and if this is true, whether different eye-sensitivity curves are obtained for a single observer with different photometers. Similar difficulties have been encountered in other laboratories. The investigations on this subject are by no means complete. The fact that there is uncertainty in this respect, however, necessitates great care in the application of visual photometry for the determination of the physically defined photometric quantities.

Which photometric method offers the best guarantee of a correct and accurate result?

As we have seen in the foregoing, fulfilment of Ives' conditions offers no sufficient guarantee that the transitive and additive laws are valid. Nevertheless, the validity of these laws must be considered a primary requirement for obtaining correct results by means of a photometric arrangement.

Photometry with adjustment to equal brightness has the great disadvantage that reproducible measurements are practically impossible when there is an appreciable colour difference. Therefore it is extremely difficult to control the validity of the transitive and additive laws directly in measurement with such a photometer. But even if it were possible to assume that the transitive and additive laws are valid, there still remains the question of whether the eye-sensitivity curve of the observer corresponds sufficiently well with the international eye-sensitivity curve. This also can only be controlled by a time-consuming and essentially inaccurate investigation.

In both respects the flicker photometer offers great advantages. Since one can use this photometer even in the presence of large colour differences, a direct control of the transitive and additive laws is immediately possible As far as our experience goes these laws are found to be satisfied exactly. For the same reason it is quite easy to obtain information about the eye-sensitivity curve of an observer. It is possible to form in this way a group of observers whose average more or less agrees with the international eye-sensitivity curve.

A simple method of doing this has already been worked out by Ives and Kingsbury. They give a method of preparing two different coloured light sources (a blue and a yellow one) which must have exactly the same intensity for an observer with a normal eye-sensitivity curve [3]). If an individual observer is allowed to determine the ratio of the light intensities (yellow: blue) with the help of a flicker photometer, he will in general find a result which differs from 1.00. If, however, a number of observers is chosen so that the average yellow-blue ratio of the whole group is exactly equal to 1.00, then according to Ives and Kingsbury the average shape of the eye-sensitivity curve of all the observers may be considered as normal. Later measurements have changed this value somewhat. In order to obtain the best agreement with the international eye-sensitivity curve the average yellow-blue ratio of the group of observers must not be exactly equal to unity but to 0.984 [4]).

[3]) The coloured light sources are composed of a carbon filament lamp and a coloured filter. The carbon filament lamp must burn at a colour temperature of 2077° K. The yellow filter consists of a solution of 72 grams of potassium bichromate per litre of solution; the blue filter of a solution of 57 grams of copper sulphate per litre of solution. Both filters are used in cuvettes with an internal thickness of 1 cm.

[4]) It cannot yet be concluded how accurately the average eye-sensitivity curve of a group of observers formed in this way agrees with the international eye-sensitivity curve. In addition to accidental deviations which are determined by the choice of the observers, systematic deviations are not held impossible. Various investigators are now working on this question. From the result of these investigations will depend whether the method of direct flicker photometric comparison of the gas-discharge lamp with the standard lamp presents the possibility of obtaining correct results.

It is now important to know to what degree the result of measurement by an observer can be determined by the yellow : blue ratio. For this purpose the candle power of a mercury lamp was compared with that of a gas-filled incandescent lamp by a number of observers with a known yellow : blue ratio. From the individual results for the candle power ratio the average for the group of observers was formed. The deviation of the individual results from this average is plotted in *fig. 2* as a function

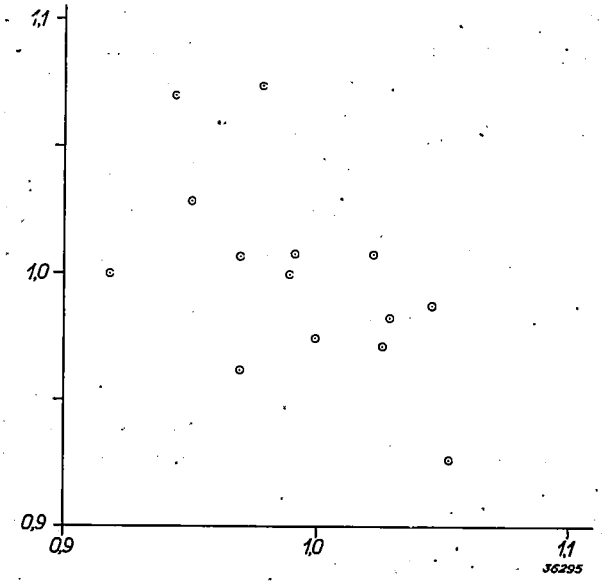

Fig. 2. For each of a number of observers the ratio measured by him between the intensities of a mercury lamp and a gas-filled incandescent lamp is plotted as ordinate, while as abscissa the value is plotted of his "yellow-blue" ratio. The average value of the ordinate for the whole group is set equal to 1.00.

of the yellow : blue ratio. The points obtained show indeed a general tendency, but it is evident that fairly divergent values of the candle power of the mercury lamp can be measured by different observers having the same value of the yellow : blue ratio. This is to be ascribed to the fact that the eye-sensitivity curves of different observers may be of relatively strongly diverging shapes, even when the yellow : blue ratio is the same. It is thus possible for example that the maximum should lie at the correct wave-length of 5 550 Å, but that the curve falls too rapidly or too slowly toward the red or blue. In comparing a gas-discharge lamp with an ordinary incandescent lamp, where the spectral energy distributions of the light curves to be compared are very different, such differences may be very significant.

In order to combat this source of uncertainty the obvious method would be to match the spectral energy distribution of the comparison lamp by means of a filter to that of the gas-discharge lamp to be measured. If it were possible to make the spectral distributions of the two light sources exactly the same, it would then be a matter of indifference, as far as the photometric adjustment is concerned, what the shape of the eye-sensitivity curve of the observer was. In practice only a relatively rough matching of the spectral energy distribution of an incandescent lamp to that of a gas-discharge lamp can be obtained with a filter. It is found nevertheless that by this rough matching the possible difference between the adjustments of different observers with the same yellow : blue ratio can be considerably reduced, as may be seen when *fig. 3* is compared with fig. 2. The possible difference between the average adjustment of a group of observers with an average yellow : blue ratio of 0.985 and the adjustment according to the international eye-sensitivity curve is obviously also decreased at the same time.

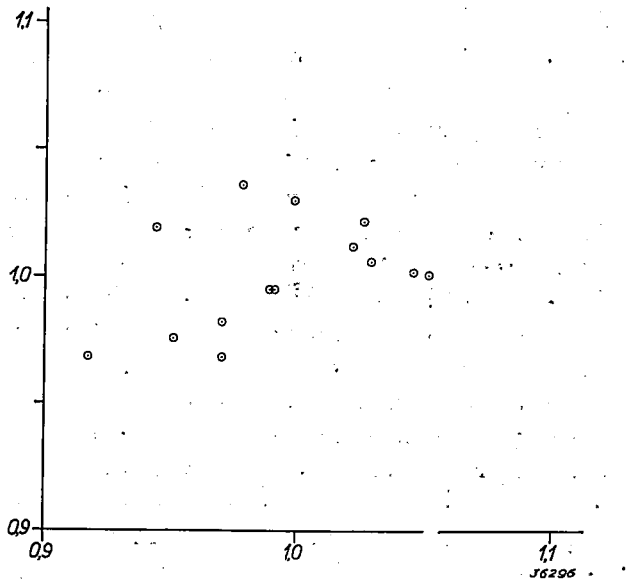

Fig. 3. Same as fig. 2 for the case where the spectral energy distribution of the comparison lamp is adapted to that of the mercury lamp by means of a filter which transmits only the wave length region from 5 300 Å to 5 900 Å. The intensity ratios measured by the different observers between the mercury lamp and the comparison lamp are now much less divergent.

If one now attempts to apply this concept in practice, one arrives at the so-called filter method in which the determination of the intensity of a gas-discharge lamp takes place in two stages. In the first stage the ratio K_g/K_f is determined between the candle power of the gas-discharge lamp and the candle power of the filtered comparison lamp in the second stage the ratio K_f/K_0 between the intensities of the filtered and the non-filtered light of the comparison lamp. The required candle power of the gas-discharge lamp is then obviously:

$$K_g = \left(\frac{K_g}{K_f}\right)\left(\frac{K_f}{K_0}\right) K_0.$$

The first factor can, as stated above, be measured with sufficient accuracy with the flicker photometer, if the observers are so chosen that the average yellow-blue ratio has a value of 0.985. The second factor, the transmission of the filter could not, however, be determined accurately enough by this method, since the spectral composition of the filtered and the non-filtered radiation of the electric lamp differ too widely from each other. It is therefore better to measure the transmission of the filter objectively. This can for example be done by measuring the spectral transmission of the filter and calculating from this with the help of the known intensity distribution of the comparison lamp and of the international eye-sensitivity curve the visual transmission τ. This amounts to

$$\tau = \frac{\int E(\lambda)\ \tau(\lambda)\ V(\lambda)\,\mathrm{d}\lambda}{\int E(\lambda)\ V(\lambda)\ \mathrm{d}\lambda}.$$

where $E(\lambda)\mathrm{d}\lambda$ is the intensity of the comparison lamp in the wave length interval $\lambda \to \lambda + \mathrm{d}\lambda$, $\tau(\lambda)$ the spectral transmission and $V(\lambda)$ the relative eye-sensitivity. If an objective photometer is available the quantity τ can of course be determined by direct measurement.

We thus reach the conclusion that for visual photometry the best method is the filter method with objectively determined filter transmission and use of a flicker photometer for the comparsion of the gas-discharge lamp with the filtered light of the standard lamp. This method of measurement has been tested in this laboratory by comparing its results with those given by the previously described objective photometer in the same measurements. From the results we may conclude that the systematic errors of this method in the case of mercury and sodium lamps are not greater than 1 per cent.

Appendix

The use of the flicker photometer for gas-discharge lamps burning on alternating current

Until now we have tacitly assumed that the intensity of the lamp being measured is constant during the measurement. In the case of gas-discharge lamps, however, this is generally not the case; such lamps are usually operated with alternating current, and the light intensity in the first approximation exhibits the same variation as the absolute value of the current. If one looks at the lamp or at a surface brightly illuminated by the lamp the flicker can scarcely be seen, since the eye cannot follow the rapid light changes. If, however, the lamp is measured with a flicker photometer, these fluctuations lead to stroboscopic effects which make the adjustment of the photometer difficult, and, moreover, cause doubt as to whether or not the adjustment is indeed correct, *i.e.* whether it indicates the average value of the light flux to be measured.

For this reason the flicker photometer is often replaced by a photometer with adjustment to equal brightness for the measurement of A.C. lamps, in spite of the difficulties which we have outlined above. If the matching of the spectral composition of the light of the comparison lamp to that of the lamp to be measured were perfect, there would be no objection to this, since in the measurement of identical light sources the adjustment is independent of the photometric method used. In practice, however, due to the limited choice of types of filters, the matching is far from perfect, and due to this, photometry with the equal brightness photometer has still other objections in addition to the uncertainties explained above.

The limited choice of filter types particularly has the result that the filtered light with the best spectral matching which can be attained differs considerably in colour from the lamp to be measured, which is decidedly not permissible with an equal brightness photometer. Thanks to the fact that two lights with the same colour by no means need have the same spectral composition, it is nevertheless still possible to find a filter which gives a practically perfect colour matching; this filter will, however, in general by no means lead to the best possible matching in the spectral energy distribution.

An example of this is encountered with the mercury lamp. The blue and violet radiation of this lamp contribute almost nothing to the light flux, but they affect the colour very strongly. The colour adaptation of the comparison lamp can best be realized with the help of filters which absorb in the red. The filtered light then contains considerable blue-green in contrast to the mercury light. From the point of view of adaptation of the spectral energy distribution, it is better to neglect the blue and violet radiation of the mercury lamp and to choose a filter which gives only an adaptation to the green and yellow mercury lines, by transmitting the light between 5 300 Å and 5 900 Å, for example. Such a filter could not be used with a photometer for adjustment to equal brightness. When the filter method is used with the flicker photometer, such a filter can nevertheless be employed.

The requirement of a very close colour adaptation for the adjustment to equal brightness has, moreover, another practical disadvantage. In practice lamps are often encountered whose spectral energy distribution varies relatively little. while the colour is clearly different. For all these types of lamps different filters would have to be used. If a flicker photometer is used fewer filters are needed.

Summarizing, we may therefore say that the use of a photometer with adjustment to equal brightness has three disadvantages. In the first place the result depends upon the type of photometer used; in the second place it is often necessary to make the adaptation of the spectral energy distribution of the comparison lamp to that of the gas-discharge lamp poorer than when it is unnecessary to consider the colour adaptation, so that the result becomes more dependent on the individual eye-sensitivity curve of the observer. In the third place, for the same number of types of lamps to be measured a larger number of filters is needed. Over against these disadvantages is the advantage that the light fluctuations of gas-discharge lamps operated with alternating current are not disturbing.

In order to ascertain whether this advantage is of decisive importance, the reproducibility was investigates in the measurement of different gas-discharge lamps operating on alter-

nating current according to the filter method with a photometer for equal brightness and with the flicker photometer. It was found that the adjustment of the flicker photometer was just as reproducible as that of the equal brightness photometer in spite of the apparance of beats. Moreover, it could be determined in a different way that with the flicker photometer the true average value of the light intensity of the lamp was actually found within the limits of error of the measurement. We therefore conclude that the objections to the photometry of alternating current lamps with the flicker photometer are without foundation.

ABSTRACTS OF RECENT SCIENTIFIC PUBLICATIONS OF THE N.V. PHILIPS' GLOEILAMPENFABRIEKEN

1494: J. H. de Boer and J. D. Fast: Electrolysis of solid solutions of oxygen in metallic zirconium (Rec. trav. chim. Pays-Bas **59**, 161-167, Febr. 1940).

The lattice constants and the density of zirconium are determined with varying amounts of dissolved oxygen. According to the results the oxygen atoms are situated in the interstices of the zirconium lattice. At high temperature they possess a great mobility in the lattice. Under the influence of an electric field the oxygen moves through the lattice as a negative ion, so that the oxygen concentration (and thereby also the electrical resistance) increases at the anode end and decreases at the cathode end.

1495*: M. J. O. Strutt: Modern multigrid electronic valves. Construction, Functioning, Properties, Electrophysical Foundations. Second enlarged and improved edition, Springer, Berlin 1940, 283 pages. (German language).

A review of the first edition was given under **1279*** and **1350***. The second edition also takes into account the newest types of valves developed since the publication of the first edition.

1496: A. Bouwers: On the behaviour of slow neutrons in water and paraffine (Physica **7**, 193-198, Mar. 1940).

The yield from a powerful source of neutrons can be measured in a simple way with the help of a very thin detector for slow neutrons, which is placed in a substance rich in hydrogen surrounding the source. Two quantities are discussed which are important for the interpretation of the experiments: the average length of trajectory δ of a neutron in this thin detector, and the average number of collisions before the neutron is captured. In the case of the number of collisions, the reflection coefficient (albedo) of a smooth limiting plane plays a part; the value of this coefficient could be determined by elementary considerations.

1497: W. de Groot and K. F. Niessen: Note on the "albedo" of a hydrogenated substance for slow moving neutrons (Physica **7**, 199-204, Mar. 1940).

O. Halpern, R. Lüneberg and O. Clark (Phys. Rev. **53**, 173, 1938) have given for the reflection coefficient β of a hydrogenated substance for slow moving neutrons, the so-called albedo, the formula: $\beta = 1 - 2.31/\sqrt{N}$, where N is the average number of collisions which a neutron undergoes before its capture. By a process of estimation of the second term, this formula is extended to:

$$\beta = 1 - 2.31/\sqrt{N} + 2.86/N.$$

1498: N. Warmoltz: Some properties of an anchored cathode spot of a mercury arc at low pressure (Physica **7**, 209-216, Mar. 1940).

The cathode spot of a mercury arc, which generally executes a dancing motion on the surface of the mercury, can be anchored by immersing in the pool of mercury a metal electrode (the "anchor"). For different forms of anchor the velocity of evaporation of the mercury is determined, and it is ascertained how the maximum current, at which the cathode spot still remains on the anchor, depends upon the temperature. The experiments confirm the impression that it is very important for the anchorage that the anchor should be wetted by the mercury.

---

*) An adequate number of reprints for the purpose of distribution is not available of those publications marked with an asterisk. Reprints of other publications may be obtained on application to the Natuurkundig Laboratorium, N.V. Philips' Gloeilampenfabrieken, Eindhoven (Holland), Kastanjelaan.

1499: J. A. M. van Liempt and J. A. de Vriend: A new method for adjusting synchronizers, also suitable for testing focal-plane shutters (Physica 7, 217-224, Mar. 1940).

A new method is described for the adjustment of the synchronizer necessary for the simultaneous operation of shutter and flash lamp. As measuring instrument a falling plate oscillograph is used, whereas in the apparatus previously described a cathode ray oscillograph had to be used. Additional advantages of the new apparatus are that it can be calibrated without wasting flash lamps, and that it can also be used in testing focal-plane shutters.

1500: J. A. M. van Liempt and J. A. de Vriend: A clarification of the conception of certain quantities in light technology with reference to photo-flash lamps (Physica 7, 255-264, Mar. 1940) (Original in German).

A survey is given of the commonly used constants for photo-flash lamps, such as the total flash time, practical flash time, 50% flash time, median time, median light intensity and photographic lumens-second. The existing definitions of these quantities are criticized and partially replaced by new definitions which are better adapted to practical use.

1501: J. F. Schouten: The residue, a new component in subjective sound analysis (Proc. Kon. Akad. Wet. A'dam 43, 356-365, Mar. 1940).

It has long been known, that when the ear picks up a series of harmonic tones in which only the fundamental is missing, an impression is received as if this fundamental were present in the sound observed, and even as if it were fairly intense. Previous experiments have convinced the author that this "missing" fundamental is not observed because, as is often assumed, of non-linear deformation in the ear. From the experiments here described, which are a repetition with the optical syren of experiments done by Seebeck nearly 100 years ago, it becomes reasonable to assume that the colaboration of those higher harmonics which are no longer observed individually by the ear (above the twelfth, for instance), and which the author proposes to call the "residue", is the cause of the observation of the "missing" fundamental. This concept makes necessary a modification of Ohm's acoustic law, which was suspected by Seebeck, but not clearly expressed by him. Besides the fact that it gives a very acceptable explanation of the fine experiments of Seebeck which were repeated, the theory of the residue is found to be of use in other acoustic problems also, several of which the writer promises to deal with in the future.

1502*: F. A. Heyn: De wisselwerking tusschen neutronen en materie (II) (The reaction between neutrons and matter) (Ned. T. Natuurk. 7, 107-123, Feb. 1940).

The main subject of part I was the reaction between fast electrons and matter. In this communication (II) the reaction is discussed between matter and slow neutrons which is of great importance due to the appearance of the resonance of atomic nuclei. Following several theoretical remarks about the effective diameter of the atomic nucleus for the capture of a slow neutron, in which it is shown that for all nuclei there is a region in which the diameter is inversely proportional to the speed of the neutron, methods are indicated of obtaining low-speed neutrons (with a velocity of the order of thermal velocity). With the help of these, resonance levels have been determined which are summarized in a table. The width of these levels, which has been determined in certain cases, is discussed, as well as their Doppler broadening. A table is given summarizing the effective diameters for capture and scattering of slow neutrons. In connection with this several observations are given on the scattering power of matter which cannot be explained from the scattering power of the atomic nuclei alone.

1503: J. L. Snoek: Over de inwendige demping van vaste stoffen (On the internal damping of solid substances). (Ned. T. Natuurk. 7, 133-146. Mar. 1940).

Several quantities which are measured of the internal friction in solid substance are defined and their mutual relations considered. An important cause of the internal friction is the local heat currents in the material, *i.e.* the so-called thermo-elastic effect. In many cases this is almost exclusively responsible for the damping observed. These heat currents may extend over relatively great distances (for instance, the thickness of transversally vibrating rods) or over much smaller distances (for instance, the distance between two adjacent crystallites). In all cases the losses are at a maximum at a frequency $\nu_k = cDa^{-2}$, where c is a constant of the order of magnitude 1, D the heat diffusion constant (coefficient of heat conductivity) and a the average distance between regions of opposite temperature fluctuation (for transversally vibrating rods this is the diameter of the rod, for longitudinally vibrating rods an estimation can be made in another way).

VOL. 5 No. 10 OCTOBER 1940

Philips Technical Review

DEALING WITH TECHNICAL PROBLEMS
RELATING TO THE PRODUCTS, PROCESSES AND INVESTIGATIONS OF
N.V. PHILIPS' GLOEILAMPENFABRIEKEN

EDITED BY THE RESEARCH LABORATORY OF N.V. PHILIPS' GLOEILAMPENFABRIEKEN, EINDHOVEN, HOLLAND

A CATHODE RAY OSCILLOGRAPH FOR USE IN TOOL MAKING

by S. L. de BRUIN and C. DORSMAN. 621.317.755 : 621-752

The cathode ray oscillograph is not only suitable for recording rapidly alternating electrical quantities, but it may also be used for the investigation of mechanical vibration phenomena. Since the frequencies of the mechanical phenomena to be investigated are usually considerably lower than those of electrical vibrations it was found desirable to develop a special oscillograph for this purpose, whose amplifier and time-axis deflection are so constructed that the frequency of a phenomenon, varying in any desired way, may fall to about 1 c/s., without the oscillogram being distorted to any serious extent. — In this article the cathode ray oscillograph GM 3 156 is described, which has been constructed on this basis. After a description of the amplifier and the time-axis generator several applications are dealt with.

An oscillograph is an instrument which serves to make visible or to record rapidly varying phenomena. Since electrical voltage variations must be supplied to the ordinary oscillograph, the latter was originally constructed almost exclusively from the point of view of measuring electrical phenomena. It was only gradually that auxiliary apparatus was developed to convert [1]) rapidly occurring mechanical phenomena into electrical phenomena, so that the oscillograph can now be used to an increasing extent in tool making also.

If one compares the applications of the oscillograph in tool making with those in electrotechnology, great differences will be found, especially with regard to the highest and the lowest frequencies of the phenomena to be investigated. In high-frequency technology one is often concerned with waves of a few metres in length, *i.e.* of vibration times of the order of 10^{-8} sec. Times of this order of magnitude also play a part in the non-periodic voltage and current changes which occur for example due to breakdown or to sparking upon breaking a contact [2]). In tool making, on the other hand, there is not the slightest necessity of reproducing such rapidly occurring phenomena. The mechanical vibrations of foundations, etc. are usually caused by rotating machines, and in such cases rotation frequencies of 3 000 r.p.m., *i.e.* 50 c/s. may already be considered high. If one is concerned with impact phenomena, the vibrations caused by the impact are determined by the mechanical resonance frequencies of the structural components, and these practically always lie within the acoustic region, *i.e.* not higher than a few thousand c/s.

Such a difference between electrical and mechanical problems is encountered at the lower limit of the frequency region which must be able to be covered in the reproduction. Alternating current technology generally works with a frequency of 50 c/s., lower frequencies seldom occur. In tool making, however, rotating engines with 120 r.p.m. are quite common, *i.e.* machines which show a fundamental frequency of 2 c/s. For the reproduction of these low frequencies the previously described cathode ray oscillograph (GM 3 152) is unsuitable, so that the need was felt of developing a separate oscillograph for tool making.

The frequency region in which the new cathode ray oscillograph, GM 3 156, produces an undistorted image is adapted to mechanical uses. The lowest fundamental frequency in this region amounts to 0.5 to 2 c/s. (30 to 120 cycles per minute) according to the nature of the phenomena to be

[1]) On the subject of the conversion of mechanical voltages or vibrations into electrical voltages see Philips techn. Rev. 5, 26 and 241, 1940.

[2]) The electron beam of a cathode ray oscillograph is capable of following these rapid phenomena, but this is not true of the electrical apparatus of the oscillograph. In Philips techn. Rev. 4, 198, 1939 it is explained in detail what measures are taken in the amplifier of the cathode ray oscillograph GM 3 152 to obtain an undistorted reproduction up to as high frequencies as possible.

recorded, while the upper limiting frequency amounts to about 10 000 c/s. In the case of the oscillograph GM 3152 previously described, which is intended primarily for electrotechnical application, the lower limiting frequency was 10 c/s and the upper 10^6 c/s; both limiting frequencies are therefore much higher in that case.

In this article we shall discuss the results of the downward shift of the effective frequency region on the construction of the oscillograph. Several examples of applications will then be dealt with.

The amplifier

In order to make visible on the screen of a cathode ray tube the very small A.C. voltages which are obtained upon the conversion of alternating mechanical quantities into electrical voltages, an amplifier with two stages is used. The input voltage of the second stage of this amplifier comes from the anode current alternations of the first stage. When an attempt is made to adapt such an amplifier to the amplification of very low frequencies, the difficulty is encountered that the slow, but sometimes quite considerable variations in the anode current, which are caused by fluctuations in the mains voltage when the amplifier is fed from the mains, are also transmitted to the following stage and lead to a distortion of the oscillogram. This difficulty can, however, be overcome by constructing the whole amplifier on the push-pull principle.

The application of the push-pull principle was of course obvious, since, as has previously been explained, the vertical deflection of the cathode ray is best brought about with a balanced voltage. For this reason even in the case of the amplifier of the oscillograph previously described the last stage was in push-pull connection. The necessity of limiting the influence of mains voltage variations has, however, led to the application of the push-pull principle in the first stage of the amplifier also.

In *fig. 1* the connections employed are shown. With the help of several variable resistances the input signal of the valve B_1 coming from the externally applied A.C. voltage, can be changed continuously and in steps. The alternating anode current of this valve passes through the resistance R_k and thereby causes such a variation of the cathode potential that the voltage difference between grid and cathode of the valve becomes smaller (inverse feed-back). At the same time an input voltage with opposite sign occurs between grid and cathode of the valves B'. In this way therefore a balanced voltage is obtained from the very beginning. The A.C. voltages in opposite phases over the anode resistances R_a are supplied *via* the condensers C to the second stage of the push-pull amplifier and again amplified. The output A.C. voltage of the second stage is fed *via* two coupling condensers to the first set of plates for vertical deflection of the cathode ray tube.

If a fluctuation of the mains voltage occurs, the

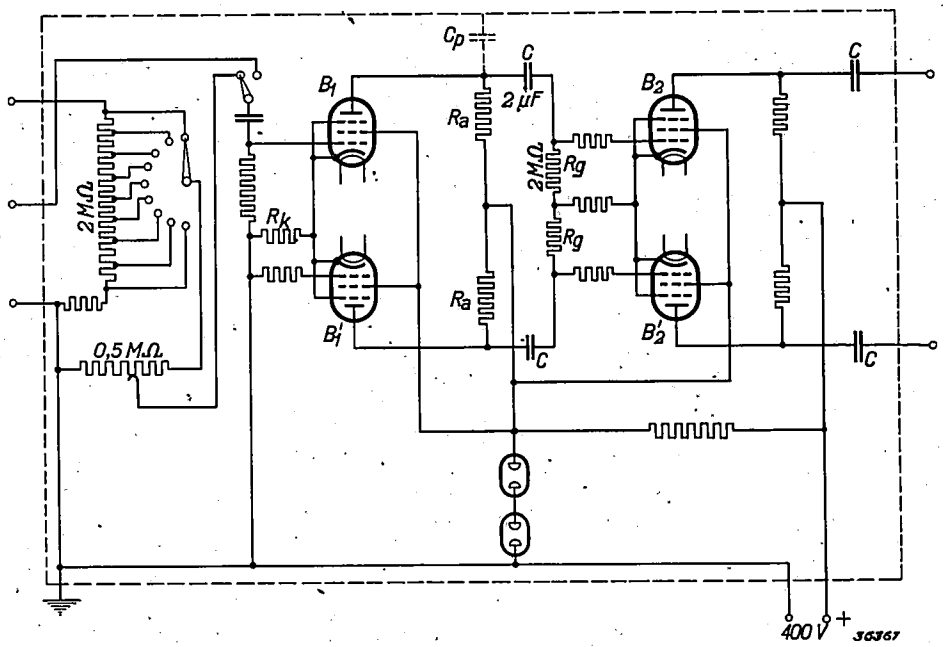

Fig. 1. Connections of the amplifier for the cathode ray oscillograph GM 3 156. It consists of two stages in push-pull connection and in the frequency region between 0.1 and 10 000 c/s it gives a voltage amplification by a factor 10 000.

anode voltages of the valves B_1, B'_1 and B_2, B'_2 will change in equal phases and not in opposite phases as takes place upon application of an input signal. Such a voltage fluctuation thus finally has the result that both deflection plates undergo the same change of potential, so that the difference of potential remains the same. The deflecting force on the electron beam is therefore unaltered; the beam merely undergoes an additional acceleration of retardation, which of course also results in a shift, although much smaller, of the oscillogram. It is therefore desirable to limit the voltage fluctuations themselves at the same time. This could be done with the help of two neon lamps in series as stabilizers, as indicated in the diagram. The result of these measures is that a sudden variation in the mains voltage of one per cent in the most unfavourable case causes a shift of the spot on the screen of 1.5 mm, and a slow change of the mains voltage has no observable results.

The reproduction characteristic of an amplifier stage at low and high frequencies is mainly determined by the anode resistance R_a, the gridresistance R_g, the capacity of the coupling condenser C and the capacity C_p between the coupling elements and earth. In the article already referred to several times about the cathode ray oscillograph GM 3152 it was explained that the lower limit f_1 of the frequency region within which the amplification is satisfactorily constant is determined by the condition

$$2\pi f_1 R_g C = 1, \quad \ldots\ldots \quad (1)$$

while the upper limit is determined by [3]):

$$2\pi f_2 R_a C_p = 1 \quad \ldots\ldots \quad (2)$$

In the oscillograph for use in tool making $R_g = 2$ MΩ and $C = 2$ μF. Thus according to equation (1)

$$f_1 = \frac{1}{2\pi \cdot 2 \cdot 2} = 0.04 \text{ c/s.}$$

The length of the cycle is thus 25 seconds. The definition of f_1 in equation (1) is such that the amplification for this limiting frequency with the connections here used would only amount to 35 per cent of its value in the flat part of the characteristics. If higher requirements are made with respect to lack of deformation in the reproduction, for instance if it is required to know the frequency region in which the amplification does not lie more than 10 per cent below the maximum value, then instead of equation (1), one obtains the following:

$$2\pi f_1 R_g C = 4 \quad \ldots\ldots \quad (1a)$$

and one calculates a lower limit of 0.17 c/s (10 c/min.)

In the case of the previously described oscillograph the lower limiting frequency for a faithful reproduction was considerably higher, because the coupling condensers C were much smaller. An enlargement of the coupling condensers was undesired in that case in connection with the reproduction of high frequencies. The coupling condensers contribute considerably to the capacity C_p, which according to equation (2) determines the upper limit of the flat part of the frequency characteristic. In the oscillograph under consideration a large value of this capacity is no objection, since the upper limiting frequency is chosen much lower. The product $R_a C_p$ in equation (2) may be larger by a factor 100 than in the oscillograph GM 3 152, and thus in spite of the larger value of C_p, the anode resistance R_a could also be made larger, whereby the amplification in the flat part of the characteristic could be increased by a factor 6. In *fig. 2* the variation of the amplification is given as a function of the frequency.

It might be supposed that the extension of the region of constant amplification to lower frequencies has been carried too far. A signal which alternates with a frequency of only a few cycles per second can easily be recorded with registering pointer instruments so that there is no need of an oscillograph for this purpose. It is found, however, that an undistorted reproduction at these low frequencies is only possible for sinusoidal vibrations, while in the case of non-sinusoidal vibrations deviations already begin to occur at considerably higher frequencies. We shall demonstrate this by calculation of the amplification of a signal of a rectangular form.

As connections for the amplifier we shall choose the simplified scheme according to *fig. 3*. If an A.C. voltage of any given form $V(t)$ is applied *via* the condenser C to the grid leakage resistance R of the first amplifier valve, then one finds for the voltage V_1 over this resistance the following differential equation:

$$\frac{dV_1}{dt} + \frac{V_1}{RC} = \frac{dV}{dt}.$$

The general solution is

$$V_1 = \left(V_0 + \int_0^t \frac{dV}{dt} e^{t/RC}\, dt\right) e^{-t/RC} \quad (3)$$

[3]) The amplification of a stage is practically constant over the greatest part of the region between these limits, and at the limits themselves it falls to $1/\sqrt{2}$ (71%) of its constant value.

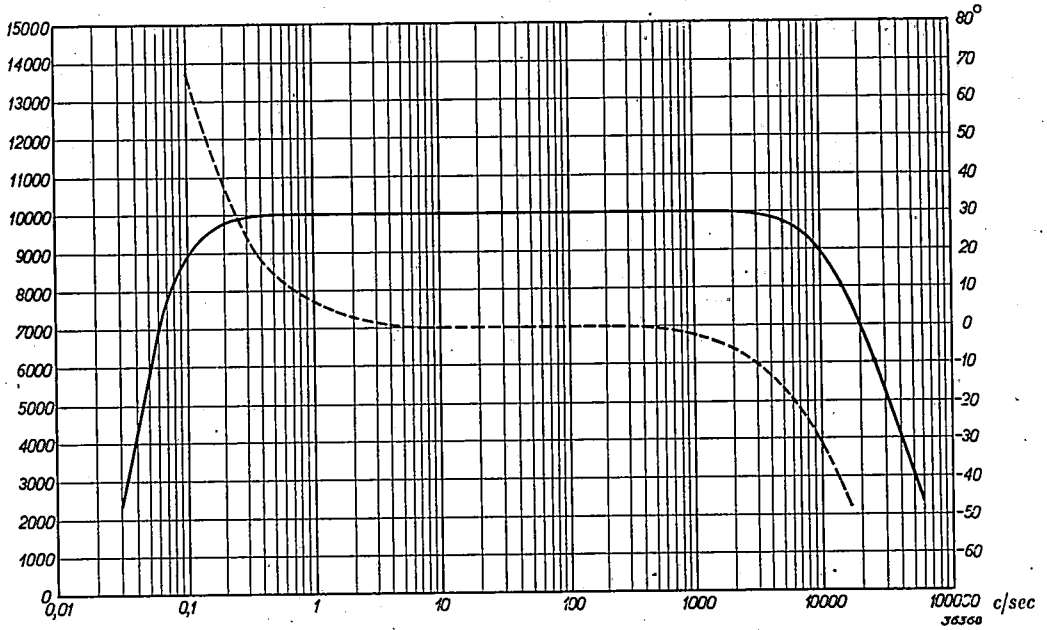

Fig. 2. Frequency characteristic of the amplifier. Full line, amplification, broken line, phase shift, as functions of the frequency. If a decrease in the amplification of 10% is allowed, the useful reproduction range extends from 0.1 to 10 000 c/s. If a phase shift of 5° is allowed, which, as far as the possible distortion af a given oscillogram is concerned, corresponds approximately to the decrease of 10% mentioned, the amplifier can only be considered useable in the frequency range from 1.5 to 1 500 c/s.

Let us assume that the signal voltage $V(t)$ is equal to zero until the moment $t = 0$, then suddenly assumes a definite value V_1 and is later constant for some time. From equation (3) it then follows that

$$V = V_0 \, e^{-t/RC} \quad . \quad . \quad . \quad . \quad . \quad . \quad (4)$$

The output voltage of the amplifier valve amounts to $AV_1(t)$, where A is the amplification of the first

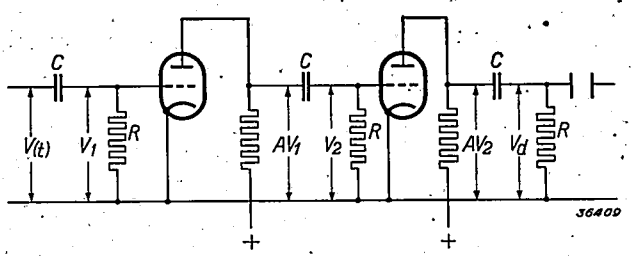

Fig. 3. Simplified diagram of the amplifier.

stage. This voltage has exactly the same significance for the second stage as the voltage $V(t)$ for the first stage, so that for the control grid voltage of the second valve we may immediately write

$$V_2(t) = \left(AV_0 + \int_0^t A \frac{dV_1}{dt} e^{-t/RC} dt \right) e^{-t/RC},$$

where V_1 must be substituted according to equation (4). When the integration is performed one obtains:

$$V_2(t) = AV_0 \left(1 - \frac{t}{RC} \right) e^{-t/RC} \quad . \quad . \quad . \quad . \quad (5)$$

This voltage is again amplified by a factor A in the second stage, and *via* a condenser C again applied to a resistance R. The final deflection voltage V_d can therefore again be calculated according to equation (3), where V must be set equal to AV_2. One then obtains

$$V_d(t) = A^2 V_0 \left(1 - \frac{2t}{RC} + \frac{t^2}{2R^2C^2} \right) e^{-t/RC}. \quad (6)$$

It is thus clear that the voltage surge V_0 amplified at the first moment by a factor A^2 is transmitted to the deflection plates. Instead of remaining constant, however, the voltage then decreases exponentially. (An oscillation occurs thereby, as shown in *fig. 4* in which the calculated variation of the voltage is given.) If we consider relatively

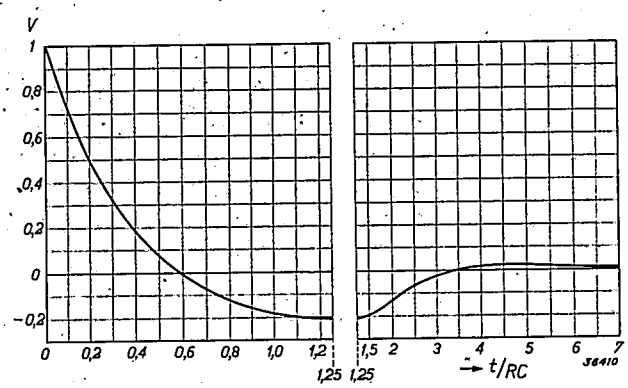

Fig. 4. Variation of the voltage on the deflection plates as a function of the time upon a commutation surge, see equation (6).

short times ($t \ll RC$) we may approximate the variation of the voltage by taking the first term of the series of e functions, and we obtain

$$V_d \approx A^2 V_0 \left(1 - \frac{3t}{RC}\right).$$

For faithful reproduction the requirement must be made that this shall be a fairly constant voltage. The corresponding input voltage is constant in any case. If V_d is allowed to decrease 10 per cent the maximum value for the time t becomes

$$t_m = \frac{1}{30} RC .$$

The input voltage may not remain constant longer than t_m if non-permissible distortion is not to occur. If RC is expressed by the lower limiting frequency according to equation (1a) one finds

$$t_m = \frac{1}{15\pi f_1} = \frac{1}{47 f_1}.$$

The maximum duration of a surge upon switching on which can be reproduced with satisfactory reliability is therefore 47 times shorter than the maximum duration of a cycle of a sinusoidal curve which is reproduced with the same accuracy. For a rectangular A.C. voltage which may be considered as a succession of such starting surges, the same considerations are valid in principle as for one such surge; the duration of one period of the square sine then amounts to $2t_m$. Good reproduction of sinusoidal vibrations to a lower limit of 0.17 c/s thus corresponds to a good reproduction of rectangular vibrations ("square sines") to a lower limit of $47 \times 0.17/2 = 3.75$ c/s. It is thus clear that upon consideration of non-sinusoidal vibrations the region of undistorted reproduction is by no means carried too far toward low frequencies. We shall see in the following oscillograms how this is manifested in practice.

In *fig. 5* three oscillograms of square sines are reproduced. Diagram *a* was obtained by applying the voltage which had a frequency of 2 c/s directly to the deflection plates of the cathode-ray tube. Diagram *b* shows that this shape can still be reproduced by the amplifier without too great distortion. Finally it may be seen from diagram *c* that this is no longer the case at appreciably lower frequencies, at a frequency of 0.5 c/s, instead of the horizontal sections, the oscillogram shows exponentially falling lines, thus a strong distortion, although no noticeable decrease in the amplification yet occurs at this frequency.

The fact that the square sine of low frequency is so much more badly reproduced than the pure sine, seems somewhat paradoxical; the square sine may be considered as composed of a pure sine and higher harmonics, and when the component with the lowest frequency is not yet appreciably weakened, this is decidedly not the case with the higher harmonics. It must, however, be kept in mind that, due to the amplification of a composite vibration, not only can the relative amplitudes of the harmonics change, but also the relative phases, and the latter effect already appears at considerably higher frequencies than the former, as may be seen from the broken-line curve in fig. 2. By the disturbance of the relative phases the sum of two vibrations in the output signal may take on a quite different form than that possessed by the original vibration, even though the relation between the amplitudes is not changed by the amplification.

In addition to distortions due to an amplification which varies with the frequency and distortions due to a phase shift which varies with the frequency, an amplifier in general also possesses a so-called non-linear deformation, which means that a sinusoidal input signal does not lead to an exactly sinusoidal output signal. The deviation from the sine shape increases with the amplitude of the

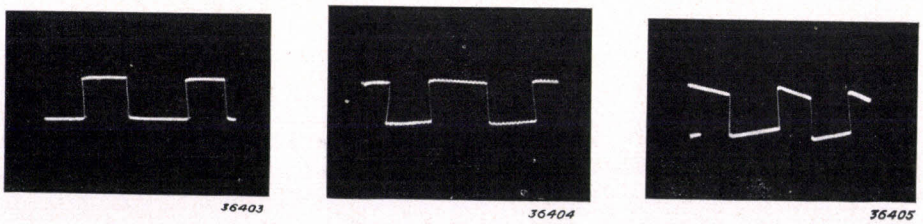

a *b* *c*

Fig. 5. Oscillograms of a rectangularly alternating voltage.
a) The voltage in question (square sine of 2 c/s) is applied directly to the plates for vertical deflection of the cathode ray tube.
b) The same voltage is fed to the cathode ray tube *via* the amplifier. Practically the same diagram results.
c) The frequency of the square sine is decreased to 0.5 c/s. A distortion of the oscillogram can now be clearly observed.

input signal, and with the amplifier of the cathode ray oscillograph in question it amounts to about 2 per cent in the least favourable case, *i.e.* with a signal corresponding to an image height of 6 cm. This deviation can scarcely be observed on the screen of the tube, and may therefore be considered permissible.

The time axis generator

The function of the time axis generator is to supply a voltage which is proportional to the time, and which suddenly falls to its initial value after reaching a given maximum, so that a saw-tooth form is obtained (*fig. 6*). If this voltage is applied to the plates for horizontal deflection of the cathode ray tube, and the voltage of the phenomenon to be recorded is simultaneously applied to the plates for vertical deflection, one sees on the screen of the tube a diagram which represents the quantity to be recorded as a function of the time.

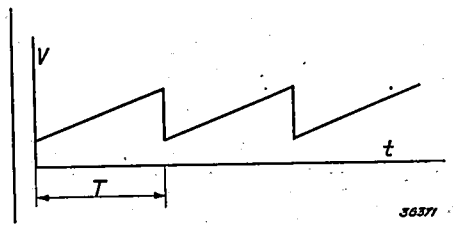

Fig. 6. Variation of the horizontal deflecting voltage, generated by the time axis generator, as a function of the time. At an amplitude of the horizontal deflection of 8 cm the "sawtooth" period T can be varied from 0.005 sec to 4 sec.

The velocity of the sawtooth motion must be able to be adapted to the frequency of the phenomenon to be recorded. This means that the region within which the frequency of the sawtooth motion can be varied must also be chosen considerably lower with the oscillograph for use in tool making than in the cathode ray oscillograph GM 3 152. The periodic falling back of the voltage can in this case be realized very easily by means of gas triodes, which could not be used in the previously described oscillographs, because they have too much time lag for the highest time axis frequencies of more than 100 000 c/s occurring in those oscillographs. For the maximum time axis frequencies of the cathode ray oscillograph for use in tool making, however, gas triodes may very well be used. Moreover, the circuit of the sawtooth generator obtained with gas triodes offers great advantages when it is desired to pass over to a much lower limiting frequency than is the case with the existing oscillographs.

In *fig. 7* the connections used are given. The pentode L_p charges the condenser C with a constant current, and the cathode potential of the gas triode L_g decreases proportionally to the time. Between the cathode and the anode of the gas triode a potential difference thus occurs, which will lead to breakdown as soon as it exceeds a certain

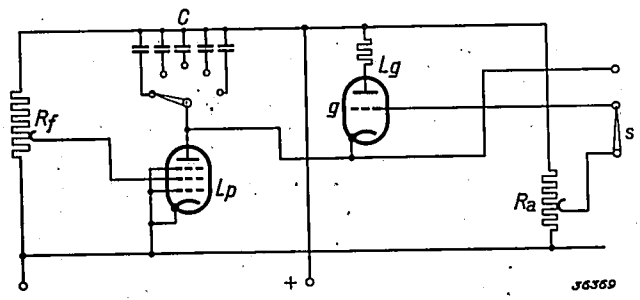

Fig. 7. Connections of the time axis generator. L_p pentode, L_g gas triode. By changing the capacity C and adjusting the potentiometer R_f the sawtooth frequency is regulated; with the help of the potentiometer R_a the sawtooth amplitude is regulated.

value. This value is mainly determined by the bias of the grid g. The breakdown occurs approximately when the potential of the cathode has fallen below that of the grid. Due to the breakdown the condenser C is discharged with a high current, so that the cathode potential again rapidly increases to its initial value; the discharge of the gas triode is hereby extinguished and the process begins anew.

By commutation of the condenser C the frequency of the time axis voltage can be affected in steps within wide limits, while a continuous regulation is possible by changing the screen grid voltage of the pentode L_p with the help of the potentiometer R_f, and regulating in this way the charging current of the condenser C. The amplitude of the sawtooth motion is adjusted with the potentiometer R_a from which the D.C. voltage for the grid of the gas triode is taken. Finally it is possible to synchronize the period of the sawtooth voltage with the help of an externally applied voltage, which is applied instead of the short circuit to the terminals s, *i.e.* to the grid of the gas triode. For this purpose the voltage of the phenomenon to be investigated may itself be used and this is taken from the output of the amplifier.

If it is desired to record non-periodic phenomena, such as those occurring upon throwing a switch, instead of the oscillating sawtooth deflection it is in many cases advantageous to use a single non-periodic linear horizontal deflection of the fluorescent spot which begins at a suitable moment. This can be obtained by applying to the grid of the gas triode such a high voltage before the beginning of the linear motion, that the discharge is never extinguished and the condenser C remains practically uncharged. At the moment when the phenom-

enon to be investigated begins, the normal voltage is applied to the grid of the gas triode with a suitable synchronizing arrangement, a mechanically driven contact, for instance. At that moment the discharge is extinguished and the fluorescent spot begins its linear motion. After having covered a certain distance the spot will jump back to the initial position and begin its motion again. The mechanically driven contact will therefore preferably be so arranged that before this first period of the sawtooth has elapsed the grid is again brought to a high voltage, so that the spot jumps back and then remains in its resting position.

By moving the sliding contact on the resistance Rf and commutation of the condenser C the velocity of the linear motion of the spot can be regulated continuously or in steps between 2 cm/sec and 16 000 cm/s. For the sawtooth motion this means a variation of the time axis frequency between 1/4 and 2 000 c/s for a length of the time base of 8 cm.

The cathode ray tube

The oscillograph for use in tool making is provided with a cathode ray tube DN 9-3 or with the post-acceleration tube DN 9-5 which was described in detail in the previous issue of this periodical [4]). The cathode of the tube is at a potential which is 1 000 volts negative with respect to earth, while the space between the deflection plates is at about earth potential, so that a voltage to be investigated with respect to earth can also be connected directly to the plates of the cathode ray tube, *i.e.* without the use of the amplifier. The electrons which have passed the deflecting systems can be accelerated a second time when the post-acceleration tube is used, as was explained in the article referred to, by means of a positive voltage on the post-acceleration electrode. For this purpose there is a special supply apparatus (GM 4 198) which can give an adjustable high D.C. voltage with respect to earth (see *fig. 8*). The highest voltage which may be applied to the post-acceleration electrode amounts to 4 000 volts with respect to earth (5 000 volts with respect to the cathode).

Due to the stronger acceleration of the electrons the picture is much brighter, so that photographic recording of the oscillogram even with simple cameras with relatively small relative aperture is possible, while at the same time there is the possibility of projecting the image and thereby making it visible to more persons at one time. For this purpose there is an auxiliary projection apparatus (GM 4 198) with a lens of 50 mm diameter and a focal length of 150 mm. The distance from the projection screen may be 1 to 5 m, and an enlargement by a factor 6 to 30 is thereby obtained.

Fig. 8. The 5 000-volt supply apparatus GM 4 198 for the post-acceleration tubes of the cathode ray oscillograph GM 3 156. The apparatus contains a high-voltage transformer, a rectifier valve and a filter for smoothing the D.C. voltage obtained. As may be seen it can be set at five different voltages with the help of a switch.

Several applications

The oscillograph for use in tool making will be chiefly employed to investigate vibration phenomena and rapidly alternating tensions in parts of machines. Since these subjects have been dealt with in detail previously [5]) we shall here only discuss a few less obvious applications.

Measurements on rotating components

With the help of a coil and a permanent magnetic core the roundness of shafts and flywheels can be tested in a very simple way. In *fig. 9* an arrangement used for this purpose is shown schematically, while *fig. 10* is a photograph of the arrangement. The iron shaft A turns at a distance of 1 mm from the magnet M with the coil S. If the air gap L

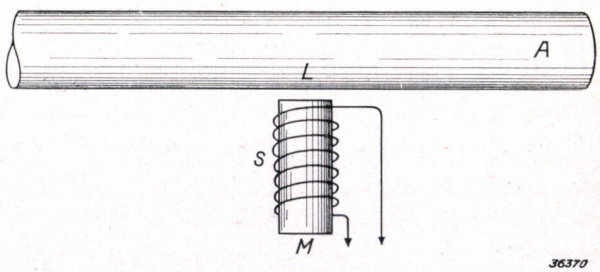

Fig. 9. Arrangement for the measurement of the lack of roundness and excentricity of shafts. A shaft, L air gap, S coil, M permanent magnet. The variation of the width of the air gap due to lack of roundness and excentricity excites an alternating voltage in the coil.

[4]) A cathode ray oscillograph with post-acceleration Philips techn. Rev. **5**, 257, 1940.

[5]) See the articles referred to in footnote [1]).

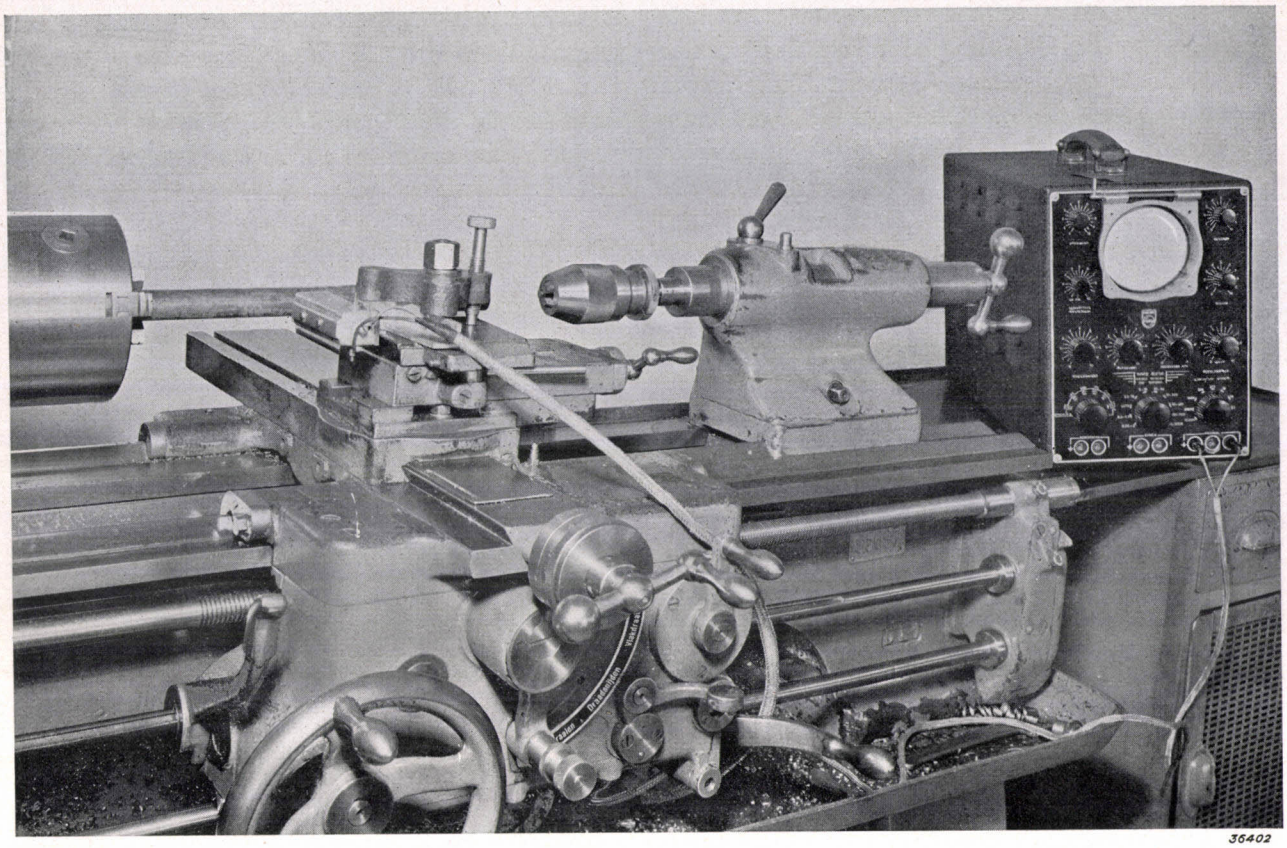

Fig. 10. Arrangement for the measurement of the lack of roundness of shafts.

between the shaft and the magnet varies in width, a voltage will be induced in the coil S which is proportional to the velocity of the change in width. When the shaft is perfectly round and does not vibrate as it turns, the induced voltage will be zero. The oscillogram thus indicates by its shape whether there is a lack of roundness, excentricity or mechanical vibration.

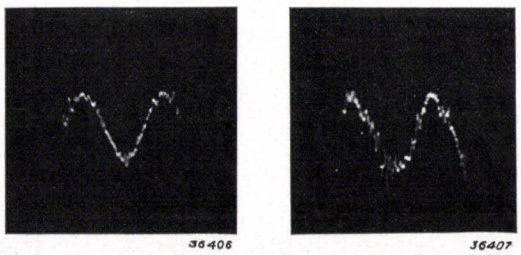

a *b*

Fig. 11. Two oscillograms obtained with an arrangement according to fig. 9. The sinusoidal vibration indicates an excentricity, while the indentations which are deeper in case *b* than in *a* are caused by irregularities of the surface.

Fig. 11 gives an example recorded with a shaft with a speed of 1000 r.p.m. and a diameter of 50 mm. In *a* we can distinguish voltage variations caused by slight irregularities and an excentricity. In *b* the same may be seen for a shaft with a rougher surface.

The frequency of the vibration which is caused by the excentricity amounts in this case to 16 2/3 c/s, so that the previously described oscillograph which gives a practically constant amplification to a lower limit of 10 c/s would also be able to indicate this excentricity practically undistorted. The use of the oscillograph specially constructed for tool making has the advantage, however, that the phase of the excentricity is also given quite correctly, since the phase deviation above 4 c/s is less than 1°.

Phase measurements at low frequencies are not only important in tool making, but also in electrotechnology, especially in the construction of inverse feed-back amplifiers. If the output voltage of the amplifier is greater than 10 volts it can be applied directly to the set of plates for horizontal deflection of the cathode ray tube, while the input signal causes the vertical deflection of the cathode ray *via* the amplifier of the oscillograph. If output voltage and input voltage are in the same or opposite phase, a straight line results; in other cases an ellipse from which the relative phase shift can be deduced [6]).

[6]) On the subject of this and other methods of phase measurements with the help of the cathode ray tube see Philips techn. Rev. **5** 210, 1940.

The measurement of varying wind velocities

In aerodynamics, wind velocities or flow velocities in turbulent air currents are measured from the cooling experienced by thin heated filaments in the air. The temperature variations of the filament cause resistance variations which can easily be converted into voltage variations. The latter can be observed with an oscillograph.

Fig. 12. Variation of the resistance of an anemometer filament in the air current of a fan.

An example of the diagrams thus obtained is given by the oscillogram of *fig. 12* which was recorded in the air current of a fan. Since this current does not have a periodic character, the non-periodic linear horizontal deflection is used. The starting point of the horizontal motion is marked as a white line at the left.

In the following number of this periodical we hope to describe additional examples of practical applications of the cathode ray oscillograph GM 3 156.

THE PERCEPTION OF PITCH

by J. F. SCHOUTEN.

534.321

Although the human ear is capable of breaking up a complex sound into harmonics, which is understandable physiologically by the so-called localization theory, upon superficial listening the ear perceives only a single pitch which is in general that of the fundamental tone. The fact that this is often true even when the fundamental tone is almost or entirely missing has been explained as due to non-linear distortion in the ear. Experiments done in this laboratory have shown that this explanation cannot be correct, and have led to the hypothesis that the low pitch observed is to be ascribed to a collective perception of the higher harmonics. This component of the sound is called the "residue". The low pitch of the residue is found to be correlated with the periodicity of the vibration which occurs due to the conjunction of the higher harmonics. It is physiologically understandable that such a conjunction should occur, considering the limited resolving power of the ear. This is made clear by means of a model. In conclusion several phenomena are discussed, some of which have long been familiar, which can be given a simple explanation by means of the hypothesis of the residue; the sound of church bells is discussed in particular.

Subjective sound analysis

Every periodic air vibration can be decomposed into the sum of a number of sinusoidal vibrations (harmonics) whose frequencies are integral multiples of a fundamental frequency (Fourier series). If only the fundamental frequency is present, and if this is in the audible region, the ear observes the air vibrations as a pure tone whose pitch is determined by the frequency. If in addition to the fundamental frequency the vibration contains a number of harmonics, other perceptions are also experienced. In general one observes a sound to which one ascribes a single definite pitch, and which is distuinguished from a pure tone with the same pitch by a certain timbre. After some practice, however, it is often possible to observe the different harmonics in the sound separately as pure tones, by concentrating the attention sharply upon the different components to be heard. The fact that the ear is capable of such a Fourier analysis was stated a century ago by Ohm (his so-called acoustic law).

The analytic power of the ear can easily be tested with the help of a piano. For instance we strike the note C (fundamental frequency 131 c/s.) In addition to the fundamental tone a series of harmonics is then heard whose frequencies (at least approximately) correspond to the fundamental frequencies of other notes on the piano. These notes are given for the first ten harmonics of C in *fig. 1*. The fact that these harmonics are actually produced by the wire C, can be proved objectively by first soundlessly depressing a key corresponding to one of the harmonics, for instance G′ (third harmonic of C) and then energetically striking the key C. Upon releasing the key C the G′ wire is clearly heard to sound, having been brought into resonance by the third harmonic of C.

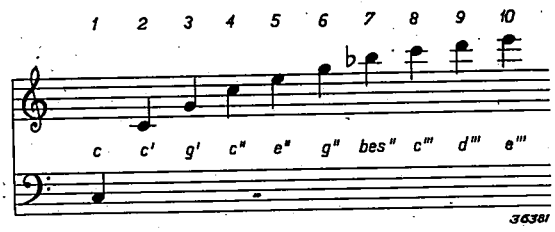

Fig. 1. The harmonics of a note on the piano correspond very closely to the fundamental tones of other notes. They are given here for the first ten harmonics of C.

In order now to observe the third harmonic in the note C subjectively also, the key G′ must first be struck softly (in order to concentrate the attention on that tone) and then released, then the key C must be struck. This can also be done for several higher harmonics up to about the eighth. When one has succeeded in observing the harmonics they are often so suprisingly clear that one is inclined to believe a resonating wire responsible for the sound.

The fact that it is not a question of a resonating wire can be beautifully demonstrated in the following way. The fifth harmonic of C is of course the major third of the C″, this interval is distinguished by the frequency ratio $5 : 4 = 1.250$. In the equally tempered scale of the piano, however, the major third lies somewhat higher ($2^{4/12} = 1.260$), so that the fifth harmonic of C must be heard slightly lower than the E″ (third of C″). This is actually found to be true. When C and E″ are struck at the same time, upon dying out of the sound the E″ is clearly heard to give a beat with a frequency of 5 c/s, corresponding to the difference in frequency between the two tones.

These experiments illustrate how the harmonics

of the vibration of a string are perceived as separate pure tones, each with the pitch corresponding to its frequency. As to the mechanism by which the ear is capable of carrying out such a Fourier analysis, the following hypothesis has been developed. In the cochlea (the spiral cavity of the internal ear) there is a membrane, the basilar membrane; see the diagram in *fig. 2*. Due to a sound vibration of a given frequency a local sensation is felt in the cochlea, in the sense that only a certain more or less limited region of the basilar membrane is brought into motion and only the fibres of the auditory nerve originating in this region are stimulated. The old and much contested localization theory has been beautifully confirmed by experiments on animals in which the electrical voltages were investigated which occur in the cochlea under the influence of sound, and which partially leak off to the outside. It was found that especially for high tones a maximum of the voltage could be observed at different points on the cochlea, depending upon the frequency.

If it is assumed, as is often tacitly done, that each of the nerve fibres will, upon stimulation, cause the perception of a definite pitch, a physiological explanation of subjective sound analysis according to Ohm's law is obtained: a composite sound brings into vibration narrow regions of the basilar membrane determined by the Fourier spectrum of the sound, and each of these regions gives the sensation of a separate tone with a pitch which is determined by the region involved.

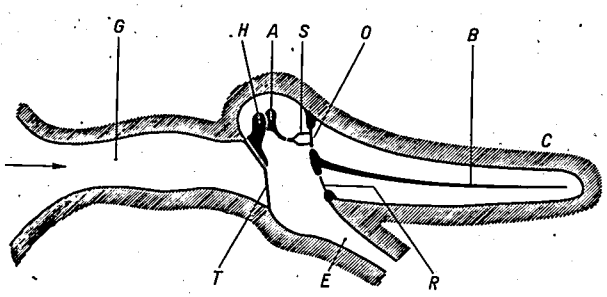

Fig. 2. Diagram of the inner ear. *G* meatus, *T* ear drum, *C* cochlea. The last organ is divided by the basilar membrane *B* into an upper and a lower half. Actually the cochlea, which is drawn extended, is rolled up in a spiral. The bones of the ear (hammer *H*, anvil *A*, stirrup *S*) act upon the oval window *O* in the upper part of the cochlea. The lower part has a circular window *R*, which opens into the Eustachian tube *E*.

We have thus briefly outlined the current conception of subjective sound analysis. Investigations which we are about to describe have led us to the conclusion that these conceptions must undergo a fundamental modification. With the help of an improved formulation of subjective sound analysis, moreover, a number of long familiar paradoxical phenomena in the perception of pitch are provided with a ready explanation. We shall deal with these in the conclusion.

The problem of the missing fundamental tone

We have already stated that in the observation of a sound consisting of different harmonics the ear generally makes no use of its analytic capacity, but only perceives the sensation of a sound with a definite pitch and timbre. This is also the case, for example, when a note on the piano is struck without attention being concentrated especially on one of the harmonics. The pitch ascribed to the sound then simply corresponds to the fundamental tone of the note, which is understandable considering the fact that the fundamental tone is usually much stronger than the accompanying harmonics in the case of the piano.

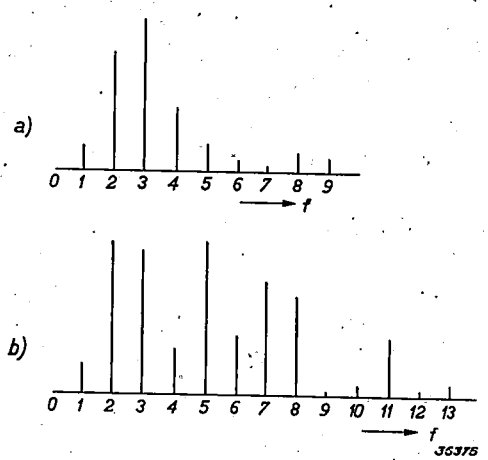

Fig. 3. *a*) Spectrum of the harmonics of the vowel A, sung at a pitch of 290 c/s.
b) The same for the G string of the violin bowed in G. In both cases the fundamental tone is only weakly represented.

When the study of sound spectra had made further progress, it was discovered that with many sounds the fundamental tone was represented to only a very slight degree. This is true for instance for the vowel A and for the G string of the violin bowed in G[1]), see *fig. 3*. Nevertheless, we ascribe to these sounds the pitch of the fundamental tone, and we are not in the least inclined to estimate the pitch an octave or a twelfth higher (*i.e.* that of the strongest component of the spectrum).

This remarkable behaviour of the ear was manifested in a still more striking way in telephony. Here it was found that without changing the pitch of the voice of the speaker the whole frequency region below 300 c/s can be cut off. It is just in this region, however, that the fundamental tones

[1]) See also: Philips techn. Rev. 4, 290, 1939 fig. 8 and 9.

of the male speaking voice lie and to some degree also those of the female voice, see *fig. 4*.

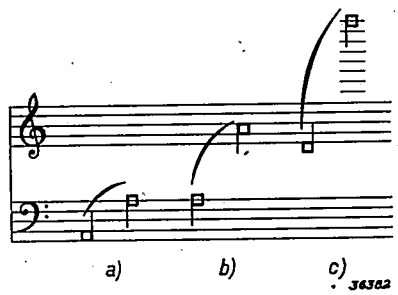

Fig. 4. Region of fundamental tones *a*) of the male and *b*) of the female speaking voice. In telephony (frequency region *c*) the fundamental tones of the man are never transmitted and those of the woman only for high voices.

make no difference whether or not the sound contains the fundamental tone objectively; in any case the subjective fundamental tone would always be dominant due to non-linear deformation.

In opposition to this statement it may be remarked that with non-linear distortion it is a case of a phenomenon which must of necessity disappear at sufficiently low sound level, while the phenomenon to be explained — the perception of the missing fundamental — continues to take place at a low level. The statement referred to is, however, entirely refuted by experiments with the optical syren, an instrument which has already been described in this periodical [3]). With this

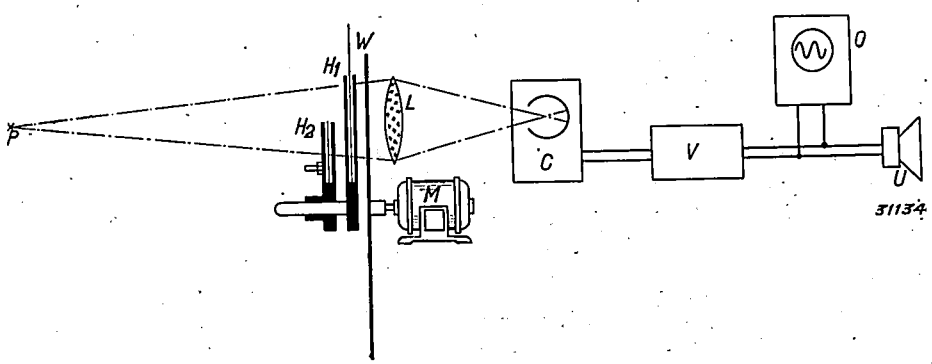

Fig. 5. Optical syren for the production of "synthetic sound". A vibration form which is to be converted into sound is cut out as a paper stencil (such stencils may be seen in fig. 6 to the left), placed in a holder H, and homogeneously illuminated by a point source of light P placed at a great distance. Behind the holder there is a disc W with a number of narrow radial slits, which is driven at an adjustable speed by a motor M. The light transmitted through the slits is concentrated by a lens L on a photocell C. The photocurrents are converted into sound *via* an amplifier V and a loud speaker U. Since upon rotation of the disc W the slits repeatedly scan the vibration form cut out in polar coordinates, the sound obtained also has this vibration form, which may be checked with the cathode ray oscillograph O. In front of the stencil holder H_1 is a second holder H_2 which can be rotated, and in which a second stencil can be inserted.

The explanation of the fact that in these cases, in spite of the absence of the fundamental, the pitch of the fundamental is ascribed to the sound has been explained as due to the non-linear distortion which the sound vibrations undergo in the transmission within the human ear [2]). Due to this distortion differential tones, among others, of the components present in the sound will occur. Each pair of adjacent harmonics will give a differential tone with a frequency just equal to that of the fundamental tone (see for instance the spectra in fig. 3). In this way therefore it would be possible that a sound which is lacking objectively (*i.e.* outside the ear) in the fundamental tone should possess this tone in the internal ear. If this phenomenon were really very pronounced, it would even

instrument, a diagram of which is given in *fig. 5* with a short description in the text under the figure, it is possible to convert into sound a series of arbitrary vibration forms cut out in the form of stencils, separately or in combination; in particular it is possible to make one of the components disappear while listening to the "synthetic sound" thus obtained, by covering the stencil in question, or to change its phase by rotating the stencil.

In this way a periodic impulse was investigated whose oscillogram and spectrum are given in *fig. 6a*. The fundamental frequency was 200 c/s. This vibration was observed as a sharp sound wih the pitch 200 c/s. By adding to the sound with the help of a second stencil a vibration with a fundamental frequency in a phase opposite to that of the fundamental vibration of the periodic

[2]) Non-linear distortion in the ear is discussed in J. F. Schouten, Synthetic sound, Philips techn. Rev. 4, 167, 1939; see especially p. 172.

[3]) See the article referred to in footnote [2]).

impulse and with a suitable amplitude, the fundamental vibration could be removed from the objective sound (present outside the ear), see fig. 6c. The observed pitch of the sharp sound remained the same. If this is to be explained on the assumption of non-linear distortion in the inner ear, it would still now be possible to compensate the fundamental tone subjectively, by adding the fundamental vibration in suitable phase and amplitude, so that the pitch would have to change. This expectation was not fulfilled, the pitch remained the same, which is all the more remarkable since a subjective compensation is indeed found possible in the investigation of the second and higher harmonics. The separate perception of these harmonics — which is particularly easily realized in these experiments by alternately covering and uncovering the corresponding stencils — can be made to disappear entirely (see fig. 6c). At not too high a sound level the subjective compensation of these higher harmonics is found to occur simultaneously with the objective compensation, so that in this case the non-linear distortion can play no appreciable part.

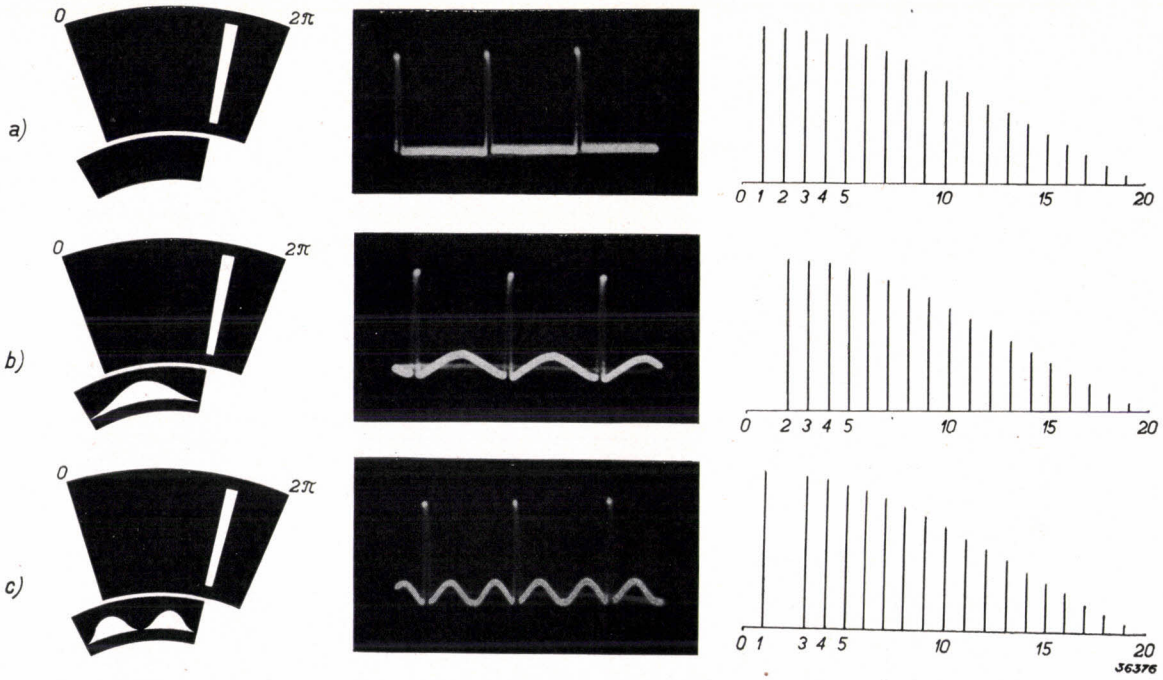

Fig. 6. Stencil, vibration form (recorded with the oscillograph) and spectrum of
a) a periodic impulse whose peaks have a width of 1/20 of the length of a period;
b) the same periodic impulse with (objectively) compensated fundamental frequency;
c) the same periodic impulse with compensated second harmonic.

The hypothesis of the residue

Experiments with the periodic impulse mentioned at a sound level at which, according to the above, it is certain that no non-linear distortion occurs, brought to light the following remarkable behaviour. Whether or not the fundamental vibration was present, a strong sharp sound with the pitch of 200 c/s continued to be observed. Addition and subtraction of the fundamental vibration is heard, however, independent of the sharp sound, as the occurrence and disappearance of a weak, pure tone with the pitch 200 c/s. This is the separately observed fundamental tone; it exactly disappears when the fundamental vibration is compensated objectively. The loudness with which we now hear the fundamental tone in the total sound is also practically the same as when we listen to the fundamental tone alone by covering the stencil of the impulse. Furthermore, upon the addition of an extra frequency of for instance 204 c/s, beats with the fundamental tone are heard which disappear completely when the latter is compensated. The sharp sound of the same pitch, which one continues to hear, on the other hand, exhibits no beats with the added frequency of 204 c/s.

The total sound thus contains two components of the same pitch. That this phenomenon has until now escaped the attention of observers must be ascribed to the difficulty of observing the fundamental tone as a separate weak component in the sound without the above-described means.

As concerns the strong, sharp sound with the

pitch of 200 c/s, this is found also to persist, not only when the fundamental vibration is removed from the sound, but also when a number of low harmonics are removed as well. It is, however, very much diminished when the highest harmonics are taken away. We are therefore compelled to assume that a collective observation of these high harmonics is the source of this sharp sound. Such a sound component will be called a residue.

A very simple solution of the problems of subjective sound analysis is furnished by the introduction of the conception of the residue. For complex sounds the rule, assumed in the foregoing to be obvious, is valid, that the pitch ascribed to the sound is that of the loudest component [4]). For all sounds which contain a large number of hamonics the residue will be the component which determines the pitch [5]); the fundamental tone itself then plays an entirely minor part. If it is practically missing, as in the case of the vowel A or the G of the violin, or if it is removed, as in telephony or in the above-described experiments, the residue continues to exist unchanged, so that the pitch remains the same.

In the case of such sounds, and there are after all many of them, it is no longer reasonable to say that the ear carries out a Fourier analysis of the sound. This is, however, true for the lower harmonics, but the most obvious component, the residue, owes its existence to the fact that the group of highest harmonics is not analysed into different pure tones but is observed as a single sound.

Correlation of residue and periodicity

It is not strange that the highest harmonics cannot be observed individually, since they lie very close together; the resolving power of the ear is clearly inadequate to distinguish them from each other. The question arises, however, as to why they form collectively a component of such a low pitch. There are two quantities which may play a part in the explanation of this: in the first place the distance between the harmonics which is equal to the fundamental frequency, and in the second place the periodicity of the collective vibration form of these harmonics. In the case of practically all vibration forms this periodicity (*i.e.* the frequency corresponding to it) is again equal to that of the fundamental vibration. Thus in the periodic impulse used by us (fig. 6*a*) not

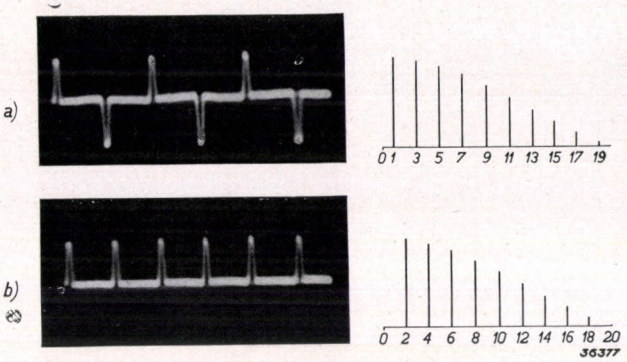

Fig. 7. Oscillogram and spectrum of two vibrations which have the same distance between the harmonics but different periodicity.

only the distance between the harmonics, but also the periodicity of several groups of adjacent harmonics is 200 c/s. Vibration forms can also be realised in which the two quantities mentioned differ. The vibration given as an example in *fig. 7a* has the same spacing of the harmonics as the periodic impulse in fig. 7*b*, the periodicity, however, not only of the total vibration but also of each group of adjacent harmonics, is twice as great in the second case as in the first. In observing these vibrations with the help of the optical syren it was found that the residue observed in the second case was an octave higher than the residue in the first case. The pitch of the residue is thus not correlated with the distance between the harmonics but with the periodicity of the collective vibration form of the constituent harmonics.

How can the existence of the residue be explained physiologically?

For the theory of the mechanism of hearing the most important consequence of the existence of this residue is that motion of a single region of the

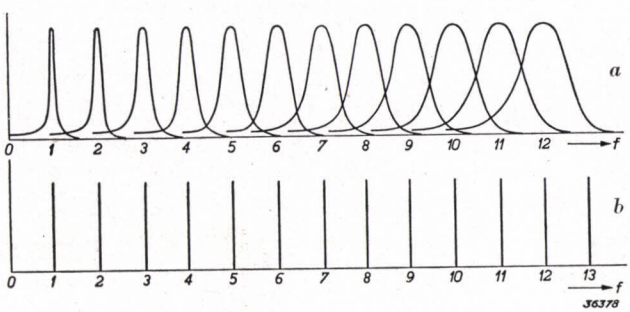

Fig. 8. *a*) Resonance curves of an series of resonators of the type of the basilar membrane. The resonators may be imagined to succeed one another in infinite density.
b) Spectrum of the harmonics of an ideal (infinitesimally narrow) periodically repeated impulse.

[4]) The pitch may also be determined by that component which draws the most attention by contrast with previous sounds or in some other way.

[5]) In principle it is possible for more than one residue to occur in a single sound.

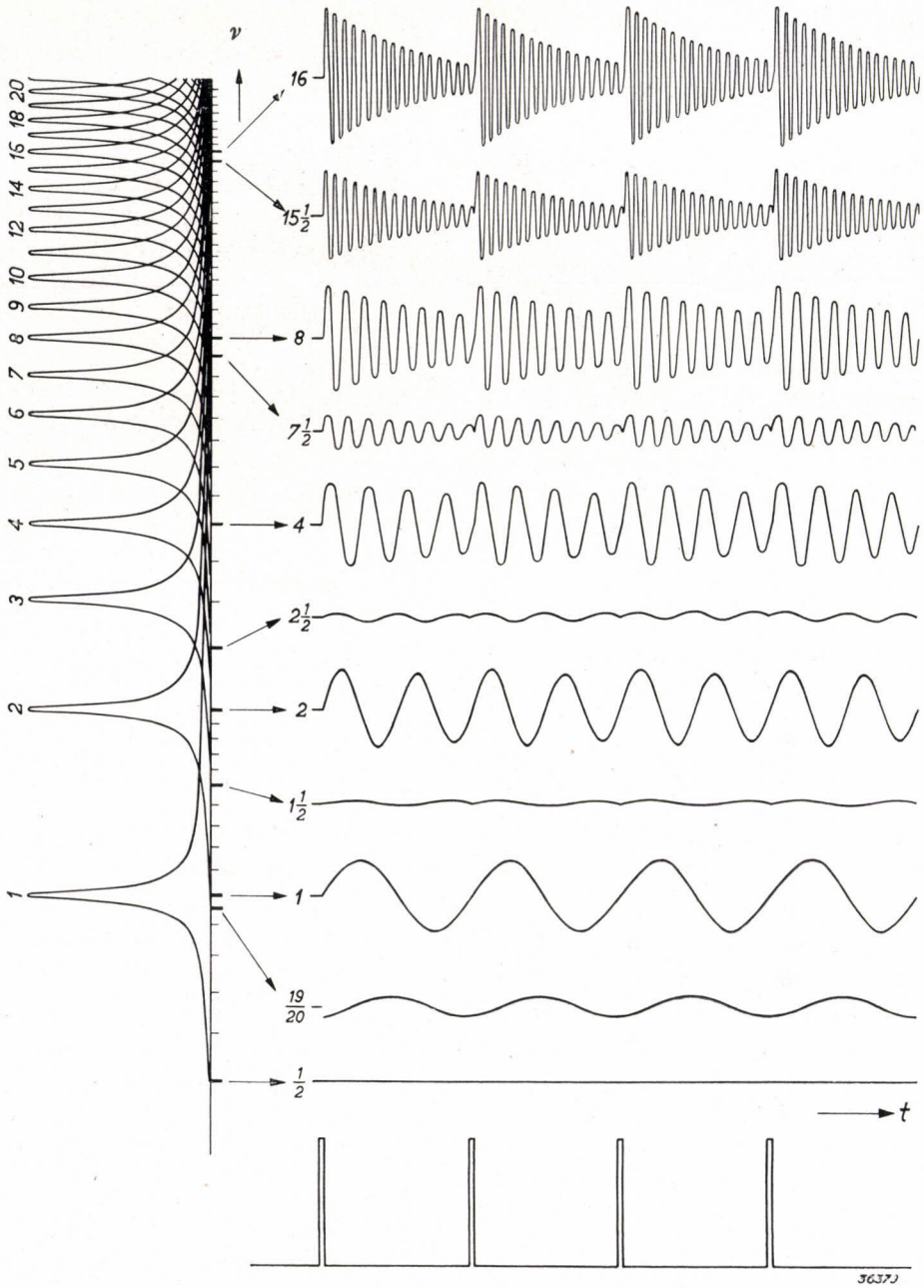

Fig. 9. To the left on a logarithmic frequency scale the excitation curves which indicate for each harmonic of the force (periodic impulse) acting on the model which resonators (characteristic frequency ν) are set in motion and to what extent. The motion occurring is here drawn for a number of resonators (relative characteristic frequency $^1/_2$, 19/20, 1, $1^1/_2$, 2, $2^1/_2$, 4, $7^1/_2$, 8, $15^1/_2$ and 16). It may be seen that in the region of the higher harmonics, where the excitation curves overlap each other very much, the vibration of all the resonators clearly shows the periodicity of the fundamental frequency.

basilar membrane may lead to perceptions of very divergent pitches. The frequencies 2 000, 2 200, 2 400 c/s, etc. will separately cause perceptions of pure tones with pitches of 2 000, 2 200, 2 400 c/s. Together, however, they will lead to the perception of a sharp sound with a pitch of 200 c/s. This means that for determining the pitch it is not the spot on the basilar membrane which moves (nor the particular nerve fibre stimulated) which is the deciding factor. We must rather ascribe to the nerve fibres the power of transmitting not only the quantity of the stimulus (loudness) but also the quality (pitch).

A comparison with the eye shows that this is very well possible from a neurological point of view. The basilar membrane must be considered as an analogue of the retina. The acoustic system in the inner ear represents in the optical analogy a spectroscope which "focusses" vibrations of different frequencies upon different parts of the

retina. In the older conception the ear was looked upon as a colour blind eye gazing into the spectroscope: it was able to determine the frequency from the position of the lines, for instance with the help of a scale division. According to the conception made necessary by the theory of the residue, we must, however, consider the ear as comparable to a colour-distinguishing eye looking into the same spectroscope. This eye will be able to draw a conclusion about the frequency of the light from the colour, aside from the position of the lines. In a grating spectroscope, in which spectra of different orders may overlap, this eye will even be able to recognize for instance a red line at a position where only blue lines are usually visible. In acoustic language, a component of low pitch (the residue) may originate in a region of the basilar membrane which in the case of pure tones gives the perception of high pitch.

We shall not enter more deeply into the forms in which such a "sense of colour" of the ear might be supposed to be realized [6]). We shall, however, show that the current conceptions about a local stimulation of the basilar membrane in principle do not exclude the possibility that a periodicity of the sum of a number of harmonics should occur as an actual quantity in this stimulus.

For this purpose we consider a mechanical model of the basilar membrane, which consists of a system of mechanical resonators of progressive characteristic frequency (a kind of harp). For the sake of simplicity we assume that the sensitivity of all the resonators is the same, and that the width of the resonance curves for all resonators is equal to the same percentage of the characteristic frequency, see *fig. 8a*. An ideal periodic impulse is allowed to act upon this system, the spectrum of which is given in fig. 8*b*. Each of the harmonics will set in motion a whole region of resonators to the degree given by the excitation curves which can easily be deduced from figs. 8*a* and *b*. In *fig. 9* on the left these excitation curves are drawn on a logarithmic frequency scale for the first 20 harmonics. For higher harmonics the excitation curves begin to overlap one another more and more, or in other words, one resonator will react simultaneously to a continually larger number of adjacent harmonics. Fig. 9 shows that for low frequencies, where the excitation curves do not yet overlap appreciably, regions of stimulation alternate with regions in which the stimulation is practically zero. The excited resonators here vibrate almost sinusoidally. At high frequencies, however, the seperation between the regions is lost, and the resonators now exhibit vibration forms in which the fundamental period of the periodic impulse is clearly manifested, and which possess exactly the perodicity of the fundamental tone.

If the transmitting mechanism (the nerves) were able to distinguish this periodicity, the existence of the residue as well as its pitch would be explained. In *fig. 10* we give in conclusion a comparison of the objective sound spectrum, the excitation of the system of resonators (the basilar membrane) and the components of the subjective analysis for a periodic impulse of a given width.

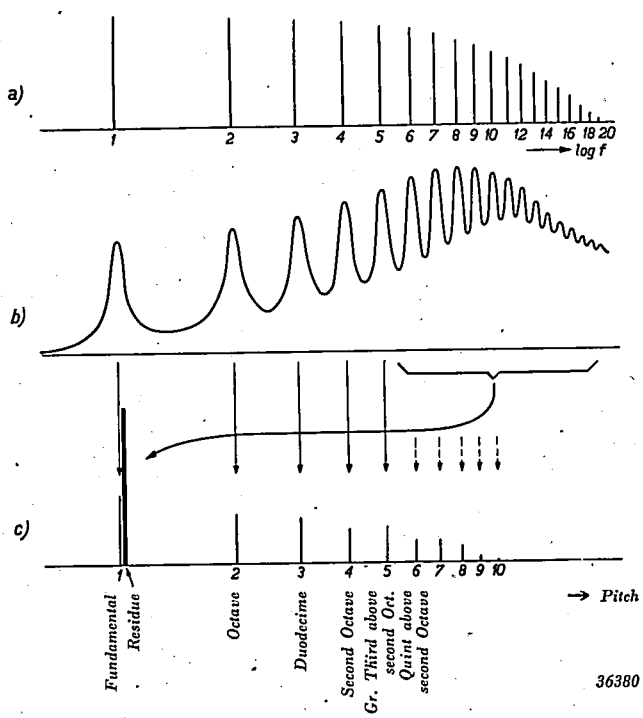

Fig. 10. Diagram of the occurrence of the subjective sound spectrum.
a) The objective spectrum of a periodic impulse with a width equal to 1/20 of the length of the period.
b) The stimulus caused by this impulse on the basilar membrane.
c) The subjective spectrum in which the ear analyses the stimulus represented by (*b*). The stimuli coming from those parts of the basilar membrane upon which the higher harmonics are localized are perceived collectively as a component of low pitch, the residue.

Applications of the hypothesis of the residue

We shall now discuss several remarkable phenomena in which the hypothesis or the residue can be applied.

Anharmonic sounds

While in the case of stringed and wind instruments, in which strings and air columns,

[6]) See in this connection: J. F. Schouten, Proc. Ned. Akad. Wet. Amsterdam **41**, 1086, 1938; **43**, 356, 1940 and **43** October 1940 (not yet published).

respectively, serve as oscillators, the frequencies of the constituent tones (harmonics) of a sound are integral multiples of the fundamental frequency, this is not the case with musical instruments with less simple oscillators. Examples of the latter are the triangle [7]) and, perhaps the most familiar, church bells. The sounds of these instruments whose vibration form is no longer purely periodic, are called anharmonic.

In the case of church bells the remarkable and long familiar phenomenon occurs that the tone by which a bell is known, the so-called strike note does not in general appear in the spectrum of the sound of the bell. While it is possible, by placing tuning forks of the corresponding frequencies upon the bell in a suitable manner, to bring them into resonance in each of the bell's characteristic frequencies, this cannot be done for the strike note. In *fig. 11a* an example of a bell spectrum is given which is characteristic of the bells cast by the Hemony brothers (seventeenth century) [8]).

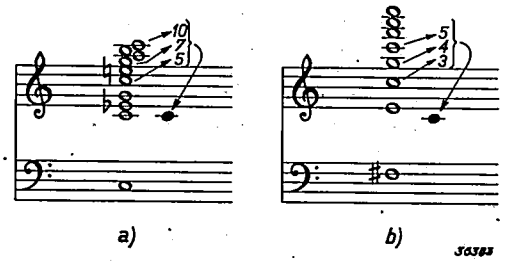

Fig. 11. *a*) Components of the sound of a church bell. The strike note is not to be found among the characteristic frequencies of the bell. Its pitch, however, usually lies very close to that of the second characteristic tone. The fifth, seventh and tenth characteristic tones form a more or less harmonic series, their frequencies are almost exactly in the ratio of 2 : 3 : 4. The strike note may be considered as the residue of these, and it therefore lies an octave below the fifth characteristic tone.
b) Components of the sound of a steel spring (of a kind of Westminster chime). The strike note is here the residue of the third, fourth and fifth characteristic tones, whose frequencies are approximately as 2 : 3 : 4. The strike note thus lies an octave below the third characteristic tone.

To what must the existence of the strike note be ascribed? Its pitch is often almost equal to that of the second characteristic frequency. The latter, however, can clearly be distinguished from the former not only by its quality — the strike note is sharp, metallic, the characteristic notes soft and pure — but also by the fact that the strike note (like the high characteristic notes) dies out relatively quickly and the second characteristic note (also called resultant tone or "hum note") only slowly [9]). Another empirical rule has been set up by Rayleigh; this may be formulated as follows. The strike note lies an octave below the pitch of the fifth characteristic frequency. The rule has also been proposed that the pitch of the strike note corresponds to the frequency difference between the fifth and seventh characteristic frequency, and this has been considered from the physical and technical point of view as the reason for explaining the strike note simply as a differential note appearing due to non-linear distortion. The Netherlander Arts [10]), however, has shown anew from extensive factual material that Rayleigh's rule is almost always better obeyed than the differential note rule. Moreover, in the case of the differential note hypothesis, the question remains unsolved as to why just the fifth and seventh characteristic notes should give a strong differential note, and why the strike note has a different sound than the other components.

The hypothesis of the residue throws some light on this problem. It may be expected that when a number of frequencies in an anharmonic spectrum chance to be integral multiples of a certain "fundamental frequency", the latter will become audible as the residue. In the case of the bell, see fig. 11*a*, the frequency ratio between the 5th, 7th and 11th characteristic frequency is in good approximation 2 : 3 : 4. These characteristic frequencies therefore would actually result in a residue whose pitch would lie an octave below the 5th characteristic tone. It is now possible to understand also why in some "ugly" bells the strike note is less clear or almost lacking: this must be the case when there is no series of characteristic frequencies in the bell spectrum which can be expressed reasonably approximately by whole numbers.

A nice confirmation of this conception was found in an investigation of the sound of a series of steel springs (a kind of Westminster chime). In fig. 11*b* a spectrum of this is reproduced. The strike note was, within 1 per cent, an octave below the third

[7]) See fig. 11 of the article referred to in footnote [1]).

[8]) This bell spectrum has the same composition for bells of different pitch, as far as the intervals of the components are concerned. In playing a melody on a chime of bells the same chord (in this case mainly the minor chord of the strike note) is heard in every sound. Debussy made an elaborate use of this property in imitating the sound of bells in his piano prelude "La cathédrale engloutie".

[9]) Here we find the perception, clearly pronounced, of two simultaneously occurring components of the same pitch and different quality, just as was found for the fundamental tone and the residue of the periodic impulse. This was already referred to by P. J. Blessing, Phys. Z. **12**, 597, 1911.

[10]) J. Arts, J. Acoust. Soc. Amer. **9**, 344, 1938 and **10**, 327, 1939.

characteristic note. The third, fourth and fifth characteristic frequencies in this case had approximately the ratio: 2 : 3 : 4.

Sounds made anharmonic artificially

It is possible to shift all the frequencies of a sound by the same number of c/s. If the sound was originally harmonic, *i.e.* if the frequencies of the components were integral multiples of the fundamental frequency, it becomes anharmonic by this treatment. The experiment can easily be carried out with the help of an apparatus for carrier-wave telephony [11]). A low frequency signal of frequency f is modulated on a carrier wave of frequency ν. The frequency $\nu + f$ obtained by filtering is modulated with a carrier wave of frequency $\nu - \Delta$ and a low frequency signal is again obtained which now has the frequency $f + \Delta$. If the repeatedly used periodic impulse with the fundamental frequency of 200 c/s is treated in this way with Δ made equal to 40 c/s, the components become 240, 440, 640 ..... c/s.

What pitch perception must now be expected of this sound? If the pitch were determined by the fundamental tone itself, it would then have to be $\Delta = 40$ c/s, *i.e.* a minor third, higher. If the pitch were determined by the differential tone, it would have to remain constant, since the distance between the harmonics is not changed by the shift. Neither of these two cases actually occurs; the pitch does change, but very little, less than half a tone. In the case of music also we found the same slight increase in pitch. This increase was measured by the comparison of two identical gramophone records, one of which was played at the normal speed and the frequencies shifted by a small amount Δ, while the other was played without the frequency shift but at such a speed (*i.e.* with multiplication of all the frequencies by such a factor), that the sound of the two records corresponded as well as possible in pitch. The result can be described by saying that the pitch is shifted relatively to the same extent as would be expected in the case of pure tones with frequencies of 1 000 to 2 000 c/s.

With the help of the residue this behaviour can be understood. Assume that a residue of the pitch 200 c/s is mainly caused by the 9th, 10th and 11th harmonics with the frequencies 1 800, 2 000, 2 200 c/s. If these frequencies are shifted to 1 840, 2 040, 2 240 c/s, respectively, they may be considered to be approximately the 9th, 10th and 11th harmonics of the frequency 204 c/s. The residue is thus shifted from 200 to 204 c/s, *i.e.* proportionally by the same amount as the frequency 2 000 c/s is shifted when $\Delta = 40$ c/s.

Partial deafness

In conclusion we should like to point out a remarkable consequence of the new hypothesis. In the case of certain defects in the sense of hearing it is only the observation of certain frequency regions which is defective. A person who is "partially deaf" in this way for all low frequencies, below 1 000 c/s for example, will not be able to hear the harmonics lying in this region, but he will be able to hear a residue with a pitch of say 200 c/s. Still more paradoxical is the behaviour which must be expected in the case of deafness for high tones. Since the high tones in a complex sound cause the residue, deafness for high tones will result in the fact that upon listening to sharp sounds one of the lowest components of the sound, the residue, will not be heard. These phenomena have not yet been investigated experimentally.

---

11) H. Fletcher, Phys. Rev. **23**, 427, 1923. In this article it is described how the complex sounds of musical instruments lose all musicality with values of Δ which are not too small.

THE FORCED AIRCOOLED TRANSMITTING VALVE TAL 12/10

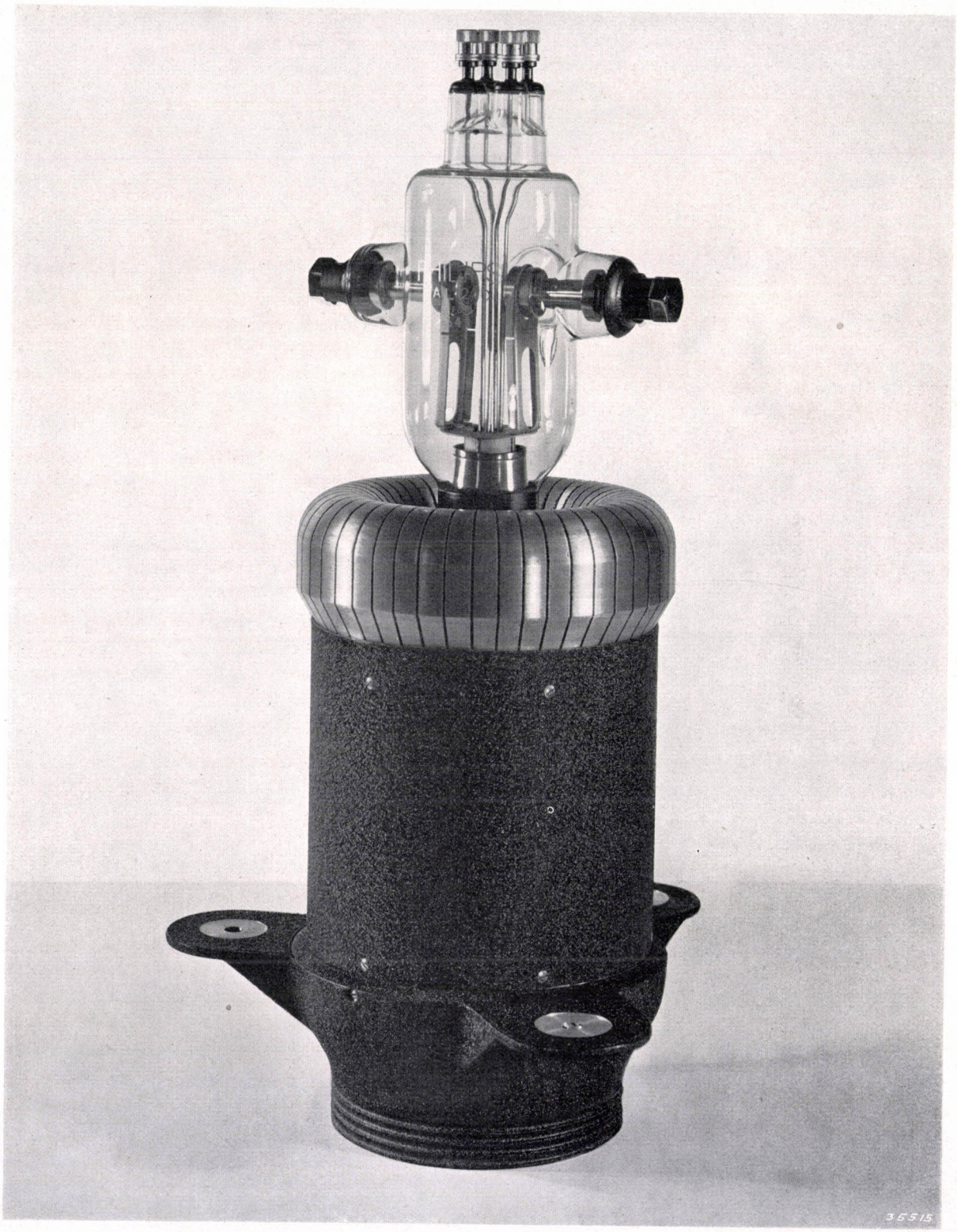

The maximum allowable anodedissipation of 4 kW is conducted from the anode by about 7.5 m^3 air per minute. In class C telegraphy adjustment the output power amounts to 10 kW and to about 6 kW in the carrier wave for anodemodulation. The air is circulated by means of a blower, enters through a number of slits. Overall length 446 mm, diameter at the cooling slits 195 mm.

NATURAL ILLUMINATION AND VISIBILITY AT NIGHT

by P. J. BOUMA. 535.241.44: 612.843.612: 628.92.024

In connection with air-raid defence it is important to know what illumination is present and what the possibility of observation is at night due to natural sources of light (moon, planets, stars, etc.). Some data are given about these facts, and these data are compared with corresponding data which were used in prescribing the legally permissible black-out illumination.

The latest branch of illuminating technology, that of black-out illumination [1]), (also called air-raid defence illumination) has stimulated fresh interest in the question of the possibilities of observation which exist at night in the complete absence of artificial illumination.

In order to judge this question two types of data are important: data about the light sensitivity of the eye, and data about the intensity of the natural illumination prevailing at night (moon, stars, planets, etc.). In the following we shall give a short survey of these data.

The absolute threshold values of the eye

Under the most favourable conditions it is possible for the eye to observe a point source of white light which produces an illumination intensity of 10^{-9} lux on the eye. If atmospheric conditions were without disturbing influence, this illumination intensity could be obtained by placing a candle at a distance of 32 km (on a tower 80 m high in order to project above the horizon)!

The pupil of the eye (8 mm in diameter) receives under these circumstances about 5×10^{-14} lumen. It is interesting to compare this with the sensitivity of photocells. When photocells are used very special measures must be taken in order to measure light fluxes of the order of 10^{-11} lumen [2]). The great sensitivity of the eye is even more clearly realized when we calculate the minimum amounts of energy necessary to cause an impression of light. If we use monochromatic light of the wave length for which the dark-adapted eye is most sensitive (5 100 Å), an energy of 4.4×10^{-17} watt or 4.4×10^{-10} erg per sec is found to be sufficient to give an impression of light [3]). An erg is approximately the amount of energy which is liberated when a weight of 1 mg is allowed to fall 1 cm. This small amount of energy, if completely converted into light of 5 100 Å, would be capable of producing in the eye a light impression during a period of 72 years. We would then receive more than 100 light quanta per second. The lowest brightness which the eye can observe under the most favourable circumstances amounts to about 3×10^{-10} stilb $= 3 \times 10^{-6}$ c.p./m^2. Such a brightness would occur if we illuminated a snow surface with a candle placed about 300 m above it; the brightness of the snow would then be a factor 30 lower than it is during a clear moonless but starry night.

Astronomical light units

In order to be able to compare the low values of illumination intensity, brightness, etc. which prevail in black-out problems, with those which occur at night naturally, we must make a few statements about the light units which are used in astronomy. There is danger of confusion in this subject because a quite different nomenclature is used in astronomical literature from that used in illumination technology. We shall therefore confine ourselves to a single universally applied concept, namely that of the magnitudes of the stars, and we shall otherwise use the nomenclature of ordinary light technology.

The magnitude of a star is a logarithmic measure of the illumination intensity which a star produces on the eye, and may be related to the light technological quantities in the following way:

a) a difference of 5 magnitudes means a factor 100 in the illumination intensity on the eye [4]);
b) a star of the first magnitude gives 8.3×10^{-7} lux at the eye.

If we also keep in mind that the astronomer ascribes a greater value to the magnitude, the weaker the star, we can formulate the relation between magnitude m and illumination intensity E in the following way:

$$m = -14.2 - 2.5 \log E$$

[1]) See also Philips techn. Rev. 4, 15, 1939, and 5, 93, 1940.

[2]) Philips techn. Rev. 4, 66, 1939.

[3]) The sensitivity of the eye expressed in energy is practically the same as that of the ear. The maximum ear sensitivity is 10^{-16} watt/cm^2 (see the article referred to in footnote [4])), while a value of 0.3 to 0.5 cm^2 is given as the effective area of the ear.

[4]) The magnitude plays the same rôle in astronomy as the decibel (phon) in acoustics (See Philips techn. Rev. 2, 47, 1937). A magnitude corresponds to 4 decibels.

The following table gives several examples

Sun	$m = -26.7$	$E = 100\,000$ lux
Full moon	$m = -12.5$	$E = 0.2$ lux (1 candle at 2.2 m)
Venus (maximum)	$m = -4.3$	$E = 1.1 \times 10^{-4}$ lux (1 candle at 100 m)
Sirius	$m = -1.6$	$E = 9 \times 10^{-6}$ lux (1 candle at 330 m)
Star of first magnitude	$m = 1$	$E = 8 \times 10^{-7}$ lux (1 candle at 1100 m)
Star of 6th magnitude	$m = 6$	$E = 8 \times 10^{-9}$ lux (1 candle at 11 km)
Star of 21st magnitude	$m = 21$	$E = 8 \times 10^{-15}$ lux (1 candle at 11 000 km)

The sun therefore gives 10^{13} times as much light to the eye as the weakest star visible with the naked eye (6th magnitude). The most powerful telescopes, aided by photography as integrating factor, add to this range of 33 magnitudes an additional range of 15 magnitudes, or a factor of 10^6 (21st magnitude).

Brightness of the night sky; illumination intensity during a clear moonless night

During a clear moonless night an average illumination intensity of about 3×10^{-4} lux occurs upon a horizontal plane. This value, derived from measurements carried out at different times and at different places on the earth's surface, is still a factor 10 to 20 smaller than the illumination level permitted in the black-out [1]). The expressions current in England such as "artificial starlight", "starlight lamps", etc. are thus rather unfortunately chosen.

To what is this illumination intensity due? One would be inclined to say: in the first place to the fixed stars which can be observed all about with the naked eye. Remarkably enough, however, this conclusion is quite incorrect. In the following we shall make an estimation of the different contributions.

a) *The direct light of the fixed stars visible to the naked eye*

It is known from star counts how many stars of each magnitude there are. If one calculates the number of stars of the first magnitude to which each of these groups is equivalent, and adds together in this way the amounts of light of all the stars to the 6th magnitude, one finds that all the visible stars together are equivalent to 148 stars of the first magnitude. If all these stars were at the zenith they would give an illumination intensity of 1.23×10^{-4} lux. This value must, however, be divided by two, since only half the stars are above the horizon, and then again divided by two, since the stars are distributed over the whole celestial hemisphere, so that the contribution of each star must be multiplied by the cosine of its angle of incidence (distance from the zenith). For the direct light of the fixed stars visible to the naked eye we obtain in this way a total contribution of $\mathbf{0.3 \times 10^{-4}}$ **lux.**

b) *The direct light of the fixed stars which are not observed individually by the naked eye*

Telescopic observations show the distribution of the fixed stars among the different magnitudes up to the 21st magnitude. The contribution of still weaker stars may be neglected. All stars from the 6th to the 21st magnitude are found to be equivalent to about 540 stars of the first magnitude. Upon application of the two corrections mentioned, we find for the total contribution to the illumination intensity $\mathbf{1.1 \times 10^{-4}}$ **lux.** The "invisible" stars thus furnish four times as large a contribution as the "visible" ones!

c) *The direct light of the planets*

When the magnitudes of the different planets are examined, the first conclusion will be that their contributions may by no means be neglected compared with that of the fixed stars. The magnitudes of Mercury, Venus, Mars and Jupiter are, respectively,

$$-0.9, \quad -4.30, \quad -1.85, \quad -2.29$$

If they were all together at the zenith the four planets would furnish a contribution of 1.45×10^{-4} lux, thus about as much as all the fixed stars together!

Actually they contribute much less, since at our latitude they are never at the zenith, while, moreover, Mercury and Venus never reach greatest height during the hours of darkness. The maximum contributions of the planets mentioned during the night amount at our latitude to about the following [5]):

Mercury 4×10^{-7} lux, Venus 4.8×10^{-5} lux,
Mars 1.1×10^{-5} lux, Jupiter 1.6×10^{-5} lux.

Thus a total of 7.5×10^{-5} lux.

[5]) Mars and Jupiter at the mean opposition, Venus and Mercury in their most favourable phases, as far as these may occur at least 1 hour after sunset.

Since these maxima, especially in the case of Mercury and Venus, prevail for very short times, the average contribution is much less still; it is estimated to be about $\mathbf{0.1 \times 10^{-4}}$ **lux.**

d) The scattered light of stars and planets

The order of magnitude of the part of the starlight which is scattered by the atmosphere can be estimated by noting that in this country (the Netherlands) the brightness of the unclouded sky in the summer at noon is an average of about 0.4 stilb, and would therefore furnish about 12 600 lux on the earth. This is about one eighth of the contribution furnished by the direct sunlight. If the same rule holds for scattered starlight, we obtain a contribution of $\mathbf{0.2 \times 10^{-4}}$ **lux.**

e) Other sources

The contributions mentioned until now give a total of 1.7×10^{-4} lux, so that about $\mathbf{1.3 \times 10^{-4}}$ **lux** must be ascribed to other sources (zodiacal light, northern lights, unknown sources). The table below gives a survey of the values found.

	E	%
a) Direct light of "visible" fixed stars	$0.3 \cdot 10^{-4}$ lux	10
b) Direct light of "invisible" fixed stars	$0.1 \cdot 10^{-4}$ lux	37
c) Direct light of planets (Mean valve)	$0.1 \cdot 10^{-4}$ lux	3
d) Scattered light of stars and planets	$0.2 \cdot 10^{-4}$ lux	7
e) Other sources	$1.3 \cdot 10^{-4}$ lux	43

About 13 per cent of the light thus comes directly from the visible sources, the other 87 per cent is observed as the brightness of the night sky itself. From this we calculate an average brightness of the night sky of 8.4×10^{-9} stilb, in good agreement with direct measurements of this quantity. This brightness is higher than the lowest observable brightness by a factor of about 30. It also shows why we can only observe stars to the 6th magnitude with the naked eye, and not to the 8th, as would follow from the threshold value of the eye mentioned at the beginning.

Possibilities of observation at these low levels of brightness

In order to obtain an idea of the possibilities of observation at very low levels of brightness, we shall mention several quantities which characterize the power of the eye under three different conditions:

I) with full moon,
II) at the illumination level which is considered just permissible in a black-out,
III) under a clear moonless sky with stars.

The illumination intensities on the ground amount to about the following for these three cases:

I) 0.2 lux, II) 0.004 lux, III) 0.0003 lux.

If it is assumed that the average reflection coefficient of the earth is about 15 per cent, the eye of a pilot will become adapted to the following levels of brightness:

I) 10^{-2} c.p./m^2,
II) 1.9×10^{-4} c.p./m^2, III) 1.5×10^{-5} c.p./m^2.

The sensitivity to contrast of the eye under these conditions can best be characterized by the percentage contrast which large dark objects must have with the surroundings, in order to reach the limit of observability for the pilot. As laboratory values we find:

I) 16 per cent, II) 46 per cent, III) 74 per cent.

Since in practice observation is always considerably less favourable, we may draw the following conclusion: large objects which are considerably darker than their surroundings can never be observed by a pilot by the light of the moonless starry sky; at the level of brightness II of the legally permissible black-out illumination they may under very favourable conditions just reach the limit of observability, while by moonlight, dark objects can often be observed.

The situation is quite different for objects which are considerably brighter than their surroundings. This case will be avoided as far as possible by blacking out; such objects will, however, occur on clear moonless nights. It may be remarked that when the eye is sufficiently adapted, the trees and the roofs of houses may very clearly be seen against the bright sky. The pilot will therefore also be able to observe large objects clearly if their brightness is at all comparable with that of the night sky. The situation may occur in the case of surfaces of water in which the sky is reflected. Experience has indeed shown that even on moonless nights coastal regions, lake regions, broad rivers are clearly observable. Very light coloured roads (with a reflection coefficient of 25 to 30 per cent) may under the most favourable circumstances still just reach the limit of visibility.

Concerning the possibility of recognizing objects it may be remarked that the visual acuity for objects which are a factor two brighter than their sur-

roundings amounts to about the following for the three levels of brightness mentioned:

$$\text{I) } 4', \quad \text{II) } 40', \quad \text{III) } 1^\circ\,50';$$

for objects which are a factor ten brighter than their surroundings:

$$\text{I) } 2', \quad \text{II) } 20', \quad \text{III) } 55'.$$

If we assume that in practice these figures lie about a factor two higher than the laboratory values here given, this means that by moonlight and at an altitude of 500 metres the pilot can still observe details of 1.2 and 0.6 metres, respectively. At the level II) of the blacked out city care must be taken that such objects do not occur. On a moonless night only those objects which are very much brighter than their surroundings can be observed. For these objects details of 16 metres will lie on the limit of distinguishability from an altitude of 500 metres. This estimation agrees with the fact that narrow brooks cannot be seen, while broad rivers, on the other hand, can be very well followed along their whole course.

In conclusion it must be noted that the illumination intensity which a point source of light must throw upon the eye of the observer in order to reach the limit of visibility was found in laboratory experiments to be the following:

With absolutely dark blackground 10^{-9} lux. With adaption level I) 3×10^{-8} lux, II) 6×10^{-9} lux, III) 2×10^{-9} lux.

The practical values lie about a factor 6 higher, thus I) 1.8×10^{-4} lux, II) 3.6×10^{-8} lux, III) 1.2×10^{-8} lux. It is quite clear from these values that, as the general illumination level becomes lower, we must be more and more careful to avoid the occurence of small points of light: on a moonless night it is possible to observe light points 15 times weaker than by full moon!

THE MEASUREMENT OF VERY SMALL PHASE DISPLACEMENTS

by C. G. KOOPS.

621.317.374 : 621.319.4

For various applications in the sphere of telephony, condensers and coils are needed with extremely small losses (phase displacements of the order of 10^{-5} to 10^{-6} radians). In order to measure such small loss angles in one of the ordinary bridge connections, standard condensers are necessary, which themselves have practically no losses. A standard condenser is here described in which the phase displacement has been successfully limited to several times 10^{-8}. The standard condenser has the character of a so-called three-point capacity: the capacity between two of the three electrodes only is free of losses. The two other capacities are rendered harmless for the purposes of the measurement by means of an auxiliary bridge connection and by the application of a substitution method. The influence of the drift of the capacities which have been rendered harmless is limited by means of a second auxiliary bridge connection. Consideration of the possible errors of measurement shows that with the measuring arrangement arrived at in this way phase displacements can be determined with an absolute accuracy of 3×10^{-8}.

In alternating current technology when one speaks of self-inductances and capacitances, impedances are meant in which the current lags or leads 90° in phase with respect to the voltage. In the coils and condensers intended for the practical realization of these impedances the phase shift is always a certain angle δ, depending more or less upon the frequency, smaller than 90°. While in the case of a phase shift of exactly 90° the impedance dissipates no energy, when the phase angle is smaller this is no longer true, and it is for this reason that the phase displacement from 90° is also called the loss angle. Phase displacement is usually indicated by its tangent; for small values of δ, $\tan\delta \approx \delta$ (in radians).

Wherever self-inductances or capacitances are applied technically attempts will be made to keep the losses, and thus the phase displacement δ, low. The requirements thereby made are very different. In the case of power condensers, for example, which are used for the improvement of the power factor, it is already enough if the phase displacements are not greater than several times 10^{-3} or 10^{-2}. Considering the other losses occurring in high power installations, this energy loss is practically unimportant, and the heat development which accompanies it can relatively easily be controlled. In other cases on the other hand, particularly in telephony, in the condensers and coils for filters and in the coils for loaded cables, the problem is to limit the losses to the very minimum. This is particularly important in the case of the filter elements, in order to be able to make the boundary of the transmitting region as steep as possible; in the case of coils for loaded cables, in order to make the damping of the cable small and at the same time the distance to be bridged (without amplification) as large as possible.

The reduction of the phase displacement of these coils and condensers is one of the most important branches of development in the subject of telephony. Because of this fact one must be able to measure very small phase displacements with great accuracy in order to detect causes of losses and to test improved constructions. The installation which has been constructed for the purpose in this laboratory will be described in the following. It is first necessary to discuss briefly the nature of the phase displacement and several concepts used in this connection.

Interpretation of the phase displacement

In order to interpret the phase displacement by means of familiar concepts in alternating current technology an equivalent circuit can be made for the coil or condenser, *i.e.* connections which (at the frequency in question) have the same electrical properties, but consist only of ideal self-inductions, capacities and resistances (in an ideal resistance current and voltage are exactly in phase). Two equiv-

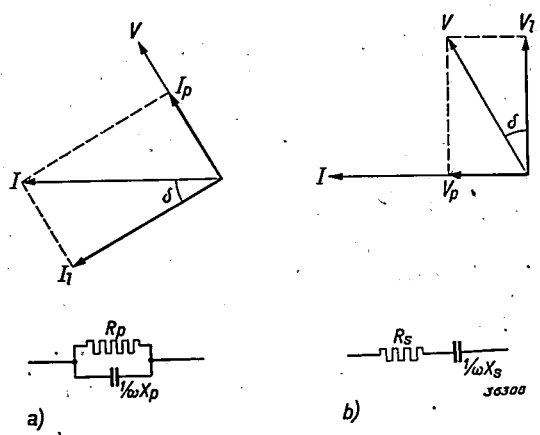

Fig. 1. The vector diagram of a condenser with phase displacement δ can be interpreted in two ways, which lead to two different equivalent circuits. The losses are thereby expressed in a certain parallel conductance $1/R_p(a)$ or a certain series resistance $R_s(b)$.

alent circuits are possible, and these are shown in *fig. 1* for the case of a condenser. In the vector diagram fig. 1*a* the current vector I is divided into two components I_p and I_l, which are parallel and perpendicular, respectively, to the voltage vector V. This vector diagram may be considered as a diagram of a connection in parallel of an ideal resistance $R_p = V/I_p$ and an ideal condenser with the reactance $X_p = V/I_l$. It may be seen that

$$\tan \delta = I_p/I_l = X_p/R_p \quad \ldots\ldots \quad (1)$$

$1/R_p$ is called the effective parallel conductance. The smaller it is, the more closely the ideal case ($\delta = 0$) is approached.

In the vector diagram fig. 1*b* the voltage vector V is divided into two components V_p, V_l. This is the diagram of a connection in series of an ideal resistance $R_s = V_p/I$ and an ideal condenser with the reactance $X_s = V_l/I$. Thus

$$\tan \delta = V_p/V_l = R_s/X_s \quad \ldots\ldots \quad (2)$$

R_s is called the effective series resistance. For the ideal case it approaches zero.

If in practice one is concerned with a connection in parallel of several condensers, it is often easy to use the method of representation of fig. 1*a*, since then all the parallel conductances $1/R_p$ may simply be added together, like all the "effective" capacities $1/\omega X_p$. In connections in series it is easier for a similar reason to use the interpretation according to fig. 1*b*. The figures and symbols are also valid *mutatis mutandis* for a self-induction.

When δ is very small, *i.e.* when only very small losses occur in the condenser or the coil, $I_l \approx I$ and $V_l \approx V$. Then

$$X_p = \frac{V}{I_l} \approx \frac{V}{I} \approx \frac{V_l}{I} = X_s = X.$$

In that case one may speak of a definite capacity $C = 1/\omega X$ or self-inductance $L = X/\omega$, practically independent of the frequency. The quantities R_p and R_s, however, will in general depend fairly closely upon the frequency.

If a coil and a condenser are connected in series the diagram of fig. 1*b* may again be applied for each, and the series resistance of the resulting equivalent circuit is the sum of the two separate series resistances R_s. This sum can be measured directly when the condenser is variable and has been brought into resonance with the coil; in that case of course current and voltage are in phase. If the value of R_s for the condenser is known, it is found for the coil in this way, and it is clear that in arranging a method of measuring its phase angle one may decide to investigate either coils or condensers. Our method of measurement was developed for condensers, and we shall in the following speak only of condensers.

General method of measurement

For the investigation of condensers bridge connections are universally used which permit very sensitive and accurate measurements. In the course of time a large number of such connections have been developed, each of which has its particular advantages and disadvantages. They have, however, one property in common: they always give the result in the form of the difference in $\tan\delta$ of the condenser being examined and that of a comparison condenser. We shall explain this for a simple bridge, the equal-armed bridge represented in *fig. 2*.

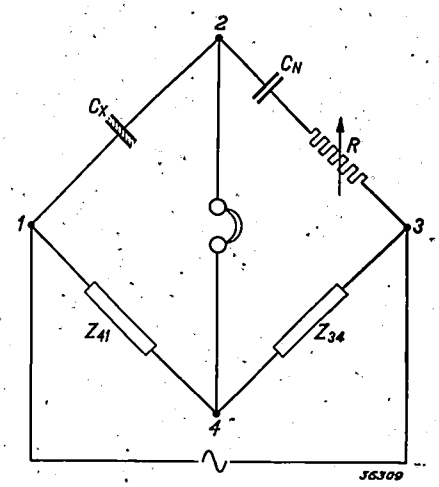

Fig. 2. Equal-armed bridge for the determination of the phase displacement of a condenser C_X. C_N is a standard condenser. The impedances Z_{41} and Z_{34} are made equal, the bridge is then brought into equilibrium by the adjustment of C_N and R.

The condenser to be investigated C_X may have a certain phase displacement δ_X, the variable standard condenser C_N a phase displacement δ_N. R is a variable resistance, Z_{41} and Z_{34} are two impedances which are made accurately equal to each other with regard to magnitude and phase angle. If an A.C. voltage is applied to the points *1* and *3* with the frequency for which δ_X is required, C_N and R_N can be so adjusted that the points *2* and *4* take on the same potential. This is controlled by means of a detection apparatus connected between *2* und *4*, an amplifier with telephone, for instance. With the correct adjustment the impedance between *1* and *2* is equal to that between *2* and *3* with respect to magnitude and phase angle, *i.e.* the effective series resistances of both arms are the same and the effective reactances also; therefore

$$R_X = R + R_N,$$
$$C_X = C_N.$$

From this it follows with equation (2) that

$$\tan \delta_X = R\omega C_N + \tan \delta_N \quad . \quad . \quad . \quad . \quad . \quad (3)$$

From the quantities to be read off R, C_N, ω therefore, it is only possible to calculate the difference $\tan \delta_X - \tan \delta_N$. Similar considerations lead to corresponding results for other bridge connections.

In order to be able to determine $\tan \delta_X$, $\tan \delta_N$ must either be known or else be so small that it may be neglected as compared with inevitable measuring errors. In practice the latter case will always be aimed at, because $\tan \delta_N$ may vary somewhat with the temperature, etc. and with a large value of $\tan \delta_N$ it would be necessary to know these fluctuations accurately and take them into account.

If for instance C_X is a paper condenser in which $\tan \delta$ may amount to several times 10^{-3} or even to 10^{-2}, an air condenser or a good mica condenser may be used as standard C_N. Such condensers have a $\tan \delta_N$ of the order of magnitude of 10^{-5} to 10^{-4}, which is small enough to be neglected, since the phase displacement of paper condensers may vary as much as 5 per cent with the temperature, the humidity of the air, etc., and it is therefore of no use to measure it more accurately.

If, however, one is concerned with smaller phase displacements, the requirements made of the standard condenser are more severe. In our case it was required that it should be possible to determine the phase displacement of a (variable) air condenser with an absolute maximum error of 10^{-6}. This meant, therefore, that we needed a standard condenser (or several standard condensers, since the measurement had to be carried out at different values of the capacity) with a value of $\tan \delta_N$ smaller than 10^{-6}.

Construction of the standard condenser

How can a condenser be constructed with such slight losses? This is in fact again the problem which formed the point of departure of this article, namely the problem of reducing the phase displacement of a condenser to the extreme minimum. The difference is only that in constructing a standard condenser we are not bound to the same degree by consideration of expense and size, etc., as in the construction of condensers and coils for technical use.

The physical causes of losses in condensers are chiefly the following:

1) The ohmic resistance of the connections and condenser plates, which would already involve a dissipation with direct current, while at higher frequencies the dissipation becomes still greater due to the eddy currents which appear.
2) A conductivity of the dielectric (insulation resistance for direct current is not infinitely high).
3) A conductivity in limited regions of the dielectric, for instance in parts with lattice disturbances in crystals, or in semi-conductive impurities in an otherwise insulating dielectric. These losses are not manifested with direct current, but at sufficiently high frequencies they may play a very important part.
4) If the dielectric contains polar molecules, *i.e.* molecules which form permanent dipoles, such, for example, as the molecules of water, these molecules tend to orient themselves in the direction of the applied electric field. With alternating current the dipoles must therefore turn back and forth with the frequency of the voltage. In doing this they experience a kind of frictional resistance in the medium, which results in the dissipation of energy. At very low frequencies (direct current) these losses disappear, and the same is true at very high frequencies, since in that case the dipoles are no longer able to follow the alternations, and thus remain practically at rest.

If it is desired to decrease the phase displacement of a condenser to the utmost, provision must therefore be made for very small resistance of contacts and connections, and a substance must be chosen as dielectric which everywhere possesses a very low conductivity and which contains no polar molecules. These requirements are very well satisfied by dry, dust-free air; the molecules of air are not polar and the insulation resistance is very high when the voltage to be applied remains below the value at which ionization by collision begins to occur.

There are, however, other things to consider. We must now assemble the electrodes of the condenser

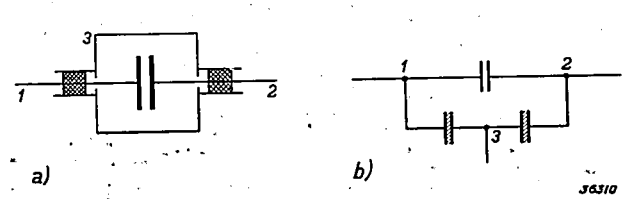

Fig. 3. Principle of the standard condenser. The electrodes *1* and *2* are so assembled (*a*) that no leakage current can flow directly from one to the other, and that no lines of force can pass from one to the other through solid insulation material. In parallel with the loss-free capacity *1-2* are the two capacities *1-3* and *3-2* in series which are not free of loss (three-point capacity, see *b*). The auxiliary capacities are rendered harmless in the measurement by a method discussed later.

so that they are insulated from each other. To do this it is unavoidable that some kind or other of solid insulation material must be introduced into the electric field between the electrodes or connections, and in this solid dielectric losses again occur, much larger than those in air, not only due to the smaller insulation resistance of the solid substance, but also due to the polarisation always occurring in it.

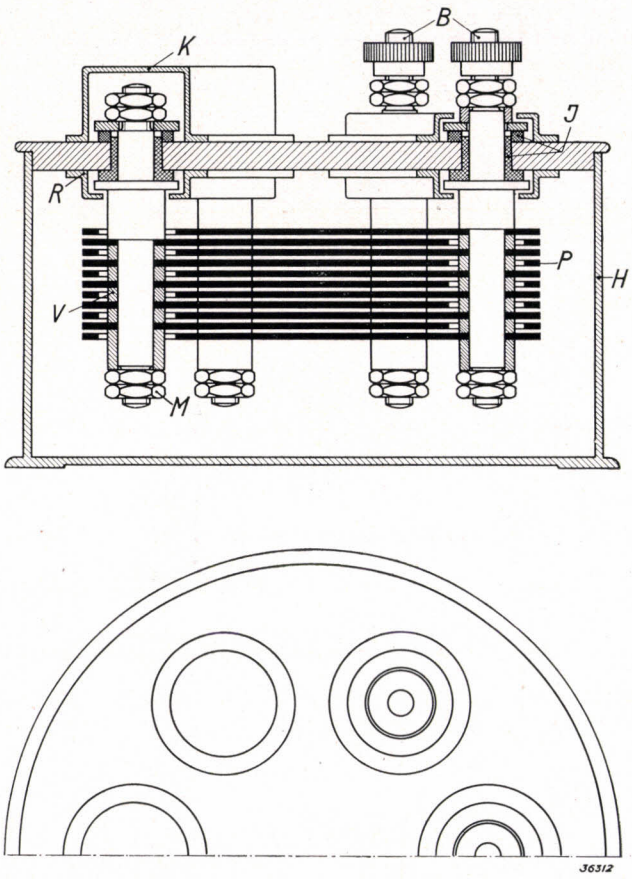

Fig. 4. Construction of the standard condenser. Three pillars, placed in a triangle, support one set of plates *P*, three other pillars in a triangle rotated 60° with respect to the first support the second set of plates lying between the first. This is shown clearly in the detail sketch. The plates are held the correct distance apart by means of distance pieces *V* which are secured by the nuts *M*. The pillars are fastened into the metal housing *H* (the third electrode, see fig. 3) with an insulation of high-frequency "Philite". The metal guard rings *R* and caps should be noticed, which shield the insulation and the free ends of the pillars in order to prevent an undesired "leakage of lines of force". *B* are the two binding posts.

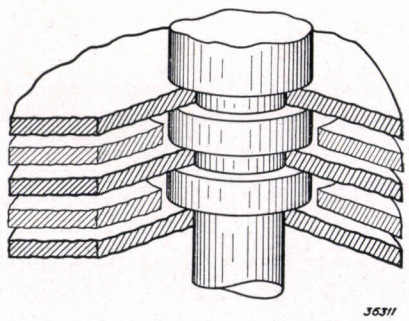

Fig. 4*a*. Detail of the construction.

These losses can now be rendered harmless by application of the principle illustrated in *fig. 3a*. The two electrodes are assembled with mutual insulation in, and entirely surrounded by a metal housing which serves as third electrode, and which can be brought to a certain potential. No leakage current can now flow directly from pole *1* to pole *2*, and with suitable construction no lines of force running from *1* to *2* can anywhere encounter a solid substance. The direct capacity between the points *1* and *2* is therefore practically entirely free of losses. It is, however, true that we have gained two additional capacities in parallel with *1-2* (fig. 3*b*), namely between *1* and *3* and between *2* and *3*, which may have quite considerable losses. By means of a special bridge connection which will be discussed later, it can, however, be brought about that only the capacity between *1* and *2* of the three-point capacity *1-2-3* makes itself felt in the measurement.

Fig. 4 shows how the principle described is realized. The condenser plates are borne by two sets of pillars which are fastened in the upper plate of the metal housing with an insulation of high-frequency "Philite". It is essential that metal guard rings and caps should be placed on the plates to which the pillars are fastened as well as on the free ends of the pillars and connected to the housing, in order to avoid as far as possible the danger that lines of force between poles *1* and *2* should cut the "Philite".

When we have rendered the insulation material harmless in this way, there still remains a spot where the electric field passes through a solid dielectric, namely on the condenser plates themselves. In the case of the metals usually used for this purpose the surface is never entirely clean, but always bears a semi-conducting film of oxide. This could only be avoided by using a precious metal such as gold. If, however, massive plates are used, this would be much too expensive, since in order to avoid any microphone effect (the capacity must be fixed within 10^{-4} per cent) the plates must be very thick, and in order to obtain the desired capacities a fairly large surface of plate is required. Gilding the plates was also found to be impossible, since alloys were formed with the underlying metal. The evil of the oxide film could, however, be very much limited when the plates were made of aluminium or covered with a layer of aluminium. An oxide film is then formed, it is true, but it is much

thinner than with other metals (several microns), and thanks to its poor conductivity it has only a very small phase displacement.

Determination of the remaining losses of the standard condensers

What will be the error in the determination of tan δ in the measurements if we neglect the losses of the standard condenser itself? In other words how large may the losses be which the standard condenser still has in spite of the preventive measures described above?

The phase displacement due to the losses in the metals, *i.e.* the resistance of pillars, plates and contacts (as well as eddy current losses occurring at higher frequencies) still remains below the accuracy of measurement attained with our bridge connections, even at the highest frequency with which we are concerned (8 000 c/s), as calculations show. The same is true of the estimated losses in the air. We have therefore still to consider only *a*) the losses in the oxide films which cause a phase displacement δ_a and *b*) the remaining losses in the solid insulation material which lead to a phase displacement δ_b. The total phase displacement of the condenser is then

$$\delta = \delta_a + \delta_b.$$

(Since we are concerned with very small angles we may here consider the angle itself instead of its tangent).

In order to determine δ we have constructed different standard condensers — as has already been stated, a number of them were needed —, whose construction differed in such a way that either δ_a or δ_b was changed in a known manner. The differences in δ for each pair of standards can be measured directly, according to equation (3), and in this way sufficient equations were obtained to calculate all the values of δ_a and δ_b separately.

In practice this was done in the following way. Two standard condensers C_1 and C_2 were made each of 100 pF [1]), furthermore a condenser C_3 of 200 pF. In the case of C_1 and C_3 the distance between the plates was 1 mm. In C_2 it was 5 mm (C_2 therefore also had a surface 5 times as large as C_1) while in other respects the construction of all was the same. It is obvious that if the oxide film is much thinner than the distance between the plates, δ_a is inversely proportional to the latter. Thus for the condenser C_1 δ_a is 5 times as large as for C_2, while for both condensers δ_b must have the same value, since the condensers are identical in all details which can influence δ_b. By measuring the difference in δ for C_1 and C_2, δ_a can be calculated for both condensers. The measurement was carried out at 1 000 c/s and at 8 000 c/s, and gave for both frequencies a value $\delta_a \approx 5 \times 10^{-8}$ for C_1 and $\delta_a \approx 10^{-8}$ for C_2. The value of δ_a for C_3 is the same as for C_1 since the two condensers have the same distance between the plates.

C_1 and C_2 were now connected in parallel giving a capacity of 200 pF which could be compared in the bridge with C_3. The parallel conductance of type b) in C_3 is equal to that in C_1 or C_2, and in $C_1 + C_2$ it is twice as much. By measurement of the difference in δ for C_3 and $C_1 + C_2$, δ_b could also be calculated for all three, since δ_a is already known for all three. The value of δ_b was found to lie below the limit of accuracy of our bridge.

In order to cover the whole desired capacity region a standard of 1 000 pF had also to be constructed; by a measurement in different steps the above result could be tested and confirmed with this standard.

[1]) The abreviation *p* (pico) is equivalent to $\mu\mu$ and means a factor 10^{-12}; 1 pF is thus 1 $\mu\mu$F = 10^{-12} F.

The total phase displacement of the standard condenser obtained amounts, according to these results, to several times 10^{-8}, and may therefore certainly be neglected in the measurements which we had in mind, where an accuracy of 10^{-6} was required.

Connections of the measuring bridge

From the description of the standard condenser it has already appeared that our measurements would be entirely wrong if we introduced the standard condenser into the bridge connections of fig. 2 in place of C_N without further precautions. If this were done, the two auxiliary capacities of the standard condenser connected in series would then be in parallel with C_N (see fig. 3*b*). Moreover, it is necessary to surround the whole bridge by an earthed screen in order to avoid disturbing influences from the outside (hand effect). By this means considerable additional parasitic impedances between points on the bridge and earth are introduced. If the housing of the normal condenser is also earthed, it is easy to divide the disturbing parasitic impedances into two groups: those between bridge points and earth, and those between points on an arm of the bridge and earth. We shall consider these in succession.

Parasitic impedances between corners of the bridge and earth

The error which is caused by parasitic impedances between corners of the bridge and earth may be understood as follows. The bridge is so balanced that the detection apparatus is silent, and from this we conclude that the current in the bridge arm from *1* to *2* is the same as in the arm from *2* to *3*, from which Wheatstone's condition follows. The conclusion as to the equality of the currents from *1* to *2* and from *2* to *3*, however, is only justified when from point *2* no appreciable current flows

to earth, *i.e.* when there is no parasitic impedance between *2* and earth.

The parasitic impedance actually present can now be rendered harmless by means of an auxiliary bridge connection (earth connection according to Wagner) which is given in *fig. 5*. The corner *5* of

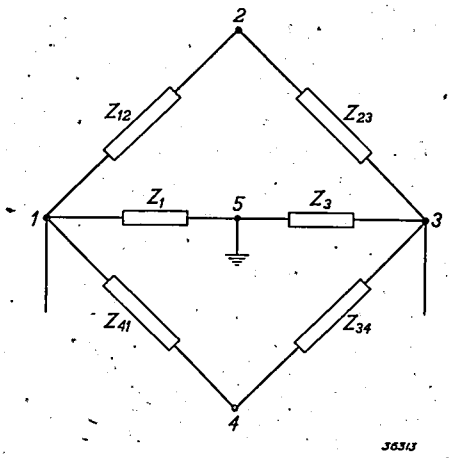

Fig. 5. Auxiliary bridge connection (earth connection according to Wagner). By balancing the (partially parasitic) impedances Z_1 and Z_3 all the parasitic impedances between the corners of the bridge and earth are rendered harmless.

the auxiliary bridge arms is earthed, and the impedances Z_{12}, Z_{23}, Z_{34}, Z_{41} of the four arms of the main bridge, as well as the impedances Z_1, Z_3 of the auxiliary bridge are so balanced that the detector gives no signal when connected between *2* and *5* and between *4* and *5*. In this case *2* and *4* are at earth potential and therefore no current can flow through parasitic impedances between *2* or *4* and earth. The current from *1* to *2* is thus indeed equal to that from *2* to *3*, and that from *1* to *4* is equal to that from *4* to *3*, so that Wheatstone's equation is valid

$$Z_{12}Z_{34} = Z_{23}\,Z_{41} \quad . \quad . \quad . \quad . \quad . \quad (4)$$

At the same time the corresponding condition for the auxiliary bridge:

$$Z_{41}Z_3 = Z_{34}\,Z_1 \quad . \quad . \quad . \quad . \quad . \quad . \quad (5)$$

must also be satisfied, where the parasitic impedances between *1* and *3* and earth are taken into account in Z_1 and Z_3, respectively. The parasitic impedances of all four corners of the main bridge are rendered harmless in this way.

The method consists practically in the fact that we introduce into the equal-armed bridge of fig. 2 the arms *5-1* and *5-3*, each of which consists of a variable condenser with a variable resistance in parallel with it. By adjustment of the condenser and the resistance we can make the total impedance between *5* and *1* (*i.e.* including the parasitic impedance) equal to that between *5* and *3*.

The drift of the parasitic impedances

A new difficulty now appears: the parasitic impedances are not constant. They are formed by all kinds of capacities, especially those between connections, transformers, etc. and earth, all of which have large phase displacements. These phase displacements, and with them the effective capacities also, depend very much upon the temperature and other circumstances. The result is that the adjustment of the auxiliary bridge would have to be continually controlled, or, since this is scarcely possible in practice, that a certain error Δ is continually made in the balancing of the main bridge. By this we mean that the detection apparatus is silent when it is not true that

$$Z_{12}Z_{34} - Z_{23}Z_{41} = 0$$

(equation (4)), but when

$$Z_{12}Z_{34} - Z_{23}Z_{41} = \Delta.$$

Let us now consider the bridge in fig. 5 once more, including the (parasitic) impedances Z_2 and Z_4 between *2* and *4*, respectively, and earth (see *fig. 6*).

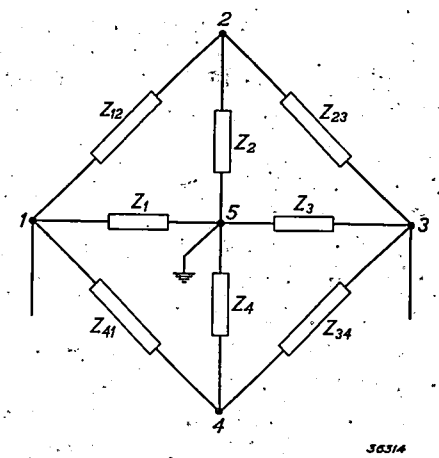

Fig. 6. Entirely symmetrical bridge with two auxiliary bridge connections. By balancing the (originally exclusively parasitic) impedances Z_2 and Z_4, the influence of the drift of all the parasitic impedances is limited.

The general proposition can then be proved: that from the fact that a detector introduced between *2* and *4* is silent, equation (4) may be considered to hold, if

$$(Z_1Z_{34} - Z_3Z_{41})\,(Z_4Z_{12} - Z_2Z_{41}) = 0 \quad . \quad (6)$$

That is, all the parasitic impedances of the corners of the bridge are harmless if we make either

$$Z_1Z_{34} - Z_3Z_{41} = 0 \quad . \quad . \quad . \quad . \quad . \quad (5a)$$

(this was the earth connection according to Wagner described above) or

$$Z_4Z_{12} - Z_2Z_{41} = 0 \quad . \quad . \quad . \quad . \quad . \quad (5b)$$

If, however, in the adjustment of the first auxiliary bridge (Z_1, Z_3) an error Δ_1 was made, and in that of the second auxiliary bridge (Z_2, Z_4) an error Δ_2, so that instead of (5a, b) the following is valid:

$$Z_1Z_{34} - Z_3Z_{41} = \Delta_1,$$
$$Z_4Z_{12} - Z_2Z_{41} = \Delta_2,$$

then the error in the main bridge is found to be proportional to these two errors:

$$\Delta \sim \Delta_1 \cdot \Delta_2 \quad . \quad . \quad . \quad . \quad . \quad . \quad . \quad (7)$$

In the case of the simple earth connection according to Wagner first described, we attempted to make $\Delta_1 = 0$, but disregarded the error Δ_2. The result, since Δ_2 may have an appreciable value, was that there was immediately a considerable error Δ at the least deviation of Δ_1. The remedy is now obvious. While the conditions (4) and (5a) for the balancing of the bridge remain valid, Z_2 and Z_4 will at the same time be so chosen that equation (5b) is satisfied. In the bridge which we constructed Z_2 was a fairly large parasitic capacity. By connecting in parallel with the parasitic impedance between 4 and earth, another variable self-induction with a variable resistance in series, Z_4 could be so adjusted that $Z_4 Z_{12} - Z_2 Z_{41} = \Delta_2 = 0$. Upon a drift in the impedance both factors which cause an error in the adjustment of the main bridge (equation (7)), now remain sufficiently small.

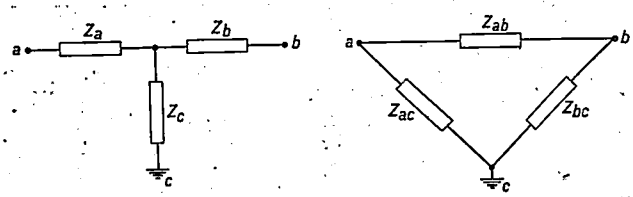

a) b)

Fig. 7. The parasitic impedance Z_c between a point on the arm of the bridge a-b and earth is equivalent to two parasitic impedances between the corners of the bridge a and b and earth, in which the effective impedance of the bridge arm Z_{ab} is not equal to $Z_a + Z_b$.

Parasitic impedances between points on the bridge arms and earth

In the case of the second group of parasitic impedances, those between points on an arm of the bridge and earth, we must pay particular attention to the auxiliary capacities of the standard condenser. In the bridge given in fig. 2 (see also fig. 8*a*) the standard condenser C_N was situated in one arm in series with the resistance R, from whose adjustment the phase displacement δ_X was calculated. Between the condenser pole connected to R and the earthed condenser housing there exists a considerable parasitic impedance. What results may this have on the measurements?

The configuration is of the type represented in *fig. 7a*. The impedances Z_a (*i.e.* the loss-free capacity C_N) and Z_b (*i.e.* the resistance R) together form the arm of the bridge, Z_c is the parasitic impedance. The star connection of fig. 7*a* is equivalent to a triangle which is represented in fig. 7*b*. The impedance Z_{ab} in the latter is

$$Z_{ab} = Z_a + Z_b + \frac{Z_a Z_b}{Z_c} \quad . \quad . \quad . \quad . \quad (8)$$

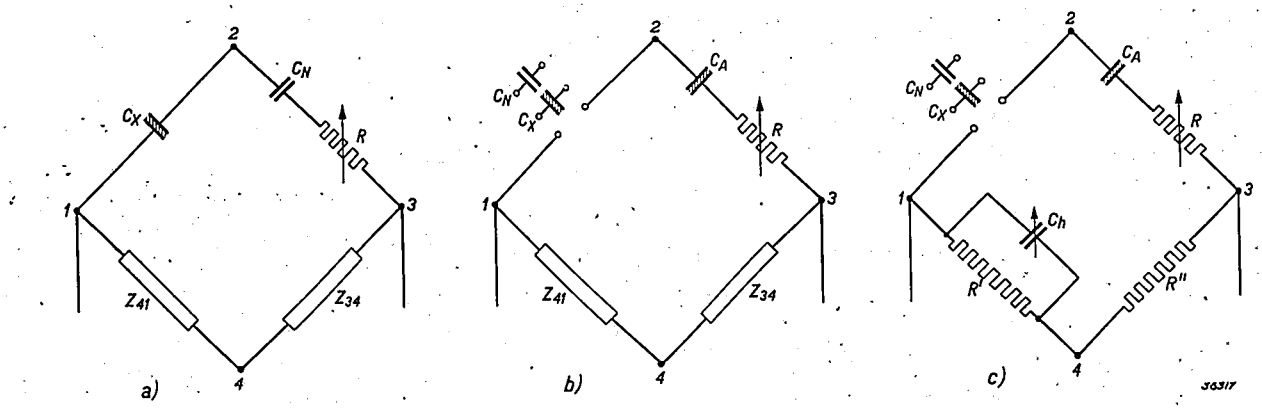

Fig. 8.*a*) Equal-armed bridge, as fig. 2.
b) Equal-armed bridge with application of a substitution method. As comparison condenser C_A a condenser is taken of about the same quality as the condenser C_X being examined. Since C_A has losses and C_N has none, negative values of the series resistance R would be necessary to bring the bridge into equilibrium.
c) By taking for Z_{41} and Z_{34} two equal resistances R' and R'' and introducing a variable auxiliary condenser C_h in parallel with R' the bridge can be brought into equilibrium with positive values of R.

The impedances Z_{ab} and Z_{bc} may be considered as parasitic impedances between corners of the bridge and earth, and thus play no part in the application of the auxiliary bridge connections. The effective impedance of the bridge arm is given by (8), while neglecting Z_c, we had considered the sum $Z_a + Z_b$ as the effective impedance. We thus make an error

$$\Delta Z_{ab} = Z_a Z_b / Z_c.$$

In our standard condenser of 100 pF the auxiliary capacity $C_p \approx 80$ pF, therefore

$$\Delta Z_{ab} = R \cdot C_p / C_N = 0.8\, R.$$

Thus, while in our measurements of loss R must be determined accurately to within fractions of a hundredth of one per cent, we must here introduce a correction of 80 per cent! It is unnecessary to state that this would make the measurements very difficult and unreliable, considering the lack of constancy of C_p.

We have avoided this difficulty by the application of a substitution method, see *fig. 8b*. In the arm *1-2* the condenser being examined C_X and the standard condenser C_N are successively introduced, while the adjustable resistance R, which is connected in the arm *2-3* in series with an arbitrary comparison condenser C_A is in each case so adjusted that the bridge reaches an equilibrium. The difference between the two values of R gives the effective series resistance, and thus the phase displacement of C_X. The difficulty mentioned — that of the parasitic impedance between the condenser pole at the middle of the bridge arm and earth — does not occur at the point of connection between C_A and R, if we take for C_A a variable air condenser of the ordinary type which can be purchased (C_A must be of about the same quality as C_X). With these condensers, which have no third electrode, the housing is connected to one electrode, so that the other electrode is entirely surrounded by it, see *fig. 9*. By connecting the housing to point *2* of the bridge, and also by surrounding the resistance R with a screen which is connected to point *3* of the bridge and which surrounds the connecting wire between C_A and R up to close to C_A, it is possible to make the remaining capacity between the dangerous connection point and earth only very small.

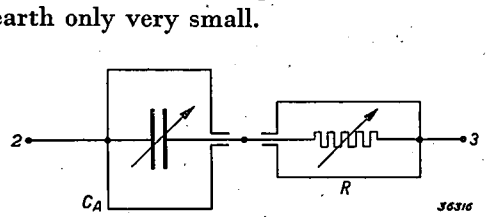

Fig. 9. If C_A is an air condenser of the ordinary type (two-point capacity), the parasitic capacity between the connection point of C_A and R and earth can easily be made very small.

In the practical execution of the substitution method it must still be kept in mind that since C_A has losses and C_N has none, a negative resistance R would be necessary to bring the equal-armed bridge into equilibrium. The bridge, however, need not be equal-armed. If we take for Z_{41} and Z_{34} two equal resistances R' and R'', and if we then connect a variable auxiliary condenser C_h (fig. 8c) in parallel with R', by regulation of this condenser we can bring the bridge so far out of equilibrium that a positive value of R is required to restore the equilibrium not only upon switching in C_X but also upon switching in C_N [2]).

In order to be able to measure a phase displacement $\tan\delta = 3 \times 10^{-8}$ with a capacity $X_X = 100$ pF and at a frequency of 8 000 c/s, R must be able to be adjusted with an accuracy of 0.005 ohm,

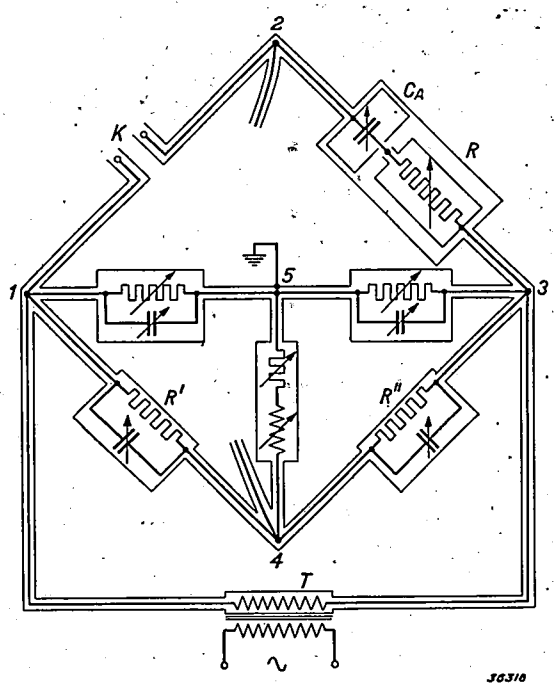

Fig. 10. Complete connections for the bridge used by us. In order to avoid disturbances from the outside the bridge is entirely surrounded by an earthed shield. At the terminals K, C_X or C_N is connected. The elements used to realize the impedances Z_1, Z_3 and Z_4 of the auxiliary bridge arms (see fig. 6) may be seen. These impedances must be balanced. A small variable auxiliary condenser is connected in parallel with R'' as well as with R', in order to facilitate the balancing. The bridge is supplied from the shielded transformer T. The detector, which is not shown, is connected successively at the points *2-4*, *2-5* and *4-5*.

[2]) Actually one ought also to be able to omit the resistance R entirely, and to bring the bridge exactly into equilibrium each time only by regulating C_h. The difference between the two adjustments of C_h necessary upon switching in C_X and C_N, respectively, would then give $\tan\delta_X$. This is the principle of Schering's bridge. We have not used this method because of the fact that extremely heavy requirements would be made of the condenser C_h: it would have to assume capacities up to 20 pF which would have to be accurately adjustable within 0.0005 pF!

at a total value of $R = 200$ ohms. Such a resistance can very well be realized.

In *fig. 10* we give finally the complete connections of the bridge as it has been developed on the basis of the above considerations. In the text below the figure certain details are explained.

Accuracy of measurement

As to the accuracy of measurement obtained, it is limited in principle by the accuracy with which the bridge can be adjusted to silencing the detector. The accuracy of adjustment is higher, the higher the voltage applied to the bridge and the greater the amplification applied in the detection apparatus. The voltage cannot be raised indefinitely because of the limited permissible load on the resistances R' and R'' (fig. 10). A limit is set to the effective amplification of the signal to be detected by the noise. This limit has been set as high as possible by sifting out a very narrow frequency range on both sides of the measuring frequency with the help of sharp cut-off filters, so that only this small section of the whole noise spectrum can become audible in the telephone as a tone fluctuating in intensity. When this fluctuating tone is heard, further amplification serves no useful purpose. The smallest measurable impedance change in the bridge is that at which the signal caused by it is just audible above the noise tone; it is found that in this way a change in tan δ of 3×10^{-8} can just be observed. Since the systematic errors in the substitution method used, as has been shown in different tests, are certainly smaller than the adjustment error mentioned of 3×10^{-8}, this is also the limit of the absolute accuracy with which we can measure a phase displacement with the apparatus described.

ABSTRACTS OF RECENT SCIENTIFIC PUBLICATIONS OF THE N.V. PHILIPS' GLOEILAMPENFABRIEKEN

1504: W. de Groot: Miscellaneous observations on the rise and decay of the luminescence of various phosphors (Physica 7, 432-446, May 1940).

With the apparatus described in **No. 1425** the rise and decay of the photoluminescence of different crystals is further studied. Crystals of ZnS-Ag, ZnS-Cu, ZnSCdS-Ag, ZnSMnS, $CaWO_4$-Sm, Zn_2SiO_4-Mn_2SiO_4 were investigated at different temperatures and different wave lengths of the irradiating light. The effective diameter of the luminescent centres for excitation by electrons, calculated from the rise of the luminescence, for the last mentioned phosphor agrees very well with the value derived from the saturation of the luminescence from data of Nottingham, while, with the help of data also from this author, a very acceptable value is found for the number of centres per unit of volume. In the quantitative interpretation of the experimentally obtained curves for the variation of the luminescence, the influence of various causes of deformation must be taken into account, among others, for instance, the weakening of the irradiating light upon penetration into the crystal. The effect of this is calculated. Furthermore with the help of an ultramicroscope the penetration of monochromatic light beams of different wave lengths into a single crystal of ZnSCdS-Ag is investigated.

1505: J. L. Snoek: On the dispersion of the initial permeability (Physica 7, 515-518, June 1940). (Original in German).

Experiments have shown that a sample of carefully purified iron, well annealed and at frequencies of 1 c/s has an initial permeability which is many times greater than the initial permeability found from measurements of the skin effect at frequencies of 10^6 to 10^8 c/s. The present theory offers no explanation of this discrepancy.

VOL. 5 No. 11 NOVEMBER 1940

Philips Technical Review

DEALING WITH TECHNICAL PROBLEMS
RELATING TO THE PRODUCTS, PROCESSES AND INVESTIGATIONS OF
N.V. PHILIPS' GLOEILAMPENFABRIEKEN

EDITED BY THE RESEARCH LABORATORY OF N.V. PHILIPS' GLOEILAMPENFABRIEKEN, EINDHOVEN, HOLLAND

THE LOCALIZATION OF OBJECTS IN THE HUMAN BODY

by A. BOUWERS.

621.386.16 : 616.073

X-ray photographs of objects in the human body permit the localization of an object in two dimensions. In order to determine the third coordinate, the depth, stereoscopic X-ray photographs, so-called planigraphic X-ray photographs and finally an apparatus by which the object is localized as the point of intersection of two beams of X-rays may be used. A description is given of such an apparatus, which has recently been developed in the Philips factories, and which is intended especially for the finding of projectiles in the body.

Introduction

One of the tasks of medical diagnostics is the accurate determination of the position of objects in the human body. As examples we may mention the localization of tumors in the stomach or other organs, or of cavities in the lungs due to a tubercular process. In wartime the problem takes on a particular significance due to the fact that the surgeon is often concerned with wounds where projectiles have remained in the body. In order to remove such projectiles with the least harm to the patient the first essential is an accurate determination of their position.

Ever since the discovery of X-rays, the X-ray shadow photograph has been used as a guide in such cases. In the first instance, however, this gives only a localization of the object in two dimensions. Methods have long been sought of obtaining information from the X-ray photographs about the position in the third dimension also (the depth under the skin). When the possibilities are reviewed which present themselves for this purpose, it seems obvious to start from the phenomena which make it possible for the eye to obtain a plastic impression in normal vision. There are in the main three such phenomena: the partial screening of distant objects by those lying closer, the decrease with increasing distance of the angle of vision within which an object of a given size is seen, and finally the parallax occurring due to the collaboration of the two eyes.

The first possibility mentioned — plastic impression due to partial screening — is missing in the X-ray photograph, since only shadows are seen, and in the first instance the shadow picture obtained of two objects lying one behind the other is independent of the order in which they are traversed by the X-rays.

The second possibility also — perspective diminution — cannot offer much aid in the X-ray picture. Since the thickness of the body is generally much smaller than the distance to the source of X-rays, the angle within which a given object is seen from the source can only vary slightly with its position, and, moreover, in order to translate the slight differences in size of the shadows in the X-ray picture into differences in distance, it would be

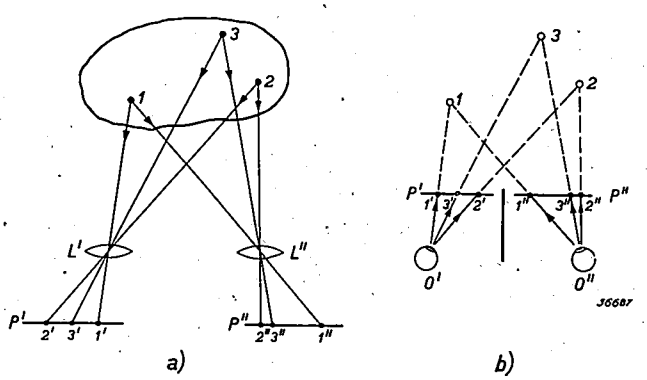

Fig. 1. When a three-dimensional object (points *1*, *2*, *3* in *a*) is seen, two different images are formed on the retina P', P'' of the two eyes (L', L'' eye lens). A plastic impression is obtained upon the flowing together of these two images into one. Stereoscopic photography is also carried out in the manner indicated in *a*), where P', P'' are two photographic plates and L', L'' two photographic lenses. When the two plates are observed in the manner indicated in *b*) (O', O'' eyes) the impression of a three-dimensional image is again obtained.

necessary to know accurately the size of the objects themselves. This is generally not the case.

The third possibility remains — the parallax. In *fig. 1* it is shown how normal stereoscopic vision or observation of stereoscopic photographs takes place with the help of the parallax. The essence of the method consists in the fact that *each point on the object is localized as the point of intersection of two rays of light.* This principle can also be applied in X-ray diagnostics and forms indeed the basis of all the usual methods of determination of depth in X-ray pictures. We shall here review several of these methods and describe in more detail an apparatus for finding projectiles which has been developed in the Philips laboratory.

Stereoscopic X-ray photographs

The diagram of fig. 1 cannot serve directly for X-ray pictures, since in taking such pictures the points of the object cannot emit any radiation but only intercept it. *Fig. 2* shows the principle of the photography and observation of X-ray stereoscopic pictures.

It is obvious that in order to superpose the two different pictures to give a (plastic) whole, the observer must be able to see every point of the one on the other. In X-ray pictures this is not so easy as in the observation of ordinary photographs. The sharp contours are often missing which could immediately be identified, and in their place there are more or less vague shadows whose lack of definition may sometimes be of the same order of magnitude as the shift due to parallax! It is therefore very difficult or even impossible to obtain a plastic impression of many objects, such as diseased spots in the lungs, by the observation of stereoscopic X-ray photographs.

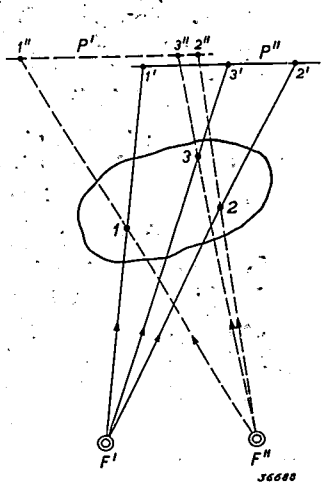

Fig. 2. In taking stereoscopic X-ray photographs shadow images are thrown by two foci F', F'', at a distance apart of 5 cm, successively upon two correspondingly placed plates P', P'' and photographed. The observation of the photograph may in principle take place in the same way as if the eyes occupied the same position as the X-ray foci.

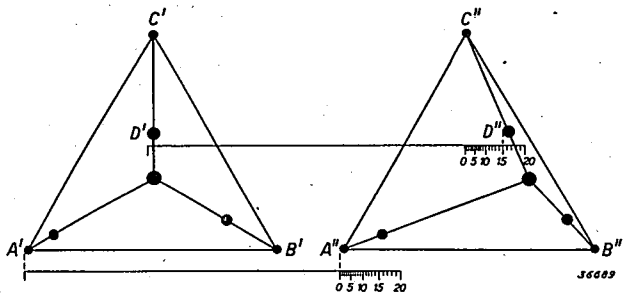

Fig. 3. In the application of a standardized method in which the two X-ray stereophotographs are taken side by side on a single film, the depth of each point can be measured directly with a calibrated ruler. In the case here represented a tetrahedron with small spheres at certain points on its edges is photographed. It may be read off directly that point D lies 15 cm above the plane of the points ABC.

The stereoscopic X-ray pictures taken according to the scheme of fig. 2 can also be used for an *objective* determination of the "depth" of the different points, without trying to see a plastic picture. For this purpose the relative displacement of corresponding points on the two pictures must be measured and calculated, a procedure which is very much facilitated when the geometrical relations prevailing during the making of the exposures are permanently fixed, and a ruler is used to measure the displacement, which is calibrated directly in depths (with respect to a given plane of comparison) [1]), see *fig. 3*. When this method is used the visualization of the object is of course entirely lost; the doctor must reconstruct the situation of the object in the body from a series of values which he has obtained in this way.

Planigraphy

An interesting method of obtaining an objective determination of depth and at the same time a physical visualization of it is by means of planigraphy [2]) (also called tomography). Suppose that the projections of the object from the two foci which were used in taking the stereoscopic X-ray pictures are not photographed on two different plates, but successively on the same plate (see *fig. 4*). By moving the plate after the first exposure

[1]) This is described by W. Hondius Boldingh, Vereinfachte und standardisierte Stereotechnik, Röntgenpraxis **1**, 561, 1929.

[2]) This method was published independently and almost simultaneously by D. L. Bartelink (Fortschr. Röntgenstr. **47**, 399, 1933), B. C. Ziedses des Plantes (Fortschr. Röntgenstr. **47**, 407, 1933) and A. Vallebona (Fortschr. Röntgenstr. **48**, 599, 1933). However, A. E. M. Bocage had already obtained a patent on it in 1921 (French patent No. 536.464).

from position *1* to position *2*, the shadow of point *A* can be made to fall on the same point in both exposures $A' = A''$. Point *A* is thus sharply focussed, and this is still true when instead of making two separate exposures plate and focus are shifted continuously during the exposure from position *1* to position *2*. If we now consider point *a*, we see that its shadow on the plate is displaced from a' to a''. The shadow of point *a* thus loses all definition. Further consideration shows that in the exposure described with moving plate and focus, not only point *A* but all points on plane *V* are sharply focussed, while the shadow of points above this plane (*a*) and below it (*b*) are spread out along a line of a certain length, and therefore lose all definition. An X-ray picture is thus obtained in which all objects in the cross section *V* of the irradiated body are visible as sharply defined shadows, while the rest of the body causes a more or less uniform fog over the picture. In practice focus and plate are usually not made to move along a straight line, but over a longer traject which as nearly as possible fills a whole area (for instance a spiral or a narrow sine curve) and over which traject focus and plate always maintain proportional velocity in opposite direction. The blotting out of the undesired planes is thereby considerably improved. If, for instance, it is desired to find the position of a cavity in the lungs by this method, a number of such planigraphic exposures can be made in each of which a different cross section (of known depth) through the body is brought into focus; afterwards the exposure can be picked out upon which the cavity is sharply (or most sharply) defined. In *fig. 5* an example is given of such exposures of different cross sections, together with an ordinary X-ray photograph of the same patient [3]).

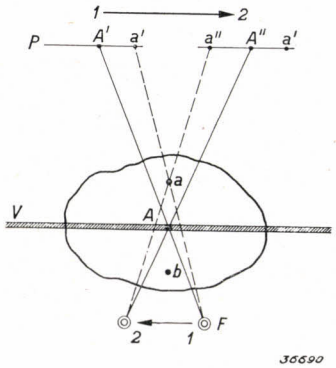

Fig. 4. Principle of planigraphy. During the exposure the X-ray focus *F* is moved from *1* tot *2*, and at the same time the photographic plate *P* is moved correspondingly. All points in the plane *V* are sharply focussed. while the shadows of points outside this plane (*a*, *b*) are rendered undefined.

The Philips "bullet finder"

For the finding of projectiles mentioned in the introduction the methods described are less suitable. In such a case it is particularly important to be able to determine the position quickly and

[3]) It must be noted that only under certain circumstances conclusions may be drawn from the planigraphic image obtained about the shape of the objects. Various investigations have been carried out in recent years on this subject, among others by the Medical Department of the Philips concern, see for instance G. C. E. Burger and J. G. A. van Weel, Fortschr. Röntgenstr. **57,** 143, 1938; further R. H. de Waard, Ned. T. Geneesk. **83,** 368, 1939.

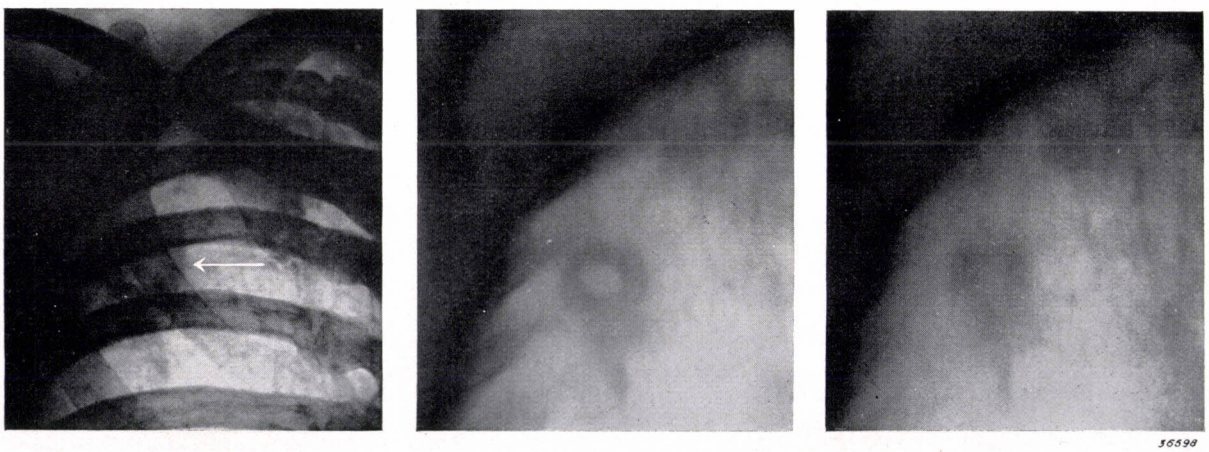

a b c

Fig. 5. *a*) Ordinary X-ray photograph of part of the chest of a patient. A ring-shaped shadow (indicated by the arrow) is visible, which indicates the presence of a cavity in the lung.
b) "Planigram" of the same patient. The photograph shows a cross section 7 cm below the skin of the back. The cavity is very clear and sharply defined.
c) Planigram at a depth of $8^1/_2$ cm. The cavity in this case has lost almost all definition.

in a simple way, and to obtain the result in such a form that it can serve the surgeon immediatly as a guide during the operation. It will be clear that the methods described would be much too elaborate in such cases, when it is kept in mind that a shift in position of the object to be removed may often occur during the operation. It is then impossible to wait for the required new determination of position by the exposure and development of one or more photographs.

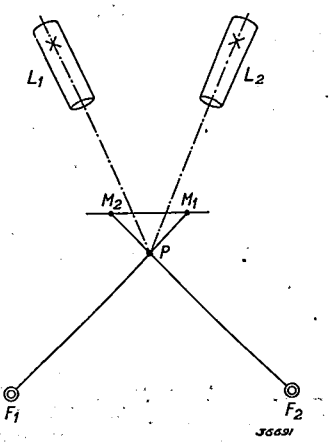

Fig. 6. Principle of the "bullet finder". Four beams meet at point P: two beams of light (broken lines) emitted by the lamps L_1, L_2, and two beams of X-rays along the lines joining two foci F_1, F_2, and two marks M_1, M_2 on a fluoroscope screen.

The numerous methods which have been worked out to satisfy the requirements of this particular application [4]) are all based upon the principle already mentioned: the localization of a point as the point of intersection of two beams. The "bullet finder" which has recently been developed at Philips is also based upon this principle. In this apparatus four ray directions intersect each other at a definite point P (see *fig. 6*): two light rays L_1 and L_2 and two rays R_1 and R_2 which are fixed as the lines joining two X-ray foci F_1 and F_2 and two marks M_1 and M_2 on a fluorescent screen. If the body of the patient is placed in the path of the rays so that the shadow of the projectile which F_2 casts falls on M_2, and that from F_1 on M_2, the projectile is obviously situated exactly at point P which is distinguishable to the surgeon as the point of intersection of the two light rays [5]).

Since the position of the patient is fixed by other factors concerned with the operation, the body with the projectile is not brought to point P, but point P to the projectile. Furthermore, two X-ray tubes are not used simultaneously, but only one tube whose focus is brought successively into the positions F_1 and F_2. This is desirable in order not to administer to the patient an unnecessarily large dose of X-rays, and in order not to obtain two superposed images on the fluorescent screen, which would be very disadvantageous as concerns the image contrast, and if several projectiles are present it would also make the images confusing. In *fig. 7* the apparatus and its method of functioning is shown diagrammatically. The standard which supports the X-ray tube, the fluoroscope screen and the light sources on a sliding frame is pushed close to the operating table in such a way that the X-ray tube, first set in position *1*, is beneath the patient, and the shadow of the projectile falls upon the mark M, of the fluoroscope screen D. This is checked by an assistant who can easily observe the fluorescent image in the mirror S by looking into the tube K, without it being necessary to darken the room. After this adjustment, by which the focus is placed directly under the projectile, the assistant fixes the standard by means of a foot brake with

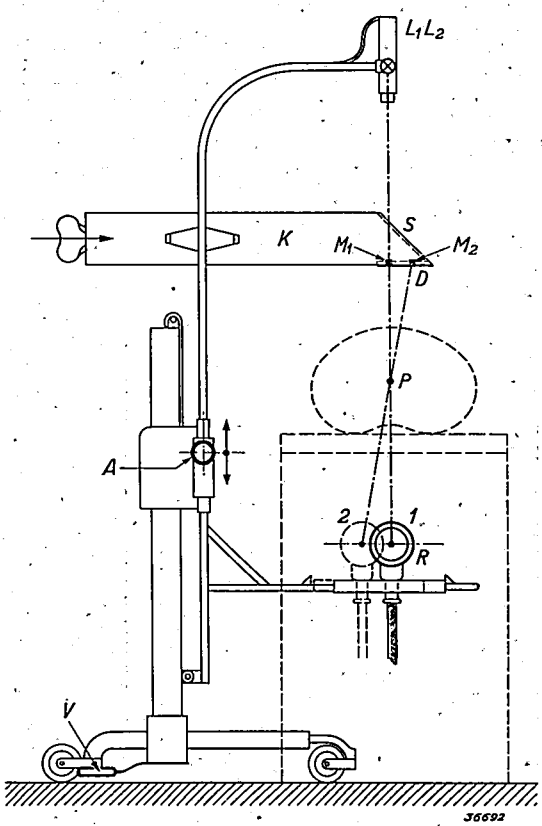

Fig. 7. Construction of the "bullet finder". *1*, *2* positions into which the X-ray tube R can be brought. M_1, M_2 marks on fluoroscope screen D, S mirror, K tube; the arrow indicates the direction of observation of the operator of the apparatus. L_1, L_2 two projection lamps lying exactly one behind the other in this sketch. The point P is made to coincide with the projectile. A handle for manipulation, V foot brake.

[4]) A survey is given in the book of R. Grashey, Steckschuß und Röntgenstrahlen, G. Thieme, Leipzig 1940.

[5]) Light beams have already been used for this purpose, although in a manner different from that here described, by C. Chaussée; see J. belge Radiol. **23**, 305. 1939.

respect to horizontal displacement, brings the X-ray tube into position *II* (see fig. 7) and then shifts the movable frame in a vertical direction until the shadow of the projectile falls upon mark M_2. The tube with the fluorescope screen is then pushed back and the operation can be begun. The two light spots which are thrown upon the patient's skin by the projection positions L_1 L_2 (these can be seen better in the photographs *fig. 8* and *9*) serve to guide the surgeon. The directions of the two light beams make an angle of about 20° with each other, so that the depth of the point *P*, *i.e.* of the projectile, under the skin of the patient is about 3 times the distance between the two light spots.

It is of essential importance for a rapid localization that the first adjustment should not be destroyed later by the second adjustment. This is guaranteed by the fact that in the second adjustment the imaginary line I-M_1 coupled to the movable frame is displaced vertically, *i.e.* in its own extension, and therefore always continues to pass through the point *P*. Experience has shown that in this way the position of the object can be determined within a few millimeters in one minute. During the operation also the two beams of light continue to indicate the direction. If necessary the observation can be repeated without appreciable interruption of the operation in order to find out whether the object has moved. In fig. 8 a photograph is given of the whole set up [6]).

The fluoroscope screen must lie at least as far above the point *P* as the thickness of a patient may be. Due to this relatively large distance the geometric lack of sharpness of the X-ray picture (half shadow width, caused by the finite dimensions of the focus), is about $^3/_4$ of the width of the focus. In order to make a sufficiently sharp localization pos-

[6]) The apparatus described has already given good service to hundreds of wounded, see J. Schlaaff, Zentralbl. Chirurgie **67**, 1924, 1940.

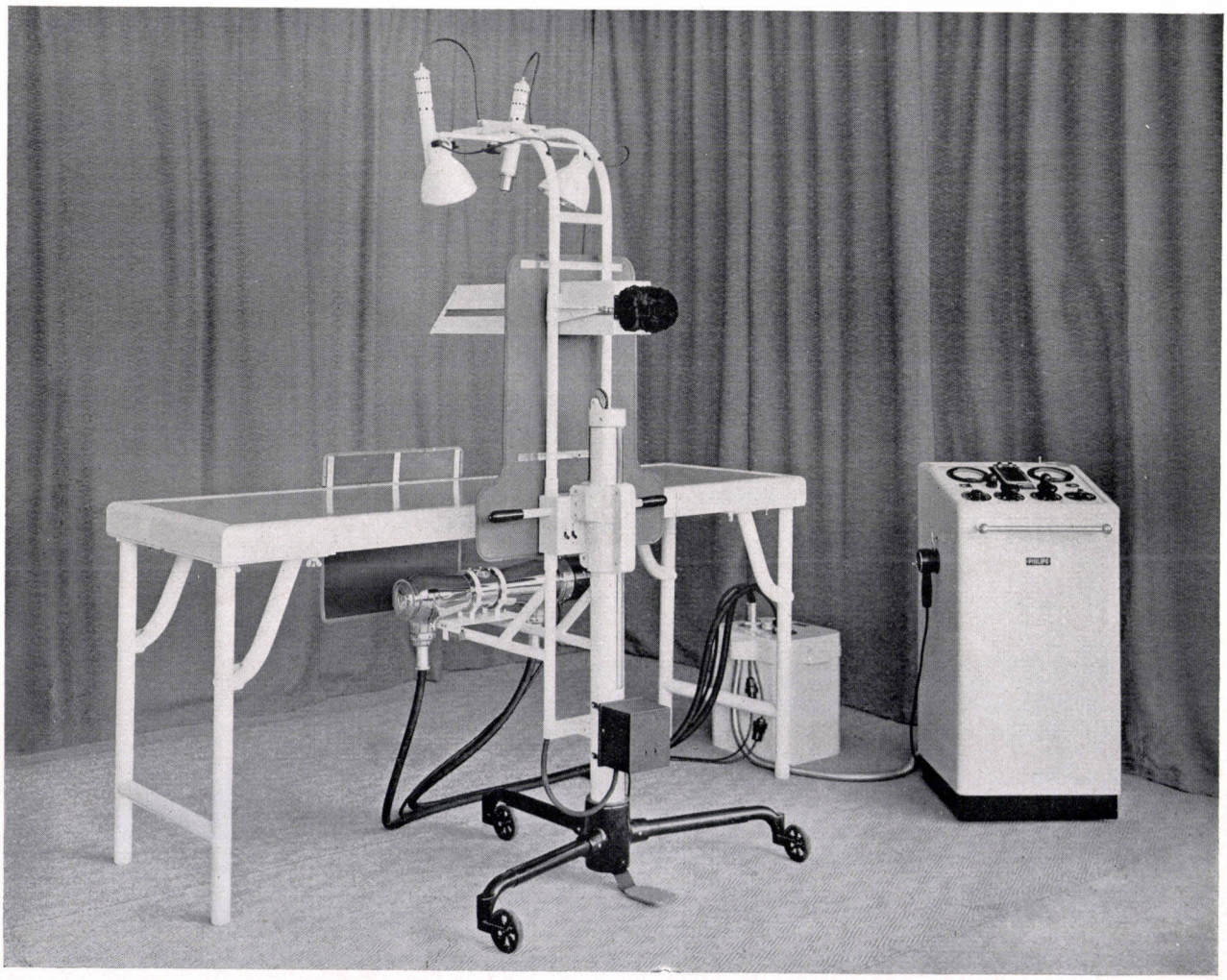

36667

Fig. 8. Complete arrangement for the localization of projectiles. In the middle the bullet finder beside the operating table. On the right the desk from which the X-ray tube is operated.

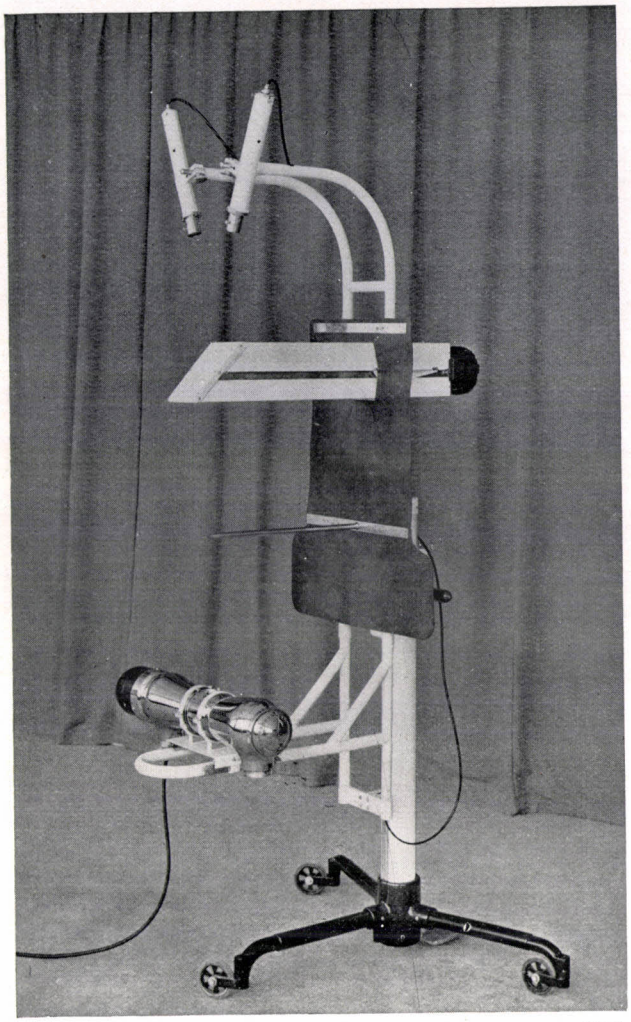

sible, therefore, an X-ray tube with a very fine focus (apparent dimensions 1.7 × 1.7 mm) is used.

When the adjustment of the apparatus, *i.e.* the intersection at point P of all four beams, is destroyed by slight deformations of the standard, such as might occur due to transportation, it can be adjusted anew with the help of the iron rod visible in fig. 9. The point of the rod is placed at the intersection of the two X-ray beams, $1\text{-}M_1$ and $2\text{-}M_2$, and the two projectors L_1 and L_2 are then turned so that the two light beams again intersect each other on the point of the rod.

Fig. 9. Photograph of the "bullet finder". The two projection lamps may be seen at the top, below them the tube with the fluoroscope screen, which can be pushed back for the operation. The rod between the tube and the X-ray tube is only inserted for the adjustment of the whole apparatus.

WIRELESS TELEPHONY WITH MOVING MOTOR-CARS

by C. G. A. von LINDERN. 621.396.5.029.6 : 621.396.931

In order to obtain an easy method of communication between the central station and motor-cars of various public services (fire department, police, etc.) the cars may be provided with a small ultra-short wave transmitter and receiver. The transmitting-receiving installation DR 38, which works on a wave length of 4 to 4.5 m has been constructed for this purpose. A description is here given of the transmitter and of the receiver, which contains a super-regenerative detector. The method of functioning of this detector is explained. In conclusion the supply, the aerial and other details of the installation are discussed. In experiments in which the aerial of the central station was set up at a height of 45 m, it was found possible to obtain a good connection over distances of from 10 to 20 km.

It has become more and more customary to equip motor-cars which are used by the police, the fire department, large garages and other services, with radio transmitters and receivers which make a telephonic connection possible between the motor-car and the central station. The great practical importance of such a possibility of communication for the services in question is obvious: the central station can by this means give orders to the cars out on patrol duty or en route to render assistance, and conversely the cars can report, ask instructions or reinforcements if necessary, etc.

In the case of other means of conveyance such as ships and aeroplanes, the use of transmitter-receiver installations has long been familiar. The requirements made of such an apparatus for cars are, however, considerably heavier in certain respects than for ship or aeroplane installations. Only a very limited amount of space is available either for the apparatus or the aerial; the energy consumption is limited to that which the accumulator battery of the car can provide; furthermore in the case of a moving car in a city the very high level of interference must be taken into account. Finally the installation must of course be able to be operated by a layman, since it would be impossible to have a radio-telegraphist in every car.

The consequence of these and other requirements for the construction of such an installation will be discussed here, and the construction of the Philips car installation, type DR 38, which has been developed on the initiative of the "Committee for special radio services at very high frequencies" will be described in particular.

Choice of the wave length

In order to obtain satisfactory radiation with a limited energy consumption, an aerial with a high radiation efficiency must be used. This amounts practically to the fact that the length of the aerial must be $^1/_4$ or $^1/_2$ of the wave length. The choice of the wave length is hereby immediately limited to the region below 10 m, because it is obvious that it is impossible to mount a structure many metres high as aerial on a car. The high level of interference in the cities also leads to a similar limitation in the choice of the wave length: with the small power available the car transmitter has no chance of dominating over the prevailing interferences; it must therefore try to avoid the frequency spectrum of those interferences as far as possible. At very high frequencies, above about 60×10^6 c/s, the interference level is sufficiently low. The installation DR 38 works on wave lengths from 4 to 4.5 m ($75 - 67 \times 10^6$ c/s). These very short waves already experience an appreciable shadow effect due to obstacles in their path such as hills, woods, groups of buildings, etc., so that for a good connection between the car and the central station it is desirable that there should be no obstacles in a straight line between the two aerials. This, however, offers no difficulty since the aerial on the central station can, without much trouble, be mounted at such a great height that it is "visible" 20 or 30 km away, and for the services mentioned this is sufficient, since the cars need in general only to travel within a relatively limited district.

The transmitter

As oscillator the transmitter contains a back-coupled triode (TE 05/10). Tuning and maintaining a constant frequency of the oscillator at such short waves is often accomplished with the help of a Lecher system (a socalled long line); because of the limited amount of space, however, this method was not used in our case. An *LC* circuit was therefore used, which corresponds in principle to the circuits for broadcasting wave lengths, but which is constructed quite differently because of the losses occurring at high frequencies. In *fig. 1* the construction is shown and explained. The ohmic, dielectric and radiation losses are here limited to a minimum,

so that a very sharp resonance curve, and thus a high frequency stability, is obtained. By screwing the cover D more or less tight the capacity can be varied and the resonance frequency thus regulated

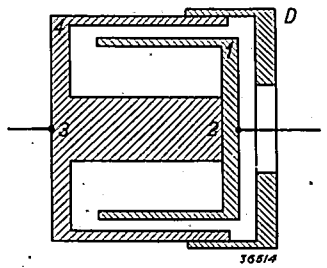

Fig. 1. Construction of the low-loss oscillation circuit which fixes the frequency of the transmitter. The construction can be considered to be formed by a rectangular current loop *1234*, in which between *1* and *4* a capacity is connected, while the whole is allowed to rotate about the axis *23*. The magnetic lines of force which are responsible for the self-induction run in circles about the axis *23*, entirely within the solid of revolution obtained. The gap of the "loop" in which run the electrical lines of force which are responsible for the capacity, is so narrow that here also practically no lines of force reach the outside, so that the losses by induction in the surroundings and by radiation are only very small. Due to the large copper cross section of the current loop the ohmic losses are also slight, while by the use of air as a dielectric the dielectric losses are small enough to be neglected.

between 75 and 67 $\times$ 10^6 c/s; the regulation, however, need be carried out only after the wave length to be used, which must of course be different for different services in the same district, has been determined.

The circuit described is connected between grid and cathode of the transmitter valve, see the diagram of *fig. 2*. The frequency is therefore partially determined by the capacity between grid and

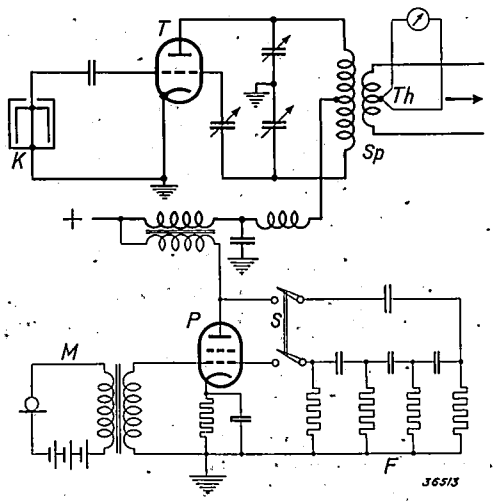

Fig. 2. Simplified diagram of the transmitter. T transmitter-triode, K low-loss circuit, Sp aerial coupling coil, Th thermo-element. The part of the connections drawn with thin lines serves for modulation. In this part P is a low-frequency pentode, M microphone circuit, F phase-rotating element for excitation of the call tone, S switch (signalling key) for calling (or telegraphy).

cathode in parallel with the circuit capacity, which is apparently increased by the capacity C_{ag} between anode and grid by an amount $gC_{ag}R_a/(R_i + R_a)$, where g is the amplification factor and R_a and R_i the external and internal resistances, respectively, of the valve. Since R_a depends upon the aerial circuit, which is coupled with the anode circuit, the frequency will therefore be somewhat influenced by the aerial, and the previously regulated wave length may therefore change slightly upon mounting the apparatus in the car. When the car is moving the frequency will then still be able to vary slightly, due to the continually changing environment which affects the aerial circuit. In modulation, which is done by changing the anode voltage, the frequency will also vary, since changes hereby occur in the valve capacities, among others. In order to keep all these frequency variations small, the valve mentioned, TE 05/10, is so constructed that the capacities have only low values. (An acorn or button valve, which satisfies very high standards in this respect [1]) because of its small dimensions, could not be used here, since it cannot deliver enough power). At a modulation depth of 90 per cent the frequency now varies about 25 000 c/s, which is no longer disturbing because of the great band width which the receivers may have in this wave length region.

For modulation a low-frequency pentode is used whose grid A.C. voltage is supplied directly by the microphone. The modulator valve is used at the same time for the generation of the call signal which consists of a tone of 1 000 c/s. For this purpose part of the anode A.C. voltage of the valve is fed back to the grid *via* a filter (see fig. 2) which rotates the phase of voltages with different frequencies to different degrees, in such a way that the phase rotation only has the correct value to cause a building up of the vibration for a frequency of about 1 000 c/s. This feed-back can be set in operation with a switch in the form of a signalling key; in this way it is possible to give Morse signals as well as the call signal.

In the coupling coil with which the aerial is coupled with the anode circuit, a thermo element is included with which the current at this point can be measured. This permits a check on the functioning of the transmitter. The power delivered to the aerial by the transmitter amounts to 5 to 6 watts.

The receiver

The primary aim in the construction of the re-

[1]) See the photograph in Philips techn. Rev. 5, 177, 1940.

ceiver was to have as few stages as possible, in order that it should occupy as little space as possible, and in order to limit the possibilities of defects as far as possible. On the other hand the receiver must in any case have a high sensitivity, while, due to the considerable variations in field strength which may occur while the car is moving, a good quick-acting automatic volume control is desired.

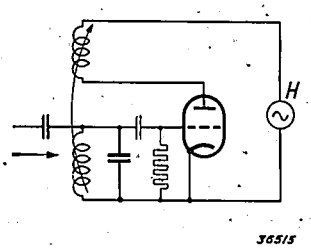

Fig. 3. Diagram showing the principle of a superregenerative detector. By means of the auxiliary oscillator H the anode voltage is so influenced that the circuit begins to oscillate periodically.

These requirements can be satisfied particularly well by the application of a so-called **superregenerative detector**. We shall examine this in somewhat more detail [2]).

Upon switching on an oscillator, for instance an amplifier valve with a back-coupled oscillation circuit (see *fig. 3*), the amplitude E of the oscillation generated at first increases according to an exponential law: $E = E_0 \exp(\alpha t)$, and then reaches a definite final amplitude due to the limitation by the valve characteristic. The time τ necessary for the building up of the oscillation to this final amplitude (we mean by this the amplitude at which the deviation from the exponential variation occurs) will depend upon the initial amplitude E_0. It is of importance in this connection that the difference $\tau_1 - \tau_2$ between the times for the building up with two different initial amplitudes E_1, E_2 is determined exclusively by the relation E_2/E_1, since

$$\tau_1 - \tau_2 = \frac{1}{\alpha} \ln E_2/E_1.$$

If we apply a signal to be received, for instance a modulated carrier wave, to the grid of the oscillator valve (the superregenerative detector), and if we change the anode voltage of the oscillator periodically in such a way that it can oscillate during a time T and the oscillation is then suddenly suppressed, the signal amplitude prevailing at the beginning of every period T functions each time as initial amplitude. During a period of time $\Delta = T - \tau$ in every period T the oscillator oscillates with maximum amplitude and large anode currents flow. In charging of the grid condenser by the grid current which increases simultaneously with the anode A.C., detection occurs in the ordinary way, *i.e.* the operating point on the characteristic of the valve continually shifts so that the anode D.C. varies in the same way as the envelope of the high frequency anode alternating current. In *fig. 4* this is shown diagrammatically. The time Δ during which the maximum anode direct current flows, therefore also the amount of charge flowing through the anode impedance per period T, varies from period to period with the signal amplitude. By a suitable choice of the anode impedance one obtains in this way relatively high low-frequency A.C. voltages whose variation with sufficiently small value of T forms a faithful picture of the variations of the signal amplitude received (modulation), and whose magnitude, according to the explanation given, is independent of the **magnitude** of the signal amplitude E and determined solely by the maximum ratio E_2/E_1, *i.e.* the **depth of modulation** of the signal. Thus on the one hand, with one valve one can obtain a very great amplification, and on the other hand an ideal "automatic volume control" is obtained. If there is no signal to be received then the spontaneous voltage fluctuations due to the thermal agitation of the electrons, etc. functions as initial signal for the periodic building up, and this is heard clearly as noise, just as is the case with a superheterodyne receiver with automatic volume control in the absence of a signal.

The periodic functioning of the oscillator can be accomplished with the help of a separate small

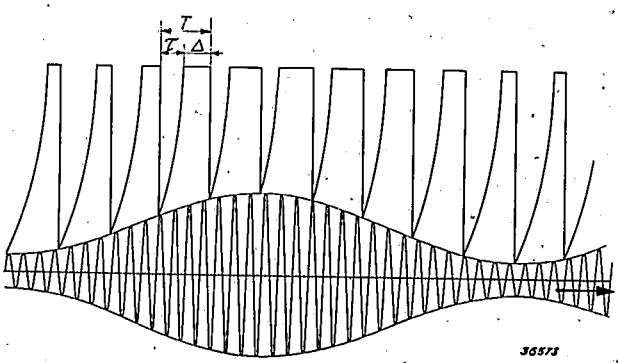

Fig. 4. The signal to be received (modulated carrier wave) and the variation of the rectified current through the valve. The high-frequency vibration is built up each time from the given signal amplitude, according to the envelope here drawn, to a constant final amplitude (time for building up a), and after a constant time T suppressed. For the sake of simplicity it is here assumed that after the exponential increase the amplitude suddenly becomes constant and upon suppression suddenly falls to the (new) initial value. (The oscillations are built up respectively much higher than according to this drawing).

[2]) *Cf.* E. H. Armstrong, Proc. Inst. Rad. Eng. **10**, 244, 1922; P. David, Onde él. **7**, 217, 1928; H. O. Roosenstein, Hochfrequenztechn. u. Elektroakust. **41**, 85, 1933.

oscillator valve, which, for instance, changes the anode voltage in the desired rhythm. As already pointed out, the period T must be chosen small enough to record a sufficient number of points on the modulation curve in the "scanning" (fig. 4). The auxiliairy frequency must therefore be considerably higher than the highest speech frequency to be reproduced. On the other hand, T may not be chosen indefinitely small. Above, in speaking of the times A of maximum generation, we assumed tacitly that T is always greater than the time for building up τ. For a sufficiently small initial amplitude, however, this will no longer be true, the oscillations then do not reach the final amplitude drawn in the figure at all. Signals below a certain amplitude limit, which is higher the smaller T is, are practically no longer reproduced. By variation of the auxiliairy frequency (T), therefore, the sensitivity of the receiver can be regulated, and at the same time, when it is possible to count on relatively strong signals, the noise in the intermissions of the reception can be decreased.

In the construction of the receiver in the installation here described, another valve was saved in the following way. The periodic generation of the oscillator is not accomplished here by an auxiliary oscillator, but takes place automatically, thanks to a suitable choice of dimensions for the condenser and the leakage resistance in the grid circuit and a sufficiently tight back-coupling. Upon oscillation the negative grid voltage rapidly becomes so large that the oscillations suddenly break off just after they have reached a certain value. The grid condenser is then discharged and the process begins anew (so-called "blocking") [3]. The action of the arrangement is now different is so far as the intervals of oscillation do not follow each other strictly periodically, but the oscillations, and thanks to the detection the anode D.C. also, vary in such a way that during each interval of oscillation about the same charge flows through the valve. The intervals succeed each other rapidly at high signal amplitude, at lower, less rapidly (see *fig. 5*). Further consideration shows that now also the variation of the average time value of the charges (*i.e.* the sound intensity obtained) is determined practically only by the depth of modulation of the signal received.

It must be pointed out that the automatic volume control, which can be applied in a superheterodyne receiver, must always work with a certain time lag in order not to regulate the modulation of the carrier wave out of existence; in superregenerative receivers on the other hand the regulation acts without any time lag, any interferences occurring (suddenly occurring signal with greater carrier wave amplitude) are therefore rendered harmless more satisfactorily.

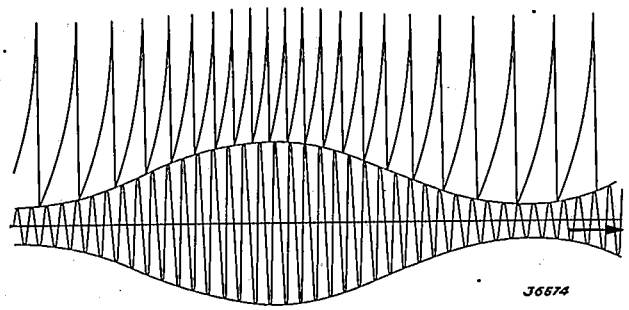

Fig. 5. Same as in fig. 4 upon making use of super-regeneration The building up now does not take place at constant intervals, but with large signal amplitude the intervals are smaller, with small signal amplitude, larger.

The oscillator valve used as superregenerative detector is an acorn valve (4 671). A stage of high-frequency amplification precedes the detector. This has certain advantages. A lower sensitivity of the detector is needed and the noises occurring in the intermissions of the reception are thereby decreased. The radiation of the receiving aerial caused by the periodic generation of the detector is considerably decreased so that other receivers in the neighbourhoud experience less interference. Furthermore, the high-frequency amplifier stage prevents the regular "blocking" of the detector in the correct manner and in the desired frequency region, which requires a very careful adjustment of all parts of the connections, from being endangered by a variable impedance in the grid circuit (namely by the coupling with the aerial).

Two stages of low-frequency amplication with a double pentode (ELL 1) follow the detector. One half of the pentode acts as output amplifier and can deliver two watts to a loud speaker connected to it. A loud speaker is used only for calling the car (see below). Two watts are more than enough to make the call tone clearly audible, even when the car is riding through a noisy street. The conversation itself is carried out with an ordinary telemicrophone, the taking up of which automatically switches off the loud speaker [4]).

[3]) See Philips techn. Rev. **3**, 248, 1938.

[4]) Since only one definite tone frequency is necessary for calling, a filter may if desired be connected in front of the loud speaker which only passes a narrow frequency range around the call tone frequency. In this way the noise heard in the absence of a signal to be received is very much reduced. Other possibilities of avoiding the noise are for example the use of a call lamp instead of a loud speaker or the short circuiting of the loud speaker by the voltages in the frequency region above 3 500 c/s (wich occur only in the noise and are eliminated during the reception of a signal).

The supply

The cathodes of the valves, which consume a total of about 20 watts, are fed directly from the 6 volt accumulator battery of the car. The anode voltages are obtained from it by means of a vibrator-converter [5]). This contains a vibrating tongue with two pairs of contacts, see *fig. 6*. By means of one set of contacts one of the poles of the accumulator is alternately connected to the ends of a transformer winding, whereupon an A.C. voltage is produced therein. This voltage is transformed up to the desired value and then with the help of the second set of contacts, converted into a (pulsating) D.C. voltage which is afterwards smoothed. Since the power to be dealt with (60 W) is too high for one such vibrator, two vibrators are connected in parallel in the converter.

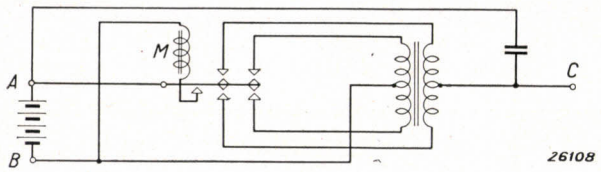

Fig. 6. Diagram of the vibrator. The electromagnet M keeps a vibrating tongue in motion, upon which there are two sets of contacts which simultaneously reverse the current direction in the primary and in the secondary winding of the transformer. After smoothing a D.C. voltage of 250 volts is obtained in this way from the 6-volt accumulator battery AB. This can be taken off between A and C.

Since it was desired to house the converter in the same cabinet as the receiver, the avoidance of interferences required special attention. Sparks from the vibrator contacts are eliminated as well as possible by shunting with suitable condensers and resistances; this is also necessary in connection with the wear on the contacts. Furthermore, the whole converter is shielded, and filters are introduced in the connection to the receiver, by means of which the interferences are reduced to a harmless level.

The current in the primary circuit of the converter amounts to 10 A, the connections to the accumulator must therefore be short and thick, and transition resistances in the contacts must be kept small. A resistance of 0.1 ohm, for instance, in this circuit would already cause a fall in the anode voltage of 15 per cent.

At the central station of the service in question the same transmitter and receiver is used as in the cars. The supply, however, can here be taken from the A.C. mains, and the converter replaced by a normal plate voltage apparatus.

[5]) Sec: J. W. Alexander, Car Radio, Philips techn. Rev. **3**, 112, 1938.

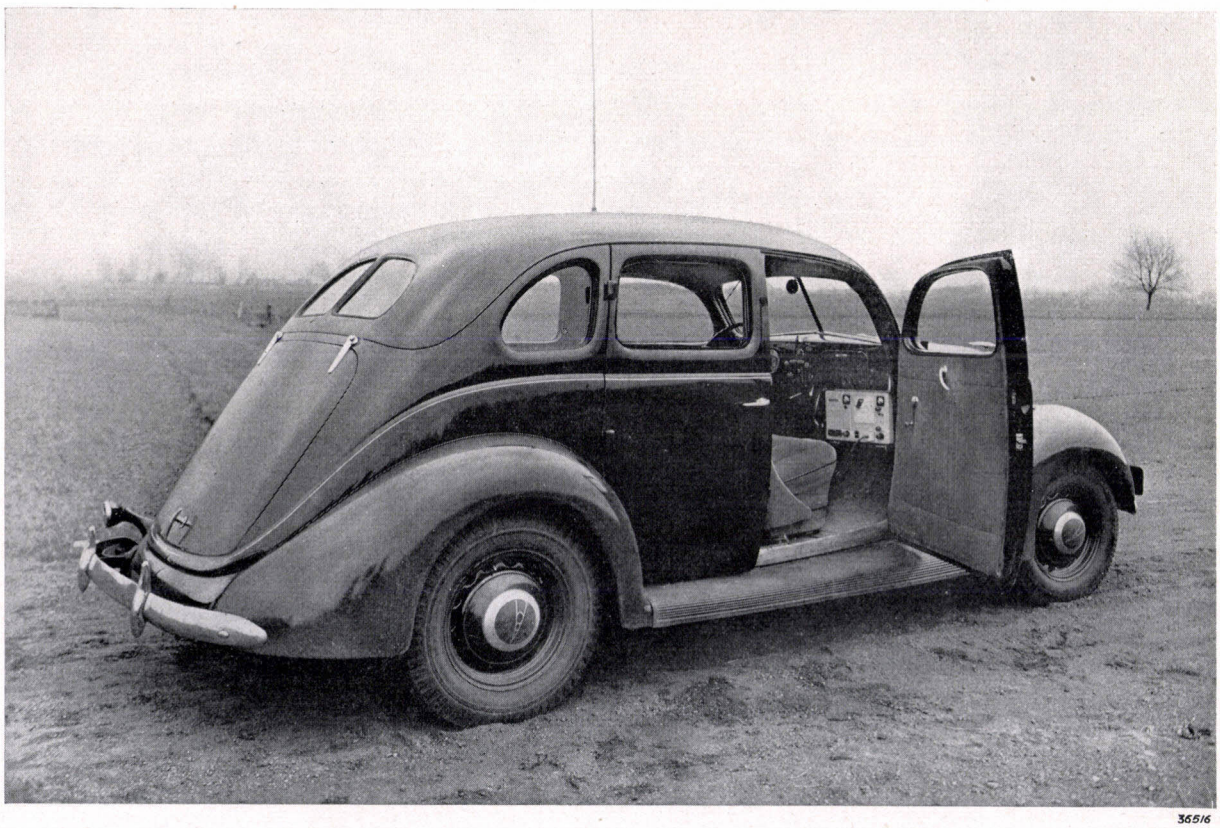

Fig. 7. The aerial rod is screwed into the middle of the roof of the car which acts as counter capacity. Under the dashboard of the car the transmitter receiver DR 38 may be seen.

The aerial

The aerial of the mobile station is a quarter wave length aerial, *i.e.* a vertical rod of about 1 m in length, with the steel top of the car for counter capacity. *Fig. 7* shows how the aerial is installed. In order to prevent damage to the fairly thin top of the car the aerial must be as thin and light as possible, so that upon braking and accelerating and jolting the mass forces occurring are not too great. The rod is best made slightly conical. In order to enter garages and drive under all kinds of obstacles such as low hanging branches, a small spring construction is built into the aerial at the height where it is fastened to the roof of the car.

The aerial is used not only for transmitting but also for receiving. Switching the aerial over to the transmitter or receiver is accomplished by means of the switch altready menioned (see *fig. 8*), which at the same time switches the anode voltage from the transmitter to the receiver, and interrupts the supply of the carbon microphone when receiving. In the third position of the switch the previously mentioned aerial current meter is switched in. In ordinary operation this is short circuited in order to prevent any interruption during transmission due to a possible defect of the thermo element.

In the case of the aerial of the central station the same limitations are not experienced as in the case of the aerials of the cars; an aerial of a half wave length, or, better, several such aerials one above the other, can be used. By using several aerial rods one above the other a concentration in the horizontal plane of the energy radiated is obtained. With three aerial rods, for instance, about the same result is obtained as with a transmitter with three times the power.

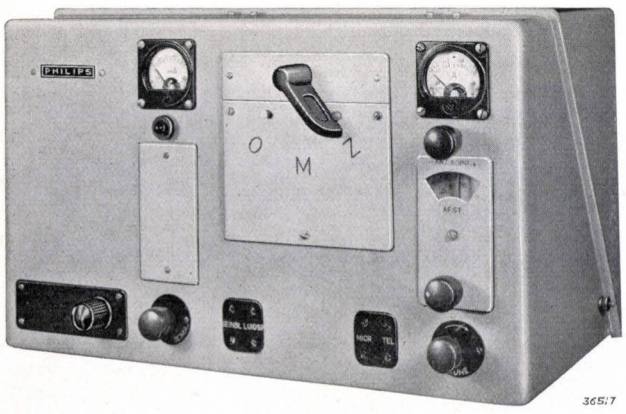

Fig. 8. The transmitter-receiver DR 38. In the middle, the switch with three positions for reception, measuring and transmitting. Below, the connections for the tele-microphone and the call loud speaker.

Use of the installation and results

When the car is moving the switch of the apparatus normally stands at reception, and the telemicrophone lies on its hook, so that the call loud speaker is in connection. If one station, either the central or one of the cars, wishes to make a communication, this station switches over to "transmission" and then transmits the call tone by means of the above-described arrangement in the modulation system. Hereby all the stations of the service are called at the same time and may therefore all receive the communication. In many cases there will be no objection to this, it may even be desirable in order that the different cars may know each others's instructions and whereabouts. If, however, it is desired to be able to call a single car individually, this can be provided for by means of a number choosing arrangement as in the case of the telephone.

Experiments have been carried out with the installation described, with the aerial of the fixed station at a height of 45 m above the ground. Good communication was possible with the mobile station in the moving car at distances of from 10 to 20 km. The greatest distance over which a communication could just be made was 45 km. At this and greater distances, where the field strength becomes very small. stationary waves, which occur upon reflection at all kinds of obstacles in the landscape, begin to play an appreciable part. It is often found in such a case that a displacement of the apparatus by several metres influences the communication considerably. In large cities, as already mentioned in the introduction, the level of interference is of special importance. This is found, however, not to be too great an objection at the frequencies here chosen. Passing cars, however, sometimes give an unpleasant interference which is caused by the sparking plugs. The car in which the apparatus in installed must of course be rendered absolutely free of interference from this source. This is done not only by the usual devices for a car radio receiver, but also by introducing resistances of about 10 000 ohms in series with the sparking plugs.

OPTICAL EXPERIMENTS WITH MODELS ON THE DIRECTIONAL DISTRIBUTION OF SOUND IN HALLS

by R. VERMEULEN.

534.846.6 ; 534.846.3

The sound distribution in a hall can be imitated in a simple way by the light distribution in a small model of the hall. With the help of a small camera obscura the directional distribution of the light can be determined at definite spots in the model, and in this way some information is obtained about the directional distribution of sound in the hall. Serveral records are shown which were made in a model of a broadcasting studio.

In order to study the distribution of the radiation of a source of sound in a hall, use may well be made of small models in which the source of sound is replaced by a light source, and the walls are made of a material which as far as possible reflects the light in the same way as the sound is reflected by the walls in the actual hall.

In a previous article in this periodical it was explained how the acoustics of theatre auditoria can be studied with the help of such models [1]). The principle of the models used for this purpose is given in *fig. 1*. The part of the auditorium in which the audience is seated is left open. This may be done since the sound which is incident on the audience is practically completely absorbed. The light source occupies the position of the stage or of the orchestra.

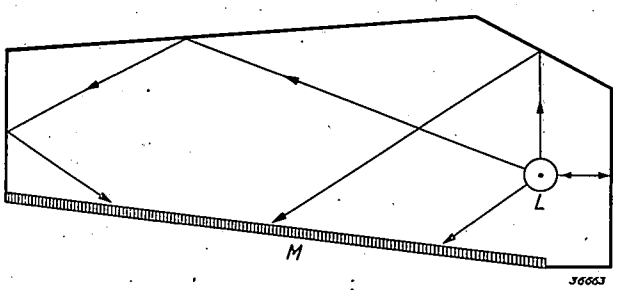

Fig. 1. Optical model for the investigation of the sound distribution in a hall. The source of sound is represented by a lamp *L*. The walls of the model are made of polished aluminium. At the spot where the audience is seated a frosted glass plate *M* is introduced. The light distribution over this plate gives a picture of the sound distribution over the audience.

If a photographic plate or a frosted glass plate is placed over the opening it will receive the direct light from the lamp and the light reflected by the ceiling and walls. The distribution of the intensity of illumination over the floor space will correspond to the distribution of the intensity of sound over the audience. This holds at least as far as the propagation of sound takes place according to the rules of geometric optics. It is true for high tones whose wave length is small compared with the dimensions of the surfaces at which the sound is reflected; for low tones, however, it does not hold. A further restriction of the fidelity of the model lies in the fact that it is almost impossible to make the optical reflection coefficients as large as the acoustic reflection coefficients of many ordinary wall coverings [2]. For this reason there is always a considerable amount of sound radiation in a hall which is due to repeated reflections which are not reproduced by the optical model. This sound radiation has usually covered a fairly long distance and has therefore experienced such a retardation that it no longer contributes to the intelligibility of speech, but is observed as reverberation or echo.

Phenomena of reverberation or echo will therefore often be incapable of being investigated by means of optical models. If we are primarily concerned with intelligibility, however, optical models can be successfully employed. The components with high frequency in the sound, whose propagation obeys the geometric optical laws very well, are of primary importance for the intelligibility [3]). Moreover, only those rays contribute to the intelligibility which are not longer than 20 m from the source to the hearer. These are rays which, in a hall of ordinary dimensions, will usually only have undergone one or two reflections [3]), and in the case of which the too great absorption in the

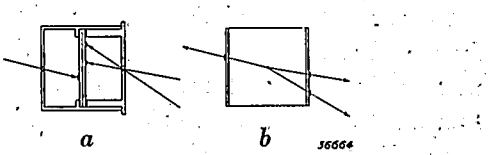

Fig. 2. *a*) Camera obscura (actual size) for the determination of the directional distribution of light at a given spot in a room.
b) The photographs obtained, pasted to a cube of the same size as the camera, give a clear picture of the directional distribution.

[1]) Philips techn. Rev. **1**, 46, 1936.

[2]) The models were made of aluminium which when entirely clean and polished has an optical absorption coefficient of about 15 per cent. This is about equal to the acoustic absorption coefficient of a carpet, while a hard wall has an absorption of only about 3 per cent.

[3]) See on this subject the article: Auditorium acoustics and intelligibility, Philips techn. Rev. **3**, 139, 1938.

optical model does not yet have a disturbing effect. For this so-called effective sound it may therefore be stated, that not only the intensity but also the directional distribution of the radiation corresponds at every point in the hall with the intensity and directional distribution of the light at the corresponding point in the model.

The previously described experiments only provide information about the total sound intensity at a given spot, but not about the direction from which the sound is incident. In the investigation of theatre auditoria this latter information is not usually required; it is, however, required in the investigation of broadcasting studios, where it is desired to know not only the intensity but also the directional distribution at the point occupied by the microphone.

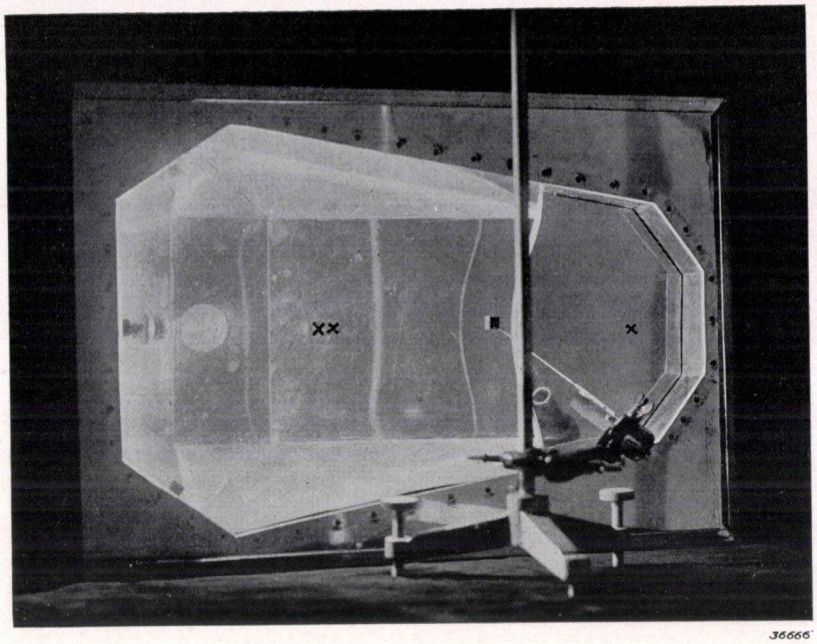

Fig. 3. Measurement with the camera obscura at a given spot in the model of a hall. Three other measuring spots are indicated by crosses.

In order to be able to determine the directional distribution of the radiation which is incident upon a given point, a "camera obscura" was constructed (see *fig. 2*). This has the form of a cube with an edge of 1 cm. At the centres of two opposite sides small holes are bored, while halfway between these holes a piece of photographic paper is inserted which is light-sensitive on both sides. When this camera is placed at a spot in the model at which one desires to investigate the directional distribution of the sound (see *fig. 3*), an image will be formed on both sides of the photographic paper from which it can be judged from which main direction the light was incident upon the front and rear of the camera obscura.

The acceptance of the camera obscura to the front and rear side amounts to only about 90°. By making three exposures with the holes of the camera first front and back, then right and left and finally top and bottom, a complete picture can be obtained of the directional distribution of the sound at the spot investigated.

This picture can be made very clear by pasting the photographs obtained upon a cube so that the line joining the centre of the cube and a blackened point of a photograph pasted on one side corresponds to the direction of the ray which caused the blackening of that point (fig. 2*b*).

Experiments were done with a model of a broadcasting studio which is shown in *fig. 4*. The arrangement shown in fig. 3 also refers to this studio. The directional distribution of the sound (the light) was determined at four points in the room which may be considered as positions for the microphone.

In the cross section sketch the path of several rays is given between the orchestra (the lamp) and the microphone (the camera obscura). It may be seen how the different facets of the walls and the ceiling above the orchestra contribute to the concentration of the sound rays and serve to send the sound toward the back of the hall. At the same time from this drawing it may be seen from which direction the sound rays reflected by the different walls are incident upon the microphone. These directions are also indicated for the three other measuring points, but without the reproduction of the entire path of the rays.

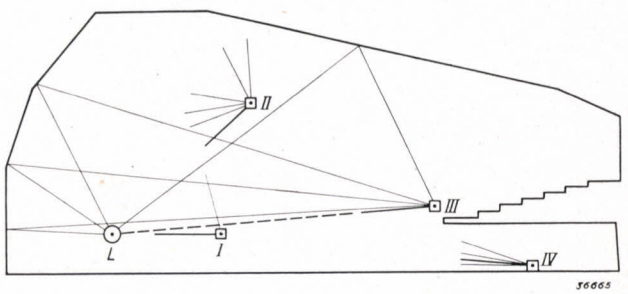

Fig. 4. Model of a broadcasting studio in Hilversum (Netherlands). *L* lamp; *I*, *II*, *III*, *IV* positions where the directional distribution of the sound was investigated with the help of a camera obscura. For position *III* the possible sound rays are drawn from the lamp to the measuring point. For the other positions these rays are indicated by short lines.

The photographs obtained with the camera, pasted to a cube in the manner described, are shown in *fig. 5a* and *b*. Most of the ray directions indicated in fig. 4 can easily be found in fig. 5. In addition to points which correspond to these ray directions, however, numerous other spots may be seen, which must be ascribed to reflections by the oblique surfaces which are situated between ceiling and walls (see fig. 3). The high intensity of these spots indicates that by a suitable construction of these oblique surfaces a considerable amplification of the sound can be obtained at the back of the hall.

In fig. 5*b* where the cubes are seen from the rear, it is striking that it is the cubes placed toward the front of the model which exhibit an appreciable blackening on their rear sides. Since the sound contribution corresponding to this covers a considerably longer path than the direct sound in the front of the hall, it might lead to disturbing echo phenomena. For this reason the rear wall of the hall was covered with a material which damps the sound very much.

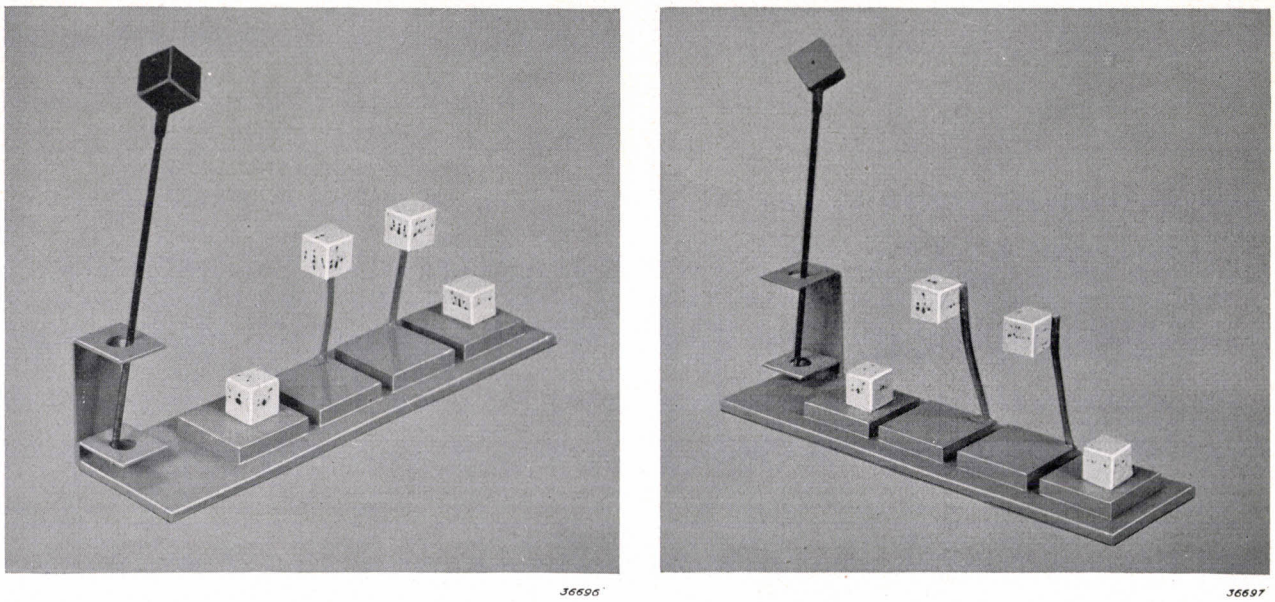

a *b*

Fig. 5. From left to right: records of the directional distribution of the sound at the positions *I-IV* of fig. 4 pasted to cubes according to the method given in fig. 2. *a*) gives the front and *b*) the rear side. From the photograph of the rear side it may be seen that a considerable amount of sound energy is reflected by the rear wall to the measuring points *I* and *II*, which in the actual hall would lead to echoes. In the stand may be seen the camera fastened to an axis in the direction of a cube diagonal. Simply by rotating this axis the camera can be brought successively into the three desired positions for the three exposures.

GEOMETRICAL CONFIGURATIONS AND DUALITY OF ELECTRICAL NETWORKS

by B. D. H. TELLEGEN.

513.84 : 621.392

Two networks may have such a relation to each other that one behaves with respect to the current flowing in it in a way entirely analogous to the way in which the other behaves with respect to the voltages prevailing in it. Such a "duality" between two networks can, however, only exists when the geometrical configuration according to which the networks are built up satisfies the condition that it can be drawn in one plane without two branches crossing each other. After a consideration of the possible geometrical configurations, this condition is illustrated by means of examples.

In calculations of electrical networks analogous formulae are often obtained when in one network the currents are calculated and in another the voltages. A simple example of two such networks is shown in *figs. 1a* and *b*. In order to present the analogy mentioned as clearly as possible we shall introduce the following concepts: an arbitrary electrical element (resistance, coil, condenser, source of voltage, source of current, etc.) we shall call a branch of the network; the end of a branch, which at the same time forms the connecting point of two or more branches, we shall call a junction; a closed circuit, which is formed by any arbitrarily chosen branches of the network, will be called a mesh.

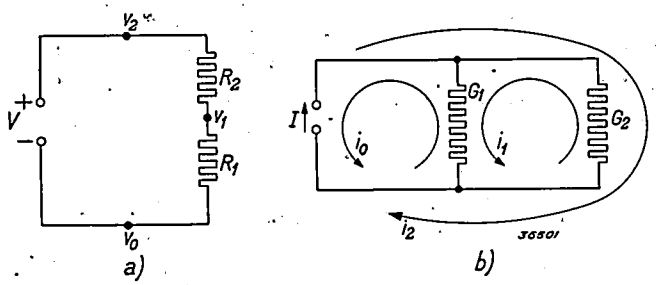

Fig. 1. Two simple networks which are dual with respect to each other.

The following statements may then be made about the network of fig. 1*a*.

A source of voltage V is applied to two resistances R_1 and R_2 in series. The current through the resistances is:

$$I = \frac{V}{R_1 + R_2}.$$

The voltages V_1 and V_2 on R_1 and R_2 are:

$$V_1 = \frac{R_1}{R_1 + R_2} V, \qquad V_2 = \frac{R_2}{R_1 + R_2} V.$$

The system contains three branches and three junctions. The voltages on the three branches are in each case equal to the differences between the potentials of the junctions, v_0, v_1 and v_2:

$$v_1 - v_0 = V_1, \quad v_2 - v_1 = V_2, \quad v_2 - v_0 = V.$$

Since the voltages on the branches do not change when the potentials of all the junctions are increased by the same amount, the latter are determined except for an additive constant.

Correspondingly the following may be stated about the network of fig. 1*b*.

A source of current I is applied to two conductances G_1 and G_2 in parallel. The voltage on the conductances is:

$$V = \frac{I}{G_1 + G_2}.$$

The currents I_1 and I_2 through G_1 and G_2 are:

$$I_1 = \frac{G_1}{G_1 + G_2} I, \qquad I_2 = \frac{G_2}{G_1 + G_2} I.$$

The system contains three branches and three meshes. The currents through the three branches are in each case equal to the differences between two of the mesh currents i_0, i_1 and i_2:

$$i_1 - i_0 = I_1, \quad i_2 - i_1 = I_2, \quad i_2 - i_0 = I.$$

Since the currents through the branches do not change when all the mesh currents are increased by the same amount, the latter are determined except for an additive constant [1]).

If we compare the statements about the two systems we see that they become identical when we interchange the words voltage and current, resistance and conductance, connection in series and connection in parallel, junction and mesh. Networks which also contain capacities and self-inductions can in the same way be compared with each other by interchanging the words capacity and self-induction. Networks which can be compared in this way are said to be dual with respect to each other [2]). If one has studied the properties of one network, the properties of the dual network are thereby also known.

---

[1]) In the customary method of calculating with mesh currents, one of these is usually set equal to zero. For the purpose in view, however, this cannot be done here.

[2]) Instead of dual the words reciprocal or inverse are also used.

The purpose of this article is to show how we can generalize the duality found in the example of fig. 1 in order to be able to indicate a dual system in the case of networks of more complex composition also.

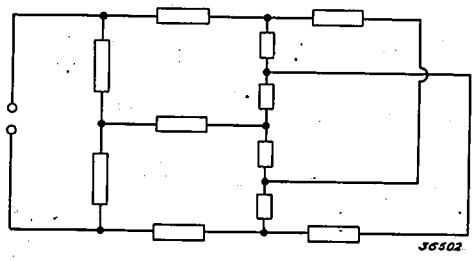

Fig. 2. Example of a network for which no dual system can be found.

We shall not consider mutual inductions in doing this, although it is possible to include them in the discussion. It will be found that this generalization is not always possible, in other words, that networks exist which have no dual system. An example of such a network is drawn in *fig. 2*. The conditions which a network must satisfy in order to have a dual system can be found by the help of topological considerations of the network. One is thereby not concerned with the electrical significance of the branches occurring in the network, but with the geometrical configuration of the network, in which it is only the way in which the junctions are connected to each other, and not the position of the junctions and the length and form of the branches which is significant. The branch of geometry which considers figures in this way is analysis situs or topology, and the configurations in question are known as graphs.

Geometrical configurations of the networks

We shall begin with a general investigation of the geometrical configurations of the networks [3]). In the case of networks which have pairs of terminals, we consider each pair of terminals as a branch of the configuration. If we are, for example, concerned with a quadripole, such as is represented in *fig. 3a*, consisting of two pairs of terminals connected by three resistances in star connection,

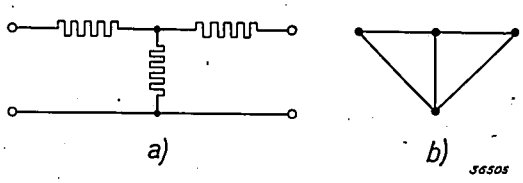

Fig. 3. A network with two pairs of terminals (*a*) and its configuration (*b*).

[3]) R. M. Foster, Geometrical circuits of electrical networks, Trans. A.I.E.E. **51**, 309. 1932.

the system contains four junctions connected by five branches, and we may draw the configuration of this quadripole as indicated in fig. 3*b*. Due to the fact that we consider the pairs of terminals as branches, the currents flow entirely within the configuration. In this way we can leave out of consideration configurations which consist of two parts which are either unconnected or connected at only one point, since in such configurations no current can flow from the one part of the configuration to the other, and the two parts are therefore entirely independent of each other electrically.

We now draw successively all the configurations which are possible with a given number of branches. This is done in *fig. 4* for up to and including seven branches. With two branches, only one configuration is possible. With three branches two configurations are obtained, with four branches five, with five there are six, with six branches 13, with seven branches 28, etc. The two configurations with three branches are formed from the configuration with two branches, by replacing one branch in the latter by two branches in parallel or two branches in series. In the same way all the configurations with four branches can be derived from the configurations with three branches, and similarly all the configurations with five branches, from those with four branches. This can be easily verified by means of fig. 4. In the case of the configurations with six branches, however, this derivation is no longer entirely valid. Among these configurations there is one (indicated in fig. 4 with heavy lines) in which no single pair of branches is in series or in parallel, so that this configuration cannot therefore be derived in the manner described from a configuration with one branch less. The configurations with seven branches can again all be derived from those with six branches, whereby two configurations with seven branches are formed from the configuration with six branches printed with heavy lines.

Since the number of configurations with more than seven branches becomes very large, in drawing them we shall confine ourselves to those configurations which contain no branches in series or in parallel, since the others can always be derived in the manner described from the configurations with one branch less. Configurations without connections in series or in parallel are only possible with definite numbers t and k of branches and junctions, as will appear from the following.

If a configuration contains no branches in series, then at least 3 branches come together at every junction. If we count the number of branches coming together at every junction and multiply by the

number of junctions, we arrive at the total of at least $3k$ branches. Every branch is hereby counted twice, so that

$$t \geqq 3k/2 \quad \ldots\ldots\ldots \quad (1)$$

If a configuration contains no branches in parallel, it cannot contain more branches than when each junction is connected to every other junction by one branch. At every junction, therefore, not more than k—1 branches come together. If for all the junctions we count the number of branches coming together at that point, we therefore arrive at the total of not more than $k(k-1)$ branches, whereby every branch is again counted twice, so that

$$t \leqq k(k-1)/2 \quad \ldots\ldots\ldots \quad (2)$$

From (1) and (2) it follows that $k\ (k-1) \geqq 3k$, and therefore $k \geqq 4$, from which with (1) it follows that $t \geqq 6$. Actually, among the configurations reproduced in fig. 4, it was with six branches that we first found a configuration which contains no connections in series or in parallel. The values of k which are possible at certain values of t on the basis of (1) and (2) are given by the following table:

t =	6	7	8	9	10	11	12
k =	4	—	5	5 6	5 6	6 7	6 7 8

In *fig. 5* these configurations are drawn for up to and including 11 branches.

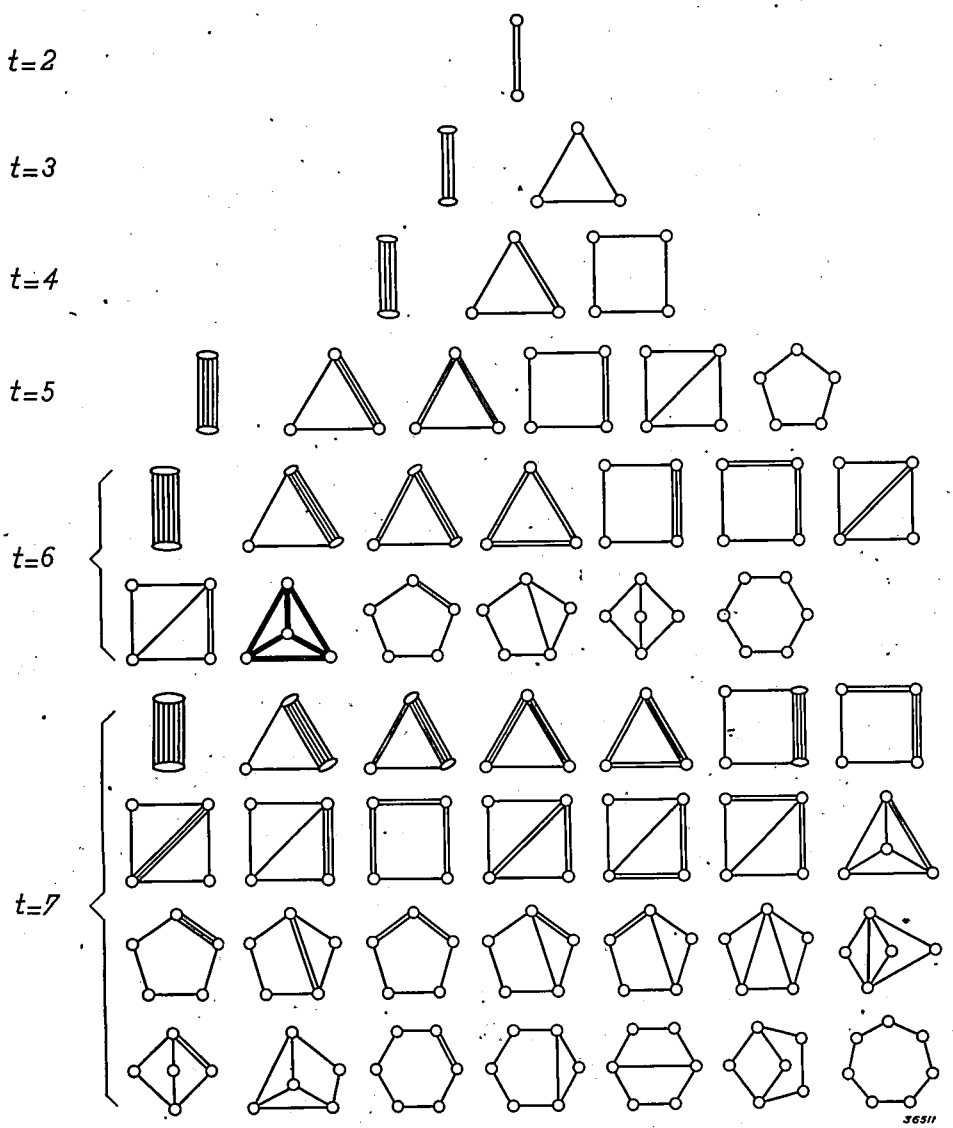

Fig. 4. Possible configurations with t branches, for t up to and including 7. The heavily printed configuration in the series with $t = 6$ differs from the others by the fact that it contains no connections in parallel or in series.

The configuration with six branches which already occurs in fig. 4 is that of Wheatstone's bridge. All the branches and junctions in it are equivalent, which can best be seen when the figure is imagined as a tetrahedron (*fig. 6a*). In a corresponding way the configuration with $t = 8$ can be imagined as a square pyramid (fig. 6*b*), that with $t = 9, k = 5$ as two tetrahedrons base to base (fig. 6*c*).

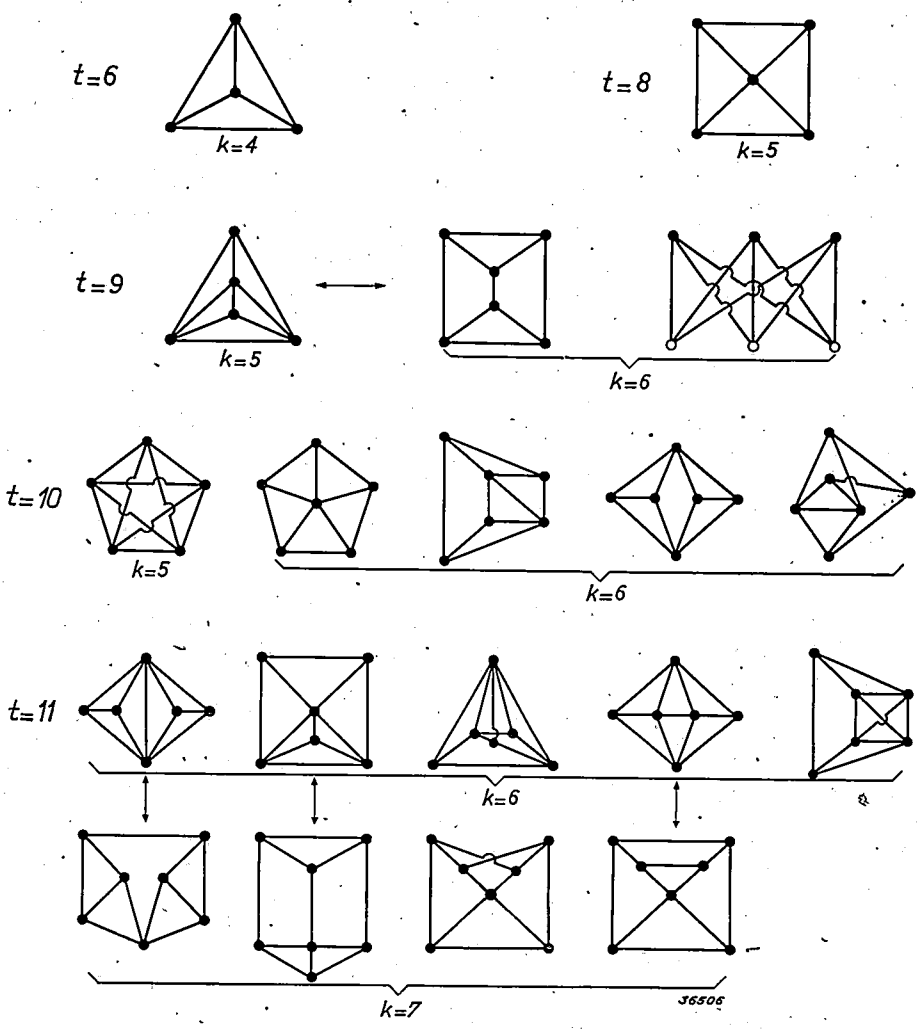

Fig. 5. Configurations for t up to and including 11, in which no connections of branches in parallel or in series occur. All planar configurations (see below) are drawn without crossings. The configurations connected by arrows are dual with respect to each other, the other planar configurations are dual in themselves.

With $t = 9$, $k = 6$ two configurations are possible, the first of which can be conceived as a triangular prism (fig. 6*d*). In the case of the second, which consists of two sets of three junctions, with each junction of one set connected to each junction of the other set, such an interpretation as a simple solid (a polyhedron) is, however, no longer possible, and the same is true of the configuration with $t = 10$, $k = 5$, in which each junction is connected to every other junction (the complete pentagon). Since these facts are of decisive importance for the duality, we shall subject them to a closer examination.

The two last-mentioned configurations, which we shall indicate by A and B in the following, and which are again shown separately in *fig. 7*, cannot be drawn in a plane without at least two branches crossing each other. This can be easily verified by attempting to do so, and it can also be proved directly (see below). Configurations which can be drawn in a plane without crossed branches we shall call planar; A and B are therefore not planar. It can be shown that all non-planar configurations can be reduced to the opening or short circuiting of branches of A and B, so that A and B are the fundamental types of non-planar configurations [4]).

[4]) C. Kuratowski, Sur le problème des courbes gauches en topologie, Fundamenta Math. **15**, 271, 1930. H. Whitney, Planar graphs, Fundamenta Math. **21**, 73, 1933.

The fact that A and B are not planar is related to the above-mentioned fact that it is impossible to conceive the branches of these configurations as the edges of a polyhedron. This may be understood

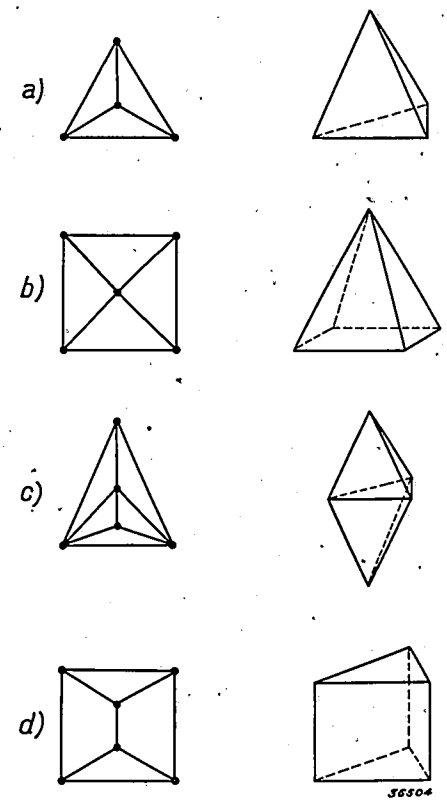

Fig. 6. Certain configurations can be imagined as polyhedrons: *a*) tetrahedron, $t = 6$, $k = 4$; *b*) square pyramid, $t = 8$, $k = 5$; double tetrahedron, $t = 9$, $k = 5$, *d*) triangular prism, $t = 9$, $k = 6$.

as follows. A planar configuration can also be drawn on a sphere without two branches crossing each other. The surface of the sphere is then divided by the configuration into a number of side surfaces, so that the part of the plane originally surrounding the configuration also becomes a side surface of the sphere. Since a sphere and a polyhedron are topologically equivalent, we may also consider the configuration drawn on the sphere as a polyhedron, and we may imagine the polyhedrons given in fig. 6 as being formed in this way from the corresponding configurations. Conversely every configuration drawn on a sphere without crossing can also be drawn without crossing in a plane [5]).

The boundary of every side surface in which a sphere is divided by a configuration drawn upon it, forms a mesh in the sense defined at the beginning. Between the number m of these side surfaces or meshes, the number t of the branches and the number k of the junctions there is a relation, called the *Euler polyhedron formula*, of the following form:

$$k - t + m = 2 \quad \ldots\ldots \quad (3)$$

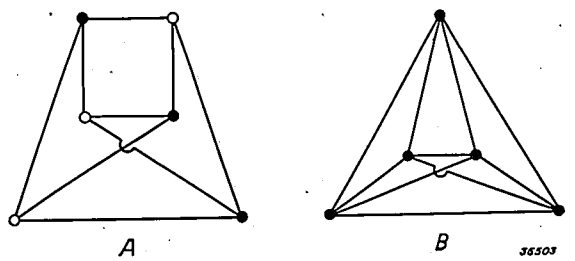

Fig. 7. The two fundamental types A and B of all non-planar configurations. The configuration A, with $t = 9$, $k = 6$ is built up of three sets of three junctions, each junction of one set (circles) is connected to each junction (points) of the other set. The configuration B with $t = 10$, $k = 5$, consists of five junctions, each of which is connected to every other. Both configurations. which occurred also in fig. 5, are here so drawn that there is only one point where two branches cross.

With the help of this formula we can demonstrate the lack of planarity of the configurations A and B. Assume that A (with $t = 9$, $k = 6$) is planar. Drawn on the sphere, it must be true that $m = t - k + 2 = 5$. Since every branch must belong to two of these meshes, $2t = 18$ branches are available for these meshes. However, A contains no triangles, so that for the meshes at least $5 \times 4 = 20$ branches are necessary, thus more than those available. From this it follows that A cannot be planar. Similar reasoning can be applied in the case of B [6]).

A and B can be drawn on other surfaces [7]) without crossing, since for such surfaces $k - t + m < 2$ is always true. For a torus for example $k - t + m = 0$. A may be drawn on a torus as is done in *fig. 8*; the torus is thereby divided into $m = 9 - 6 = 3$ meshes. B can also be drawn on a torus, in two ways, as indicated in *fig. 8*. In both cases the torus is divided into 5 meshes. Another type of surface is Möbius' strip which is obtained by giving a half turn to an open strip and then joining the ends. On this surface, starting from any point and passing around the strip, we can reach the corresponding point on the other side of the strip. Such surfaces are called unilateral surfaces. For Möbius' strip $k - t + m = 1$. The configurations A and B can also be drawn upon it, as indicated in *fig. 9* and B can again be drawn in two ways.

Conditions for duality and construction of the dual network

When generalizing the duality found in the case

[5]) Each side surface of the sphere may be transformed into the part of the plane surrounding the configuration. Drawn on the sphere, the configuration with eight branches, for example, from fig. 5, contains four triangles and one quadrangle. In fig. 5 it is so drawn in a plane that the quadrangle forms the periphery. It may, however, also be drawn so that one of the trangles forms the periphery.

[6]) F. Levi, Streckenkomplexe auf Flächen, Math. Z. **16**, 148, 1923.

[7]) I. N. Kagno, The mapping of graphs on surfaces. J. Math. and Phys. **16**, 46, 1937.

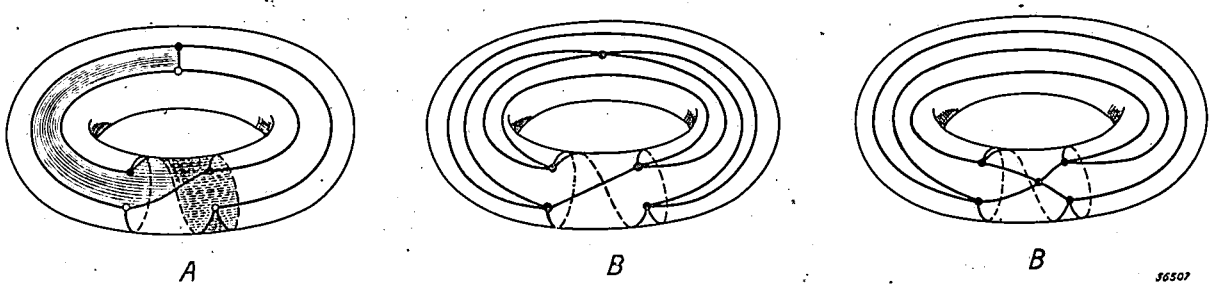

Fig. 8. The non-planar configurations A and B drawn on a torus. Configuration A divides the torus into 3 meshes, each of 6 branches. One of the side surfaces which are bounded by these meshes is here indicated by shading. Configuration B divides the torus either into 2 meshes of 5, 1 mesh of 4 and 2 meshes of 3 branches, or into 5 meshes of 4 branches.

of the example in fig. 1 we begin with the requirement that the junctions of the dual system shall correspond to certain meshes of the original system. This leads to the following result [8]):

A network has a dual system when and only when it is planar.

The network of fig. 2 is not planar, since it can be derived from the configuration A, as is shown in *fig. 10*, when the branch indicated is opened and one each of the resulting pairs of branches in series is short circuited. The network therefore has no dual system.

If a network is planar, the dual system can be found in the following way. If we draw the configuration of the network without crossings on a sphere (or in a plane) certain meshes are emphasized, namely the meshes which bound the side surfaces of the sphere. These meshes must now correspond to the junctions of the dual system. Within each of these meshes (in the plane, outside the outermost mesh also) we therefore assume a new junction and connect every pair of these new junctions which lie in adjacent meshes by a new branch, which crosses the common branch of these meshes (see *fig. 11*). If the meshes have more than one branch in common, the corresponding new junctions are also joined by more than one branch. We arrive in this way at a new planar configuration which is the dual of the original, and in which each of the original junctions lies in a mesh of the new system. *The duality is thus reciprocal.* In fig. 5 arrows indicate which configurations are dual with respect to each other. The other planar configurations in this figure are dual in themselves.

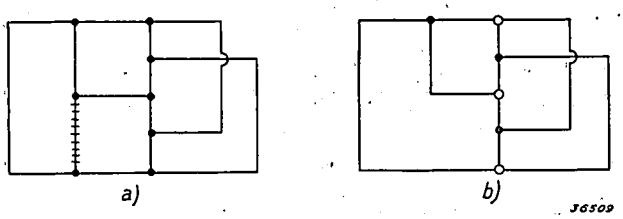

Fig. 10. The network reproduced in fig. 2 can be converted into configuration A by opening one branch and short circuiting two others.

In order to provide that to every equation which can be written for the original system there is a corresponding, entirely analogous equation for the dual system, we must, in the manner indicated at the beginning, change the electrical quantities in the original system into corresponding quantities of the dual system. A current I, for instance, becomes a voltage V. Since these quantities have

[8]) H. Whitney, Non-separable and planar graphs, Trans. Amer. Math. Soc. 34, 339, 1932. Since the derivation of the theorem is rather elaborate and involves abstract considerations it is not given here; it will be published in T. Ned. Rad.-Genoot.

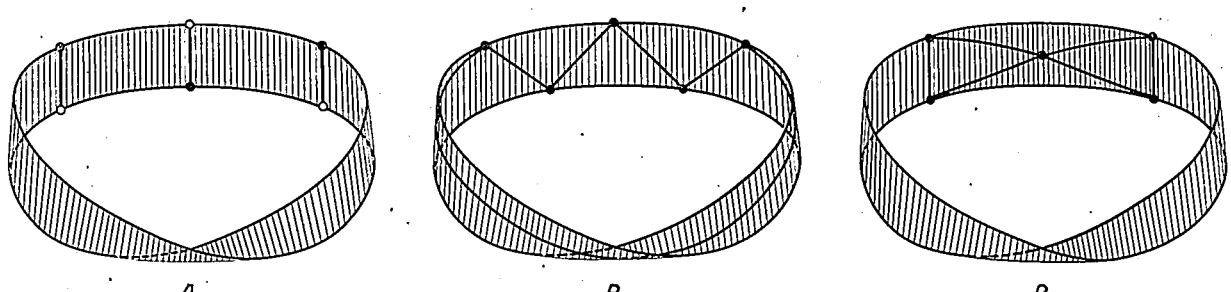

Fig. 9. The non-planar configurations A and B drawn on Möbius' strip. On this surface A forms 3 meshes of 4 and one of 6 branches, B forms either 5 meshes of 3 and 1 of 5 branches, or 4 meshes of 3 and 2 of 4 branches.

different dimensions we may not immediately set them equal to each other, but we must introduce a dimension factor K which has the dimension of a resistance, and whose magnitude we may choose arbitrarily. When we have made $V = KI$ in this way, then the product of every pair of impedances of the two dual networks compared with each other is equal to K^2.

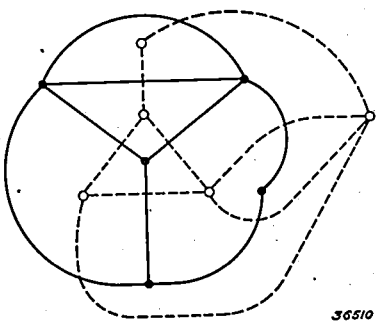

Fig. 11. Construction of the dual configuration (broken lines) for a given configuration (full lines).

If the system contains connections in series, for instance a self-induction, a resistance, a capacity and a source of voltage in series, these must be considered as four branches which are therefore replaced in the dual system by a capacity, a conductance, a self induction and a source of current connected in parallel.

As an example let us consider the oscillation circuits given in *fig. 12a*, which are coupled over a self induction, and the first of which contains a source of voltage. The dual system is drawn in fig. 12*b*. If we assume in the first system two mesh currents i_1 and i_2, the equations for these meshes become:

$$\left(\frac{1}{j\omega C} + R + j\omega L_1\right) i_1 + j\omega L_2 (i_1 - i_2) = V,$$

$$\left(\frac{1}{j\omega C} + R + j\omega L_1\right) i_2 + j\omega L_2 (i_2 - i_1) = 0.$$

If in these we replace the quantities of the first system by the quantities of the dual system in accordance with the above, be replacing C by L/K^2, L_1 by K^2C_1, L_2 by K^2C_2, R by K^2G, V by KI, i_1 by v_1/K, i_2 by v_2/K, where v_1 and v_2 are the voltages on the circuits of the dual system, the above mesh equations pass over into the following equations:

$$\left(\frac{1}{j\omega L} + G + j\omega C_1\right) v_1 + j\omega C_2 (v_1 - v_2) = I,$$

$$\left(\frac{1}{j\omega L} + G + j\omega C_1\right) v_2 + j\omega C_2 (v_2 - v_1) = 0.$$

These are actually the junction equations of the dual system.

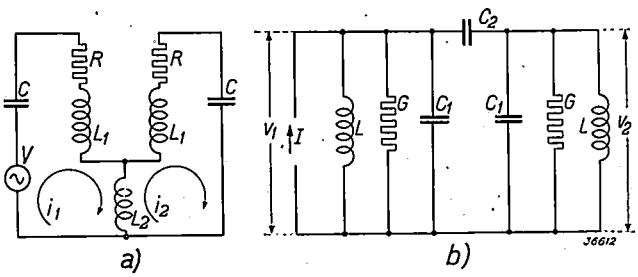

Fig. 12. Example of a network (*a*) for which the dual network (*b*) has been constructed according to the directions given in the text.

AN APPARATUS FOR THE MEASUREMENT OF THE PHOTOGRAPHIC DENSITY OF FILMS

by J. M. LEDEBOER.

771.534.531.5

In measuring photographic density different values can be obtained according to the apparatus used. In the case of the photographic measurement of radiation this is without effect as long as a given arrangement is used. For the recording of density curves of photographic films or plates in order to judge the qality of the picture, however, the arrangement must be adapted to the method of observing (or copying) the film or plate. An apparatus is described which is intended particularly for density measurements of X-ray films. The density can be read off directly on a scale. By the application of an amplifier with automatic control a linear density scale is obtained.

The quality of a photograph, whether a simple amateur photograph or an X-ray photograph for medical or industrial purposes, with given exposure conditions, is mainly determined by the density curve of the photographic film (or plate), *i.e.* by the curve which indicates the relation between the intensity of the radiation incident on the film and the blackening caused by it. In order to judge the value of a film (or of the method of development employed), therefore, this curve must be known. In other cases also, where it is not a question of the quality of the picture, a knowledge of the density curve is required, especially when use is made of the blackening of the film in order to determine quantitatively radiation intensities. Examples of this may be found in spectrography (intensity distribution in spectra), in astronomy (magnitude of stars) and in many other branches of applied physics. Less familiar applications are the determination of the distribution of brightness on road surfaces [1]) and the control of X-ray dosages [2]).

Not only in these measurements themselves, but also in recording the density curve which is required in these cases for calibration, and in general for the estimation of film quality, the problem is encountered of determining the density of a film. We shall here explain briefly how this can be done and then describe a simple, directly indicating instrument for such measurements.

Definition of the density and principle of its measurement

If an amount of light I_0 is allowed to fall upon a blackened film, only a part I of this light will be transmitted. The density of the film is then

$$Z = {}^{10}\log I_0/I.$$

This definition gives some idea of what is meant by "density"; it is, however, inadequate for a quantitative measurement. The value obtained according to the definition by the measurement of I_o and I will still depend very much upon the way in which the light is made to fall upon the film being investigated, and upon the way in which the light is captured which has been transmitted by the film. The loss of light in the blackened film is caused partly by absorption and partly by reflection and lateral scattering [3]). If for example a light ray (I_0) is allowed to fall perpendicularly upon the film and the light emerging at the back in the same direction as the ray is measured (*fig. 1a*), then for that direction the absorbed and reflected light as well as the scattered light is lost. If on the other hand the light emerging within a certain angle is measured (fig. 1*b*) — and this is practically always the case, thanks to the finite aperture of the receiver of the light — then part of the scattered light is also measured, and therefore a lower density is found. In *fig. 2a* this effect is given for different densities.

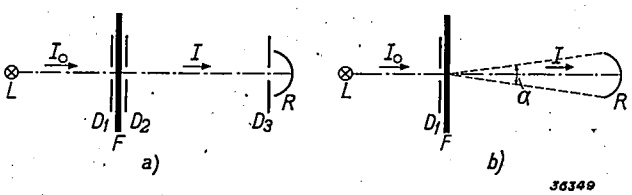

Fig. 1. Arrangements for density measurements. The source of light L radiates on the blackened film F a quantity of light I_0, only part of which I passes through to the receiver R. In *a*) R receives only the direct ray because of the diaphragms D_1-D_3, in *b*); it receives in addition all the rays scattered within the angle α.

The absorption in the blackened film will be greater for a light ray which passes obliquely through the film than for a perpendicular ray. If the light is incident, not in a parallel beam, but dif-

[1]) See P. J. Bouma. Measurements carried out on road lighting systems already installed, Philips techn. Rev. 4, 292, 1939, especially p. 294-5.

[2]) See A. Bouwers and J. H. van der Tuuk, Fortschr. Röntgenstr. **41**, 767, 1930.

[3]) The considerations in this section are borrowed from: J. E. de Graaf, Zur Densitometrie von Röntgenfilmen und ihrer Normung. Z. wiss. Photogr. **37**, 147, 1938.

fusely upon the film to be investigated, then, due to this effect, a smaller value of I/I_0, and thus a higher density, may be found with a greater aperture of the receiver, since in this case the rays incident upon the receiver pass more obliquely through the film and are thus more attenuated.

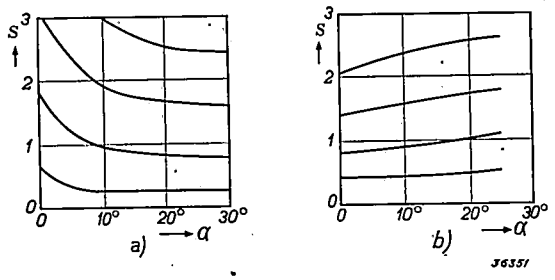

Fig. 2. Density value Z which is found in measuring the same film with receivers of different acceptance angles α (see fig. 1*b*) according to de Graaf [3]). The four curves were obtained with four different heavily blackened films. *a*) A parallel beam was incident on the film. *b*) The film was diffusely illuminated.

This is shown clearly in fig. 2*b*. For a quantitative explanation of the curves there shown the relation between absorption and ray direction as well as the effect of scattering represented in fig. 2*a* must be taken into account.

Finally the colour of the light used for the measurement and the spectral sensitivity of the receiver will affect the value of I_0 found, since the scattering by the grains of the blackened layer depends upon the wave length.

If the purpose of the density measurement is the determination of radiation intensities, it is of little importance what colour of light or direction of beam one uses, if the density measurement is carried out in the same way in calibration and in the measurement itself. The density is in this case only an intermediate quantity. If the density measurement is for the purpose of judging the photographic quality of a film or plate, however, it must be kept in mind that the density differences are the component element of the picture to be obtained, and thus that the manner in which the eye (or the copying material) registers the density also plays a part in the quality which may be assigned to the picture. In this case it is necessary to adapt the density measurement to the manner of observation of the picture (or to the method of copying).

The apparatus which we shall describe in the following was especially developed for the measurement of the density of X-ray films. X-ray films are usually examined by transmitted light with the help of a light box, *i.e.* with diffuse illumination. The eye of the observer is at a distance of about 30 cm from the film. The diameter of the opening of the "receiver", *i.e.* the diamter of the pupil of the eye, is about $^1/_2$ cm. We have therefore chosen exactly the same dimensions for our apparatus (*fig. 3*). As receiver a photocell was used. The spectral sensitivity of this cell should actually be matched to the spectral eye sensitivity; in our case, however, this was unnecessary, since according to a proposal of de Graaf [3]) we used the practically monochromatic light of a sodium lamp for the measurements. For the observation of X-ray films with the light box the use of sodium light is not yet generally customary, it is, however, to be recommended in connection with the relatively slight fatique experienced by the eye upon long continued observation with sodium light.

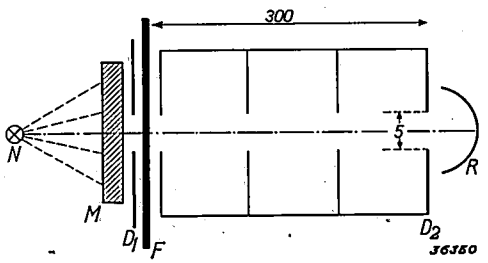

Fig. 3. Arrangement for density measurement of X-ray films, adapted to the method by which the films are examined with the light box. N sodium lamp, M frosted glass, D_1 diaphragm, F film. The aperture of the photocell R is reduced by means of the diaphragm, D_2 to the diameter of the pupil of the eye (5 mm), the distance F-D_2 is equal to the ordinary distance between eye and film (300 mm).

Construction of the apparatus

Arrangement for direct indication

The sodium lamp used in the apparatus burns on alternating current (50 c/s), so that a light flux is obtained which alternates at 100 c/s. The photocell serving as receiver for I therefore gives an alternating current of the same frequency. This is amplified in a two-stage A.C. amplifier, and after rectification the output signal is measured with an ordinary voltmeter (see the diagram of *fig. 4*). The meter can be calibrated directly in density values when care is taken that the extremities of the scale always correspond to the value $Z = 0$ and $Z = \infty$, respectively. For $Z = \infty$, $I = 0$, and this is therefore the pointer indication with no input signal. The pointer can be set accurately on the line for ∞ of the scale by means of a setting screw on the meter. For $Z = 0$, *i.e.* $I = I_0$, the pointer, which here has its greatest deviation (it is best to have it move from right to left) must coincide with the zero line of the scale. This is accomplished with the help of a variable shunt (B in fig. 4) across the meter. The adjustment is only

valid of course for a given value of the light flux I_0, and this must be kept constant during the measurement (see below).

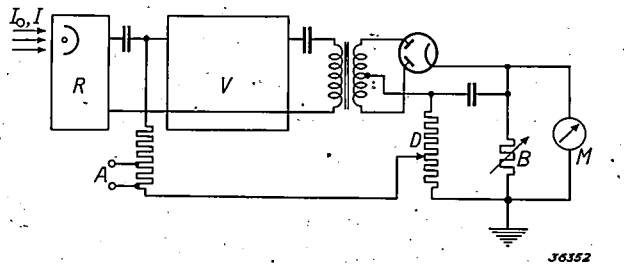

Fig. 4. Connections of the density meter. *R* photocell, *V* two-stage amplifier containing a variable mu pentode EF 9 and an output pentode. *M* voltmeter indicating directly the density, with shunt *B*. *D* potentiometer for regulating the fraction of the output voltage fed back to the valve EF 9. A calibration voltage can be applied at *A*.

The method of obtaining a linear density scale

If an ordinary amplifier with a linear amplification were used, the meter deviation would be proportional to I, *i.e.* we would obtain a logarithmic scale for the density: 90 per cent of the available scale length would be occupied by the region $Z = 0$ to $Z = 1$, the following 9 per cent by the region $Z = 1$ to $Z = 2$, and the last one per cent by the values of Z greater than 2. This is very undesirable, not only for radiation measurements, where the same degree of accuracy throughout the whole measuring region is desired, but also for judging the quality of the picture, because the impressions produced on the eye, according to the law of Weber and Fecher, are approximately proportional to the density.

In order to obtain a density scale which is approximately linear in the region of densities which is of practical importance, an amplifier would be needed which amplifies less with a large input signal (I) than with a small input signal. This requirement recalls the automatic volume control which is employed in radio receiving sets, and indeed the problem can here be solved in an entirely analogous manner [4]). As first amplifier valve we use a variable mu pentode EF 9; the negative grid bias of this valve is influenced by the rectified output voltage of the amplifier, so that the operating point on the valve characteristic is shifted to sections with steeper slope, as the input signal becomes smaller. The "control" characteristic, *i.e.* the relation obtained between output and input signal, still depends upon the fraction of the output voltage (adjustable with potentiometer D in fig. 4) fed back to the input, but in the case of the valve EF 9 it always has an approximately logarithmic section, with which a linear density scale can be obtained in the desired region (*fig. 5*).

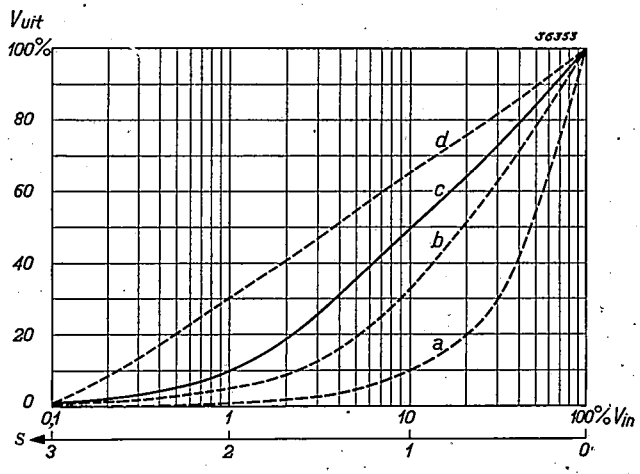

Fig. 5. Control characteristic (output voltage as a function of the input voltage, both in per cent of the value at $I = I_0$) for different adjustments of the potentiometer D in fig. 4.
a) No control; linear characteristic, very unfavourable scale.
b) Weak control (loss in amplification, a factor 4); for $0<Z<1$ the characteristic is already approximately logarithmic.
c) Control as used by us (loss in amplification, a factor 20); the characteristic is about logarithmic for $0<Z<2$.
d) Very strong control. While the density scale hereby obtained is linear up to $Z = 3$, the loss in amplification becomes undesirably great.

Calibration of the scale

By adjustment of the potentiometer D mentioned, the form of the control characteristic can be so influenced that the desired measuring region falls in a favourable position. Since in the case of X-ray films the region between $Z = 0$ and $Z = 2$ is of special importance, it was desirable in the case of the apparatus in question that the point $Z = 1$ should stand in the middle of the scale. This was accomplished in a very simple way. The signal caused by I_0 at the input of the amplifier was replaced by a calibration voltage (applied at A in fig. 4) which causes the same meter indication ($Z = 0$). This voltage was then lowered by a factor 10. Since the current of the photocell is exactly proportional to the light flux at the illumination intensities here prevailing, the attenuation of the calibration voltage by a factor 10 is exactly equivalent to the attenuation of the light flux by a film with the density $Z = 1$. By adjustment of D it was now brought about that the pointer of the measuring instrument coincided with the desired scale line in the middle of the scale (fig. 5 full line curve). In a similar way, namely by successively lowering the calibration voltage by known factors, the rest of the scale was then calibrated. In *fig. 6* it may be seen that the scale is fairly approximately linear

[4]) See C. W. Miller, A linear photoelectric densitometer, Rev. sci. instrum. **6**, 125, 1935.

up to about $Z = 2$. The calibration was controlled by attenuating the light falling upon the photocell by known amounts, by changing the distance of the light source. The "density" measured always showed excellent agreement with the attenuation calculated from the inverse square law.

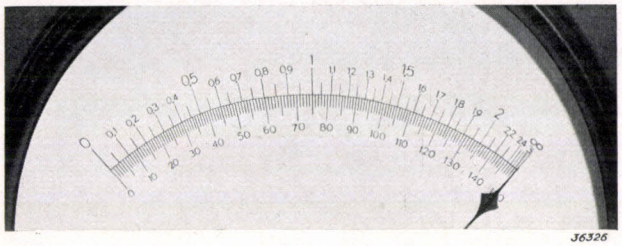

Fig. 6. Density scale of the apparatus with a linear scale below. It may be seen that the density scale is approximately linear in the region between $Z = 0$ and $Z = 2$, which is the most important for X-ray films. The ends $Z = 0$ and $Z = \infty$ of the scale must be checked before the beginning of every measurement and readjusted if necessary. The mechanical resting position of the pointer is on the extreme right, slightly beyond the point $Z = \infty$.

Several details of the construction

In *fig. 7* a photograph is given of the complete apparatus. In the horizontal box is the sodium lamp with the accompanying supply transformer. The supply voltage is stabilized. Since the light flux of the sodium lamp varies only very little with variations in the supply voltage, the light flux I_0 is practically entirely independent of mains voltage fluctuations. The lamp is cooled by a slight aïr current, since otherwise the outer bulb might become too hot.

The lamp illuminates a frosted glass plate (see fig. 3) which in turn serves as secondary light source for the diffuse illumination of the film being examined. The light passes through a diaphragm in the smoothly-finished upper surface of the box into a vertical tube blackened on the inside (fig. 7), and falls upon the photocell used as receiver. When the film is slid over the smooth plate so that the light falls upon the desired spot, the lower section of the tube is pulled down until it touches the film, so that the path of the light ray is entirely shielded from stray light. The diaphragm in the plate has a diameter of 5 mm and therefore the average-density of a circle of that diameter is measured. If desired a smaller diaphragm can also be used.

The amplifier and the accompanying supply apparatus are housed in the vertical box. The supply voltage for the amplifier and the photocell is also stabilized, so that the calibration of the density scale is quite independent of fluctuations of the mains voltage.

The operation of the apparatus is limited to the control and if necessary to the readjustment of the two extremities of the scale before the beginning of each measurement. For setting the point $Z = 0$ with the shunt across the measuring instrument (B in fig. 4, the corresponding knob may be seen above on the left in fig. 7); one must of course wait until the light flux of the sodium lamp has reached its final value, which is the case about 15 minutes after switching on. The potentiometer D for choosing the correct control characteristic is not accessible from the outside; its adjustment needs only seldom to be verified, namely when the variable mu valve is exchanged.

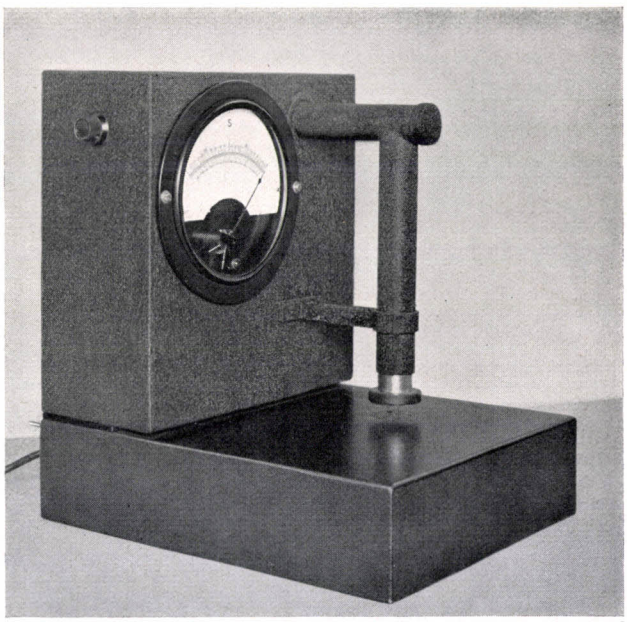

Fig. 7. Photograph of the apparatus. The sodium lamp is in the horizontal box, on the smooth upper surface of this box the film being examined is placed. The light shines through the film into the vertical tube at whose upper end in the horizontal tube the photocell is mounted. The amplifier and the accompanying supply apparatus are housed in the upright box.

REAR LIGHTS AND REFLECTORS FOR BICYCLES

by H. A. E. KEITZ.

683.848.8 : 683.852 : 629.113.8

To protect the cyclist against the danger of being run into from behind by motorvehicles, rear lights or reflectors may be used. In certain countries fixtures are prescribed which function both as rear light and reflector. In this article the principles are discussed upon which the construction of these three types of safety devices is usually based. The Philips bicycle rear lamps, which are of the last-mentioned type, are dealt with in conclusion. The special measures are discussed which have been taken in order to determine easily whether or not the rear light is burning.

In recent years it has become more and more evident that cyclists must be protected at night against the danger of being run into from behind by motorist, and the use of rear lights and reflectors is being made compulsory in more and more countries. It is therefore of interest to examine the optical principles upon which the modern rear lights and reflectors for bicyles are based. Beginning with these optical principles we shall then discuss the way in which a rear lamp can at the same time be made to serve as a reflector, as is now prescribed in various countries. Finally a description will be given of the Philips bicycle rear lamps which belong to this type.

Rear lights

In the case of lamps which are intended only as rear lights, little need be said. Such lamps consist simply of a case with a window of red glass behind which a small lamp burns. This rear light need have an intensity of only a few millicandle power. In general lamps are used which are connected in parallel with the head lamp of the bicycle, and which consume a current of about 0.5 A with the normal running voltage of the bicycle dynamo. Since the current of a modern bicycle dynamo varies only little with the resistance of the lamps connected to it, when a rear light is required it is best to choose for the head lamp a lamp with a correspondingly lower nominal current, for instance 0.45 A instead of 0.5 A. A loss of light of 10 per cent is then experienced which will hardly be noticed, while with a lamp of nominally 0.5 A a loss of about 30 per cent would result, since the lamp would burn at a considerably lower temperature than with normal consumption.

The light intensity of the rear lamp is usually adequate with the simple arrangement mentioned [1]). If, however, an increase in the light intensity toward the rear is desired, this can be obtained at the expense of the acceptance angle of the beam by using a lens instead of the cover glass, and placing the lamp at a suitable spot between the lens surface and the focus. The closer the lamp is placed to the focus, the narrower the beam becomes and the greater the light intensity toward the rear.

Reflectors

Since the cyclist who may be considered to be in danger is practically always in the light beam emitted by the head lamps of the car overtaking him, it was at first thought sufficient if instead of a rear light a reflector was used which reflects the light incident from the head lamp to the car-driver's eye.

The rays falling upon the reflector may be considered as a parallel beam which must therefore be reflected as a practically parallel beam, and in the direction from which the light originally comes. A slight spreading about this direction is permissible and even necessary, since the direction from the reflector to the eye of the car driver does not exactly coincide with the direction from the reflector to the head lamp. The legal regulations existing in different countries about bicycle reflectors take this into account not only by specifying the intensity of the reflection in the direction of incidence, but also by requiring a definite reflective capacity within a definite solid angle around the direction of the incident light. This reflective capacity is usually given as the number of millicandle power reflected per lux of the incident light.

For the solution of the problem of reflecting an incident light beam in the direction of incidence there are two main principles which have led to practically useful constructions:

[1]) According to the legal regulations of different countries the opinions about the necessary light intensity of a rear light are very divergent. A value of several millicandle power may in general be regarded as sufficient. The power of the ordinary rear lamps amounts to about 250 mW, which would in itself be more than adequate for the required light intensity. It must, however, be kept in mind that the cover glass may have quite a strong absorption, while, moreover, from considerations of safety margins, it is desirable to allow the rear light to burn at a relatively low temperature, so that the specific light yield is also quite low.

1) the triple mirror,
2) a lens with a mirror at the focus.

The triple mirror

In 1887 it was demonstrated by Beck [2]) that a system of three mutually perpendicular plane mirrors possesses the property that every light ray which is incident upon it is exactly reversed in direction, so that, apart from a lateral displacement whose maximum value is equal to the diameter of the opening between the three mirrors, it returns exactly to the point from which it was emitted (*fig. 1*).

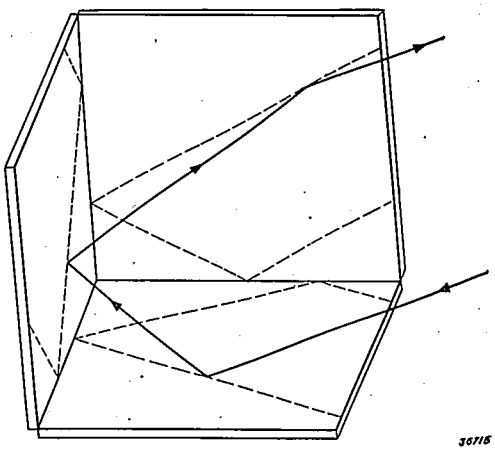

Fig. 1. Triple mirror. A ray, which is reflected by three mutually perpendicular planes, emerges from the third plane in a direction exactly opposite to the direction of incidence on the first plane.

This property of the triple mirror can be demonstrated quite simply by a slightly different interpretation of the law of reflection, which states that the angle of reflection is equal to the angle of incidence. For this purpose we resolve the direction vector of the incident rays into three mutually perpendicular components, two of which lie in the surface of the mirror, while the third is perpendicular to it (see *fig. 2*). It is now evident that upon reflection the component of the ray vector which is perpendicular to the mirror is reversed in direction, while the components parallel to the mirror remain unaltered. A glance at the figure shows immediately that in this case the angle of reflection is equal to the angle of incidence, while the incident ray, reflected ray and normal to the surface lie in a common plane as required by the law of reflection.

If we now pass over to the triple mirror we can best choose for the three components of the ray direction the normals to the three mirrors. Each normal is parallel to two other mirrors, so that we are again concerned with the case discussed above.

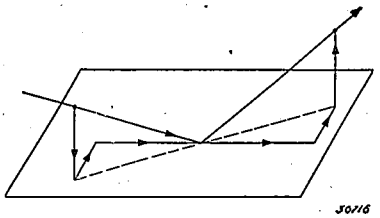

Fig. 2. Reflection on a plane mirror. The direction vector of the reflected ray may be found by reversing the component of the incident ray which is perpendicular to the reflecting surface, and leaving the components parallel to that surface unchanged.

If a ray is successively reflected by the three mirrors, one component of the ray vector is reversed in direction by each mirror, while the other two components remain unchanged. Finally all three components are reversed in direction, which means that the ray itself has been reversed in direction.

In the practical construction of a reflector on the principle of the triple mirror use may be made of the reflection experienced by a ray incident upon a glass surface. If a ray of light is allowed to fall perpendicularly upon the basal plane of a pyramid which has the shape of an obliquely cut off corner of a cube (see *fig. 3*), the ray is totally reflected at the three side surfaces of the pyramid (boundary surfaces glass-air) and then emerges again from the basal plane in a normal direction. The angle of incidence on the three side surfaces in this case is 54.7°. Since toatal reflection already takes place at considerably smaller angles, it is obvious that some-

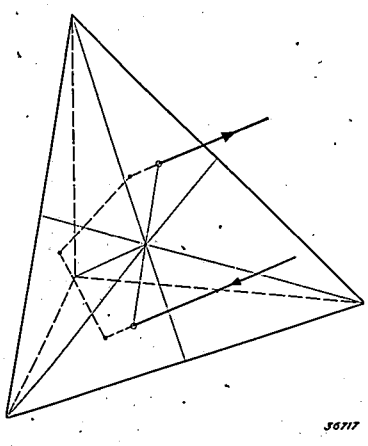

Fig. 3. A pyramid with three mutually perpendicular surfaces has the action of a triple mirror. The direction vector of a ray incident upon the basal plane of the pyramid is resolved into three components parallel to the three perpendiculars to the surfaces of the pyramid. Each of these components is perpendicular to one mirror surface and is reversed in direction when the ray is reflected by the surface in question.

[2]) A. Beck: Über einige neue Anwendungen ebener Spiegel, Z. Instr., 7, 380-389, 1887.

what obliquely incident rays will also be totally reflected. For rays which have an angle of incidence on the basal plane of the pyramid of more than about 20°, the reflection is no longer total, but still very considerable; the reflectivity therefore decreases only slightly with increasing angle of incidence.

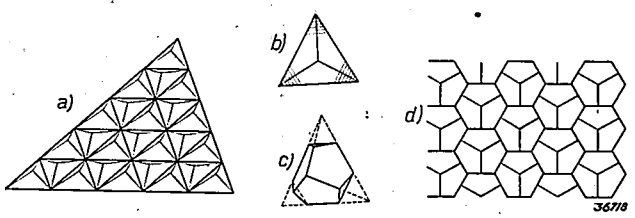

Fig. 4. Pyramid glass. *a*) Plane, covered with rectangular pyramids. A ray which is incident from below vertically upon one of these pyramids will also be reflected vertically downward, except when it is too close to one of the basal angles of the pyramid, namely in the shaded part of *b*). By cutting off this part of the pyramid as in *c*) the surface can be more completely covered with pyramids, for instance as in *d*), and in this way the efficiency of the reflector in the axis direction is increased.

The glass of the pyramid is red in order to give the reflected light the customary red warning colour. Since the path of the light through the glass is quite long, and since the loss of light must be limited in order to obtain the greatest possible efficiency, the coloration of the glass would have to be made extremely light with this type of construction. Such a weak coloration is difficult to obtain in mass production with sufficient constancy. Therefore in the construction of bicycle reflectors on this principle it is almost universally customary to limit the path of the light through the glass by impressing in the glass a large number of small pyramids side by side as indicated in *fig. 4a*, instead of using a single large pyramid. The part of the surface which is shaded in fig. 4*b* contributes no useful effect upon illumination in a perpendicular direction. If one considers how the reflected rays travel it is found that a ray which falls upon the shaded portion of the pyramid (the "dead angles") after two reflections emerges in an oblique direction without touching the third side. By cutting off the dead angles vertically according to fig. 4*c* a closer packing of pyramids can be obtained (see fig. 4*d*), and the efficiency of the reflector for perpendicularly incident rays is improved.

If the pyramid glass acted exactly as a triple mirror, the light of a head lamp would be reflected back to the head lamp in such a narrow beam that it would not meet the eye of the driver. It is therefore desirable that the surfaces of the pyramids should not reflect perfectly, but should have a certain spreading. This spreading is found in practice always to be present, because even the best constructed reflectors have deviations from the ideal form, particularly in the smoothness of the side surfaces of the pyramids. It is therefore no problem to obtain this spreading. On the contrary, great care must be taken to keep it small, since every increase in the spreading is accompanied by a decrease in the light intensity in the desired direction and therefore in the quality of the reflector.

In addition to careful finishing of the surfaces of the pyramids, a correct choice of the colour of the glass is of great importance for the quality of the reflector. Insufficient reflection may of course also be due to too dark a colour of the glass. It is therefore advantageous to choose the colour of the glass as light as is compatible with the requirement that the reflected light must be unequivocally observed as red.

Lens with a mirror at the focus

A lens with a mirror at its focus, like a triple mirror, has the property of reflecting every light ray which falls upon it in the direction from which it came (see *fig. 5*). On this basis bicycle reflectors can also be constructed which, although theoretically imperfect, since every lens possesses a spherical aberration, are practically just as satisfactory as reflectors which use a pyramid glass. As to the practical structure of a lens with a mirror, a distinction may be made between two types: one in which the rear surface of the lens forms the focal plane and is silvered so that it acts as a mirror, and one in which lens and mirror are separate. Several models of these two types may be seen in *fig. 6*.

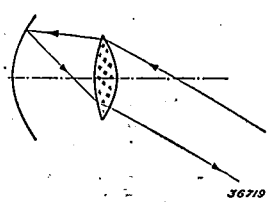

Fig. 5. Combination of lens and mirror. A ray which is reflected by a mirror at the focus of a lens emerges from the lens in a direction opposite to that of incidence.

With the large acceptance angle of the lenses, which is necessary to make possible a compact form of the reflectors, lenses with spherical surfaces cannot be used without obtaining non-permissible losses in the intensity of the reflected light, due to the very incomplete convergence of the rays at the focal plane. Since, however, the lens of the bicycle reflector is not ground, but pressed, the use of a non-spherical surface offers no difficulty in manufacture. A plane-convex lens is usually used, with the

convex side outermost. In order to be able to obtain an exact focussing in a single point, at least of the rays parallel to the axis, the curved surface of the lens must have approximately the form of an ellipsoid.

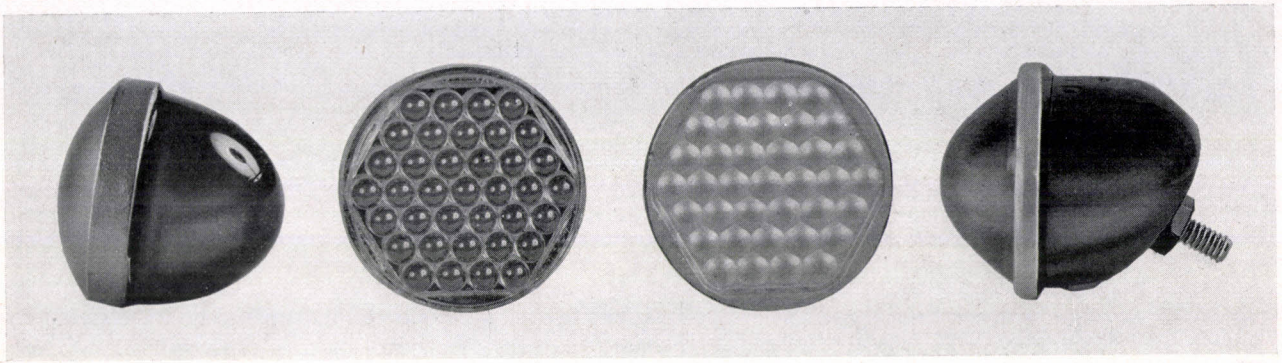

Fig. 6. Bicycle reflectors with combination of lens and mirror. In the types a, b_1 and b_2 the focal plane of the lens coincides with its rear surface; by covering the latter with a reflecting layer the desired effect is achieved (b_1 and b_2 are the front and back of the same reflector). In the type c) a separate mirror is used.

For obliquely incident light the focussing of the rays by the ellipsoid is not complete, so that the reflected beam is spread more and more with increasing angle of incidence. Since, however, for obliquely incident rays, less rigid requirements need be made than for rays parallel to the axis, this property of the lens-mirror combination is not objectionable.

Combination of rear light and reflector

The use of a reflector will in general furnish less perfect protection than the use of a rear light, but it has certain advantages; in the first place a reflector acts even when the bicycle is stationary, in the second place it is absolutely sure, while a rear light fails to act when the lamp or the connection between the lamp and the dynamo is defective. This objection to the rear light is particularly conclusive, since such a defect can scarcely be observed directly by the cyclist himself, and often escapes his attention for some time.

In order to meet this objection it is required in certain countries that a rear light must continue to act as a reflector when the lamp is extinguished. In addition methods have been sought in recent times of making the non-functioning of the rear light directly visible to the cyclist. These two possibilities will be considered further in the following.

As to the combination of rear light and reflector, different solutions are arrived at according as a reflector of the pyramid glass type or of the lens-mirror combination type is used. In the case of the first type it might be considered that it would be sufficient simply to place the lamp behind a covering of pyramid glass. This is found, however, not to constitute a possible solution of itself, since the pyramid glass is entirely opaque, at least in the direction perpendicular to the basal plane. The truth of this fact can easily be understood when it is kept in mind that light incident perpendicular to the front surface of the pyramids cannot pass through the glass but is totally reflected. From the reversibility of the light rays it follows directly that no light from a lamp behind the front surface can emerge in a direction perpendicular to it [3]).

If it is, nevertheless, desired to use a pyramid glass as cover of a rear light, care must be taken that the whole surface is not covered with pyramids. In *fig. 7* two types of such cover glasses are shown: in the case of the first small windows are left open between the pyramids at the spots where the dead

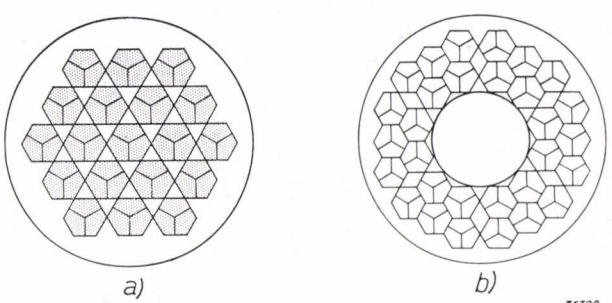

Fig. 7. Two types of pyramid glasses which may be used for rear lights.

[3]) This property may be used to pick out the poorly reflecting glasses. When a pyramid glass is held in front of a source of light the pyramids should remain dark. If, however, the side surfaces of the pyramids are very uneven they may allow light to pass through, and when this is the case it is a proof that the glass has poor reflective qualities.

angles of the pyramids would occur, in the case of the second a lens occupies the centre of the field and is surrounded by pyramids. The second type has been chosen for the rear light type 7/312 constructed by Philips and shown in *fig. 8*.

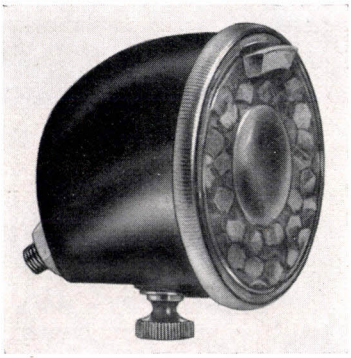

Fig. 8. The Philips bicycle rear light type 7 312 with pyramid glass.

If we now consider the possibilities which are offered by the combination of lens and mirror for the combining of reflector and rear light, we must make a distinction between the two forms of construction according to fig. 6*b* and 6*c*. The construction according to fig. 6*b* can be used by placing a large lens in the centre, instead of the small mirrored lenses, and behind it the lamp. If one wishes to use the combination of a lens and a mirror separated from each other (fig. 6*c*), the lamp can simply be placed between the lens and the mirror. Care must be taken that the path of the rays between lens and mirror is not too much interfered with by the presence of the lamp. A practical construction on this principle, the Philips rear light type 7 309, is shown in the cross section sketch *fig. 9*.

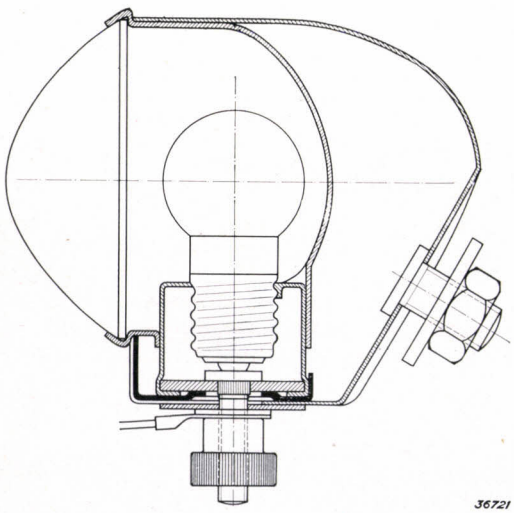

Fig. 9. The Philips rear light type 7 309 with the combination of a lens and a mirror.

Control of the rear light

As already mentioned, attempts have been made recently to find some method of making it directly evident to the cyclist whether or not the rear lamp is burning. The simplest solution is to construct the rear light so that by turning his head the cyclist can see for himself.

In order to be able to ascertain without stopping whether the rear light is burning, it is necessary that the lamp should emit a small amount of light in a forward direction obliquely upwards. In the case of the construction given in fig. 9 with a convex lens, this could be done simply by providing that the lens does not lie too deeply in the holder. By internal reflection and scattering a sufficient amount of light is then refracted in the desired direction. In constructions with a plane cover glass, for instance a pyramid glass, no lighted parts usually project beyond the holder. In the construction of

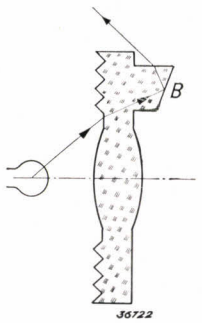

Fig. 10. Path of the rays in the prismatic projection of the Philips rear light type 7 312. The ray is totally reflected at the oblique front surface *B* of the prismatic projection and emerges from the glass in a direction such that it can be seen by the cyclist by turning his head.

the Philips rear light type 7 312 (fig. 8) a special solution was therefore devised of making the rear light visible to the cyclist without dismounting. This was accomplished by means of a prismatic projection at the upper edge of the glass, which can easily be seen by the cyclist as demonstrated in *fig. 10* where the path of the rays in this projection is sketched. It is obvious that the device described has no effect when the rear light is shielded from above, as is at present the case in many countries in connection with the black-out for air-raid defense.

Aside from this objection, the turning about of the cyclist also has other disadvantages connected with safety in traffic. Therefore in recent times another method has been adopted, namely that of connecting in series with the rear light a second lamp which is so placed that it may be seen without turning, and which indicates by remaining lighted that the circuit to the rear light is unbroken. In the case of certain models of Philips bicycle

lamps there is a special fitting for this control lamp in the back of the head lamp (see *fig. 11*). The control lamp is of the same type as the rear lamp; its burning temperature is, however, lower, since a resistance is connected in parallel with it.

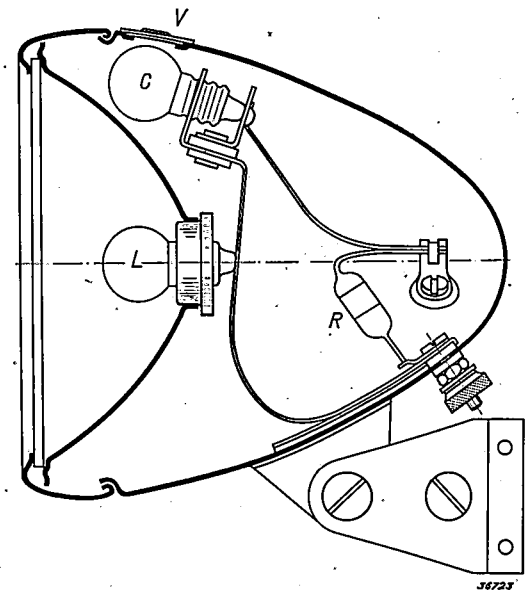

Fig. 11. Cross section of a Philips bicycle lamp with built-in control lamp for the rear light. *L* head lamp, *C* control lamp, *V* window, *R* resistance in parallel with the control lamp.

This construction has various favourable properties. In the first place it is convenient to have the same type of lamp for control lamp and rear light, it is consequently unnecessary to have two different types of spare lamps. In the second place the control lamp is only very lightly loaded due to the resistance in parallel with it, so that it practically never burns out [4]). If, however, due to some other cause, such as heavy shocks, the control lamp becomes defective, the circuit remains closed thanks to the resistance, so that the rear light continues to burn. If on the other hand the rear light becomes defective it can immediately be replaced by the control lamp; in this respect also therefore the control lamp contributes to the reliability of the rear light.

[4]) The fact that the light intensity of the control lamp is thus made very small is no disadvantage, but even an advantage, since it prevents blinding of the cyclist on dark roads.

VOL. 5 No. 12 DECEMBER 1940

Philips Technical Review

DEALING WITH TECHNICAL PROBLEMS RELATING TO THE PRODUCTS, PROCESSES AND INVESTIGATIONS OF N.V. PHILIPS' GLOEILAMPENFABRIEKEN

EDITED BY THE RESEARCH LABORATORY OF N.V. PHILIPS' GLOEILAMPENFABRIEKEN, EINDHOVEN, HOLLAND

THE BLENDED-LIGHT LAMP

AND OTHER MERCURY LAMPS WITH IMPROVED COLOUR RENDERING

by E. L. J. MATTHEWS.

621.327.3 : 621.327.9

Compared with ordinary electric lamps gas-discharge lamps have the advantage of a much higher efficiency; for certain applications, however, they have the disadvantage that the colour of the objects illuminated deviates disturbingly from that by daylight. In this article the methods are examined by which this objection can be met in the case of high-pressure mercury lamps. There are two methods which may be considered: the application of fluorescent substances, and the blending of mercury light with the light of ordinary electric lamps. The first method led to the development of mercury lamps with fluorescent bulbs, the second to the design of fixtures for blended light and to the development of a blended light lamp which combines incandescent lamp and mercury lamp in one system. The degree to which the light sources obtained approach daylight is studied by means of the block method.

Upon the appearance of metallic vapour lamps which were suitable for practical use it was to be expected that the pronounced colour of the light of these lamps and the resulting unnatural colour of the illuminated objects would prevent the unrestricted application of this type of light source. Since, however, the unusually high efficiency made their use very attractive, means have been sought of improving their colour rendering.

In an earlier article in this periodical [1]) the method was discussed by which "white" light [2]), *i.e.* light which makes a satisfactory colour rendering possible, can be obtained with tubular luminescence lamps of low mercury pressure. We shall here examine the method by which the same problem can be brought to a satisfactory practical conclusion in the case of high-pressure mercury lamps.

For this purpose several new types of lamps were developed from the high-pressure mercury lamp, particularly the high-pressure mercury lamp with luminescent bulb (HPL) and the blended light lamp (ML), the latter of which combines a filament and a mercury discharge tube in one bulb. Before dealing with these lamps and the way in which white light can be obtained with the lamps alone or in combination with incandescent lamps, we shall first discuss briefly the properties of the high-pressure mercury lamp itself.

High-pressure mercury lamp, type HP

In the first volume of this periodical [3]) the high-pressure mercury lamp HP 300 was described which differed from the earlier low-pressure mercury lamps by its greater efficiency, its extremely small size and its low electrical power consumption (75 W), which made it possible to use the lamp for indoor illumination also. With the same consumption and providing the same light flux (3 000 lm), a new type of lamp has since been developed which, in different models, has found increasing application within the last few years. This lamp differs from its predecessor chiefly by its lower ignition and burning voltage, which for 220 V mains voltage makes it possible to replace the leakage transformer formerly needed by a choke, which is cheaper and which, moreover, causes fewer electrical losses. As to the external appearance of the lamp, this also made it possible, thanks to the lower working voltage, to replace the special base with pins by an ordinary Edison or Swan base, which did much to promote the use of the new lamp. In the ordinary model the bulb is inside-frosted. The base is provided with a green ring as a warning

[1]) Philips techn. Rev. 4, 337, 1939.

[2]) Philips techn. Rev. 2, 1, 1937; 4, 66, 1939.

[3]) Philips techn. Rev. 1, 129, 1936.

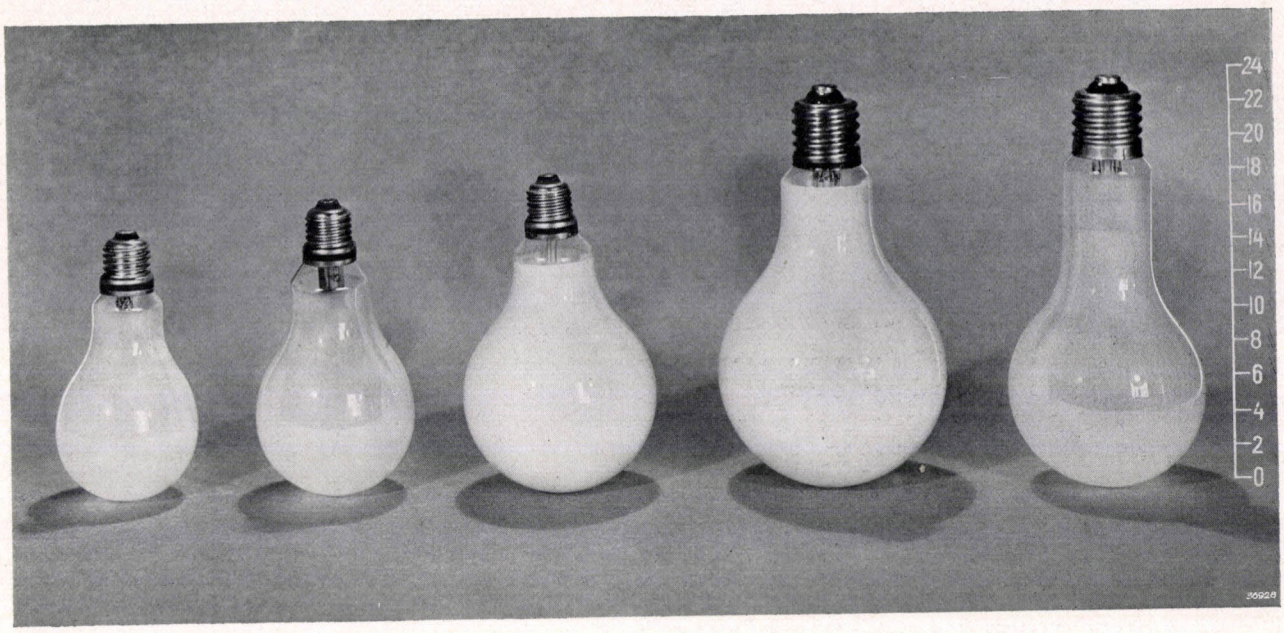

a *b* *c* *d* *e*

Fig. 1. The high-pressure mercury lamps HP 300, HP 500, HPL 300. HPL 500 and the blended-light lamp ML 500. The HPL lamps have a bulb which is covered on the inside with a layer of a fluorescent material, the blended-light lamp ML 500 contains, in addition to the mercury discharge tube, a filament which provides half the total light flux. To the extreme right a cm scale. The first three lamps have an Edison base and are also made with Swan base; the last two lamps have a Goliath base.

that the lamp may not be screwed into any socket but only in a special holder which is part of a circuit containing a suitable series apparatus. This measure is especially important when mercury lamps and incandescent filament lamps are used at the same time, as for instance in the fixtures for blended light mentioned later. In such cases it is best, if possible, to use mercury lamps and ordinary lamps with different bases.

In addition to this new lamp, which has kept the old type number HP 300, a somewhat larger type HP 500 of 120 W, 5 000 lm is also manufactured. The action of these two lamps corresponds almost exactly with that of the previously described high-pressure mercury lamp, except for the fact that the ignition voltage is now lowered by an auxiliary electrode which, inside the lamp itself, it connected to one of the main electrodes *via* a current-limiting resistance.

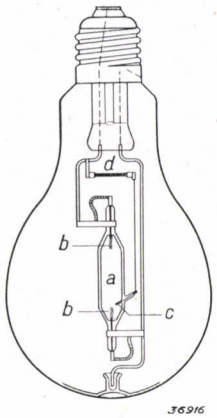

Fig. 2. The mercury lamp HP 300. In the discharge tube *a*, in addition to the main electrodes *b*, there is an auxiliary electrode *c* to one side, which is connected with one of the main electrodes *via* a resistance *d*.

Figs. 1a and *b* show these two types of lamp while in *fig. 2* a cross section is given of the mercury lamp HP 300. In *table 1* the most important data are given. The starting time, *i.e.* the time necessary for the lamp to reach its normal working state, is several minutes. During this time the power consumed and the light flux developed increase gradually. After switching off, the lamp must first cool for several minutes before being able to ignite again. This peculiarity limits the use of the lamp to cases where it is unnecessary to switch the lamp on and off in rapid succession.

Table 1. Properties of HP lamps.

	HP 300	HP 500
light flux	3 000 lm	5 000 lm
consumption (lamp alone)	75 W	120 W
losses in choke (220 V A.C. mains)	8 W	12 W
ditto with leakage transformer (115—125 V A.C. mains)	17 W	23 W
efficiency with choke	36 lm/W	38 lm/W
ditto with leakage transformer	32.5 lm/W	35 lm/W
starting time	4-5 min	4-5 min

The latest models of the series apparatus, over which the HP lamps must be connected, are of such small dimensions that no difficulty is experienced in building them into fittings, etc. *Fig. 3* shows the choke coil (220 volt mains) and the leakage transformer (115-125 volt mains) for the mercury lamp HP 300. The corresponding appliances for the mercury lamp HP 500 are about 1 cm higher.

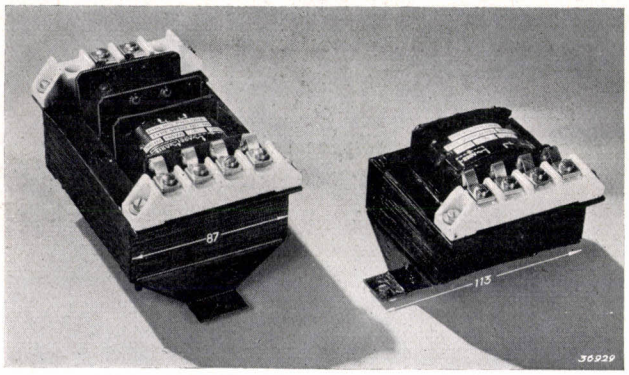

a *b*

Fig. 3. Series apparatus for the mercury lamp HP 300: *a*) leakage transformer for mains of 115-125 V. *b*) choke coil for 220 V mains. The corresponding apparatus for the mercury lamp HP 500 are 14 and 12 mm higher, respectively (113 mm is not the width of the core, but the total width of the choke coil including the feet).

The light of the HP lamps consists mainly of the well-known yellow, green and blue-violet mercury lines with a very weak continuous background (*fig. 4*). The use of these lamps with no colour correction will as a rule result in a pronounced colour change of the illuminated objects.

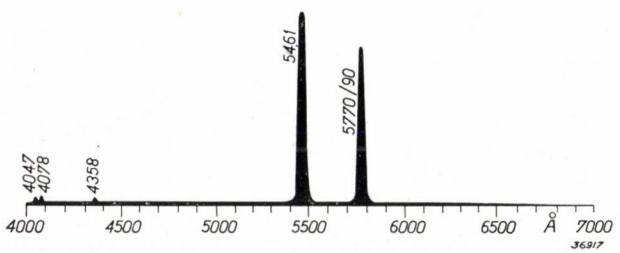

Fig. 4. Spectral distribution of the light of the high-pressure mercury lamps HP 300 and HP 500.

Nevertheless an extensive and varied sphere of use for these lamps has grown up, partly in spite of the peculiar colour of the light, in cases where the high efficiency is the deciding factor, and partly just because of that colour or of other properties of the light such as the greater acuity of vision which can be attained with mercury illumination [4]). HP lamps are widely used for public lighting in cities or for general illumination in the metal industry, while they are also used with great success for the illumination of white or coloured advertising signs and for flood lighting lawns or groups of trees which assume an especially natural appearance in this light because of the high content of green radiation in the mercury light. Applications based upon improved colour contrast are found in the illumination of coal sorting belts where the mercury light increases the contrast between coal and stone, or in the marking department of construction workshops and plate workshops, where the lines drawn with a copper stylus on the iron come out very clearly in the mercury light. Surface flaws in tin plate, nickel plate or chromium plated objects, on enamelled products, on porcelain, on glossy paper are more easily observed by the light of HP lamps than by ordinary white light. The inspection of plate glass before it is placed in the cooling ovens is based not only upon colour contrast but also upon visual acuity. In conclusion the use of HP lamps in photographic enlarging apparatus [5]) may be mentioned.

High-pressure mercury lamp with colour correction, type HPL

The colour rendering of the HP lamps, which is inadequate for ordinary purposes, has been improved in different ways. In the first place it is possible to cover the inside of the bulb of the HP lamp with a layer of fluorescent material. In this fluorescent layer the conversion into light takes place of the ultra-violet radiation which is excited in the mercury discharge and which is otherwise lost by absorption in the glass of the bulb. The fluorescent material, which gives a continuous spectrum, is so chosen that as much red light as possible is obtained upon conversion, which red light is entirely missing in the natural mercury light. This brings about a very considerable colour correction. The light flux hereby remains unchanged: the fluorescence light approximately compensates for the loss of primary mercury light which is absorbed in the fluorescent layer. Electrically also the lamps with fluorescent bulb HPL 300 and HPL 500 (fig. 1*c* and *d*) are exactly like the mercury lamps HP 300 and HP 500, respectively. The bulb of the HPL lamps is made slightly larger than that of the HP lamps since this makes the efficiency of the fluorescent layer higher.

Although important, the colour correction in the HPL lamps is nevertheless not such that the lamps can be recommended for every use: they do not

[4]) Philips techn. Rev. **1**, 215, 1936.

[5]) Philips techn. Rev. **3**, 91, 1938.

give "white" light. This could hardly have been expected since the available quantity of ultraviolet radiation in the discharge, even with the optimum conversion efficiency, is insufficient to provide a complete colour correction. The HPL lamps are nevertheless suitable for all cases where it is unnecessary to be able to determine accurately the finer shades of colour. They can therefore be used for street lighting as well as for factories, workshops, garages, storerooms, etc. For photography on extra red-sensitive panchromatic material the HPL lamp may also very well be used and even gives an extraordinarily faithful reproduction of the colour relations [6]).

Blended light of mercury and incandescent filament lamps

For cases in which the HPL lamp is unable to render the colour gradation satisfactorily, the mercury light may be blended with ordinary electric light. There are special fixtures for this purpose, for interior lighting (*fig. 5*) as well as for use out

Fig. 5. Blended-light fitting. Enamelled reflector for workshop illumination, containing three ordinary electric lamps and one mercury lamp.

of doors. In the blended light thus obtained the excess of red rays from the electric lamp serves to make up the corresponding shortage in the light of the mercury lamp. By a well chosen construction of the fixture and a correct relative arrangement of the different lamps, a satisfactory blending of the two kinds of light can be obtained without the formation of coloured shadows. An extra advantage of this blended light is, that upon switching on, a large part of the normal light flux is immediately available, namely that part which is due to the incandescent lamps. Upon repeated switching on also, it is unnecessary to wait for the mercury lamp to cool, since the filament lamps are always ready for action. In order to obtain a better blending of the two kinds of light it is necessary to divide the total amount of ordinary electric light necessary per mercury lamp over a number of small lamps. The proportions of the mixture can then be adapted to the needs of each case. When no particular requirements are made the proportions 1 : 1 will be satisfactory. *i.e.* a mixture consisting of equal quantities of the two kinds of light. In practice this can be attained for instance with one HP 300 or HP 500 and one or more electric lamps with a total consumption of 200 or 300 watts, respectively. If higher requirements are made of the colour rendering, the content of ordinary electric light will often have to be increased. Conversely, the percentage of ordinary electric light can be decreased when the colour rendering is not the primary requirement, but, for instance, visual acuity, or when the objects being observed are mainly white. If it is desired to suppress the violet light of the mercury lamp, which gives blue objects especially an unnatural appearance, it is best to replace the HP lamp by an HPL lamp, or to use a suitable yellow-green filter around the mercury lamp. So little light need be absorbed by the glass of the filter that the total efficiency of the lamp is scarcely affected by it. This is due to the fact that the violet radiation in the mercury light comprises less than 1 per cent of the light flux.

When blended light is used the total efficiency of the combined light sources will necessarily be lower than that of the mercury lamps. Nevertheless it is always higher than that of ordinary electric lamps alone, and it is strikingly better than the efficiency of the so-called daylight blue lamps which were formerly used almost exclusively for a correct colour rendering, and which consist of ordinary electric lamps in a blue glass bulb. While the latter gave good results, it was only at the expense of a very low efficiency, and therefore in some cases of an unpleasant rise in temperature of their surroundings.

It would be difficult to give a survey of all the cases in which mercury blended light can be successfully used. As an indication therefore a few typical applications are given in *table 2* with the most important practical data referring to those uses. These can be varied according to taste and circumstances.

[6]) Philips techn. Rev. **4**, 27, 1939.

Table 2. Blended light of mercury and incandescent lamps.

Application	Proportions of mixture $\frac{\text{lumen mercury light}}{\text{lumen incand. light}}$	Remarks
Show windows		
flowers	1/2	for light colours and green: mercury lamp HPL
textiles	1/2	preferably with yellow-green filter
gold	1/1	
zilver	2/1	
fancy goods	2/1	with yellow-green filter in some cases
bicycles, tools, stoves, etc.	1/1	
Interior illumination		
general	1/1 - 1/1.5	indirect, if necessary
drafting rooms	1/1 - 1/1.5	indirect
offices	1/1 - 1/1.5	
exhibition halls	1/1 - 1/1.5	
printing offices:		
hand composing room	3/1	
rotating press	1/1	
colour printing	1/2	indirect, mercury lamp HPL
offset	1/1.5	
binder	2/1	
shops (textiles)	1/2	
Outdoor illumination		
streets	2/1 - 1/1	

Blended-light lamp, type ML

In a number of cases the use of blended light can be considerably simplified by the application of the new blended-light lamp ML 500. This lamp, which, except for the inside-frosting of the bulb, does not differ in appearance from an ordinary 300 W electric lamp (fig. 1*e*) combines in itself a mercury discharge tube and a filament, which are connected in series and placed in a bulb filled with the mixture of argon and nitrogen which is ordinarily used for electric lamps. The filament, which furnishes half of the total light flux of the lamp, also serves as a stabilizer for the discharge, so that the separate series apparatus which would otherwise be necessary may be omitted.

Since not only the filament, but also the mercury discharge in the blended-light lamp functions under conditions which deviate from the usual ones, we shall discuss them briefly. Upon ignition the mercury discharge has at first an arc voltage of about 15 volts, so that the filament must take up the whole difference between this voltage and the mains voltage. When burning normally, on the other hand, the voltage to be taken up by the filament is considerably lower. The filament is therefore heavily overloaded in the starting period, so much indeed that during the first minute after the lamp has been switched on it evaporates as much as during an hour of ordinary use. This periodic overloading of the filament while the discharge is starting results in the fact that the life of the blended-light lamp depends to a greater degree than is the case with most other light sources on the number of times it is switched on, or on the average length of burning after each time it is switched on. Furthermore it must be noted that the ever present fluctuations in the mains voltage are transmitted entirely to the filament, since the arc voltage of the mercury discharge tube is constant in normal use. The result is that the percentage of fluctuations for the filament, which takes up only a part of the mains voltage, will be considerably higher than that for the whole lamp. In connection with this it is absolutely essential that the blended-light lamp be used at the correct mains voltage.

As concerns the mercury-discharge tube, it here acts in series with the ohmic resistance of the filament, instead of with the inductive resistance of a choke coil. The lag of the current is thus eliminated which is due to the inductive resistance in series with the lamp, and the result is an increase in the "re-ignition voltage" in the following half cycle. If the current lags in phase behind the voltage, then at the moment when the current changes from the positive to the negative direction there is already a considerable negative voltage, so that the lamp can immediately re-ignite. If, however, current and voltage have the same phase, at the moment when the current direction changes the voltage is zero, and it is a fraction of the following half period before the voltage has reached the re-ignition value. In this short time, however, the ionization in the tube falls back so that the re-ignition voltage increases.

The filament as well as the gas-discharge tube therefore work under less favourable conditions than if they were connected separately to the mains, and the result is that the efficiency of the blended-light lamp is somewhat lower than that of a corresponding combination of incandescent lamps and mercury lamps. Compared with blended light obtained from a mercury lamp and one or more incandescent lamps, however, the blended-light lamp offers the advantage of requiring no series apparatus. Furthermore it is important that the blended-light lamp burns with full light intensity immediately after being switched on, since the overloaded filament gives slightly more light at the moment when it is switched on than filament and mercury dis-

charge together in the normal working state. A third advantage of the blended-light lamp is that the starting time of the mercury discharge, which is about 5 minutes with the HP lamps, could be reduced to about 1 minute, by allowing the heat development of the filament to serve for the evaporation of the mercury.

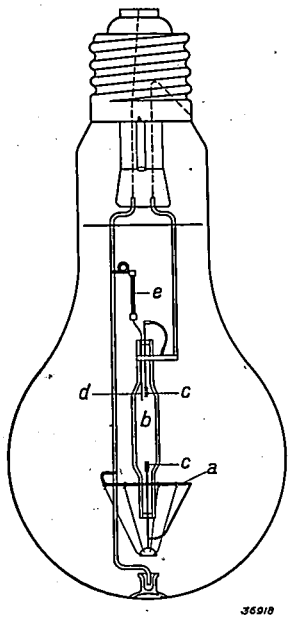

Fig. 6. Construction of the blended-light lamp ML 500. *a* filament in argon-nitrogen mixture, *b* mercury discharge tube, *c* main electrodes, *d* auxiliary electrode, *e* current-limiting resistance.

Like the other ordinary metallic vapour lamps, the blended-light lamp is intended for use on alternating current. The lifetime is calculated for an average of 2 000 hours, with the assumption that the average duration of burning after every switching on amounts to about 3 hours. The lamp is easily proof against mains voltage fluctuations of ± 5 per cent, while the mains voltage may fall to 170 volts without the lamp being extinguished. The relative positions of discharge tube and filament as shown in *fig. 6* ensure a very good blending of the light, so that the lamp exhibits a completely uniform appearance. The most important practical data of the lamp are collected in *table 3*.

Table 3. Properties of the blended-light lamp ML 500

	mercury discharge	filament	total
light flux	2 500 lm	2 500 lm	5 000 lm
power consumption	65 W	185 W	250 W
voltage	78 V	156 V	220 V
current	1,19 A		
starting time	1 min		
cooling time *)	1-2 min		

*) Within this interval of time after switching off it is impossible to re-ignite the lamp. The cooling time depends upon the circumstances.

The blended-light lamp ML 500 is still too new to have been able to conquer all the territory which it deserves. It may, however, be assumed that before long it will find its way into public lighting systems, while furthermore it should be considered for factories, offices, shops, warehouses, hospitals, churches, schools, theatres, halls and many other large covered spaces where larger lamp units are desired for the illumination.

Spectral data of the different kinds of light

In addition to the method of trying by practical experiments to find the most suitable composition of the light which is to be used for a given type of illumination, there is the block method [7]). According to the latter method the entire visible spectrum is divided into 8 adjacent regions (see *table 4*). Different lamps can then be compared with each other block by block with respect to the colour of the light. Two light sources will give practically the same colour gradation when the light fluxes in corresponding blocks are equal, or in a constant ratio to each other, notwithstanding the actual spectral distribution within the blocks themselves. The eye is, however, incapable of observing deviations from the colour equality defined in this way which are smaller than 10 to 25 per cent, or at least it is incapable of finding them disturbing. Sometimes a deviation in a given block can more or less compensate an opposite deviation in the adjacent block, especially when the colour difference between such blocks is not too great. On the other hand this tolerance will be found too great when two neighbouring blocks exhibit deviations in the same sense.

The kinds of light mentioned in table 4 are all compared with average daylight which is set equal to 1 in each block. In order to approach average daylight as closely as possible a given kind of light must therefore be represented in each block by a number differing as little as possible from one. At first glance the table seems to give little hope. A comparison with universally familiar kinds of light, however, (direct sunlight or electric light) shows how far one may deviate from the requirement without obtaining an illumination which is unnatural or unpleasant in colour. This is true at least as long as the spectrum exhibits no great lack of balance. In an otherwise satisfactorily uniform

[7]) See the articles referred to in footnote [2]).

Table 4

Light flux of various sources of white light in certain blocks of the spectrum; values for daylight set equal to unity.

Blocks (boundaries in Å)	4 000	1	4 200	2	4 400	3	4 600	4	5 100	5	5 600	6	6 100	7	6 600	8	7 200
average daylight		1		1		1		1		1		1		1		1	
sunlight		0.64		0.69		0.70		0.83		0.96		1.06		1.16		1.30	
incandesc. electr. lamp ("Bi-arlita")		0.19		0.20		0.25		0.48		0.80		1.17		1.79		2.60	
"Daylight blue lamp"		0.35		0.36		0.44		0.68		0.97		1.09		1.18		1.40	
HP lamp		0.68		3.19		0.10		0.08		1.26		1.26		0.07		0.09	
ditto with yellow-green filter		0.37		2.34		0.06		0.08		1.37		1.14		0.10		0.09	
HPL lamp		0.29		0.88		0.16		0.14		1.14		1.31		0.41		0.41	
HP-blended light 2 : 1		0.52		2.19		0.15		0.21		1.11		1.23		0.65		0.91	
ditto 1 : 1 *)		0.44		1.69		0.17		0.28		1.03		1.22		0.93		1.33	
ditto 1 : 2		0.36		1.24		0.20		0.39		0.95		1.20		1.21		1.74	
HPL-blended light 1 : 2		0.24		0.42		0.19		0.37		0.91		1.21		1.33		1.86	
HP-blended light 1 : 2 with yellow-green filter around mercury lamp		0.26		0.92		0.19		0.35		0.99		1.16		1.22		1.74	

*) Blended-light lamp ML 500

spectrum, for example, one stronger spectral line, especially when it belongs to the blue-violet part of the spectrum, can make the light in question entirely unsuitable.

The spectrum of the HP lamp, which actually consists of lines (fig. 4), has a very irregular appearance. There can be no question of any analogy with average daylight. In the case of the HPL lamp this irregularity is much reduced, the excess of blue-violet is removed, but the red is not sufficiently reinforced. The HP lamp with yellow-green filter lies between the two preceding ones as concerns these colours which present the greatest difficulty for every mercury lamp.

The different kinds of mixed light form, according to the table, so many compromises between an optimum red rendering and the best possible blue rendering. According as the incandescent lamp light in the HP blended-light makes up a larger portion, the emphasis may be seen to shift from blue to red. The HPL blended light in the proportion indicated is found to possess a blue radiation relatively uniformly distributed over the first three blocks, but which is relatively too weak, so that the rendering of blue seems somewhat faded, while the red is rather reinforced and vitalized. The HP blended light with a yellow-green filter over the mercury lamp is especially remarkable for its excellent rendering of blue, and the red remains about as with the ordinary HP mixed light without filter in the same ratio.

This all agrees entirely with practical experience, where, according to the needs of every separate case, the emphasis may now be placed upon the red end of the spectrum, and then again on the blue end, thanks to the flexibility of the mixed light, so that a whole series of variants with respect to the composition is formed. It is therefore clear that with the help of blended light when used with judgment, not only with respect to the system chosen but also with respect to the proportions of the mixture, more satisfactory results can be obtained than with ordinary electric light alone.

AN ELECTRICAL PRESSURE INDICATOR FOR INTERNAL COMBUSTION ENGINES

by P. J. HAGENDOORN and M. F. REYNST.

531.787.9 : 621.43

In order to satisfy the severe requirements made of the indicator for measuring the pressure in modern internal combustion engines an electrical measuring apparatus (pressure indicator, type GM 3 154) has been developed which employs a cathode ray tube. A membrane is set into the wall of the cylinder, and together with an opposing electrode forms a condenser. The condenser is part of a bridge connection which is fed with a high frequency voltage. When the capacity of the membrane condenser varies due to the movement of the membrane, the high-frequency voltage taken from the bridge is modulated with these variations, which form a picture of the variations in pressure. After amplification and rectification the deflection voltage is obtained for the vertically deflecting plates of the cathode ray tube. The horizontal deflection can be made proportional to the time as well as to the displacement of the piston. The construction of the indicator on this principle is discussed and the most important details are explained.

The classical device for controlling the functioning of steam engines and internal combustion engines is the mechanical pressure indicator which traces the pressure in the cylinder as a function of the position of the piston. In this way a pressure volume diagram is obtained (*fig. 1*), from which conclusions may be drawn about the different processes taking place in the cylinder, and from which by planimetry the work done by the burning gas per revolution of the crank shaft (the "indicated power") can directly be determined.

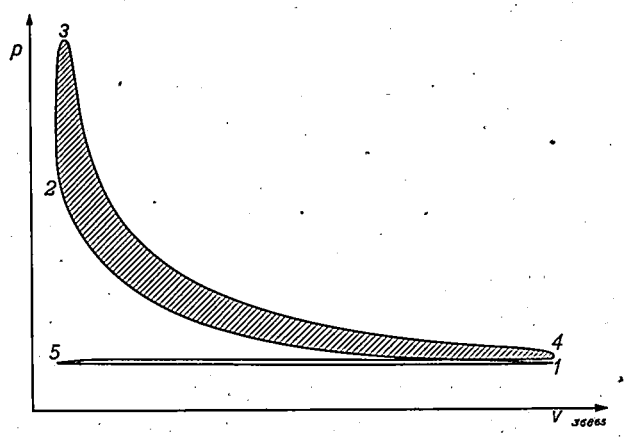

Fig. 1. Normal appearance of the pressure-volume diagram of a four-stroke internal combustion engine. Upon movement of the piston from *1* to *2* the air in the cylinder is compressed, at *2* the fuel (oil) is sprayed in, a moment later the mixture begins to burn and the pressure rises quickly to the peak value at *3*. From *3* to *4* the gas expands. Upon the following stroke of the piston the burned gas is driven out (*4* to *5*) and fresh air sucked in (*5* to *1*), whereupon the process begins anew. The shaded area indicates the work done by the cylinder during two revolutions of the crank shaft.

The new engine constructions of the last 10 or 20 years, which work at higher speeds of revulution (up to 6 000 r.p.m. in aeroplane engines) and involve a heavier loading of the material than was formerly the case, on the one hand make an indication of the pressures prevailing more necessary, and on the other hand they make heavier requirements of the indicating instrument. This instrument must be adapted to the higher speed of revolution mentioned, and furthermore a single diagram will often not be sufficient, but a continuous indication during operation will be desired, while at the same time the fine details of the diagram will be more important than formerly, such as those which correspond to the moment when the fuel is sprayed in and to the progress of the combustion of the gas mixture.

As has often been affirmed in this periodical, in the investigation of such mechanical phenomena where higher frequencies are concerned electrical methods of measurement offer great advantages over mechanical methods, since the cathode ray tube which can thereby be used as indicating instrument is practically free of time lag. A continuous indication can easily be obtained with this instrument, while at the same time the indicator can be situated at a central point where various phenomena — for instance the variation of the pressure in several cylinders — can be examined.

An indication of the pressure with the help of the cathode ray tube can be realized as follows. The pressure variations in the combustion chamber are converted into electrical voltage variations by means of a pressure indicator connected with the said chamber, which, as regards function, may be compared with a microphone. The voltage variations are amplified and fed to the set of plates for vertical deflection of a cathode ray tube. At the same time a voltage is applied to the plates for horizontal deflection which varies proportionally to the displacement of the piston. On the fluorescent screen of the tube the above-mentioned pressure-volume diagram appears. If, as is more usual in oscillography, the horizontal deflection voltage is allowed

to vary proportionally to the time, a pressure-time diagram is obtained which may sometimes also be useful.

The problems which are encountered in the realization of these principles, and the solutions which have been found in the pressure indicator (type GM 3 154) developed by Philips, will be discussed in the following. The realization of this pressure indicator and its adaptation to the requirements of internal combustion engines would have been impossible without the stintless collaboration of the Laboratory at Delft of the *Bataafsche Petroleum Maatschappij* and of the N.V. *Werkspoor* at Amsterdam who placed there experimental plant at our disposal and contributed to these experiments by word and deed.

Principle of the arrangement

The pressure recorder

In the pressure recorder an elastic deformation of some kind of body is caused by the variation in pressure. This deformation can give rise to an electrical voltage variation in various ways as in the different ordinary microphones [1]), namely by the piëzo-electric effect (crystal microphone), by a change in resistance (carbon microphone), by a change in capacity (condenser microphone) or by an electrodynamic or electromagnetic method (ribbon microphone). If it is required that the relation between voltage and change in pressure shall be independent of the frequency over a long range, only the first three methods mentioned can be considered, as is explained in the article already referred to [1]), with the additional condition that the (lowest) characteristic frequency of the body upon which the varying pressure acts must lie sufficiently far above the frequency range with which we are concerned. If we assume a maximum velocity of 9 000 r.p.m. (this has already been employed in test models of engines), then the fundamental frequency of the diagram to be recorded (with a two-stroke engine) is 150 c/s. In order to reproduce all the details of the diagram satisfactorily, such as the steepest pressure peaks, detonation vibrations, etc., the 20th harmonic must still show no appreciable change in amplitude and phase. It is therefore desirable [2]) that the resonance frequency of the recorder should be at least 8 times as high, *i.e.* at about 25 000 c/s.

In order to obtain satisfactory sensitivity with such a high characteristic frequency it is important to use for the pressure recorder a vibrating system with as small a mass as possible. In this respect the condenser microphone is particularly suitable: the vibrating mass here consists only of a thin membrane which is bent more or less by the pressure variations. Together with a rigid counter electrode in the shape of a plate, the membrane forms a condenser whose capacity varies with the movement of the membrane. The Philips indicator is constructed on this princple. *Fig. 2* shows diagrammatically how the membrane condenser can be built into the wall of the engine cylinder. For the sake of simplicity in fastening it, the membrane is earthed and the counter electrode insulated.

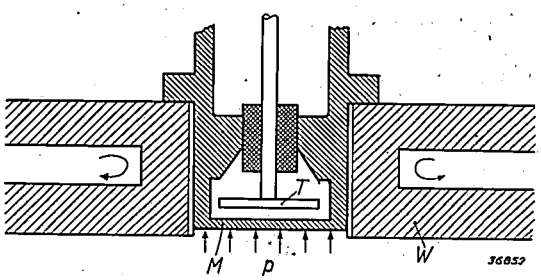

Fig. 2. The membrane M which is fixed into the wall W of the cylinder and which is moved more or less by the pressure p in the cylinder, forms, together with the counter electrode T, a condenser of variable capacity.

The conversion of the capacity variations into voltage variations

In the case of the condenser microphone the membrane condenser, which is charged by a direct current source, is included directly in the grid circuit of an amplifier valve. When the charge is kept constant the changes in capacity cause changes in the grid voltage which are then further amplified. For the pressure recorder, however, this connection, although simple in principle, cannot be considered. In this case it is also necessary to be able to measure unchanging pressures as well (this is especially important for the calibration), so that it would become necessary to use a D.C. amplifier. In many respects it is more difficult to use such an amplifier. Moreover very severe requirements which can hardly be satisfied are made of the insulation of the connection between the condenser and the grid of the first amplifier valve. In order to avoid these difficulties a quite different principle is applied in the Philips pressure indicator. The membrane condenser is included in a bridge circuit to which a high-frequency A.C. voltage is applied, see *fig. 3*. When the bridge is in equilibrium, there is no voltage between the points *c-d*. When the equilibrium is disturbed by a variation in capacity ΔC of the membrane condenser, a high-frequency A.C. voltage

[1]) J. de Boer, Microphones, Philips techn. Rev. **5**, 140, 1940.

[2]) See for example K. J. de Juhasz and J. Geiger, Der Indikator, Springer, Berlin 1938, p. 240.

acts between *c-d*, whose amplitude is proportional to ΔC when the variations are not too great. In this way a high-frequency voltage (carrier wave) is

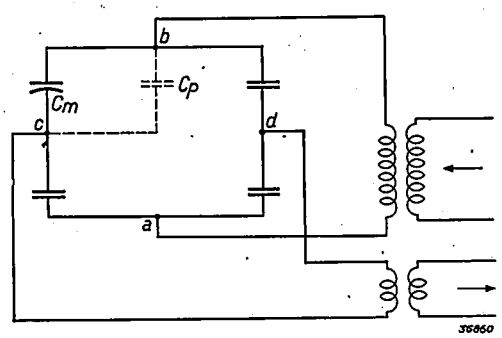

Fig. 3. The membrane condenser C_m is included in a bridge connection. At *a-b* (*via* a cable and matching transformer) a high-frequency A.C. voltage is fed to the bridge. If the bridge is balanced for a given value of C_m, then upon a variation ΔC of the latter a high-frequency voltage with an amplitude approximately proportional to ΔC will act across the points *c-d*. This "modulated carrier wave" is taken off by a cable with matching transformer.

obtained which is modulated with the pressure changes to be recorded. From this, after amplification and rectification, the desired deflection voltage for the vertical deflection of the cathode ray is obtained.

In *fig. 4* the main features of the whole circuit are given. The oscillator for the excitation of the carrier wave is built into a cabinet together with the amplifier, the cathode ray tube and several auxiliary apparatus, the bridge connections on the other hand are placed in the immediate neighbourhood of the membrane condenser for reasons which will be discussed later. The high-frequency voltage is applied to the bridge, or taken from it, with a cable which may have a length of for instance 10 m, or in some cases 50 m, in order to ensure the necessary freedom in setting up the indicating instrument.

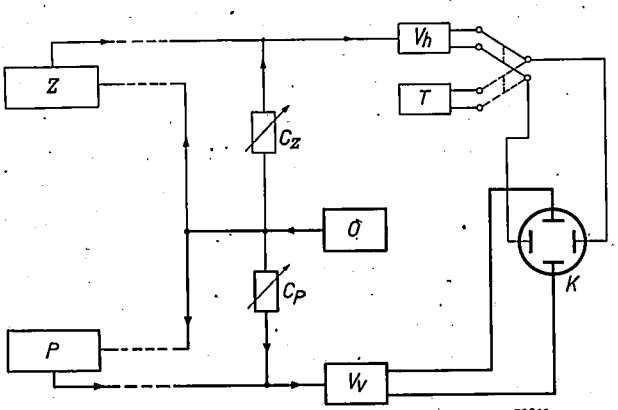

Fig. 4. Main features of the whole connection. *O* oscillator, *P* pressure indicator, V_v amplifier for the vertical deflection voltage, *K* cathode ray tube, *Z* piston-stroke indicator, *T* time-base generator, V_h amplifier for the horizontal deflection voltage. C_p and C_z compensation arrangements discussed in the following.

As carrier-wave frequency 450 c/s is chosen. This value is so low that the damping of the carrier wave in the cable can be made small enough to be neglected, and so high that the construction of an amplifier with the desired band width (namely twice the maximum modulation frequency of the carrier wave, *i.e.* the highest frequency occurring in the oscillogram) still offers no difficulties.

Time base and piston-stroke base

A time-axis generator is included in the apparatus similar to that which is used in the cathode ray oscillograph recently described in this periodical [3]). With the sawtooth voltage given by this generator the cathode ray is given the necessary horizontal deflection to trace a pressure-time diagram. For tracing a pressure-volume diagram, however, the horizontal deviation of the fluorescent spot must be proportional at every moment to the displacement of the piston with respect to its position at the "dead point" near the top of the cylinder. The deflection voltage which is necessary for this is obtained by a "piston-stroke indicator" which functions as follows. A revolving cylinder of the shape shown in *fig. 5* is coupled to the crank

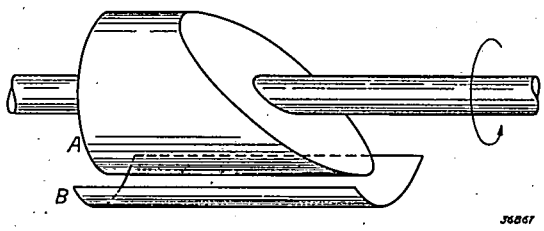

Fig. 5. Principle of the piston-stroke recorder. The cylinder *A* which is cut off in a certain way and coupled with the crank shaft, forms, together with the fixed counter electrode *B*, a condenser whose capacity varies as *A* rotates with the displacement of the piston in the cylinder of the engine.

shaft of the engine. Together with a fixed plate this cylinder forms a condenser whose capacity varies as the cylinder turns. By choosing a suitable shape for the cylinder the capacity of the cylinder condenser at every moment can be made proportional to the displacement of the piston. The cylinder condenser is included in a bridge connection in the same way as the membrane condenser of the pressure indicator, and the bridge is fed *via* a cable with the same high-frequency voltage. The output of the bridge is again amplified and rectified and applied to the horizontal deflection plates of the cathode ray tube. The piston-stroke indicator thus acts in exactly the same way as the pressure indicator itself (see also the diagram fig. 4).

[3]) A cathode ray oscillograph for use in tool making, Philips techn. Rev. 5, 277, 1940.

Construction of the pressure indicator

Having given a general idea in the foregoing of the construction of the apparatus, we shall now give some details of the connections and of the construction of the components. Especially the pressure indicator deserves attention. It is a component which must satisfy rigid requirements in three respects: electrically, mechanically, and thermally. In the first place it may be noted that the capacity in the branch *bc* of the bridge (fig. 3) is composed of that of the membrane condenser C_m and the capacity C_p, in parallel with it and independent of the pressure, between the counter electrode plus connections and earth. Since C_p may vary somewhat due to different influences, especially temperature changes, it is necessary to keep C_p as small as possible. To this end the connection is made as short as possible, *i.e.* the whole bridge is placed as close as possible to the membrane condenser. Nevertheless there still remains a considerable stray capacity of the enclosed counter electrode (fig. 2), so that C_p could not be made smaller than about 18 $\mu\mu$F. In order to limit the influence of variations in C_p one must therefore try to make the capacity C_m which changes with the pressure as large as possible by making the air gap between membrane and counter electrode very small. In doing this, however, care must be taken that no short circuit can occur during use between the membrane and the counter electrode. Short circuiting was found to be promoted especially by the freeing of particles of material from the membrane — a phenomenon which need cause no surprise when it is remembered that the membrane may become red hot due to contact with the hot gases in the cylinder, and that it continually undergoes pressure shocks of up to 100 atmospheres. By careful ageing of the membrane, however, this phenomenon could be rendered harmless to such an extent that the air gap could be reduced to 0.2 mm. Since the area of the surface of the membrane was determined by the consideration that the pressure indicator should be able to be fastened into the wall of the cylinder in the same way as a sparking plug, the capacity of the membrane condenser was approximately determined at the same time. The value obtained is $C_m \approx 1.5$ $\mu\mu$F.

The relatively small values of C_m compared with that of the stray capacity C_p make it necessary to work with as large as possible capacity variations of the membrane condenser. The membrane is therefore so constructed that at the maximum pressure the displacement f at the centre is almost equal to the width of the air gap, namely 0.18 mm. The tensile stresses hereby occurring in the membrane may not become too large. The following general relation holds for the maximum tensile stress δ_{max} in a circular membrane fastened around its circumference:

$$\sigma_{max} = K \frac{E}{c} f \nu_1 \quad . \quad . \quad . \quad . \quad . \quad (1)$$

Here ν_1 is the lowest resonance frequency of the membrane, c the velocity of sound in the material of the membrane, E its modulus of elasticity and K a constant which depends only upon the rigidity with which the membrane is clamped [4]). In our case the constant K is approximately 4.5. When the values of c and E for steel: $c = 5\times10^5$ cm/s, $E = 20\times10^5$ kg/cm^2, are filled in, and for ν_1 the value 25 000 c/s which is desired according to the above, then for $f = 0.18$ mm one arrives at a maximum tensile stress $\delta_{max} = 8\,000$ kg/cm^2.

With an ordinary good quality of steel this value is permissible. In our case, however, the unusual thermal load on the membrane had still to be taken into account. During combustion in the cylinder peak temperatures of 1 600° C occur, while the average working temperature of the membrane may amount to about 550° C. With ordinary kinds of steel the permissible value of δ_{max} thereby decreases very considerably, to only 2 000 kg/cm^2, for example. In order to be able to obtain the desired values of f and ν_1 and at the same time to ensure reliability in operation and sufficient constancy of the properties of the membrane, a specially tough and heat-resistant kind of steel was used and its yield value was further raised as much as possible by extra hardening.

In order to protect the membrane against becoming too hot, *i.e.* to limit the average temperature to the value of 550 °C already mentioned, a perforated cap is placed in front of it, see *fig. 6*. This helps to conduct the heat of the gases to the cooled walls of the cylinder, and at the same time supports the whole pressure indicator. The cap has an ex-

[4]) If p is the excess pressure, r the radius of the membrane and δ its thickness, then

$$f = C_1 \frac{r^4}{\delta^3} \frac{p}{E}, \qquad \sigma_{max} = C_2 \frac{r^2}{\delta^2} p, \qquad \nu_1 = C_3 \frac{\delta}{r^2} c,$$

where C_1, C_2, C_3 are constants, which depend upon the rigidity of the fastening of the membrane. When the two last equations are divided by each other and the pressure p eliminated, the dimensions r and δ are also found to disappear from the resulting equation, and equation (1) is obtained where C_2/C_1C_3 is set equal to K. A similar relation is also found for other vibrating systems. This has already been pointed out in this periodical in connection with a discussion of the sound cutter of the Philips-Miller-system: Philips techn. Rev. 1, 136, 1936.

ternal screw thread like a sparking plug and is screwed into the wall of the cylinder. This construction has the advantage that the material in the neighbourhood of the point where the membrane is clamped is kept free of forces which occur during the screwing in (actually the membrane is not clamped but simply forms the bottom of the cylinder B). These forces would otherwise cause a deformation and in that way be able to change the sensitivity of the pressure indicator (*i.e.* its calibration).

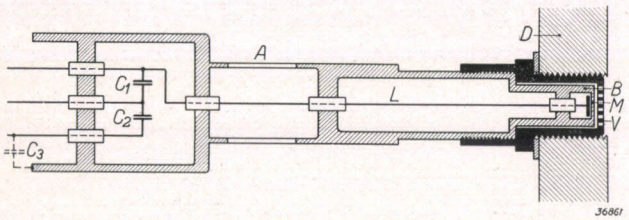

Fig. 6. Construction of the pressure indicator. The membrane M forms the bottom of a cylinder B. V perforated cap, D cylinder wall, L lead of the counter electrode, C_1, C_2, C_3 condensers of the bridge.

In the cross section sketch fig. 6 the condensers of the bridge may also be seen which is situated in the immedate neighbourhood of the membrane condenser. As already stated, it is by means of this precaution that the value of the stray capacity C_p, and with it the influence of its variations are kept small. On the other hand, however, this precaution introduced the danger that the impedances of the other bridge elements would vary much due to the vibrations and the transmission of heat from the engine cylinder, so that it would be a case of out of the frying pan into the fire. This could be avoided by a very compact and strong construction of the bridge with high-frequency porcelain used in most places for insulation, and by a heat insulating separation between the membrane condenser and the bridge. The section A which supports the bridge is provided with holes so that only a small cross section is available for heat conduction and the air can flow freely through it, see *fig.* 7. Furthermore the whole rear section as well as the connection L is made of chrome-iron which is a poor heat conductor. In this way the bridge portion of the pressure indicator was kept at a temperature no higher than 50° C without a special water-cooling system being needed.

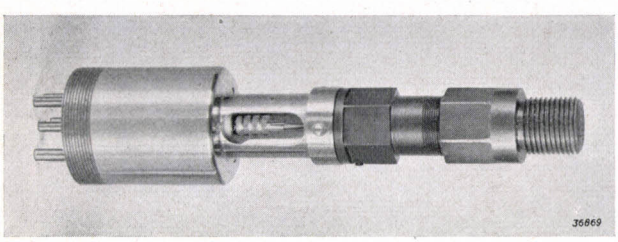

Fig. 7. Photograph of the pressure indicator. On the right the cap with sparking plug screw thread which is screwed into the wall of the cylinder. On the left the cable to the indicating instrument is connected and fastened.

Compensation arrangement

The bridge can be brought out of equilibrium by an increase as well as by a decrease in the capacity of the membrane condenser. In both cases the amplitude of the high-frequency output voltage of the bridge will increase from zero to a certain value, and therefore a corresponding deviation of the fluorescent spot will appear on the screen of the cathode ray tube. This is made clear in *fig. 8a*. In order to obtain a linear relation between the pressure and the deviation on the screen, the bridge must be brought into equilibrium for such a low (or high) capacity C_0 that it never passes this equilibrium at any capacity variation occurring (*i.e.* at any pressure occurring).

Now, however, the following complication appears. The amplifier for the vertical deflection of the cathode ray can receive a high-frequency input voltage due to other causes besides capacity variations of the membrane condenser. In the first place the cables and transformers for leading in and leading out the high-frequency voltage of the bridge are always capacitively and inductively coupled to a certain extent, notwithstanding careful mutual shielding; the voltage thereby induced reaches the amplifier entirely outside of the bridge. The balance of the bridge, which requires not only a regulation of the effective capacities, but also of the loss resistances of the four condensers, is always more or less disturbed due to the fact that a drift in the value of the loss resistances caused by temperature influences can never entirely be avoided. This again results in a certain initial voltage at the input of the amplifier.

The different contributions to the total input voltage of the amplifier must be added vectorially since they may differ in phase. The magnitude of the resultant voltage vector determines the deviation of the fluorescent spot obtained. Suppose for instance that the initial voltage E_1 (made up of different contributions) is shifted 90° in phase with respect to those voltages ΔE which occur due to the pressure variations. The magnitude of the resultant vector E, and therefore also the deviation y observed on the screen, then varies with the pressure according to fig. 8*b*; in the region of low pressures the diagram is somewhat compressed. An even greater distortion occurs when the vector

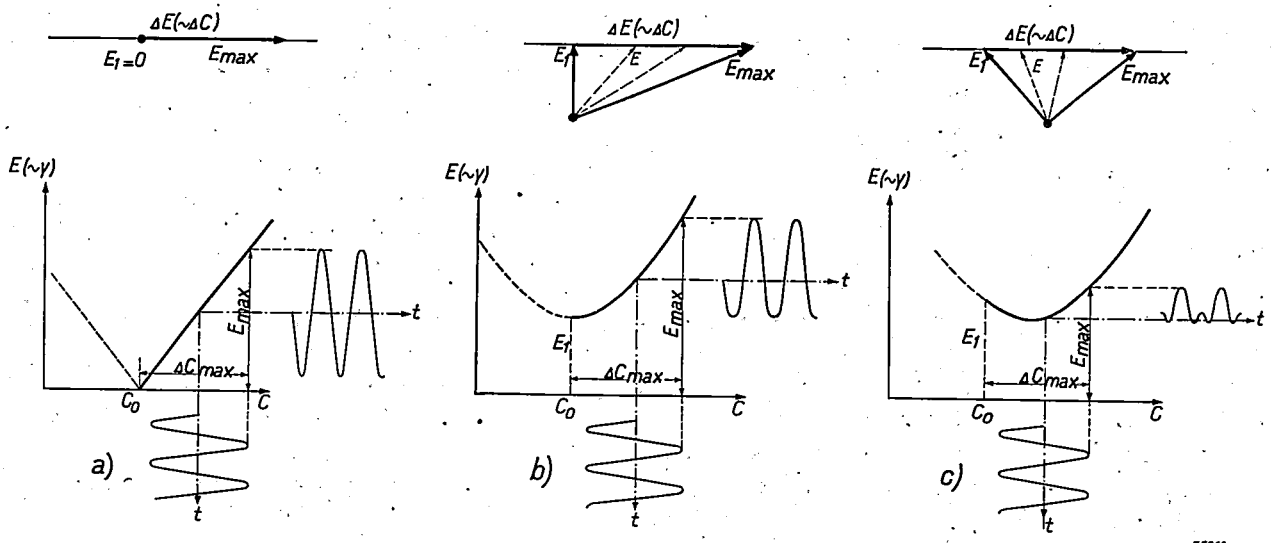

Fig. 8. Relation between the deviation γ on the screen, which is proportional to the input voltage E of the amplifier, and the capacity C of the membrane condenser.
a). No undesired initial voltage E_1 at the input of the amplifier. At C_3 the bridge is in equilibrium. C_3 must lie outside the region in which C varies with the pressure prevailing. Then γ is a faithful representation of C (thus of the pressure) as shown in the oscillogram constructed for a sinusoidal variation of C.
b) Undesired initial voltage E_1, shifted 90° in phase with respect to the voltage ΔE which is obtained by the capacity variations ΔC. γ is proportional to the magnitude of the resultant vector E. The oscillogram is flattened at the low-pressure values.
c) Arbitrary initial voltage E_1. The relation between γ and C is now no longer singular throughout the whole range of variations. In the oscillogram a reversing of the troughs as well as flattening may occur.

of the initial voltage E_1 has a direction like that indicated in fig. 8*c*. The magnitude of the resultant vector E then varies according to the curve drawn, the relation between deviation and pressure is no longer singular in the whole range of pressures; with a sinusoidally varying pressure the troughs are reversed in the oscillogram (see the figure).

In order to avoid these deformations it is necessary to make the initial voltage E_1 at the input of the amplifier disappear. This has been made possible in a very simple way in the case of the indication here described: part of the oscillator voltage is fed directly to the amplifier, while phase and amplitude of this voltage are so adjusted that the initial voltage E_1 is exactly compensated.

Since the phase of the initial voltage E_1 may vary between 0 and 360°, the phase of the compensation voltage must also be able to be varied within these limits. The connections shown in *fig. 9a* are used for this purpose. They consist chiefly of two similar resistance bridges which are fed from the oscillator. The two supply voltages (E_0) differ 90° in phase. By moving contact *a* the voltage between *c* and earth can be regulated between $+E_0/2$ and $-E_0/2$. The same is true upon moving *g*, for the voltage between *e* and earth which differs by 90°. The vector of the resulting voltage between *c-e*, which is used for the compensation, can therefore take on any position within the square drawn in fig. 9*b*, *i.e.* the compensation voltage can be varied 360° in phase and at least between 0 and $E_0/2$ in amplitude.

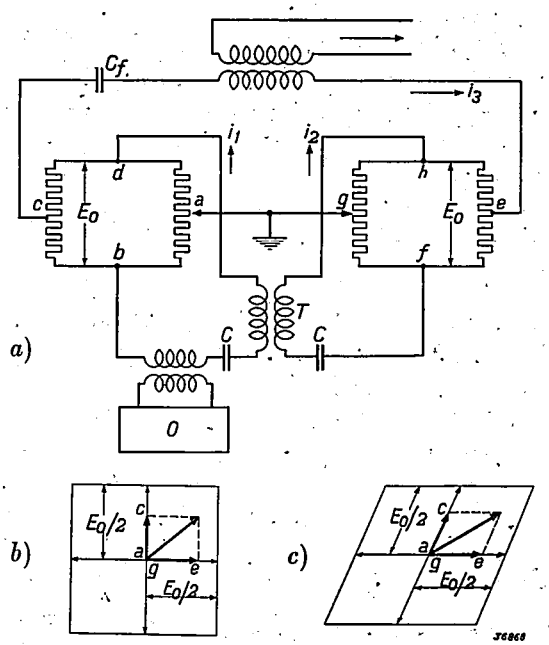

Fig. 9. Connections (*a*) consisting of two bridges *a-b-c-d* and *e-f-g-h* for obtaining the compensation voltage. By means of a condenser C in each bridge, current and voltage are brought into phase. Since the secondary voltage of the transformer T is always shifted 90° in phase with respect to the primary current, i_1 and i_2 are therefore shifted 90° in phase. The compensation voltage is taken off between *c* and *e*, and can be varied 360° in phase by moving the contacts *a* and *g*. This is shown in the vector diagram: *b*) for the case where the currents i_1 and i_2 differ exactly 90° in phase; *c*) for the case where this condition is not satisfied.

If an appreciable current i_3 is taken off between c-c, the phase relation between the currents i_1 and i_2 in the two bridges changes; instead of fig. 9*b* a vector diagram like fig. 9*c*, for instance, is obtained. The range of variation of the amplitude has here become smaller for some phase angles. This effect is found to reach a minimum at a certain phase relation between the current taken off and the voltage. This phase relation is realized by means of the condenser C_f.

Compensation takes place practically as follows. The initial voltage on the amplifier causes a certain initial deviation of the fluorescent spot. The contact a is now moved until this deviation is a minimum. The same is now repeated with contact g. In general, however, the deviation cannot be reduced to zero in this way, but can be again reduced by a further moving of a, etc. Further consideration shows that this alternate regulation of a and g converges rapidly.

In order to avoid all deformation the compensation voltage must be adjusted to an accuracy of several per mille. To attain this great accuracy of adjustment the potentiometers *b-a-d* and *f-g-h* (fig. 9*a*) are so constructed that in order to cover the region of regulation seven complete turns of the knob for that purpose are required.

The amplifier

If it is necessary to be able to determine the indicated cylinder power directly by planimetry from the pressure-volume diagram obtained, there must be a linear relation between the deviation on the screen and the cylinder pressure. Now without special measures the relation between these two quantities is by no means linear. The deviation on the screen when a normal linear amplifier is used is indeed proportional to the capacity variation of the membrane condenser, this capacity variation is not, however, proportional to the pressure variation. Proportionality would only exist if the movements of the membrane were small compared with the width of the air gap — a condition which, according to the description given of the pressure indicator, is far from satisfied. The relation between the capacity of the membrane condenser and the pressure is shown in *fig. 10* for the range of variations for practical use.

In order nevertheless to obtain a linear relation between the deviation on the screen and the pressure it is obvious that an ordinary linear amplifier should not be used, but the amplification should be made to decrease with increasing amplitude of the input voltage (increasing capacity variation), in such a way that the deviation from linear variation shown in fig. 10 is just corrected. For this purpose, as in the case of automatic volume control in radio receiving sets [6]), part of the rectified output voltage of the amplifier is fed back to the grids of the amplifier valves (the amplifier contains two stages), so that the operating point on the characteristic, and at the same time the slope of the valves, is changed according to the magnitude of the input voltage. While without this amplification regulation the relation between the deviation on the screen and the pressure would have the shape of the full line curve of fig. 10, by means of the regulation the broken-line curve in the same figure is obtained. The remaining deviation from linearity is slight, the difference amounts to about 2 per cent of the maximum pressure at the middle of the whole pressure range, while without regulation it amounts from 10 to 15 per cent.

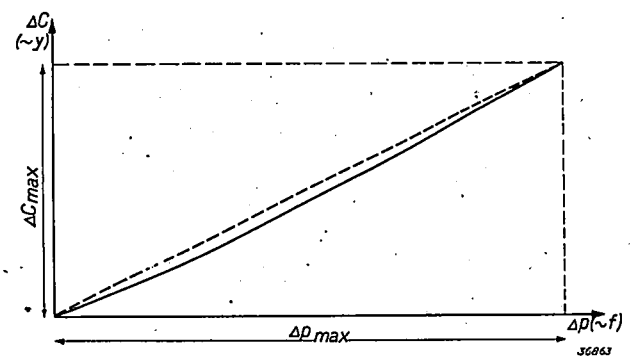

Fig. 10. Relation between the capacity C of the membrane condenser and the pressure p on the membrane. When a linear amplifier is used this is also the relation between the deviation y on the screen and the pressure. By automatic regulation of the amplification the broken-line curve is obtained in its place.

Instead of "the whole pressure range" we might better speak of the variation range of the movement of the membrane. For different applications of the prssure indicator the pressure range will be very different; for these applications a series of pressure indicators have been developed which differ chiefly only in the thickness of the membrane, and in which, as a result, the maximum movement of the membrane (0.18 mm) occurs at different pressures, for instance at 30, 50, 100 atmospheres, etc. The variation of the capacity as a function of the movement is almost independent of the thickness of the

[5]) As a first, rough approximation we may consider the membrane condenser as consisting of two parallel plane plates whose separation diminishes with increasing pressure. With a small separation a given decrease in that distance will obviously cause a greater increase in capacity than with a large separation, which leads to the curvature of the full line in fig. 10.

[6]) A similar linearity correction has recently been described in this periodical for a density meter for X-ray films: Philips techn. Rev. 5, 333, 1940.

membrane, so that for all pressure indicators the same linearity correction can be used.

Although it is best always to use the pressure indicator which is adapted to the measuring range [7]), it may happen that the pressure varies less and that therefore the diagram only occupies a part of the screen of the cathode ray tube. In that case, in order to take advantage of the whole area of the screen, the sensitivity of the amplifier should be increased, which can be done by changing the bias of the control grid (the operating point) of the first amplifier valve with a potentiometer. Since when this is done one works with smaller capacity variations of the membrane condenser, and therefore with a smaller part of the full-line curve of fig. 10 which more nearly approaches linearity, the regulation range of the linearity correction must also be decreased, *i.e.* only a smaller fraction of the rectified output voltage must be fed back. This reduction is obtained by changing the fraction mentioned with a potentiometer which is coupled mechanically with the potentiometer for the regulation of the sensitivity.

According to fig. 8*a* the bridge is so balanced that the deflection voltage of the amplifier obtained becomes equal to zero for the smallest pressure occurring. In order to use the whole area of the screen, the fluorescent spot must be at the bottom of the screen at this pressure, it must therefore have a certain initial deviation. This is obtained by means of the output connections of the amplifier shown in *fig. 11*. The rectified output voltage, as

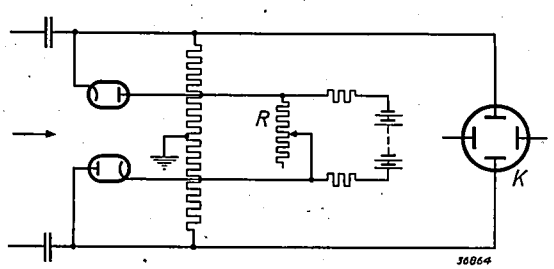

Fig. 11. Output connections (diagrammatic) of the amplifier for the vertical deflection voltage. The voltage rectified by the two diodes is fed in push-pull connection to the deflection plates of the cathode ray tube *K*, while by the likewise balanced bias on the resistance *R* an initial deviation can be given to the fluorescent spot.

well as the constant extra voltage for the initial deviation, is applied to the deflection plates of the cathode ray tube in push-pull connection; this is necessary in order to avoid distortion of the oscillogram on the screen [8]). By short circuiting the resistance *R* more or less the magnitude of the initial deflection can be further varied.

The band width of the amplifier which is tuned to the oscillator frequency of 450 c/s was fixed at 30 000 c/s. In the pressure diagrams of internal combustion engines it is unnecessary, as was explained at the beginning, to count on frequencies higher than 3 000 c/s, so that a band width of 6 000 c/s would be sufficient. Because of the higher value chosen, however, the pressure indicator can also be used for pressure measurements in quite different cases, namely for measuring fluid pressures in pressure lines of turbines, of hydraulic presses, etc. where considerably steeper pressure wave fronts (higher frequencies) occur than in engines cylinders.

Calibration and application of the indicator

It has already been pointed out that thanks to the carrier-wave principle chosen, static pressures can also be measured. The calibration is thus very simple: the pressure indicator is connected for instance to a cylinder with compressed gas whose pressure is regulated with a valve and read with an ordinary manometer. The modulus of elasticity of the material of the membrane is found to be practically independent of the temperature so that the calibration can be carried out with the membrane cold. The calibration is of course valid only for a given adjustment of the sensitivity of the amplifier. Furthermore it is valid only for a given amplitude of the carrier wave with which the bridge of the pressure indicator is fed. It is this amplitude which determines the proportionality factor between the input voltage of the amplifier and the capacity variation of the membrane condenser. In order to prevent changes in the carrier-wave amplitude which might occur due to voltage fluctuations of the mains from which the oscillator is fed, the feeding voltage of the latter is stabilized with neon lamps. At the same time this precaution serves to keep the carrier-wave frequency constant. If this frequency should change, the phase relation between the various voltage components at the input of the amplifier would change, and this would upset the compensation of the undesired initial voltage. For the rest, thanks to the carrier-wave principle, the whole arrangement is to a high degree insensitive to disturbances by induction from electric mains and the like.

In a coming article in this periodical the appli-

[7]) When this is done the sensitivity of the amplifier need only be small. The greater the sensitivity, the greater the displacement of the zero line obtained on the screen upon a drift in the bridge connections (fig. 8*b* and *c*).

[8]) This is for instance explained in Philips techn. Rev. 4, 198, 1939.

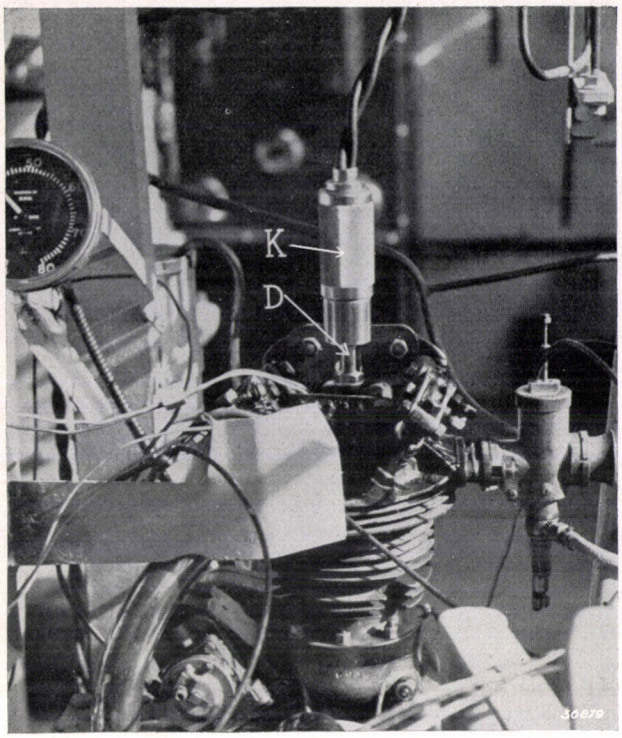

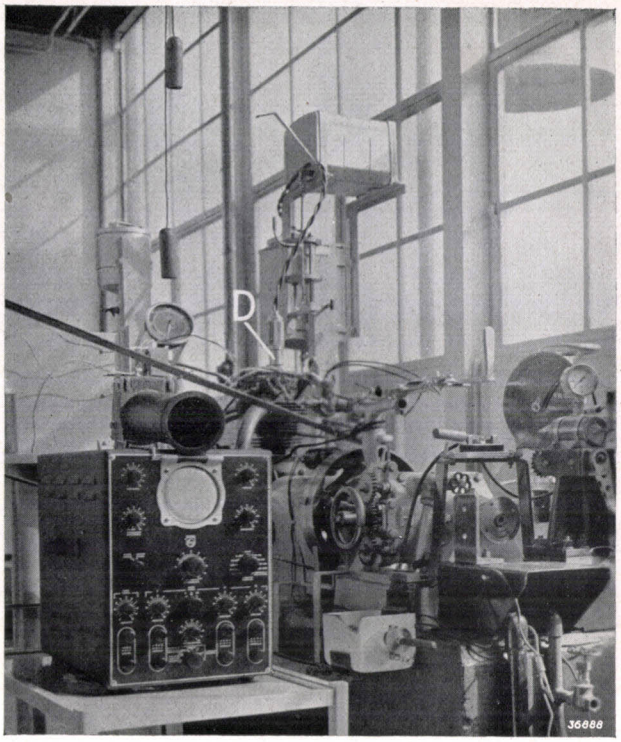

a *b*

Fig. 12. The pressure indicator GM 3 154 in operation. *a*) The pressure indicator *D* shown on the engine cylinder; *K* is the connecting piece for the 10 m cable connecting the pressure recorder to the indicating instrument. The latter may be seen in the left foreground of *b*).

cation of the apparatus for the investigation and control of internal combustion engines will be discussed in detail. We shall here merely draw attention to another possibility of application, namely the investigation of mechanical vibrations. If the membrane of the pressure indicator is omitted and the rigidly fixed counter electrode is placed opposite a vibrating body, the capacity between the electrode and earth varies, and the vibration becomes visible on the screen of the cathode ray tube. By giving the counter electrode suitable dimensions vibrations with amplitudes of several μ up to several cm can be measured. In the control of internal combustion engines also this possibility is important, namely for recording the so-called needle-stroke diagram.

Fig. 12 shows the pressure indicator in use. In order to be able to compare various phenomena, for instance the variation in pressure in different cylinders, the apparatus is so arranged that three, different pressure (or vibration) recorders can be connected at the same time with cables. By a simple switching operation the three different diagrams can be made to appear on the screen in rapid succession. Since the required compensation voltage for the three cables plus pressure indicators will in general differ, each of the three connections is provided with its own compensation arrangement as in fig. 9*a*. A fourth compensation set is necessary for the amplifier of the horizontal deflection voltage (piston-stroke base). In fig. 12*b* may be seen the four pairs of regulation knobs of the compensation arrangements, placed at bottom of the panel of the cabinet.

A VARIABLE AMPLIFIER VALVE WITH DOUBLE CATHODE CONNECTION SUITABLE FOR METRE WAVES

by M. J. O. STRUTT and A. van der ZIEL.

621.396.645.3.029.6

A great disadvantage of ordinary amplifier valves in the amplification of very high frequencies is the damping of the oscillator circuit connected with the control grid, due to the coupling between control grid circuit and anode circuit *via* the self-induction of the cathode connection. This disadvantage can be avoided by providing the cathode with two connections, which belong respectively to the control grid circuit and the anode circuit. By using these two connections of the cathode in a suitable manner numerous possibilities of connection occur so that it is possible to eliminate the damping of control grid circuit and anode circuit simultaneously, and at the same time to influence the reactance in a favourable manner. In this article a variable amplifier valve with a double cathode connection (EF 51) is described, which for wave lengths not shorter than 1.5 m gives approximately as satisfactory results as the (non-variable) push-pull amplifier valve EFF 50, and considerably better results than the existing button pentodes.

For the satisfactory performance of electronic valves which are intended for the amplification of very short waves it is essential that particularly the noise resistance, the input damping and the output damping should be low, while at the same time a steep slope must be retained. A steep slope, however, as explained previously in this periodical [1]), causes great damping of the input circuit due to the self-induction of the cathode connection. In the second article referred to, a valve was described in which this objection is met by the application of the push-pull principle. This valve, type EFF 50, can be used successfully for the amplification of signals with frequencies up to 6×10^8 c/s (wave length 50 cm), at which frequency an amplification by a factor 8 can still be obtained.

The principle upon which the push-pull amplifier valve is based consists in the fact that two systems which work in exactly opposite phase are connected to a common cathode connection. Since the sum of the high-frequency currents in the two systems is equal to zero, no high-frequency current flows through this cathode connection, and its self-induction can therefore have no damping effect on the input circuit.

The result obtained in this way answered fully to the expectations. In practice, however, it is not always possible to use a push-pull valve. It therefore became necessary to find out whether the aim in view — combatting the damping effect of the cathode connection — could not be attained by some other method as well.

A constructively simple principle, which offers many possibilities of influencing the input damping, the output damping and in addition the reactance in a favourable way, consists in the use of a double cathode connection. The anode current which returns to the cathode *via* one of the cathode connections then no longer needs choose a path which comprises part of the input circuit which is connected to the other cathode connection between grid and cathode (see *fig. 1b*).

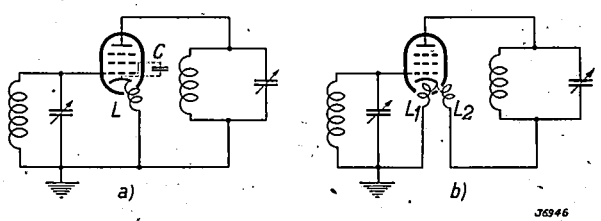

Fig. 1. Connections of a valve with single cathode connection (*a*) and of a valve with double cathode connection (*b*) in a stage for high-frequency amplification. Only the impedances important for high-frequency currents are given. In case *a* the self-induction L forms part of the input circuit and part of the output circuit at the same time, so that a back coupling occurs which is lacking in case *b*.

In order to show that by this means the damping effect of the anode current on the control grid circuit actually does disappear, we shall briefly review the theory of the input damping due to the self-induction of the cathode connection. If v is the A.C. voltage on the input circuit of fig. 1*a* and i_a the anode A.C., then the A.C. voltage between control grid and cathode is approximately:

$$v_g = v - j\omega L\, i_a$$

and therefore the A.C., which will flow to the control grid due to the presence of the grid-cathode capacity C, amounts to

$$i_g = j\omega C\, v_g = j\omega C v + \omega^2 LC\, i_a$$

In the first approximation $i_a = Sv$ where S is the slope of the valve, and therefore

[1]) M. J. O. Strutt and A. van der Ziel, The behaviour of amplifier valves at very high frequencies, Philips techn. Rev. **3**, 103, 1938; A new push-pull amplifier valve for decimetre waves, Philips techn. Rev. **5**, 172, 1940.

$$i_g = (j\omega C + \omega^2 LCS)\, v.$$

The second term in parentheses represents a current component which is in phase with the voltage, so that energy is taken from the input circuit. The equivalent input parallel resistance is

$$R_L = 1/\omega^2 LCS \quad . \quad . \quad . \quad . \quad . \quad . \quad (1)$$

(The subscript L indicates that the self-induction of the cathode connection is the cause of the damping).

In the connections with two cathode connections given in fig. 1*b* the anode current has no effect on the voltage between control grid and cathode, so that the above-discussed damping effect is entirely absent.

We need not stop at this result, however, but by the addition of suitable circuit elements we may even obtain negative damping of the input circuit, as will be explained in the following. After having shown further that the output damping and the reactance can also be favourably affected by suitable use of two cathode connections, we shall describe the construction of a valve, namely the high-frequency amplifier valve EF 51 which, for waves no shorter than 1.5 m, possesses properties which are much more favourable than those of the existing button pentodes and only slightly less satisfactory than those of the push-pull amplifier valve EFF 50. Compared with the push-pull amplifier valve the new high-frequency valve has the advantage that it offers the possibility of varying the amplification by varying the slope of the valve.

The influence of two cathode connections on the input damping

For the sake of simplicity of expression in the following we shall define several of the terms to be used. By the first cathode connection we mean the cathode connection which belongs to the input circuit, while the second cathode connection belongs to the output circuit. The end of the cathode connection which extends outside the valve will be called the lower end; the upper end is thus connected to the cathode.

In order to profit by the double cathode connection for the purpose of decreasing the damping of the input circuit, another condenser C_1 must be added to the circuit elements given in fig. 1*b* between the lower end of the second cathode connection and the control grid. In this way the diagram of *fig. 2* is obtained. It is immediately clear that the A.C. voltage which occurs due to the self-induction of the second cathode connection, *via* the condenser C_1 will now lead to a grid A.C., as was the case in the ordinary connections according to fig. 1*a*. Since the condenser C_1 is connected to the lower end of L_2, however, this A.C. is opposite in phase to that which occurred in the case of fig. 1*a*, so that instead of a damping a negative damping is obtained.

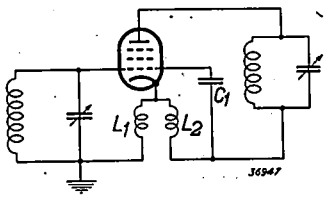

Fig. 2. Connection to two cathode connections and an auxiliary condenser C_1 for the purpose of eliminating the damping of the input circuit.

By analogy with equation (1) we obtain as value of the equivalent parallel resistance by approximation:

$$R_{L_2} = -1/\omega^2 L_2 C_1 S \quad . \quad . \quad . \quad . \quad . \quad (2)$$

This negative damping can be used for instance to decrease, or even entirely to eliminate the damping of the input circuit which occurs as a result of the finite transit time of the electrons between cathode and control grid [2]). This damping of the transit time, in the case of the valve EF 51 discussed later, corresponds approximately to a resistance

$$R_e = \frac{36}{f^2}\, 10^{+6}\ \Omega$$

where f is expressed in megacycles per second. If we attempt to compensate this damping with the help of the negative damping action of the second cathode connection, the sum of the damping by R_e and R_{L_2} must disappear as follows:

$$\omega^2 L_2 C_1 S = \frac{f^2}{36} \cdot 10^{-6} \quad . \quad . \quad . \quad . \quad . \quad (3)$$

The slope S of the valve EF 51 amounts to about 10 mA/V. Moreover $\omega = 2\pi f \times 10^6$, so that for the unknown circuit elements C_1 and L_2 we obtain the condition:

$$L_2 C_1 = \frac{10^{-15}}{10 \cdot 36 \cdot 4\pi^2} = 7 \cdot 10^{-20} \text{ farad henry.} \quad (4)$$

If we choose for C_1 a capacity of 1 picofarad then the self-induction of the cathode connection L_2 must be 7×10^{-8} henry, which is obtained by a wire about 6 cm long and 1 mm in diameter. We thus obtain elements which can easily be realized

[2]) See C. J. Bakker, Philips techn. Rev. **1**, 171, 1936.

in practice. The damping elimination indicated is valid for the whole range of short waves, since the value of L_2C_1 determined by equation (4) is independent of the frequency.

The influence of two cathode connections on the output damping

If in addition to the input damping we also wish to influence the output damping in a favourable direction, a second auxiliary condenser C_2 must be placed between the anode and the lower end of the first cathode connection (see *fig. 3*). If e_a is the

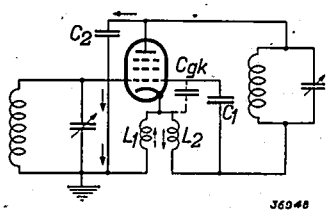

Fig. 3. Connection with two cathode connections and two auxiliary condensers C_1 and C_2 for the purpose of eliminating the input and the output damping. At the same time C_2 leads to a reactance capacity between anode and control grid, and thereby compensates the negative reactance capacity which is present at short waves due to other causes.

anode A.C. voltage over the oscillator circuit, then by approximation the following A.C. flows through this condenser:

$$i_{C_2} = e_a\, j\omega C_2,$$

along the path indicated by arrows *via* the self-inductions L_1 and L_2. Between cathode and earth therefore an A.C. voltage occurs:

$$v_k = -j\omega\, L_1\, i_{C_2} = e_a\, \omega^2\, L_1 C_2.$$

This change in the cathode potential leads to an extra anode current $-Sv_k$, thus $-e_a\, \omega^2 L_1 C_2 S$. From this it is evident that a negative damping also occurs in the anode circuit, which is determined by a formula quite analogous to the negative damping of the grid circuit.

In almost all connections occurring in practice the anode circuit of the high-frequency amplifier valve is coupled with the input circuit of a second stage, for instance a second amplifier valve or a mixing valve. The negative damping of the anode circuit is at the same time a negative damping of the input circuit of the following stage so that in the latter the damping need not be eliminated or only to a smaller extent.

The influence of the two cathode connections on the reactance of the cathode on the control grid

As was stated in the discussion of the output damping, the A.C. voltage e_a over the anode circuit leads to an A.C. along the path indicated by arrows (in fig. 3). This A.C. causes the A.C. voltage mentioned between cathode and earth:

$$v_k = e_a\, \omega^2\, L_1\, C_2$$

The A.C. flows further through the second cathode connection (self-induction L_2), so that the lower end of the latter possesses the following A.C. voltage with respect to earth:

$$v = e_a\, \omega^2\, (L_1 + L_2)\, C_2$$

These two A.C. voltages result in alternating currents to the control grid *via* the capacities C_{gk} and C_1, respectively. These capacities connect the control grid to points on which an A.C. voltage acts which is in phase with the anode A.C. voltage, but which has a much smaller amplitude. The effect of the A.C. voltages v_k and v on the control grid circuit is therefore exactly the same as if the capacities C_{gk} and C_1 were connected between control grid and anode, not with their whole magnitude, however, but reduced by a factor v_k/e_a and v/e_a. The total apparent capacity hereby caused between control grid and anode thus amounts to:

$$C_{ag}' = C_{gk}\frac{v_k}{e_a} + C_1\frac{v}{e_a} =$$

$$= \omega^2 C_2\,[L_1\,(C_{gk} + C_1) + L_2 C_1] \quad . \quad . \quad (6)$$

This apparent capacity is now found to reduce the reactance at high frequencies, since the reactance already present due to other causes has at high frequencies the character of a negative apparent capacity [3]), which like that of equation (6) is proportional to the square of the frequency. The size of this apparent capacity C_{ag}'' depends upon the manner of connection, and at a wave length of 2 m, for example, may amount to 0.2 pF. This would correspond to a behaviour according to the formula

$$C_{ag}'' = -2.25\cdot 10^{-19}\, \omega^2\ \text{pF} \quad . \quad . \quad . \quad . \quad (7)$$

If the total reactance must just be made to disappear, care must be taken that

$$C_2 = \frac{2.25\cdot 10^{-19}}{L_1\,(C_{gk} + C_1) + L_2 C_1} \quad . \quad . \quad . \quad (8)$$

The capacity C_2 to be calculated from this, as was already indicated in the previous section, gives at the same time a negative damping of the anode circuit; in the case of the valve EF 51 this is found to be more than enough to combat the causes of damping present.

[3]) See the first article referred to in footnote [1]), p. 113.

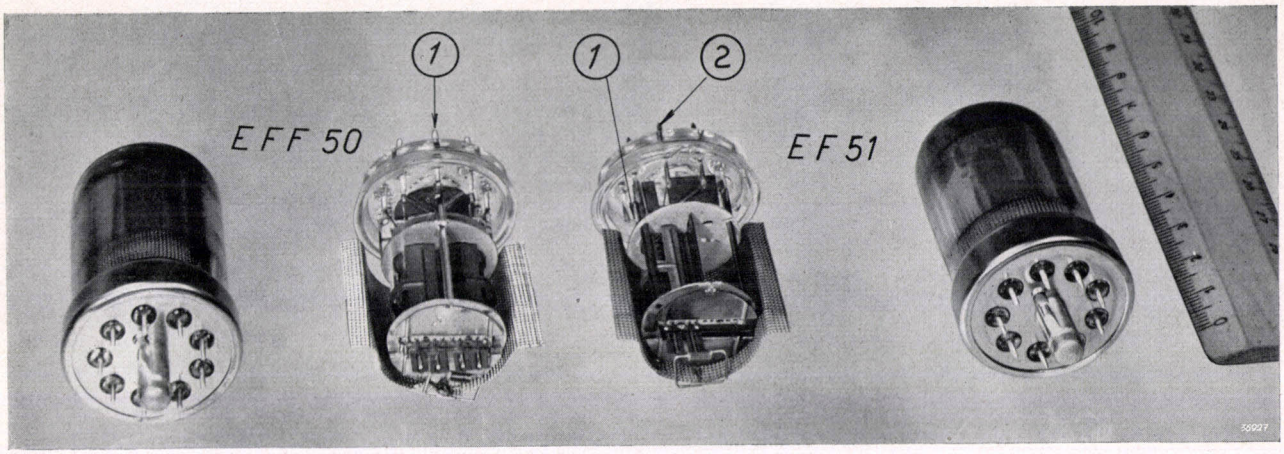

Fig. 4. Exterior and interior of the push-pull amplifier valve EFF 50, and of the valve with double cathode connection EF 51. The interior, from which the gauze screen has been removed, is mounted unsymmetrically in the case of the valve EF 51; *1* and *2* are the two cathode connections. In the case of the valve EFF 50 two identical systems are placed side-by-side and connected to a common cathode connection (*1*).

Construction of the amplifier valve with double cathode connection

In designing the amplifier valve with double cathode connection an attempt was made to make the harmful effect of the self-induction of the cathode connection as small as possible, even without the measures previously discussed. For this purpose the cathode connections, and particularly the first cathode connection, were kept extremely short, which could be done without changing the relative arrangement of the pins in the valve by placing the system unsymmetrically in the bulb, so that one end of the cathode falls exactly above the pin of the first cathode connection.

The construction of the valve with double cathode connection, type EF 51, is given in *fig. 4*. It may be seen that the appearance of this valve corresponds somewhat to that of the push-pull amplifier valve EFF 50 which is shown for the sake of comparison. In the case of the valve EF 51 the two cathode connections marked by arrows *1* and *2* may be distinguished; in the case of the push-pull amplifier valve, on the other hand, the two systems have a common cathode connection which is indicated by *1* in the photograph of the internal system.

The control grid of the valve EF 51, contrary to the case with EFF 50, has an irregular pitch (see *fig. 5*). In this way the magnitude of the negative control grid voltage, which is necessary to suppress the anode current, is made different for different parts of the cathode. In *fig. 6* it may be seen what effects this has on the characteristic. In the case of the valve EFF 50 the anode current is practically entirely suppressed by a control grid voltage of −6 V, and slightly above this "cut off voltage" the slope of the I_a-V_g characteristic (slope S_1 in fig. 6) decreases very sharply with falling control grid voltage. In the valve EF 51, on the other hand, the cut off voltage is different from point to point, in other words, the cutting off takes place quite gradually. The result is that the change in the slope also takes place quite gradually. Thanks to this property of the EF 51 it is possible to regulate the amplification of the valve by changing the grid bias, without experiencing much difficulty with non-linear distortion.

The non-linear distortion is characterized in fig. 6 by the quotient S_3/S_1. The coefficients S_1 and S_3 are thereby derived from the series:

$$S = S_1 + S_2 (V_g - V_{g0}) + S_3 (V_g - V_{g0})^2 + \ldots$$

which represents the behaviour of the slope S in the neighbourhood of the operating point (grid voltage V_{g0}). The strength of the cross modulation and of certain other undesired phenomena is found to be directly proportional to S_3/S_1 [4]), so that it is desirable to have this quotient as small as possible. As may be seen in fig. 6, S_3/S_1, in the case of the

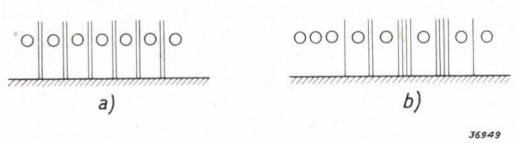

Fig. 5. *a*) Regular (*b*) irregular pitch of the control grid. For a control grid voltage in the regulation region the emission of the cathode is suppressed locally in the case of the irregularly wound grid.

[4]) On this subject we refer the reader to the book: Moderne Mehrgitter-Elektronenröhren, by M. J. O. Strutt, Springer (Berlin), 2nd edition 1939, p. 17.

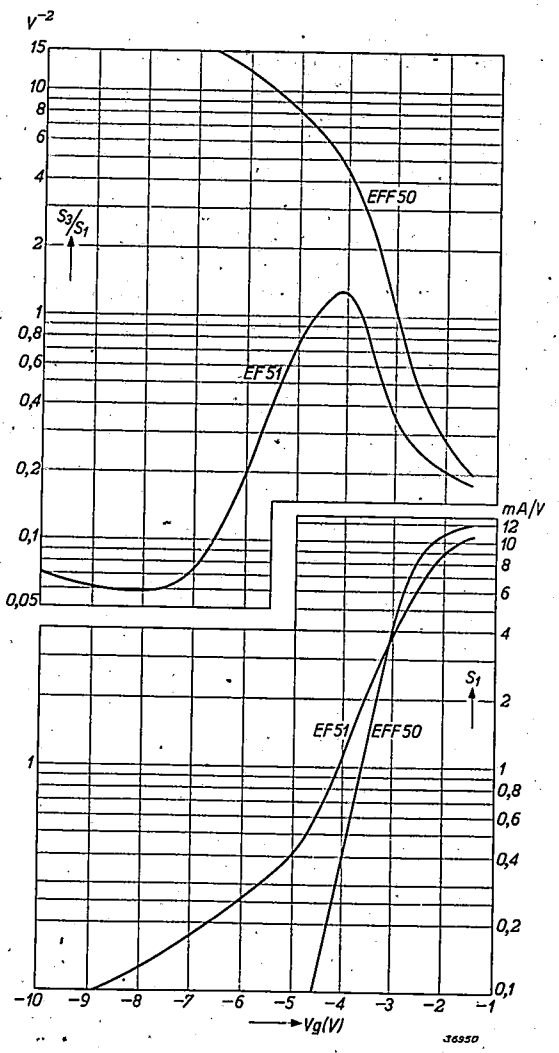

Fig. 6. Slope S_1 and distortion factor S_3/S_1 as a function of the grid voltage for the push-pull amplifier valve EFF 50 and for the valve with double cathode connection EF 51. The factor S_3/S_1 in the case of the valve EF 51, especially for large negative control grid voltages, is much smaller than in the valve EFF 50.

valve EF 51 is much smaller, especially for large negative grid voltages, than in the valve EFF 50.

Like all amplifier valves, the valve EF 51 exhibits a change in the input capacity upon regulation. This capacity variation may be unfavourable since due to it a detuning of the input circuit occurs. If only one cathode connection is used this capacity variation can for the most part be compensated in a simple way, for instance by the introduction of a resistance of about 30 ohms in this cathode connection. If both cathode connections are used the connections undergo several additional alterations.

The screen grid of the valve with double cathode connection is wound with a lower pitch than that of the push-pull amplifier valve. By this means the static capacity between control grid and anode is reduced and the internal resistance enlarged, which means an improvement of the valve qualities especially for not very short waves. In the following table the most important properties of the button pentode, the push-pull amplifier valve and the new amplifier valve with double cathode connection are shown side-by-side.

Table I

Properties of amplifier valves for very short waves.

Valve type	Button pentode 4 672	Push-pull amplifier valve EFF 50	Valve with double cathode connection EF 51
Slope (mA/V)	1,4	11*	10
Noise resistance R_r (ohms)	8 000	600*	900
Damping resistance R_e for $\lambda = 3$ m (ohms)	18 000	2 700*	3 600
R_r/R_e	0.44	0.22	0.25
C_{ag} for low frequencies (pF)	< 0.007	< 0.02	< 0.006

*) Per system (the valve contains two identical systems).
**) By this is meant the input parallel resistance which is equivalent to the damping due to the transit time of the electrons between cathode and control grid.

The noise qualities of the different valves are characterized in the table by the ratio between the socalled noise resistance R_r and the damping resistance R_e which occurs at the input side of the amplifier valve due to the finite transit time of the electrons between cathode and control grid. This quantity R_r/R_e is found in many practical cases to determine the maximum attainable ratio between signal voltage and noise voltage. From table I we see that the valve EF 51, as far as noise is concerned, is almost as good as the valve EFF 50 and considerably better than the button pentode 4 672.

Application of the valve with double cathode connection

The amplifier valve with double cathode connection will be used in the first place for the amplification of ultra short waves to a lower limit of 1.5 metres. These waves are of great importance, for example for telephony with directional aerials and possibly for television; in addition these frequencies are encountered as intermediate-frequency in superheterodyne receivers for still shorter waves.

The connections of the amplifier valve with double cathode connection can be based upon the diagram given in fig. 2, for example. This scheme

[5]) The capacity C_1 in many cases need not be realized by a separate condenser, but can be obtained by using the capacity between control grid and screen grid present in the valve. For this it is necessary that the screen grid should be connected for high frequency to the end of the second cathode connection, as is the case in the connections given in fig. 7.

is valid only for high-frequency currents, and must still be supplemented by the connection lines necessary for obtaining the desired biases of the different electrodes. In this way a scheme is arrived at like *fig. 7*, the functioning of which will be clear after the discussion of fig. 2.

If an attempt is made to apply these connections to practical cases, difficulties are found to occur due to parasitic capacities. The oscillation circuit LC in the anode circuit usually has a fairly considerable capacity with respect to earth or with respect to the chassis, and this capacity is in parallel with the capacity C_2. We have seen that C_2 causes a reaction which need only be very small to eliminate the small negative reactance present. If C_2 becomes too great a positive reactance occurs which, like the negative reactance, may have unfavourable effects on the amplification, for instance, a tendency to oscillation [6]). Therefore with these connections it is necessary to reduce the parasitic capacity between the oscillating circuit and earth, which can be done by housing the oscillating circuit in a closed container connected to the second cathode connection, as indicated in the figure.

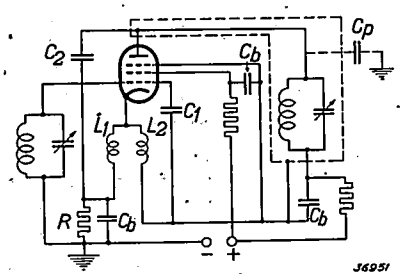

Fig. 7. Complete connections of a high-frequency amplifier stage with the valve EF 51 as amplifier valve. In order not to make the capacity C_2 too large due to the parasitic capacity C_p, the output circuit must be shielded. C_b block condensers. The resistance R serves to obtain the negative control grid bias.

If no other amplifier stage follows the connections just discussed, the method of shielding indicated can easily be realized. If, however, there are a number of stages in cascade, this is practically impossible. The anode A.C. voltage of the first valve must always be transmitted to the control grid of the following valve, which itself already possesses a capacity of about 10 pF with respect to earth.

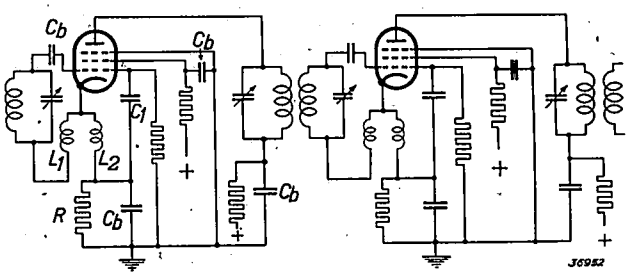

Fig. 8. Connections with the valve EF 51 in which no shielding of the output circuit is necessary. By inductive coupling any desired number of stages of this kind can be connected in succession. C_b block condensers. The resistance R serves for obtaining the negative control grid bias.

In order to be able to form cascade connections, therefore, it is desirable to use a connection with which no shielding of the anode circuit with respect to earth is necessary. Such a connection can be obtained very simply by connecting the second cathode connection in fig. 2, instead of the first, to earth. The scheme of connection thus obtained may be seen in *fig. 8*; it is also shown in this figure how by the use of an inductive coupling a second identical amplifier stage may be connected to the first stage. In this way any desired number of amplifier stages can be connected in succession. Instead of the magnetic coupling, electrostatic coupling can also be applied as shown in *fig. 9*. In this case two coupling condensers are required to take off the A.C. voltage to be transmitted from the two ends of the oscillation circuit. Apart from this the connections show no fundamental difference from the ordinary coupling with normal valves between successive stages.

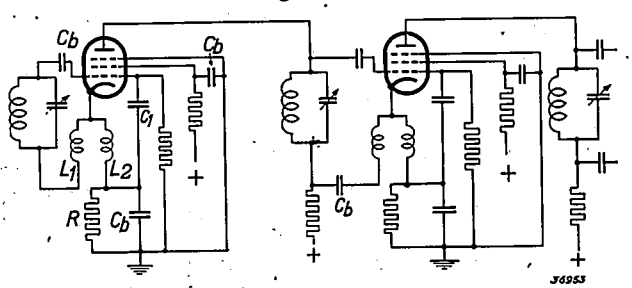

Fig. 9. Like fig. 8, but with a capacitative coupling between the stages.

[6]) On the disturbing effect of reactance see the article on transmitting pentodes, Philips techn. Rev. **2**, 257, 1937, especially fig. 3 and page 261.

ALPHABETICAL INDEX VOLUMES 1—5

The number in heavy print by each subject indicates the volume, the following number the page. If it is desired to know the complete title and the author of the article in which the subject in question is discussed, this can be looked up by means of the volume and page found in the chronologic index (pp. 000).

Adsorption phenomena at metal contacts 5,238

Aerials:
communal — („Antennaphil") 1,246
receiving — („Philastatic") . 4,320
rotating directional — PCJ transmitter 3,59

Aerodromes:
illumination and beaconing . 4,93
radio beacons 2,370

Aeroplane radio:
position and course finding . 2,184
transmitter-receiver V.R. 18 1,114
transmitter-receiver with course finder (plate) . . . 2,182

Amplifier installations, see **Sound amplification Amplifiers**
negative feed-back, see under that title noise of — 2,136
use intelephony 2,209

Amplifier valves, see **Radio valves**

Analysis:
mixtures of argon and nitrogen 5,88
polarography 4,231
X-ray diffraction for — . . 1,158; 5,157

Apparatus for defective hearing . 4,316
Architecture and illumination . . 2,8
Armatures, testing 4,88

Artificial resin:
X-ray diffraction diagrams . 2,256
see further „Philite"

Artificial respiration, apparatus . 4,325

Auditorium acoustics:
intelligibility 3,139
reverberation 3,65
sound absorption 3,363
optic0ls models:
investigation directional distribution. 5,321
principe; investigation intensity distribution . . 1,46

Automobile radio:
receiving set 3,112
transmitting-receiving set . . 5,315

Band spread 4,286
Baretters 3,74

Beacons for aerodromes:
light beacons 4,93
radio beacons 2,370

„Bi-Arlita" lamp 1,97
Bicycle dynamo 3,87
Bicycle rear lights and reflectors . 5,335

Biological effect of ultraviolet radiation:
cure of rickets (Vitamin D) . 3,33
erythema and conjuctivitis . 2,20

„Biosol" lamp 2,18

Black-out illumination, see **Illumination Blocking-layer rectifiers,** see **Rectifiers (blocking-layer rectifiers)**

„Blocking" of oscillators, investigation with oscillograph . . . 3,251

Brightness:
definition and significance . 1,142
of mercury lamp and sun . . 1,62
of night sky 5,296

Broadcasting:
motor van for — 4,73
studio installations 4,135
studio K.R.O. investigation with optical model 5,321

Bulbs, flower, influence of X-ray treatment on 2,321
Bullet finder 5,309

Cancer Institute, Amsterdam, X-ray installation 4,153
Candle power, new 5,1

Carrier-wave telephony, see **Telephony**

Cathanode 1,367

Cathode-ray oscillograph:
applications:
armatures, testing in mass production . . . 4,88
„blocking" of oscillators 3,251
chemical analysis (polarography) 4,231
depth of modulation . . 3,249
electron switch as auxiliary 3,148; 4,267
frequency measurement. 3,341
frequency modulation, control 3,248
fuses 4,118
gas-discharge lamps, current and voltage . . . 3,148
hysteresis loop 3,341
I_a-V_a diagrams 3,339
mechanical stresses . . . 5,26
mechanical vibrations . 5,230
pith of orchestra, control 4,205
power mains 3,30
resonance curves of receiving sets 4,85
construction:
GM 3150 1,147
GM 3152 4,198
GM 3156 (tool making) 5,277
see also **Cathode-ray tube**

Cathode-ray tube:
electrode system, potential field (plate) 4,229
focussing of electron beam . . 1,33
post-acceleration tube . . . 5,245
applications:
characteristics of output valves 5,61
characteristics of transmitter valves 4,56
phase angles, measurement 5,208
pressure indication . . . 5,3
recording oscillograms . . 2,148
scanning speed:
apparatus for measuring 3,216
calculation, measurement, practical conclusions 2,148
enlargement by post-acceleration 5,245
seondary emission of screen . 3,214
ray intensity, regulation . . . 1,91
television tube with magnetic deflection 4,349
television tube with projection of image 2,249
applications in which an ordinary oscillograph apparatus is used, see under **Cathode-ray oscillograph**

Chrome iron for metal-glass joints 2,306
Cold emission 4,103
Colour photography, additive method 5,48

Colour rendering of light sources:
improvement:
electric lamps („Philiphane" glass) 3,46
mercury lamps (luminescence) 3,272
mixed light 5,353
method of comparison of sources of „white" light . . . 2,1
photometer for investigation 4,66

Coulours
colour vision 1,282
diagram (ICI triangle) . . . 2,39

Condensers:
electrolytic — 2,65
heavy current — 1,178
linear action — 4,277
pressure —. 4,254
standard — 5,300

Contact resistance:
convergenxe resistance . . . 4,332
transition resistance (influence of adsorption) 5,238

Contrasts and visibility:
in road lighting 1,166
in X-ray fluoroscopy 4,114

Converter of direct current, see **Vibrator**

Course finder for aeroplanes . . . 2,184

Crystal structure, see **Structure analysis**

Damping mechanical vibrations . 1,370
Decibel, definition and use . . . 2,47
Decimal classification 3,27
Density meter 5,331

Diamond:
crystal defects 2,254
dies 5,14

Dies:
diamond 5,14
hard-cemented carbides . . . 4,309

Direct-current dynamo's, voltage regulation with triodes 3,97

Disc test for machinability . . . 1,183; 1,200

Distortion:
in coil-load cables 4,79
in the ear 4,172
due to magnetic causes . . . 2,193
measurement of — in loud speakers 4,353
reduction by negative feed-back, see **Negative feed-back**
Dynatron 3,133

Ear:
distortion 4,162
perception of pith 5,286
sensitivity 2,50
Electric lamps, see **Light sources**
Electrolytic condenser 2,65
Electrometer triode 5,54
Electron diffraction diagrams . . 5,161
Electron microscope:
construction and applications 1,312
investigation of α-γ transition in iron 1,317
Electron multipliers:
construction 3,134
use in television transmitter . 2,72
Electron switch:
description 4,267
example of application . . . 3,150
Electron trajectories:
in magnetron 4,193
model for investigation of — . 2,338
in multigrid valves 5,131
Electronic valves, see **Radio valves**
Enamelled wire 3,39
Equivalent networks with highly saturated iron cores 2,276
Exposition illumination, see **Illumination**
Eye:
characteristics with reference to level of illumination of roads 1,102
colour perception 1,283
colour space diagram 2,39
contrast sensitivity 1,166
glare 1,225
sensitivity 5,296
speed of vision 1,215
visual acuity 1,215

Fastness-to-light meter:
description 1,277
radiation intensity 2,282
Field strength measurement:
accuracy 5,149
recording apparatus 2,216
Film projection with water-cooled mercury lamps 4,2
Filters, electrical:
general theory 1,240
high and band-passN . . . 1,327
low-passN 1,298
practical calculation 1,270
table 1,332
transmitting of impulse . . 1,363
Filters, magnetic, for oil 2,295
Flashlight lamps:
peak time 4,148
„Photoflux" 1,289
synchronizers 2,334
Flicker, gas-discharge lamps, improvement by luminescence . . 3,277
Fluorescence, see **Luminescence**
Foundry:
high-frequency furnace . . . 1,53
X-ray testing of castings . . 2,377
Frequency characteristic, recording:
automatic recording apparatus 4,354
tone generator for — 5,263
Frequency measurement of, with oscillograph 3,341
Frequency moduation, control with oscillograph 3,248
Fuses, electrical testing with oscillograph 4,118

Gas-discharge lamps:
alternating current connection 2,103
oscillographic investigation . 3,148
see also **Gas discharges** and **Light sources** (mercury and sodium lamps)
Gas-discharges:
comparison of sodium and mercury lamp 1,2 1,70
excitation and ionization in positive coumn 3,157
light emission in positive column of mercury, sodium, neon 3,197
luminescent tube-wall with low-pressure mercury column 3,272
Gas-filled photocells, inertia . . . 4,48
Gas-filled rectifier valves:
physical principles 2,122
see also **Rectifiers (hot-cathode rectifiers)**
Getters 5,217
Glare instreet lighting 1,225
Glass:
composition properties, use . 2,87
joints with metals (chrome iron) 2,306
metal leads through — . . . 3,119
Gramophone records:
simple apparatus for recording 4,106
speed of playing 2,56
stereophony on — 5,182

Hard metal ("hard cemented carbides") 4,309
Hardness, definition and measurement 2,177
High-frequency furnace with valve generator 1,53
High-voltage:
assembly of 10^6 volt generator (plate) . . . . . .
generator for 10^6 volts on the cascade principle 1,6
installation of Cavendish Laboratory 2,161
X-ray tube construction . . . 4,153
impulse voltOge generators, see under that title
Hysteresis loop:
measuring apparatus for soft iron 2,84
oscillographic recording . . . 3,341

Iconoscope 1,18
Illumination:
aerodromes 4,93
architecture and — 2,8
blackout illumination:
brightness of night sky . 5,296
filter method 5,93
principles 4,15
cruiser „de Ruyter", festive — (plate) 1,282
expositions:
Liége 1939 5,42
Paris 1937 2,361
"Well lighted house" 4,174
general principles of public — 2,110
indirect —, light distribution on reflection 5,125
League of Nations Palace, Geneva 3,322
linear light sources:
illumination intensity, shadows, reflection . . 4,181
reflecting surfaces . . . 5,16
mixed light 5,353
railway yards 4,62
road lighting, see under that title
ships („Nieuw Amsterdam") 3,356
streets:
principles 2,142
reflector 5,222
tennis courts 1,252
work benches 3,53
Impulse-voltage generators:
for 2×10^6 V 1,236
for 4×10^6 V and 8 kW sec . 3,306
Indicator fir unternal combustion motors 5,360
Infra red radiation, surveillance system 1,306
Intelligibility 3,139
Iverse feed-back:
principles and possibilities of application 2,289
use for expansion in sound reproduction 3,204
use in receiving sets 1,268
use in repeaters 2,209
Iron filament resistances 3,74
Iron lung 4,325

Lamps, see **Light dources**
Laryngophone 5,6
Leads, metal, through hard glass and silica 3,119
Lueague of Nations Palace, Geneva:
electro-acoustic equipment . 3,322
illumination 3,175
Liége, illumination of Water Exposition 1939 5,42
Light-house lamps 4,29
Light intensity, unit 5,1
Lighting, electrical data 2,225
Light sources:
alternating current connections of gas-discharge lamps 2,103
bicycle rear lights 5,335
colour rendering, see under that title
incandescent electric lamps:
assembly of 10 kW lamp (plate) 4,41
„Bi-Arlita" lamp . . . 1,97
light-house lamps . . . 4,29
"Protector" lamps . . . 4,15
tungsten ribbon lamps . 5,82
linear —, see **Illumination**
luminescence lamps, tubular 4,337
mercury lamps:
„Biosol" lamp 2,18

comparison with sodium lamps 1,2 1,70
high-pressure —, air-cooled;
HP 300 1,129
HPL (luminescence) 5,
for enlarging apparatus 3,91
for photography . . 4,27
high-pressure —, water-cooled;
brightness 1,62
for film projection . 4,2
HP and SP 2,165
lox-pressure —, with luminescence . . . 4,337
mixed-light lamp 5,353
sodium lamps:
applications in photography 2,24
comparison with mercury lamps 1,2 1,70
high-frequency oscillations 1,87
principles and development 2,353
Linear light sources:
application, see **Illumination**
luminescence lamps . . . 4,337
Loading coils:
magnetic core material . . . 2,77
use, see **Telephony**
X-ray examination of core material 2,93
Loud speakers:
directional effect, sound diffusers 4,144
efficiency 4,301
testing 4,354
Luminescence:
application:
in high-pressure mercury lamp 5,353
in low-pressure mercury lamp:
practical application 4,337
principles 3,272
for testing and research . 3,5
fluorescence and phosphorescence, different forms 3,241
fluorescence phenomena, theory 3,125

Machinability, estimation by disk test 1,183 1,200
Magnetrons:
theory 4,189
use in transmitter 2,299
Magnets:
calculation 5,29
lifting power 5,195
Magnet steel:
theory, properties of different kinds 2,233
use for magnets 5,29
Mains:
oscillographic investigation . 3,50
protection against surge voltages 2,225
Manometers for low gas pressures 2,201
Manufacture, methods of checking:
cathode-ray oscillograph for testing 4,85
universal testing set for radio valves 2,57
X-ray control of assembly . . 3,186
Material testing:
automatic — with ionization chambers and X-rays . . . 3,228
electron microscope for — . . 1,313 1,321
hardness 2,177
machinability 1,183 1,200
structure analysis; see under that title
X-ray —:
apparatus 5,69
examples:
assembly 3,186
castings 2,377
rivetted joints . . . 2,350
welds 3,92
method 2,314
Measuring bridge, simple apparatus 2,217
Mechanical stresses, investigation:
with cathode-ray oscillograph (varying —) 5,26
with X-ray diffraction 1,373
Mechanical vibrations:
damping of — 1,370
vibration recorder for investigation of — with oscillograph 5,230
Megaphone, electrical 4,272
Mercury cathode, metal rectifier with 1,65
Mercury lamps, see **Light sources**
Metal-vapour lamps, see **Gas-discharge lamps**
Microphones:
absolute calibrated — . . . 1,84
laryngophone 5,6
review of different kinds . . 5,140
Mixing valves, four beam electrode 3,266
Modulation depth, measurement with oscillograph 3,248
Motor van for sound recording . . 4,73
Music:
fortissimo and pianissimo . . 1,266
pitch intervals 2,47
pitch of orchestras, statistics 4,205
pitch, standard 5,243
playing speed of gramophone records 2,56
Musical instruments:
church bells 5,293
compass of various — . . . 2,49
violin, amplification of sound 5,36

Neon lamps for irradiation of plants 1,193
Networks:
duality of — and geometric configurations 5,324
equivalent —, with highly saturated iron core 2,276
filters, see under that title
Neutrons production and use . . . 3,331
„Nieuw Amsterdam", illumination 3,356
Nipkow disc:
construction 4,42
interlaced scanning 3,285
use in television transmitter . 2,72
Noise:
in amplifiers 2,136
in amplifier valves 2,329
in receiving sets 3,189
in ultra short wave reception 5,172
„Normandie", sound distribution 1,22
Nuclear physics 2,97

Octave and decibel 2,47
Oil filters, magnetic 2,295
Optical models for investigation of auditorium acoustics:
investigation of directional distribution 5,321
principle; investigation of intensity distribution 1,46
Optical telephony 1,152
Oscillograms, distortion:
causes in the amplifier . . . 5,281
causes in the tube 4,199 5,251
Output valves, see **Radio valves**

Paris, illumination world exposition 1937 2,361
Pearls, X-ray testing for genuineness 1,60 2,156
Pentodes, see **R0dio valves** and **Transmitter valves**
Perception of pitch 5,286
Phase angles, measurement with cathode-ray tube 5,208
Phase displacement, measurement 5,300
"Philiphane" glass, influence on colour rendering 3,46
Philips-Miller system of sound recording:
machine for recording and reproduction 5,74
principle 1,107
recording strip 1,231
sound recorder 1,135
sound-track cutter 1,211
use in motor van 4,73
"hilishave" shaving apparatus . . 4,350
„Philite":
— presses with 1000 ton pressure (plate) . . . . . .
properties and manafacture . 1,257
use, table of properties . . . 3,9
"Philiscope" measuring bridge . . 2,270
pH measurement with electrometer triode 5,54
Phosphorescence, see **Luminescence**
Photocells:
amplification by secondary emission 5,253
application of:
optical telephony . . . 1,152
photometry 4,66 5,166 4,260
surveillance system . . . 1,306
television 2,72
iconoscope 1,18
inertia, gas-filled — 4,48
principles and development . 2,13
Photocurrent, measurements with electrometer triode 4,66 5,54
"Photoflux" lamp 1,289
Photography:
colour photography, additive method 5,48
erlarging apparatus with mercury lamps 3,91
flashlight lamps, see under that subject
— with mercury light (HPL lamp) 4,27
— with sodium light 2,24

Photometry:
definitions of brightness . . 1,142
genral problems 1,120
physical — 4,260
spectral — (block method) . 4,55
subjective — 5,270
technical — 5,166
tungsten ribbon lamps for — 5,82
unit of light intensity . . . 5,1
Planigraphy 5,309
Plants, irradiation of 1,193
Polarography 4,231
Positive column, see **Gas discharges**
Potential fields, recording with electrolytic tank 4,223
Powder metallurgy 4,309
Pressure condensers 4,254
Pressure indicator 5,360
„Protector" lamps 4,15
Push-pull amplifier valve (EFF 50) 5,172

Quartz glass, metal leads 3,119

Radiation measurements:
density meter 5,331
with ionization chamber and electrometer triode 5,54
Photographic (X-ray) dosages 1,62
Radio interferences:
causes and method of transmission 3,235
combatting 4,237
— due to sodium lamps . . . 1,87
Radio receiving sets:
band spread 4,284
car radio 3,112
compression and expansion . 3,204
frequency characteristics . . 5,115
magnetic tuning; negative feed-back 1,264
noise of — 3,189
push-button tuning:
with linear action condenser 4,277
with motor 3,253
resonance curves, control in mass production 4,85
superheterodyne principle, demonstration 1,76
superregenerative reception . 5,315
Radio valves:
characteristics, recording with oscillograph 3,339; 5,61
construction; all-glass — . . . 4,162
electron trajectories in — . . . 5,131
influence of transit times, self induction, mutual induction of connections 3,103
influence of transit times and space charge; amplification with negative anode . . . 1,171
measuring apparatus for — . 2,57
noise of — 2,329
pumping plant for — (plate) 3,147
secondary emission in —:
application 3,133
harmful results 3,211
special valves:
double cathode connection (EF 51) 5,369
electrometertriode . . . 5,54
four-beam electrode . . 3,266
gas-filled triodes 1,371
output valves, power and distortion 5,189
output valves, testing with oscillograph . . . 5,61
push-pull amplifier valve (EFF 50) 5,172
Radio waves, propagation . . . 4,245
Railway yards, illumination . . 4,62
Rare gases:
analysis of argon-nitrogen mixtures 5,88
manufacture of — 4,128
Rear lights for bicycles 5,335
Recrystallization, X-ray investigation 2,29
Rectifiers:
blocking-layer rectifiers:
theory 4,100
use of selenium valves . 5,199
controllable unit 20 kV, 18 amp 1,161
hot-cathode rectifying valves:
high-voltage valves . . 1,8
principles of gas-filled rectifier valves 2,122
relay valve (DCG 5/30) 1,163
mercury cathode, metal valve with 1,65
for telephone exchanges 1,295
Receiving sets, see **Radio receiving sets**
Reflexion:
brightness coefficients of road surfaces 3,313
light distribution upon — by different materials 5,125
triple mirror (bicycle reflectors) 5,335
Reflector for street lighting . . . 5,222
Relaxation oscillations 1,39
Relay valves:
controllable rectifier unit with — DCG 5/30 1,161
— as timing devices in seam welding 1,11
Resistance measurements:
apparatus for — 2,270
— of liquids 3,183
Resonance curves of receiving sets, measurement 4,85
Reverberation 3,65
Ribbon lamps 5,82
Rivitted joints, X-ray investigation 2,350
Road lighting:
installed systems:
measurements 4,292
Purley Way, Croyden (plate) 1,230
physiological principles:
brightness and apparent brightness 1,142
general properties of the eye 1,102
glare 1,225
sensitivity to contrast and wealth of contrast 1,166
visual acuity and speed of vision 1,215
reflection of road surface:
desired brightnesses and contrasts 2,239
distribution of brightness 3,313; 5,222
visibility meter for judging . 1,349
„Rotalix" X-ray tube 3,292

Scanning speed, see **Cathode-ray tube**
Secondary emission:
applications:
cathode-ray tube . . . 3,214
dynatron, electron multiplier, amplifier valves . 3,133
photocell 5,253
emission of different matials 3,80
undesired effects in amplifier valves 3,211
Selenium valves:
principles, preparation . . . 4,100
use in rectifiers 5,199
Shaving apparatus „Philishave" 4,350
Soapstone, X-ray tests 1,60; 2,157
Sodium lamps, see **Light sources**
Sound:
amplication:
apparatus for improving defective hearing . . . 4,316
League of Nations Palace . 3,312
megaphone 4,272
"Normandie" 1,22
principles, applications . 3,221
auditorium acoustics, see under that title **distribution,** see — **amplification**
intensity of different sources 2,54
radiation:
pressure measurements . 1,82
theory and models . . . 4,213
recording:
gramophone records, simple apparatus . . 4,106
machines for sound film 5,74
motor van for — . . . 4,73
Philips-Miller system, see under that title stereophone records 5,182
reproduction:
compression and expansion 3,204
fortissimo and pianissimo 2,266
in radio apparatus . . . 5,115
stereophonic — 5,107
spectra:
acoustic spectroscope . . 4,290
light diffraction by sound film 3,298
synthetic sound 4,167
tone generator 5,263
units 2,47; 5,243
Sound diffusers in loud speakers . 4,144
Sound film:
light diffraction by — . . . 3,298
machines for recording and reproduction 5,74
Philips-Miller system, see under that title
Spring balance 1,126
Stabilizer with highly saturated iron core 2,276
Starting resistances, automatic . 1,205
Stereophony:
principles 5,107
stereophone records 5,182
stereophonic apparatus for the deaf 4,316
Street lighting, see **Illumination**
Structure analysis, X-ray:
applications:
analysis of mixtures . . 1,158
crystal defects 2,254
crystal size 2,255

identification 1,31, 1,158, 1,188
mixed crystals 1,220, 1,252
recrystallization 2,29
strains 1,373
survey 5,157
texture 1,60, 1,95, 2,93, 2,156
method:
general 1,29
"sensitive" lines 1,253
X-ray tube for — . . . 3,259
Studio equipment 4,136
Superheterodyne reception, destration model 1,76
Superregenerative receiver . . . 5,315
Surface layers, X-ray investigation 1,31, 1,95
Surge voltages, protection of mains against 2,225
Surveillance system with infra red rays 1,306
Synchronizers for flash light photography 2,334
Synthetic sound 4,167

Telephony:
carrier-wave telephony:
on coil-loaded cables . . 4,20
distortion in coil-oaded cables 4,79
filters, see under that title
loading coils:
core material 2,77
use 1,357
optical telephony 1,152
rectifiers for exchanges . . . 1,295
repeaters 2,209
ultra short wave telephone connections:
Eindhoven-Nijmegen . . 2,299
Eindhoven-Tilburg . . . 2,173
with moving automobiles 5,315
Telescope mirrors 1,362
Television:
experimental transmitter . . 1,16
Nipkow disc, construction . 4,42
projection of image 2,249
receiving sets 2,33, 4,342
transmitter with iconoscope . 1,325
odem; portable 3,1
transmitter with Nipkow disc 2,72
idem with interlaced scanning 3,285
Temperature measurement with thermo-elements 5,214
Texture investigation, see **Structure analysis**
Thermo-elements for temperature measurement 5,214
Thermojuctions 3,165
Tone generaotr 5,263
Topological consideration of networks 5,324
Transmitters:
broadcastin transmitter Rio de Janeiro (plate) 3,58
short wave station P.C.J. . . 3,17
television transmitters, see **Television transmitting-receiving installations**
transmitter-receiver installations:
for aeroplanes 1,114
for automobiles 5,315
Eindhoven-Mijmegen . . 2,299
Eindhoven-Tilburg . . . 2,171
Transmittind valves:
air-cooled — 4,121
characteristics, recording with cathode-ray tube . . . 4,56
development, manufacture of — 2,115
gas-filled triodes 1,367
hum of — 5,100
pentodes 2,257
Triodes, see **Radio valves** and **Transmitting valves**
Tuberculosis detection by large scale X-ray examination 1,339
Tungsten:
preparation 4,309
thorium in — 1,189
working (plate) 5,121
α and β modification 1,190
Tungsten ribbon lamps 5,82

Ultra short waves:
amplifier valves:
double cathode connection 5,369
genral behaviour on ultra short waves 1,171, 3,103
push-pull amplifier valve 5,172
automobile transmitter receiver 5,315
magnetron 4,189
propagation of — 4,245
telephone connections, see **Telephony**
Ultra violet radiation:
biological effects:
general 2,18
vitamine D 3,33
technical application for luminescence research . . . 3,5
Units:
decibel 2,47
new candle power 5,1
phon 5,243

Vibration recorder 5,230
Vibrator:
converter direct into alternating current 2,346
transforming direct current voltage 3,114
Violin, perspectives in development 5,36
Visibility meter:
principle and construction . . 1,351
use, results of measurements 4,292
Vitamine D 3,33
Voltage regulation of direct current generators with triodes . . 3,97

Welding:
efficiency of welding rods . 3,352
fusing of welding rod, X-ray cinematic investigation . . 1,26
methods and kinds of rods . 2,129
relay valves as timing devices 1,11
tensile strength of weld material 3,279
transfer of material (overhead welding) 4,9
twin current welding unit . . 1,338
X-ray control of welds . . . 3,92
Work bench illumination 3,53

X-ray:
apparatus for testing material 5,69
diagnostics:
camera photographs 5,258
fluoreoscopy (protection against radiation, observation of objects) . . . 4,114
localization of objects projectiles) 5,309
tuberculosis detection . 1,335
diffraction diagrams:
special applications, see under **Structure analysis**
survey of interpretation and applications . . . 5,157
material testing, see under that title
photographs:
camera photographs . . . 5,258
density meter for X-ray films 5,331
short exposure times (10^{-6} sec) 5,22
stereoscopic — 5,309
welding process (transfer of drop) 1,26, 4,9
protection from radiation . . 1,62, 4,114
radiation of flower bulbs . . 2,321
structure analysis, see under that title
tubes:
for diagnosis ("Rotalix tube) 3,292
for structural analysis . 3,259
for therapeutics, up to 10^6 volts 4,153

Zirconium:
preparation and use 3,345
use as getter 5,217

CHRONOLOGICAL INDEX VOLUMES 1–5

VOLUME 1, 1936

	Page
Introduction - G. Holst	1
Comparison between discharge phenomena in sodium and mercury vapour lamps I - G. Heller	2
A modern high-voltage equipment - S. Gradstein	6
Relay valves as timing devices in seam-welding practice - D. M. Duinker	11
An experimental television transmitter and receiver - J. van der Mark	16
The loudspeaker and sound-amplifying installation on the T.S.S. "Normandie" - N. A. Halbertsma	22
How does a welding electrode fuse? - J. Sack	26
Practical applications of X-rays for the examination of materials I - W. G. Burgers	29
The production of sharp fluorescent spots in cathode ray tubes - G. P. Ittmann	33
Relaxation oscillations - S. Gradstein	39
Optical model experiments for studying the acoustics of theatres - R. Vermeulen and J. de Boer	46
A high-frequency furnace with valve generator - G. Heller	53
Practical applications of X-rays for the examination of materials II - W. G. Burgers	60
Dosage control in X-ray laboratories and works	62
A new metal rectifying valve with mercury cathode - J. G. W. Mulder	65
Comparison between discharge phenomena in sodium and mercury vapour lamps II - G. Heller	70
Demonstration model illustrating superheterodyne reception - H. J. J. Bouman	76
Absolute sound-pressure measurements - J. de Boer	82
High-frequency oscillations in sodium lamps - L. Blok	87
Control of the beam intensity in cathode ray tubes - G. P. Ittmann	91
Practical applications of X-rays for the examination of materials III - W. G. Burgers	95
The development of the coiled-coil lamp - W. Geiss	97
Characteristics of the eye with special reference to road lighting - P. J. Bouma	102
The Philips-Miller system of sound recording - R. Vermeulen	107
The V.R. 18 transmitting and receiving equipment - C. Romeyn	114
The photometry of metal vapour lamps - G. Heller	120
A very sensitive spring balance - C. J. Dippel	126
The mercury vapour lamp HP 300 - G. Heller	129
The sound recorder of the Philips-Miller system - A. Th. van Urk	135
The definitions of brightness and apparent brightness and their importance in road lighting and photometry - P. J. Bouma	142
An oscillograph apparatus - G. P. Ittmann	147
Optical telephony - J. W. L. Köhler	152
Practical applications of X-rays for the examination of materials IV - W. G. Burgers	158
A controllable rectifier unit for 20 000 Volts/18 Amperes - J. G. W. Mulder and H. L. van der Horst	161
The reception of brightness contrasts in road lighting - P. J. Bouma	166
Some characteristics of receiving valves in shortwave reception - C. J. Bakker	171
Heavy-current condensers - H. Ehrnreich	178
A speed-increment test as a short-time testing method for estimating the machinability of steels - P. Clausing	183
Practical applications of X-rays for the examination of materials V - W. G. Burgers	188
Irradiation of plants with neon light - J. W. M. Roodenburg and G. Zecher	193
The disk test as a rapid method for estimating the machinability of steel - P. Clausing	200
Automatic starting resistances ("Starto" tubes) - P. C. van der Willigen	205
The sound-recording cutter in the Philips-Miller system - A. Cramwinckel	211
Visual acuity and speed of vision in road lighting - P. J. Bouma	215
Practical applications of X-rays for the examination of materials VI - W. G. Burgers	220
The problem of glare in highway lighting - P. J. Bouma	225
The new sodium lighting scheme of the Purley Way, Croydon (picture)	230
The recording strip in the Philips-Miller system - C. J. Dippel	231
An impulse-voltage generator for two million volts - A. Kuntke	236
Electrical filters I - Balth. van der Pol and Th. J. Weijers	240
The communal aerial - J. van Slooten	246
Sodium lighting of tennis courts	252
Practical applications of X-rays for the examination of materials VII - W. G. Burgers	253
Properties and applications of artificial resin products - R. Houwink	257
Improvements in radio receivers - C. J. van Loon	264
Electrical filters II - Balth. van der Pol and Th. J. Weijers	270
A new apparatus for testing the fastness-to-light of materials - J. F. H. Custers	277
Festive illumination of the Netherlands cruiser "De Ruyter" (picture)	282
The perception of colour - P. J. Bouma	283
The "Photoflux", a light-source for flashlight photography - J. A. M. van Liempt and J. A. de Vriend	289
Rectifiers for telephone exchanges - H. J. J. Bouman	295
Electrical filters III - Balth. van der Pol and Th. J. Weijers	298
A surveillance system using infra-red rays - A. L. Timmer and A. H. van Assum	306
The electron microscope as an aid in metallographic research - W. G. Burgers and J. J. A. Ploos van Amstel	312
Electron-optical observations on the transition of alpha to gamma iron - W. G. Burgers and J. J. A. Ploos van Amstel	317
Television - J. van der Mark	321
Electrical filters IV - Balth. van der Pol and Th. J. Weijers	327
Systematic X-ray examination for the detection of pulmonary tuberculosis - J. G. A. van Weel	335
The Philips twin current welding unit - H. A. W. Klinkhamer	338
How can one judge the efficiency of road lighting? - G. Holst and P. J. Bouma	349
The use of loading coils in telephony - W. Six	353
Telescope mirrors - H. J. Meerkamp van Embden	358
Electrical Flters V - Balth. van der Pol and Th. J. Weijers	363
Gas-filled triodes - H. G. Boumeester and M. J. Druyvesteyn	367
The damping of mechanical vibrations - A. Cramwinckel, C. J. Dippel and G. Heller	370
Practical applications of X-rays for the examination of materials VIII - W. G. Burgers	373

VOLUME 2, 1937

	Page
Colour reproduction in the use of different sources of "white" light - P. J. Bouma	1
Illumination and architecture - L. C. Kalff	8
The photo-electric effect and its application in photo-electric cells - M. C. Teves	13
Spectral distribution of the radiation from the „Biosol" - A. van Wijk	18
The "Philora" sodium lamp and its importance to photography - J. A. M. van Liempt	24
Practical applications of X-rays for the examination of materials IX - W. G. Burgers	29
A television receiver - C. L. Richards	33
The representation of colour sensations in a colour space-diagram or colour triangle - P. J. Bouma	39
Octaves and decibels - R. Vermeulen	47
The playing speed of gramophone records - J. de Boer	56
A universal testing set for radio valves - D. Eringa	57
Electrolytic condensers - W. Ch. van Geel and A. Claassen	65
Television system with Nipkow disc - H. Rinia and C. Dorsman	72
Magnetic cores for loading coils - J. L. Snoek	77
An apparatus for hysteresis measurements on soft magnetic materials - J. J. Went	84
Glass for modern electric lamps and radio valves - J. Smelt	87
Practical applications of X-rays for the examination of materials X - W. G. Burgers	93
Nuclear physics - W. de Groot	97
Alternating-current circuits for discharge lamps - E. G. Dorgelo	103
Public lighting, principles of road lighting - G. B. van der Werfhorst	110
Development and manufacture of modern transmitting valves - H. G. Boumeester	115
Physical principles of gasfilled hot-cathode rectifiers - M. J. Druyvesteyn and J. G. W. Mulder	122
Welding and welding rods - J. Sack	129
The causes of noise in amplifiers - M. Ziegler	136
Public lighting, principles of street illumination - G. B. van der Werfhorst	142
The recording of rapidly occurring electric phenomena with the aid of the cathode ray tube and the camera - J. F. H. Custers	148
Practical applications of X-ray analysis to the testing of materials XI - W. G. Burgers	156
A generator for very high direct current voltage - A. Kuntke	161
Water-cooled mercury lamps - E. G. Dorgelo	165
An ultra short wave telephone link between Eindhoven and Tilburg - C. G. A. von Lindern and G. de Vries	171
The measurement of the hardness of metals and alloys - E. M. H. Lips	177
Transmitting and receiving equipment V.R. 35 combined with the automatic pilot V.P.K. 35 (picture)	182
Position finding and course plotting on board an aeroplane by means of radio - G. P. Ittmann	184
Non-linear distortion phenomena of magnetic origin - J. W. L. Kôhler	193
High-vacuum gauges - F. M. Penning	201
The use of amplifiers (repeaters) in telephony - W. Six and H. Mulders	209
A recording field-strength meter of high sensitivity - M. Ziegler	216
Surge protection of low-tension overhead lines - J. W. G. Mulder	225
Magnet steels - J. L. Snoek	233
Technical considerations in the lighting of country roads - G. B. van der Werfhorst	239
The enlarged projection of television pictures - M. Wolf	249
Practical applications of X-rays to the examination of materials XII - W. G. Burgers	254
Five-electrode transmitting valves (pentodes) - J. P. Heyboer	257
The relationship between fortissimo and pianissimo - R. Vermeulen	266
A simple electrical measuring bridge - P. G. Cath	270
Equivalent networks with highly-saturated iron cores with special reference to their use in the design of stabilisers - H. A. W. Klinkhamer	276
The radiation intensity of the Philips fastness-to-light meter - J. F. H. Custers	282
Inverse feed-back - B. D. H. Tellegen	289
The application of magnetic oil filters to lubricating systems - L. H. de Langen	295
A decimetre wave radio link between Eindhoven and Nijmegen - C. G. A. von Lindern and G. de Vries	299
Joints between metal and glass - H. J. Meerkamp van Embden	306
Illumination of the Eiffel-tower at the Paris World Exhibition (1937) (Picture)	313
The examination of the macro-structure of raw materials and products with the help of X-rays I - J. E. de Graaf	314
The influence of X-ray treatment on flower bulbs (hyacinths and tulips) - W. E. de Mol	321
Noise in amplifiers contributed by the valves - M. Ziegler	329
The adjustment of synchronizers for the "Photoflux" photo flash bulb - J. A. M. van Liempt and J. A. de Vriend	334
The motion of an electron in two-dimensional electrostatic fields - P. H. J. A. Kleynen	338
A vibrator for the connection of alternating current receiving sets to the direct current mains - J. W. Alexander	346
The investigation of the macro-structure of raw materials and products by means of X-rays II - J. E. de Graaf	350
The sodium lamp, from laboratory experiment to street lighting - E. G. Dorgelo and P. J. Bouma	353
Illumination at the International Exhibition in Paris 1937 - L. C. Kalff	361
Radio landing beacons for aerodromes - P. Zijlstra	370
The examination of the macro-structure of materials and products with the help of X-rays. III - J. E. de Graaf	377

VOLUME 3, 1938

	Page
A transportable television installation - J. van der Mark	1
The use of ultraviolet radiation in industrial luminescence research - A. van Wijk	5
"Philite" as a structural material - L. L. C. Polis	9
The experimental short wave broadcasting station PCJ - P. J. H. A. Nordlohne	17
The universal decimal classification - L. C. J. te Bockhorst	27
Lamp manufacture and vitamine research - A. van Wijk	33
Properties and applications of enamelled wire - J. Hoekstra	40
The colour reproduction of incandescent lamps and "Philiphane glass" - P. J. Bouma	47
Applications of cathode ray tube I - H. van Suchtelen	50
Work-bench illumination - N. A. Halbertsma	53
Broadcasttransmitter Rio de Janeiro (Picture)	58
A rotating directional aerial for short wave broadcasting - P. J. H. A. Nordlohne	59
Auditorium acoustics and reverberation - A. Th. van Urk	65
Barretters - J. G. W. Mulder	74
Secondary electron emission - H. Bruining	80
An alternating current dynamo with a flat characteristic for bicycle illumination - H. A. G. Hazeu and M. Kiek	87
The use of the "Philora" HP mercury discharge lamp in an enlarging apparatus - J. A. M. van Liempt	91
The examination of the macro-structure of materials and products with the help of X-rays IV - J. E. de Graaf	92
Voltage regulation of direct current generators by means of triodes - N. A. J. Voorhoeve and F. H. de Jong	97
The behaviour of amplifier valves at very high frequencies - M. J. O. Strutt and A. van der Ziel	103
A car radio - J. W. Alexander	112
The sealing of metal leads through hard glass and silica - B. Jonas	119
Fluorescence - W. de Groot	125
Technical applications of secondary emission - J. L. H. Jonker and M. C. Teves	133
Auditorium acoustics and intelligibility - R. Vermeulen	139
Pumping plant for radio valves (Picture)	147
Applications of cathode ray tubes II - H. van Suchtelen	148
Electrical phenomena in the positive column at low pressure - W. Uyterhoeven	157
Thermojunctions - J. W. L. Köhler	165
Assembly of wireless receivers (Picture)	174
The illumination of the new League of Nations Palace in Geneva - L. C. Kalff	175
A simple arrangement for the measurement of the specific resistance of liquids - A. Claassen	183
The examination of the macro-structure of materials and products with the help of X-rays V - J. E. de Graaf	186
Noise in receiving sets - M. Ziegler	189
Emission of light in the positive column at low pressure - W. Uyterhoeven	197
Compression and expansion in sound transmission - V. Cohen Henriquez	204
Phenomena in amplifier valves caused by secondary emission - J. L. H. Jonker	211
An apparatus for the measurement of scanning speeds of cathode ray tubes - L. Blok	216
Sound amplification and public address - J. de Boer	221
Automatic macroscopic examination of materials with X-rays - J. E. de Graaf and J. H. van der Tuuk	228
Radio interference - L. Blok	235
Fluorescence and phosphorescence - J. H. Gisolf and W. de Groot	241
Applications of cathode-ray tubes III - H. van Suchtelen	248
Radio receivers with push-button tuning - A. Horowitz and J. A. van Lammeren	253
X-ray tube for the analysis of crystal structure - J. E. de Graaf and W. J. Oosterkamp	259
A new frequency-changing valve - J. L. H. Jonker and A. J. W. M. van Overbeek	266
Low-pressure mercury discharge within a luminescent tube - W. Uyterhoeven and G. Zecher	272
The tensile strength of deposited weld metal - J. Sack	279
Television with Nipkow disc and interlaced scanning - H. Rinia	285
The "Rotalix" tube for X-ray diagnosis - J. H. van der Tuuk	292
The diffraction of light by sound film - J. F. Schouten	298
Impulse voltage installations - W. Hondius Boldingh	306
The brightness of road surfaces under artificial illumination - J. Bergmans	313
The electro-acoustic installation in the League of Nations Palace in Geneva - N. A. J. Voorhoeve and P. J. Bourdrez	322
The production and use of neutrons - F. A. Heyn	331
Applications of cathode ray tubes IV - H. van Suchtelen	339
Zirconium and its compounds with a high melting point - J. D. Fast	345
Quantitative considerations of electric welding - J. ter Berg	352
The illumination of passenger ships - L. C. Kalff	356
Auditorium acoustics and sound absorption - R. Vermeulen	363

VOLUME 4, 1939

	Page
A film projection installation with water-cooled mercury lamps - G. Heller	2
Overhead welding - J. Sack	9
Illumination and black-outs - P. J. Bouma	15
Carrier-telephony on loaded cables - F. de Fremery and G. J. Levenbach	20
The role of mercury lamps with fluorescent bulbs in photography - J. A. M. van Liempt	27
Lamps for lighthouses - Th. J. J. A. Manders and L. J. van der Moer	29
Picture taken during the assembly of a large filament lamp for 110 V. 10 kW	41
The Nipkow disc - H. Rinia and L. Leblans	42
Time lag phenomena in gas-filled photoelectric cells - A. A. Kruithoff	48
Recording the characteristics of transmitting valves - Tj. Douma and P. Zijlstra	56
The illumination of railway yards with sodium lamps - H. Zijl	61
A photometer for the investigation of the colour rendering reproduction of various light sources - P. M. van Alphen	66
A motor van for sound recording by the Philips-Miller system - M. J. C. van der Meulen	73
Non-linear distortion in loaded cables - G. J. Levenbach and H. van de Weg	79
Application of cathode ray tubes in mass production - H. van Suchtelen	85
The illumination and beaconing of aerodromes - G. L. van Heel	93
Blocking layer rectifiers - W. Ch. van Geel	100
A simple apparatus for sound recording - K. de Boer and A. Th. van Urk	106
Several problems of X-ray fluoroscopy - B. van Dijk	114
The testing of electric fuses with the cathode ray oscillograph - J. A. M. van Liempt and J. A. de Vriend	118
Air-cooled transmitting valves - M. van de Beek	121
The manufacture of rare gases - H. C. A. Holleman	128
The equipment of broadcasting studios - S. Gradstein.	136
Sound diffusers in loud speakers - J. de Boer	144
The significance of a constant peak time in photo flash bulbs - J. A. M. van Liempt and P. Leydens	148
A million volt X-ray tube - J. H. van der Tuuk	153
A new principle of construction for radio valves - P. G. Cath	162
Synthetic sound - J. F. Schouten	167
The well-lighted house - L. C. Kalff	174
Illumination by means of linear sources of light - N. A. Halbertsma and G. P. Ittmann	181
The magnetron as a generator of ultra short waves - G. Heller	189
A cathode ray oscillograph - J. D. Veegens	198
The pitch of musical instruments and orchestras - Balth. van der Pol and C. C. J. Addink	205
The radiation of sound - A. Th. van Urk and R. Vermeulen	213
Measurements of potential by means of the electrolytic tank - G. Hepp	223
Rapid chemical analysis with the mercury dropping electrode and an oscillograph or measuring bridge as indicator - J. Boeke and H. van Suchtelen	231
Combating radio interferences - L. Blok	237
The propagation of wireless waves round the earth - Balth. van der Pol and H. Bremmer	245
Pressure condensers - C. de Lange	254
Physical photometry - J. Voogd	260
An electron switch - C. Dorsman and S. L. de Bruin	267
An electrical megaphone - J. de Boer	271
Radio receiving sets with linear action tuning condensers. - S. Gradstein	277
Radio sets with station dials calibrated for short waves - G. Heller	284
An acoustic spectroscope - J. F. Schouten	290
Measurements carried out on road lighting systems already installed - P. J. Bouma	292
The efficiency of loud speakers - J. de Boer	301
The preparation of metals in a compact form by pressing and sintering - J. D. Fast	309
On improving of defect hearing - K. de Boer and R. Vermeulen	316
Receiving aerials - J. van Slooten	320
An apparatus for artificial respiration ("Iron lung") - J. B. Aninga and G. C. E. Burger	325
The electrical resistance of metal contacts - J. J. Went	332
Tubular luminescence lamps - P. Schouwstra and G. Zecher	337
Television receivers - G. Heller	342
The dry shaving apparatus "Philishave" - A. Horowitz, A. van Dam and W. H. van der Mei	350
The testing of loud speakers - R. Vermeulen	354

VOLUME 5, 1940

	Page
The new luminous standard - G. Heller	1
The laryngophone - J. de Boer and K. de Boer	6
Drilling diamond dies	14
Reflecting surfaces in the neighbourhood of linear sources of light - N. A. Halbertsma	16
X-ray photographs with extremely short exposure times - W. J. Oosterkamp	22
The investigation of rapidly changing mechanical stresses with the cathode ray oscillograph - S. L. de Bruin	26
The use of modern steels for permanent magnets - A. Th. van Urk	29
Perspectives in the development of the violin - R. Vermeulen	36
Interesting lighting effects of the Liege Water Exposition - L. C. Kalff	42
Quantitative considerations in colour photography by the additive method - J. F. H. Custers	48
The electrometer triode and its applications - H. van Suchtelen	54
Testing amplifier output valves by means of the cathode ray tube - A. J. Heins van der Ven	61
X-ray apparatus for the macroscopic examination of materials - J. E. de Graaf	69
The transport of sound film in apparatus for recording and reproduction - J. J. C. Hardenberg	74
Tungsten ribbon lamps for optical measurements - J. Voogd	82
Measurements in the Philips rare gas plant - H. C. A. Holleman	88
Black-out by the filter method - E. L. J. Matthews and J. A. M. van Liempt	93
The hum due to the magnetic field of the filaments in transmitting valves - K. Posthumus	100
Stereophonic sound reproduction - K. de Boer	107
The reproduction of high and low tones in radio receiving sets - V. Cohen Henriquez	115
The swaging of tungsten rods (Picture)	121
The distribution of the light reflected by different ceiling and wall materials - Joh. Jansen	125
Electron trajectories in multigrid valves - J. L. H. Jonker	131
Microphones - J. de Boer	140
The accuracy of measurements of field strength - J. D. Veegens and J. J. Zaalberg van Zelst	149
The use of X-rays and cathode rays in chemical and metallographic investigations - W. G. Burgers	157
Technical photometry of gas-discharge lamps - P. J. Oranje	166
View of a part of the industrial plant of N. V. Philips' Gloeilampenfabrieken, Eindhoven (Picture)	171
A new push-pull amplifier valve for decimetre waves - M. J. O. Strutt and A. van der Ziel	172
Experiments with stereophonic records - K. de Boer	182
Output and distortion of output amplifier valves under different loads - A. J. Heins van der Ven	189
A permanent magnet which can lift 3 500 times its own weight - J. L. Snoek	195
The use of selenium valves in rectifiers - D. M. Duinker	199
Measurement of phase angles with the help of the cathode ray tube - W. Nijenhuis	208
Technical temperature measurement with thermo-elements	214
Metals as getters - J. D. Fast	217
A new fitting for Roadlighting - J. Bergmans	222
An electrodynamic pick-up for the investigation of mechanical vibrations - J. Severs	230
Absorption phenomena at metal contacts - J. J. Went	238
Standardization of acoustic quantities - R. Vermeulen	243
A cathode ray tube with postacceleration - J. de Gier	245
A photocell with amplification by means of secondary emission - M. C. Teves	253
X-ray photographs with the camera - A. Bouwers and G. C. E. Burger	258
A tone generator - L. Blok	263
Subjective photometry - J. Voogd	270
A cathode ray tube for use in tool making - S. L. de Bruin and C. Dorsman	277
The perception of pitch - J. F. Schouten	286
Natural illumination and visibility at night - P. J. Bouma	296
The measurement of very small phase displacements - C. G. Koops	300
The localization of objects in the human body - A. Bouwers	309
Wireless telephony with moving motorcars - C. G. A. von Lindern	315
Optical experiments with models of the directional distribution of sound in halls - R. Vermeulen	321
Geometrical configurations and duality of electrical networks - B. D. H. Tellegen	324
An apparatus for the measurement of the photographic density of films - J. M. Ledeboer	331
Rearlights and reflectors for bicycles - H. A. E. Keitz	335
The blended-light lamp and other mercury lamps with improved colour rendering, by E. L. J. Mathews	341
An electrical pressure indicator for internal combustion engines, by P. J. Hagendoorn and M. F. Reynst	348
A variable amplifier valve with double cathode connection suitable for metre waves, by M. J. Strutt and A. van der Ziel	357
Alphabetical index, volumes 1-5	363
Chronological index, volumes 1-5	368